International co-tutorial Ph.D. thesis

in agreement between

Université de Lille
Faculté de Sciences et Technologies
École Doctorale Biologie Santé
Cell Phisiology Lab INSERM U1003
Rue Paul Langevin, SN3
59655 Villeneuve d'Ascq, France

Università degli Studi di Torino
Department of Life Sciences and Systems Biology
PhD School in Complex Systems for Quantitative Biomedicine
Cellular and Molecular Angiogenesis Lab
Via Accademia Albertina 13
10123 Torino, Italy

TRP CHANNELS FUNCTIONAL ROLE IN PROSTATE CANCER ANGIOGENESIS AND INVASION

by **Chinigò Giorgia**

defended the September 9th, 2022 - 1 pm
Department of Life Sciences and Systems Biology
University of Turin

Committee for PhD Defense:

Pr. Alessandra Fiorio Pla, University of Turin (Italy)	Tutor
Pr. Dimitra Gkika, Université de Lille (France)	Tutor
Pr. Annarosa Arcangeli, University of Florence (Italy)	Referee - President
Pr. Halima Ahidouch-Ouadid, Université de Picardie Jules Verne (Amiens, France)	Referee
Pr. Rosa Angela Cardone, University of Bari (Italy)	Committee
Pr. Xuefen Le Bourhis, Université de Lille (France)	Committee

Ph.D. thèse en cotutelle internationale

en accord entre

Université de Lille
Faculté de Sciences et Technologies
École Doctorale Biologie Santé
Cell Phisiology Lab INSERM U1003
Rue Paul Langevin, SN3
59655 Villeneuve d'Ascq, France

Università degli Studi di Torino
Department of Life Sciences and Systems Biology
PhD School in Complex Systems for Quantitative Biomedicine
Cellular and Molecular Angiogenesis Lab
Via Accademia Albertina 13
10123 Torino, Italy

RÔLE FONCTIONNEL DES CANAUX TRP DANS L'ANGIOGENÈSE ET L'INVASION DU CANCER DE LA PROSTATE

par **Chinigò Giorgia**

soutenue le 9 septembre 2022 - 1 pm
Département "Life Sciences and Systems Biology"
Université de Turin

Membres du jury:

Pr. Alessandra Fiorio Pla, University of Turin (Italy)	Directeur de thèse
Pr. Dimitra Gkika, Université de Lille (France)	Directeur de thèse
Pr. Annarosa Arcangeli, University of Florence (Italy)	Rapporteur - Président
Pr. Halima Ahidouch-Ouadid, Université de Picardie Jules Verne (Amiens, France)	Rapporteur
Pr. Rosa Angela Cardone, University of Bari (Italy)	Examinateur
Pr. Xuefen Le Bourhis, Université de Lille (France)	Examinateur

To my beloved father

Table of contents

Abstract 1

Resumé 3

Glossary 5

Lists of figures 9

Lists of Tables 13

1. INTRODUCTION 15

1.1 TRP CHANNELS 16

1.1.1 Introduction to TRP 16

1.1.2 TRPA1 24

1.1.3 TRPM8 37

1.2 TRP CHANNELS IN PROSTATE CANCER 51

1.2.1 TRP channels and cancer 51

1.2.2 Transcriptional regulation of TRP channels during carcinogenesis 54

1.2.3 TRP channels and prostate tumor growth 60

1.2.4 TRP channels and prostate cancer invasiveness 64

1.2.5 TRP channels and prostate angiogenesis 68

1.2.6 The intringuing case of TRPM8 in prostate cancer 71

1.3 TRP CHANNELS AND SMALL GTPases INTERPLAY IN THE MAIN HALLMARKS OF METASTATIC CANCER 76

1.3.1 ***Introduction: TRPs and small GTPases*** 77

1.3.2 ***TRPs-small GTPases interplay in metastatic cancer*** 82

1.3.3 ***Conclusions and perspectives*** 95

1.4 THERAPEUTIC APPROACHES TO TARGET PROSTATE CANCER 98

1.4.1 Prostate cancer: diagnosis and prognosis 98

1.4.2 Conventional therapeutic approaches 101

1.4.3 TRP channels as innovative therapeutic targets 103

1.4.4 Photodynamic therapy in prostate cancer 132

1.5. References for the introduction 143

2. PhD PROJECT 187

3. RESULTS 195

3.1.1 Role of TRPA1 in prostate cancer angiogenesis 196

"Transient Receptor Potential Channel Expression Signatures in Tumor-Derived Endothelial Cells: Functional Roles in Prostate Cancer Angiogenesis" 196

3.1.2 Role of TRPM8 in prostate cancer invasion 244

"TRPM8-Rap1A interaction sites as critical determinants for adhesion and migration of prostate and other epithelial cancer cells" 244

"TRPM8 as an Anti-Tumoral Target in Prostate Cancer Growth and Metastasis Dissemination" 302

3.2 Lipid nanoparticles as nanodelivery systems: incorporation of polymethine dyes 338

"Polymethine dyes-loaded Solid Lipid Nanoparticles (SLN) as promising photosensitizers for biomedical applications" 338

"Quatsomes as powerful nanovesicles for Photodynamic Therapy" 366

4. GENERAL DISCUSSION 389

4.1 TRP channels to target prostate cancer progression 390

4.1.1 TRPA1 channel to target PCa angiogenesis 390

4.1.2 TRPM8 channels to target PCa invasion 392

4.2 Lipid nanoparticles as drug delivery systems: incorporation of polymethine dyes 397

4.3 References for general discussion 400

5. CONCLUSIONS & FUTURE PERSPECTIVES 405

Author's contributions 407

Aknowledgements 413

Annex 414

"TRP channels in Brain Tumors" 414

Abstract

Prostate cancer (PCa) is the second most lethal tumor among men and its mortality is mainly due to metastasis. Thus, it is critical to understand the mechanisms by which tumors grow and how metastases can diffuse throughout the body. Cell migration of both epithelial and endothelial cells (EC) is required for cancer cell invasion of neighboring tissues as well as for the formation of tumor vasculature. Several Transient Receptor Potential (TRP) channels are deregulated in cancer cells and have been suggested as valuable markers in predicting cancer progression as well as potential targets for pharmaceutical therapy. In the present Ph.D. thesis, I established the role of TRP channels regulating Ca^{2+} signature in PCa cells and vasculature focusing, in particular, on the channels that affect migration, a common key step in tumor vascularization and invasion.

The role of TRP channels in prostatic angiogenesis was studied in prostate tumor-derived EC (PTEC): we fully profiled the expression of all TRPs in normal ECs and TECs derived from PCa, breast, and renal tumors. We identified three 'prostate-associated' genes whose expression appears selectively upregulated in PTECs: TRPV2, TRPC3, and TRPA1. Among them, TRPA1 seems to play a critical role in regulating PCa angiogenesis, promoting PTEC migration, vascular network formation, and angiogenic sprouting both *in vitro* and *in vivo*.

As regards, instead, epithelial PCa cells' motility, emerging evidence indicates that TRPM8 may exert a protective role in metastatic PCa by impairing the motility of these cancer cells. Investigating the molecular mechanism underlying this biological effect, we found that, as previously described for ECs, TRPM8 inhibits PCa cell migration and adhesion independently from its channel function by intracellularly trapping the small GTPase Rap1A in its inactive form and thus avoiding its translocation and activation on the plasma membrane. Moreover, we identified and validated the residues involved in the interaction between TRPM8 and Rap1A: residues E207 and Y240 in the sequence of TRPM8 and Y32 in that of Rap1A.

Our data shed new light on the roles played by TRPA1 and TRPM8 in prostate cancer angiogenesis and invasion by affecting cell migration of endothelial and epithelial cells, respectively.

In the fight against metastasis, the development of efficient nanodelivery systems can be as crucial as the identification of new molecular targets in cancer therapy to fill the gap between "drug discovery" and "drug delivery" which is one of the most challenges in clinical perspectives. In this context, a second part of this Ph.D. project focused on the study of lipid nanoparticles as suitable drug delivery systems. In particular, the use of solid lipid nanoparticles (SLN) and quatsomes (QS) for the incorporation of polymethine dyes (PMD) suitable for both diagnostic and therapeutic purposes was investigated. We demonstrated that lipid nanocarriers not only increase the solubility of PMD in physiological conditions but even enhance their

spectroscopic performances, making PMD-loaded nanocarriers potential and appealing candidates for *in vivo* imaging and/or PDT applications.

Overall, the present Ph.D. thesis deepens our knowledge of the role of TRP channels in PCa progression, providing new insight into their possible use as new therapeutic targets in PCa treatment and, at the same time, proposes new therapeutic tools to improve drug delivery in cancer therapy.

Résumé

Le cancer de la prostate (CaP) est la deuxième cause de mortalité par cancer chez l'homme et sa lethalité est principalement due aux métastases. Il est donc essentiel de comprendre les mécanismes par lesquels les tumeurs se développent et comment les métastases peuvent se diffuser dans le corps. L'agressivité des tumeurs prostatiques est étroitement liée à la migration des cellules épithéliales et endothéliales (EC) provoquant l'invasion des tissus voisins ainsi que la vascularisation tumorale. Plusieurs canaux de la famille TRP (Transient Receptor Potential) sont dérégulés dans les cellules cancéreuses et ont été suggérés comme marqueurs pronostiques et diagnostiques ainsi que comme des cibles potentielles pour la thérapie du cancer. Dans cette thèse doctorale , j'ai établi le rôle de certains canaux TRP régulant la signature calcique des cellules endothéliales et cancéreuses de la prostate , en se concentrant en particulier sur les canaux qui affectent la migration, une étape clé commune dans la vascularisation et l'invasion tumorales.

Le rôle des canaux TRP dans l'angiogenèse prostatique a été étudié dans les EC dérivées de tumeurs de la prostate (PTEC): nous avons etabli le profil complet d'expression de tous les TRP dans les EC normales et les TEC dérivées des tumeurs prostatiques, mammaires et rénales. Nous avons identifié trois gènes « associés à la prostate » dont l'expression est corrélée positivement dans les PTEC : TRPV2, TRPC3 et TRPA1. Parmi eux, TRPA1 joue un rôle essentiel dans la régulation de l'angiogenèse du CaP, favorisant la migration des PTEC, la formation du réseau vasculaire et l'angiogenèse par bourgeonnement *in vitro* et *in vivo*.

En ce qui concerne la motilité des cellules cancéreuses d'origine épithéliale, je me suis concentrée sur TRPM8, canal pour lequel un rôle protecteur dans le CaP métastatique a été proposé via l'altération de la motilité cellulaire. Nous avons tout d'abord validé le rôle anti-métastatique de TRPM8 *in vivo*, montrant que la surexpression et l'activation de TRPM8 réduisent significativement la croissance tumorale et la dissémination des métastases dans un modèle murin de xénogreffe orthotopique de la prostate. De plus, en étudiant le mécanisme moléculaire sous-jacent à la fonction inhibitrice de TRPM8 sur la migration des cellules du CaP, nous avons constaté que, comme décrit précédemment pour les EC, TRPM8 inhibe la migration et l'adhésion des cellules du CaP indépendamment de sa fonction canalaire en piégeant au niveau intracellulaire la petite GTPase Rap1A sous sa forme inactive et en évitant ainsi sa translocation et activation sur la membrane plasmique. De plus, nous avons identifié et validé les résidus impliqués dans l'interaction entre TRPM8 et Rap1A : résidus E207 et Y240 dans la séquence de TRPM8 et Y32 dans celle de Rap1A. Nos données révèlent donc le mécanisme moléculaire de TRPA1 et TRPM8 expliquant leur rôle dans l'angiogenèse et l'invasion du CaP en affectant la migration des cellules endothéliales et épithéliales, respectivement.

Dans la lutte contre les métastases, le développement de systèmes de nano-administration efficaces est aussi crucial que l'identification de nouvelles cibles moléculaires afin de combler le fossé clinique entre la

«découverte de cibles pharmaceutiques » et la « livraison de médicaments ». Dans ce contexte, une deuxième partie de ce projet de doctorat était axé sur l'étude des nanoparticules lipidiques en tant que systèmes d'administration de médicaments appropriés. En particulier, l'utilisation de nanoparticules lipidiques solides (SLN) et de quatsomes (QS) pour l'incorporation de colorants polyméthine (PMD) adaptés à des fins diagnostiques et thérapeutiques a été étudiée. Nous avons démontré que les nanoparticules lipidiques non seulement augmentent la solubilité de la PMD dans des conditions physiologiques, mais améliorent même leurs performances spectroscopiques, faisant des nanoparticules chargés de PMD des candidats potentiels et attrayants pour l'imagerie *in vivo* et/ou les applications PDT.

Dans l'ensemble, cette thèse de doctorat approfondit nos connaissances sur le rôle des canaux TRP dans la progression de la CaP, fournissant de nouvelles cibles potentiellles dans la thérapeutique contre le CaP et, en même temps, propose de nouveaux outils thérapeutiques pour améliorer l'administration de médicaments dans le traitement du cancer.

Glossary

AA	*Arachidonic-acid*
AC	*Adenylate cyclase*
AD	*Atopic dermatitis*
ADPKD	*Autosomal dominant polycistic kidney disease*
ADT	*Androgen deprivation therapy*
AITC	*Allyl isothiocyanate*
AJCC	*American Joint Committee on Cancer*
AM	*Adrenomedullin*
Ang II	*Angiotensin II*
AnkR	*Ankyrin repeat*
AR	*Androgen receptors*
α_{1D}-AR	*α_{1D} adrenergic receptor*
ASIC	*Acid-sensing ion channels*
bFGF	*basic fibroblast growth factor*
BK	*Bradykinin*
BPA	*Bisphenol A*
BPH	*Benign prostate hyperplasia*
BT	*Brachytherapy*
BTEC	*Breast tumor-derived endothelial cells*
Ca^{2+}	*calcium*
$Ca^{2+}{}_i$	*intracellular free calcium*
CAF	*Cancer-associated fibroblasts*
CaM	*Calmodulin*
CaMKII	*Calmodulin-dependent protein kinase II*
cAMP	*cyclic AMP*
CDK	*Cyclin-dependent kinase*
CGRP	*Calcitonin gene-related peptide*
CK8/CK18	*Cytokeratin 8/18*
COPD	*Chronic obstructive pulmonary disease*
COX-2	*Cyclooxygenase 2*
$cPLA_2$	*Cytosolic phospholipase A2*
CPP	*Cell penetrating peptides*
CRPC	*Castration-resistant prostate cancer*
CT	*Computed tomography*
CTD	*C-terminal domain*
CTL	*cytotoxic T lymphocytes*
DAG	*Diacyl glycerol*
DC	*Dendritic cells*
DED	*Dry eye disease*
DLI	*Drug-to-light interval*
DNBS	*Dinitrobenzene sulphonic acid*
DRG	*Dorsal root ganglion*
EC	*Endothelial cells*
ECM	*Extracellular matrix*
EGF	*Endothelial growth factor*
EM	*Electron Microscopy*

EMA	*European Medicines Agency*
EMT	*Epithelial to mesenchymal transition*
EPC	*Endothelial progenitor cells*
EPR	*Enhanced permeability and retention*
ePLND	*Extended pelvic lymph node dissection*
ER	*Endoplasmic Reticulum*
ER_α	*Estrogen receptor α*
FA	*Focal adhesions*
FAK	*Focal adhesion kinases*
FDA	*Food and Drug Administration*
FEPS	*Familial episodic pain syndrome*
FLS	*Fibroblast-like synoviocytes*
FN	*Fibronectin*
FSGS	*Focal segmental glomerular sclerosis*
GABAA	*γ-aminobutyric acid type A*
GABAARAP	*γ-aminobutyric acid type A receptor-associated protein*
$G\alpha_q$	*α subunit of G protein-coupled receptors*
GF	*Growth factors*
GnRH	*Gonadotropin-releasing hormone*
GPCR	*G-protein coupled receptors*
GTPases	*Guanosine triphosphatases*
GAP	*GTPases activating protein*
GDI	*Guanine-nucleotide dissociation inhibitors*
GEF	*Guanine exchange factors*
HGF	*Hepatocyte growth factor*
HMEC	*Human dermal microvascular endothelial cells*
hK2	*Human glandular kallikrein 2*
HS	*Hydrosulfide*
HUVEC	*Human umbilical vein EC*
H_2O_2	*Hydrogen peroxide*
IBD	*Inflammatory bowel disease*
IEC	*Intestinal epithelial cells*
IGF	*Insulin-like growth factor 1*
IGRT	*Image-guided radiotherapy*
IL-1β	*Interleukin 1-beta*
IL-6	*Interleukin 6*
IL-6 R	*Interleukin 6 receptor*
IMRT	*Intensity modulation radiotherapy*
IP_3	*Inositol triphosphate*
IP_3R	*Inositol triphosphate receptor*
$iPLA_2$	*Ca^{2+}-independent phospholipase A2*
ISC	*Intersystem conversion*
ISUP	*International Society of Urologic Pathologists*
JNK	*Jun N-terminal kinase*
KLK3	*serine protease kallikrein 3*
KO	*Knockout*
LC	*Leukotrienes*
LNC	*Lipid nanocapsules*
LPC	*Lysophosphatidylcholine*
LPI	*Lysophosphatidylinositol*

LPL	*Lysophospholipids*
LTB_4	*Leukotriene B4*
MAM	*Mitochondria-associated ER membranes*
mCRPC	*Metastatic castration-resistant prostate cancer*
MDCK-F	*Madin–Darby Canine Kidney-Focus*
MDR	*Multi-drug resistance*
Mg^{2+}	*magnesium*
MHR	*TRPM homology regions*
MLC	*Myosin light chain*
MLCK	*Myosin light chain kinase*
MMP	*Matrix metalloproteinase*
MRI	*Magnetic resonance imaging*
Na^+	*sodium*
NFAT	*activated T cell nuclear factor*
NFkB	*nuclear factor kappa-light-chain-enhancer of activated B cells*
NIR	*Near-infrared*
NO	*Nitric oxide*
NOX	*NADPH oxidase*
NP	*Nanoparticles*
NSAID	*Non-Steroidal Anti-Inflammatory Drugs*
O_2	*Oxygen*
$^1O_2$	*Singlet oxygen*
OD	*Oropharyngeal dysphagia*
PAR-1/2	*Protease-activated receptor 1/2*
PCa	*Prostate Cancer*
PCNA	*Proliferating cell nuclear antigen*
PDD	*Photodynamic diagnosis*
PDGF	*Platelet-derived growth factor*
PDT	*Photodynamic therapy*
PET	*Positron emission tomography*
PG	*Prostaglandins*
PheoA	*Pyropheophorbide A*
PI3K	*Phosphatidylinositol 3-kinase*
PIP_2	*Phosphatidylinositol bisphosphate*
PKA	*Protein kinase A*
PKC	*Protein kinase C*
PLC	*Phospholipase C*
PM	*Plasma membrane*
PMA	*Phorbol 12-myristate 13-acetate*
PMD	*Polymethine dyes*
PPI	*Protein-protein interactions*
PRGF-1	*Plasminogen related growth factor-1*
PS	*Photosensitizer*
PSA	*Prostate-specific antigen*
PSMA	*Prostate specific membrane antigen*
PtdIns(n,n2)P_2	*Phosphatidylinositol n,n2-bisphosphate*
PTEC	*Prostate tumor-derived endothelial cells*
pTNM	*pathological tumor-node-metastasis*
Pyk2	*Proline-rich tyrosine kinase 2*
PZQ	*Praziquantel*
QS	*Quatsomes*

RES	*Reticuloendothelial system*
ROS	*Reactive oxygen species*
RP	*Radical prostatectomy*
RT	*Radiation therapy*
RyR	*Ryanodine receptors*
SAR	*Structure-activity relationship*
SERCA	*Sarco-Endoplasmic Reticulum Calcium ATPase*
SF	*Scatter factor*
SLN	*Solid lipid nanoparticles*
SMA	*Scapuloperoneal spinal muscular atrophy*
SMOC	*Second messenger-operated channel*
SNP	*Single Nucleotide Polymorphisms*
SOC	*Store-operated channels*
SOCE	*Store-operated calcium entry*
TCAF	*TRP channel-associated factors*
TEC	*Tumor-derived endothelial cells*
TM	*Trans-membrane*
TMD	*Trans-membrane domain*
TGF-β1	*Transforming growth factor β1*
TNF-α	*Tumour necrosis factor alpha*
TRP	*Transient Receptor Potential*
TRPC	*TRP Canonical*
TRPV	*TRP Vanilloid*
TRPVL	*TRP Vanilloid-like*
TRPM	*TRP Melastatin*
$TRPM8_{FA}$	*TRPM8 from Ficedula albicollis*
$TRPM8_{PM}$	*TRPM8 expressed on the plasma membrane*
$TRPM8_{ER}$	*TRPM8 expressed on the endoplasmic reticulum*
4TM-TRPM8/ sTRPM8 α	*Short TRPM8 isoform α (35-40kDa – 4 TM)*
sM8	*non-channel cytoplasmic small TRPM8 isoform*
TRPA	*TRP Ankyrin*
TRPN	*TRP No mechanoreceptor potential C*
TRPS	*TRP Soromelastatin*
TRPP	*TRP Polycystic*
TRPML	*TRP Mucolipin*
TRUS	*Transrectal ultrasound*
TX	*Thromboxanes*
UAE	*European Association of Urology*
UCP-1	*Uncoupling protein 1*
uPA	*Urokinase plasminogen activator*
uPAR	*Urokinase plasminogen activator*
VEGF	*Vascular endothelial growth factor*
VEGF-A	*Vascular endothelial growth factor A*
VGIC	*Voltage-gated ion channels*
VMRT	*External beam volumetric arc radiotherapy*
VSLD	*Voltage sensor module*
$3\text{-}T_1AM$	*3-iodothyronamine*
5-ALA	*5-aminolevulinic acid*

Lists of figures

INTRODUCTION

TRP channels

Figure 1. Phylogeny and distribution of TRP channels superfamily in Eukarya. 18

Figure 2. Structural divergences among TRP subfamilies. 20

Figure 3. Protein-protein interactions (PPI) network of TRP channels. 23

Figure 4. TRPA1 structure. 26

Figure 5. Signaling pathways modulating TRPA1 activity. 34

Figure 6 TRPM8 structure. 38

Figure 7. Structural basis of the binding of cooling agents and PIP_2 to TRPM8. 39

Figure 8 Schematic summary of the pathways involved in TRPM8 modulation. 48

TRP channels in prostate cancer

Figure 9. TRP regulation during carcinogenesis/tumor progression. 55

Figure 10. TRP isoforms. 58

Figure 11. TRP channels and prostate tumor growth. 64

Figure 12. TRP channels and prostate cancer invasiveness. 67

Figure 13. TRP channels and tumor vascularization. 70

Figure 14. TRPM8 expression profile during PCa development. 71

Figure 15. TRPM8 localization and function depending on androgens and the differentiation status of human prostate epithelial cells. 72

TRP channels and small GTPases interplay in the main hallmarks of metastatic cancer

Figure 16. TRP-small GTPases signaling pathways interplay in cell migration. 83

Figure 17. TRP- small GTPases signaling pathways interplay in cell invasion. 88

Figure 18. TRP- small GTPases signaling pathways interplay in aberrant tumour vascularization. 91

Therapeutic approaches to target prostate cancer

Figure 19. Prostate cancer statistics. 98

Figure 20. Representative histological staining on PCa tissues. 100

Figure 21. TRP channels in diseases. 105

Figure 22. Properties of nanoparticles and their impact on systemic delivery. 125

Figure 23. Passive and active targeting of nanoparticles. 127

Figure 24. Historical development of nanonystems. 129

Figure 25. Key steps and biological mechanisms underlying PDT treatment. 132

Figure 26. Jabłoński diagram illustrating the photophysical principles of PDT. 133

Figure 27. Structures of selected porphyrins (porfimer sodium), chlorins (verteporfin) and bacteriochlorins (redaporfin) currently in clinical use. 134

Figure 28. Diagram depicting prostate PDT apparatus. 136

Figure 29. General structure of polymethine dyes. 139

RESULTS

3.1.1 "Transient Receptor Potential Channel Expression Signatures in Tumor-Derived Endothelial Cells: Functional Roles in Prostate Cancer Angiogenesis"

Figure 1. Identification of the trp expression signature in PTEC. 209

Figure 2. Protein expression of 'prostate-associated' genes in PTEC and HPrMEC. 212

Figure 3. TRPV2 modulates EC viability. 215

Figure 4. hTERT PTEC validation as cellular model for TEC studies. 217

Figure 5. TRPA1 increases EC migration. 220

Figure 6. TRPC3 has a role in PCa cell attraction. 222

Figure 7. TRPA1 promotes *in vitro* tubulogenesis and *in vivo* angiogenesis. 225

Figure 8. TRPA1 is implicated in PTEC chemotaxis and function in tip-like cells. 227

Figure 1S. Assessment of external and internal controls of real-time qPCR used for the normalization of expression data. 236

Figure 2S. Assessment of external and internal controls of real-time qPCR used for the normalization of expression. 237

Figure 3S. hTERT PTEC characterization. 238

Figure 4S. Validation of 'prostate-specific' channel overexpression in HMECs for their functional characterization in ECs. 240

Figure 5S. Validation of 'prostate-specific' channel in tubulogenesis *in vitro*. 241

3.2.1 "TRPM8-Rap1A interaction sites as critical determinants for adhesion and migration of prostate and other epithelial cancer cells"

Figure 1. TRPM8 inhibits cell migration and adhesion independently of its channel activity. 260

Figure 2. TRPM8 decreases Rap1 activation. 262

Figure 3. TRPM8 ER localization. 264

Figure 4. Identification of the residues involved in TRPM8-Rap1 interaction. 266

Figure 5. Rap1 mutants' characterization. 269

Figure 6. TRPM8 mutants' characterization. 272

Figure 7. TRPM8 mutant's functional validation. 275

Figure 8. Validation of TRPM8 E207A Y240A on other epithelial cancer cell lines. 277

Figure 9. TRPM8 and Rap1A expression during carcinogenesis in different cancers. 279

Figure 10. Graphical abstract. 285

Figure S1. Validation of TRPM8 pore mutant. 292

Figure S2. Original uncropped blot referring to Fig. 2ai. 293

Figure S3. TRPM8 and Rap1A basal expression in PC3, MCF-7, and HeLa cell lines. 294

Figure S4. RCA of the interaction between TRPM8 and Rap1A. 296

Figure S5. Role of K31 and Y32 in mediating the direct interaction between the inactive (GDP-bound) form of Rap1 and TRPM8 N terminus. 297

Figure S6. Original uncropped blots referring to Fig. 6 and 7. 298

Figure S7. TRPM8-Rap1A interaction in cancer cells viability. 299

Figure S8. TRPM8-Rap1A interaction in healthy and cancerous prostate tissues. 300

3.2.2 "TRPM8 as an Anti-Tumoral Target in Prostate Cancer Growth and Metastasis Disseminations"

Figure 1. TRPM8 overexpression inhibits prostate primary tumor growth *in vivo*. 312

Figure 2. TRPM8 overexpression affects cell proliferation but not apoptosis. 314

Figure 3. TRPM8 overexpression inhibits clone's formation capability. 316

Figure 4. TRPM8 overexpression inhibits PCa cells' metastatic dissemination. 318

Figure 5. TRPM8 overexpression in PC3 inhibits metastatic dissemination. 320

Figure 6. Effects of lipid nanocapsules (LNC) containing a TRPM8 agonist on migratory and invasive properties. 323

Figure 7. TRPM8 doesn't affect MMPs secretion but modulates Rho-GTPases signaling pathway. 325

Figure 8. TRPM8 affects ERK and FAK phosphorylation assessed by western blot. 326

Figure S1. PC3-luc or PC3-M8-luc intravenous injection on mice and invasion assay 336

3.3.1 "Polymethine dyes-loaded Solid Lipid Nanoparticles (SLN) as promising photosensitizers for biomedical applications"

Figure 1. PMD and SLN. 346

Figure 2. SLN AF4 characterization. 348

Figure 3. Dyes and dye-loaded SLN optical characterization. 350

Figure 4. *In vitro* cytotoxicity of CY-SLN and SQ-SLN on MCF-7. 352

Figure 5. Dyes and dye-loaded SLN in vitro phototoxicity. 354

Figure 6. Dye-loaded SLN uptake and intracellular localization. 357

Figure S1. SLN stability. 362

Figure S2. *In vitro* cytotoxicity of CY-SLN and SQ-SLN on HMEC. 363

Figure S3. CY uptake and intracellular localization. 364

3.3.2 "Quatsomes as powerful nanovesicles for Photodynamic Therapy"

Figure 1. Br-Squaraine-C12 loaded QS. 376

Figure 2. Absorbance and fluorescence spectra of a) free Br-Sq-C12 in ethanol and b) dye-loaded QSs in water. 378

Figure 3. Physicochemical and Photophysical properties of QS-Sq. 381

Figure 4. Colloidal stability and photostability of QS-Sq. 383

Figure 5. Comparative generation of reactive oxygen species (ROS) by QS_Sq. 384

Figure 6. *In vitro* cytotoxicity of QS and QS-Sq. 386

Figure 7. *In vitro* phototoxicity of QS and QS-Sq. 387

ANNEX

Figure 1. TRPs-mediated signaling pathways in gliomas. 423

Lists of Tables

INTRODUCTION

TRP channels

Table 1. TRPA1 agonists. 28

Table 2. TRPA1 antagonists 31

Table 3. TRPM8 agonists. 41

Table 4. TRPM8 antagonists. 43

TRP channels in prostate cancer

Table 5. TRP channels in prostate cancer. 53

TRP channels and small GTPases interplay in the main hallmarks of metastatic cancer

Table 6. TRPs expression in cancer and correlation with patient survival prognosis. 78

Table 7. TRPs-small GTPases relationship in metastatic cancer hallmarks. 95

Therapeutic approaches to target prostate cancer

Table 8. Prostate cancer stages and classification. 100

Table 9. Potential repurposing of FDA-approved drugs against ion channels in cancer therapy. 103

Table 10. Drugs targeting TRP channels in clinical trials. 107

Table 11. Patented TRPA1 antagonists/agonists and drug repositioning. 112

Table 12. Patented TRPM8 antagonists/agonists and drug repositioning. 119

Table 13. Approved nanodelivery systems with anticancer indications. 127

Table 14. Photosensitizers in clinical studies for prostate PDT. 136

RESULTS

3.1.1 “Transient Receptor Potential Channel Expression Signatures in Tumor-Derived Endothelial Cells: Functional Roles in Prostate Cancer Angiogenesis”

Table 1. Primers sequences used for trp profiling in PTEC. 201

3.2.1 "TRPM8-Rap1A interaction sites as critical determinants for adhesion and migration of prostate and other epithelial cancer cells"

Table 1. Primers sequences used for single and double mutagenesis of TRPM8 (E207A and Y240A) and Rap1 (K31 and Y32A). 248

3.3.1 "Polymethine dyes-loaded Solid Lipid Nanoparticles (SLN) as promising photosensitizers for biomedical applications"

Table 1. Physicochemical properties of BLK-SLN, SQ-SLN and CY-SLN. 347

Table 2. Particle size obtained from DLS analysis of AF4 fractograms, elution volume (mL) and peak width. 348

Table 3. Optical properties of CY and SQ dissolved in organic solvent and after encapsulation into SLN in aqueous solution. 351

3.3.2 "Quatsomes as powerful nanovesicles for Photodynamic Therapy"

Table 1. Concentrations (nM) and dilution rates of quatsomes, and exposure times used in PDT tests. 374

Table 2. Summary of the parameters obtained by lyophilization and UV-vis spectroscopy on PMD-loaded quatsomes. 377

Table 3. Photochemical properties of Br-Sq-C12, QS_Sq_200 and QS_Sq_300. 377

Table 4. Summary of DLS and ELS parameters measured on quatsomes. 380

ANNEX

Table 1. TRP channels expression and functionality in gliomas/glioblastomas. 420

1. INTRODUCTION

1.1 TRP CHANNELS

1.1.1 Introduction to TRP

Transient Receptor Potential (TRP) channels are a class of non-selective ion channels, mostly permeable to calcium (Ca^{2+}), sodium (Na^{+}), and magnesium (Mg^{2+}) although with varying cation selectivity. Their discovery dates back to the early '70 when an interesting *Drosophila* mutant was characterized by defective light-sensing resulting in blindness in the presence of constant bright light. This defect was due to the lack of a functional copy of the gene subsequently named *trp* as responsible for the transient rather than sustained receptor potential observed following *Drosophila*'s continuous exposure to light (Cosens and Manning 1969; Minke, Wu, and Pak 1975; Montell and Rubin 1989; Hardie and Minke 1992). Therefore, the name "TRP" is a misnomer, since, the wild-type channel induces a persistent and not transient current; the second is the result of a gene mutation.

Since its first discovery in 1969, the **function** of the *TRP* gene product remained unclear for 20 years. The first evidence that the trp gene could encode an ion channel dates back to 1985 when the gene was cloned for the first time (Montell et al. 1985) and the amino acid sequence started to be deduced (Montell and Rubin 1989). Then, an *in vivo* study on a TRP isoform carrying a mutation (Asp^{621}) in the pore loop responsible for the ion selectivity definitively demonstrated that the TRP is a superfamily of Ca^{2+}-permeable channels (Liu et al. 2007). Since 1995 with the discovery of human TRP proteins (Wes et al. 1995), interest in these proteins has grown exponentially and the further pieces of evidence of TRP as key global sensors of sensory input completely redefined our understanding of sensory physiology. In particular, a milestone in the field of TRPs was the discovery of additional mammalian "thermoTRPs" (Bandell, Macpherson, and Patapoutian 2007; Caterina 2007; Talavera, Nilius, and Voets 2008). Moreover, within the animal kingdom all senses, including vision, smell, taste, hearing, and touch, appear mediated by TRP channels. Consistently, mutations in many of the 27 human TRP have been associated with a large variety of diseases ranging from episodic pain syndrome (TRPA1), stationary night blindness (TRPM1), kidney diseases (TRPP2 and TRPC6), hypomagnesemia and hypocalcemia (TRPM6), skeletal diseases and neuropathies (TRPV4), cardiac disease (TRPM4) and neurodegenerative disorders (TRPM2 and TRPML1) (Dietrich 2019; Nilius and Owsianik 2010). In the last 20 years, the interest in TRP channels has grown exponentially until reaching its peak in 2021 with the awarding of the Nobel Prize in Physiology or Medicine to David Julius for the discovery of the capsaicin receptor TRPV1 in 1997 (Caterina et al. 1997; Julius 2022).

TRP channels likely developed early in eukaryotic evolution, as no evidence of TRP channels has been reported in Archaea or Bacteria, while in Eucarya the TRP superfamily has been found to be highly conserved from worms to humans (**Fig. 1**) (Wes et al. 1995). TRP channels have diversified considerably in the course of evolution, acquiring different structural domains, gating modalities, and being recruited into various types of tissue (Himmel and Cox 2020). The great interest aroused by TRP channels over the last three decades together with the considerable enhancement of -omics techniques has led to a radical change in the definition and characterization of the subfamilies belonging to this class of channels compared to the original classification (Himmel and Cox 2020). Based on sequence homology, TRPs in animals may be classified into nine subfamilies: TRPC (Canonical), TRPV (Vanilloid), TRPVL (Vanilloid-like), TRPM (Melastatin), TRPA (Ankyrin), TRPN (NompC, or no mechanoreceptor potential C), and TRPS (Soromelastatin) which are categorized as group 1, TRPP (Polycystic) and TRPML (Mucolipin) which define group 2 (**Fig. 1**).

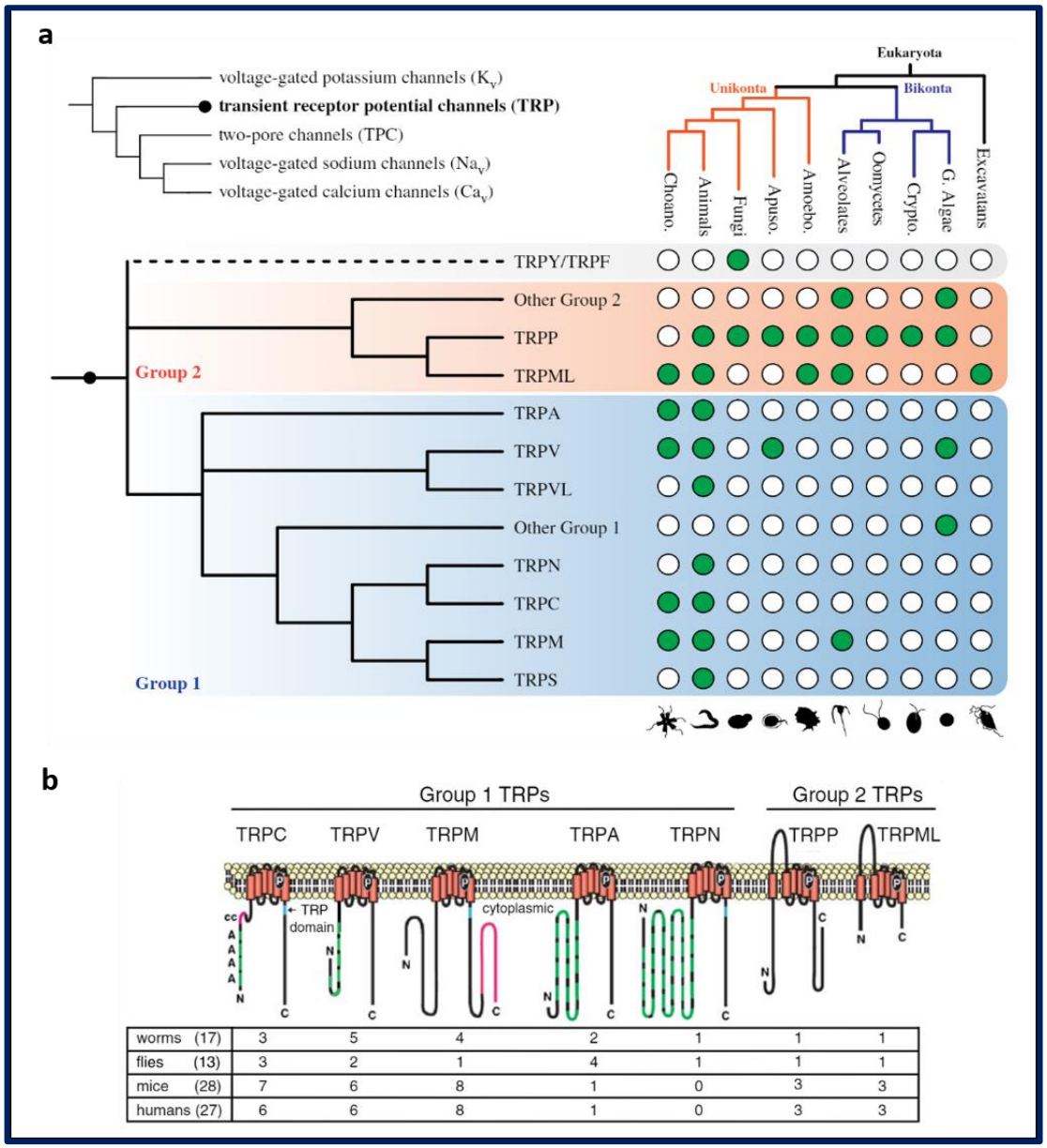

Figure 1. Phylogeny and distribution of TRP channels superfamily in Eukarya.

a) Top left: TRP superfamily within the voltage-gated ion channel clade; Taxa shown: Choano.: Choanoflagellates (unicellular flagellates closely related to animals), animals, fungi, Apuso.: Apusozoans (flagellate eukaryotes), Amoebo.: Amoebozoans (amoeboid eukaryotes), Alveolates (including dinoflagellates), Oomycetes (fungus-like eukaryotes), Crypto.: Cryptophyte, G. Algae: green algae, and excavatans (basal eukaryotes). Filled circles indicate the presence of the family reported on the left in the taxon above; blank circles indicate no evidence for that family in the indicated taxon. The dashed line for TRPY/TRPF indicates that its placement is especially uncertain. Images from (Himmel and Cox 2020).

b) Distribution of TRP subfamilies in worms (C. elegans), flies (D. melanogaster), mice and humans; the total numbers of TRP channels are indicated in parentheses, and the numbers of TRP within each subfamily are shown. TRPP1 channels are not included in the tabulation. Image from (Montell 2011).

At the **structural level,** TRP channels are homo-tetramers based on subunits formed by 6 transmembrane (TM) spanning domains (S1 to S6) (**Fig. 2**). Each subunit forms a conductive pore through a loop between S5 and S6 segments within the plasma membrane (PM) and has two cytoplasmic tails (N- and C- terminal domains). Moreover, the first four helices (S1–S4) define the so-called voltage sensor–like domain (VSLD), connected to the pore domain by the S4–S5 linker and responsible for the modest voltage sensitivity exhibited by TRP channels. The latter is mainly due to the presence of gating charges in their S4 helices which, in analogy to the voltage-gated ion channels (VGIC) although to a lesser extent, drive the movement of the S4 helix in accordance with the electric field of the membrane and consequently affect channel gating through S4–S5 linker (Cao 2020). Although the general architecture is the same for all TRP channels, the overall structure of the channels can diverge significantly due to the wide variety of intracellular domains responsible for the different responsiveness to functional modulators. In general, the length and nature of the domains present in the intracellular amino and carboxylic terms mainly define the members of the different subfamilies (**Fig. 2**). To date, 28 TRP channels have been identified in mammals including 27 in humans, classified as follows:

- TRPC (1-7): "*Canonical*" because of the high homology shown by the 7 TRPC members with TRP protein from *Drosophila*; to be noted that TRPC2 is a pseudogene not expressed in humans;
- TRPV (1-6): the name "*Vanilloid*" is due to the fact that the first member cloned (TRPV1) is activated by capsaicin, a vanilloid chemicals
- TRPM (1-8): "*Melastatin*" since the first member of this family (TRPM1) has been discovered from the comparison between a benign nevus and a murine melanoma nevus (Duncan et al. 1998); this subfamily is characterized by the presence among its members of chanzymes, combining two functions of an ion channel and an enzyme, as TRPM2 and TRPM7 (Huang et al. 2020);
- TRPA (1): this family includes just one member (TRPA1) and its name refers to the about 14 *Ankyrin* repeats present in the TRPA1 N-terminal tail;
- TRPP (2,3,5): the members of this family are also referred to as PKD (polycystic kidney disease) ion channels, hence the name "*Polycystic*"; to be noted that TRPP1 protein (PKD1) is not a TRP channel;
- TRPML (1-3): "*MucoLipin*" refers to the association between TRPML1 channel and the neurodevelopmental disorder mucolipidosis IV.

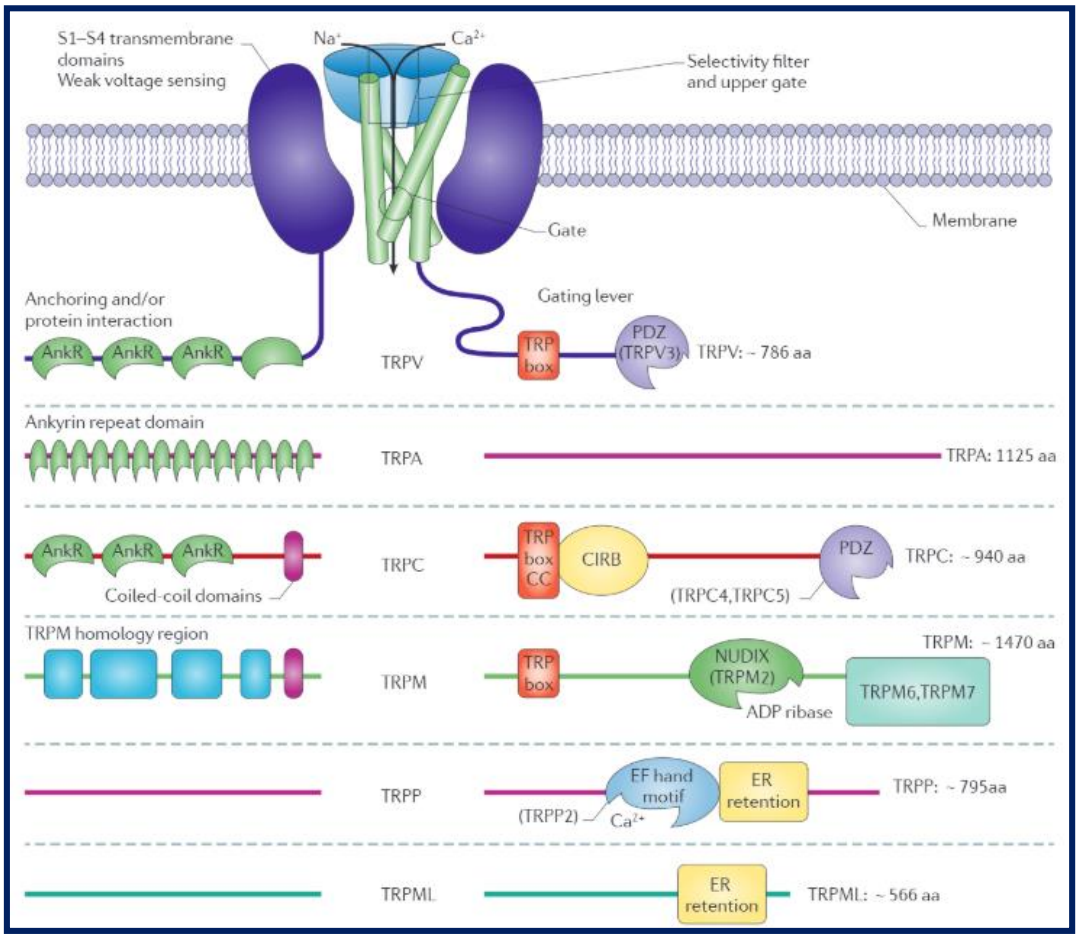

Figure 2. Structural divergences among TRP subfamilies.

Different motifs exhibited by each TRP subfamily in its amino (N) and carboxyl (C) termini. TRPV, TRPA, and TRPC families have N terminal ankyrin repeat (AnkR) domains that are absent in other TRP channel subfamilies. A TRP box, thought to be involved in gating, has been found in TRPV, TRPM and TRPC families. TRPP and TRPML channels both have endoplasmic reticulum (ER) retention domains that may be due to their functional localization on intracellular organelles.
aa: amino acids; CIRB: calmodulin/inositol-1,4,5-trisphosphate (Ins(1,4,5)P_3) receptor binding domain; NUDIX: nucleoside diphosphate-linked moiety X; PDZ: postsynaptic density protein 95 (PSD95); DLGA: Drosophila disc large tumour suppressor; ZO1: zonula occludens protein 1. Image from (Moran et al. 2011).

Different TRP subunits within or across subfamilies can then organize and associate to form hetero-tetramers (TRPC1-TRPC3 (Lintschinger et al. 2000), TRPC1-TRPC4 (Phelan et al. 2012), TRPC1-TRPC5 (Strübing et al. 2001), TRPC1-TRPP2 (Bai et al. 2008), TRPV4-TRPP2 (Du et al. 2012), TRPV5-TRPV6 (Hoenderop et al. 2003), TRPML1-TRPML2 (Curcio-Morelli et al. 2009), and TRPML1-TRPML3 (Curcio-Morelli et al. 2009) with new and peculiar conductive and regulatory properties, as described in some studies in particular on the TRPC family (Hofmann et al. 2002; Earley and Brayden 2015). However, little is known about the stoichiometry of the subunits of TRP heteromers in physiological conditions and it is not entirely clear how much the different

electrophysiological properties exhibited by heterotetramers depend directly on the interaction of the different subunits, how much on different protein-protein interactions and how much environmental conditions (Chun et al. 2014).

Recently, the structures of several TRP channels have been elucidated with cryo-electron microscopy (EM). Moreover, the high potential of this technique allowed us to appreciate different conformational states for almost all TRP, such as open/closed, activated/inhibited, and unligated/ligated conformations, and thus to better understand their mechanism of action.

Most TRP channels are Ca^{2+}-permeable, except for TRPM4 and TRPM5 which are only permeable to monovalent cations and do not conduct Ca^{2+} and Mg^{2+}. However, relative Ca^{2+} permeability varies widely among the isotypes from low ($P_{Ca}/P_{Na} < 10$) to very high Ca^{2+} selectivity ($P_{Ca}/P_{Na} > 100$; TRPV5 and TRPV6) (Owsianik et al. 2006).

TRP channels are **polymodal molecular sensors**. Indeed, they can be activated by several chemical as well as physical stimuli, including light, temperature, pH, voltage, pressure, and tension. Most TRP channels involved in sensory perception have intrinsic voltage sensing probably associated with the presence of positively charged lysine and arginine residues located in transmembrane segment S4 and S4-S5 linker (Nilius et al. 2005). Specific ligands or temperature changes may trigger the voltage-dependent activation of TRP by altering their midpoint by hundreds of millivolts. Another well-established mechanism of TRP activation is related to membrane phospholipids, which may directly or indirectly affect TRP function mainly by acting on their voltage sensing and/or their sensitivity to ligands or Ca^{2+} (Nilius, Owsianik, and Voets 2008). For instance, many TRP channels including TRPV1, TRPM8, and TRPM5 can be modulated directly or indirectly by the PM level of phosphatidylinositol 4,5-bisphosphate (PtdIns(4,5)P_2) as well as by membrane-associated enzymes sensitive to alterations in PtdIns(4,5)P_2 levels as Pirt (Kim et al. 2008). Moreover, the phospholipase C (PLC) through the hydrolysis of phosphatidylinositol bisphosphate (PIP_2) into diacylglycerol (DAG) and inositol triphosphate (IP_3) may trigger the PLC-DAG-IP_3 pathway which ultimately results in TRP modulation induced by store depletion. Indeed, some TRP channels including TRPC1 and other members of the Canonical subfamily are Store-Operated Channel (SOC) meaning that they can be activated by the depletion of intracellular calcium stores mainly the endoplasmic reticulum. Another general mechanism of TRP channel gating concerns phosphorylation. In particular, protein kinase C (PKC) and protein kinase A (PKA) have been shown to influence the activity and sensitization of TRPV1 and TRPM8 albeit with opposite effects. In particular, PKC and PKA sensitize TRPV1 to heat or capsaicin potentiating its responses (Bhave et al. 2003; Jeske et al. 2008), whereas lead to the downregulation of TRPM8 activity (Premkumar et al. 2005). In addition to all these mechanisms, TRP channels may be activated by several exogenous and endogenous ligands both natural and synthetic. For instance, TRPC channels are activated by DAG, TRPV1, and TRPV4 by arachidonic-

acid (AA)-related compounds, and TRPM3 by sphingosine. Moreover, temperature-sensitive TRP channels can be activated by natural and chemical compounds that mimic thermal sensation: the “hot” sensor TRPV1 is activated by capsaicin and piperine, extracted by hot and black pepper respectively, whereas the “cold” sensor TRPM8 is sensitive to compounds that mimic cold sensation like menthol, eucalyptol, and icilin. To be noticed that some compounds are relatively highly selective for a particular TRP channel (olvanil for TRPV1; 4α-phorbol-12,13-didecanoate, lumiphorbols, phorbol-hexonates, and GSK 1016790A for TRPV4), whereas others can activate more than one TRP channel (2-aminoethyl diphenylborinate activates TRPV1, TRPV2, and TRPV3; icilin activates both TRPM8 and TRPA1). Finally, the activity of many TRP channels may also be controlled by indirect activation that arises downstream of receptor-mediated signaling, either via G-protein coupled receptors (GPCR) or receptor tyrosine kinases.

Thanks to their ability to sense changes in the cellular environment TRP have a profound impact on animal behavior and survival mechanisms. TRP are expressed in most tissues and cell types both excitable and non-excitable and, in response to a large number of different stimuli, mediate countless cellular functions. Basically, TRP channels integrate different signaling pathways converting them into electrochemical signals to finally elicit different cellular responses. This is often achieved through the interaction of TRP channels with a great number of intracellular proteins to form “signalplexes” and “channelosomes” which significantly affect their trafficking, positioning, and activity of the channels (Planells-Cases and Ferrer-Montiel 2007). Beyond their contribution to sensory functions like nociception, taste transduction, pheromone signaling, and temperature sensation TRP channels are key modulators of intracellular Ca^{2+} and Mg^{2+} homeostasis through which they affect many physiological processes within the cell including cell cycle and cell motility. Alterations in the activity of TRP channels have been widely associated with a broad array of disorders involving the skin (Caterina and Pang 2016), peripheral and central nervous system (Vennekens, Menigoz, and Nilius 2012; Morelli et al. 2013), gastrointestinal (Holzer 2011), genito-urinary (Skryma et al. 2011), respiratory (Preti, Szallasi, and Patacchini 2012), cardiovascular (Watanabe et al. 2013), and immune systems (Schwarz 2007; Smith and Nilius 2013) as well as metabolic disorders including obesity and diabetes (Zhu et al. 2011; Suri and Szallasi 2008). Furthermore, mutations in the *TRP* gene have been linked to human inherited diseases known as ‘TRP channelopathies’ affecting the kidney, the skeleton, cardiovascular and nervous systems as well as nociception (Wu, Sweet, and Clapham 2010; Nilius and Owsianik 2010; Prevarskaya, Skryma, and Shuba 2018). For example, autosomal dominant polycystic kidney disease (ADPKD), distal and scapuloperoneal spinal muscular atrophy (SMA), and focal segmental glomerular sclerosis (FSGS), and have been related to mutations on TRPP2 (Igarashi and Somlo 2002), TRPV4 (Auer-grumbach et al. 2012), and TRPC6 (Winn et al. 2005) genes, respectively. However, most inherited or acquired TRP dysfunctions rely on impaired TRP protein-protein interactions (PPI) (Chun et al. 2014). Therefore, in recent years, great efforts

have been dedicated to the study of the TRP interactome in order to elucidate the molecular mechanisms underlying the role of these channels in physio-pathological processes. Indeed, based on the biological knowledge existing on TRP binding proteins, it is reasonable to think that unknown TRP functions can be deduced. In this context, certainly, that the integration of TRP channel PPI data with gene expression profiles would further unravel new and promising interactions and molecular mechanisms underlying TRP functions (**Fig. 3**).

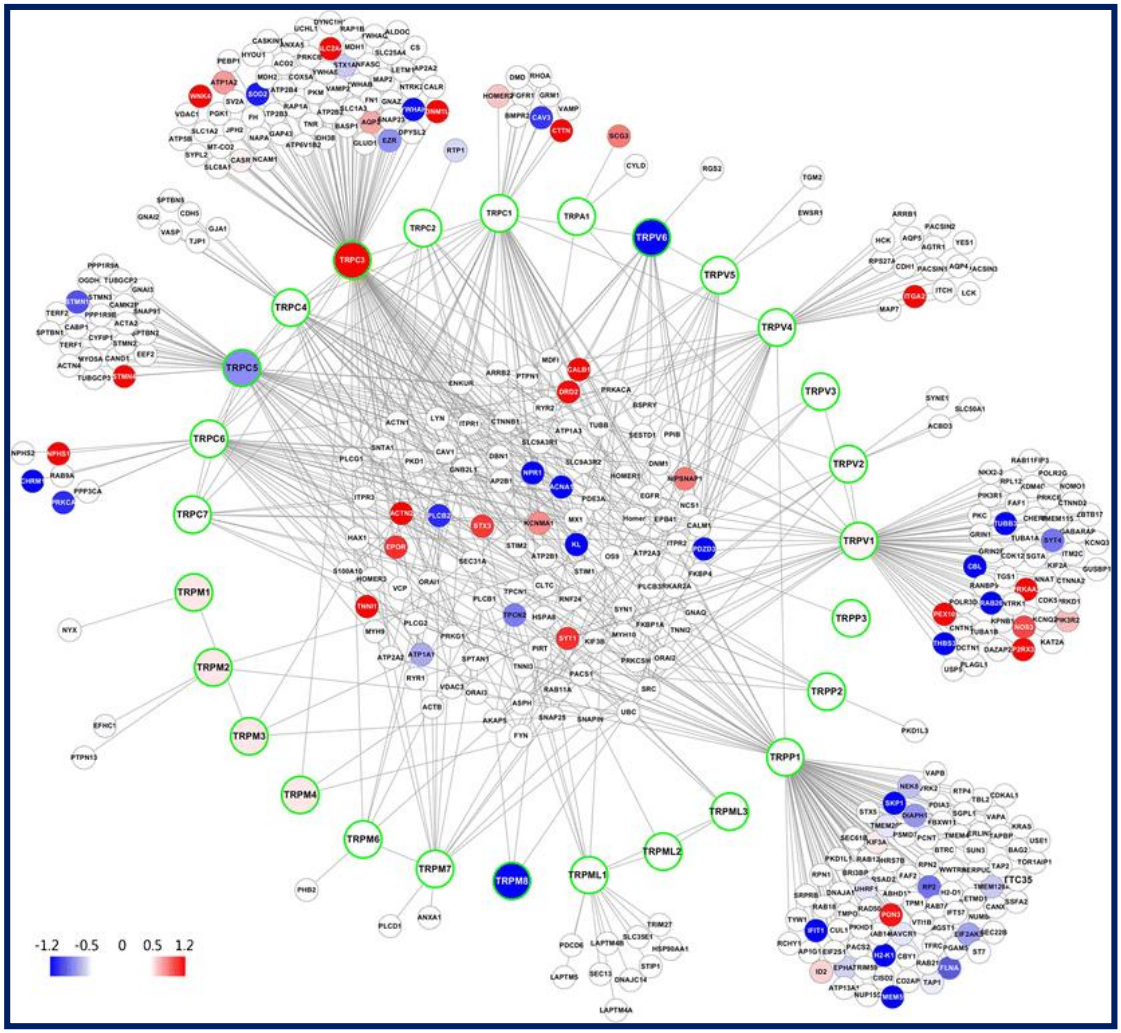

Figure 3. Protein-protein interactions (PPI) network of TRP channels.

Example of integration of PPI data with gene expression profile data on TRP channels provided by (Chun et al. 2014). The PPI data were downloaded from the TRIP database 2.0 (Shin et al. 2012) and visualized using the Cytoscape. TRP channels and their interacting proteins are represented by nodes with green and white borders, respectively; gene expression values (log scale) for each node are displayed along a color gradient between red and blue.
Image from (Chun et al. 2014).

Most TRP channels are mainly localized at the PM and their surface expression is mainly controlled by vesicular trafficking. In this regard, several studies have demonstrated that TRP translocation to the PM may be induced by several factors such as hormones, growth factors, and G protein-coupled receptors' agonists. However, TRP channels are also expressed in intracellular membranes like mitochondria and endoplasmic reticulum (ER). Based on their specific location, the TRP channel can bind to different accessory proteins forming signaling complexes involved in the modulation of different signaling pathways (Nilius and Owsianik 2011).

In the following paragraphs, I will describe in more detail two TRP channels that have been the subject of my research project, namely TRPA1 and TRPM8.

1.1.2 TRPA1

TRPA1, originally named ANKTM1, is a non-selective cation channel and it is the only member of the ankyrin subfamily so far identified in mammals. It is mainly permeable to Ca^{2+} and Na^{+}, but it is also permeable to K^{+}, rubidium, cesium, lithium, and zinc (Story et al. 2003).

TRPA1 was first discovered in 1999 in human fetal lung fibroblasts as a gene product associated with oncogenic transformation (Jaquemar, Schenker, and Trueb 1999). Afterward, TRPA1 expression was found in sensory neurons of dorsal root ganglion (DRG), nodose ganglion, and trigeminal ganglion neurons, suggesting an interesting role of this channel in the propagation of noxious and inflammatory stimuli (Andrade, Meotti, and Calixto 2012; Viana 2016). In addition to different types of sensory neurons (Anand et al. 2008), TRPA1 expression has also been detected in numerous tissues that actively participate in homeostasis such as the skin (keratinocytes, melanocytes, and fibroblasts) (Atoyan, Shander, and Botchkareva 2009; Tsutsumi et al. 2010), lungs (alveolar epithelial cells, smooth muscle cells, and fibroblasts) (Mukhopadhyay et al. 2011; Nassini et al. 2012), blood vessels (Gratzke et al. 2009; Qian et al. 2013), urinary tract (Streng et al. 2008; Gratzke et al. 2010), and pancreatic beta cells (Cao et al. 2012).

Structure

TRPA1 is an 1119 amino acid protein encoded by the *TRPA1* gene located on chromosome 8q13. The TRPA1 structure was first solved by the Moiseenkova-Bell laboratory in 2011 with a resolution of ~ 16 Å (Cvetkov et al. 2011). Hence, it was further described more finely at near-atomic resolution (~ 4 Å) using cryo-EM (Paulsen et al. 2015). Commonly to the other TRP channels, TRPA1 has a transmembrane domain (TMD) consisting of six putative transmembrane segments (S1–S6) and a pore loop between S5 and S6, which

resembles those of TRPV1 and V2 structures except for the pore region (**Fig. 4**). The latter is gated at the top by Asp915 (Gly643 and Met644 in TRPV1) and at the bottom by two hydrophobic residues Ile957 and Val961 (Ile679 in TRPV1) (Paulsen et al. 2015). Moreover, the outer region of the pore exhibits two short pore helices similar to those observed in Na_v channels. However, the biggest peculiarity of the TRPA1 channel, to which it also owes its name, is the presence of 14/18 ankyrin repeats (AnkR) in the N-terminal domain (out of which only five were solved by cryo-EM), similar to those observed in the TRPV and TRPC channels albeit in smaller numbers (3-6) (**Fig. 4**). Basically, AnkR are protein units of about 33 amino acids that make up 3 α-helices connected by a β-sheet. These motifs play key roles in the mediation of protein-protein interactions and, consequently, in the activation of the channel, as well as in the insertion of the channel in the PM (Gaudet 2008). In fact, although these activation modes are controversial, it would seem that the AnkR attend to the opening of the channel linked to mechano-sensation as well as to thermo-sensation, functioning as a molecular spring that connects the channel to the cytoskeleton matrix to allow it to open (Nagata et al. 2005; Sotomayor, Corey, and Schulten 2005; Lee et al. 2006) upon mechanical stimuli or at temperatures below 17° C. However, results from different studies are contradictory on this point (Bautista et al. 2006; Kwan et al. 2006). In addition, the pre-S1 region within the N-terminus exhibits a large number of cysteines and lysines which may form a complex network of protein disulfide bridges within and between monomers. Consistent with the possible involvement of these key electrophile sensing residues in allosteric modulation of the channel gating, 3D reconstruction showed that the TRP-like domain in TRPA1 is located close to the pre-S1 region and the S4–S5 linker with which it establishes numerous interactions. Binding sites for Ca^{2+}, responsible for TRPA1 sensitization/desensitization, have been suggested to be present in both the N- and C-termini (Zygmunt and Hogestatt 2014). In particular, the N-terminal domain shows an EF-hand site that allows the binding of intracellular Ca^{2+} to the channel, thus directly regulating its activity or increasing its sensitivity to agonists (Doerner et al. 2007; Zurborg et al. 2007). The C-terminus of TRPA1 forms a coiled-coil central stalk-like domain, flanked by the AnkR of the N-terminus. Finally, TRPA1 possesses two putative N-glycosylation sites (N747 and N753) which influence the sensitivity of the channel to different agonists (Egan et al. 2016). The structure solved by Paulsen provided new insights into the binding of a known selective TRPA1 antagonist, A-967079. Indeed, it has been suggested that A-967079 binds at a potential binding pocket formed by S5, S6, and the first pore helix between S5 and S6 and that through an " induced-fit " mechanism it prevents the movement of these elements, thus acting as a molecular wedge that inhibits the opening of the lower gate (Paulsen et al. 2015). However, to better elucidate the binding sites and mechanisms of action for other known classes of TRPA1 antagonists, new Cryo-EM structures of TRPA1 bound with different classes of antagonists at higher resolutions would be needed. To note, several higher resolution Cryo-EM structures of TRPA1 have been recently solved including the ligand-free form of TRPA1 with a resolution of 2.8 Å, the

TRPA1 complex with irreversible covalent agonist JT010 (2.9 Å), as well as the complex with reversible covalent agonist BITC (3.1 Å) (Suo et al. 2020). These structures provided new insights into the electrophile recognition by Cys621 of TRPA1 agonists and the subsequent electrophile-dependent conformational changes. In fact, the authors suggested that TRPA1 agonists following binding to a "shell" binding pocket on the cytoplasmic side lead to conformational changes in the upper half which then translate into a conformational change in the β sheet (Suo et al. 2020). The latter, in turn, repositions a newly identified interfacial helix (IFH) allowing it to interact with the S4-S5 linker and finally open the S6 gate (Suo et al. 2020).

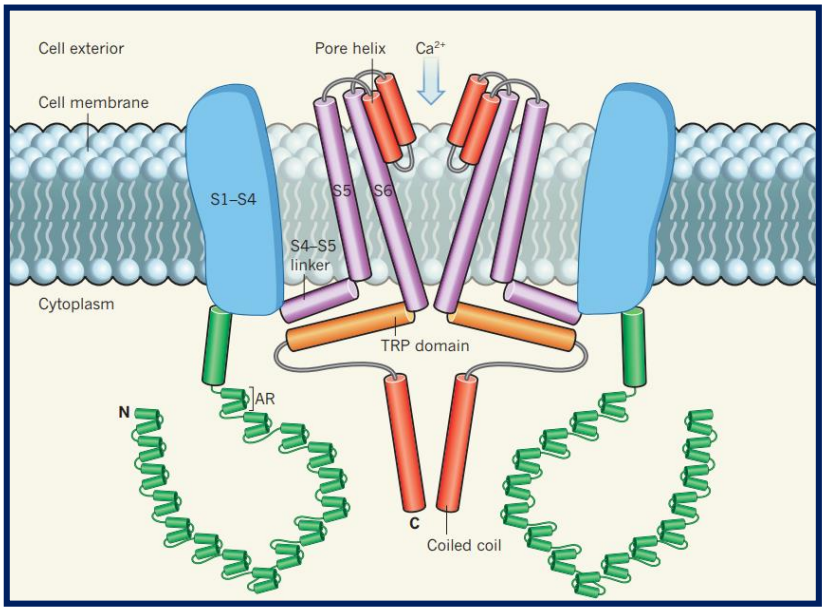

Figure 4. TRPA1 structure.
Image from (Clapham 2015).

Further advances in Cryo-EM technology and the emergence of higher-resolution TRPA1 structures bound with different classes of antagonists, would enhance the structure-based design and the discovery of novel TRPA1 antagonists (Chen and Terrett 2020).

Activation and modulation

TRPA1 is a polymodal channel capable of sensing numerous signals related to tissue damage, oxidative stress, and inflammation, from both outside and inside the cell, in order to translate them and ensure specific biological effects by modulating the membrane potential or intervening in calcium signaling.

Activators

Endogenous

The TRPA1 channel can be considered a sensor of oxidative stress. Indeed, it can be activated directly by the accumulation of endogenous substances produced by oxidative reactions (Takahashi and Mori 2011; Takahashi et al. 2011; Arenas et al. 2017), including hydrogen peroxide (H_2O_2) (Andersson et al. 2008), reactive oxygen species (ROS), oxidized lipids such as 4-hydroxy-2-nonenal (4-HNE) (Taylor-Clark et al. 2008; Trevisan et al. 2014), 4-oxo-nonenal (Andersson et al. 2008) or even 8-*iso*-prostaglandin A_2 (Taylor-Clark et al. 2008) and 15-Deoxy-$\Delta^{12,14}$-prostaglandin J_2 (Andersson et al. 2008), and nitrated lipids like nitro oleic acid (Sculptoreanu et al. 2010) (**Table 1**). Activation of TRPA1 by these compounds can occur by conjugate addition or by the formation of disulfide bridges (Andersson et al. 2008). Moreover, the capability of TRPA1 to sense O_2 in bronchopulmonary C-fibers has also been detected. More specifically, it has been shown that in normoxia conditions TRPA1 is inhibited by the hydroxylation of specific proline residues, whereas in hyperoxia O_2 directly abolishes TRPA1 inhibition thanks to the high sensitivity of the channel to cysteine-mediated oxidation (Takahashi et al. 2011). Along with several molecules involved in cellular stress and tissue damage (Arenas et al. 2017), TRPA1 can also be indirectly activated by pro-inflammatory agents via the PLC signaling pathway. In that case, cytosolic Ca^{2+} plays an important role in regulating channel gating (Zygmunt and Hogestatt 2014). As an example, it has been observed that TRPA1 may be activated by the accumulation of compounds that contribute to inflammatory pain like bradykinin (BK), which mediates inflammation by causing vasodilation, by increasing vascular permeability, and by stimulating the synthesis of prostaglandins (Bandell et al. 2004), or methylglyoxal, a reactive metabolite that accumulates during diabetes (Brownlee 2001; Nakayama et al. 2008) and induces painful peripheral neuropathies through the direct activation of TRPA1 (Eberhardt et al. 2012; Andersson et al. 2013).

Exogenous

TRPA1 is activated by temperature changes (Laursen et al. 2015; Bandell et al. 2004) as well as by mechanical perturbations (Corey et al. 2004) and a plethora of chemical compounds (**Table 1**). TRPA1 is a well-known receptor for a wide range of plant-derived, food (allicin, carvacrol, cinnamaldehyde, gingerol, mustard oil, thymol, and wasabi) or polluting irritant products thanks to key cysteine and lysine residues accessible to solvents present in a putative highly integrated nexus that converges on an unexpected TRP-like allosteric domain (Macpherson et al. 2007). Electrophilic compounds and oxidants able to modify, in an alkylative or oxidative fashion, nucleophilic cysteine residues, highly conserved in the channel's N-terminus across species (Kang et al. 2010), are strong activators of this channel. For example, pollutants from smoke and gases harmful to health have the ability, thanks to their electrophilic carbon nucleus, to form reversible

covalent adducts with the SH thiol groups of the lysine and cysteine residues of the N-terminal, thus activating the channel (Hinman et al. 2006; Macpherson et al. 2007; Takahashi et al. 2008; Sadofsky et al. 2011). Several residues have been found to be critical for this type of bond: cysteines C415, C421, C422, C619, C621, C622, C639, and C663 as well as lysine K708. Therefore, TRPA1 may act as a sensitive, low-threshold electrophilic receptor (Paulsen et al. 2015). The most well-characterized TRPA1 agonists are allyl isothiocyanate (AITC), the active ingredient in mustard oil and wasabi, cinnamaldehyde which is an extract from cinnamon, allicin from garlic extract, and acrolein from fume exhaust (Bautista et al. 2006; Bandell et al. 2004) Nilius, Appendino, and Owsianik 2012). Additionally, TRPA1 is also activated by non-electrophilic molecules which do not covalently bind to the channel protein like menthol (Karashima et al. 2007), nifedipin (Fajardo et al. 2008), nicotine (Talavera et al. 2009) and cannabinoids (Jordt et al. 2004). However, the molecular mechanism of TRPA1 channel modulation by non-reactive ligands is still largely unknown and controversial. Consistent with its function in pain perception, recent data have shown that analgesics and vasodilators such as paracetamol and dihydropyridines as well as general anesthetics are able to stimulate the TRPA1 channel questioning the use of these clinical drugs for inducing non-negligible side effects (Fajardo et al. 2008; Matta et al. 2008; Nassini et al. 2010; Andersson et al. 2011).

TRPA1 agonists			
Compound	Structure	EC_{50} (µM)	Ref.
Endogenous			
H_2O_2 (Hydrogen peroxide)		230	(Andersson et al. 2008)
NO_3 (Peroxynitrite)	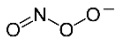		(Andersson et al. 2015)
NO (Nitrogen monoxide)			(Eberhardt et al. 2015)
ClO^- (Hypochlorite)		~ 10	(Bessac et al. 2008)
H_2S (Hydrogen sulfide)			(Eberhardt et al. 2015; Chung et al. 2020)
5-6-EET (5,6-Epoxy-eicosatrienoic acid)	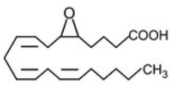		(Sisignano et al. 2012)

Nitro-oleic acid	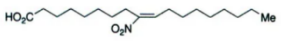		(Sculptoreanu et al. 2010)
Alkenyl aldehydes (4-hydroxynonenal 4-oxo-nonenal 4-hydroxyhexenal)	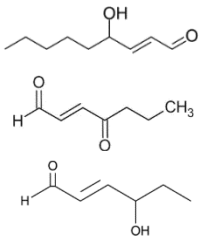	19.9 1.9 38.9	(Taylor-Clark et al. 2008; Trevisani et al. 2007; Trevisan et al. 2014; Andersson et al. 2008)
Prostaglandins (8-*iso*-prostaglandin A_2 15-Deoxy-$\Delta^{12,14}$-prostaglandin J_2)	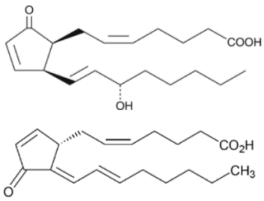	5.6	(Taylor-Clark et al. 2008; Andersson et al. 2008)
methylglyoxal	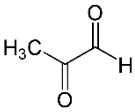	744	(Eberhardt et al. 2012)
Exogenous			
Cinnamaldehyde (cinnamon)	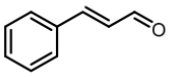	19	(Bandell et al. 2004)
Allyl isothiocyanate (AITC) (mustard and wasabi)	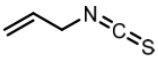	2.7	(Jordt et al. 2004; Uchida et al. 2012)
Allicin (garlic and onion)	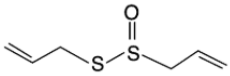	1.91	(Macpherson et al. 2005)
Toluene diisocyanate	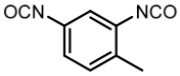	10	(Taylor-Clark et al. 2009)
Acrolein (cigarette smoke, fume exhaust, and tear gas)		5	(Bautista et al. 2006; Macpherson et al. 2007)

Cannabinoids (Marijuana - Δ^9-tetrahydrocannabinol)	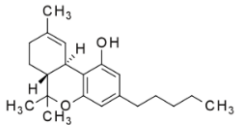	12	(Jordt et al. 2004)
Menthol	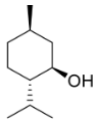	95	(Karashima et al. 2007)
Nifedipin	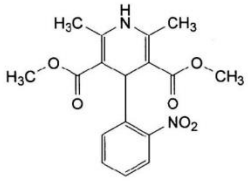	$400*10^3$	(Fajardo et al. 2008)
Nicotine	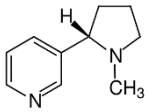	~ 10	(Talavera et al. 2009)
JT-010	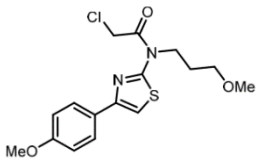	0.000065	(Takaya et al. 2015)
PF-4840154	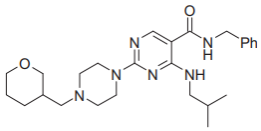	0.023	(Ryckmans et al. 2011)
DNCB (2,4-Dinitrochlorobenzene)	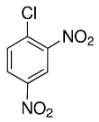	0.167	(Saarnilehto et al. 2014)

Table 1. TRPA1 agonists.

Inhibitors

Unlike agonists like irritants, oxidative stress products, and inflammation mediators, natural TRPA1 channel inhibitors have only begun to be identified (**Table 2**). The main natural inhibitors of TRPA1 are camphor (Xu, Blair, and Clapham 2005), curcumin (Leamy et al. 2011), eucalyptol (Takaishi et al. 2012), α-

lipoic acid (Trevisan et al. 2013) as well as powerful antioxidants like resveratrol (Yu et al. 2013; Nalli et al. 2016), a natural polyphenol found in red wine and food (grapes and peanuts) with multiple beneficial effects (cardioprotection and anti-cancer), caffeine (Nagatomo and Kubo 2008), and cardamon from medicinal herbs (Wang et al. 2016). Consistently, some dietary antioxidants have proved to significantly reduce pain associated with peripheral neuropathies caused by chemotherapeutic agents in animal models. All these molecules are accumulated by antioxidant properties, however, the inhibition mechanisms mediated by them can be very different and are not yet fully known. For instance, camphor and curcumin activate the channel before completely desensitizing it, while other molecules such as α-lipoic acid exert a purely inhibiting effect. Furthermore, the effects of these molecules may depend on the species considered, such as caffeine which inhibits the human form of the TRPA1 channel while activating the mouse form. While most natural channel blockers are promising, they have only recently been discovered and remain for the most part ineffective and not very specific. Thus, to compensate for this lack of antagonists, drug molecules have been developed to selectively and more effectively inhibit the channel. The best known of these pharmacological inhibitors is HC-030031 (IC_{50} = 6.2 µM for the response to AITC) whose efficacy *in vitro* has been demonstrated in numerous studies (McNamara et al. 2007; Eid et al. 2008). Unfortunately, however, this molecule has shown considerable limitations in its applicability *in vivo* due to its poor pharmacokinetic properties, a very short half-life (32 min), and the tendency to bind to over 90% of plasma proteins as was demonstrated in rat models (Rech et al. 2010). To date, new, other TRPA1 antagonists have been developed by several pharmaceutical companies like Glenmark, Hydra Bioscience, Janssen, and Merck; among them, A-967079 (IC_{50} 67 nM for the inhibition of the human form of the channel), developed by Abbott (Chen et al. 2011; Copeland et al. 2014; Rooney et al. 2014), GRC 17536 by Glenmark and HX100 by Hydra Biosciences currently in the clinical stage (2 and 1 respectively) for the treatment of diabetic neuropathies and asthmatic diseases. Finally, monoclonal antibodies were produced such as the 2B10 antibody directed against the pore domain of the channel, which showed great efficacy with an inhibition of the AITC response greater than 70% (Lee et al. 2014).

TRPA1 antagonists			
Compound	Structure	IC_{50} (µM)	Ref.
Curcumin	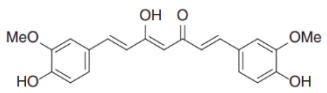	3.3	(Nalli et al. 2017)

Resveratrol	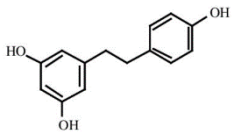	19.9	(Nalli et al. 2016)
Eucalyptol (1,8 cineole)	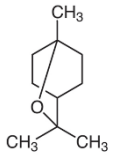	500	(Takaishi et al. 2012)
Camphor	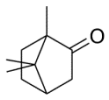	1260	(Takaishi et al. 2014)
α-lipoic acid	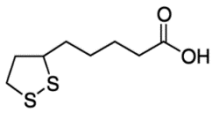		(Gualdani et al. 2015)
caffeine	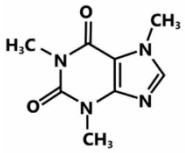	1000	(Nagatomo and Kubo 2008)
Chembridge-5861528	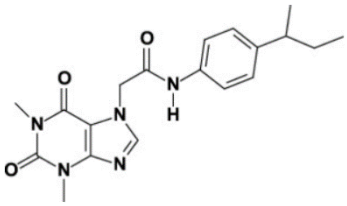	14.3	(Wei et al. 2009)

Table 2. TRPA1 antagonists.

Due to the great interest aroused by TRPA1 in the therapeutic field, many TRPA1 modulators, mainly inhibitors, have been proposed and patented by pharmaceutical companies as well as academic groups. Many of the most relevant TRPA1 antagonists patented in the last years are summarized in **Table 11** and will be discussed further in **Chapter 1.4.3**.

Modulators

G protein-coupled receptors

In addition to the various ligands mentioned above, it has been shown in DRG neurons that the TRPA1 channel can be activated by GPCR-induced transduction pathways like that involving the BK receptor, a vasodilator peptide hormone involved in inflammation, or the PAR2 (protease-activated receptor 2) (**Fig. 5**). Indeed, the activation of these GPCR induces activation of the TRPA1 channel and/or sensitization of the channel to various agonists such as AITC, cinnamaldehyde or endogenous agonists. These effects mainly involve the activation of PLC with the generation of inositol triphosphate (IP_3), which, following binding to its receptor, will allow depletion of reticular calcium store and the possible binding of Ca^{2+} on the TRPA1 channel sensitizing it to agonists or activating it directly (Jordt et al. 2004) (**Fig. 5**). Having been shown that phosphatidylinositol bisphosphate (PIP_2) is capable of inhibiting the TRPA1 channel, activation of the PLC would remove the inhibition by hydrolyzing PIP_2 into IP_3 and DAG (Dai et al. 2007; Wang et al. 2008). Furthermore, this channel activation *via* the PLC pathway would not be PKC dependent, as experiments showed neither inhibition with GF109203X, a potent PKC inhibitor, nor PKC activation with PMA (phorbol 12-myristate 13-acetate) did not affect bradykinin-mediated sensitization of the channel to agonists. Conversely, PKA may also play a role in the modulation of the channel activity (Wang et al. 2008). Finally, about the transduction pathway generated by chloroquine in DRG neurons also capable of activating TRPA1, it was observed that the βϒ subunits constituting the G proteins could interact directly with the TRPA1 channel to regulate its activity. More specifically, their inhibition with gallein significantly decreases the Ca^{2+} influx generated by the TRPA1 channel, regardless of PLC whose inhibition had no effect in this model (Wilson et al. 2011; Lieu et al. 2014). TRPA1-GPCR interplay is bidirectional. Indeed, TRPA1 was found to activate the FGFR2 receptor in lung adenocarcinoma cells by establishing a direct physical interaction between its N-

terminal ankyrin repeats and the C-terminal proline-rich motif of FGFR2. This interaction and subsequent oncogenic activation of FGFR2 can be hindered by miRNA-142-3p (Berrout et al. 2017).

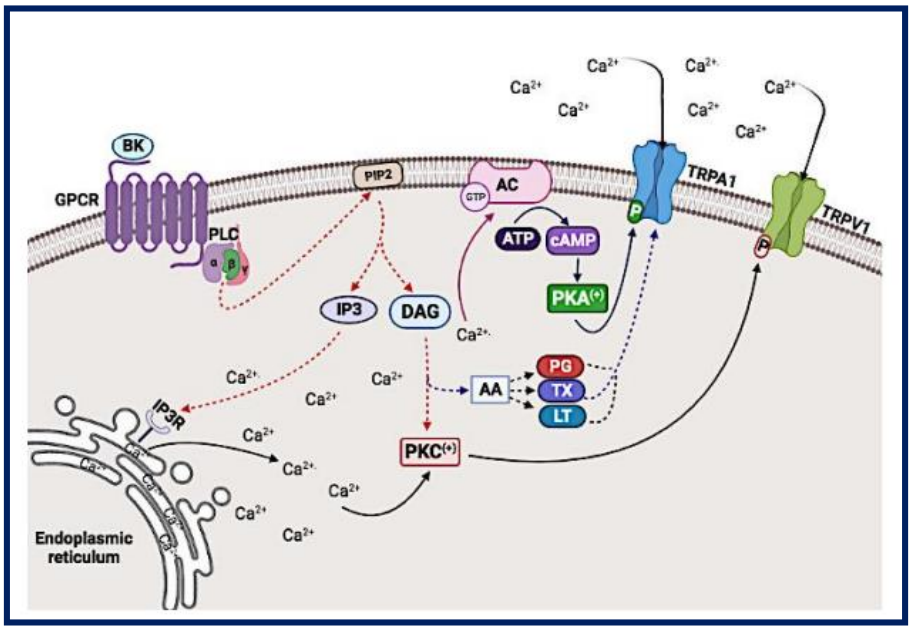

Figure 5. Signaling pathways modulating TRPA1 activity.
BK: bradykinin; PLC: phospholipase C; PIP_2: phosphatidylinositol bisphosphate; IP_3: inositol triphosphate; DAG: diacylglycerol; PKC: protein kinase C; AC: adenylate cyclase; AA: arachidonic acid; PG: prostaglandins; TX: thromboxanes; LC: leukotrienes.
Image from (Duitama et al. 2022)

Ca^{2+}

As previously said, Ca^{2+} plays a very important role in regulating the activity of TRPA1 channel by activating it directly and/or sensitizing it to the agonists following its binding to an EF-hand domain present on the N-terminal domain of the channel. This putative domain is present at the level of AnkR between amino acids 466 and 479. In fact, electrophysiological and calcium imaging studies have shown that when mutations were induced in this area, in particular AA 474 (L474A), the sensitivity to Ca^{2+} was suppressed and the activation of the channel following the depletion of ER Ca^{2+} store was significantly reduced (Doerner et al. 2007; Zurborg et al. 2007). Furthermore, other studies have shown that an influx of Ca^{2+} is also able to inactivate the channel in the presence of high concentrations of localized intracellular Ca^{2+} (Wang et al. 2008), being able to bind to a domain other than the EF-hand also located at the N-terminal (Cordero-Morales, Gracheva, and Julius 2011).

Biological functions and pathological implications

Based on localization and functional properties, TRPA1 is considered a key player in acute and chronic (neuropathic) pain and inflammation. Indeed, TRPA1 is expressed in sensory neurons (both peptidergic and non-peptidergic neurons like Aδ and C-fiber and in some myelinated Aβ-fibers) as well as in non-neuronal cells such as epithelial cells, melanocytes, mast cells, fibroblasts, and enterochromaffin cells (Zygmunt and Hogestatt 2014). TRPA1 mainly acts as a promiscuous chemical nocisensor but it is also involved in noxious cold and mechanical sensation. Moreover, a recent study suggested a role of TRPA1 in heat detection, since upon stimulation by agonists like AITC and cinnamaldehyde the resultant sensation is burning pain rather than cold (Nozazde et al. 2016). In primary sensory neurons, the TRPA1-mediated Ca^{2+} and Na^{+} influx within the cell cause membrane depolarization, action potential discharge, and neuro-transmitter release both at peripheral and central neural projections (Zygmunt and Hogestatt 2014). The overall effect of strong TRPA1 activation in the nervous system ultimately elicits pain. For instance, it has been shown that intraplantar cinnamaldehyde (Tsagareli et al. 2010) and AITC (Nozadze et al. 2016) induce dose-dependent heat hyperalgesia lasting more than 2 hours, mechanical allodynia, and cold hyperalgesia. Therefore, TRPA1 is of special interest in the treatment of pain and itching (Radresa et al. 2013; Nozazde et al. 2019; Tsagareli et al. 2019). Furthermore, the high co-expression of TRPA1 with TRPV1 in the cutaneous sensory nerves explains its involvement in itching. In particular, activation of TRPA1 by leukotriene B_4 (LTB_4) induces scratching behavior as does TRPV1 albeit through a different mechanism involving superoxide release instead of neutrophil migration (Fernandes et al. 2013). Accordingly, TRPA1 genetic and/or pharmacological suppression reduces the scratching responses induced by pruritogen compounds like chloroquine and BAM8–22 (Wilson et al. 2011). TRPA1 is also co-expressed with TRPV1 in sensory neurons innervating the bladder (Streng et al. 2008). Its expression is upregulated in patients with bladder outlet obstruction (Du et al. 2008) and its activation leads to an increased micturition frequency in rats through the C-fiber pathway (Du et al. 2007; Streng et al. 2008). Conversely, TRPA1 pharmacological inhibition attenuated hyperalgesia and bladder overactivity thus suggesting a potential role of TRPA1 as a drug target for bladder disorders (Andrade et al. 2011; Meotti et al. 2013). In addition, TRPA1 has been linked to secretory functions of the digestive tract. In particular, it has been implicated in insulin release from pancreatic beta-cells (Cao et al. 2012), eliciting interest as a potential therapeutic target in the treatment of diabetes and its complications related to peripheral neuropathy, nephropathy, retinopathy, as well as cardiovascular disease. In this regard, TRPA1 has been studied together with TRPV1 as an analgesic target in diabetic neuropathic pain (Koivisto et al. 2012). A possible link between high glucose levels and pain can be found in methylglyoxal, a glucose metabolite capable of directly activating TRPA1 (Ohkawara et al. 2012).

On the other hand, in addition to pain TRPA1 has been associated with several other diseases. Among them, TRPA1 expression in lung fibroblasts (Mukhopadhyay et al. 2011) suggested an interesting role of the channel in the pathogenesis of asthma, chronic cough, and chronic obstructive pulmonary disease (COPD). Indeed, it has been shown that genetic and/or pharmacological suppression of TRPA1 in murine models significantly reduces cytokine and mucus production as well as leukocyte infiltration in the airways (Caceres et al. 2009; Nassini et al. 2012). Consistently, the cough induced by the inhalation of acrolein and other irritants present in cigarette smoke and able to activate TRPA1, seemed to be abolished by the treatment with the selective TRPA1 antagonist HC-030031 (Andrè et al. 2008; Andrè et al. 2009).

Good pieces of evidence support the important involvement of TRPA1 in the development and maintenance of the inflammatory bowel disease (IBD). In inflamed mouse gut TRPA1 expression appears upregulated and both the pharmacological and genetic inactivation of the channel ameliorate dinitrobenzene sulphonic acid (DNBS)-induced colitis (Engel et al. 2011). Somewhat surprisingly, also TRPA1 activation by cannabichromene has been shown to reduce colitis in mouse models through the inhibition of nitric oxide production in macrophages, thus indicating a more complex involvement of TRPA1 in IBD (Romano et al. 2013).

1.1.3 TRPM8

TRPM8 is a nonselective Ca^{2+} permeable, outwardly rectifying cation channel (McKemy, Neuhausser, and Julius 2002) belonging to the Melastatin TRP (TRPM) subfamily which is, indeed, very diversified in terms of structure, ion permeation, gating mechanism and tissue distribution of its members (Chen et al. 2019). In this regards, within the TRPM subfamily, TRPM8 is the most selective for Ca^{2+} with a selectivity ratio (P_{Ca}/P_{Na}) of 3.3 (Zholos et al. 2011).

Originally cloned from prostate cancer tissue (Tsavaler et al. 2001), the human TRPM8 gene was later found in peripheral sensory neurons (Aδ and C fiber afferents), where it plays a crucial role in cold temperature detection, and also on deep visceral afferents in urogenital tract, prostate, bladder and bronchopulmonary tissues. Although at much lower levels, TRPM8 expression has recently also been detected in the central nervous system, particularly in the hypothalamus, septum, thalamic reticular nucleus, some cortices and other limbic structures, as well as some specific nuclei of the brain stem (Ordás et al. 2021).

Structure

The human TRPM8 is a 1104 amino acid protein with a homotetrameric quaternary structure. Like other TRP channels, TRPM8 has a TMD containing six transmembrane helices (S1-S6) with a transmembrane loop between S5 and S6, and cytosolic N-terminal and C- terminal domains (**Fig. 6**). As a member of the Melastatin subfamily, TRPM8 structure is specifically characterized by a well-defined C-terminal tetrameric coiled-coil domain (Fujiwara and Minor 2008), a peculiar N-terminal with 'TRPM homology regions' (MHR) that are involved in channel assembly and trafficking (Kraft and Harteneck 2005), and the lack of N-terminal AnkR that is commonly seen in other subfamilies (Kraft and Harteneck 2005) (**Fig. 6**). TRPM8 C-terminal is characterized by a peculiar umbrella-like shape defined by a vertical coil-coiled domain (coil-coiled "pole") and an horizontal coiled-coil domain (helical "ribs") (**Fig.6**). The voltage sensor-like domain (VSLD) is defined by the first four TM helices (S1-S4) which also contain the binding sites for menthol and icilin (Bandell et al. 2006). More specifically, mutagenesis experiments and molecular modelling studies identified Y745 (located in the middle of S2 or at S1 but anyway still in the VSLD cavity) as a key residue for menthol binding (Bandell et al. 2006) as well as for cold and voltage activation of the channel (Malkia et al. 2009). Moreover, the same residue was found involved in TRPM8 blocking by SKF96365 but not by other antagonists such as BCTC, capsazepine, clotrimazole, and econazole, thus suggesting the existence of allosteric points of interaction (Malkia et al. 2009; Pedretti et al. 2009; 2011). The pore module of TRPM8 is, instead, formed by the last two TM helices (S5-S6) and it is characterized by a highly conserved hydrophobic region and a conserved aspartate residue, responsible for ion selectivity. Homology models of TRPM8 built on the basis of the of the cryo-EM

structure of TRPV1 (Liao et al. 2013), lead to the identification of Y981 residue as a crucial inter-monomer point of interaction that might influence channel gating through the connection of the TRP domain and the S4–S5 linker of the different subunits (Taberner et al. 2014).

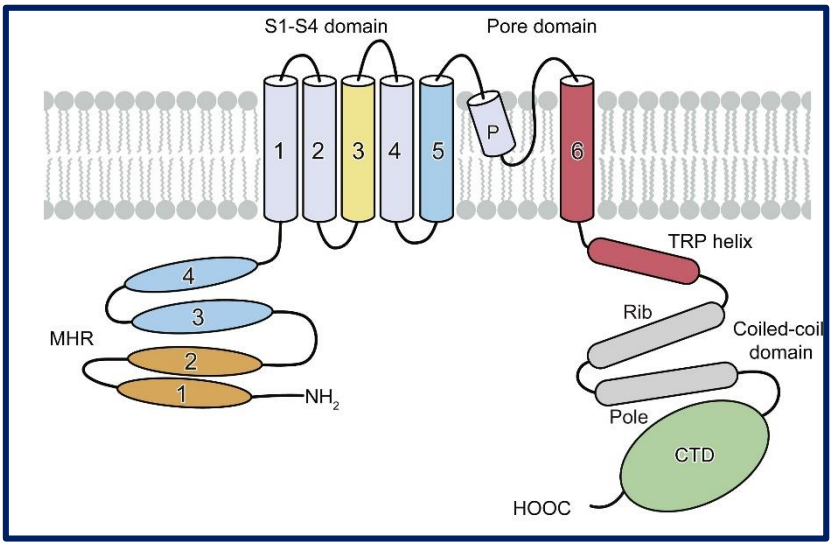

Figure 6 TRPM8 structure.

Domains of a monomer of human TRPM channels, characterized by 6 transmembrane helices (1-6) and peculiar N- and C-terminal domains. MHR: TRPM homology regions 1-4; CTD: C-terminal domain; Pole: vertical coiled-coil domain; Rib: horizontal coiled-coil helix. Image from (Huang et al. 2020)

The full-length TRPM8 structure (from the collared flycatcher *Ficedula albicollis* ($TRPM8_{FA}$) was only recently solved in 2018 by the group of Seok-Yong with a resolution of ~ 4.1 Å (Yin et al. 2018). To note, the final model (aa 122-1100) lacks several loops and some regions including three β-strands in pre-MHR, C-terminal domain (CTD) helix 1, and the C-terminal coiled coil has been built as polyalanine. This structure pointed out some peculiarity of TRPM8 structure with respect to other TRP. For instance, the selectivity filter organization seemed different since the pore loop is much longer and positioned away from the central axis. Moreover, the TMD consists exclusively of α-helical elements, and S1 as well as the cytosolic pre-S1 helix are connected by three short helices which are not present in other TRP. Furthermore, it has been postulated that a possible site of interaction for PIP_2 could be located at the interface between TRP domain, pre-S1 helix, and N-terminal MHR4.

The binding sites for icilin and the menthol analogue WS-12 (in the presence of the allosteric effector PIP_2 too) have been further investigated (Yin et al. 2019). They showed that icilin and WS12 bind to the cavity formed by the VSLD and the TRP domain (**Fig. 7 a**). More specifically, in the presence of intracellular Ca^{2+}, icilin positions itself on the TM segment 4 (S4) in the VSLD cavity, thus triggering substantial structural

rearrangements mainly concerning the VLSD and the pore (Yin et al. 2019). However, the channel cooling agents sensing is allosterically increased by the membrane lipid PIP_2, which, in contrast to what observed in TRPV1 structure (Cao et al. 2013), binds TRPM8 at the membrane interfacial cavity by engage subdomains from both the transmembrane domain (pre-S1 domain and S4-S5 junction) and the cytoplasmic domain (TRP domain on C-terminal tail and MHR4 on N-terminal tail) (**Fig. 7 a**) (Yin et al. 2019).

WS-12 seemed to bind TRPM8 within the VSLD cavity and, more specifically, through an H-bond between the WS12 central amide and R841 side chain (S4) beyond to other direct interactions with other residues in the TRP domain (Y1004 and R1007), while Y745 (S1) was at the top of the binding site (**Fig. 7 b**). Also icilin was found to bind the channel in correspondence of a cavity between VSLD and TRP domain flanked by Y745 and Y1004 and to establish interactions with the side-chains of residues at S4 (R841 and H844) (**Fig. 7 b**). As regards the allosteric coupling between the PIP_2 and the agonist, it has been observed that by binding TRPM8 on opposing sides of S4 in the VSLD cavity, both triggers structural rearrangements that favor binding of the other (Yin et al. 2019).

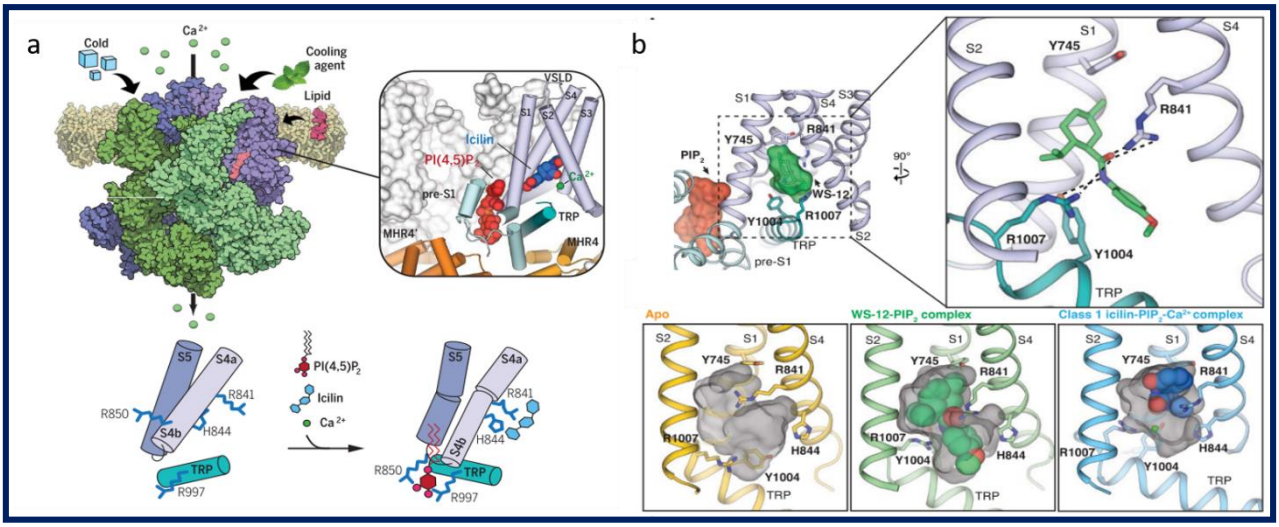

Figure 7. Structural basis of the binding of cooling agents and PIP_2 to TRPM8.

a) Suggested allosteric coupling between cooling agents PIP_2 in TRPM8 structure. b) Binding sites for Icilin- and WS12-PIP_2 complex in TRPM8 structure.
Image rearranged from (Yin et al. 2019)

Using the $TRPM8_{FA}$ structure as template, a homology model of human TRPM8 has been generated and used to study the interaction between the channels and some antagonists such as tryptamine derivatives discussed in the following section. These studies, highlighting a role of residue Y745, characterized as site of interaction with menthol and SKF963635 as previously mentioned, suggested a competitive mechanism of inhibition for this class of compounds (Bertamino et al. 2016).

Activation and modulation

Activators

TRPM8 may be gated by voltage, pressure, low temperatures (8°-28°C) as well as by cooling compounds (menthol, eucalyptol, icilin, WS12) (McKemy, Neuhausser, and Julius 2002; Peier et al. 2002; Liu et al. 2016). Based on the classification proposed by Voets *et al.*, TRPM8 agonists can be divided into two groups: menthol-like (type I) and AITC-like (type II). These two classes of compounds differ not only in their structure but also in their kinetic activity. Indeed, in addition to a different sensitivity (**Table 3**), the mechanisms brought into play by the different agonists are different. In particular, menthol-like compounds seem to stabilize the opening of the channel, while AITC-like destabilize its closure (Janssens et al. 2016). Furthermore, the mode of action of one of the best known TRP agonists, icilin, was found to be dependent on the intracellular concentrations of Ca^{2+} unlike the action of menthol or the menthol analogue WS12 which can activate the TRPM8 channel even in the absence of intracellular Ca^{2+} (Yin et al. 2019). This difference is mainly based on the fact that the binding of different agonists doen't involve the same residues on the structure of TRPM8.

Belonging to the menthol-like group, the rotundifolone revealed a higher selectivity than menthol and an interesting antinociceptive activity; eucalyptol (EC_{50} = 145 µM) proved to increase the temperature of the intrascapular brown adipose tissue and colon (Urata, Mori, and Fukuwatari 2017) and to provide TRPM8-mediated anti-inflammatory and analgesic effects in mouse models (Caceres et al. 2017). In recent years, several menthol derivatives have been described to activate TRPM8. Among them borneol, a terpene derivative, is able to activate TRPM8 in a temperature- and dose-dependent (10 µM to 2 mM) manner increasing tear production in guinea pigs without evoking nociceptive responses at 25°C (Chen et al. 2016). Moreover, a series of exocyclic olefin analogues of menthol was synthesized from cubebol, a natural sesquiterpene patented as a cooling agent by Firmenich SA (Velazco, Wuensche, and Deladoey 2000), and, based on specific structural modification of this compound, a promising antagonist, agonist and allosteric modulator of TRPM8 able to minimize the menthol-induced channel desensitization were obtained (Legay et al. 2016) (**Table 12** in **Chapter 1.4.3**). In addition, triazole-based menthol derivatives with EC_{50} values in the micromolar range have been proposed as potent TRPM8 agonists for the prevention and treatment of dry eye disease (DED), vaginal dryness, and burning mouth syndrome (Ferrer Montiel, Fernandez Carvajal, Belmonte Martinez et al. 2017). Two new patents have recently been applied by the Procter and Gamble Company on a series of menthol-based carboxamides and esters with activity on TRPM8 activity in the nanomolar range (Yelm et al. 2017; Wos et al. 2017). Most of the more recent patents on TRPM8 agonists will be summarized in **Chapter 1.4.3** (see **Table 12**).

Among non-menthol derivatives, Shirai *et al*. reported the agonist activity (EC_{50} = 332 nM) of a new neolignan from nutmeg (a diastereoisomer mixture of erythro- and threo-Δ8,7-ethoxy-4-hydroxy-3,3',5'-trimethoxy-8-O-4'neolignan) which binds to TRPM8 channels at different sites from that of menthol (Shirai et al. 2017). Five new series of potent TRPM8 agonists have been developed by Senomyx, Inc. using pyrazol-5-one, pyrimidine-2,4,6-trione, imidazolidine-2,4-dione, 2-phenyl propanamide, and phenoxyacetylamide as scaffolds. These compounds revealed *in vitro* EC_{50} values ranging from 0.2 to 74 nM (Priest et al. 2012; Chumakova et al. 2014) which have been recently further improved till picomolar range thanks to SAR studies (Noncovich et al. 2017). However, the pharmacokinetic properties of this class of compounds are not optimal yet.

TRPM8 agonists			
Compound	Structure	EC_{50} (μM)	Ref.
Menthol*	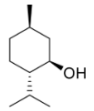	80 10.4	(McKemy, Neuhausser, and Julius 2002) (Bödding, Wissenbach, and Flockerzi 2007)
Icilin	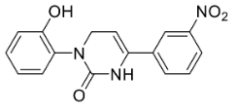	0.360 1.4	(McKemy, Neuhausser, and Julius 2002) (Bödding, Wissenbach, and Flockerzi 2007)
WS-12	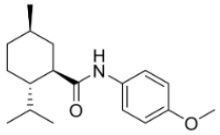	0.193	(Bödding, Wissenbach, and Flockerzi 2007)
Rotundifolone	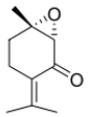	1000	(Silva et al. 2015)
Eucalyptol		3400 145	(McKemy, Neuhausser, and Julius 2002) (Caceres et al. 2017)
Borneol	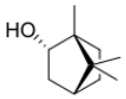	n.d.	(Chen et al. 2016)

Neolignan from nutmeg	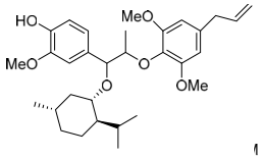	0.332	(Shirai et al. 2017)
MPO*	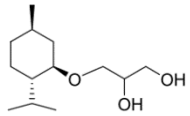	6	(Misery et al. 2019) (González-Muñiz et al. 2019)
D-3263 hydrochloride *	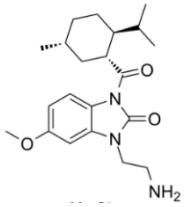	< 0.02	(Genovesi et al. 2022)
3-T_1AM	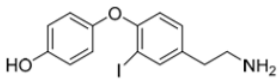		(Khajavi et al. 2015; Khajavi, Mergler, and Biebermann 2017; Schanze et al. 2017; Bräunig et al. 2018; Lucius et al. 2016; Mergler et al. 2012; Walcher et al. 2018)
*currently in clinical stages of development			

Table 3. TRPM8 agonists

Inhibitors

Natural plant-derived cannabinoids including cannabidiol, cannabinol and cannabiogerol as well as some phenethyl analogues have been shown to exert nonselective antagonist properties against several thermo TRPs, including TRPM8 (De Petrocellis et al. 2008; 2011; Pollastro et al. 2017) (**Table 4**). Similarly, the anti-inflammatory and analgesic activities exerted by the alkaloid riparin II seem to be mediated by the activation of TRPM8 together with a plethora of other targets (i.e., TRPV1, TRPA1, acid-sensing ion channels (ASIC), and bradykinin and histidine receptors) (Rodrigues de Carvalho et al. 2018). Moreover, as mentioned in the previous section, a cubebol-derived unsaturated menthol benzoate synthesized by Firmenich SA displayed a dose-dependent inhibition of TRPM8 with an IC_{50} of 2 ± 1 µM (Velazco, Wuensche, and Deladoey 2000).

However, despite the great interest of both the academic and the pharmaceutical field in the discovery of TRPM8 antagonists, most of the molecules developed to date have important limitations due to their poor selectivity, often interacting also with TRPV1 and TRPA1.

Importantly, De Petrocellis's group has recently confirmed the importance of both the urea function and tetrahydroisoquinoline ring for TRPM8 antagonist activity, proposing two series of tetrahydroisoquinoline-derived ureas (symmetric and asymmetric) and another of pyrazino[1,2-b]isoquinolin-1-ones (De Petrocellis et al. 2016). Accordingly, Amgen proposed a related tetrahydronaphthyridine-derived asymmetric urea as a good TRPM8 antagonist able to inhibit cold-induced arterial blood pressure and wet-dog shaking in rat models (Horne et al. 2014). Linear urea derivatives could, therefore, represent suitable scaffolds in the optimization of new TRPM8 antagonists (Horne et al. 2018).

Also tryptamine derivatives, described by Gómez-Monterrey *et al*. have shown an interesting inhibitory action on the activity of TRPM8 (high nanomolar range in patch clamp experiments) and the ability to reduce cold allodynia induced by oxaliplatin and icilin-induced wet-dog shakes in mouse models (Bertamino et al. 2016; 2018). More specifically, a key role of the methoxycarbonyl group as well as a chiral center in the molecule for interaction with the TRPM8 channel has been suggested. Molecular modelling investigations suggested that this type of antagonist could act by inducing a conformational perturbation in the interaction network established between the TRP domain and the S1–4 transmembrane segments of the channel subunits (Bertamino et al. 2018).

Finally, a class of β–lactam derivatives acting as negative allosteric modulators with a nanomolar potency and a high selectivity toward TRPM8, TRPV1, TRPA1, K_v1.1, and Na_v1.6. have been described to block all modalities of channel activation (voltage, menthol, and temperature) by the group of González-Muñiz (De La Torre-Martínez et al. 2017).

TRPM8 antagonists			
Compound	Structure	IC_{50} (μM)	Ref
AMTB	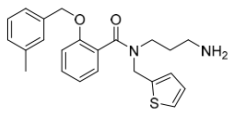	0.588	(Lashinger et al. 2008)
PF-05105679	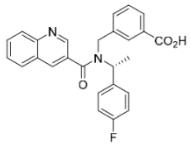	0.103	(Andrews et al. 2015) (Gaston and Friedman 2017) (Horne et al. 2018)

AMG-333	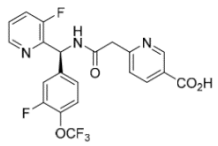	0.013	
AMG2850	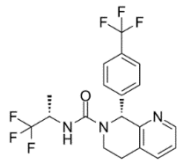	0.041	(Lehto et al. 2015)
SKF96365	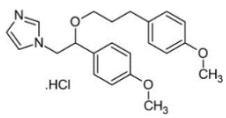	1	(Malkia et al. 2009)
PBMC	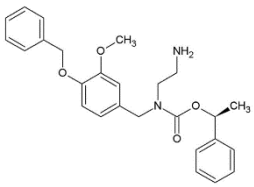	0.0156	(Gardiner et al. 2014)
RQ-00203078	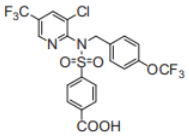	0.0083	(Ohmi et al. 2014)
M8-An	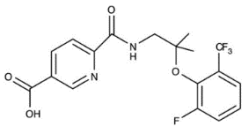	0.0109	(Patel et al. 2014)
Cannabinoids (Δ^9-tetrahydrocannabinol)	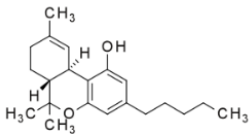		(De Petrocellis et al. 2008; 2011; Pollastro et al. 2017)

Cannabidivarin	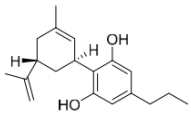	0.9	(Gaston and Friedman 2017; De Petrocellis et al. 2011)
Cannabigerol	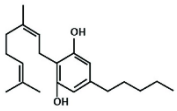	0.11	(Borrelli et al. 2014)
Clotrimazole	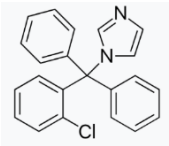	0.2	(Meseguer et al. 2008)
Riparin II	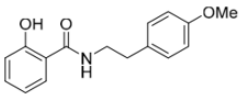		
Linear urea derivatives	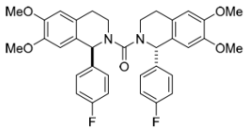	0.072	(De Petrocellis et al. 2016)
	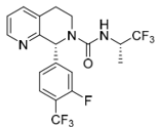	0.012	(Horne et al. 2014)

Table 4. TRPM8 antagonists.

Due to the great interest aroused by TRPM8 in clinical applications, many TRPM8 modulators, mainly activators, have been proposed and patented by pharmaceutical companies as well as academic groups. Many of the most relevant TRPM8 agonists/antagonists patented in the last years are summarized in **Table 12** and will be discussed further in **Chapter 1.4.3**.

Modulators

Chemical compounds described in the previous section as TRPM8 agonists generally act as positive allosteric modulators, meaning that, since the activation of TRPM8 is also voltage-dependent, these agonists

shift the activation threshold toward more negative potentials by eliciting a sensation of cold, thus enabling the channel to open at higher than normal temperatures; by contrast, TRPM8 antagonists exert their effect by shifting the threshold of TRPM8 activation toward more positive potentials (Brauchi, Orio, and Latorre 2004; Voets et al. 2004; Mälkiä et al. 2007). However, in non-temperature sensitive tissues in which the aforementioned physical and chemical stimuli are absent, the activation of TRPM8 must be induced by different mechanisms (Gkika et al. 2010; Yudin and Rohacs 2012). The main signaling pathways involved in the regulation of TRPM8 known to date are represented in **Figure 8**.

Prominent rundown of TRPM8 activity in excised patches (Voets et al. 2004) raises the possibility that some endogenous ligands might be necessary for the channel activation. **PIP_2** has been found to be such a factor, as it is capable not only restoring menthol-activated TRPM8 current after its rundown in excised patches, but also of activating the current independently of menthol by interacting with the TRP domain of the channel (Liu and Qin 2005; Rohács et al. 2005). The functional importance of the PIP_2-dependent TRPM8 gating has thus become evident in the cold sensation since any of the well-known PIP_2 depletion scenarios (e.g. activation of $G_{\alpha q}$/11- PLC-coupled receptors or Ca^{2+}-dependent activation of some PLC isoforms) would limit TRPM8 activation by shifting its gating towards lower temperatures or higher voltages (**Fig. 8 - panel 1**). However, the possibility of channel activation (rather than desensitization) with the involvement of PIP_2 seems more remote. Interestingly, PIP_2 also plays a role in desensitizing TRPM8 channel after its activation. In fact, following the activation of TRPM8 and the entry of Ca^{2+} into the cell, the Ca^{2+}-dependent activation of PLC_δ allows the hydrolysis of PIP_2 and, therefore, the depletion of PIP_2 inside the cell. Then, this depletion of PIP_2 desensitizes the TRPM8 channel and therefore limits its activity (Rohács et al. 2005).

Beyond to inhibit TRPM8 by decreasing PIP_2 levels, **PLC** can also enhance TRPM8 activity by activating the **IP_3**-mediated store depletion (**Fig. 8 - panel 4**). This evidence seems puzzling but can be explained by assuming differential roles for the two lipid messenger pathways: the PIP_2 primarily controlling TRPM8 desensitization (Rohács et al. 2005) and the IP_3 lysophospholipids providing the main chemical activation input (Vanden Abeele et al. 2006).

Furthermore, a novel concept of Ca^{2+}-independent TRPM8 activation has been proposed by Vanden Abeele *et al*. (Vanden Abeele et al. 2006). Indeed, the group of Natasha Prevarskaya described a mechanism of TRPM8 stimulation involving the Ca^{2+}-independent phospholipase A_2 (**$iPLA_2$**). As depicted in **Figure 8 - panel 2**, they suggested that the products of $iPLA_2$ stimulation as lysophospholipids (LPL), lysophosphatidylcholine (LPC), and lysophosphatidylinositol (LPI) promote the opening of TRPM8 on the PM and its activation as well as that of SOC in a “membrane delimited” fashion (Vanden Abeele et al. 2006). $iPLA_2$ stimulation may result from the store depletion evoked by the cold/menthol-induced activation of TRPM8 localized on the ER and the subsequent displacement of the inhibitory Ca^{2+}-dependent calmodulin (CaM)

(Vanden Abeele et al. 2006). The same pathway (store/iPLA$_2$/LPC/LPI) can also be recruited by store depletion *via* ER-leak channels as a result of the inhibition of the Sarco-Endoplasmic Reticulum Ca^{2+} ATPase (SERCA) pump by thapsigargin. An iPLA$_2$-dependent mechanism of TRPM8 activation has been also confirmed in dorsal root ganglia neurons, thus suggesting its ubiquitous character (Andersson, Nash, and Bevan 2007). Moreover, the activation of cytosolic phospholipase A$_2$ (cPLA$_2$) through the M3 muscarinic acetylcholine receptor-coupled signaling cascade was found to inhibit TRPM8 activity in an AA-dependent way (**Fig. 8 - panel 5**) (Bavencoffe et al. 2011). Indeed, as previously described for LPL, AA as well as other polyunsaturated fatty acids are known to directly inhibit TRPM8 activity (Andersson, Nash, and Bevan 2007). Furthermore, PM lipids have also been shown to play a role in regulating TRPM8 activity. In fact, the localization of TRPM8 within lipid rafts, that is specific areas of PM rich in cholesterol and sphingomyelin, has been shown to be important for its activity (Morenilla-Palao et al. 2009). In particular, the cholesterol depletion induced by methyl-β-cyclodextrin causes the delocalization of TRPM8 outside the lipid rafts and this significantly modifies the properties of the channel: as an example, its cold-induced activation is shifted to 37° C when TRPM8 it is not associated with lipid rafts (Morenilla-Palao et al. 2009).

Another signalling pathway involved in the modulation of TRPM8 activity is that of the G_i-coupled α_{2A} adrenergic receptor which inhibits TRPM8 channel function *via* the $G_{\alpha i}$-induced blockade of the adenylate cyclase (**AC**)/cyclic AMP (**cAMP)**/**PKA** signaling cascade (**Fig. 8 - panel 3**) (Bavencoffe et al. 2010). Indeed, Ser-9 and Thr-17 are two critical sites for PKA phosphorylation regulating TRPM8 channel activation (Bavencoffe et al. 2010). This pathway can be restored by the β AR-mediated activation of AC through $G_{\alpha s}$ (**Fig. 8 - panel 3**) (Bavencoffe et al. 2010). Interestingly, Zhang *et al.* brought to light another not conventional mechanism through which G-proteins may modulate TRPM8 activity (Zhang et al. 2012). More specifically, they showed that the $G_{\alpha q}$ (but not $G_{\beta\gamma}$) subunit of the G-protein is able to bind directly to TRPM8 and inhibit its activity once activated by a $G_{\alpha q}$-coupled receptor (Zhang et al. 2012).

Furthermore, the regulated translocation of TRP channels appears to be a key mechanism for the gating of constitutively active subunits (Shapovalov et al. 2013). Basically, TRPM8 can be kept in readiness in a dynamic pool of vesicles under the cell surface and this dynamic TRPM8 pool could be activated by intracellular factors known to modulate TRPM8 activity, including second messengers generated during the activation of surface receptor-coupled signaling pathways (Bavencoffe et al. 2010; Yudin and Rohacs 2012; Zhang et al. 2012; Shapovalov et al. 2013). In this regard, the prostate-specific antigen (**PSA**) too proved to be a physiological/natural modulator of TRPM8. Indeed, it has been shown that PSA enhances TRPM8-mediated currents by increasing TRPM8 channel expression on the PM through the bradykinin 2 receptor (B2R)/PKC signalling pathway (**Fig. 8 - panel 4**) (Gkika et al. 2010). Therefore, TRPM8 regulation by PSA is mediated via G-protein coupled receptor(s) and downstream signaling cascade (Gkika et al., 2010).

Interestingly, several studies have supported TRPM8 agonist activity for the thyroid hormone metabolite 3-iodothyronamine (3-T_1AM) (Khajavi, Mergler, and Biebermann 2017) in rat thyrocyte (PCCL3 cells) (Schanze et al. 2017), human conjunctival epithelial cells (HCjEC) (Khajavi et al. 2015), and a murine hypothalamic cell line (Bräunig et al. 2018). In particular, it has been observed that 3-T_1AM induces Ca^{2+} responses similar to those evoked by menthol. Moreover, the 3-T_1AM-induced TRPM8 activation displayed an inhibitory action on TRPV1-induced Ca^{2+} influxes in human corneal epithelial cells (Lucius et al. 2016), WERI-Rb1 retinoblastoma (Mergler et al. 2012), and human uveal melanoma (UM 92-1) (Walcher et al. 2018). This negative feedback mechanism relies on a complex interplay between TRPs and GPCR which are also targets of this metabolite (Hoefig, Zucchi, and Köhrle 2016).

Finally, some proteins were shown to exert their modulator activity on TRPM8 *via* direct interaction with the channel. Among them, androgen receptors (AR), TRP channel-associated factor (TCAF) 1 and their action on TRPM8 function in the prostate will be discussed in the **Chapter 1.2** (Grolez et al. 2019; Gkika et al. 2015).

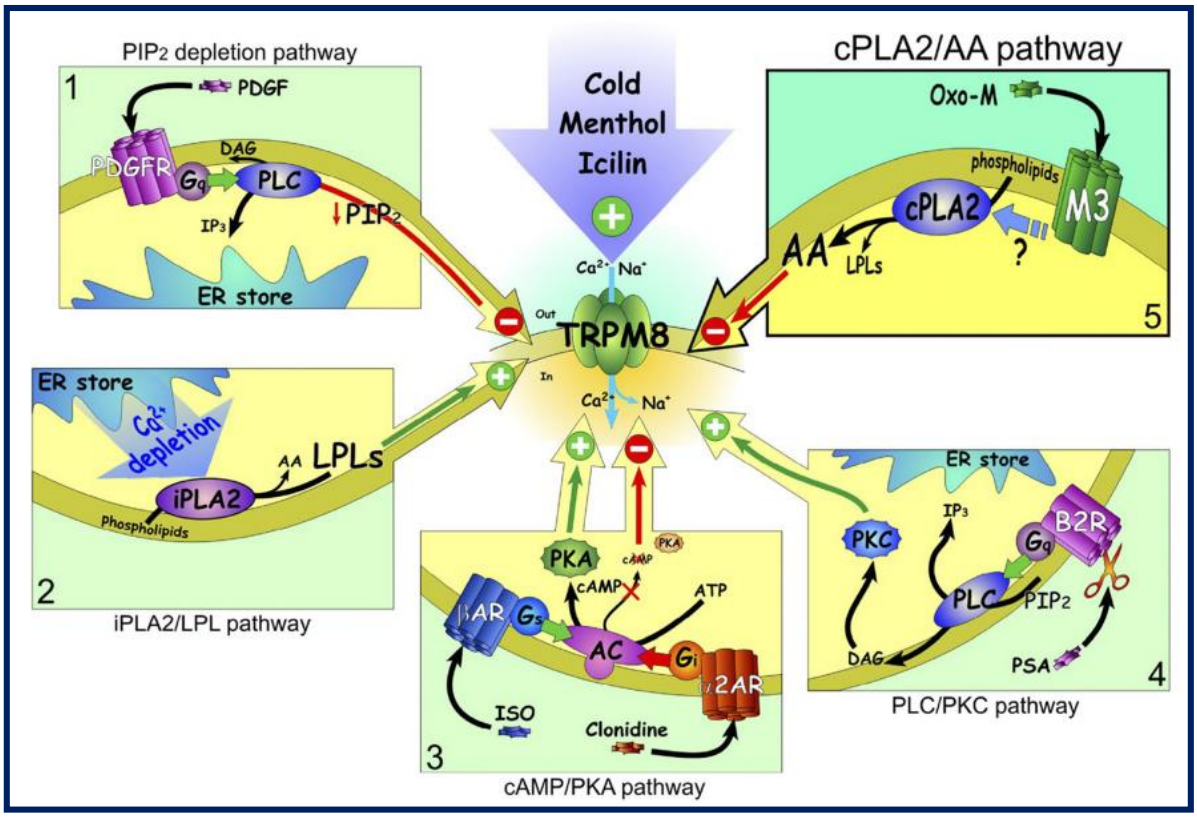

Figure 8 Schematic summary of the pathways involved in TRPM8 modulation.

PIP_2: phosphatidylinositol 4,5-bisphosphate; PLC: phospholipase C; IP_3: inositol 1,4,5-trisphosphate; $iPLA_2$: Ca^{2+}-independent phospholipase A_2; AR: adrenergic receptor; AC: adenylate cyclase; PKA: protein kinase A. Image from (Bavencoffe et al. 2011).

Biological functions and pathological implications

TRPM8 is mainly known as "cold" sensor. Indeed, in peripheral sensory neurons (nociceptive Aδ and C-fibre afferents) TRPM8 activation by cold temperatures in the range of 8°-28°C and/or by cooling agents as menthol induces a Ca^{2+}-mediated cold response signals at the application site (McKemy, Neuhausser, and Julius 2002). In addition to cold thermal transduction, TRPM8 is also involved in pain sensation; in particular, in cold allodynia after inflammation or nerve injury. Indeed, it has been shown that menthol-induced TRPM8 activation leads to analgesia thanks to the synergistic excitation of GABA receptors and sodium ion channels (Pergolizzi et al. 2018; Farco and Grundmann 2013).

In central neurons TRPM8 may affect multiple aspects of thermal regulation, including autonomic and behavioural thermoregulation (Ordás et al. 2021). Moreover, along with TRPA1, TRPV1 and TRPV4, TRPM8 has been hypothesized to be involved in migraine through a mechanism of activation of meningeal nociceptors possibly involving the Calcitonin Gene Related Peptide (CGRP) (Benemei and Dussor 2019). In this regard, it has been proposed a strong correlation between migraine processes and specific Single Nucleotide Polymorphisms (SNP) in the gene encoding TRPM8 (Dussor and Cao 2016).

Furthermore, TRPM8 is expressed in a subset of autonomic nerves that innervate the bronchopulmonary system and are responsible for airway resistance (Xing et al. 2008). Consequently, it can be reasonably assumed that this channel is involved in the cold-induced exacerbation of respiratory disorders such as asthma. It has been consistently shown that menthol can alleviate the effects of respiratory irritants found in cigarette smoke and that its action is blocked by administration of the TRPM8 antagonist AMTB (Willis et al. 2011). Interestingly, TRPM8 is also markedly overexpressed in the bronchial epithelium of COPD patients and its expression and / or activation has been linked to MUC5AC expression, thus more strongly supporting an active role of TRPM8 in the development of respiratory disorders such as COPD as well as asthma (Li et al. 2011).

Recently, it has been observed that TRPM8 co-localizes with the acid-sensing ion channel ASIC3 on the submucosal sensory fibers innervating the human oropharynx. Moreover, the selective activation of TRPM8 in combination with acidic solutions was found to improve the swallow response in patients with oropharyngeal dysphagia (OD), showing that (Alvarez-Berdugo et al. 2018).

Furthermore, due to a role in transducing signals of chemical irritation and temperature change from the ocular surface to the brain, dysfunctions of TRPM8 have been related to dry eye disease (DED) (Yang et al. 2018).

TRMP8 expression has been also found in bladder afferent neurons (Shibata et al. 2011) and it results upregulated after bladder outlet obstruction in rats (Hayashi et al. 2011) as well as in patients with bladder disorders in which correlates with clinical grades (Mukerji et al. 2006). TRPM8 antagonists AMTB and BCTC

have been shown to be effective in the treatment of overactive bladder and painful bladder syndrome by reducing volume-induced bladder contraction and nociceptive reflex responses to noxious bladder distension (Lashinger et al. 2008) and menthol- or cold stress-induced detrusor hyperactivity (Lei et al. 2013), respectively.

TRPM8 also revealed a role in IBD, supported by its upregulation in colon during inflammation and the reduction of inflammatory responses in a mouse model of colitis upon icilin treatment (Ramachandran et al. 2013). In addition, TRPM8 has been recently associated with obesity, due to the observation that chronic administration of menthol in the diet prevent obesity in wild-type mice but not in TRPM8-deficient mice, probably triggering uncoupling protein 1 (UCP-1)-mediated thermogenesis in brown adipose tissue (Ma et al. 2012).

Finally, a recent evidence linked TRPM8 with hypertension demonstrating that TRPM8 expression in vascular smooth muscle cells can be downregulated by angiotensin II (Ang II), whose role in hypertension and other cardiovascular disorders is well-established (Huang et al. 2017). In this regard, TRPM8 activation was observed to reduce the upregulation of NADPH oxidase (NOX) 1 and NOX4 as well as the increase of ROS and H_2O_2 production both induced by Ang II (Huang et al. 2017).

1.2 TRP CHANNELS IN PROSTATE CANCER

1.2.1 TRP channels and cancer

In addition to the different pathological conditions mentioned in the previous chapter, TRP channels have recently been linked to cancer showing altered expression during cancer development and progression (Nilius et al. 2007). It is not yet possible to say whether these changes in TRP expression are central steps in the progression of cancer or are secondary to other changes, although the latter is most likely (Prevarskaya, Zhang, and Barritt 2007). However, several TRP proteins may prove to be valuable markers in predicting the progress of cancers and are potential targets for pharmaceutical treatment (Tsavaler et al. 2001; Fuessel et al. 2003; Wissenbach, Niemeyer, and Flockerzi 2004).

Due to their key role in the modulation of spatial and temporal patterns of the intracellular distribution of Ca^{2+}, dysregulation of the function or expression of TRP channels can interfere with multiple downstream effectors involved in the pathophysiology of cancer, which influence tumor growth, invasion, and vascularization (Prevarskaya, Skryma, and Shuba 2018). Indeed, intracellular free calcium ($Ca^{2+}{}_i$) is the most abundant second messenger within the cell and plays a critical role in multiple signaling pathways controlling gene expression, cell cycle, autophagy, apoptosis, and cell motility (Berridge, Lipp, and Bootman 2000). Cellular Ca^{2+} signals are temporally and spatially tightly regulated within the cell (Csordás et al. 2010; Parekh 2011; Berridge, Bootman, and Roderick 2003) to avoid prolonged $[Ca^{2+}]_i$ increase that is toxic and lethal (McConkey and Orrenius 1997). More specifically, based on the duration, frequency, and amplitude of Ca^{2+} peaks, oscillations or waves, the cell controls the selective and specific activation of transcription factors for cell proliferation and migration. (Parekh 2011). Hence, the generated selective oscillatory $Ca^{2+}{}_I$ signals are decoded by downstream effectors, such as nuclear factor kappa-light-chain-enhancer of activated B cells (NF-κB), activated T cell nuclear factor (NFAT), calmodulin (CaM), calmodulin-dependent protein kinase II (CaMKII), calpain, etc. (Smedler and Uhlén 2014; Cullen 2003). Therefore, alteration of $[Ca^{2+}]_I$ due to the dysfunction of membrane channels and transporters, may change cellular fate towards a tumor phenotype (Prevarskaya, Skryma, and Shuba 2018). TRP channels are no exception (Bödding 2007; Prevarskaya, Zhang, and Barritt 2007): mutations, dysregulation of TRP channels gating or expression levels by disrupting normal spatiotemporal patterns of local Ca^{2+} distribution contribute to tumor phenotype. However, alteration of $[Ca^{2+}]_i$ is not the only way TRP channels influence tumor progression. Indeed, it is increasingly evident that another probable pathway through which TRP channels interfere with the onset and progression of cancer underlies their interaction with other intracellular proteins (Bödding 2007).

In the next sections, the role of TRP channels in different hallmarks of cancer will be discussed (Yang and Kim 2020; Shapovalov et al. 2016; Hantute-Ghesquier et al. 2018), with emphasis on TRP channels in prostate cancer (PCa). Indeed, as summarized in **Table 5,** many TRPs have been found deregulated in the prostate and suggested to play key roles in the physiology, pathology, and carcinogenesis of the prostate (Prevarskaya, Flourakis, et al. 2007; Van Haute, De Ridder, and Nilius 2010; Gkika and Prevarskaya 2011).

TRP	CHANGES IN EXPRESSION			REF.	LOCALIZATION	BIOLOGICAL EFFECTS	REF.
	HEALTHY/ BENIGN	TUMOR	INVASIVE				
TRPC1	Yes	Yes	↓	(Riccio et al. 2002; Pigozzi et al. 2006)	PM ER	pro-apoptotic (TNF-α/NF-κB)	
TRPC3	Yes / very low	low (Increased by store depletion)		(Riccio et al. 2002; Pigozzi et al. 2006)		pro-apoptotic (TFII-I)	(Misra et al. 2011)
TRPC4	Yes			(Riccio et al. 2002)		pro-apoptotic (SOCE)	(Abeele et al. 2004)
TRPC6	Yes	↑	↑	(Yue et al. 2009; Riccio et al. 2002)		pro-proliferative (α_{1D}-AR/NFAT) pro-invasive	(Thebault et al. 2006; Wang et al. 2010) (Wang et al. 2014)
TRPV1	Yes	↑	↑	(Sánchez et al. 2005; Czifra et al. 2009)		pro-proliferative (α_{1D}-AR) pro-apoptotic	(Morelli et al. 2014; Malagarie-Cazenave et al. 2009) (Sánchez et al. 2006; Ziglioli et al. 2009)
TRPV2	n.d.	yes	↑	(Monet et al. 2010)	PM	pro-proliferative pro-migratory	(Monet et al. 2009; 2010; Oulidi et al. 2013)
TRPV4	Yes (EC)	↓ (TEC)		(Adapala et al. 2016)		anti-angiogenic	(Adapala et al. 2016; Thoppil et al. 2016; Cappelli et al. 2019)
TRPV6	No/ very low	↑	↑	(Wissenbach et al. 2001; Fixemer et al. 2003; Peng et al. 2001)	PM	pro-proliferative (SOCE /NFAT) and anti-apoptotic	(Lehen'kyi et al. 2007; Raphaël et al. 2014)
TRPM2	Yes	↑	↑	(Zeng et al. 2010; Hantute-Ghesquier et al. 2018)	PM lysosomes nuclei	pro-apoptotic (ROS-mediated)	(Zeng et al. 2010; Wang, Huang, and Yue 2017)
TRPM4	Yes (kept low by miR-150)		↑	(Hong and Yu 2019; Schinke et al. 2014)		pro-proliferative (β-catenin) pro-EMT (Snail1) pro-migratory (SOCE)	(Armisén et al. 2011; Sagredo et al. 2018) (Holzmann et al. 2015; Sagredo et al. 2019; Hong and Yu 2019)
TRPM7	Yes	↑				anti-apoptotic (TRAIL) pro-EMT	(Sun et al. 2013; Lin et al. 2015)

						pro-migratory pro-invasive	(Sun et al. 2014; Chen et al. 2017)
TRPM8	Yes	↑	↓	(Tsavaler et al. 2001; Fuessel et al. 2003; G Bidaux et al. 2007)	PM ER MAM	pro-proliferative pro-apoptotic (ER depletion) anti-migratory	(Zhang and Barritt 2004; Prevarskaya et al. 2007; Thebault et al. 2005; Yang et al. 2009) (Gkika et al. 2010; 2015; Z. H. Yang et al. 2009)
TRPA1	Yes	Yes (prostate CAF)		(Du et al. 2008; Gratzke et al. 2010; Vancauwenberghe et al. 2017)		pro-secretory (VEGF-HGF) anti-apoptotic	(Vancauwenberghe et al. 2017)

Table 5. TRP channels in prostate cancer.

Abbreviations: (↑) increment (↓) reduction; PM: plasma membrane; ER: endoplasmic reticulum; TNF-α: tumor necrosis factor α; NF-κB: nuclear factor kappa-light-chain-enhancer of activated B cells; TFII-I and Snail: transcription factors; SOCE: store-operated calcium entry; α_{1D}-AR: α_{1D} adrenergic receptor; NFAT: nuclear factor of activated T-cells; ROS: reactive oxygen species; EMT: epithelial to mesenchymal transition; TRAIL: TNF-related apoptosis-inducing ligand; MAM: mitochondria-associated membranes; VEGF: vascular-endothelial growth factor; HGF: hepatocyte growth factor.

1.2.2 Transcriptional regulation of TRP channels during carcinogenesis

What accompanies the transformation of normal cells into tumorigenic cells is a long and complex process that also involves the progressive accumulation of mutations in multiple oncogenes and tumor suppressor genes that code for key signaling proteins. The subsequent alteration of several intracellular pathways drives the transition from normal differentiated cells to hyperplastic, dysplastic, neoplastic, and then metastatic cells. Over the past twenty years, a considerable number of studies have found a correlation between carcinogenesis/tumor progression and alterations in the expression of TRP channels (Nilius et al. 2007; Bernardini et al. 2015). To date, most changes involving TRP proteins do not involve mutations in the TRP gene, but rather increased or decreased expression levels of the wild-type TRP protein, depending on the

stage of cancer (Gkika and Prevarskaya 2009). In particular, the expression levels of members of the TRPC, TRPM, and TRPV families have been correlated with the emergence and/or progression of multiple cancers including melanoma, glioma, breast and prostate cancer (Duncan et al. 1998; Wissenbach et al. 2001; Tsavaler et al. 2001; Thebault et al. 2006).

Modulation of TRP expression/activity concerns different levels: transcriptional and translational, trafficking of the channel to the PM, or direct stabilization of the channel on PM. At all of these levels, TRP can be regulated by hormones, growth factors (GF), and alternative splicing isoforms (**Fig. 9**), with the subsequent consequences on the signaling pathways that involve them (Gkika and Prevarskaya 2009).

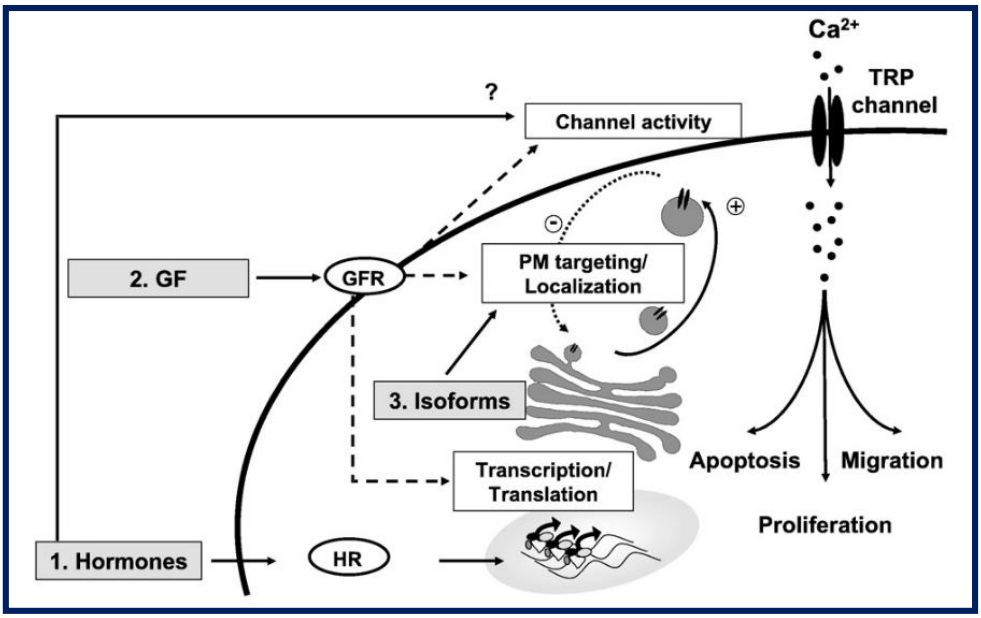

Figure 9. TRP regulation during carcinogenesis/tumor progression.

GF: growth factors; GFR: growth factor receptors; PM: plasma membrane
Image from (Gkika and Prevarskaya 2009)

Hormonal regulation

In some cases, TRP channels' expression displays a hormone dependence. This is, for example, the case with TRP channels associated with cancers that are subject to hormonal regulation, such as prostate and breast cancer. In particular, two TRP channels revealed a transcriptional regulation by androgens and estrogens, which are TRPM8 and TRPV6.

Consistent with an up-regulation during the androgen-dependent phase of PCa and a dramatic down-regulation during the late androgen-independent stage, **TRPM8** expression was proved to be directly

controlled by androgen receptors (AR). More specifically, it was observed that the gene encoding TRPM8 is a primary androgen-responsive gene having 10 presumed androgen-responsive elements, one of which is in the promoter region and the others in correspondence with the intronic sequences (Bidaux et al. 2005; Zhang and Barritt 2004). The expression of TRPM8 is induced by the binding of the testosterone-AR complex to the androgen-responsive sequence. In addition, androgens seem to differentially regulate two different TRPM8 isoforms and their subcellular localization in the PM or the ER (Bidaux et al. 2005; Gkika and Prevarskaya 2011). This aspect of androgen regulation will be discussed in more detail in **section 1.2.6**.

TRPM8 expression was also found to be regulated by estrogen receptor (ER) α in breast cancer (Chodon et al. 2010). Indeed, TRPM8 up-regulation in breast adenocarcinomas is correlated with the ER^+ status of the tumors and steroid deprivation as well as silencing of ERα were demonstrated to reduce TRPM8 expression (Chodon et al. 2010)

The gene encoding **TRPV6** also appears to be subject to androgenic regulation in the prostate, although this mechanism is currently less characterized than that of TRPM8 regulation. Indeed, although an androgen-responsive element on the 5' TRPV6 gene flanking sequences has been observed, further investigations on it are needed to better define the mechanism by which TRPV6 transcriptional regulation occurs. Contrary to TRPM8, TRPV6 is subject to negative regulation by androgens (Lehen'kyi et al. 2007) consistent with the different expression pattern shown by TRPV6 which, unlike TRPM8, has been seen to increase progressively and proportionally to the aggressiveness of the tumor. However, the evidence that androgen-sensitive LNCaP display higher levels of TRPV6 compared to androgen-insensitive PC-3 or DU-145 cell lines seems to suggest the presence of different regulatory mechanisms and a ligand-independent way for AR regulation in LNCaP cells (Lehen'kyi et al. 2007).

The dependence of TRPV6 expression on estrogens and its consequences in breast cancer is better characterized. Indeed, it has been described that estrogens are able to positively regulate TRPV6 transcription through the direct binding to the estrogen-responsive element present in the TRPV6 promoter sequence (Weber et al. 2001). Consistently, TRPV6 expression progressively increases during breast cancer (Zhuang et al. 2002). TRPV6 transcription is also affected by several Ca^{2+}-sensitive transcriptional regulators including the serum responsive element and the cAMP/Ca^{2+}-responsive element (Gallin and Greenberg 1995; Hoenderop, Nilius, and Bindels 2005), synergistically with estrogens. Interestingly, TRPV6 transcripts are enhanced by long-term stimulation with estrogen and mildly reduced by short-term treatment as well as by inhibition of estrogen receptors, indicating a direct involvement of estrogen receptors in TRPV6 gene regulation (Bolanz, Hediger, and Landowski 2008). In addition, it has been demonstrated that estrogens affect TRPV6 regulation not only at the transcriptional level but also directly enhancing channel function as a Ca^{2+}-permeable channel (Weber et al. 2001).

Regulation by growth factors

During the onset and progression of cancer, TRP channels also undergo growth factor-mediated regulation. As an example, the hepatocyte growth factor/scatter factor (**HGF/SF**), also known as plasminogen-related growth factor-1 (PRGF-1), was shown to potentiate the agonist-induced stimulation of TRPV1 and TRPM8 thus enhancing Ca^{2+} influx and cell migration in hepatoblastoma and glioblastoma, respectively (Zhang and Vande Woude 2003; Wondergem et al. 2008; Waning et al. 2007). Moreover, HGF/SF together with the endothelial growth factor (**EGF**) stimulates the proliferation of hepatoma cells by up-regulating TRPC6 expression (Boustany et al. 2008). The latter is also regulated by two other growth factors crucial in the angiogenic process, i.e. vascular endothelial growth factor (**VEGF**) and platelet-derived growth factor (**PDGF**) (Jung et al. 2002). In particular, it has been shown that the VEGF-induced Ca^{2+}-mediated increase of microvessel permeability is mediated by store-independent TRPC including TRPC6 (Pocock, Foster, and Bates 2004; Cheng et al. 2006). As regards PDGF, it up-regulates TRPC6 transcription *via* the c-Jun/STAT3 signaling pathway thus leading to a more sustained proliferation of pulmonary artery smooth muscle cells (Yu et al. 2003). Finally, in bladder cancer, the insulin-like growth factor 1 (**IGF-1**) seems to play an important role in regulating cell growth (Zhao et al. 2003) by promoting TRPV2 translocation to the PM (Kanzaki et al. 1999; Qin et al. 2008).

Modulatory TRP isoforms

Alternative splicing by which multiple protein isoforms can be generated from the same gene is another regulatory mechanism of TRP channels in cancer. Indeed, TRP splice variants exhibit different properties in terms of functionality, protein/ protein interaction, or subcellular localization (Stamm et al. 2005) which lead to different biological effects. Alternative splicing may also produce non-functional isoforms of the gene which revealed regulatory properties on functional proteins. Indeed, these inactive isoforms may contribute to the formation of non-functional heteromers by blocking their activity and/or translocation on the plasma membrane. Basically, most TRP channels feature at least two or more splice variants with different expression profiles according to the tissue, type, and stage of cancer. This is especially the case with TRPV1, TRPM1, TRPV2, and TRPM8 (**Fig. 10**).

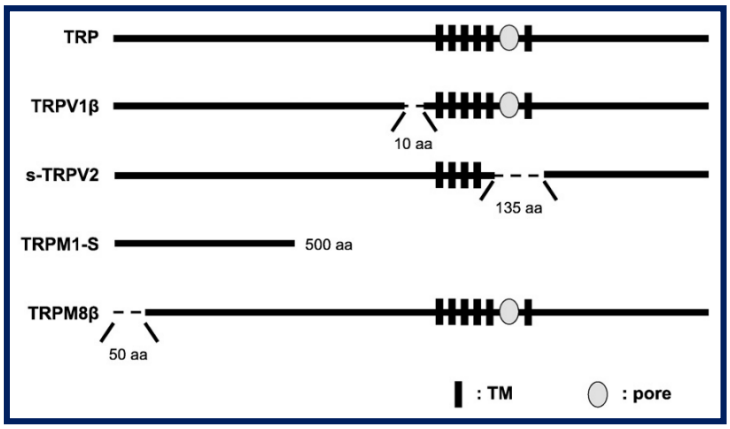

Figure 10. TRP isoforms.
Examples of TRP isoforms showing changes at the protein level (shortened proteins or deletion of small fragments) in cancer: TRPV1 (TRPV1β) and TRPV2 (s-TRPV2) isoforms are implicated in bladder cancer, TRPM1 (TRPM1-S) and TRPM8 (TRPM8β) isoforms in melanoma and prostate cancer, respectively; (aa: amino acids)
Image from (Gkika and Prevarskaya 2009)

Short **TRPV1** isoform (TRPV1β) lacks 10 amino acids in the N-terminal tail and acts as a dominant-negative mutant against the full-length isoform by affecting the tetramerization, stability, and activity of TRPV1 channel (Wang et al. 2004). The short/full TRPV1 form ratio could play a role in controlling urothelial carcinoma progression (Lazzeri et al. 2005). Similarly, metastatic melanoma seems to be correlated with the loss of the full-length **TRPM1** protein probably due to its proteolysis by shorter TRPM1 products (Duncan et al. 1998; Fang and Setaluri 2000; Zhiqi et al. 2004) which have also revealed the capability to retain TRPM1 full-length in the ER (Xu et al. 2001). Indeed, it has been shown that **TRPV2** expresses a full-length isoform showing upregulation during bladder cancer and a short variant (s-TRPV2) whose expression, on the other hand, gradually decreases with tumor progression (Caprodossi et al. 2008). A different s-TRPV2 isoform characterized by a lack of the pore-forming region and the S5 and S6 TM has been observed in human macrophages (Nagasawa et al. 2007). To date, more than one splice variant has been characterized for **TRPM8** protein. Similarly to TRPV1, TRPM8 expresses short splice variants (sTRPM8α, sTRPM8β, and sTRPM8-6, 6-18 kDa) which exert a dominant-negative action against the full-length channel since they are in a closed configuration with its C-terminal tail and thus impair both its cold sensitivity and activity (Fernández et al. 2012; Bidaux et al. 2012). These isoforms are freely diffusing in the cytosol (sTRPM8, 6-18 kDa) and share an antagonist functional effect compare to the channel isoforms (Bidaux, Borowiec, Dubois, et al. 2016). Moreover, an altered N-terminus variant displaying a preferential ER localization and a specific role in controlling cold air-induced inflammation has been cloned from lung epithelia (Sabnis, Reilly, et al. 2008; Sabnis, Shadid, et al. 2008). Other TRPM8 isoforms have been observed and further characterized in PCa (Lis,

Wissenbach, and Philipp 2005). In particular, two TRPM8 isoforms with different localization on the PM ($TRPM8_{PM}$) and ER ($TRPM8_{ER}$) have been identified (Bidaux et al. 2007). Despite the controversy existing in the literature on the presence and functionality of $TRPM8_{ER}$ which could be explained by the different concentrations of agonist used and/or with the specific culture conditions used ((Mahieu et al. 2007; Kim et al. 2009) versus (Thebault et al. 2005; Bidaux et al. 2005; Zhang and Barritt 2004)), the expression of $TRPM8_{ER}$ was confirmed on freshly-isolated primary epithelial PCa cells (Bidaux et al. 2007). It has been shown that the expression of these two isoforms strongly depends on the degree of differentiation of the cells and their dependence on androgen regulation, thus suggesting that the two variants may derive from an alternative promoter of the *TRPM8* gene with different sensitivity to androgens. However, it cannot be excluded that the distinct subcellular localization of the two isoforms results from differences in the primary sequences encoding an ER-specific retention signal and/or involves modulatory mechanisms that influence TRPM8 trafficking. Confirming the existence of TRPM8 isoforms expressed at the intracellular level shorter than the canonical full-length isoform present on the PM (110-128 kDa), an isoform of 95 kDa was found specifically in various endothelial cell lines (EC) showing a strong down-regulation in tumor-derived endothelial cells (TEC) (Genova et al. 2017) as well as in glioblastoma cells (Wondergem et al. 2008). Recently, peculiar N-terminal truncated TRPM8 isoforms domains have been cloned from keratinocytes (eTRPM8) (Bidaux et al. 2015; Bidaux, Borowiec, Prevarskaya, et al. 2016) as well as from PCa cells (Bidaux et al. 2018). These short isoforms, deriving from alternative splicing mechanisms (Bidaux et al. 2015; Bidaux, Borowiec, Prevarskaya, et al. 2016; Borowiec et al. 2016), are characterized by an unconventional structure with 4 instead of 6 TMD (sTRPM8; 35-40kDa – 4TM) as they lack TM1 and TM2 domains. Consistent with their partial localization in mitochondria-associated ER membranes (MAM) 4TM TRPM8 isoforms were found to mediate the uptake by mitochondria of Ca^{2+} released from ER (Bidaux et al. 2018). Another study demonstrated that inhibition of the proteasome machinery in PCa cells results in the up-regulation of the canonical full-length TRPM8 isoform and the simultaneous down-regulation of a short 55 kDa isoform presumably similar to the 4TM TRPM8 isoform, clearly suggesting that $TRPM8_{ER}$ isoforms can derive both from alternative transcriptional splicing as well as from protein degradation mechanisms (Asuthkar et al. 2017).

1.2.3 TRP channels and prostate tumor growth

Tumor growth, cell proliferation and apoptosis

Cancer development and progression are characterized by cell cycle dysregulation, which results in increased cell growth and concomitant suppression of the mechanisms responsible for cell death (Monteith et al. 2007). Most of the mechanisms regulating cell proliferation, cell death, and survival are strongly dependent on $[Ca^{2+}]_i$ homeostasis and thus are affected by Ca^{2+}-permeable ion channels including TRP (Fliniaux et al. 2018). Basically, pro-proliferative pathways involve the entry of Ca^{2} through TRP channels expressed on the plasma membrane (PM) (Berridge, Bootman, and Roderick 2003; Monteith et al. 2007), as well as fluxes of Ca^{2+} mediated by cytoplasm, mitochondria, lysosome or ER inducing pro-apoptotic pathways (Orrenius, Zhivotovsky, and Nicotera 2003; Pinton et al. 2008).

During the cell cycle, calcium oscillations occur during both the G_1/S and G_2/M phases and play a role in centrosome duplication and separation by inducing the expression of transition **cyclins (D and E)** and associated cyclin-dependent kinases (**CDK4 and CDK2**) (Matsumoto and Maller 2002; Roderick and Cook 2008). Furthermore, through effector molecules such as **CaMKII** and **NF-κB**, calcium has been shown to affect proliferation components from transcription to cytokinesis (Matsumoto and Maller 2002). The CaMKII kinase plays an essential role in Ca^{2+}- calmodulin-regulated calcium reuptake and has been recently found to induce apoptosis resistance in PCa in an androgen-sensitive way (Rokhlin et al. 2007). The NF-κB is a transcriptional factor that, in response to different stimuli including a transient rise in intracellular Ca^{2+}, ROS (Sée et al. 2004; Kriete and Mayo 2009), tumor necrosis factor-alpha (TNF-α) (Chandel et al. 2000), and interleukin 1-beta (IL-1β) (Renard et al. 1997), controls the expression of several genes associated with inflammatory and immune responses as well as cell survival and proliferation (Gilmore 2006). For instance, NF-κB has been shown to interfere with caspase-induced apoptosis through the regulation of the anti-apoptotic genes TRAF1 and TRAF2, and its suppression in cancer cells leads to inhibition of tumor cell proliferation and improvement of their sensitivity to chemotherapy drugs (Liu et al. 2012; Sheikh and Huang 2003; Escárcega et al. 2007). Other important Ca^{2+}-dependent players in the regulation of the cell cycle are calpains (Ca^{2+}-dependent cysteine proteases) and calcineurin (Ca^{2+}-dependent serine-threonine phosphatase) (Wu, Tomizawa and Matsui 2007). **Calpains**, upon activation by local Ca^{2+} entry (Smith and Schnellmann 2012) affect not only cytoskeletal remodeling and cell motility (Santella et al. 2000) but also proliferative and apoptotic pathways (Sanvicens et al. 2004; Gómez-Vicente, Donovan, and Cotter 2005) through the proteolytic cleavage of various cytoplasmic proteins including calcineurin (Wu, Tomizawa, and Matsui 2007). **Calcineurin**, in turn, upregulates the expression of interleukins by the activation of specific nuclear transcription factors including

NFAT, and thus stimulates cellular growth and differentiation (Heit et al. 2006). Finally, another Ca^{2+} -associated mechanism of central importance in the regulation of the cell cycle is the so-called store-operated calcium entry (**SOCE**) mediated by ion channels expressed on the PM (Parekh, Fleig, and Penner 1997; El Boustany et al. 2010). Basically, these channels can be activated by the emptying of intracellular Ca^{2+} stores and thus give rise to a sustained calcium entry through the plasma membrane that influences mitochondrial and cytoplasmic apoptotic pathways (Prevarskaya, Skryma, and Shuba 2004; Vanden Abeele et al. 2002; Vanoverberghe, Abeele, et al. 2004). Moreover, it has been shown that Ca^{2+} release from internal stores can itself compromise apoptosis and improve the proliferation and aberrant differentiation of tumor cells (Bidaux et al. 2007; Xin et al. 2005). This observation points out that some ion channels are not only expressed on the PM but also on the membranes of intracellular organelles like lysosomes, mitochondria, and ER from where they support the passage of Ca^{2+} through various intracellular compartments (Pedersen, Owsianik, and Nilius 2005). Among these, there are the well-known IP_3 receptors and ryanodine receptors (RyR) expressed on ER membranes and involved in the regulation of apoptosis (Hoyer-Hansen and Jaattela 2007; Johnson et al. 2004) but also some members of the TRP family such as TRPC1 (Ambudkar, de Souza, and Ong 2017), TRPM2 (Zeng et al. 2010), and TRPM8 (Bidaux et al. 2012; 2015).

TRP channels in PCa growth

Some TRP channels have revealed pro-proliferative effects on PCa cells (**Fig. 11**). Among these, **TRPV6** is certainly the best characterized to date for its strong pro-proliferative role in PCa as well as in other cancers involving the pancreas, colon, ovary, breast, and thyroid gland (Stewart 2020; Lehen'kyi, Raphaël, and Prevarskaya 2012). TRPV6 has been shown to promote proliferation and survival probably through a SOCE-dependent mechanism and under transcriptional regulation by progesterone, estrogen, tamoxifen, and vitamin D (Van Cromphaut et al. 2003; Song et al. 2003). TRPV6 expression significantly increases with the progression of PCa towards aggressive forms and correlates with the Gleason grading > 7 (Wissenbach et al. 2001; Peng et al. 2001; Fixemer et al. 2003). Moreover, TRPV6 up-regulation is known to be driven by AR: it results inhibited by the AR agonist dihydrotestosterone and stimulated by the AD antagonist bicalutamide (Bödding, Fecher-Trost, and Flockerzi 2003; Vanden Abeele et al. 2003). However, TRPV6 impact on PCa growth is not only affected by its differential expression according to cancer stage but also by its trafficking to the plasma membrane regulated by Orai1/TRPC1/Annexin I/S100A11 pathway in a SOCE-dependent manner (Raphaël et al. 2014). Prevarskaya's group demonstrated that TRPV6 contributes to LNCaP proliferation basically decreasing proliferation rate, cell accumulation in the S-phase of the cell cycle, and the expression of proliferating cell nuclear antigen (PCNA) (Lehen'kyi et al. 2007). Mechanistically, it has been suggested that the increase in cell viability and resistance to apoptosis conferred by TRPV6 to LNCaP cells

might be caused by the TRPV6 mediation of the Ca^{2+}-induced activation of NFAT and NF-κB signaling pathways, known to induce the expression of genes conferring resistance to apoptosis (Lehen'kyi et al. 2007; Schwarz et al. 2006; Raphaël et al. 2014).

Also **TRPC1** expression is regulated by androgen receptor in the prostate although displaying the opposite pattern during PCa progression compared to TRPV6. Indeed, TRPC1 is down-regulated from the androgen-dependent to the androgen-independent phase of PCa. Accordingly, TRPC1 exerts a pro-apoptotic role in PCa probably through the TNF-α-induced NF-κB signaling pathway (Marasa et al. 2006).

Furthermore, it has been observed that treatments that induce neuroendocrine differentiation like androgen deprivation could up-regulate **TRPV2** expression thus associating this channel with the castration-resistant prostate cancer (CRPC) progression (Monet et al. 2010). TRPV2 is expressed in androgen-independent and metastatic phases of PCa and its suppression has been shown to slow down PCa growth and invasiveness in nude mice xenografted with PC3 cells (Monet et al. 2009; 2010). The mechanism through which TRPV2 may affect cell proliferation has not been yet elucidated, whereas **TRPV1** involvement has been linked to a cross-talk with α_{1D}-AR which ultimately results in a more sustained PCa cells proliferation (Morelli et al. 2014). Similar results were also observed in LNCaP cells where capsaicin activation of TRPV1 enhances cell proliferation through the Akt and ERK pathways (Malagarie-Cazenave et al. 2009). Consistently, TRPV1 expression levels appear to be increased in high-grade PCa when compared with benign prostate hyperplasia (BPH) (Sánchez et al. 2005; Czifra et al. 2009). However, TRPV1 also displayed a pro-apoptotic role in PCa induced by vanilloid stimulation and the subsequent Ca^{2+} overloading within the cell, and the fast decrease of the transmembrane mitochondrial potential (Ziglioli et al. 2009). At the same time, capsaicin has been shown to inhibit PC3 growth *via* a receptor-independent mechanism involving coenzyme Q inhibition, ROS accumulation, and caspase activation (Sánchez et al. 2006).

Regarding the TRPM family, a pro-proliferative role in PCa has been assigned to TRPM4 and TRPM7. Significant increases in **TRPM4** transcripts were observed in PCa patients supporting a pro-proliferative role of TRPM4 through the promotion of β-catenin function as a transcriptional cofactor and Wnt signaling pathway (Armisén et al. 2011; Sagredo et al. 2018). Another player in the growth of PCa is **TRPM7**, although it has been better characterized for its impact on PCa invasiveness. Indeed, TRPM7 inhibition was shown to promote the TRAIL-induced apoptotic pathways in PC3 cells (Lin et al. 2015), whereas its activation by cholesterol supports PCa cells proliferation through the activation of the Ca^{2+}-dependent AKT and/or ERK pathways (Sun et al. 2013). This mechanism may explain the correlation found between high circulating cholesterol levels and the higher risk of aggressive PCa in general (Pelton, Freeman, and Solomon 2012).

Other TRP channels appear to play a protective role in the progression of prostate cancer by exercising pro-apoptotic functions as described above for **TRPC1** (**Fig. 11**). As an example, some early studies proposed

the involvement of **TRPC4** in ATP-stimulated SOCE-dependent mechanisms in PCa cell lines (Vanden Abeele et al. 2004). Although its role has not yet been fully investigated, it appears that TRPC4 may be implicated in SOCE-induced cell proliferation mechanisms due to its tendency to form heteromers with TRPC1 (Antoniotti et al. 2006). Moreover, the prolonged depletion of intracellular Ca^{2+} stores has been shown to up-regulate **TRPC3** expression, as well as that of TRPC1, in LNCaP cells *via* Ca^{2+}/calmodulin/calcineurin/NFAT pathway (Pigozzi et al. 2006). In addition, in DU145 cells it has been described an interesting co-localization of TRPC3 channel with transcription factor TFII-I, known to interfere with apoptosis (Misra et al. 2011). Of note, within the TRPC family, compensatory pathways relying on their tendency to aggregate and function interdependently should always be considered in defining their roles in physiological and/or pathological conditions. Another member of the TRPC family associated with PCa growth is **TRPC6**, whose expression was associated with the histological grade, Gleason score, and extra-prostatic extension of PCa (Yue et al. 2009). TRPC6 act as a second messenger-operated channel (SMOC) being involved in the α_{1D}-AR-mediated stimulation of PCa cell proliferation (Thebault et al. 2006) as previously described for TRPV1. Indeed, agonist-mediated activation of α_{1D}-AR enhances PCa cell proliferation thus inducing a store-independent TRPC6-mediated Ca^{2+} entry which ultimates in the activation and nuclear translocation of the Ca^{2+}/calcineurin-dependent NFAT (Thebault et al. 2006). Moreover, TRPC6 has been implicated in the HGF-induced proliferation of PC3 and DU145 cells (Wang et al. 2010). Taking into account these data, basal prostate cancer cell proliferation has been proposed to be under the control of the basal calcium entry provided by TRPV6, and that TRPC6 is involved in the catecholamine-induced mitogenic effect (Prevarskaya, Skryma, and Shuba 2010).

Finally, a pro-apoptotic role in PCa has been assigned to TRPM2 (Zeng et al. 2010). The selective suppression of **TRPM2** expression in PCa cells has been shown to inhibit tumor growth without affecting cell proliferation in healthy cells (Zeng et al. 2010). In addition to a higher level of expression in tumor cells, TRPM2 exhibits markedly different subcellular localization between cancerous and non-cancerous cells: in benign cell lines, TRPM2 is expressed on the PM and in the cytosol (lysosomes), while in tumor cells it is also expressed in a cluster pattern in the nuclei (Zeng et al. 2010). It has been shown that TRPM2 can inhibit nuclear ADP-ribosylation in PCa, thanks to the enzymatically active adenosine diphosphoribose hydrolase domain present in its C-terminus (Wang, Huang, and Yue 2017b). However, the TRPM2-mediated inhibition of cell proliferation does not depend on the activity of poly (ADP-ribose) polymerases (Zeng et al. 2010). Although the link between TRPM2 and cell survival is still elusive, it could be associated with the ROS-induced TRPM2-mediated Ca^{2+} release from the lysosomal stores and the subsequent trigger of apoptotic pathways as observed in rat β pancreatic cells (Lange et al. 2009; Starkus, Fleig, and Penner 2010). In this regard, it has been shown that oxidative stress in cancer cells can activate CaMKII in a TRPM2-dependent mechanism which

ultimately results in a positive feedback loop characterized by intracellular ROS accumulation, mitochondrial fragmentation, and loss of mitochondrial membrane potential (Wang, Huang, and Yue 2017b).

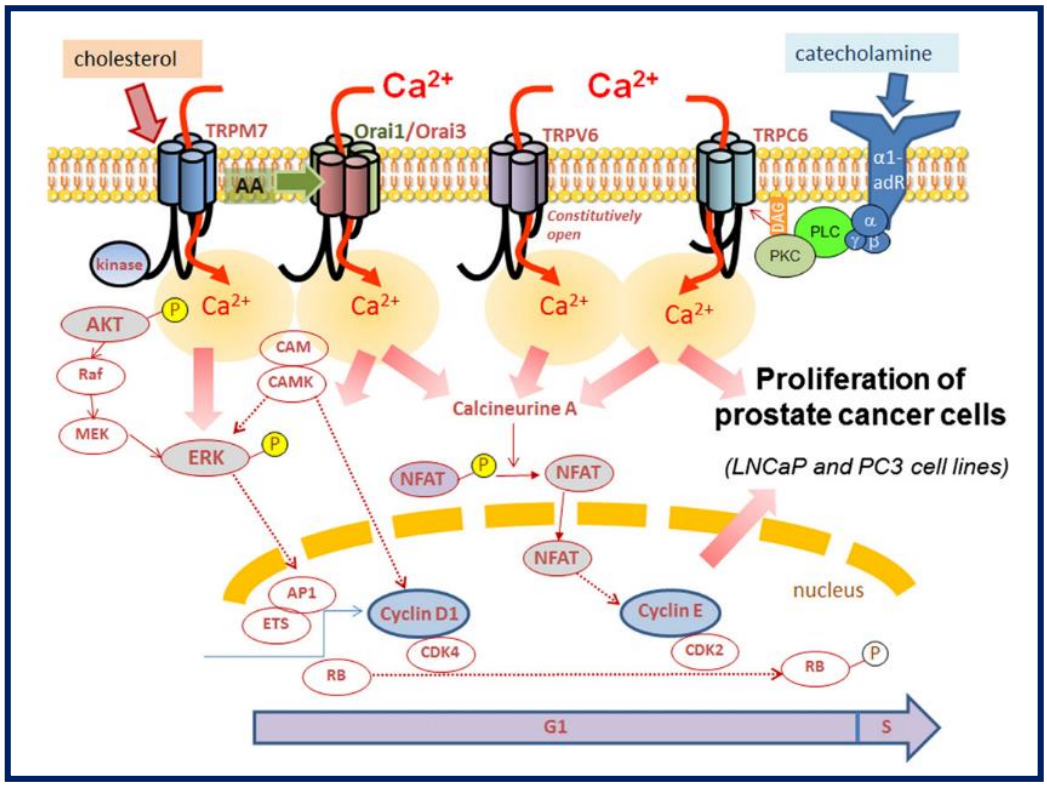

Figure 11. TRP channels and prostate tumor growth.
Scheme representing signalling pathways through which TRP channels affect PCa cells proliferation and apoptosis. AKT: serine/threonine kinase also known as protein kinase B; ERK: extracellular signal-regulated kinases; MEK: mitogen-activated protein kinase kinase; AP1: activator protein 1; RB: transcriptional corepressor 1; ETS: transcriptional factor; NFAT: nuclear factor of activated T-cells; CDK: cyclin-dependent kinases; RB: focal adhesion; CAM: calcium/calmodulin; CAMK: calcium/calmodulin-dependent kinase II; PKC: protein kinase C; PLC: phospholipase C.
Image from (Déliot and Constantin 2015)

1.2.4 TRP channels and prostate cancer invasiveness

Cell migration and invasion

To escape the primary tumor and spread to colonize other sites, cancer cells must acquire a more aggressive phenotype characterized by a greater ability to migrate and cleanse their way through the extracellular matrix (ECM) to invade surrounding tissues.

Cell migration is a Ca^{2+}-dependent multistep process basically involving cytoskeleton remodeling as well as cellular protrusion/contraction to adhere and detach from ECM. Cancer cells mainly adopt a mesenchymal mode of motility based on directional migration. This process relies on the formation of a transient increase of intracellular Ca^{2+} which produces a front-to-rear calcium gradient and polarity within the cell (Mayor and Etienne-Manneville 2016). Therefore, specific cellular responses are then triggered based on the spatial and temporal distribution of $[Ca^{2+}]_i$. Typically, at the leading edge cell membrane extensions with directed actin polymerization are formed, while contemporarily focal adhesions (FA) linking cytoskeleton with ECM are disassembled at the rear of the cell and the trailing edge is contracted (Mayor and Etienne-Manneville 2016). The directionality of the movement is determined by the so-called "calcium flickers" which are restricted at lamellipodia and confer to the cell the ability to respond to directional cues (Wei et al. 2009; 2010). Among the main players of the migratory machinery, there are Ca^{2+}-dependent myosin light chain kinase (**MLCK**) and the EF-hand Ca^{2+}-binding protein family of **S100** responsible for F-actin polymerization and myo II–actin assembly resulting in actomyosin contraction (Clark et al. 2007); focal adhesion proteins, such as **integrins**, **talin**, **vinculin** and focal adhesion kinases (**FAK**) that undergo high turnover through the cleavage by the Ca^{2+}-sensitive protease **calpain** and the restoration by proline-rich tyrosine kinase 2 (**Pyk2**), and small GTPases like **Ras** and **Rac** (Franco and Huttenlocher 2005; Lysechko, Cheung, and Ostergaard 2010; Selitrennik and Lev 2015). As responsible for the intracellular homeostasis of calcium, TRP channels can define the frequency and localization of these transient and local Ca^{2+} microdomains within the cytosol and thus orchestrate the migratory machinery.

Another feature that cancer cells must acquire to give rise to metastasis is strong invasiveness which is the ability to efficiently degrade ECM proteolytically. This process is mediated by special cellular structures named invadopodia and consists of dynamic actin-enriched cell protrusions with proteolytic activity. Ca^{2+} influx and oscillations are required to trigger invadopodia initiation, assembly through the generation of phosphatidylinositol-3,4-bisphosphate (**PtdIns(3,4)P_2**), and the activation of the non-receptor tyrosine kinase **Src**, and maturation (Mader et al. 2011; Yamaguchi et al. 2011). Focal degradation of the ECM is achieved by the upregulation of proteolytic enzymes such as zinc-dependent endopeptidases **MMP** (matrix metalloproteinase) and **cathepsins** which are incorporated into mature invadopodia and then released *via* endocytic vesicles at the degradation sites of the ECM to allow cell invasion (Beaty et al. 2013; Brown and Murray 2015).

Intracellular signaling pathways involved in tumor cell migration and invasion will be discussed more in detail in **Chapter 1.3**.

TRP channels in PCa invasiveness

The main TRP channels involved in the control of motility of transformed cells are TRPC1, TRPM1, TRPM7, TRPM8, and TRPV2 (Canales et al. 2019; Fels et al. 2018; Asghar and Törnquist 2020). Regarding prostate cancer specifically (**Fig. 12**), it has been observed that **TRPV2** enhances PCa cells invasive features by promoting cell migration and stimulating the expression of invasion markers MMP-2, MMP-9, and cathepsin B leading to the progression to androgen resistance (Monet et al. 2009; 2010). Indeed, androgen deprivation induces *de novo* expression of TRPV2, which, in turn, mediates a constitutive calcium increase in the cytosol supporting the migratory machinery of metastatic cells (Monet et al. 2010). Moreover, independently of androgens, endogenous lysophospholipids may enhance the translocation of TRPV2 to the PM *via* the phosphatidylinositol 3-kinase (PI3K) pathway, thus promoting PCa cells migration (Monet et al. 2009). Similarly, the activation of adrenomedullin (AM), a multifactorial 52-amino acid regulatory peptide involved in different cancerogenesis processes, was shown to promote the PI3K-mediated translocation of TRPV2 to the PM and the subsequent Ca^{2+}-dependent activation of β1-integrin and FAK phosphorylation responsible for increased cell migration (Oulidi et al. 2013). Therefore, TRPV2 may be considered a promising pharmaceutical target for the treatment of androgen-independent PCa.

Moreover, a driven role in CRPC progression has recently been attributed to **TRPM4** channel (Schinke et al. 2014) since it was found to sustain EMT phenotypes, migration, and invasion of PCa cells (Hong and Yu 2019). More in detail, the miR-150-mediated suppression of TRPM4 expression in PCa tissues resulted in the inhibition of metastases (Hong and Yu 2019). Consistently, TRPM4 silencing decreases EMT and cell migration in PC3 and DU145 cells through the blockade of the β-catenin signaling pathway without affecting their proliferation (Holzmann et al. 2015; Sagredo et al. 2019). Conversely, TRPM4 overexpression in LNCaP lead to higher levels of Snail1, inhibition of E-cadherin expression, and increased migratory capability (Sagredo et al. 2019).

Another member of the TRPM family affecting PCa invasiveness is **TRPM7**, which, also considering its stretch-dependent mode of activation, has been proposed as part of the complex mechanosensory toolkit driving cancer cells to metastasis development by modulation of actomyosin cytoskeleton contraction and dynamics of the FA turnover (Su et al. 2011; Gao et al. 2011; Middelbeek et al. 2012; 2016; Langeslag et al. 2007). Consistently with its up-regulation in PCa compared to BPH, TRPM7 silencing was shown to revert EMT through the reduction of MMPs and the calpain-mediated increase of E-cadherin levels and to inhibit both cell migration and invasion through a cholesterol-dependent calcium entry (Sun et al. 2014; Chen et al. 2017).

A study linking the migration of prostate cancer cells with incubation with the endocrine-disrupting compound bisphenol A (BPA) which is abundant in reusable water bottles, metal cans, and plastic food

containers, highlighted the role of SOCE in promoting the migration of androgen-dependent or -independent prostate cells (Derouiche et al. 2013). More specifically, it has been demonstrated that BPA incubation affects LNCaP migration by regulating the expression of important components of SOC such as Orai1 and TRPV6 (Derouiche et al. 2013). Therefore, the TRP and Orai channels appear to be promising pharmaceutical targets for blocking the spread of PCa cells within the body. Moreover, TRPC6 has been linked to PCa invasiveness showing that the overexpression of TRPC6 in cancer cells correlates with increased invasion ability of PC3 into a "matrigel-based" matrix (Wang et al. 2014).

Beyond their role in controlling prostate tumor growth, migration, and invasion, the possible involvement of TRP channels in castration resistance and the subsequent non-responsiveness to the current androgen deprivation therapy (ADT) has not yet been established (Yang and Kim 2020).

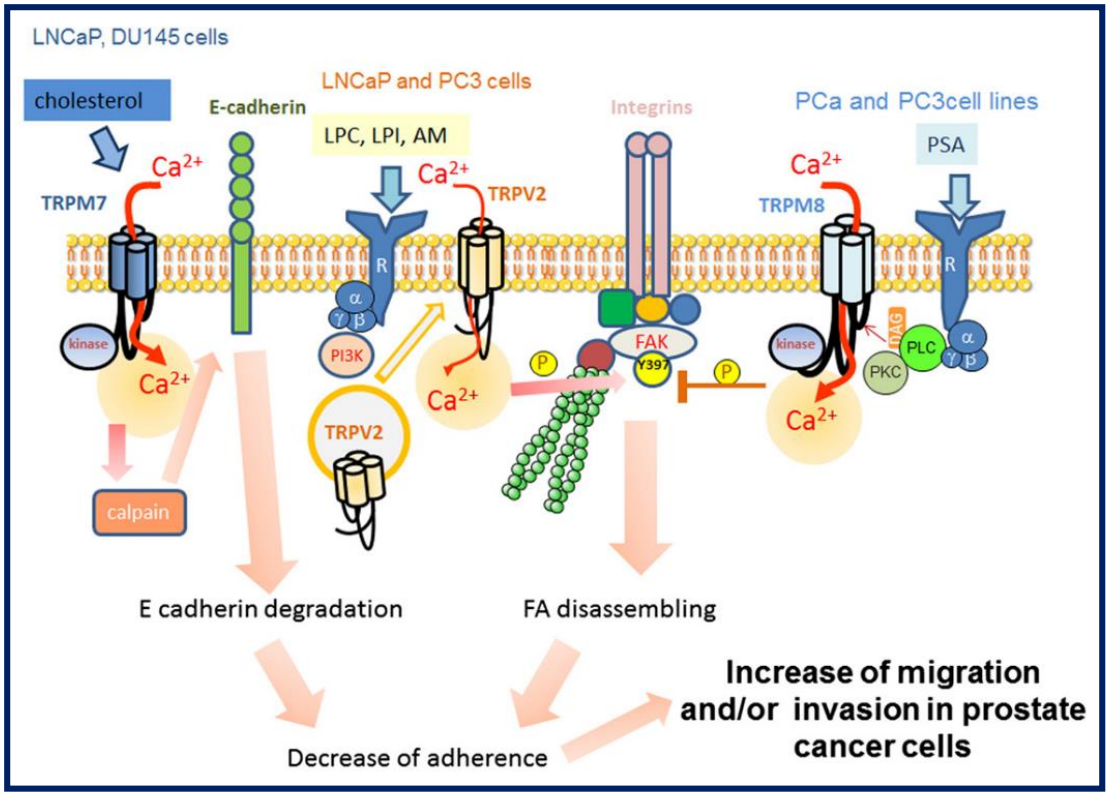

Figure 12. TRP channels and prostate cancer invasiveness.
Scheme representing signalling pathways through which TRP channels affect PCa cells migration and invasion. LPC: Lysophosphatidylcholine; LPI: lysophosphatidylinositol; AM: adrenomedullin; FAK: focal adhesion kinase; FA: focal adhesion; PSA: prostate specific antigen.
Image from (Déliot and Constantin 2015)

1.2.5 TRP channels and prostate angiogenesis

Tumor vascularization and angiogenesis

Tumor growth and metastasis require the formation of new blood vessels to provide oxygen and nutrients, as well as to allow metastatic cells to access the bloodstream, allowing them to spread and colonize new sites. The angiogenic process is promoted by the cancer cells themselves and ultimately triggered by a plethora of growth factors released in the tumor microenvironment. Among them, the **VEGF** is the indisputable protagonist of the complex angiogenic process. The role played by the vascular endothelial growth factor A (VEGF-A) is particularly important, since it activates local EC and the recruitment of endothelial progenitor cells (EPC) from bone marrow, both necessary for the angiogenic switch (Carmeliet and Jain 2000). Then, a new circulatory network characterized by abnormal morphology, irregular blood flow, and distribution, non-uniform pericyte coverage and hyperpermeability and involving proliferation, migration, differentiation and stabilization of such TEC is established (Carmeliet 2005; Folkman 2006). VEGF was found to contribute to multiple features of tumour neovascularization including permeability, motility and apoptosis (Dragoni et al. 2011; 2015; Weis and Cheresh 2005; Noren et al. 2017). Intracellular Ca^{2+} signalling play a central role in all of these processes (Iamshanova, Fiorio Pla, and Prevarskaya 2017; Moccia et al. 2019; Scarpellino et al. 2020). For instance, the expression and the secretion of several growth factor including VEGF is Ca^{2+}-dependent and thus controlled by ion channels including TRP (Negri et al. 2020). Moreover, TEC exhibit alterations in a plethora of pro-angiogenic Ca^{2+} signals pathways induced by VEGF as well as by other pro-angiogenic factors such as, ATP, AA, NO, hydrosulfide (HS), cAMP known to exert pro-migratory effects on TEC but not in normal EC (Fiorio Pla and Munaron 2014). More specifically, it has been extensively demonstrated that pro-angiogenic molecules such as those listed above enhance vessel permeability as well as EC survival, migration and tubulogenesis through Ca^{2+}-dependent pathways (Dragoni et al. 2011; 2015; Noren et al. 2017; Iamshanova, Fiorio Pla, and Prevarskaya 2017; Moccia et al. 2019). As regards TRP channels, they have proved to be involved in multiple steps of the angiogenic process by affecting vascular remodeling, permeability, tone, mechanosensing, etc. (Munaron 2015).

TRP channels in PCa angiogenesis

At least 14 TRP channels were found to be expressed in EC as well as in EPC and some of them revealed aberrant expression during tumor vascularization (Negri et al. 2020) (**Fig. 13**). However, to date, only **TRPV4** has been directly associated with prostate angiogenesis. The role of TRPV4 as a mechano-sensor intervenes in actin remodeling and cell volume regulation thanks to its ability to perceive and therefore integrate

mechanical stresses deriving from alterations in cell morphology, cell swelling, and shear stress is well known (Becker et al. 2005; Becker, Bereiter-Hahn, and Jendrach 2009). Adapala *et al*. showed a down-regulation of TRPV4 expression in TEC from a transgenic adenocarcinoma mouse prostate. This down-regulation correlates to enhanced cell motility, abnormal angiogenesis, and increased vascular leakage in TEC thus resulting in enhanced tumor growth (Adapala et al. 2016; Cappelli et al. 2019). Consistently, TRPV4 overexpression or activation "normalizes" the vascular endothelium and blocks tumor growth essentially by improving vessels' permeability to chemotherapeutic drugs (Adapala et al. 2016). Mechanistically, this effect is due to the central role played by TRPV4 in regulating TEC mechano-sensitivity towards ECM stiffness by inhibiting Rho activity (Adapala et al. 2016; Thoppil et al. 2016) and tumor vascular integrity by stabilizing the cell-cell junctions of VE-cadherin (Cappelli et al. 2019). By contrast, other studies conducted on different TEC models from human breast and renal carcinomas have reported an up-regulation of TRPV4 parallel to enhanced cell migration in TEC compared to the normal counterpart (Fiorio Pla et al. 2012). This discrepancy, which can be at least partially explained by the different tumor models used, underlines how each channel can have a specific and unique role depending on the type of cancer. In any case, the involvement of TRPV4 in tumor neovascularization processes is indisputable so much so that the angiogenesis of some tumor forms can be classified as TRPV4 oncochannelopathy (Prevarskaya, Skryma, and Shuba 2018).

Interestingly, activation of **TRPA1** was found to increase the secretion of VEGF and HGF through a Ca^{2+}-dependent pathway in prostate cancer-associated fibroblasts (CAF) and simultaneously rescue co-cultured PCa cells from apoptosis, thus suggesting a role for TRPA1 in prostatic angiogenesis (Vancauwenberghe et al. 2017).

For other TRP, their potential involvement in angiogenesis appears to be suggested by evidence of a role in controlling proliferation, apoptosis, motility, permeability, and growth factor secretion in EC, but their specific impact on tumor neovascularization has yet to be proven. As an example, **TRPC6** (Chigurupati et al. 2010) and TRPA1 (Park et al. 2016) have been associated with the control of hypoxia-induced VEGF release in PCa cells, while **TRPC6** (Zhang et al. 2015), **TRPC3** (Ampem, Smedlund, and Vazquez 2016; Smedlund, Tano, and Vazquez 2010), and **TRPM2** (Sun et al. 2012) contribute to the activation of pro-apoptotic pathways in EC in response to ER stress inducers. TRPC6 expression and activity have been related to VEGF and PDGF signaling in EC with subsequent consequences on microvessels' permeability and EC proliferation respectively (Pocock, Foster, and Bates 2004; Cheng et al. 2006; Yu et al. 2003). Moreover, TRPC6 has been recently associated with the aberrant transforming growth factor β1 (TGF-β1) signaling thus affecting stress fibers' formation and cell migration in EC (Park et al. 2017). Additionally, **TRPM7** seems to inhibit EC proliferation and NO production via the ERK pathway (Inoue and Xiong 2009; Baldoli and Maier 2012; Baldoli, Castiglioni, and Maier 2013). Furthermore, TRPC6, **TRPC1**, and TRPM2 revealed a role in increasing EC

permeability (Singh et al. 2007; Mehta et al. 2003; Hecquet et al. 2008; Mittal et al. 2015), and TRPM8 and TRPM7 were found to affect EC motility (Genova et al. 2017; Baldoli and Maier 2012; Baldoli, Castiglioni, and Maier 2013; Zeng, Inoue, et al. 2015).

The role played by TRPV4, TRPC1, TRPC6, and TRPM8 in EC and their potential role in affecting tumor neovascularization will be discussed more in detail in **Chapter 1.3**. In this context, some of the results obtained in the present Ph.D. thesis better defined the role of TRPV2, TRPC3, and TRPA1 in PCa angiogenesis as shown and discussed in **Chapters 3.1.1** and **4.1.1**, respectively.

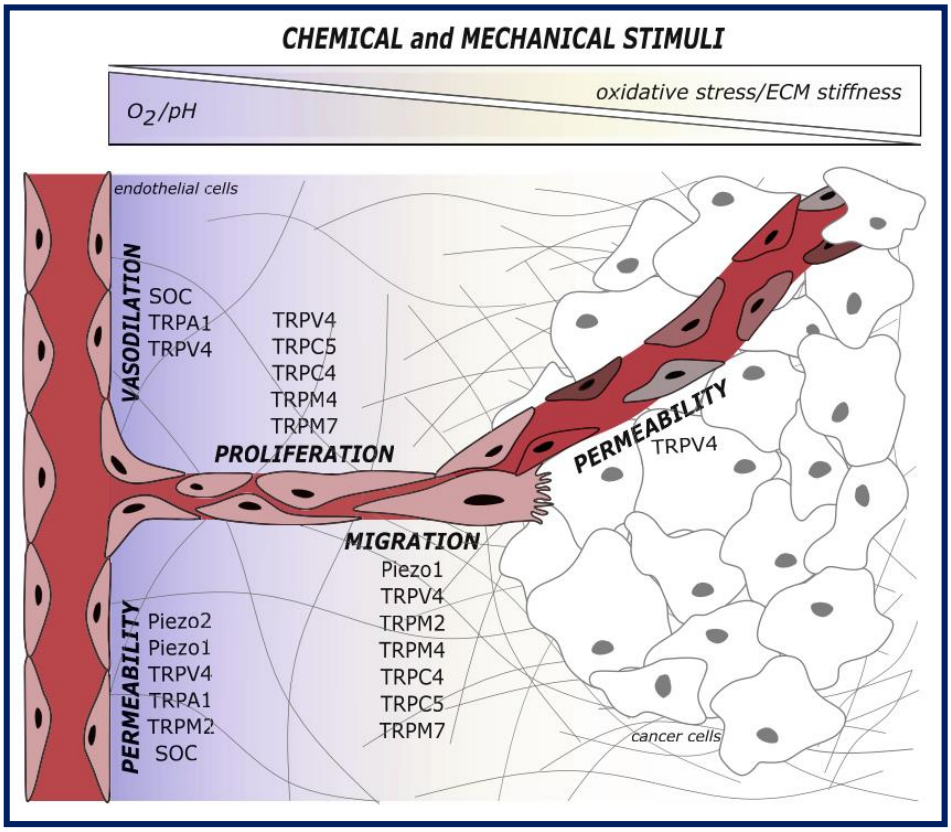

Figure 13. TRP channels and tumor vascularization.

Scheme representing processes controlled by TRP channels in EC justifying their possible involvement in tumor vascularization.
Image from (Scarpellino et al. 2020).

1.2.6 The intringuing case of TRPM8 in prostate cancer

TRPM8 expression in prostate

Contrary to most TRP channels which, according to currently available data, tend to adhere to specific roles, improving cell proliferation or apoptosis, **TRPM8** shows participation in complex modulatory mechanisms in PCa concomitantly with a cancer stage-dependent expression pattern, as previously described for TRPC1. Consequently, the role of TRPM8 in prostate cancer progression is much more complex. As previously mentioned (**Chapter 1.1.3**), TRPM8 was firstly identified in the prostate even before its classical function as cold receptor in sensory neurons was established. On paraffin-embedded sections, TRPM8 transcripts were detected by *in situ* hybridization only in prostate epithelial cells, while neither in the vascular smooth muscle cells and endothelium (Tsavaler et al. 2001). At the protein level, TRPM8 channel was found by immunohistochemistry and western blot analysis both in the apical epithelial cells and in the smooth muscle cells of the human prostate (Bidaux et al. 2005; 2007). *TRPM8* was described from the very beginning as a novel prostate-specific gene due to its peculiar expression profile during PCa development and progression (Tsavaler et al. 2001). Indeed, TRPM8 expression significantly increases in BPH and the early androgen-dependent stages of PCa (Fuessel et al. 2003), while decreases during the late androgen-independent metastatic phase (**Fig. 14**) (Bidaux et al. 2007), making TRPM8 a potential good prognostic marker for PCa.

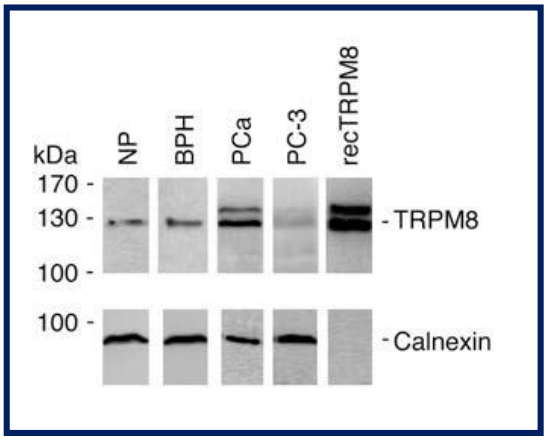

Figure 14. TRPM8 expression profile during PCa development.

TRPM8 full-length isoform (128 kDa) was detected in normal prostate (NP), benign prostate hyperplasia (BPH), androgen-dependent prostate cancer cells (PCa) and androgen-independent metastatic prostate cancer cells (PC-3)
Image from (Bidaux et al. 2007).

The peculiar expression profile exhibited by TRPM8 in PCa is based on the androgen dependence of its expression (**Chapter 1.2.2**). Indeed, it has been proven that anti-androgen therapy on patients and mouse models (Henshall et al. 2003) as well as withdrawal of androgens in PCa cell lines (Bidaux et al. 2005; Zhang and Barritt 2004) greatly reduces the expression of TRPM8. Moreover, it has been reported that a functional AR is required and sufficient to induce TRPM8 expression thanks to its binding to androgen-responsive elements present in the *TRPM8* gene sequence in its testosterone-bound form (Bidaux et al. 2005). In addition, an additional non-genomic mechanism has been recently proposed showing that AR interacts with TRPM8 within specific microdomains of the PM named lipid rafts (Bidaux et al. 2007). Consistently, a correlation between the differentiation state of prostate cells and the subcellular localization of TRPM8 has been established (Bidaux et al. 2007) (**Fig. 15**). In this regard, Bidaux *et al.* showed that TRPM8 is mainly expressed on the PM ($TRPM8_{PM}$) of highly differentiated prostate apical epithelial secretory cells expressing cytokeratins CK8 and CK18 and suggested an androgen-dependent shift of its localization to the ER ($TRPM8_{ER}$) in cells that lost androgen receptor activity during PCa development into more aggressive metastatic forms (Bidaux et al. 2007). Indeed, $TRPM8_{ER}$ was found in both luminal and basal phenotypes regardless of the differentiation status of prostate cells (Bidaux et al. 2007; Thebault et al. 2005; Zhang and Barritt 2004). This different subcellular localization was then also associated with changes in channel function and has been hypothesized to be linked and critical for carcinogenic events, such as proliferation, apoptosis, and migration. For instance, PCa cells may exploit the altered expression of $TRPM8_{ER}$ as an adaptive response to acquire a survival advantage in terms of resistance to apoptosis in the late metastatic phase thanks to the reduced Ca^{2+} release content from intracellular stores.

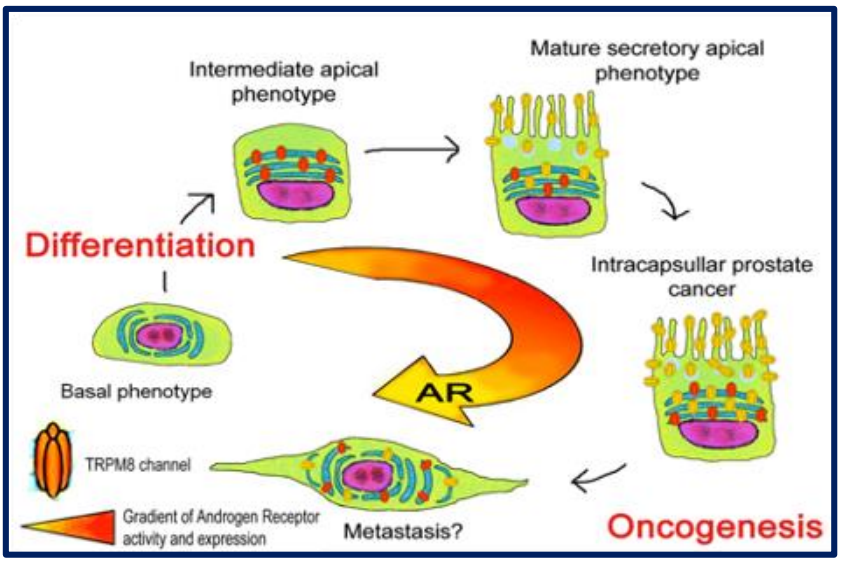

Figure 15. TRPM8 localization and function depending on androgens and the differentiation status of human prostate epithelial cells.
Image from (Prevarskaya, Flourakis, et al. 2007)

Roles of TRPM8 in prostate cancer

According to Tsavaler's hypothesis, TRPM8 can be considered an oncogene in the prostate and its overexpression/overactivity circumscribed to the androgen-dependent phase of PCa may be related to the higher rate of growth observed in these cells compared not only to normal prostatic ones but also to metastatic androgen-independent cells (Berges et al. 1995). This is mainly due to the high sensitivity to apoptotic stimuli displayed by normal prostatic cells thanks to fine and strict regulation of the Bcl-2 signaling pathway mediated by the AR. More in detail, AR enhances the expression of pro-apoptotic genes belonging to the Bax family and decreases the translation of anti-apoptotic genes belonging to the Bcl-2 family (Bonkhoff, Fixemer, and Remberger 1998). Although the involvement of TRPM8 in ensuring the survival of androgen-dependent PCa cells has been amply demonstrated by several studies, whether this occurs through a proliferative and/or anti-apoptotic mechanism is still arguable. Interestingly, the identification of different TRPM8 isoforms with distinct subcellular localization ($TRPM8_{PM}$ and $TRPM8_{ER}$) could justify the fact that TRPM8 can simultaneously regulate both proliferation and apoptosis in prostate cancer, based on the involved isoform (Prevarskaya, Zhang, and Barritt 2007). Zhang et al. have demonstrated that TRPM8 is required for PCa cell survival since its pharmacological inhibition or the siRNA-mediated TRPM8 silencing impairs the cell viability of LNCaP by perturbing intracellular Ca^{2+} homeostasis (Zhang and Barritt 2004). Other studies demonstrated that basal TRPM8 expression is sufficient to increase proliferation rates and proliferative fraction in PCa cells and not in normal cells (Valero et al. 2012; Liu et al. 2016). The underlying molecular mechanism describes the up-regulation of phosphorylated protein kinase B, cyclin D1, CDK2, and CDK6, down-regulation of glycogen synthase kinase 3β, and activation of MAPK kinases (p38 and JNK) (Peng et al. 2015). Furthermore, by using androgen-dependent LNCaP cells resistant to anti-androgen bicalutamide treatment, it has been shown that the transition of metastatic PCa cells to androgen independence is accompanied, in addition to an up-regulation of Bcl-2, and a down-regulation of PCNA, AR, and TRPM8, by reduced cell proliferation (Prevarskaya, Skryma, et al. 2007). This evidence seems to support a putative pro-proliferative role of TRPM8 in androgen-dependent PCa cells. However, in LNCaP cells activation of **$TRPM8_{ER}$** by cold or menthol results in the ER store depletion followed by SOCE (Thebault et al. 2005) and, as previously described, this pathway can be critical in **promoting growth arrest and apoptosis** of PCa epithelial cells (Prevarskaya, Flourakis, et al. 2007). Indeed, one of the hallmarks of the apoptosis-resistant cell phenotypes of advanced PCa is the reduced basal filling of intracellular Ca^{2+} stores (Prevarskaya, Flourakis, et al. 2007; Vandel Abeele et al. 2002; Vanoverberghe, Vanden Abeele, et al. 2004). Moreover, TRPM8 overexpression in PC3 cells revealed a role in promoting starvation-induced cell apoptosis by causing a significant cell cycle arrest in G_0/G_1 stage (Yang et al. 2009) and menthol-induced TRPM8 activation in DU145 cells inhibits cell proliferation (Wang et al. 2012). By contrast, the overexpression of the short TRPM8 isoform α (sTRPM8 α)

was found to reduce starvation-induced apoptosis in LNCaP cells possibly *via* inhibition of phosphorylated-c-Jun N-terminal kinase (p-JNK) thus contributing to a more malignant phenotype (Peng et al. 2015). Finally, new functional $TRPM8_{ER}$ isoforms (4TM-TRPM8 isoforms) have been recently cloned and characterized in PCa epithelial cells, showing their direct involvement in mediating Ca^{2+} flux from the ER to the mitochondria and thus in the control of PCa cell survival by affecting ATP and ROS synthesis (Bidaux et al. 2018). Furthermore, it has been shown that non-channel cytoplasmic small TRPM8 isoforms (sM8), ubiquitously expressed in PCa cells, are involved in PCa cell death by reducing ER stress, p21 expression, and apoptosis and in exploiting their action require 4TM-TRPM8 isoform activity (Bidaux, Borowiec, Dubois, et al. 2016). Therefore, it is evident that the balance between proliferation or apoptosis in prostate tissues may depend, among others, on the relative expression levels of the different TRPM8 isoforms and that to counteract PCa growth specific inhibition of different isoforms may be considered depending on the stage and androgen-sensitivity of the tumor (Bidaux et al. 2012; Prevarskaya, Skryma, et al. 2007). $TRPM8_{ER}$, being capable of influencing the filling of ER stores, can be considered an important factor in controlling the apoptosis of advanced PCa metastatic cells, whereas $TRPM8_{PM}$ may play an important role in regulating pro-proliferative pathways mediating Ca^{2+} influx within the cells. To note, the target of sM8 could represent an appropriate strategy to fight PCa (Bidaux, Borowiec, Dubois, et al. 2016).

However, **$TRPM8_{PM}$** has been mainly associated with PCa cell migration proposing a protective role of TRPM8 in PCa progression. More in detail, it has been shown that the activation of $TRPM8_{PM}$ by icilin and/or PSA significantly **reduces the motility** of PCa cells (Gkika et al. 2010). Moreover, the reduction of cell migration was even more pronounced by treating the cells with both icilin and PSA, highlighting a synergistic action of these compounds on cell migration inhibition (Gkika et al. 2010). Interestingly, this could be the second mechanism through which PSA exerts its anti-angiogenic properties on PCa beyond the well-known conversion of Lys-plasminogen to biologically active angiostatin-like fragments (Heidtmann et al. 1999). Indeed, the PSA-mediated activation of TRPM8 could sustain dormancy of prostatic hyperplasia by reducing its mobility and possible migration and the gradual loss of TRPM8 during tumor progression to a late stage is in line with this assumption. Furthermore, the gradual loss of the $TRPM8_{PM}$ during tumor progression may be an adaptive mechanism of PCa epithelial cells to reduce constant stimulation of the PSA/TRPM8 pathway (Gkika et al. 2010). TRPM8 trafficking to the PM and its subsequent impact on PCa cell migration have been proved to be also controlled by a family of TRP channel-associated factors (TCAF) (Gkika et al. 2015). TCAF co-localized with TRPM8 and interact directly with its N-terminal tail, although two different isoforms exert opposite regulatory effects on TRPM8 activity and function while both increasing TRPM8 expression on PM. Indeed, it has been shown that TCAF1 facilitates TRPM8 channel opening and subsequently contributes to the TRPM8-inhibition of PCa cells migration, whereas TCAF2 significantly increases the migration speed of

LNCaP by suppressing TRPM8 activity (Gkika et al. 2015). This difference is likely due to a PI3K domain present in the C-terminal tail of TCAF1 and absent in the TCAF2 sequence, which revealed a central role in mediating not the interaction with TRPM8 or its trafficking to the plasma membrane, but the TCAF1-mediated effects on cell migration. Consistently with the functional data, the expression levels of TCAF2 remain unchanged during PCa progression, whereas TCAF1 proteins display an expression pattern similar to TRPM8, being maximal in early-stage PCa tissue and minimal in aggressive metastatic tissue (Gkika et al. 2015). Therefore, TCAF1 can be considered a good candidate as a prognostic marker in prostate cancer as well as TRPM8, prostein, and PSA (Schmidt et al. 2006).

Regarding the molecular mechanism underlying the inhibitory effect of TRPM8 on PCa migration, it seems to involve the inactivation of FAK (Yang et al. 2009; Wang et al. 2012). By contrast, the short TRPM8 isoform α (sTRPM8 α) exhibited an opposite effect compared to the full-length TRPM8 isoform, revealing a role in promoting LNCaP cells migration and invasion through the activation of MMP-2 (Peng et al. 2015).

A recent study reinforced the applicability of TRPM8 as a pharmaceutical target to treat androgen-sensitive PCa, showing that in PCa cell-derived 3D models specific TRPM8 antagonists successfully revert the androgen-induced increase in cell spheroid size and significantly inhibit cell proliferation, migration, and invasiveness of androgen-dependent LNCaP cells (Di Donato et al. 2021). Taken together, all these data strongly support the potential use of TRPM8 as a “drugable” target in PCa treatment (**Chapter 1.4.3**).

1.3 TRP CHANNELS AND SMALL GTPases INTERPLAY IN THE MAIN HALLMARKS OF METASTATIC CANCER

Giorgia Chinigò[1,2], Alessandra Fiorio Pla[1,2] and Dimitra Gkika[2]*

[1] Laboratory of Cellular and Molecular Angiogenesis, University of Torino, Department of Life Sciences and Systems Biology, Torino, Italy
[2] Laboratoire de Cell Physiology, Université de Lille, Department of Life Sciences, Univ. Lille, Inserm, U1003 - PHYCEL - F-59000 Lille, France

*Corresponding author

Chinigò *et al.*, *Front. Pharmacol.* 2020, 11:581455

1.3.1 Introduction

Ca^{2+} signalling plays a central role in the regulation of many important cellular functions and indeed, not surprisingly, a deregulation of Ca^{2+} homeostasis has been observed in various pathological conditions, including tumorigenesis (Monteith, Prevarskaya, and Roberts-Thomson 2017). Changes in Ca^{2+} signalling leading to dysfunctions in cancer cells are due to alterations in the so-called "Ca^{2+}-signalling toolkit" (Berridge et al., 2003) which include, among others, ion channels, responsible for altered fluxes within the cell, and several Ca^{2+}-dependent effectors, which mediate various signal transduction pathways in response to altered Ca^{2+} homeostasis .

The involvement of Ca^{2+}-permeable channels in neoplastic disease has been extensively investigated in recent years and a direct correlation between their deregulation and cancer development has been shown (Monteith et al., 2017). Among them, Transient Receptor Potential (TRP) channels have revealed an important involvement in the regulation of many signalling pathways associated with tumor progression (Yang et al., 2020). One of the key features of TRP channels is their polymodal activation mechanism and their involvement in different signal transduction pathways. Among the multiple pathways TRPs are signalling through, the ones involving specific intracellular messengers belonging to the family of small guanosine triphosphatases (GTPases) are emerging as essential in tumorigenesis in the last decade. Therefore, in this review we will focus on TRPs-mediated pathways involving GTPases, whose role in the regulation of intracellular Ca^{2+} homeostasis associated with several aspects of the metastatic process has been well established (Aspenström et al., 2004; Clayton & Ridley, 2020).

Metastatic cascade, which lead to spread of malignant cells from the primary tumor through the lymph or blood circulation to establish secondary growth in a distant organ, is a multistep process involving highly complex structural and functional alterations within cancer cells. Primary tumor cells are primed for dissemination by the process of epithelial- mesenchymal transition (EMT), during which they assume a more aggressive mesenchymal-like phenotype. This phenotypic switch allows them to detach from the primary tumor mass and to acquire migratory and invasive properties, in order to move from their original location, migrate and invade the extracellular matrix (ECM) and endothelium to spread to secondary sites and form metastases (Roche 2018). All the steps involved in metastatic cascade (EMT, cell migration, invasion and tumor vascularization) are regulated by the intracellular Ca^{2+} concentration (Berridge et al., 2003) and specifically by the TRP-mediated calcium influx (Fels et al., 2018), as well as by the most important small GTPases (Rho-like and Ras-like) involved in cytoskeletal dynamics and cell polarity (Ungefroren et al., 2018). Here, we discuss TRPs and small GTPases contribution in cancer progression, focusing on signalling pathways

involving a direct interplay between TRPs and small GTPases in three main metastatic cancer hallmarks: migration, invasion and tumor vascularization.

TRP CHANNELS

TRP channels mainly act as signal transducers by altering membrane potential or intracellular Ca^{2+} concentration in response to various environmental stimuli**,** including physical-chemical stimuli, such as temperature, pH changes, tension, osmolarity, and pressure as well as endogenous and exogenous ligands (Bernd Nilius and Owsianik 2011). TRP channels have been shown to play a central role in carcinogenesis as well as in various late stages of tumor progression. In particular, it has been shown that changes in the expression of TRP channels is correlated with the progression of different types of cancers. To date, most changes involving TRP proteins do not involve mutations in the TRP gene but rather deregulation of the wild-type TRP protein expression levels, depending on the stage of the cancer (Lehen'kyi and Prevarskaya 2011; Gkika and Prevarskaya 2011; Bernardini et al. 2015; Shapovalov et al. 2016). Moreover, several recent studies have highlighted a direct correlation between cancer patient survival and TRP channel expression. Tumor differential expression of the main TRP channels discussed in this review and its correlation with patients' survival are summarized in **Table 6**.

		EXPRESSION				
CHANNEL	CANCER TYPE	HEALTHY/ BENIGN	TUMOUR	INVASIVE	PROGNOSIS	REFERENCES
TRPC1	Breast basal/ lymph nodes	Yes	↑	↑	poor	Azimi et al., 2017;
	Breast ductal adenocarcinoma	yes	↑			Dhennin-duthille et al., 2011
TRPC5	Colon	yes	↑	↑	poor	Chen et al., 2017a
TRPC6	Prostate	yes	↑	↑		Yue et al., 2009
	Glioblastoma	yes	↑	↑		Chigurupati et al., 2010
	Esophageal squamous cell carcinoma	yes	↑	↑	poor	Zhang et al., 2013
	Breast/ Invasive ductal adenocarcinoma	yes	↑			Guilbert et al., 2008; Dhennin-duthille et al., 2011
TRPM2	Breast	yes	↑	↑	Depends on subtype	Sumoza-Toledo et al., 2016
TRPM4	Prostate	yes	↑			Ashida et al., 2004; Singh et al., 2006

	Cervical	yes	↑			Narayan et al., 2007
TRPM7	Breast	yes	↑	↑	poor	Middelbeek et al., 2012; Meng et al., 2013
	Invasive ductal adenocarcinoma/ lymph nodes	yes	↑	↑		Guilbert et al., 2013; Dhennin-duthille et al., 2011
	Pancreatic ductal adenocarcinoma/ lymph nodes	yes	↑	↑	poor	Yee et al., 2015; Rybarczyk et al., 2012
	Nasopharyngeal	no	↑	↑	poor	Chen et al., 2015
	Ovarian; Prostate; Melanoma; Sarcoma			↑		Meng et al., 2013
TRPM8	Breast ductal adenocarcinoma	yes	↑	↑		Dhennin-duthille et al., 2011
	Prostate	yes	↑	loss		Tsavaler et al., 2001; Fuessel et al., 2003; Bidaux et al., 2005
	Urothelial carcinoma of bladder	yes	↑	↑	poor	Xiao et al., 2014
	Lung	Very low level	↑			Tsavaler et al., 2001
	Colon	no	↑			Tsavaler et al., 2001
	Melanoma	no	↑			Tsavaler et al., 2001
	Osteosarcoma	yes	↑	↑	poor	Zhao & Xu, 2016
TRPV2	Prostate	no		↑		Monet et al., 2010
	Bladder	yes (full isoform)	↑	↑		Caprodossi et al., 2008
		yes (short isoform)	↓	loss		
	Esophageal squamous cell carcinoma	yes	↑	↑	poor	Zhou et al., 2014
	Gastric	yes	↑	↑	poor	Zoppoli et al., 2019
	Breast (Triple negative/basal subtype)	yes	↑		better	Elbaz et al., 2018
TRPV4	Breast	yes	↑	↑	poor	Lee et al., 2016; Lee et al., 2017
	Gastric		↑		poor	Lee et al., 2016
	Ovarian		↑		poor	Lee et al., 2016
	Glioma	yes	↑	↑	poor	Ou-yang et al., 2018

Table 6. TRPs expression in cancer and correlation with patient survival prognosis.
Abbreviations: (↑) increment (↓) reduction

These observations strongly indicates that TRPs play a significant role in cancer progression and more specifically in many processes underlying the metastatic cascade, making them promising candidates as both molecular biomarker and therapeutic targets in various types of cancer (Litan and Langhans 2015; Fiorio Pla and Gkika 2013; Gkika and Prevarskaya 2011; Bernardini et al. 2015; Fels et al. 2018; Lastraioli et al. 2015). It has been shown that TRP-mediated effects on metastatic cancer cell behaviours are mainly associated to their Ca^{2+} permeability. Indeed, through the regulation of intracellular Ca^{2+} concentration, both in the cytosol and within subcellular organelles, TRP channels play a key role in many Ca^{2+}-dependent signalling pathways, including those associated with the metastatic cascade such as EMT, migration, invasion and tumor vascularization (Iamshanova et al. 2017). In response to different environmental challenges during the metastatic cascade, like hypoxic, acidic and mechanical cues, cancer cells "re-program" TRPs expression and "misuse" their functions in order to put in place and sustain a more aggressive, metastatic phenotype. However, although most of TRP-mediated pathways involved in cancer progression are due to alteration of Ca^{2+} homeostasis, it has been also demonstrated an involvement of these channels independent from their Ca^{2+} permeability. As an example, TRPM7 regulation on cell migration is mainly due to Mg^{2+} influx through the channel (Abed and Moreau 2009; Su et al. 2011). Similarly, the Na^{+}-selective TRPM4 channel, has been implicated in cancer migration, although it is inherently Ca^{2+}-impermeable (Vennekens and Nilius 2007; Holzmann et al. 2015; Cáceres et al. 2015). On the other hand, TRPs involvement in the metastatic cascade may also be pore-independent, extending the interest in TRPs beyond the field of ion channels (Vrenken et al. 2015). Indeed, TRPM7 promotes many of its biological effects through its peculiar intrinsic kinase activity (Faouzi et al. 2017; Cai et al. 2018; Desai et al. 2012). Moreover, we recently demonstrated the role of TRPM8 in inhibiting vascular endothelial cell migration which is independent from pore function of the channel (Genova et al. 2017).

It is therefore clear that, despite the innumerable progress made in recent years in the study of TRP channels, there are still many aspects to be explored in order to better characterize the main TRP-mediated pathways involved in tumor progression and thus be able to develop new cancer therapies using TRPs as therapeutic targets.

SMALL GTPases

The family of small GTPases is composed of a large group of structurally and functionally related proteins, subgrouped into six families: Ras, Rho, Arf, Rab, Ran and RGK. Among them Ras-like and Rho-like GTPases are the most well characterized. Mechanistically, small GTPases are molecular switches that cycle between an active GTP- bound form and an inactive GDP-bound form. More specifically, these enzymes, once bound GTP, are able to catalyze its hydrolysis to GDP and this reaction then results in a conformational change which

cause the inactivation of the proteins (Cherfils and Zeghouf 2013; Vetter and Wittinghofer 2001). The cycling between GTP- and GDP-bound stages is tightly regulated by specific GTPases activating protein (GAPs), which act as negative regulators, promoting the GDP-bound state by increasing several fold the hydrolysis activity of most members of the small GTPases, and by guanine exchange factors (GEFs), which act as positive regulators, guiding the replacement of the hydrolysed GDP for a GTP, thus promoting the enzyme active state (Mishra and Lambright 2016). Moreover, a third family of regulatory proteins called guanine-nucleotide dissociation inhibitors (GDIs) inhibit small GTPases activity by controlling their intracellular localization: GDIs bind to GTPases in their inactive GDP-bound state and sequester them in the cytosol, thus preventing their translocation to intracellular membranes, where activation occurs (Mishra and Lambright 2016). Indeed, it has been shown that spatial and temporal distributions of the different small GTPases, as well as of their regulators, are important determinants in signalling by small GTPases, determining many aspects of cell behaviour (Moissoglu and Schwartz, 2014; Yarwood et al., 2006; Cherfils and Zeghouf 2013).

The conformational changes following the binding to GTP allow the association of small GTPases with a large number of potential effector proteins such as enzymes and scaffold proteins, which mediate the specific biological effects of each GTPases. Thanks to their ability to interact with a wide number of downstream targets and to co-ordinately activate several molecular processes required for a particular cellular response, small GTPases function as signalling switches in numerous cellular processes. In general, it has been found that Ras-like GTPases are mainly implicated in regulating the cell cycle, differentiation and proliferation, (Shields et al., 2000), whereas Rho-like GTPases are mainly involved in cell morphology, cytoskeletal dynamics and cell polarity (Ridley 2001). Moreover, Rab GTPases play a key role in many cellular functions, by controlling intracellular trafficking between organelles through vesiculotubular carriers and thus ensuring the spatiotemporal regulation of vesicle traffic (Stenmark 2009). Considering the central role of Ca^{2+} signalling in many of these processes, it is not surprising that small GTPases activity was found to be strongly related with Ca^{2+} homeostasis (Aspenström 2004). More specifically, their activation/inactivation may be occur through Ca^{2+}-dependent mechanism acting on specific GEF/GAP proteins or directly on them. Moreover, some GTPases have revealed a direct influence on calcium signalling by regulating the activity of certain calcium channels, including TRPs, by itself or through their effectors (Aspenström 2004; Correll et al. 2008; Iftinca et al. 2007; Koopman et al. 2003). Finally, several small GTPases collaborate with calcium signalling through the activation of specific Ca^{2+}-related effectors involved in cellular processes, such as cell adhesion, cell migration and exocytosis (Aspenström 2004; Cullen and Lockyer 2002; Bader et al. 2004).

Small GTPases have been implicated in a variety of cancer-related dysfunctions and it has been shown that in some tumors their expression is deregulated and correlates with progression of disease (Svensmark and Brakebusch, 2019; Sahai and Marshall, 2002). Without a doubt, Ras is still the most small GTPase studied

in cancer, due to the role played by mutated ras genes in the pathogenesis of human tumors (Bos 1989; Hobbs et al. 2016; Li et al. 2018). Indeed, oncogenic mutations on H-ras, K-Ras and N-Ras genes have been detected in several tumor types, although the incidence varies greatly (Bos 1989; Prior et al. 2012; Li et al. 2018). Moreover, some members of the Ras superfamily like Rap1, play a key role in integrin-mediated "inside-out" signaling events and subsequently in cancer hallmark such as migration and angiogenesis (Boettner and Van Aelst, 2009; Chrzanowska-wodnicka et al., 2008; Carmona et al., 2009). As regards the Rho superfamily, instead, its role in many aspects of the metastatic cascade, including EMT, cell migration, invasion and angiogenesis, has been well established (Clayton and Ridley, 2020; Bryan and D'Amore, 2007; Ungefroren et al., 2018).

1.3.2 TRPs-SMALL GTPases INTERPLAY IN METASTATIC CANCER

Migration

One of the key step in the metastatic cascade involves the acquisition of motility by cancer cells. It results from a complex coordination between cytoskeleton dynamics, cellular contractility and cell adhesion rearrangements. Cell migration is a dynamic process characterized by the cycling of four principal steps: after an initial phase in which cell spreading increases about twice with the generation of protrusions at the leading edge and cell adhesion to the ECM increases, then spreading is reduced and thanks to the generation of traction forces cell compacts and detaches at the trailing edge, allowing for forward cellular movement (Haws et al., 2016). Due to their role as key regulators of cytoskeletal dynamics and cell polarity, it is not surprisingly that Rho GTPases play a central role in controlling cell migration (Clayton and Ridley 2020) This process is triggered by cell acquisition of a front-rear end polarity due to the formation of protrusive structures, called filopodia and lamellipodia, at the front edge, opposite to a retracting trailing edge (Llense and Etienne-Manneville 2015). Filopodia consist of actin filaments organized as long parallel bundles and their formation is dependent on Rho GTPase Cdc42 activity, whereas lamellipodia result from the subsequent Rho GTPase Rac1- mediated branching of actin filaments. The extension of actin-based protrusions is accompanied by the formation at the leading edge of new adhesions that link integrins on the plasma membrane to the F-actin cytoskeleton through talin, vinculin and focal adhesion kinases (FAKs) and which can mature into focal adhesions (FAs) in a process Rho GTPase RhoA- dependent. Contemporary, RhoA also mediates cytoskeletal rearrangements that lead to the formation of stress fibers, structures composed of bundles of actin and myosin II that have a high contractile capability. The force necessary to pull the cell body forward are engendered by the association of mature FAs with the end of stress fibers and by the actin-myosin

cytoskeleton contraction. Finally, disassembling of FAs in the rear of migrating cells support cell retraction at the trailing edge, allowing cell detachment and movement.

A direct involvement of TRP channels activity in all processes associated with cell migration, including cytoskeletal rearrangement, FA turnover and cellular contractility, has been well established (Canales et al. 2019; Fiorio Pla and Gkika 2013). Therefore, it is not surprisingly that several studies have highlighted a tight interplay between TRP channels and Rho GTPases in controlling cell migration during cancer progression. As depicted in **Figure 16**, this interplay is characterized by a bidirectional communication, in which TRP channels promotes actin cytoskeleton reorganization through a cation-dependent activation of Rho GTPases, and, conversely, some small GTPases cause changes in TRP channel location, protein–protein interactions and channel gating, thereby modulating their function. More specifically, as described in the following paragraphs, TRPC5, TRPC6, TRPC1, TRPM7, TRPM4 and TRPV4 have been found to affect cell migration through a direct interaction with some small GTPases belonging to the Rho family.

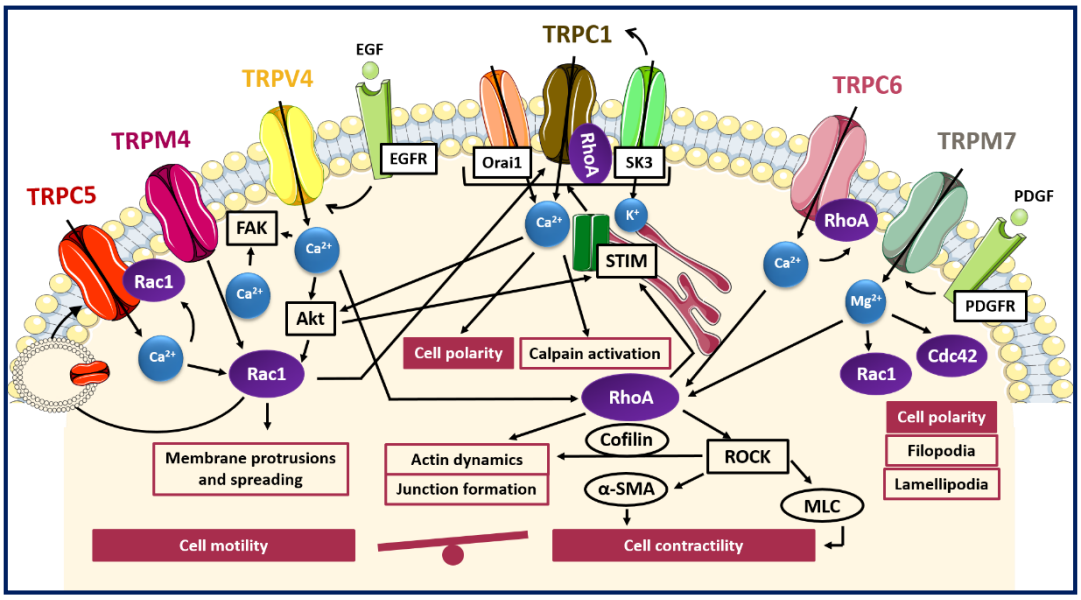

Figure 16. TRP-small GTPases signaling pathways interplay in cell migration.

Cartoon depicting TRP channels signaling pathways affecting cell motility and contractility through GTPases. TRPC5, TRPM4 and TRPV4 induce the formation of protrusions and spreading via Rac1 activation in a Ca^{2+}-dependent manner and at the same time Rac1 promote the translocation of TRPC5 into the plasma membrane; Rac1 and RhoA through SOCE activation induce TRPC1-mediated cell polarization for directional cell migration; TRPM7 control polarized cell movement through the regulation of Rac1 and Cdc42 in a Mg^{2+}-dependent way; TRPM7, TRPV4 and TRPC6 contribute to actin dynamics and cell contractility through the Mg^{2+}- or Ca^{2+}-mediated activation of RhoA/ROCK pathways.

Abbreviations: FAK = focal adhesion kinase, Akt = protein-kinase B, EGF = epidermal growth factor, EGFR = epidermal growth factor receptor, PDGF = platelet-derived growth factor, PDGFR = platelet-derived growth factor receptor, Orai1 = calcium release-activated calcium channel, SK3 = small

conductance calcium-activated potassium channel 3, STIM = stromal interaction molecule 1, ROCK = Rho-associated protein kinase, α-SMA = alfa-smooth muscle actin, MLC = myosin light chain.

Indeed, TRPC5 and TRPC6 channels have been identified as antagonist regulators of actin remodelling and cell motility in fibroblast and kidney podocytes, mediating the activation of Rac1 and RhoA, respectively (Tian et al. 2010). It has been shown that TRPC5 and TRPC6 triggered antagonistic and mutually inhibitory pathways associated with the maintenance of the balance between contractility and motility. In particular TRPC5-mediated Ca^{2+} influx induces Rac1 activation, thereby enhancing motility and cell migration. Conversely, TRPC6-mediated Ca^{2+} influx stimulates an increase in RhoA activation, thereby promoting stress fibre formation, cell contractility and the subsequent inhibition of cell migration (Tian et al. 2010) or the disruption of podocytes architecture in glomerular renal diseases, which may lead to proteinuria (Jiang, et al., 2011). Interestingly, the functional coupling between TRPC5 and TRPC6 with Rac1 and RhoA respectively, gives rise to two distinct molecular complexes predominantly localized to discrete membrane compartments, as detected by co-immunoprecipitation and immunofluorescence (Tian et al. 2010). Of note, the presence of constitutively active Rac1 has been shown to affect TRPC5 channel localization, leading to an increase in plasma membrane abundance of TRPC5 with respect to TRPC6, which, conversely, is predominant in cells expressing constitutively active RhoA. In this regard, RhoA seemed to have no effect on the dynamics of TRPC6 insertion into the membrane, whereas Rac1 was found to promote translocation of TRPC5 into the plasma membrane, according to other findings (Bezzerides et al. 2004). This close interdependence between TRPC5 and Rac1 could suggest a positive feedback mechanism in which the Rac1-mediated TRPC5 insertion from a vesicular pool into the cell membrane leads to enhanced TRPC5-mediated Ca^{2+} influx, which in turn triggers the activation of Rac1 and the subsequent migratory phenotype. Although a direct correlation between TRPC5/TRPC6 and Rac1/RhoA has not yet been established in cancer models, it is possible to speculate that a similar interplay may also occur in the regulation of cancer cells migration, taking into account evidences of a direct involvement of TRPC5 and TRPC6 in the increased migratory potential of several cell types (Rampino et al., 2007; Xu et al., 2006; Greka et al., 2003), including some tumors such as colon cancer and glioblastoma (Chen et al., 2017; Chigurupati et al., 2010). However, whether these effects on tumor migration are dependent on the impact of TRPC5 and TRPC6 activity on cell contractility and motility remains to be clarified.

Similarly, TRPC1 have shown a correlation with an increased migratory phenotype in some tumors, such as glioblastoma, osteosarcoma, thyroid, pancreatic and colon carcinoma (Lepannetier et al. 2016; Huang et al. 2015; Asghar et al. 2015; Dong et al. 2010; Guéguinou et al. 2016). One of the key step in cell migration is the establishment of a functional and morphological polarity along the axis of movement. In this context,

it has been demonstrated that TRPC1 is localized to lipid raft domains at the leading edge of migrating cells and plays a role in determining their polarity and directionality (Fabian et al. 2008; Bomben et al. 2011; Huang et al. 2015). For instance, it has been shown that in transformed renal epithelial Madin–Darby Canine Kidney-Focus (MDCK-F) cells the silencing of TRPC1 lead to a decrease in migration associated with a failure of cell polarization and an impaired lamellipodia formation. This effect is due to the partial loss of the local Ca^{2+} gradient at the front edge, needed for establish and maintain the axis of movement in migrating cells (Fabian et al. 2008). Same findings have also been shown in U2OS bone osteosarcoma cells, in which TRPC1 inhibition or knowndown lead to a decrease in the percentage of polarized cells and the subsequent reduction in cell migration (Huang et al. 2015). However, the link between TRPC1-mediated Ca^{2+} gradients and actin dynamics, as well as the possible involvement of TRPC1-mediated Rho GTPases activation in these processes has not been yet fully characterized. Nonetheless, a direct interaction between TRPC1 and RhoA has been characterized in intestinal epithelial cells (IECs) and in pulmonary arterial endothelial cells (Chung et al. 2015; Mehta et al. 2003). It has been shown that in IECs RhoA physically interacts with and regulates TRPC1-mediated Ca^{2+} influx through SOCE, stimulating cell migration after wounding (Chung et al. 2015). A reduction of RhoA/TRPC1 complexes, induced by downregulation or inactivation of either small GTPase or TRP channel, is associated with an inhibition of Ca^{2+} influx after store depletion and the subsequent obstruction to reseal superficial wounds after injury (Chung et al. 2015). Furthermore, it has been recently proposed a mechanism involving TRPC1 and Rac1 in promoting SOCE-dependent colon cancer cells migration (Guéguinou et al. 2016). Indeed, in HCT-116 colon cancer cells TRPC1 and Rac1 are involved in a complex positive feedback loop in which EGF-induced SOCE activates both Rac1 and STIM1 through Akt pathway; in turn, STIM1 activation promotes translocation of TRPC1 and Orai1 into lipid rafts where SK3 is located and thereby triggers SOCE mediated by the complex SK3/TRPC1/Orai1. At the same time Akt-mediated Rac1 activation enhances SOCE and thereby SOCE-dependent cell migration through Akt pathway, with subsequent lamellipodia formation and calpain activation. Taken together these data suggest a direct interplay between TRPC1 and Rho GTPases in controlling cell polarity and actin rearrangements during cancer cells migration.

TRPM7 is involved in directional migration in different cell types including migrating fibroblasts, osteoblasts, astrocytes and endothelial cells (ECs) (Wei et al. 2009; Abed and Moreau 2009; Zeng et al. 2015; Baldoli et al. 2013) . Similarly to TRPC1 also TRPM7 has been shown to be involved in Ca^{2+} gradient formation contributing to cell polarization and directional migration (Wei et al. 2009). In particular, TRPM7 is positively correlated with platelet-derived growth factor (PDGF)-induced Mg^{2+} influx as well as high-calcium microdomains "Ca^{2+} flickers", most active at the leading lamella of migrating cells (Wei et al. 2009; Abed and Moreau 2009). Interestingly, several evidences have shown that TRPM7 effects in controlling cytoskeleton

and polarized cell movements are independent from its kinase activity and are associated with its channel function. This has been clearly demonstrated in fibroblasts and neuroblastoma cells where re-expression of TRPM7 as well as a kinase-inactive mutant of TRPM7 on knock out cells reverted phenotypic changes in cell polarization enhancing cell spreading and adhesion (Su et al. 2011; Clark et al. 2008). In particular, it has been shown that Mg^{2+} play a central role in TRPM7-mediated control of directional migration in fibroblasts and osteoblasts (Su et al. 2011; Abed and Moreau 2009). The effects observed by TRPM7 depletion in cell morphology, disruption of actin filaments and myosin fibres and a decrease in the number of FAs, correlates with decreased activity of RhoA GTPase, suggesting a role for TRPM7 in RhoA regulation (Su et al. 2011). Beside its interaction with RhoA, TRPM7 is also functional coupled with Rac1 and Cdc42: indeed, TRPM7 knockdown prevented Rac1 and Cdc42 activation, with subsequent deficiency in their ability to form lamellipodia and impaired polarized cell movements (Su et al. 2011). Although Rho GTPases, differing from Ras and Rab proteins, did not require Mg^{2+} for high affinity nucleotide binding, it has been shown that Mg^{2+} plays a role in regulating nucleotide binding and hydrolysis kinetics in the GEF- and GAP-catalyzed reactions of Rho family GTPases (Zhang et al. 2000). In particular, RhoGAPs exploit Mg^{2+} to achieve high catalytic efficiency and specificity and conversely, RhoGEFs result negatively regulated by free Mg^{2+}, since the presence of Mg^{2+} significantly decrease the intrinsic dissociation rates of the nucleotides. This finding may suggest that one role of GEFs is to displace bound Mg^{2+} from Rho proteins in order to efficiently perform their function and dissociate nucleotide from Rho GTPases (Zhang et al. 2000). Taken together this data revealed an interesting and so far little investigated interplay between TRP channel and Rho GTPases in controlling cell migration mediated by Mg^{2+} homeostasis.

More recently, another member of the TRPM subfamily, TRPM4, has been recognized as the first TRP channel to be part of the adhesome that is the set of protein components of FAs required for migration and contractility (Cáceres et al. 2015). Indeed, it has been shown that TRPM4 localized to FAs in different cell types and that its suppression impaired FAs relocation and lamellipodia formation, leading to a reduced cellular spreading and migration in mouse embryonic fibroblasts. Actually, FA turnover plays a key role in cell migration, contributing to the generation of the traction forces necessary for cellular movements. TRPM4-mediated effects on cell migration are at least partially due, to the activation of Rac1 GTPase. Indeed, it has been observed that upon silencing TRPM4 the serum-induced activation of Rac1 was significantly reduced as well as lamellipodial distribution, suggesting a direct cooperation between TRPM4 and Rac1 in the regulation of cellular spreading. Moreover, it has been demonstrated that TRPM4 pharmacological inhibition caused a retarded skin wound healing *in vivo,* affecting cell contractility (Cáceres et al. 2015). TRPM4 has been found to affect the migratory behaviour of many cell types, including prostate cancer cells (Holzmann et al. 2015). Although TRPM4 itself is Ca^{2+}-impermeable, its contribution to cell migration through the regulation of

intracellular Ca^{2+} signalling has been well established (Vennekens and Nilius 2007). For instance, in androgen-insensitive prostate cancer cells it has been shown that TRPM4 acts as an important negative feedback regulator of SOCE, thus promoting cell migration (Holzmann et al. 2015). However, further investigations are needed to deepen the knowledge of the molecular mechanism underlying the pro-migratory effect of TRPM4 on prostate cancer cells migration.

To date, several experimental evidences have revealed a critical role of TRPV4 in regulating migratory properties of many tumors, including liver, breast and gastric cancer (Vriens et al. 2004; Lee et al. 2016; Xie et al. 2017). However, little is known about the molecular nature of this process. Nonetheless, it has been shown that TRPV4 is involved in the dynamics of trailing adhesions, likely through an interplay with other cation channels or proteins present at the FA sites (Mrkonjić et al. 2015). A direct correlation between TRPV4 and RhoA/ROCK pathways has been revealed in cardiac fibroblast remodeling and myofibroblast contraction. In particular, it has been shown that after stimulation with growth factors, TRPV4 contributed to cell contractility by increasing the actin protein α-SMA expression and incorporation into stress fibers, through the Ca^{2+}-mediated activation of RhoA/ROCK pathways (Adapala et al. 2013; Thodeti et al., 2013; Tomasek et al. 2006). Another study reported a role of TRPV4 in the modulation of adherent-junctions, mediated by the TRPV4-dependent activation of Rho GTPases, thereby promoting actin fibers organization and junctions formation (Sokabe and Tominaga 2010). Furthermore, the exogenous up-regulation of TRPV4 in breast cancer has been shown to aid actin dynamics and lead to a higher activation of cofilin, a downstream protein effector of RhoA/ROCK pathways that promotes actin filaments depolymerisation, thus conferring cellular "softness" and promoting transendothelial migration (Lee et al. 2016). Accordingly, TRPV4 knockdown reduced migration, invasion and transendothelial migration in breast cancer cells (Lee et al. 2016). Finally, a recent study of Ou-yang and co-worker (2018) has described the Akt/Rac1 signalling pathway through which TRPV4 promote migration and invasion in glioma cancer cells (Ou-yang et al., 2018). Mechanistically, agonist-mediated TRPV4 activation promoted the activation of Rac1 by targeting Akt for phosphorylation, thus enhancing glioma cells migration and invasion (Ou-yang et al. 2018). Accordingly, in gastric cancer TRPV4-mediated Ca^{2+} influx promote cell migration through the activation of the downstream Akt/β-catenin pathways (Xie et al. 2017). Collectively, these data support a direct interplay between TRPV4 and small GTPases in controlling cytoskeletal remolding aimed to confer migratory phenotypes.

Invasion

In order to reach lymph- and bloodstreams and to colonize sites distant from the primary tumor, cancer cells have to acquire, beyond migratory phenotype, the ability to degrade ECM. Consequently, invasion is another key step of the metastatic cascade. Invasiveness of cancer cells comes from their ability to produce

special protusions called invadopodia, which are actin-rich protrusions of the plasma membrane with proteolytic activity. Once matured, invadopodia recruit proteolytic enzymes such as membrane-matrix metalloproteinases (MMPs), which are endopeptidases able to locally degrade ECM, allowing cell invasion. Among them, MMP-2 and MMP-9 were considered the most important in metastasis, since they were often aberrantly expressed in tumors (Jabłońska-trypuć et al., 2016). Both TRP channels and small GTPases have been implicated in increased tumor invasiveness through the induction of MMPs expression (Yang and Kim 2020; Betson and Braga 2003). Indeed, TRPM2, TRPM7, TRPM8, TRPV2 and TRPC1 have shown to cause upregulation of MMP9 in a Ca^{2+}-dependent manner in gastric, bladder, oral squamous, prostate and thyroid cancer cells respectively (Almasi et al. 2019; Cao et al. 2016; Chen et al. 2017; Okamoto et al. 2012; Monet et al. 2010; Asghar et al. 2015). Additionally, TRPM2, TRPM7 and TRPC1 activity have been also correlated with MMP2 production in gastric, lung, pancreatic and thyroid cancer (Almasi et al. 2019; Liu et al. 2018; Rybarczyk et al. 2017; Asghar et al. 2015). Also Rho and Rac GTPases activation has been correlated with increased MMPs expression in different cancer cell types (Abécassis et al.,2003; Santibáñez et al. 2010; Jacob et al. 2013; Zhuge and Xu 2001). TRPV2 and TRPM2 have been shown to affect cell invasiveness through signalling pathways involving small GTPases, which are summarized in **Figure 17**.

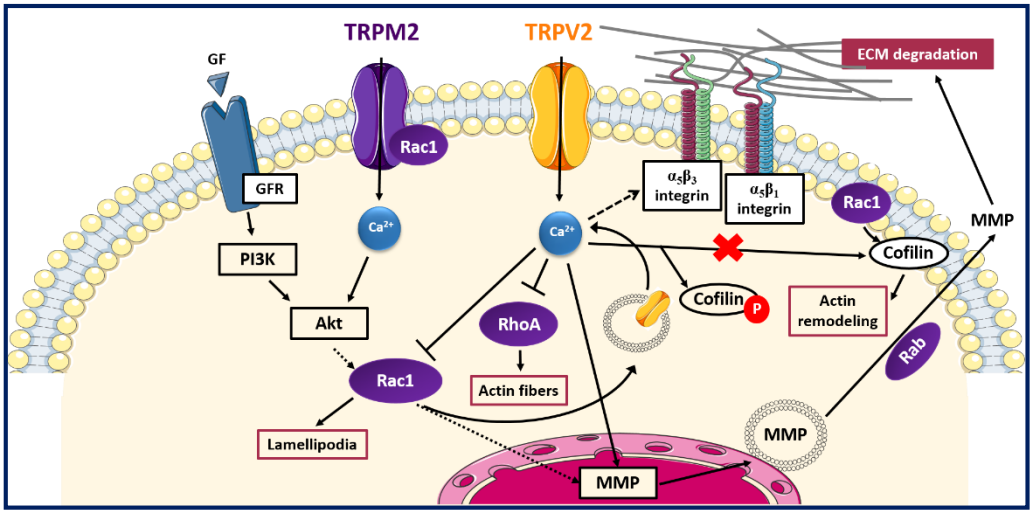

Figure 17. TRP-small GTPases signaling pathways interplay in cell invasion

Cartoon depicting TRP channels signaling pathways affecting cell invasiveness through GTPases. Rac1 promotes the translocation of TRPV2 into the plasma membrane and thus TRPV2-mediated increased in MMPs expression; TRPV2 affects also cell adhesion and invasion interfering with integrin-mediated signalling and inhibiting Rac1, RhoA and cofilin activation by Rac1 in a Ca^{2+}-dependent manner; TRPM2 and Rac1 physically interact with each other, mutually influencing their activity and lead to an increase in MMPs production; MMPs exocytosis is mediated by the Rab superfamily of small GTPases.

Abbreviations: GF = growth factor, GFR = growth factor receptor, PI3K = phosphoinositide-3 kinase, Akt = protein-kinase B, MMP = membrane-matrix metalloproteinase, ECM = extracellular matrix

TRPV2 has been found to positively correlate with prostate cancer (PCa) invasiveness, promoting PCa progression to the aggressive castration-resistant stage (Monet et al. 2010). More specifically, it has been shown that siRNA-mediated silencing of TRPV2 lead to a decrease in MMP-2 and MMP-9 invasive enzymes expression, reducing growth and invasive properties of PC3 prostate tumors established in nude mice xenografts (Monet et al. 2010). The mechanism by which the Ca^{2+} influx mediated by TRPV2 is linked with the up-regulation of MMPs has not been characterized. However, another study have revealed that in PCa TRPV2 trafficking to the plasma membrane, correlated with enhanced cell migration and invasion, is mediated by the phosphoinositide 3-kinase (PI3K) pathway (Oulidi et al. 2013). Taking into account evidences of a PI3K-mediated activation of Rac1 in several tumor models (Haws et al., 2016; Ungefroren et al., 2018) and considering that Rac1 has been found to regulate TRPV2 intracellular trafficking in fibrosarcoma cells (Nagasawa and Kojima 2015), it is possible speculated that in PCa a PI3K-mediated Rac1 activation may allow the translocation to the plasma membrane of the "*de novo*" expressed TRPV2 in PC3 cells, thus giving rise of the TRPV2-mediated increase of cytosolic Ca^{2+} concentration responsible for MMPs overexpression. Confirming this hypothesis, Rac1 have been related with the up-regulation of MMP-2 and MMP-9 in fibrosarcoma (Zhuge and Xu 2001) and transformed keratinocytes (Santibáñez et al. 2010), respectively. Unlike in PCa, TRPV2 has been found to suppress invasiveness of fibroblast-like synoviocytes (FLS), which have an aggressive and invasive behaviour resembling that of cancer cells (Laragione et al. 2015). TRPV2 activation have been associated both *in vitro* and *in vivo* with a reduced cell invasiveness and a down-regulation of the IL-1β-induced expression of MMP-2 and MMP-3 (Laragione et al. 2015). More recently, the cell signalling events mediating this TRPV2 suppressive activity has been characterized (Laragione et al., 2019). Interestingly, a direct interplay between TRPV2 channel function and RhoA/Rac1 GTPases activity in suppressing FLS cells invasion have been proposed (Laragione et al., 2019). In particular, it has been shown that, upon stimulation with the commercially-available TRPV2-specific agonist O1821, the channel nearly disappeared from the plasma membrane, as well as integrins αv, β1 and β3, involved in cell binding to ECM. Concomitantly, a decrease in cell adhesion and in the numbers of thick actin filament and a reduction in lamellipodia formation were observed. Mechanistically, it has been found that O1821-induced TRPV2 activation caused a decrease in both RhoA and Rac1 activation, giving rise of the observed inhibition of actin filaments and lamellipodia formation respectively. Moreover, TRPV2 activation significantly increased levels of phosphorylated (inactive) cofilin and affected the localization of active cofilin keeping it in the cytosol away

from cell protrusions and lamellipodia, in which normally it exerts its function on actin remodelling, upon activation by Rac1. Considering the active involvement of Rac1 in TRPV2 trafficking found by Nagasawa *et al*. (2015), the Rac1 inhibition through TRPV2 described by Larangione *et al*. might also explained the observed reduction of TRPV2 expression on the plasma membrane after channel stimulation, suggesting an intriguing negative feedback loop between TRPV2 and Rac1 regulation. Indeed, TRPV2 activation on the plasma membrane may inhibit in a Ca^{2+}-dependent manner Rac1 activation, which in turn resulted in a decrease of TRPV2 expression on the cell surface. Taken together, these data account for a possible two-sided interplay between Rac1 and TRPV2, based on which TRPV2 may exert both pro- and anti-invasiveness activities depending on cell type. In the first case Rac1 is activated by IP3K pathway, thus allowing the overexpression of the constitutively active TRPV2 on the plasma membrane and the increased calcium flow responsible for MMPs overexpression and the increased cell invasiveness; in the second case TRPV2, upon activation by external stimuli, causes Rac1 inactivation and the inhibition of pro-invasive intracellular pathways as well as the expression of TRPV2 in the membrane through a negative feedback mechanism. Therefore, in an interesting interchangeable relationship TRPV2 may act as either modulator or effector of Rac1, depending on cell type, thus reflecting the bivalent activity showed by the channel in cell invasiveness.

In addition to TRPV2, TRPM2 offers another potential field of investigation on TRP-small GTPase relationship in cancer cells ability to invade surrounding tissues. In fact, it has been recently proven that TRPM2 caused an increase in MMP-9 production in gastric cancer (Almasi et al. 2019). Also in this case, the function of the channel appeared to be regulated by the Akt pathway, known to regulate the activity of several GTPases including Rac1 (Ho et al., 2010), whose interaction with TRPM2 has been already well established in response to oxidative stress (Gao et al. 2014). On this regard, it has been demonstrated that TRPM2 and Rac1 physically interact with each other, mutually influencing their activity, similarly to what observed between TRPC5 and Rac1 in podocytes previously described (Tian et al. 2010; Bezzerides et al. 2004). Thus, we could speculate a TRPM2-Akt-Rac1 axis in the modulation of MMP-9 expression in gastric cancer.

Tumor vascularization

Tumor vascularization, is a critical step in the metastatic cascade, since the formation of new blood vessels is crucial not only to provide sufficient oxygen and nutrients and thus promoting the continuous growth of tumors but also to drive tumor spread and metastasis. Tumor vascularization, promoted by the tumor cells themselves through the secretion of several growth factors, results aberrant and leads to the formation of new vessels characterized by abnormal morphology, irregular blood flow and distribution, non-uniform pericyte coverage and hyper-permeability. TRP channels are widely expressed within vascular ECs and several

evidences correlated aberrant TRP channels expression and/or activity with tumor vascularization, thanks to their high sensitivity to both pro-angiogenic signals and subtle changes in local microenvironment (Negri et al., 2020; Brossa et al. 2019). TRP channels have been related to critical steps of tumor vascularization, including cell adhesion, cell migration, enhanced permeability and *in vitro* angiogenesis (Fiorio Pla and Gkika 2013). Similarly, several Rho and Ras small GTPases, thanks to their contribution to actin dynamics, cell contractility and integrin-mediated "inside-out" signalling events, have been found to be de-regulated during tumor vascularization (Chrzanowska-Wodnicka 2010; Carmona et al. 2009). Some common pathways involving both TRP channels and small GTPases in determining aberrant tumor vascularization have been described, such as those concerning TRPV4, TRPM8, TRPC1 and TRPC6, depicted in **Figure 18**.

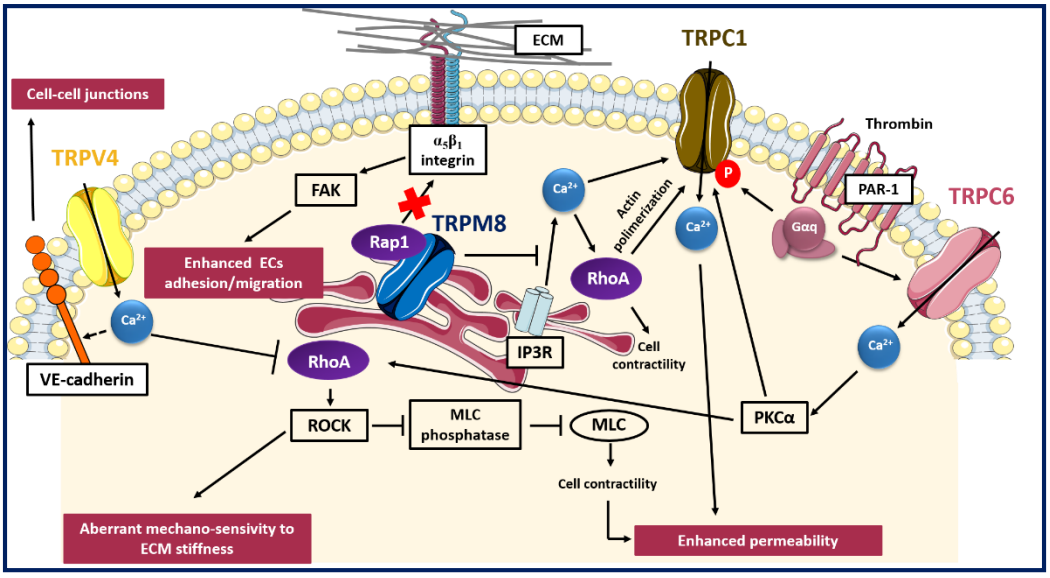

Figure 18. TRP- small GTPases signaling pathways interplay in aberrant tumour vascularization

Cartoon depicting TRP channels signaling pathways affecting tumour vascularization through GTPases. TRPV4 induces aberrant mechano-sensivity to ECM through the Ca^{2+}-dependent inhibition of Rho/ROCK pathway; TRPC1 and TRPC6 enhance vessels permeability affecting cell contractility through a Ca^{2+}-mediated regulation of RhoA; on the contrary, TRPM8 exerts a protective role in tumour vasculature permeability, inhibiting the store-operated RhoA activation and subsequent cell contraction; TRPM8 also inhibits ECs adhesion and migration, impairing activation of β1-integrin through the intracellular retention of Rap1.

Abbreviations: VE-cadherin = vascular E-cadherin, FAK = focal adhesion kinase, ROCK = Rho-associated protein kinase, MLC = myosin light chain, PKCα = protein kinase C alpha, IP3R = inositol trisphosphate receptor, PAR-1 = protease-activated receptor-1

TRPV4 has been the first TRP channel to be clearly implicated in tumor angiogenesis, although it can have both pro-angiogenic and anti-angiogenic effects depending on tumor type. In particular, TRPV4-mediated Ca^{2+} signals are implicated in tumor-derived endothelial cells (TECs) migration via a membrane stretch activated arachidonic acid release and subsequent actin remodelling and TRPV4 insertion in plasma

membrane (Fiorio Pla et al. 2012). These data are in accordance with previous results showing that TRPV4 is required for shear stress EC reorientation in an integrin dependent manner (Thodeti et al. 2009). On the other hand, in different TECs models TRPV4 resulted down-regulated as compared to normal tissues and this is correlated with aberrant mechano-sensitivity of TECs towards ECM stiffness and subsequently with enhanced cell motility and abnormal angiogenesis. The subcutaneously injection of Lewis Lung Carcinoma cells in TRPV4 knockout mice lead to increased vascular density, higher vessel diameter and reduced pericyte coverage, overall resulting in enhanced tumor growth (Adapala et al. 2016). More recently, it has also been shown by the same group that TRPV4 silencing caused a significant decrease in VE-cadherin expression at cell-to-cell junctions, with the subsequent increase in vascular leakage (Cappelli et al. 2019). Accordingly overexpression or pharmacological stimulation of TRPV4 with GSK has been shown to lead to a "normalization" of the vascular endothelium, enhancing the permeability of chemotherapeutic drugs, and basically blocking tumor growth (Adapala et al. 2016). In particular, TRPV4-mediated "normalization" of aberrant capillary-like tubules *in vitro* is achieved by restoring the mechano-sensitivity of ECs toward ECM stiffness through the blockade of basal Rho activity (Adapala et al. 2016). In this contest, it was previously shown that the aberrant TECs mechano-sensitivity of TECs in response to ECM stiffness and cyclic strain resulted, at least partially, due to constitutively high level of Rho/ROCK basal activities (Ghosh et al. 2008). TRPV4 overexpression or activation was able to significantly reduce the high basal Rho activity exhibited by prostate TECs (Adapala et al. 2016). Moreover, ECs isolated from TRPV4 knockout (KO) mice displayed higher basal Rho activity as compared to EC wt and the inhibition of Rho/ROCK pathway in TRPV4KO mice resulted able to normalize tumor vasculature, confirming the role of TRPV4 as an important modulator of Rho activity also *in vivo* (Thoppil et al. 2016).

Accordingly with other recent evidences which have highlighted non-conducting functions of TRP channels in many processes, including the regulation of cytoskeletal dynamics (Vrenken et al., 2015), our recent study (Genova et al. 2017) has unveiled that TRPM8 may inhibit ECs migration in a Ca^{2+}-independent manner. TRPM8 mainly localized close to the endoplasmatic reticulum (ER) in ECs and its expression resulted remarkably down-regulated in breast TECs (BTECs) with respect to human microvascular ECs (HMECs) and human umbilical vein ECs (HUVECs) (Genova et al. 2017). In normal ECs TRPM8 has been shown to inhibit migration and spheroid sprouting by trapping Rap1 intracellularly, thereby preventing its relocation toward the plasma membrane, which is required to activate β_1-integrin signalling. Rap1 physically interacts in its inactive form (GDP- bound) mainly with the N-terminal tail of TRPM8 and interestingly, its retention within the cytosol occurred also in the presence of a TRPM8 pore mutant, demonstrating that TRPM8 inhibitory effects on ECs migration and adhesion by trapping Rap1 are independent from its channel function (Genova et al. 2017). Curiously, TRPM8 activation through specific channel agonists (icilin and menthol) or

endogenous activators such as prostate specific antigen (PSA), significantly reduced the amount of active Rap1-GTP bound and enhanced its inhibitory effect on migration, thus raising questions about the possible effects of agonists on TRPM8 besides pore gating. The TRPM8-mediated prevention of Rap1 cytoplasm–plasma membrane trafficking impaired the activation of a major inside-out signalling pathway known to trigger the conformational activation of β_1-integrin and, consequently, cell adhesion and migration. In particular, TRPM8 has been found to modulate ECs adhesion to fibronectin (FN) through the inactivation of $\alpha_5\beta_1$ integrin, one of the major FN receptor. Coherently, upon stimulation with icilin TRPM8 significantly inhibited active-β_1 integrins as revealed by immunofluorescence assays. In addition, it has been proven that agonist-induced TRPM8 stimulation lead to a significant decrease in FAK autophopshorylation, suggesting the involvement of FAK as downstream effector of the β_1-integrin pathway affected by TRPM8 (Genova et al. 2017). This study have highlighted how TRP channels may regulate GTPases activity not only by the generation of local Ca^{2+} fluxes, but also acting as a GDI-like protein, so through physical interactions which affect their intracellular localization and thus their activity. Indeed, as well as TRP channels, also small GTPases are used for spatial and temporal control of cell behaviour, as reported by several studies (Wang et al., 2012; Moissoglu and Schwartz, 2014; Yarwood et al, 2006). Another evidence of a TRPM8 interplay with small GTPases in controlling ECs behaviour comes from a study of Sun and coworkers (2014), which have revealed a role of TRPM8 in vasoconstriction and hypertension through attenuating RhoA/Rho kinase pathway. In particular, the authors have shown that TRPM8 activation by menthol attenuated vasoconstriction by inhibiting RhoA/ROCK pathway in wild-type mice, but not in TRPM8KO mice (Sun et al. 2014) . TRPM8 effect was associated with inhibition of intracellular calcium release from the sarcoplasmic reticulum, thus reducing Ca^{2+}-mediated activation of RhoA/ROCK and ECs contraction. Since several evidences have correlated ECs contraction with vessels permeability (Hicks et al. 2010), this study could suggest a protective role of TRPM8 not only in ECs migration, but also in tumor vasculature permeability.

The increased permeability shown by tumor vessels may be induced by several factors, including hypoxia and inflammatory signals, such as thrombin. In this regard, TRPC6 and TRPC1 has been implicated in thrombin-induced hyper-permeabilization of ECs through RhoA/ROCK signalling pathway. Thrombin is a serine-protease which after binding to the endothelial cell surface protease-activated receptor-1 (PAR-1) induces a signalling cascade resulting in an increase in ECs contraction, changes in cell shape and ultimately the development of tiny inter-endothelial junctional gaps that lead to increased endothelial permeability. It has been shown that thrombin, through the α subunit of G protein-coupled receptors ($G\alpha_q$) signals TRPC6 activation (Singh et al., 2007). Then, the TRPC6-mediated Ca^{2+} influx lead to the activation of PKCα and thereby induced RhoA activity and ECs contraction, with subsequent cell shape changes and inter-endothelial gaps formation (Singh et al., 2007). Indeed, upon thrombin stimulation it has been shown that RhoA activated

its downstream effector ROCK, which in turn stimulated the phosphorylation of the myosin light chain (MLC) phosphatase regulatory subunit, which reduced the phosphatase activity (Birukova et al. 2004). Such an attenuation of dephosphorylation of MLC resulted in a net increase in phosphorylated MLC, thus sustaining ECs contraction (Birukova et al. 2004). TRPC6 have also been found to play a central role in determining the angiogenic potential of glioma cells, since its inhibition affected EC tube formation *in vitro* by reducing the number of branch points (Chigurupati et al. 2010). Moreover, TRPC6 has been shown to exert pro-angiogenic effects by affecting vascular endothelial growth factor (VEGF)-induced calcium influx in ECs. Indeed, expression of a dominant negative TRPC6 significantly reduced ECs number, migration and sprouting (Hamdollah Zadeh et al., 2008). Interestingly, TRPC6 promoted proliferation and tubulogenesis induced by VEGF, but not by basic fibroblast growth factor (bFGF), in HUVECs (Ge et al. 2009). Although to date there are not evidences of GTPases-mediated TRPC6 functions in angiogenesis, some studies have defined an important role of RhoA in ECs proliferation, migration, invasion and sprouting triggered by important angiogenesis inducers, including VEGF (Zahra et al. 2019), thus suggesting a possible interplay between TRPC6 and RhoA in VEGF-induced angiogenesis.

As well as TRPC6, also TRPC1 has been found to have a role in increasing ECs permeability through RhoA activation in response to thrombin stimulation. In this regard, an intriguing mechanism depicting RhoA as TRPC1 modulator in human pulmonary arterial endothelial cells have been proposed by Mehta and co-worker (2003). They showed that RhoA, upon thrombin-induced activation, formed a complex with IP_3R and TRPC1, which then translocated to the plasma membrane, where TRPC1 can mediate a store depletion-induced Ca^{2+} entry and the resultant increase in endothelial permeability. Moreover, it has been demonstrated that RhoA-induced association of TRPC1 with IP_3R was dependent on actin filament polymerization, since its inhibition hindered both association and Ca^{2+} entry (Mehta et al. 2003). It has been shown that also the serine/threonine phosphorylation of TRPC1 by PKCα is crucial in inducing Ca^{2+} influx, since PKCα inhibition significantly reduced Ca^{2+} entry and hindered the increase in endothelial permeability (Ahmmed et al. 2004). However, the mechanism by with PKCα integrated with RhoA in ECs to trigger TRPC1-mediated Ca^{2+} influx remained to be characterized. Nonetheless, considering the previously described role of PKCα as a downstream effector of TRPC6 (Singh et al., 2007), it is possible that the PKCα- dependent RhoA-induced TRPC1 activation gives rise to a positive feedback loop that overall lead to persistent increase endothelial permeability. This study provide an examples of pathway in which small GTPases do not act as TRP Ca^{2+}-dependent effectors, but rather as modulators of TRP channel activity, influencing protein–protein interactions and channel gating, and thus corroborating the bidirectional nature of this complex interplay.

1.3.3 Conclusions and perspectives

TRPs and small GTPases show a direct interplay in cancer progression, characterized by a bidirectional communication, whereby TRP channels have been shown to affect small GTPases activity *via* both Ca^{2+}-dependent or Ca^{2+}–independent pathways, and conversely some small GTPases may affect TRP channels activity through the regulation of their intracellular trafficking to the plasma membrane or acting directly on channel gating (**Table 7**). In most cases TRP-GTPase interaction is mediated by Ca^{2+} signals, triggered by TRP-mediated Ca^{2+} influx through the plasma membrane induced by growth factors, specific ligands or mechanical stimuli. In some specific cases, like that of TRPM7, the TRP-mediated small GTPases activation/inhibition may be supported by Mg^{2+} rather than Ca^{2+} homeostasis regulation. Moreover, also Ca^{2+}-impermeable TRP channels like TRPM4 has been found to regulated small GTPases activity, probably through an indirect control on other Ca^{2+}-signalling pathways. Finally, alternative regulatory pathway which go beyond the canonical ones involving cation homeostasis have been characterized for TRP-mediated small GTPases regulation. For instance, it has been shown that some TRPs, such as TRPM8 in ECs, may act similarly to a GDI-like protein, inhibiting small GTPases activity by physically trapping and restraining them within a specific cellular compartments and thus preventing their switch to the active form that generally occurs at the plasma membrane. Although in most cases small GTPases act as TRP effectors, there are some evidences about a role of small GTPases as modulators of TRP channel activity. Indeed, it has been shown that some small GTPases may affect TRPs channel activity by influencing channel trafficking, gene expression, protein–protein interactions and channel gating. In some cases, positive feedback loop mechanisms, wherein TRP channels activate small GTPases which in turn increase TRPs insertion to the plasma membrane, have also been described. In addition, some studies have highlighted that effector/modulator roles may be interchangeable between TRPs and small GTPases depending on cell type. For instance, it has been shown that Rac1 may act as either modulator or effector of TRPV2 activity, thus determining opposite effects on cell invasion, depending on cell type.

HALLMARK	TRP CHANNEL		GTPase	BIOLOGICAL EFFECT	REFERENCE
Migration	TRPC1	Ca^{2+} ←	RhoA	↑	(Chung et al. 2015; Mehta et al. 2003)
		Ca^{2+} ↔	Rac1	↑	(Guéguinou et al. 2016)

	TRPC5	Ca^{2+} ↔	Rac1	↑	(Tian et al. 2010; Bezzerides et al. 2004)
	TRPC6	Ca^{2+} →	RhoA	↓	(Tian et al. 2010)
	TRPM4		Rac1	↑	(Cáceres et al. 2015)
	TRPM7	Mg^{2+} →	RhoA	↑	(Su et al. 2011)
		Mg^{2+} →	Rac1 Cdc42		(Su et al. 2011)
	TRPV4	Ca^{2+} →	RhoA	↑	(Adapala et al. 2013; Thodeti, Paruchuri, and Meszaros 2013; (Tomasek et al. 2006; Lee et al., 2016)
		Ca^{2+} →	Rac1	↑	(Ou-yang et al. 2018)
Invasion	TRPM2	Ca^{2+} ↔	Rac1	↑	(G. Gao et al. 2014)
	TRPV2	←	Rac1	↑	(Nagasawa and Kojima 2015)
		Ca^{2+} ┤	RhoA/ Rac1	↓	(Laragione, Harris, and Gulko 2019)
Aberrant tumour vascularization	TRPC1	←	RhoA	↑	(Mehta et al. 2003)
	TRPC6	→	RhoA	↑	(Singh et al., 2007)
	TRPM8	┤	Rap1	↓	(Genova et al. 2017)
		┤	RhoA	↓	(Sun et al. 2014)
	TRPV4	┤	Rho	↓	(Thoppil et al. 2016; Adapala et al. 2016)

Table 7. TRPs-small GTPases relationship in metastatic cancer hallmarks.

Legend: →: TRP enhances GTPase activity; ←: GTPase enhance TRP activity; ↔: bidirectional activation; ┤: TRP inhibits GTPase activity; ↑: increase; ↓: decrease

In addition to the examples of a direct TRP-small GTPases interaction in metastatic cancer hallmarks reported in this review, many studies suggest other possible signal transduction pathways associated with tumor progression involving both TRPs and small GTPases. For instance, they have both been implicated in the regulation of MMPs production through pathways like IP3K/Akt and Hsp90α-uPA-MMP2 that offer many points of contact in between them (Luo et al., 2016; Rybarczyk et al., 2017; Liu et al., 2018; Yang et al., 2015; Zhuge & Xu, 2001; Koike et al., 2000). However, to date a direct correlation between TRPs and small GTPases in these signal transduction pathways has not yet been established, but remains to be deeper clarified. Moreover, several studies have reported a role of both these two superfamilies of molecules in promoting another key step of the metastatic cascade that is EMT. In response to the same growth factor/cytokines-induced signalling pathways both TRPs and small GTPases are able to induce the up-regulation of mesenchymal-like markers such as vimentin and the down-regulation of epithelial-like markers such as E-cadherin through the direct regulation of transcriptional factors including STAT3, Snail and Twist (Davis et al., 2014; Simon et al., 2000; Liu et al., 2014; Seiz et al., 2020; Yang et al., 2015; Liu et al., 2019; Chen et al., 2017; Kim et al., 2018). However, a synergistic cooperation between TRPs and Rho GTPases during the early stage of growth-factor induced EMT is still just a speculation, since to the best knowledge of the authors a direct correlation between TRPs and small GTPases effects on EMT has not yet been characterized. In conclusion, the interplay between TRP channels and small GTPase in cancer progression is only partially investigated to date and further investigations are required to shed light on many other aspects of this interesting crosstalk in cancer not well known.

1.4 THERAPEUTIC APPROACHES TO TARGET PROSTATE CANCER

1.4.1 Prostate cancer: diagnosis and prognosis

PCa is one of the most common non-cutaneous human malignancies. Progression of PCa is generally slow or mild in diagnosed patients, but in its metastatic stage it is the second deadliest cancer among men with 10% of total cancer death in Europe (Dyba et al. 2021) and 6.8% worldwide (Sung et al. 2021). Indeed, once the tumor escapes its primary site giving metastases, the outcome of the therapy worsens (**Fig. 19**). PCa has the highest incidence in industrialized countries with a 4% to 6% annual increase for the advanced disease since 2011 (Siegel et al. 2022) and led to 375,304 deaths around the world in 2020 ("World Cancer Research Fund International" 2022). As shown in **Figure 19**, the 5-year relative survival for PCa is 100% as long as it is diagnosed as localized or spread to the (regional) lymph nodes but drops dramatically to 32.3% for patients in which it has metastasized reaching distant organs such as lungs and bones.

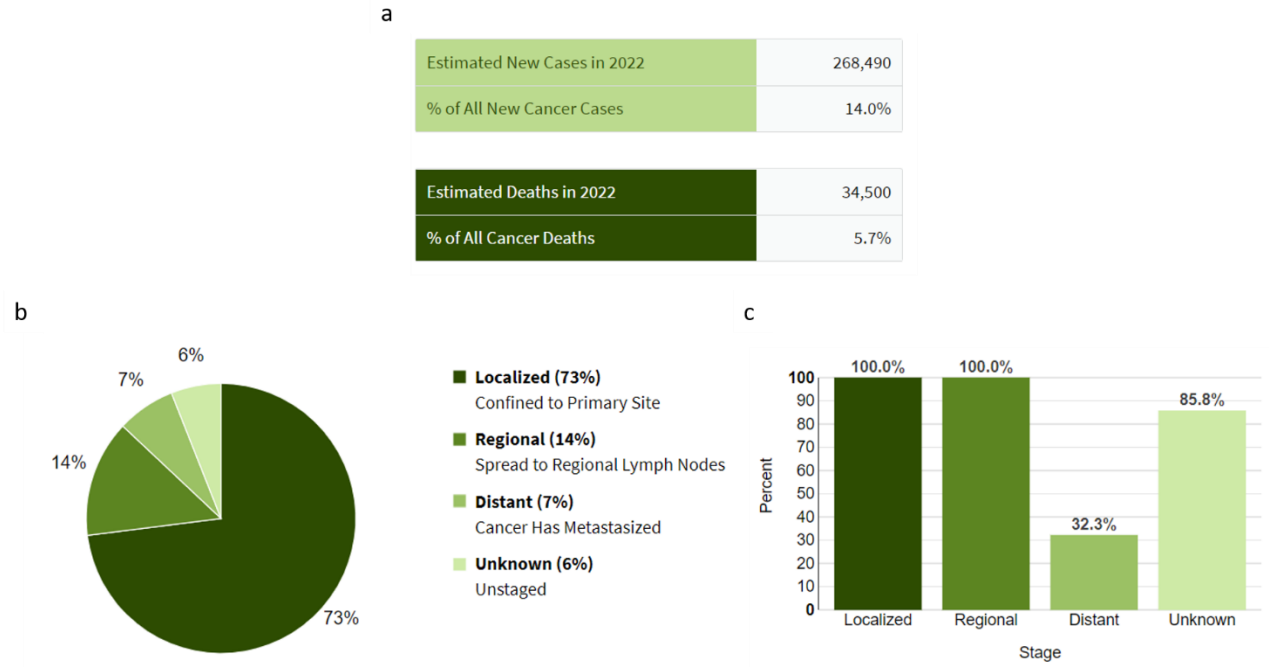

Figure 19. Prostate cancer statistics.

Estimated new cases and deaths for prostate cancer in 2022 (a); Percentage of cases (b) and 5-Year relative survival by stage at diagnosis (c) relative to prostate cancer (2012-2018). Data from SEER (Surveillance, Epidemiology, and End

Result Program), National Institute of the U.S. Department of Health and Human Services ("National Cancer Institute - Surveillance, Epidemiology, and End Result Program" 2022).

PSA serology is of course the most important screening tool for **detecting PCa** and recurrence, as well as monitoring response to therapies because blood PSA levels are elevated in both local and metastatic PCa.
PSA is also known as KLK3 (the third member of the serine protease kallikrein family) and it has been extensively studied as a biomarker for the detection and follow-up of PCa although it is not an excellent tumor marker as it lacks both selectivity and specificity (Van Haute, De Ridder, and Nilius 2010). Indeed, PSA levels are variable and not always directly correlated to cancer staging. For instance, PSA levels are high in patients with BPH whereas decrease in the late metastatic phase (Shariat et al. 2004). For this reason, PSA is often detected in combination with other blood biomarkers such as transforming growth factor-beta 1 (TGF-β1), human glandular kallikrein 2 (hK2), urokinase plasminogen activator (uPA), interleukin-6 as well as their receptors (uPAR and IL-6R) (Shariat et al. 2011).
Following an abnormal digital rectal examination or detection of elevated PSA levels in the blood, PCa diagnosis is then confirmed by transrectal ultrasound (TRUS)-guided core-needle biopsy, generally well-tolerated by patients. The biopsy can then be followed by pelvic magnetic resonance imaging (MRI), computed tomography (CT), bone scan, and most recently positron emission tomography (PET)/CT scan to determine if cancer has spread to surrounding regions and stage cases of advanced PCa (Trabulsi et al. 2020).
PCa patients are then **classified** as low, intermediate, or high-risk localized cancer or locally advanced cancer according to some parameters reported in **Table 8**, like PSA level, International Society of Urologic Pathologists (ISUP) grade, pathological tumor-node-metastasis (pTNM) classification, and Gleason score. In particular, the latter corresponds to the sum of two numbers indicating the most representative glandular differentiation patterns observed in the biopsy samples through a value ranging from 1 (for the least aggressive most differentiated tumor pattern) to 5 (for the most aggressive showing no glandular differentiations tumor pattern) (Gleason, Mellinger, and Ardving 1974) (**Fig. 20**). Consequently, the final Gleason Score ranges from 6 (very low-risk PCa) to 10 (very high-risk PCa). The ISUP classification is a new system developed in the United States as a modification of the Gleason score system easier to understand and more accurate for predicting how quickly cancer will spread and the chance of death. This classification assigns tumors a grade ranging from 1 for the least aggressive to 5 for the most aggressive forms. In particular, ISUP grade 1 corresponds to Gleason Score 3+3, grade 2 to Gleason 3+4, grade 3 to 4+3, grade 4 to 4+4 and grade 5 to 4+5, 5+4, and 5+5. As for the TNM system, it was proposed by the American Joint Committee on Cancer (AJCC) and categorizes tumors in terms of size (T1-T4), lymph node involvement (NX, N0, N1), and presence of metastases (M0-M1).

		Low risk	Intermediate risk	High risk
Localized PCa	PSA	< 10 ng/mL	10-20 ng/mL	> 20 ng/mL
	Gleason score	< 6	7	> 7
	ISUP grade	1	2-3	4-5
	Clinical stage	T1-T2a	T2b-T2c	T3a
Locally advanced PCa	Clinical stage	T3b or cN1 (lymph node metastasis) (any PSA, any Gleason score)		

Table 8. Prostate cancer stages and classification.

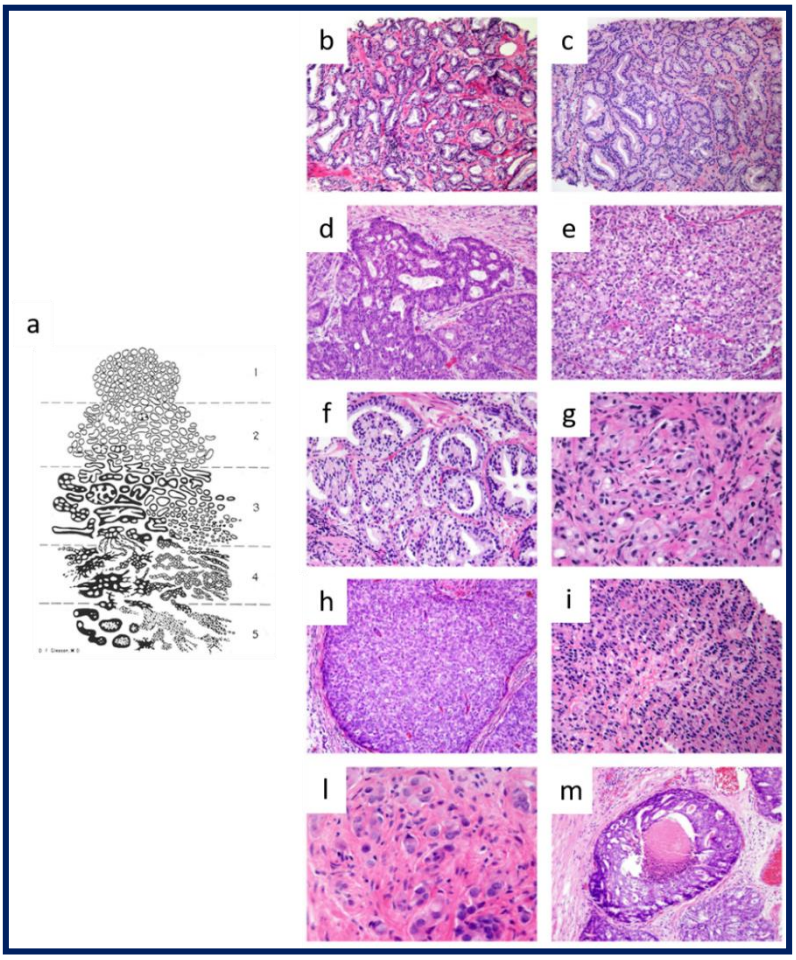

Figure 20. Representative histological staining on PCa tissues.

(a) Schematic example of the histological differences corresponding to each Gleason grade (from 1 to 5); Representation of tissues assigned to Gleason grades from 1 to 5: (b) Gleason score 3+3 (ISUP Grade Group 1); (c) Gleason score 3+4 (ISUP Grade Group 2); (d-g) Gleason score 4+4 (ISUP Grade Group 4); (h-l) Gleason score 5+5 (ISUP Grade Group 5); Gleason score 5+4 (ISUP Grade Group 5);
Image adapted from (Gordetsky and Epstein 2016).

Taking into account the androgen-dependency of PCa, the first-line standard treatment is androgen ablation either by surgical or chemical castration or by administration of androgen receptor inhibitors like Bicalutamide (Casodex®, AstraZeneca) approved in 1995 and currently used as monotherapy to treat PCa in its earlier stages or in combination with gonadotropin-releasing hormone (GnRH) analogs to treat advanced PCa (Wellington and Keam 2006). In this regard, the discovery that surgical orchiectomy is effective in countering metastatic PCa by leading to androgen ablation earned the Nobel Prize to Huggins and Hodges in 1966 (Huggins and Hodges 1972). However, the effectiveness of this treatment is limited in time and some patients relapse due to the growth and spread of cancer cells with an acquired lethal resistant phenotype (Déliot and Constantin 2015). Consequently, regarding **low-risk prostate cancer**, the significant increase in cases diagnosed following a broader screening of the population opened a debate on the potential benefits and harms of early treatment versus active surveillance (Osuchowski et al. 2021). By contrast, over the past decade, the cases of **advanced prostate cancer** diagnosed increased from 3.9% to 8.2% (Siegel et al. 2022) and the treatment options are very limited as tumors inescapably become refractory to hormonal treatments and may give rise to bone metastases that are difficult to treat.

1.4.2 Conventional therapeutic approaches

Based on the tumor classification, there are currently several therapeutic alternatives to countering PCa. The two types of therapeutic approaches recommended by the European Association of Urology (UAE) for **patients with low-risk prostate cancer** are deferred treatment and active treatment. In the first case, one of the modalities recommended above all for patients with a life expectancy of fewer than 10 years is watchful waiting, as it allows to avoid the complications associated with the side effects of the treatments. Alternatively, active surveillance with frequent and continuous follow-up by monitoring PSA levels, multi-parametric MRI, and biopsies is recommended for patients with a longer life expectancy.

As for active treatments, the main ones are: **radical prostatectomy (RP)**, **radiation therapy (RT)** with or without image-guided radiotherapy (IGRT), **hormonal therapy**, **proton beam therapy**, and **brachytherapy (BT)**. The latter provides for the temporary or permanent implantation of sealed radioactive seeds (^{125}I or ^{103}Pd) to prostate tissue. In combination with RT, brachytherapy has been shown to be effective in treating patients with intermediate-risk and high-risk diseases as in 85% of cases it increases the overall survival rate by 10 years, reduces the development of metastasis by 10%, and leads to tumor-specific mortality rate less than 5% (Zaorsky et al. 2017). An interesting comparison between a group of patients undergoing active

monitoring with patients undergoing RP or RT showed that the former had higher rates of disease progression and metastases more frequently, but overall survival rates were the same (Hamdy et al. 2016).

By contrast, **patients with localized high-risk PCa** can be treated with **RP, RT, and long-term androgen deprivation therapy (ADT)**, which ensure the best long-term effects. In particular, the treatment for high-risk patients that produces the best results in terms of survival is undoubtedly RP. However, for RP to be applied, the tumor must not have infiltrated the pelvic wall or urethral sphincter and its volume must be small (Gunnarsson et al. 2019). Furthermore, it should also be taken into account that all types of radical prostatectomy can cause postoperative incontinence and erectile dysfunction as side effects (Haglind et al. 2015). In addition, taking into account the high risk of lymph node metastases, extended pelvic lymph node dissection (ePLND) is also recommended although not often performed (Fossati et al. 2017).

The other widely used therapeutic approach in the case of high-risk patients is **RT**. In this context, photon-based therapies such as intensity modulation radiotherapy (IMRT) or external beam volumetric arc radiotherapy (VMRT) characterized by a shorter application time can be used. In both cases, precise computer-assisted dosimetry greatly increases the efficiency of the treatment. Alternatively to photon beam, proton beam therapy is also used, although its clinical benefits have not yet been clearly determined (Mottet et al. 2021). Interestingly, it has been stated that the use of RT in combination with short-term (3–6 months) and long-term **ADT** (2–3 years) can improve overall prognosis as well as extend the recurrence-free interval and overall patient survival rate (Denham et al. 2011; Mottet et al. 2021).

Several therapies have proven effective to inhibit PCa progression and have been approved in the past decade. Among them, chemotherapeutic agents including Docetaxel (Taxotere®, Sanofi-Aventis) and Cabazitaxel (Jevtana®, Sanofi-Aventis), radium-233 as radiotherapeutic that targets the bone, compounds targeting the androgen receptor–signaling pathway or androgen synthesis like Enzalutamide (Xtandi®, Pfizer) and Abiraterone acetate (Zytiga®, Janssen) respectively, as well as PARP inhibitors that interfere with DNA repair in tumor cells (Olaparib commercialized as Lynparza® by AstraZeneca and Rucaparib sold under the brand name Rubraca®, ClovisOncology), and the autologous cell-based cancer vaccine, Sipuleucel-T (Provenge®, Dendreon Pharmaceuticals). Regarding the use of **anti-angiogenic agents** to counter metastatic PCa, although promising results have been obtained in pre-clinical models, clinical trials performed on tyrosine kinase inhibitors like Sorafenib and Sunitinib failed the endpoints (Martínez-Jabaloyas et al. 2013; Dror Michaelson et al. 2009; Michaelson et al. 2014; Aragon-Ching et al. 2009; Steinbild et al. 2007). In addition, other alternative therapies like **cryotherapy**, **high-intensity focused ultrasound**, and **photodynamic therapy (PDT)** are currently under investigation to target PCa. However, unfortunately, patients with metastatic castration-resistant prostate cancer (mCRPC) still have a poor prognosis with a median life expectancy of <3 years. Indeed, no effective treatments are available for mCRPC which continues to account

for more than 250,000 cancer deaths worldwide, annually (Siegel et al. 2022). In this context, TRP channels can be very promising therapeutic tools for future perspectives (Yang and Kim 2020).

1.4.3 TRP channels as innovative therapeutic targets

One possibility to improve actual clinical treatment modalities consists in combining existing cancer drugs with each other or with new pharmaceutical agents. Among them, the target of ion transporting proteins is proving to be of clinical relevance (Imbrici et al. 2018). As evidence of this, many FDA-approved drugs that target ion channels are currently used to treat a variety of pathological conditions and are being evaluated for cancer repurposing (Prevarskaya, Skryma, and Shuba 2018) (**Table 9**). Nowadays, drug repositioning - that is, finding new uses for old drugs - is, in fact, a very popular strategy due to its high efficiency, low cost, and reduced risks.

	FDA-approved or clinically tested		Cancer Repurposing			
Drug	Primary target	Usage/condition	Cancer-relevant target	Cancer hallmark affected	Cancer type effective	Ref.
Amitriptyline	Serotoninergic, dopaminergic, adrenergic, cholinergic systems	Tricyclic antidepressant	K_v10.1 (EAG1)	Metastasis	GBM	(Martínez et al. 2015)
DHP Ca^{2+} channels antagonist (amlodipine, cilnidipine, felodipine, manidipine)	Ca_v1	Antihypertensive	Ca_v1.1, Ca_v1.3	Migration, invasion	Breast, pancreatic	(Min et al. 2011)
Imipramine	Serotoninergic, dopaminergic, adrenergic, cholinergic systems	Tricyclic antidepressant	K_v10.1 (EAG1)	Proliferation, apoptosis resistance	SCLC, pancreatic, MCC	(Jahchan et al. 2013)
Lidocaine	Na_v1.5, Na_v1.7	Local anesthetic, antiarrhythmic	Na_v1.5	Invasion, metastasis	Breast, colon	(House et al. 2015) NCT01916317
Phenytoin	Na_v1	Antiepileptic	Na_v1.5	Proliferation, apoptosis resistance	Breast	(Nelson et al. 2015)

Promethazine	Serotoninergic, dopaminergic, adrenergic, cholinergic systems	Neuroleptic antihistamine	K_v10.1 (EAG1)	Proliferation, apoptosis resistance	SCLC, pancreatic, MCC	(Jahchan et al. 2013)
Ranolazine	Na_v1	Antiarrhythmic, chronic angina	Na_v1.5	Invasion, metastasis	Breast	(Driffort et al. 2014)
Ropivacaine	Na_v1.7	Local anesthetic	Na_v1.5	Invasion, metastasis	Colon	(Baptista-Hon et al. 2014)
Senicapoc	K_{Ca}3.1	Sickle cell anemia	K_{Ca}3.1 (IK, Gardos)	Proliferation, migration, invasion, angiogenesis	Colon, melanoma, glioma	(Ataga et al. 2008; D'Alessandro et al. 2013; Grgic et al. 2005; Köhler et al. 2000; Tajima et al. 2006)
Thiorizadine	Serotoninergic, dopaminergic, adrenergic systems	Antipsychotic	K_v10.2 (EAG2)	Metastasis	MB	(X. Huang et al. 2015)

Table 9. Potential repurposing of FDA-approved drugs against ion channels in cancer therapy.

GBM: glioblastoma multiforme; DHP: dihydropyridine; SCLC: small cell lung cancer; MCC: Merkel cell carcinoma; MB: medulloblastoma.
Adapted from (Prevarskaya, Skryma, and Shuba 2018)

At the same time, the development of new efficient drug delivery systems can help overcome some limiting problems related to chemotherapeutic agents, improving their bioavailability at the desired sites of action while reducing negative side effects (Senapati et al. 2018).

"Drugable" target

Among the newly discovered ion channels, the TRP family is arguably the most appealing, proving to be a promising target for drug discovery (Kaneko and Szallasi 2014). The ubiquity of expression of TRP channels in almost all the cells of the human body and the wide spectrum of physiological processes in which they have been proven to be involved explains the recent huge hope for the development of new drugs targeting these fascinating channels (Nilius and Szallasi 2014; Moran 2018).

Early drug discovery efforts to target TRP channels have focused on pain (Patapoutian, Tate, and Woolf 2009) but to date, they have broadly expanded into other therapeutic areas covering diseases such as asthma, anxiety, cardiac hypertrophy, obesity, and metabolic disorders as well as cancer thanks to the remarkable discoveries made on the implication of TRP channels in various pathological conditions (**Fig. 21**).

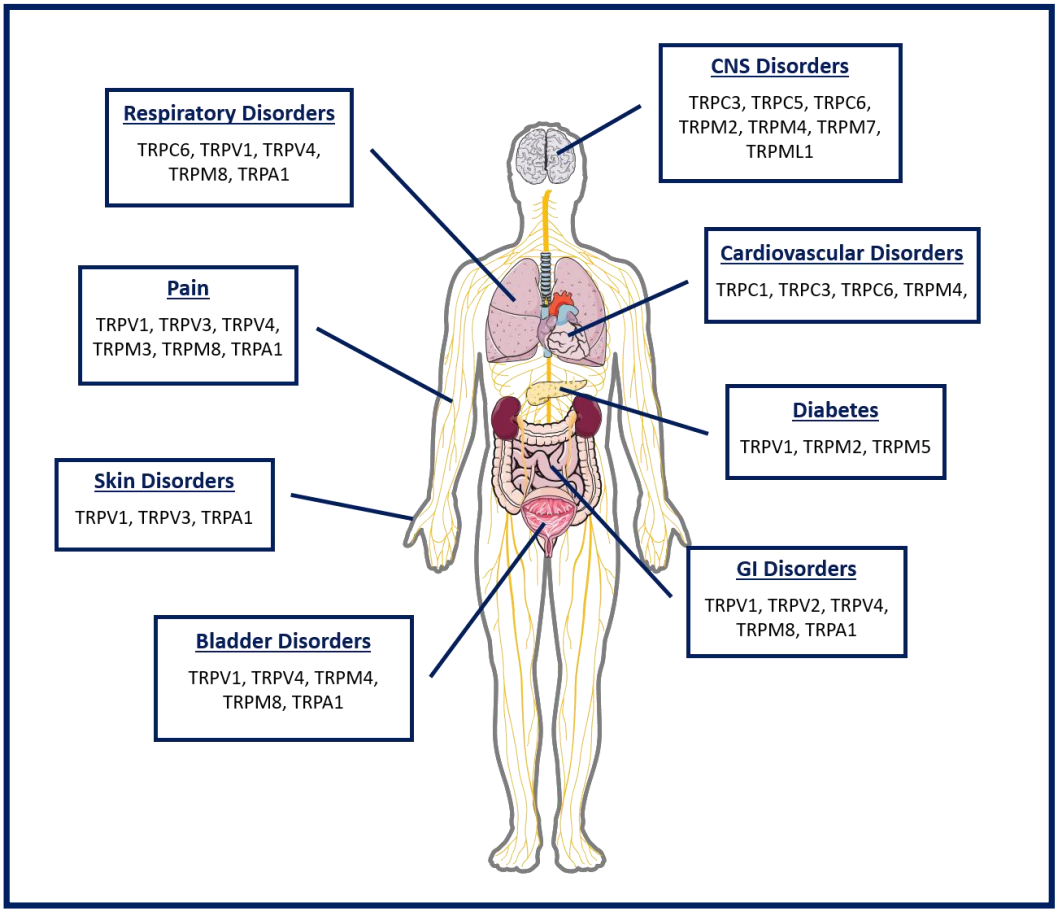

Figure 21. TRP channels in diseases.
Scheme representing putative roles of TRP channels in the pathogenesis of several human disorders affecting nervous (Vennekens, Menigoz, and Nilius 2012; Morelli et al. 2013); gastrointestinal (Holzer 2011), genito-urinary (Skryma et al. 2011), respiratory (Preti, Szallasi, and Patacchini 2012), cardiovascular (Watanabe et al. 2013), and immune systems (Schwarz 2007; Smith and Nilius 2013) as well as skin diseases (Caterina and Pang 2016), metabolic disorders including obesity and diabetes (Zhu et al. 2011; Suri and Szallasi 2008) and pain (Nozazde et al. 2016; Dai 2016).
CNS: central nervous system; GI: gastrointestinal.
Image remade from (Kaneko and Szallasi 2014).

One of the **advantages** offered by TRP-targeted drug development is the possibility to obtain truly selective modulators thanks to the relatively low sequence homology among family members and the remarkable differences in their 3D structure. For the same reason, it is neither possible nor opportune to extrapolate any consideration from one channel to another (Moran 2018). In this regard, recent advances

associated with cryo-EM have enabled near-atomic resolution structures for many TRPs, thus facilitating and improving the efficiency of drug design studies. Moreover, the prevalent TRP localization at the plasma membrane makes them promising pharmacological targets.

Nowadays, numbers of **small molecules** modulating different TRP have entered clinical trials for different diseases (Tsagareli and Nozadze 2020; Kaneko and Szallasi 2014). Considered the most recent discovery of the implication of TRP channels in cancer compared to other pathologies, it is not surprising that among the drugs currently **in the clinical phase** only one has specifically an anti-tumor purpose. Moreover, not surprisingly, most of the compounds currently in clinical studies are agonists or antagonists of TRP channels better and longer characterized for their role in nociception, that is TRPV1, TRPV3, TRPM8, and TRPA1. The only regards TRPV6, whose inhibitor has recently entered clinical trials for cancer treatment. However, all the information obtained from research on TRP-related analgesic drugs undoubtedly may represent an excellent starting point for being translated into clinical pharmacological research centered on other human pathologies including cancer. Currently, seven antagonists and five agonists of TRPV1, one antagonist of TRPV3 and one of TRPV6, five antagonists of TRPA1, as well as two agonists for TRPM8 are being under clinical investigations (**Table 10**).

Channel	action	Drug	Company	Disease	Status	ClinicalTrials.gov identifier
TRPV1	agonist	capsaicin	N.A.	Pain	Launched	
		NGX-4010	Acoda Therapeutics Inc/ Astellas Pharma Inc	Post-herpetic neuralgia	Launched	
		zucapsaicin	Sanofi-Aventis Canada Inc	Osteoarthritis	Registered	
		zucapsaicin	Winston Pharmaceuticals Inc	Cluster headache	Phase 3	NCT000338339
		MCP-101	Mt Cook Pharma	Overactive bladder	Phase 2	N.A.
	siRNA	SYL-1001	Sylentis Sau	Ocular pain	Phase 2	NCT01776658
	antagonist	DWP-05195	Daewoong Pharmaceutical Co Ltd	Neuropathic pain	Phase 2	NCT01557010
		XEN-D0501	Provesica Ltd	Overactive bladder	Phase 2	N.A.
		Mavatrep	Johnson & Johnson Pharmaceutical	Osteoarthritis / Pain	Phase 1	NCT00933582
		PHE-377	PharmEste SRL	Neuropathic pain	Phase 1	N.A.
		MR-1817	Mochida Pharmaceutical Co Ltd	Pain	Phase 1	NCT00960180
		PAC-14028	Pacific Pharmaceuticals Co Ltd	Atopic dermatitis/ IBD	Phase 1	NCT01638117
		SB-705498	GlaxoSmithKline plc	Pruritus	Phase 1	NCT01673529
TRPV3		GRC-15300	Glenmark Pharmaceuticals Ltd / Sanofi	Neuropathic pain/ Osteoarthritis	Phase 2	NCT01463397
TRPV6		SOR-C13		Cancer	Phase 1	NCT01578564
TRPA1		GRC-17536	Glenmark Pharmaceuticals Ltd	Diabetic neuropathy / Respiratory disorders	Phase 2	NCT01726413
		CB-625	Cubist Pharmaceuticals/ Hydra Biosciences	Inflammatory disease / Pain	Phase 1	N.A.
		HX-100	Hydra Biosciences	Diabetic neuropathy / Asthmatic diseases	Phase 1	N.A.
		GDC-0334	Genentech, Inc.		Phase 1	NCT03381144

TRPM8	agonist	Menthol	National Research Centre for the Working Environment	Carpal tunnel syndrome /	N.A.	NCT01716767
		Biofreeze		Neck pain		NCT01542827
		ph5 Eucerin	University Hospital Muenster	Dry Itchy Skin	N.A.	NCT00669708
		MPO	University Hospital Brest/ Beiersdorf	Atopic dermatitis	N.A	NCT03610386
		D-3263	Dendreon	Cancer	Phase 1	NCT00839631

Table 10. ***Drugs targeting TRP channels in clinical trials.***
N.A.: not assigned; IBD: inflammatory bowel disease; MPO: D-3263

However, it should be noted that only 5 of the 28 TRP channels identified in mammals have currently reached the clinical stage of drug development. This is mainly due to some **inherent problems** that hinder the translation of basic research results into clinical applications. Indeed, despite notable advances in the clinical application of TRP channels, some challenges faced by these compounds in clinical practice remain to be overcome (Koivisto et al. 2021; Tsagareli and Nozadze 2020; Kaneko and Szallasi 2014). In this context, one of the main intrinsic problems of TRP channels relates to the high risk of adverse effects associated with their wide range of tissue distribution and their polymodal activation of gating. For example, the clinical development of TRPV1 antagonists is hampered by the fact that they caused hyperthermia and increased the heat pain threshold in human volunteers (Moran et al. 2011; Kaneko and Szallasi 2014; Dai 2016; Moran 2018; Moran and Szallasi 2018). Similarly, the topical activation of TRPV4 by GSK1016790A in the skin may improve barrier function promoting intracellular junction development (Kida et al. 2012), but its systemic administration led to endothelial failure and cardiovascular collapse (Willette et al. 2008). For TRP channels showing opposite actions in a wide range of diseases depending on their localization, this issue may represent an even bigger problem. For instance, suppression of TRPM4 may, on one hand, be useful for the treatment of multiple sclerosis (Schattling et al. 2012) and anaphylaxis (Smith and Nilius 2013), but, on the other hand, may lead to cardiac arrhythmias and hypertension (Abriel et al. 2012). The goal will be to find a way for exploiting the ‘fair face’ of TRP channels without revealing the ‘ugly face’, using Nilius' terminology (Nilius 2013).

As regards the employ of TRP agonists to locally desensitize TRP channels in pain management, although severe adverse effects have not been reported, they could risk inducing initial irritation or even degeneration of the sensory nerves. It should be noted that in traditional Chinese medicine formulations containing shogaol, menthol, and cinnamaldehyde known for the activation of TRPV1, TRPM8 and TRPA1 respectively

have long been used topically or orally to relieve headache, menstrual pain, neuralgia, and arthralgia. Additionally, capsaicin is contained in many formulations (creams, occlusive patches, and liquid) currently used in the treatment of chronic painful conditions such as diabetic neuropathy, post-herpetic neuralgia and other painful ailments (Dai 2016; Moran 2018; Moran and Szallasi 2018). Therefore, the advantages and disadvantages of using TRP channels as new therapeutic targets compared to currently available therapeutic options must be carefully evaluated from time to time.

Second, another possible problem of drug discovery against TRP channels is associated with their heteromerization (not uncommon (Cheng, Sun, and Zheng 2010)). Indeed, heteromers can have distinct pharmacological properties and are not easily reproducible in heterologous expression systems (Kaneko and Szallasi 2014).

Finally, when it comes to inherited human disorders caused by TRP mutations, another problem to consider about the use of TRP channels as therapeutic targets is the fact that disorders caused by gain-of-function mutations can be clinically addressed more easily than those associated with loss-of-function mutations. Indeed, in the first case, such as the Familial Episodic Pain Syndrome (FEPS) caused by a point mutation on the TRPA1 gene (Kremeyer et al. 2010), small compounds able to antagonize the channel function could offset its overactivation; conversely, in the second case, loss-of-function mutations, especially truncation types, are difficult to target with small drugs and may require less validated approaches such as gene therapy to restore the physiological function of the TRP channel. This is the case, for example, of the loss of TRPML1 function in type IV mucolipidosis, which has proved more difficult to treat (Dong et al. 2008).

Regarding cancer therapy, as previously mentioned only two compounds targeting TRP channels have already reached clinical trials. However, the notions obtained to date on other therapeutic indications can represent an excellent starting point for the development of new first-rate anticancer drugs. Moreover, a new strategy taking advantage of the up-regulation of some TRP channels in cancer cells has been proposed. Basically, TRP channels could be used just as a target for delivering toxic chemicals or radioactive nuclide at the desired site by exploiting a tight-binding agonist or an anti-TRP antibody (Prevarskaya, Zhang, and Barritt 2007). A peptide-doxorubicin "prodrug" was tested *in vivo* and was shown to significantly reduce tumor burden following its specific activation by PSA-induced cleavage of the peptide sequence (L-377,202) (DeFeo-Jones et al. 2000; Garsky et al. 2001). Interestingly, the peptide-doxorubicin was found to be less cytotoxic on off-target cells and 15 times more effective than doxorubicin on target tumor cells that secrete PSA (DeFeo-Jones et al. 2000; Garsky et al. 2001). A similar approach has also been proposed to target TRPV1 by covalently binding capsaicin to a PSA-clearable peptide (Prevarskaya, Zhang, and Barritt 2007).

Certainly, we are still in the early stages of understanding the disease-causing dysfunctions of the TRP channels. Therefore, resolving more TRP structures as well as a better understanding of the molecular

mechanisms that link to TRP channels with cancer development and progression is essential to optimize the development of new anti-tumor drugs and thus improve the prognosis of different cancers including PCa. Furthermore, to at least partially overcome the problem associated with unacceptable side effects, it is important to study tissue-specific targeting strategies. In this context, the use of nanodelivery systems discussed at the end of this chapter could be particularly appealing.

TRPA1 in clinic: current and perspectives

Clinical investigations

To date, five TRPA1 antagonists have reached the clinical stage of development basically for pain relief (**Table 10**). Among these studies, that about ODM-108 (ClinicalTrials.gov: NCT02432664) although did not show safety problems at the doses administered, was interrupted due to the complex pharmacokinetics displayed by the molecule (Koivisto et al. 2018). By contrast, CB-625 by Cubist Pharmaceuticals and Hydra Biosciences is revealing good potential for acute surgical pain. Moreover, several pieces of evidence linking TRPA1 to non-neurogenic airway inflammation suggest that selective TRPA1 antagonists might be potential new therapeutic tools for the treatment of respiratory diseases like asthma and COPD (Belvisi, Dubuis, and Birrell 2011). Consistently, GRC-17536 manufactured by Glenmark (ClinicalTrials.gov: NCT01726413) and HX-100 by Hydra Biosciences currently undergoing clinical phases 2 and 1 respectively revealed good potential to treat not only pain associated with diabetic peripheral neuropathies but also respiratory disorders such as asthma. Finally, GDC-0334 by Genentech has recently entered safety, tolerability, pharmacokinetics, and pharmacodynamics clinical trials (Chan et al. 2021) (ClinicalTrials.gov: NCT01726413).

Patents on TRPA1 antagonists

In the last decade, a significant number of patent applications related to TRPA1 have been published thanks to the great interest aroused by the therapeutic potential of this channel in the treatment of pain, airway respiratory, and dermatological diseases (Chen and Terrett 2020) (**Table 11**). Among the most relevant, a disclosure by the biotech company Algomedix (Herz and Kesicki 2015) seems to potentially contain promising TRPA1 antagonists for the treatment of various types of acute and/or chronic pain and the company is planning to start clinical trials on lead drug candidates shortly.

One of the major players in the search for TRPA1 antagonists is definitely Glenmark Pharmaceuticals. Indeed, in addition to GRC-17536, currently undergoing clinical investigations (phase 2) on patients suffering

from diabetic neuropathies and asthma, the company has two other patent applications on thienopyrimidinedione compounds to be used, alone or in combination with analgesic agents, for the same clinical indications (Glenmark Pharmaceuticals 2015; 2016).

TRPA1 antagonists can also find use in the treatment of itching sensation by exploiting their spectrum of action different from TRPV1 antagonists. Consistently, some TRPA1 antagonists have been proposed for dermatological applications including atopic dermatitis (AD) (Galderma Research & Development 2018) by the skin health company Galderma as well as by academic groups from Duke University which proposed a formulation containing TRPA1 and TRPV4 inhibitors to topically target dermatological disorders (University 2016; Duke University 2017). About that, Mandom Corporation, mainly involved in the market of skin and hair products, has recently published a patent application for structurally unique compounds characterized by linear alkyl groups which significantly increase their skin permeability (Mandom Corporation 2018).

In the last seven years, Genentech has published eight patent applications for TRPA1 antagonists (Chan et al. 2021) and Almirall also proposed a series of TRPA1 antagonists useful to treat pain, pruritus, inflammatory dermatological diseases, as well as respiratory disorders (Almirall 2015; 2017a; 2017b). Quite interestingly, EA Pharma recently filed a patent containing 51 sulfonamide derivatives (EA Pharma Co. 2017) to treat gastrointestinal diseases through the inhibition of TRPA1.

In addition, Kao Corporation proposed compounds with distinct structural features compared to the majority of known TRPA1 antagonists (Kao Corporation 2015), and Eli Lilly and Company which acquired Hydra Biosciences' program on TRPA1 published a patent application relating to the use of xanthine-based compounds for pain and respiratory diseases (Eli-Lilly and Company 2019).

Finally, Pfizer published a series of carboxamide-containing TRPA1 antagonists with potential applications in pain and pruritus, which, however, were recently proved to induce TRPA1-mediated Ca^{2+} influx, thus acting as reversible TRPA1 agonists (Chernov-Rogan et al. 2019) (**Table 11**). Moreover, in an earlier patent, Pfizer reported the discovery of a pre-clinical TRPA1 agonist, PF-4840154 with peculiar features compared to most well-known endogenous electrophilic TRPA1 agonists, basically acting as a non-covalent binder (Ryckmans et al. 2011) (**Table 1** in **Chapter 1.1.2**).

The most recent patent applications on TRPA1 antagonists are well-reviewed and discussed more in detail in Chen and Terrett 2020.

Drug repurposing/repositioning

Regarding TRPA1 antagonists, it has recently been shown that pyrazolone derivatives, such as antipyrine, dipyrone, and propiphenazone, selectively reduce AITC-evoked calcium currents in TRPA1-expressing cells

(Nassini et al. 2015). Similarly, Non-Steroidal Anti-Inflammatory Drugs (NSAIDs), such as diclofenac, ketorolac, and lornoxicam (xefocam) seem to inactivate or desensitize TRPA1 channel (Tsagareli et al. 2018). Interestingly, it has been found that ibuprofen-acyl glucuronide, which is one of the most used NSAIDs ibuprofen's reactive compound, inhibits the pro-algesic activity of TRPA1, whereas its parent compound ibuprofen doesn't (De Logu et al. 2019). These findings shed new light on the mechanisms by which ibuprofen exerts its antinociceptive/antihyperalgesic and anti-inflammatory activity, providing new insights into the development of drugs targeting TRPA1 in pain relief.

Patented TRPA1 antagonists					
Compound	Structure	IC_{50} (µM)	Actions	Developer	Ref.
A-967079	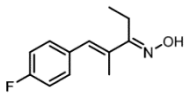	0.067		Abbott	(Perner et al. 2009)
HC-030031	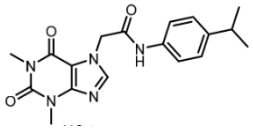	5-6		Hydra Biosciences	(Hydra Biosciences 2007)
GRC-17536*	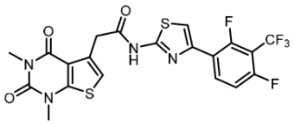	< 0.05		Glenmark Pharmaceuticals	(Glenmark Pharmaceuticals 2010)
AP-18	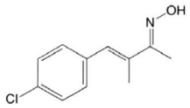	3.1		Novartis	(Patapoutian and Jegla 2007)
AZ465	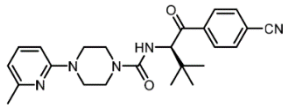			AstraZeneca	(Nyman et al. 2013)
AM-0902	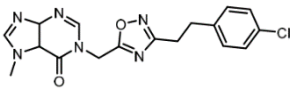	0.131		Amgen	(Schenkel et al. 2016)

A-967079	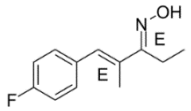	0.067		Pfizer	
Heterocyclic amides	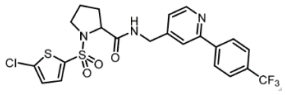	0.007		Janssen Pharmaceutical	(Janssen Pharmaceutical 2010)
CB-625*				Cubist Pharmaceutical Hydra Biosciences	
HX100*				Hydra Biosciences	
ODM-108				Orion Pharma	
GDC-0334*	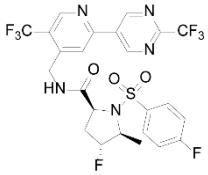			Genentech	(Chan et al. 2021)
	# 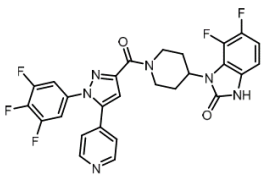	0.05-5	-Acute/ Chronic pain -Respiratory diseases	Algomedix	(Herz and Kesicki 2015)
	# 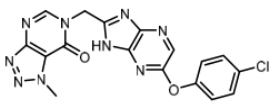	0.1-1	-Acute/ Chronic pain -Respiratory diseases -Skin inflammation -Pruritus	Almirall	(Almirall 2015; 2017a; 2017b)

	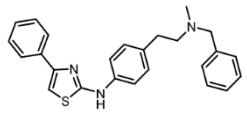		-Skin inflammation -Pruritus -Pain	Duke University	(University 2016; Duke University 2017)
Sulfonamide derivatives	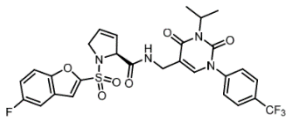	0.0036	-GI diseases	EA Pharma	(EA Pharma Co. 2017)
Xanthine-based compounds	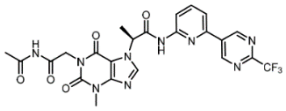	0. 0476	-Pain -Respiratory diseases	Eli Lilly and Company	(Eli-Lilly and Company 2019)
			-Actopic Dermatitis	Galderma	(Galderma Research & Development 2018)
Substituted sulfonamides	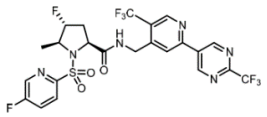	0.00269		Genentech	(Hoffmann, LaRoche, and Genentech 2018)
Cyclic ether-based compounds		0.00042 (90 min)			(Hoffmann, LaRoche, and Genentech 2019)
Thienopyrimidinedione compounds	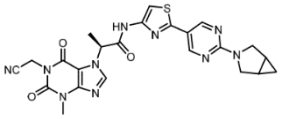	0.001	-Pain	Glenmark Pharmaceuticals	(Glenmark Pharmaceuticals 2015)
			-Diabetic neuropathy		(Glenmark Pharmaceuticals 2016)

	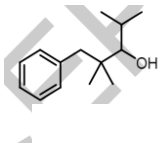	2.3	-Skin and mucous membranes irritation	Kao Corporation	(Kao Corporation 2015)
	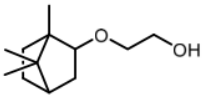		-Skin diseases	Mandom Corporation	(Mandom Corporation 2018)

*currently in clinical stages of development

: representative structures

Drug repositioned

Diclofenac Ketorolac (NSAID)			-Inflammation		

Patented TRPA1 agonists

Composition	Structure	EC_{50} (µM)	Actions	Developer	Ref.
Carboxamide-based compounds	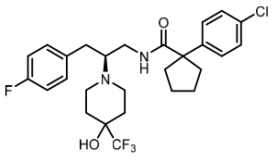	0.006	-Pain -Pruritus	Pfizer	(Pfizer 2016)

Drug repositioned

General anesthetics (Isoflurane)	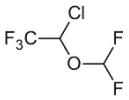	180			(Matta et al. 2008)
Acetaminophen (Paracetamol)	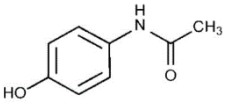	1.3-2.2			(Nassini et al. 2010; Andersson et al. 2011)

Dihydropyridines (vasodilators)	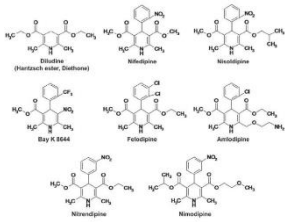	0.5-4			(Fajardo et al. 2008)

Table 11. Patented TRPA1 antagonists/agonists and drug repositioning.

GI: gastro-intestinal; NSAID: Non-steroidal anti-inflammatory drugs

TRPM8 in clinic: current and perspectives

Clinical investigations

Taking into account the significant difference in TRPM8 expression levels between malignant and non-malignant prostate tissues, TRPM8 could address the need for a more sensitive and **specific biomarker in PCa diagnosis** and staging and can be considered a potential and promising competitor to PSA currently in use. (Prevarskaya, Skryma, et al. 2007). Indeed, unlike PSA mRNA levels, TRPM8 mRNA transcripts in malignant prostate biopsy specimens were found significantly higher compared to normal samples (Fuessel et al. 2003; Schmidt et al. 2006; Kiessling et al. 2003). Moreover, it has been shown that TRPM8 levels could also give information about PCa staging and prognosis since it strongly correlates with tumor relapse after radical prostatectomy (Henshall et al. 2003). Accordingly, the TRPM8 activator WS-12 has been proposed as a diagnostic marker for prostate cancer by incorporating radiohalogens (Beck et al. 2007; Boonstra et al. 2016).

From the therapeutic point of view, TRPM8 has been proposed as a molecular **target for immunotherapy of PCa**. Indeed, an immunogenic peptide derived from TRPM8 (HLA-A*0201) and recognized by cytotoxic T lymphocytes (CTL) from PCa patients has been identified and characterized in clinical trials (Phase I) for its ability to activate CTL when loaded on autologous dendritic cells (DC) and to effectively lysate LNCaP cells (Fuessel et al. 2006; Kiessling et al. 2003).

In addition, in the last two decades, several studies have focused on the development and optimization of **small molecules targeting TRPM8** functionality. Countless TRPM8 agonists and antagonists have been developed through structure-activity relationship (SAR) studies aimed to improve the selectivity and efficiency against TRPM8. As regards TRPM8 activators, topical menthol reached clinical trials as an analgesic in patients with carpal tunnel syndrome (ClinicalTrials.gov: NCT01716767) and neck pain (ClinicalTrials.gov: NCT01542827) (**Table 10**). Other very recent clinical studies are currently evaluating the efficacy of menthol-based TRPM8 agonists as therapeutic agents in combination with other drugs (Ständer et al. 2017; Misery et al. 2019). As an example, a lotion containing two TRPM8 agonists has been proposed to treat chronic pruritus due to dry skin (ClinicalTrials.gov: NCT00669708), and a cream containing only menthoxypropanediol (MPO – **Table 3** in **Chapter 1.1.2**) is being evaluate for its anti-itching effects on patients with AD.

Interestingly, in 2009 an enteric-coated selective TRPM8 agonist, D-3263, entered a clinical Phase 1 dose-escalation study (ClinicalTrials.gov: NCT00839631) (**Table 10**), revealing a good potential in stabilizing patients with advanced PCa by inducing cell death in TRM8-expressing cancer cells through a Ca^{2+}/Na^{+}-dependent action (Genovesi et al. 2022). This important study together with that on the TRPV6 antagonist SOR-C13, being the first and only to have reached the clinical stage to date for the applications of TRP

channels in cancer therapy, could pave the way for the development of other drugs that exploit a similar approach based on the up-regulation of TRP channels in different types. of cancer, such as TRPC6 in glioblastoma and TRPV2 in ovarian cancer (Kaneko and Szallasi 2014).

Regarding TRPM8 antagonists, despite numerous have been developed as a potential treatment for pain, inflammation, migraine, and cancer (Pérez De Vega et al. 2016; Izquierdo et al. 2021), only 3 have reached the clinical stage of development (González-Muñiz et al. 2019). Among them, PF-05105679 and AMG-333 had been proposed for the treatment of migraine but they have not passed phase I studies (**Table 4** in **Chapter 1.1.3**) (Gaston and Friedman 2017). By contrast, Cannabidivarin is currently in phase II clinical assays (Gaston and Friedman 2017; De Petrocellis et al. 2011). The main problem associated with this class of compound is their low selectivity against TRPM8 due to the simultaneous activation of other TRP channels such as TRPA1 and TRPV1 (González-Muñiz et al. 2019).

Patents on TRPM8 modulators

In the last few years, numbers of TRP modulators have been patented by pharmaceutical and biotech companies as well as academic groups trying to improve their selectivity and efficiency against TRPM8 for clinical purposes (González-Muñiz et al. 2019; Izquierdo et al. 2021) (**Table 12**).

Patented TRPM8 agonists

In 2017 Hoag disclosed a topical analgesic composition mainly comprising menthol and eucalyptol as well as other natural plant extracts with anti-inflammatory properties mediated by the inhibition of the enzyme cyclooxygenase 2 (COX-2) for the treatment of inflammatory and painful diseases (Hoag 2017).

Melior Pharmaceuticals I, Inc. included different TRPM8 agonists such as icilin, menthol, WS3, and WS23 in different preparations containing an activator of Lyn kinase for potential applications in metabolic disorders (obesity, prediabetes, and type II diabetes) by reducing blood glucose levels, weight gain, or fat depot levels (Reaume et al. 2018).

The multinational chemical company BASF extended some previous patents by expanding the use of TRPM8 modulators from skin applications (Subkowski et al. 2010; Surburg et al. 2011) to bladder weakness and cancer treatment (Subkowski et al. 2013).

Finally, in recent years some DIPA- (Wei 2015) and DAPA-derivatives (Yang et al. 2017) have been developed as TRPM8 activators and patented as topical agents for the treatment of mild forms of dry eye disease (DED) (TR: ISRCTN24802609 and ISRCTN13359367 respectively). This class of compounds has also been proposed in a more recent patent as potential agents to treat lower gastrointestinal tract disorders (Wei 2017).

Patented TRPM8 antagonists

Since 2017, a considerable number of patents have been filed for new and more potent inhibitors of TRPM8 as therapeutic agents in the treatment of pain, neurodegeneration of migraine, ischemia, psychiatric disorders, urological dysfunctions, and associated pain hypersensitivity (Weyer and Lehto 2017; González-Muñiz et al. 2019). The Kissei Pharmaceutical Co. has recently patented KPR-2579 and analogs (Hirasawa, Kawamura, and Kobauashi 2016; Hirasawa et al. 2018b; 2018a) which in reducing the afferent hyperactivity of the bladder and icilin-induced wet dog shakes in rats without causing any cardiovascular side effects or changes in body temperature at the effective dose in the nanomolar range (Kobayashi et al. 2017; Aizawa et al. 2018).

Similarly, the naphthyl-derivative DFL00014817 was found effective in an overactive bladder rat model displaying nanomolar potency (IC_{50} = 7.23 nM), good pK properties although selectivity towards TRPM8, TRPA1, TRPV1, and TRPV3 (Beccari et al. 2017). Some other examples are aromatic carboxamides patented by Mitsubishi Tanabe Pharma Corporation for the treatment of different types of chronic pain (Kato et al. 2017); 4-hydroxy-2-phenyl-1,3-thiazol-5-yl methanone derivatives (Aramini, Bianchini, and Lillini 2017) and DFL23448 (Dompe Farmaceutici S.p.A.), which reduce icilin-induced wet-dog shakes, block bladder overactivity and prolong the storage phase of micturition by selectively blocking TRPM8 (Moriconi et al. 2013); RQ-00434739 (structure not disclosed) and imidazolinone derivatives (RaQualia Pharma Inc. - (Shishido and Ohmi 2017). RQ-00434739 is currently a promising drug for bladder disorders as, without affecting body temperature, it has been shown to be effective in reducing oxaliplatin-induced cold allodynia in rats and monkeys and icilin-induced wet dog shaking in rats blocking l-menthol-induced C-fiber hyperactivity and inhibiting prostaglandin E2-induced hyperactivity of primary bladder afferent nerves in rats (Aizawa et al. 2019).

In a 2017 patent, the commercially available TRPM8 antagonist SML0893, was administered alone or in combination with other substances to treat or prevent ocular pain or discomfort (Abelson, Corcoran, and Lnea 2017). Finally, in a new invention, sulfonamide compounds were used to treat or prevent vasomotor symptoms, such as hot flashes, because they lowered core body temperature (Palumbo 2017).

Drug repurposing/repositioning

In the context of drug repositioning, the anthelminthic drug Praziquantel (PZQ) has recently proved to modulate TRPM8 activity with selectivity in the micromolar range (Babes et al. 2017). More specifically, PZQ displays a partial agonist/antagonist activity on the channel by activating it or inhibiting TRPM8 in the absence and the presence of menthol respectively. Therefore, the vasodilator effect exerted by PZQ in mesenteric vessels can be associated with TRPM8 activation taking into account TRPM8 involvement in the regulation of

vascular tone (Johnson et al. 2009). Similarly, the immunosuppressant Tacrolimus revealed a role in inducing TRPM8-mediated Ca^{2+} influx within sensory neurons in different species (Arcas et al. 2019). Another example of drug repurposing is given by Riluzole, a commercial drug used in the treatment of amyotrophic lateral sclerosis. Riluzole has proved to significantly reduce cold and mechanical allodynia induced by oxaliplatin by indirectly suppressing TRPM8 overexpression in DRG neurons probably through the inhibition of sodium and calcium channels (Yamamoto et al. 2018).

Patented TRPM8 agonists					
Compound	Structure	EC_{50} (µM)	Actions	Developer	Ref.
DIPA derivatives	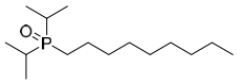	0.9	DED / GI disorders		(Wei 2015; 2017)
DAPA analogues	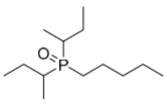	1.7			
Decahydronaphtho[1,2-c]chromene and Dihydropyrido[2,1a]isoindolone derivatives	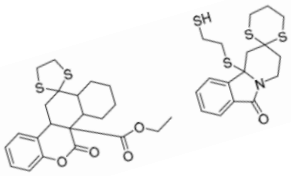	n.d.		BASF	(Subkowski et al. 2010; Surburg et al. 2011; Subkowski et al. 2013)
Triazole-based menthol derivatives		~ 1	DED		(Ferrer Montiel, A.V. Fernandez Carvajal, A. Belmonte Martinez et al. 2017)
menthol-based carboxamides and esters		~ 10		Procter and Gamble Company	(Yelm et al. 2017; Wos et al. 2017)
Cubebol and derivatives	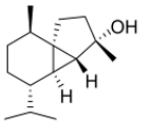	~ 10		Firmenich SA	(Velazco, Wuensche, and Deladoey 2000; Legay et al. 2016)
	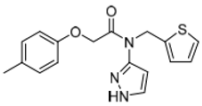	$0.2*10^{-3}$		Senomyx, Inc.	(Priest et al. 2012; Chumakova et al. 2014)
Menthol, eucalyptol + anti-inflammatory plant extracts			Topic analgesic pain		(Hoag 2017)

icilin, menthol, WS3, WS23 + Lyn kinase activator				Melior Pharmaceuticals I, Inc.	(Reaume et al. 2018)

Drug repositioned

Compound	Structure	EC_{50} (µM)	Actions	Developer	Ref.
Praziquantel (PZQ)	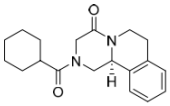	25			(Johnson et al. 2009)
Tacrolimus	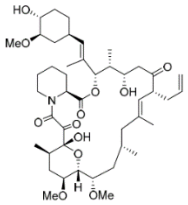				(Arcas et al. 2019)
Riluzole	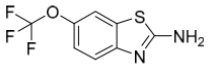				(Yamamoto et al. 2018)

Patented TRPM8 antagonists

Compound	Structure	EC_{50} (µM)	Actions	Developer	Ref.
KPR-2579 and analogues	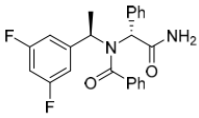	0.008	Overactive bladder	Kissei Pharmaceutical Co.	(Hirasawa, Kawamura, and Kobauashi 2016; Hirasawa et al. 2018b; 2018a; Aizawa et al. 2018)
DFL00014817	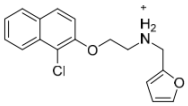	0.007	Overactive bladder		(Beccari et al. 2017)
Aromatic carboxamides	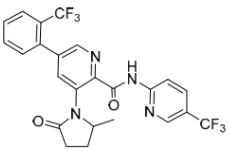	0.004	Chronic pain	Mitsubishi Tanabe Pharma Corporation	(Kato et al. 2017)
4-hydroxy-2-phenyl-1,3-thiazol-5-yl methanone	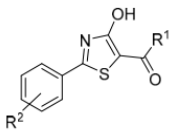				(Aramini, Bianchini, and Lillini 2017)
DFL23448	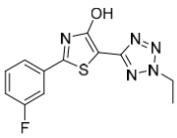	0.01	Overactive bladder	Dompe Farmaceutici	(Moriconi et al. 2013)

RQ-00434739	n.d.		Bladder disorders		(Aizawa et al. 2019)
Imidazolinone derivatives	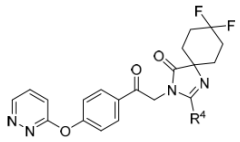	3		RaQualia Pharma Inc	(Shishido and Ohmi 2017)
SML0893	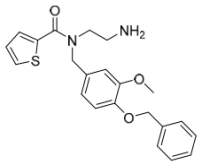		Ocular pain or discomfort		(Abelson, Corcoran, and Lnea 2017)
Sulfonamide compounds	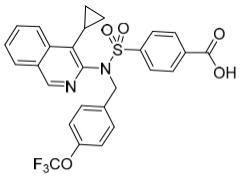				(Palumbo 2017)
Cubebol-derived unsaturated menthol benzoate	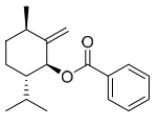	2		Firmenich SA	(Velazco, Wuensche, and Deladoey 2000)
Tryptamine derivatives	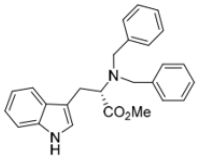	$0.2*10^{-3}$			(Bertamino et al. 2016; 2018)
β–lactam derivatives	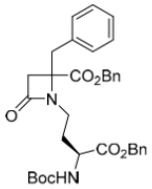	$42*10^{-3}$			(De La Torre-Martínez et al. 2017)

Table 12. Patented TRPM8 agonists/antagonists and drug repositioning.

GI: gastro-intestinal; DED: dry eye disease

Peptide therapy

Among other strategies, peptides against ion channels/receptors could be powerful pharmaceutical agents for the treatment of several diseases. Interestingly, three peptidomimetics targeting the αIIbβ3 integrin have been approved by FDA and are currently used in therapy as Eptifibatide (Integrilin, COR Therapeutics), Tirofiban (Aggrastat, Merck), and the chimeric 7E3 Fab (Abciximab, Repro) (Bledzka, Smyth, and Plow 2013; Kuo, Chung, and Huang 2019). Employing both peptides acting directly or indirectly on different ion channels including TRP channels as well as peptides engineered from protein-protein interactions between ion channels and regulatory protein could represent a reliable and innovative approach (Tsagareli and Nozadze 2020). As an example, some successful peptide agents, already in the clinics or under clinical trials, seems a reliable approach has been developed for pain management (Pérez de Vega, Ferrer-Montiel, and González-Muñiz 2018). Moreover, peptides engineered from protein-protein interactions (PPI) among pain-related receptors and regulatory proteins also led to new therapeutic approaches for pain management.

In this context, considering the growing number of 'signalplexes' and 'channelosomes' formed by TRP channels with a wide range of intra- cellular proteins, drug discovery is lately becoming interested and turning to the possible manipulation of these interactions. As an example, blocking the interplay between TRPV1 and the scaffolding A-kinase anchoring protein AKAP79 was found effective in inhibiting inflammatory hyperalgesia by preventing the PKA- and PKC-dependent sensitization of TRPV1 (Btesh et al. 2013; Fisher, Btesh, and McNaughton 2013). Indeed, it has been demonstrated that peptide antagonists to TRPV1–AKAP79 binding built based on the critical residues mediating TRPV1-AKAP79 interaction, can effectively abrogate inflammatory hyperalgesia *in vivo* without affecting pain thresholds (Btesh et al. 2013; Fisher, Btesh, and McNaughton 2013). Therefore, these peptides could represent a valid alternative strategy to treat pain sensation after inflammation avoiding the side effects related to hyperthermia and decreased sensitivity to painful levels induced by the direct blocking of TRPV1.

The intriguing research on the interactome of TRP channels could also have great potential in cancer therapy. Indeed, direct targeting of PPI involving TRP channels could minimize side effects by specifically activating/inhibiting only the cellular pathways associated with a specific interaction (Mabonga and Kappo 2019; Scott et al. 2016). Some examples of PPI inhibitors currently undergoing clinical stages of development for cancer treatment are reviewed in (Scott et al. 2016).

To date, no PPI modulators related to ion channels have been approved for human treatment. However, several *in vivo* data strongly support the great therapeutic potential of peptides capable of impairing the association between ion channel and their interactors (Fisher, Btesh, and McNaughton 2013; Schulie et al. 2020; Brittain et al. 2011; Fischer et al. 2013; Tu, Chang, and Bikle 2005). As regards TRP channels, a synthetic

peptide mimicking the PLC-γ1 SH2 domains and revealing an anti-tumoral activity in breast cancer (Katterle et al. 2004), has been found to interact with TRPC1 (Tu, Chang, and Bikle 2005). Similarly, a peptide designed on the γ-aminobutyric acid type A (GABAA) receptor-associated protein (GABARAP) has recently been proposed as a good candidate to promote TRPV1-associated suppression of breast cancer progression (Saldías et al. 2021) due to its direct interaction with TRPV1 (Laínez et al. 2010). Furthermore, the design of peptides able to promote TRPV1-TRPA1 interaction has been proposed as promising candidates to treat pain (Weng et al. 2015).

Overall, growing pieces of evidence suggest that the manipulation of protein-protein interactions involving TRP channels could represent a reliable approach to improving current therapeutic strategies for fighting cancer (Mabonga and Kappo 2020; Corbi-Verge and Kim 2016). Therefore, a deeper mechanistic understanding of these interactions is critical for improving the specificity and selectivity of this innovative approach.

However, despite its high specificity, the use of peptides also has limitations to be taken into consideration such as their poor cell/tissue specificity and membrane penetration capacity (Scott et al. 2016). Moreover, targeting PPIs is more complicated than targeting enzymes or receptors due to the broad and less structured interface of these interactions (Scott et al. 2016). Combining PPI-targeted bioactive peptides with cell-penetrating peptides (CPP) has been shown to be a good strategy to overcome these challenges as it improves cellular uptake and biocompatibility while keeping side effects low *in vivo* (Habault and Poyet 2019; Xie et al. 2020; Kang et al. 2020). Another strategy could involve the employ of nanodelivery systems able to enhance the bioavailability of lipophilic drugs, as discussed in the next section (Ray et al. 2017).

Nanodelivery systems

Although in recent years great advances have been made in biomedical research leading to the discovery and development of many new drugs, currently the main limitation aroused by pharmaceutical and biotech industries is represented by the ability to translate these advances into clinical efficacy, that is to reduce the gap between "drug discovery" and "drug delivery" (drug distribution) (Rosenblum et al. 2018; Parveen, Misra, and Sahoo 2012). As extensively discussed in the previous chapters, carefully targeted approaches are necessary to minimize potential side effects due to the multifunctional roles of TRP channels. Furthermore, nanodelivery systems can help to improve the solubility and therefore the bioavailability/pharmacokinetic profile of lipophilic drugs, thus optimizing their therapeutic action in the desired sites.

The use of many drugs is, indeed, currently limited by factors such as poor solubility and stability in biological fluids, rapid degradation *in vivo* and reduced plasma half-life, as well as non-specific distribution and the subsequent need for administration at high doses. This also applies to many TRP agonists and antagonists, since, as shown in **Tables 11** and **12** for TRPA1 and TRPM8, they are mainly highly hydrophobic aromatic compounds. For this reason, in recent decades an ever-increasing interest has been directed to the development of new systems for the delivery of diagnostic and therapeutic agents, leading to the affirmation of drug delivery as an independent and multidisciplinary research field (Dang and Guan 2020; Lu and Qiao 2018).

The development of nanotechnologies has had a significant impact on the field of drug delivery (Rosenblum et al. 2018). Indeed, the incorporation of both diagnostic and therapeutic agents into nanocarriers was found not only to increase their solubility and stability in biological fluids but also to improve their pharmacokinetic profile and distribution in peripheral tissues. Consequently, once incorporated into such systems the fate of the drug *in vivo* is no longer dependent on its properties but on those of the carrier, which can be suitably controlled (**Fig. 22**).

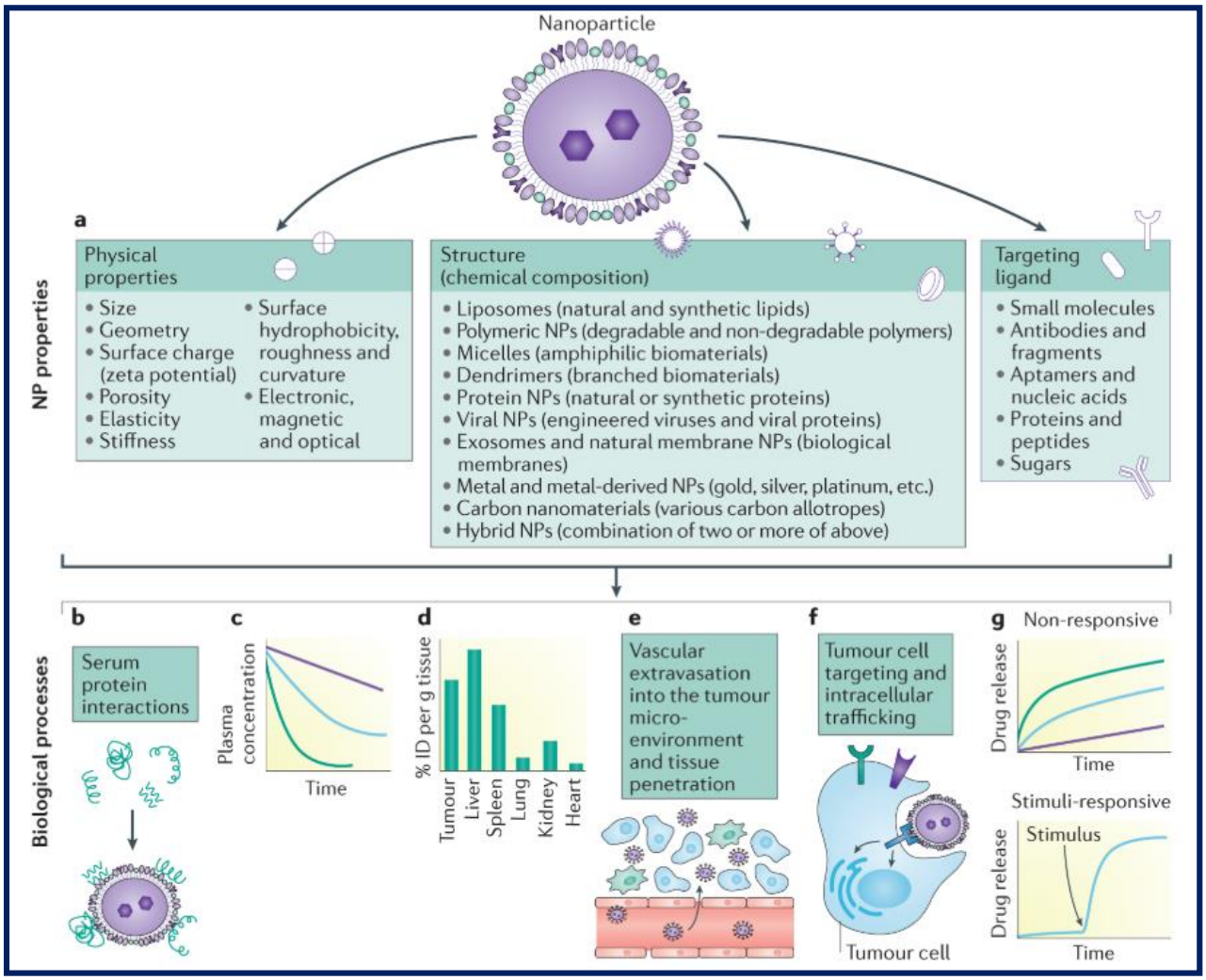

Figure 22. Properties of nanoparticles and their impact on systemic delivery.

a) Physical-chemical properties of nanoparticles (NP) that may affect different processes in vivo including the interaction with serum proteins (b), blood circulation (c), biodistribution (d), vascular extravasation and tissue penetration (e), tumor cell targeting (f), and drug release (g).
NP: nanoparticles; ID: injected dose
Image from (Shi et al. 2017)

Based on the shape, size, and surface characteristics of the nanocarrier used, it is possible to modify and control the ADME of the drug: the nanocarriers protect it from any type of chemical-enzymatic degradation and increase its permanence in the systemic circulation, thus allowing its absorption even in the peripheral districts as well as a prolonged and controlled release over time (Parveen, Misra, and Sahoo 2012) (**Fig. 22**). Furthermore, nanocarriers may also offer the advantage of significantly reducing side effects associated with a non-specific distribution of the drug thanks to targeted delivery (**Fig. 22**). In the case of anticancer diagnostics and therapy, for example, the preferential accumulation of the nanosystem in correspondence

with the tumor tissues is underlying a passive targeting mechanism, associated with the sub-micrometric dimensions of the nanocarriers and the pathophysiological characteristics of tumor tissues. The latter is, in fact, generally characterized by a greater permeability of blood vessels and by the lack of an efficient lymphatic drainage system, which together define the so-called "EPR effect" ("enhanced permeability and retention") (Fang, Islam, and Maeda 2020) (**Fig. 23**). Therefore, unlike the free drug, which diffuses in a non-specific way, the extravasation of the nanocarriers is favored only in correspondence with the fenestrations typically exhibited by the tumor vascular endothelium (gap junctions ranging in size between 100 nm and 2 µm - (Fang, Islam, and Maeda 2020)). Then, the inefficiency of the lymphatic drainage system contributes to favoring the further retention of the nanosystem at the tumor site. However, this type of targeting has some limitations, as its effectiveness depends on several variables that make it difficult to control. First, the degree of vascularization and the porosity of the vessels vary according to the type of tumor and the progress of the neoplastic tissue, and therefore the EPR effect is not always effective (Park et al. 2019); moreover, EPR can lead to the development of “multi-drug resistance” (MDR) by the tumor cells (Peer et al. 2007). However, the employ of nanocarriers allows overcoming these limits by realizing an active targeting of the therapeutic/diagnostic agent. Basically, the surface of such nanosystems may be functionalized with targeting agents (antibodies, peptides, nucleic acids, vitamins, or carbohydrates) able to specifically binding macromolecules selectively exposed on the surface of target cells (Yu, Park, and Jon 2012). In this way, following extravasation, the nanocarriers will be recognized, selectively bound, and internalized by the tumor cells, optimizing the release of the drug at the target site and therefore the effectiveness of the treatment (**Fig. 23**) (Peer et al. 2007).

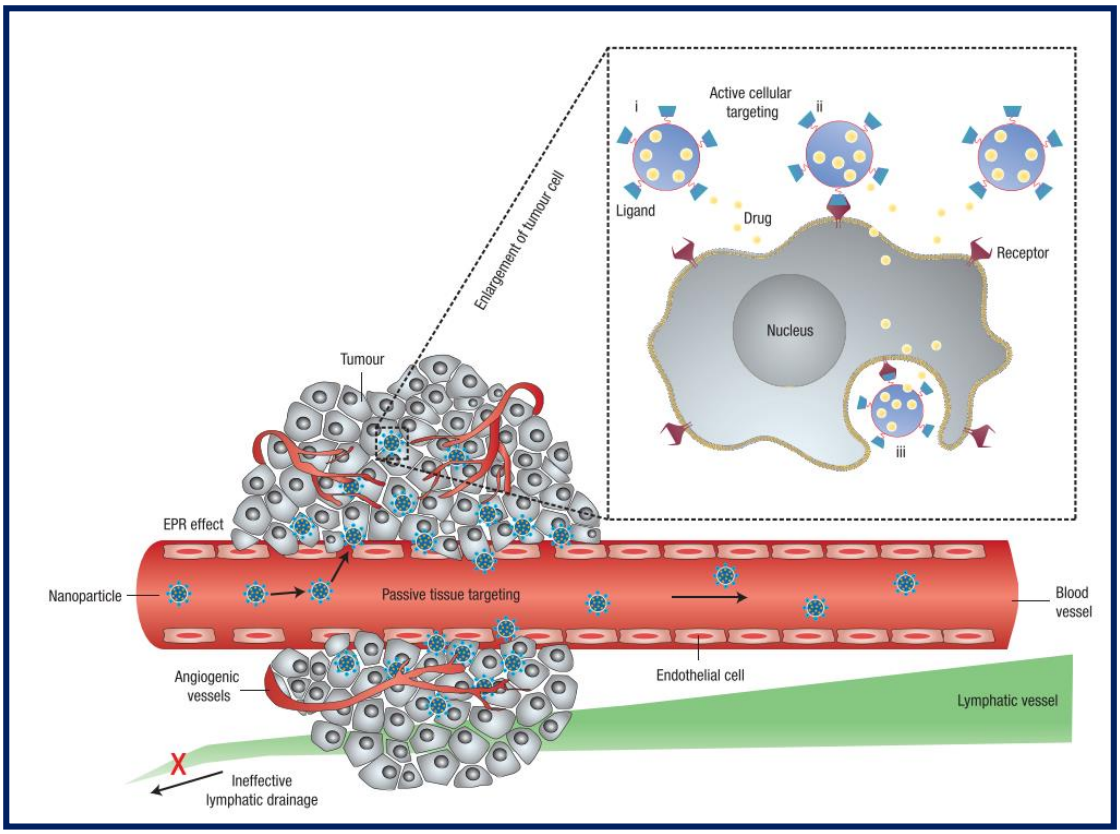

Figure 23. Passive and active targeting of nanoparticles.
Images from (Peer et al. 2007)

However, it should be noted that, despite the number of successful pre-clinical studies, among the passively targeted nanocarriers proposed only a few have been approved for clinical use in cancer therapy, whereas none of the actively targeted nanocarriers are currently on the market (**Table 13**) (Shi et al. 2017; Piscatelli et al. 2021).

Commercial name	Platform	Active drug	Indications	Year and place of approval	
Doxil™/Caelyx™	PEG-liposomes	doxorubicin	HIV-related Kaposi's sarcoma / ovarian cancer / multiple myeloma	1995	
DaunoXome™	liposomes	daunorubicin	HIV-related Kaposi's sarcoma	1996	
DepoCyt	liposomes	cytarabine	refractory Kaposi's sarcoma / recurrent breast and ovarian cancer	1999	US
Onco TCS	liposomes	vincristine	relapsed aggressive non-Hodgkin's lymphoma	1999	
Abraxane™	albumin NP	paclitaxel	metastatic breast, lung and pancreatic cancer	2005	
Marqibo™	liposomes	vincristine sulfate	acute lymphoblastic leukaemia	2012	

Onivyde™/ MM-398™	PEG-liposomes	irinotecan	combinatorial therapy of metastatic pancreatic cancer	2015	
Myocet™	liposomes	doxorubicin	combinatorial therapy of recurrent breast and ovarian cancer	2000	Europe
Mepact™	liposomes	mifamurtide	high-grade resectable non-metastatic osteosarcoma	2009	
NanoTherm	Iron oxide NP	NA	glioblastoma	2011	
Vyxeos™	liposomes	cytarabine & daunorubicin	acute myeloid leukaemia	2017	
Genexol-PM™	PEG-polymeric micelle	paclitaxel	metastatic breast and ovarian cancer / NSCLC	2006	Korea
SMANCS™	Polymer conjugate	neocarzinostatin	Liver and renal cancer	1993	Japan

Table 13. Approved nanodelivery systems with anticancer indications.
NP: nanoparticles; NA: not applicable; NSCLC: non-small cell lung cancer

Despite the precise definition of nanomaterials, i.e. objects with size in a range between 1 and 100 nm, in the context of drug delivery the term nanocarriers often refers to systems with dimensions between 10 and 1000 nm (Parveen, Misra, and Sahoo 2012). Based on their shape and composition, different types of nanocarriers can be distinguished (**Fig. 22**):

- Inorganic nanocarriers
  - ceramic nanoparticles
  - magnetic nanoparticles
  - gold nanoparticles
  - quantum dots
- Organic nanocarriers
  - polymer nanostructures
  - dendrimers
  - lipid vesicular nanosystems (micelles, liposomes, ethosomes, niosomes)
  - lipid nanoparticles and nanocapsules

In the context of cancer diagnostics and therapy, in order to allow rapid and effective translation from research to the clinical phase, the nanocarrier must have some fundamental characteristics:

- It must be soluble or be in a colloidal state in an aqueous environment

- It must have a low aggregation rate, good storage stability, and an adequate half-life in circulation
- It must exhibit a higher uptake efficiency in target cells than in healthy tissues
- It must be made of biocompatible, well-characterized, and easily functionalizable materials

As shown in **Table 13**, all nanocarriers currently approved by the Food and Drug Administration (FDA) or by the European Medicines Agency (EMA) are organic nanosystems since they exhibit greater biocompatibility than those of inorganic nature (**Table 13** and **Fig. 24**). More precisely, these are liposomes and polymer nanoparticles. The characteristics and main advantages of lipid nanocarriers for therapeutic purposes will be mentioned in the next section.

Lipid nanoparticles

Compared to polymer nanoparticles, lipid nanocarriers have further advantages, including higher biocompatibility and a wider versatility of the materials that can be used for their synthesis (Battaglia and Gallarate 2012). The first lipid system for drug delivery developed in the 1950s was an **oil-in-water nanoemulsion**, the use of which, however, is limited by problems of physical instability induced by the drug, which tends to come out quickly from lipid droplets. This drawback was overcome with the subsequent development, in the 1960s, of vesicular lipid nanosystems: the confinement of the therapeutic/diagnostic agent within these structures made it possible to reduce its release rate, allowing the development of more stable nanocarriers (**Fig. 24**).

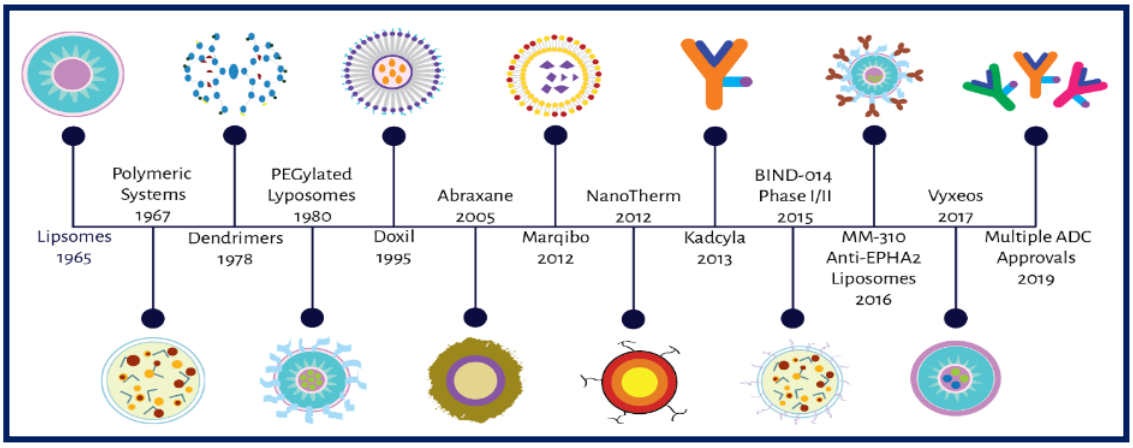

Figure 24. Historical development of nanonystems.
Image from (Piscatelli et al. 2021)

Micelles and liposomes are spherical vesicular structures made up of phospholipids, which, in the case of liposomes, are organized to form a phospholipid bilayer that encloses an aqueous internal cavity. These

systems have the advantage of allowing the trapping of both lipophilic drugs (within the phospholipid bilayer) and hydrophilic (within the aqueous core) and have been extensively investigated in recent decades in the pharmaceutical and cosmetic fields (Naseri, Valizadeh, and Zakeri-Milani 2015). Some liposomal formulations are currently on the market. However, many of their potential applications are limited by some disadvantages (Naseri, Valizadeh, and Zakeri-Milani 2015) including:

- poor physical stability
- low encapsulation efficiency
- rapid blood clearance due to the action of the reticuloendothelial system (RES)
- phenomena of absorption and intermembrane transfer due to interactions with the cell surface
- susceptibility to heat and some types of radiation that make sterilization difficult
- costs associated with their synthetic development
- difficulty in scale-up

Since the 1970s **nanocarriers with a particle structure** have been developed to overcome the limitations associated with vesicular systems such as the lack of stability over time (Grimaldi et al. 2016). Indeed, the greater structural rigidity gives nanoparticles greater chemical-physical stability. Lipid nanoparticles are then distinguished, based on their structure, into two families: nanospheres, characterized by a homogeneous structure, and nanocapsules, which instead exhibit a typical core-shell structure (Battaglia and Gallarate 2012). The main advantages associated with the use of lipid nanoparticles compared to other traditional nanocarriers are good biocompatibility, low cytotoxicity, elimination of organic solvents in the preparatory processes, the possibility of production on an industrial scale, modulation of drug release, broad application spectrum (oral, dermal, intravenous, etc.) (Battaglia and Gallarate 2012). In particular, in this Ph.D. thesis two specific types of lipid nanocarriers have been investigated, i.e. solid lipid nanoparticles (SLN) and quatsomes (QS).

Many chemotherapeutic and diagnostic agents have been efficiently incorporated into nanoparticles of various natures and, as demonstrated by the results obtained by various research groups, these nanosystems have revealed a wide potential in anticancer therapy and detection (Subramaniam, Siddik, and Nagoor 2020). As regards TRP channels, it has been reported that curcumin-loaded nanoparticles are effective in targeting PCa growth through TRPA1 activation (Yallapu et al. 2014).

Moreover, we have recently described the incorporation of the TRPM8 agonist WS12 into lipid nanocapsules (LNC) with a hybrid structure between polymeric nanocapsules and liposomes consisting of an oily liquid core surrounded by a layer of lecithins and hydrophilic surfactant (Grolez et al. 2019). The aim was to improve WS12 solubility in aqueous solutions and thus its applicability *in vivo*. Interestingly, we found that

beyond increasing its apparent aqueous solubility by a factor of at least 60, the incorporation in such as nanosystem increases the affinity of the lipophilic agonist for TRPM8 by 10 times. Functionalization of LNC using an antibody against the prostate-specific membrane antigen (PSMA) could further enhance this pharmacological tool by allowing a specific target to the prostate and thus limiting the possible side effects of TRPM8 activation in other organs (Yallapu et al. 2014). The same type of nanodelivery system was found promising to enhance the Hypericin-induced production of singlet oxygen ($^1O_2$) in PDT application (Barras et al. 2013). Similarly, the incorporation of Hypericin into SLN has been shown to improve *in vitro* the physical-chemical properties of this photosensitizer (Lima et al. 2013) as well as others (Navarro et al. 2014). Indeed, the incorporation of PS within nanoparticles not only enhances their solubility in physiological conditions by shielding their hydrophobicity but also improves their spectroscopic properties probably due to the increased stabilization of the molecule within the lipidic microenvironment.

1.4.4 Photodynamic therapy in prostate cancer

Fundamentals

The use of light as a therapeutic device has a long history, which begins with heliotherapy practiced in ancient Egypt, China, and India. Following the reintroduction of phototherapy by Reiki in 1855, the interest in this therapeutic approach, as a non-invasive treatment method, has significantly intensified in the fields of oncology, dermatology, ophthalmology, and microbiology, until approval by the FDA (1993) of the first drug used for PDT, a hematoporphyrin derivative known under the trade name of Photofrin® (Dougherty et al. 1998).

PDT is characterized by three key elements, whose combination leads to the destruction of the target tissue:

1) a photochemically active drug called photosensitizer (PS),
2) a non-thermal light source that emits at a specific wavelength
3) molecular oxygen dissolved in the tissue

As shown in **Figure 25**, the treatment begins with the administration of PS, which, after a certain time interval called “drug-to-light interval” (DLI) which may vary from hours to several days, is selectively excited with a light radiation corresponding to the maximum absorption wavelength of the PS. More specifically, the PS is irradiated *via* laser or LED through optical fibers. To allow deeper penetration of light into the tissue,

the PS must absorb in the region of the electromagnetic spectrum corresponding to the so-called transparency window of the tissues (650-900 nm) (Dąbrowski et al. 2016). Upon irradiation, PS may be embedded within or on the surface of a tumor, move freely through the tumor's vascular system, or may adhere to organelles within cancer cells or be generated in them although less commonly in Clinical PDT (i.e. protoporphyrin IX is formed in mitochondria following administration of 5-aminolevulinic acid (5-ALA)).

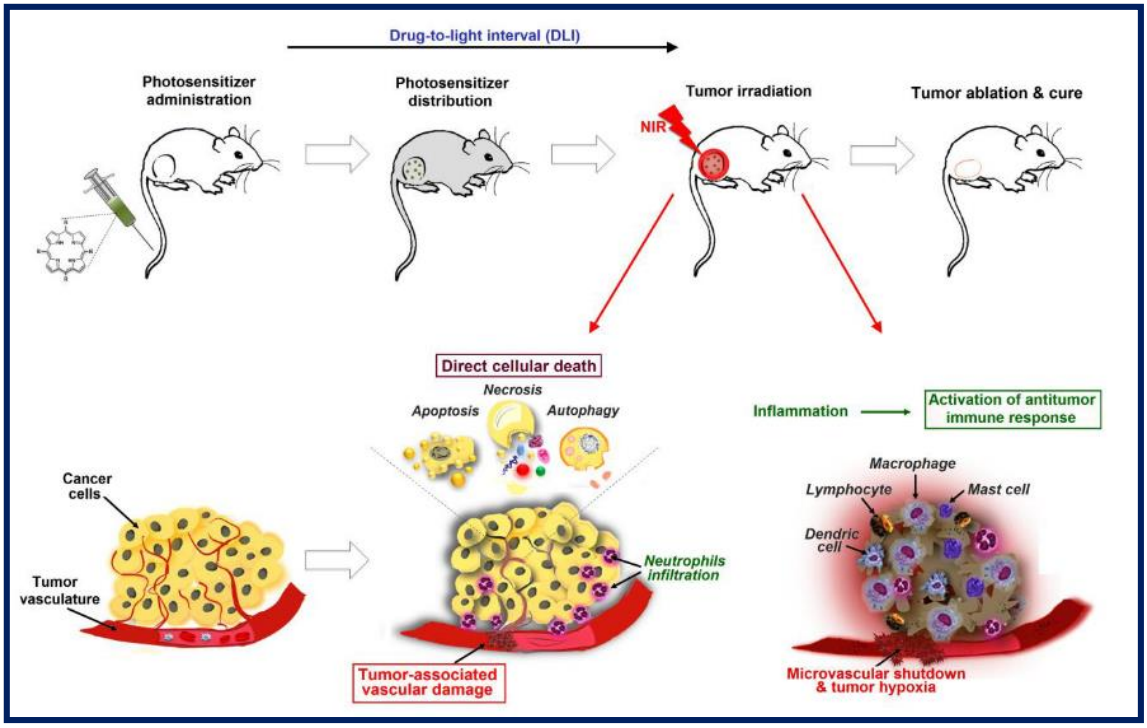

Figure 25. Key steps and biological mechanisms underlying PDT treatment.
Image from (Dąbrowski et al. 2016)

Irradiation of tumor tissue can lead to three main biological consequences:

1) Direct cell death due to necrosis, apoptosis, and/or autophagy (Dąbrowski and Arnaut 2015; Castano, Demidova, and Hamblin 2004)
2) Occlusion of intra- and peri-tumor blood vessels (Preise, Scherz, and Salomon 2011)
3) Stimulation of the immune system and induction of pro-inflammatory processes (Gollnick and Brackett 2010)

All these biological processes are caused by the oxidative stress induced by the PS at the cellular level. Basically, the PS, after being excited by the light radiation, dissipates part of the energy acquired through the so-called intersystem conversion pathway (ISC), which, *via* the excited triplet state, ultimately results in the formation of ROS and $^1O_2$ (**Fig. 26**). The latter may exert its oxidizing activity throughout the cell volume

(average distance 150 nm) by oxidizing and/or oxygenating the functional groups of various biologically relevant macromolecules such as proteins, sugars, lipids and nucleic acids (Silva et al. 2016). On the contrary, the photo-damage induced by the other ROS that originates from the type I photochemical process ($O_2^{\bullet-}$, $OH^{\bullet}$, H_2O_2), is limited to the cellular compartment in which PS is localized, as these radical species, despite being extremely reactive, have a very short diffusion radius (1 nm) and a short lifetime due to the sophisticated cellular systems responsible for their neutralization.

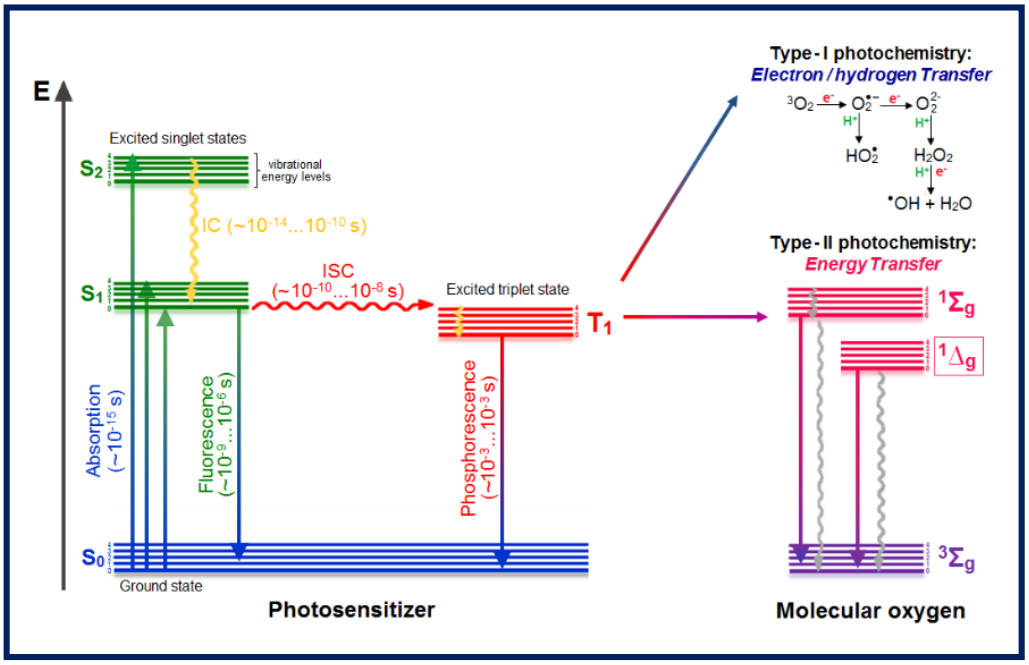

Figure 26. Jabłoński diagram illustrating the photophysical principles of PDT.

The incident light radiation promotes the passage of an electron of the PS molecule from the fundamental S_0 to the excited singlet state S_1 or S_2; then, the unstable excited state dissipates the absorbed energy via ISC, which foresees the spin inversion of the excited electron and its consequent passage to a state of multiplicity of spin 3 (excited state of singlet → excited state of triplet); starting from the triplet state, the excess energy can be then dissipated through the transfer of electrons/hydrogen (type I process) or energy (type II process) to the molecular O_2 present in the surrounding environment.
S: discrete singlet states; T: triplet states; IC: internal conversion; ISC: intersystem crossing.
Image from (Dąbrowski et al. 2016)

As previously mentioned, the oxidative damage caused at the target tissue can lead to direct cell death due to necrosis, apoptosis and/or autophagy, occlusion of intra- and peri-tumor blood vessels, and/or stimulation of the immune system with the consequent induction of pro-inflammatory processes. The contribution of each process to the final destruction of the target tissue and the final therapeutic efficacy of the treatment depends on several factors (Dąbrowski et al. 2016), including:

- subcellular localization of the PS
- binding of the PS to albumin and/or blood lipoproteins
- pharmacological dose
- duration of the DLI
- fluence rate of light
- O_2 concentration in the tumor

The photophysical and photochemical features, which define a good PS are:

- Ability to absorb electromagnetic radiation within the range of wavelengths that define the so-called tissue transparency window (650-850 nm)
- High molar extinction coefficients
- Low quantum yield of fluorescence
- Good chemical-physical stability and photostability
- High quantum yield of $^1O_2$ or ROS production

Furthermore, the PS should exhibit stability in body fluids, a preferential distribution in tumor cells, low cytotoxicity in the dark and high cytotoxicity following light excitation, a pharmacokinetic profile that allows the use of an appropriate DLI, and a reasonable body clearance which would disadvantage any phototoxic side effects in healthy tissues and hypersensitivity to light after PDT treatment (Dąbrowski and Arnaut 2015; Dąbrowski et al. 2016).

The main PS studied and approved for clinical applications of PDT are porphyrins, chlorines, bacteriochlorines, and phthalocyanines (**Fig. 27**), all derived from the tetrapirrolic macrocycle typical of many natural pigments such as hematin (porphyrins), chlorophyll (chlorophyll) and bacteriochlorophyll (bacteriochlorin).

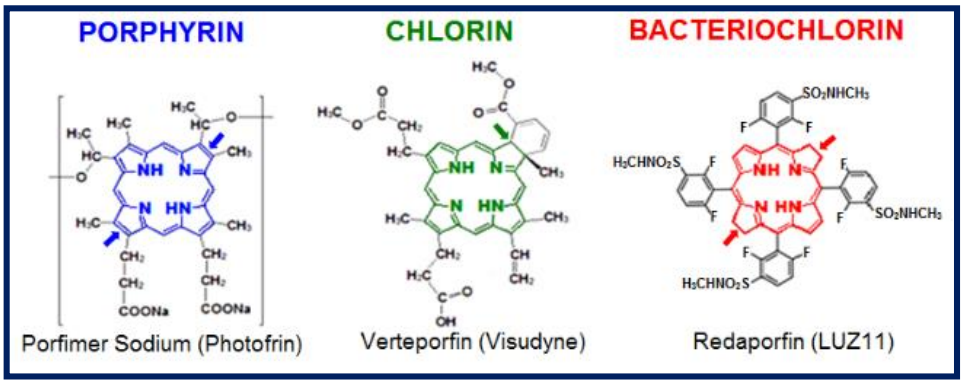

Figure 27. Structures of selected porphyrins (porfimer sodium), chlorins (verteporfin) and bacteriochlorins (redaporfin) currently in clinical use.

These molecules have many of the characteristics that define a good PS mentioned above, but also have some disadvantages including a low molar extinction coefficient (in the case of Porphyrins and Chlorines), which leads to the need to use high doses of PS, a low tissue penetration, poor tumor selectivity, a long half-life and low clearance with consequent non-negligible side effects affecting healthy tissues (Dąbrowski and Arnaut 2015; Dąbrowski et al. 2016). As an example, Photofrin®, the first photosensitizing agent approved for PDT by the FDA in 1993, in addition to being able to cause inflammatory reactions and intense necrosis at the treated site, it causes widespread and prolonged photosensitivity in the patient, which can last up to several weeks after the treatment (Dougherty, Cooper, and Mang 1990). For this reason, in recent years research has focused on the development of more effective PS. In this context, polymethine dyes (PMD) which will be discussed later, have proved to be promising candidates.

PDT in prostate cancer

Currently, significant shortcomings and uncertainties surround PDT as a treatment for low-grade prostate cancer due to the open debate about the benefits of active surveillance over the harms associated with early-stage treatment. Indeed, in 2020 the Oncologic Drugs Advisory Committee within the FDA voted against approval of padeliporfin di-potassium (water-soluble Tookad®) for PDT treatment of localized PCa in the United States, not considering it significantly more effective than active surveillance (Todak 2020; "FDA Briefing Document Oncologic Drugs Advisory Committee Meeting NDA 212578/S000 Padeliporfin Di-Potassium (TOOKAD) Applicant: Steba Oncology, Inc" 2020).

However, this methodology continues to be vigorously studied and refined to improve treatment parameters and its success while reducing side effects of concern to oncologists. Of note, this type of focal therapy is only appropriate for patients with localized prostate cancer and not in cases of advanced metastatic diseases that have already affected surrounding structures such as nodes, seminal vesicles, and extracapsular extensions (Valerio et al. 2014).

Currently, **most PS used in clinical trials for PCa** are vascular rather than tissue-based excited by low-power laser or LED within minutes following intravenous administration. The main advantages associated with vascular PS are faster clearance and reduced photosensitivity. Moreover, in contrast to other PDT applications exploiting flat tip fibers conically, in PDT PCa treatment the light is delivered by optical fibers possessing a cylindrical diffusion tip for spherical illumination (Shafirstein et al. 2017). As depicted in **Figure 28**, the optical fibers are placed within plastic catheter needles that are positioned in the prostate gland *via* the perineum (Moore, Pendse, and Emberton 2009). More specifically, catheter placement is accomplished by TRUS or MRI using a BT template and to ensure precise positioning, patients undergo general anesthesia

before the procedure so that they remain immobile. Using vascular PS, the DLI is in the order of minutes. For instance, Moore *et al*. reported a continuous illumination at 753 nm for 22 min 15 s to activate the vascular padeliporfin 10 min after administration (Moore, Pendse, and Emberton 2009). Furthermore, depending on the morphology of the tumor, the number of light applications, and consequently the total procedure time may vary.

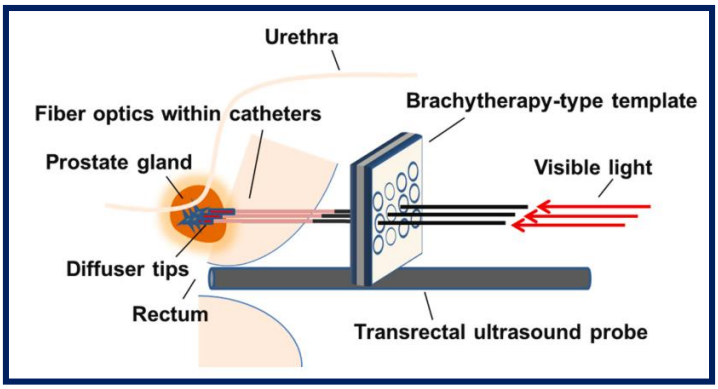

Figure 28. Diagram depicting prostate PDT apparatus.

The main PS currently evaluated for prostate PDT are summarized in **Table 14**.

Photosensitizers	Type	λ_{ex} (nm)	Drug dose (mg/Kg)	Light dose	Drug-Light Interval	Side effects	Stage	Ref.
Temoporfin (mTHPC) (Foscan® m-tetrahydroxyphenyl chloride)	Tissue-based	652	0.15	20/50 J	3 days	prolonged photosensitivity	I	(Nathan et al. 2002)
			0.15	50-100 J/cm	2-5 days			(Moore et al. 2006)
5-aminolevulinic acid (5-ALA) derived protoporphyrin IX	Tissue-based	635	20	250 J/cm	4 h	n.d.		(Zaak et al. 2003)
Motexafin lutetium (MLu)	Vascular	732	0.5-2	25-100 J/cm^2	3-24.6 h	Low grade (Grade I) genitourinary side-effects	I	(Verigos et al. 2006)
			0.5-2	25-150 J/cm	24 h			(Du et al. 2006)
Padoporfin (Tookad®)	Vascular	763	2	32 J/cm^2	20 min	lessening of voiding function and recto-urethral fistula		(Trachtenberg et al. 2008; Trachtenberg et al. 2007)
Padeliporfin (water soluble Tookad®)	Vascular	753	4-6	200-300 J/cm	10 min	prostatitis, acute urinary retention	II	(Azzouzi et al. 2013; 2017; Eymerit-Morin et al. 2013;

								Barret et al. 2013; Moore et al. 2015; Lebdai et al. 2015; 2017; Taneja et al. 2016; Gill et al. 2018; Noweski et al. 2019)

Table 14. Photosensitizers in clinical studies for prostate PDT.

Recently, several PDT conjugates have been proposed for treating prostate carcinoma. Among them, a novel unsymmetrical phthalocyanine conjugated with a cyclic arginine-glycine-aspartic acid sequence (RGDyK) was found promising for its high selectivity towards $\alpha v\beta_3$ integrin overexpressed by cancer cells as well as by tumor blood vessels (Luan et al. 2016). Then, chemical conjugation between the AR antagonist abiraterone and a cyanine used for cancer imaging and photodynamic therapy in the past (IR-780) has been proposed (Yi et al. 2016). Moreover, nano-assemblies combining 5-ALA and squalene (Babič et al. 2018) or protoporphyrin IX mixed with polyamines highly produced by rapidly growing cells have been proved to lead to better acinar adenocarcinoma selectivity and superior photodynamic therapy efficiency (Fidanzi-Dugas et al. 2017). Similarly, the combination of PS like pyropheophorbide A (PheoA) and bacteriochlorophyll with a long-circulating peptide (LC-Pyro) to prolong plasma circulation time and PSMA to address selective targeting of the prostate has proved to be a very promising approach (Harmatys et al. 2018; Overchuk et al. 2020). Indeed, combining targeting, selectivity and pharmacokinetic properties greatly increases treatment efficiency providing a significant improvement in pharmacokinetics and tumor accumulation (Harmatys et al. 2018). Other examples of PSMA-targeted photosensitizer conjugates have been proposed such as PSMA inhibitors coupled to porphyrin dyes like Ppa-CTT-54 (Liu, Wu, and Berkman 2010; Liu et al. 2009) or IRDye700DX (Wang et al. 2016; Chen et al. 2017). PSMA-1-IR700DX conjugates revealed a good potential in delaying tumor growth and prolonging survival in prostate adenocarcinoma mouse models (Watanabe et al. 2015; Lütje et al. 2014). PSMA-targeted PDT has not yet reached the stages of clinical development but is very promising. The main problem associated with this type of conjugates is that they can only be exploited for PSMA-positive tumors as they are ineffective in the absence of this specific membrane antigen. Finally, encouraging results come from the use of curcumin and some curcuminoids with improved tissue penetration on PDT treatment of LNCaP PCa cells (Kazantzis et al. 2020). Of note, curcumin is also known for its action as a TRP activator.

Despite the promising results obtained with the use of some PS, certainly including Padeliporfin, however, it remains to be determined whether the progression of the disease is reduced compared to active surveillance. Notably, as opposed to RT approaches, precise computer-aided dosimetry cannot be exploited

in PDT since light intensity can be reduced by scattering and absorbing processes involving tissues (Kim and Darafsheh 2020). Moreover, the efficiency of the process may be affected by interactions occurring between PS molecules and/or rapid bleaching which leads to lower ROS yields. Not to mention the main problem associated with the PDT of cancer which is the characteristic hypoxia of tumor tissues. Moreover, the penetration of light through tissues, the oxygen concentration within the prostate and the dynamic interactions occurring between light, PS, and O_2 during PDT treatment are highly variable (Kim and Darafsheh 2020). Hence, great inter- and intra-patient variability was observed in several clinical studies (Du et al. 2006; Trachtenberg et al. 2008). Taking into account all the parameters that may influence treatment efficiency including the photosensitizer dosage (mg/kg of body mass), the light dose (in J or J/cm), and the drug-light interval as well as all the complex interactions that can occur between them, the precise impact of PDT on patients is difficult to measure and predict.

Finally, PS are also employed for photodynamic diagnosis (PDD) helping to detect cancerous lesions and delineate tumor margins for resection (Bochenek et al. 2019). For example, PSMA-PS conjugates appear promising for intraoperative near-infrared (NIR) fluorescence imaging purposes, helping to perform a complete resection of PCa with negative surgical margins (Yossepowitch et al. 2014; Lütje et al. 2014; Eiber et al. 2017).

Polymethine dyes as new class of photosensitizer

The term "polymethine dyes" (PMD) was introduced by Koening in 1922 to indicate a class of colored organic compounds characterized by the presence, in their structure, of a chain of methine groups (-CH=) conjugated, generally in trans configuration (**Fig. 29**). In accordance with the theory of the triad of Daehne, they represent one of the three main types of conjugated systems (Daehne and Koenig 1922), i.e. systems consisting of pairs of π bonds alternating with single bonds, in which the interaction between the π bonds leads to a partial overlap of the p orbitals belonging to the two carbon atoms joined with a simple bond, giving rise to an electronic delocalization (**Fig. 29**). By virtue of this electronic delocalization, PMDs are resonant hybrids. Unlike the other conjugated systems (polyenes and aromatics), PMD have an electron-donor group (D) and an electron-acceptor group (A) at the two ends of the polymethine chain: due to the mesomeric effect, the delocalized π electrons move between D and A, giving a positively or negatively charged molecule (cationic or anionic PMD).

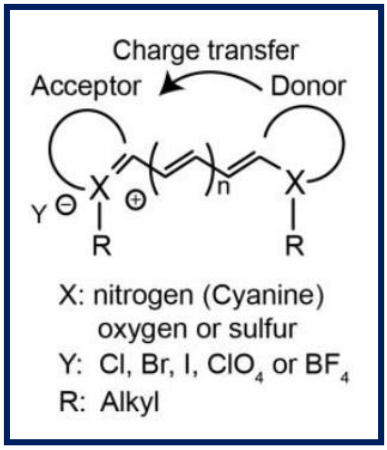

Figure 29. General structure of polymethine dyes.

n: number of vinyl groups that make up the polymethine chain
Image from (Li, Zhao, and Zhang 2020)

In recent years, some PMD belonging to the family of cyanines and squaraines have revealed a good potential in PDT applications, thanks to their excellent photophysical properties and remarkable quantum efficiency of $^1O_2$ production. Moreover, their great structural variability and the possibility of directing their synthesis in such a way as to obtain molecules with the desired chemical-physical properties has further increased the great interest in PMD for PDT (Dąbrowski and Arnaut 2015). However, due to their relatively recent investigation in this field, no PMD is currently in clinical trials.

Atchison *et al*. identified two iodinated cyanines showing good phototoxicity following light beam irradiation and low cytotoxicity in the dark both *in vitro* and in a mouse model of pancreatic cancer (Atchison et al. 2017). Furthermore, cyanines revealed an interesting preferential distribution in tumor tissues, thus providing potential for high specificity of targeting *in vivo*. In agreement with other data reported in the literature, this study by Atchison *et al*. also highlighted that the introduction of a **heavy atom** like iodine in the heterocyclic ring significantly improves $^1O_2$ production efficiency and consequently increases the photodynamic activity of the PMD (Redmond et al. 1997); by contrast, in the absence of the heavy atom, PMD have lower yields of inter-system conversion and decay from the excited state mainly through the singlet path (Redmond et al. 1997).

The nature of the substituents was found to affect not only PMD activity but also their uptake and intracellular localization, as it determines the **degree of lipophilicity/hydrophilicity** of the molecule. In this regard, a key role is played by the nature and length of the alkyl chain linked to the quaternary N atom (N-alkyl chain). In particular, chains that are too short or too long cause a rapid elimination of the molecule from the body because either they do not give the molecule a degree of lipophilicity sufficient to allow the crossing

of the cell membrane (too short) or they hinder its crossing due to the formation of aggregates(too long). Therefore, intermediate chains such as N-butyl seem to confer to the molecule the characteristics of uptake and mitochondrial localization that are ideal for PDT applications (Shi, Wu, and Pan 2016; Onoe et al. 2014).

Squaraines have a lower synthetic development than cyanines because they are more recent, but they too have revealed a great application potential in the field of PDT (Ramaiah et al. 1997; 2002; 2004; Rapozzi et al. 2010; Avirah et al. 2012; Soumya et al. 2014; Shafeekh et al. 2014; Serpe et al. 2016). In fact, in addition to exhibiting intense ($\varepsilon \approx 105\ M^{-1}cm^{-1}$) absorptions in the near-infrared region some squaraines, suitably substituted, have been shown to possess excellent photophysical properties and remarkable quantum efficiency of $^1O_2$ production (Ramaiah et al. 1997). Furthermore, this class of molecules revealed poor cytotoxicity in the dark and the ability to promote, on the other hand, a strong dose-dependent photo-induced toxic effect on various tumor cell lines (Rapozzi et al. 2010). The structure-localization-activity relationships shown by the squaraines are very similar to those found with cyanines (Soumya et al. 2014; Serpe et al. 2016). As regards, for example, the so-called "heavy atom effect", Ramaiah *et al.* have shown that when the terminal heterocycle is replaced with a heavy atom the phototoxicity of the molecule is more marked (Soumya et al. 2014). This effect was also confirmed by a recent study conducted by Serpe *et al*. on a new class of squaraines based on the indolenine ring (Serpe et al. 2016). This study, in addition to confirming the effect that the introduction of a halogen within the indolenine ring has on the photodynamic activity of this class of compounds, has also highlighted the role played in this regard by the length of the N-alkyl chain: only the molecules with a side chain consisting of four carbon atoms (C4) lead to a significant decrease in cell growth following irradiation. This is probably due to the fact that the greater lipophilicity of the structure facilitates the cellular uptake of the molecule, as observed in the case of cyanines (Onoe et al. 2014). Furthermore, also in this case, the PS showed a preferential accumulation in the mitochondria. In conclusion, from a SAR (structure-activity relationship) point of view, it is clear that the pharmacological activity of PMD is notably influenced not only by the presence of a heavy atom in the terminal donor group but also by the hydrophilic-lipophilic balance of the molecule (Serpe et al. 2016). Furthermore, by increasing the length of the polymethine bridge it is possible to shift the absorption of the PMD to gradually increasing wavelengths until it falls perfectly within the range of the so-called “tissue transparency window” mentioned in the previous section.

Taking into account their peculiar spectroscopic properties together with their preferential accumulation in cancer cells (Luo et al. 2011; Yang et al. 2010; Tan et al. 2012), PMD have also proved useful tools for cancer imaging, allowing to detect not only large tumor areas but also metastases and circulating tumor cells (Yang et al. 2010; Zhang et al. 2010). For this reason, PMD are defined as native multifunctional probes (Luo et al. 2011), as they can act simultaneously as imaging agents and targeting.

The main challenges associated with the biomedical application of PMD are due to their structural characteristics. In particular, the presence of extensive conjugated domains and highly hydrophobic aromatic structures result in poor solubility and low chemical stability, especially in aqueous solutions. Moreover, the more the dye absorption is shifted to wavelengths close to infrared and suitable for biomedical application, the less stable its structure is. Therefore, the main application limitations associated with PMD NIR are the tendency to form aggregates, the sensitivity to photobleaching, and the tendency to chemical degradation when in solution. A valid approach to overcome this limit and improve PMD bioavailability is represented by their incorporation into different nanoparticle systems. To date, several studies have reported the efficient incorporation of PMD into organic nanoparticles, such as micelles (Kirchherr, Briel, and Ma 2009; Sreejith et al. 2015), liposomes (Zhang et al. 2014) and lipid nanoparticles (Texier et al. 2009; Jacquart et al. 2013; Mérian et al. 2015).

1.5. References for the introduction

Abécassis I,, Olofsson B,, and Schmid M. **2003**. "RhoA Induces MMP-9 Expression at CD44 Lamellipodial Focal Complexes and Promotes HMEC-1 Cell Invasion." *Exp Cell Res.* 291 (2): 363–76. https://doi.org/10.1016/j.yexcr.2003.08.006.

Abed E,, and Moreau R. **2009**. "Importance of Melastatin-like Transient Receptor Potential 7 and Magnesium in the Stimulation of Osteoblast Proliferation and Migration by Platelet-Derived Growth Factor." *American Journal of Physiology - Cell Physiology* 297 (2): 360–68. https://doi.org/10.1152/ajpcell.00614.2008.

Abelson M.B., Corcoran P., and Lnea K. **2017**. Transient receptor potential cation channel subfamily M member 8 (TRPM8) Antagonist and methods of use. Patent. WO2017062570, issued 2017.

Abriel H., Syam N., Sottas V., Amarouch M.Y., and Rougier J.S. **2012**. "TRPM4 Channels in the Cardiovascular System: Physiology, Pathophysiology, and Pharmacology." *Biochemical Pharmacology*. https://doi.org/10.1016/j.bcp.2012.06.021.

Adapala R.K., Thoppil R.J., Ghosh K., Cappelli H., Dudley A.C., Paruchuri S., Keshamouni V., et al. **2016**. "Activation of Mechanosensitive Ion Channel TRPV4 Normalizes Tumor Vasculature and Improves Cancer Therapy." *J Autism Dev Disord* 35 (3): 314–22. https://doi.org/10.1097/CCM.0b013e31823da96d.Hydrogen.

Adapala R.K., Thoppil R.J., Luther D.J., Paruchuri S., Meszaros J.G., Chilian W.M., and Thodeti C.K. **2013**. "Cellular Cardiology TRPV4 Channels Mediate Cardiac Fi Broblast Differentiation by Integrating Mechanical and Soluble Signals." *Journal of Molecular and Cellular Cardiology* 54: 45–52. https://doi.org/10.1016/j.yjmcc.2012.10.016.

Ahmmed G.U., Mehta D., Vogel S., Holinstat M., Paria B.C., Tiruppathi C., and Malik A.B. **2004**. "Protein Kinase Cα Phosphorylates the TRPC1 Channel and Regulates Store-Operated Ca 2 ⁄. Entry in Endothelial Cells *." *The Journal of Biological Chemistry* 279 (20): 20941–49. https://doi.org/10.1074/jbc.M313975200.

Aizawa N., Fujimori Y., Kobayashi J.I., Nakanishi O., Hirasawa H., Kume H., Homma Y., and Igawa Y. **2018**. "KPR-2579, a Novel TRPM8 Antagonist, Inhibits Acetic Acid-Induced Bladder Afferent Hyperactivity in Rats." *Neurourology and Urodynamics* 37 (5): 1633–40. https://doi.org/10.1002/nau.23532.

Aizawa N., Ohshiro H., Watanabe S., Kume H., Homma Y., and Igawa Y. **2019**. "RQ-00434739, a Novel TRPM8 Antagonist, Inhibits Prostaglandin E2-Induced Hyperactivity of the Primary Bladder Afferent Nerves in Rats." *Life Sciences* 218 (December 2018): 89–95. https://doi.org/10.1016/j.lfs.2018.12.031.

Almasi S., Sterea A.M., Fernando W., Clements D.R., Marcato P., Hoskin D.W., Gujar S., and El Hiani Y. **2019**. "TRPM2 Ion Channel Promotes Gastric Cancer Migration , Invasion and Tumor Growth through the AKT Signaling Pathway." *Scientific Reports* 9 (1): 4182. https://doi.org/10.1038/s41598-019-40330-1.

Almirall SA. **2015**. New TRPA1 antagonists. WO2015155306, issued 2015.

———. **2017**a. New TRPA1 antagonists. WO2017060488, issued 2017.

———. **2017**b. New TRPA1 antagonists. WO2017064068, issued 2017.

Alvarez-Berdugo D., Rofes L., Casamitjana J.F., Enrique A., Chamizo J., Viña C., Pollán C.M., and Clavé P. **2018**. "TRPM8, ASIC1, and ASIC3 Localization and Expression in the Human Oropharynx." *Neurogastroenterology and Motility* 30 (11): 5–7. https://doi.org/10.1111/nmo.13398.

Ambudkar I.S., Brito de Souza L., and Ling Ong H. **2017**. "TRPC1, Orai1, and STIM1 in SOCE: Friends in Tight Spaces." *Cell Calcium*. https://doi.org/10.1016/j.ceca.2016.12.009.

Ampem P.T., Smedlund K., and Vazquez G. **2016**. "Pharmacological evidence for a role of the Transient Receptor Potential Canonical 3 (TRPC3) channel in endoplasmic reticulum stress-induced apoptosis of human coronary artery endothelial cells." *Vascular Pharmacology* 76: 42–52. https://doi.org/10.1016/j.vph.2015.07.011.

Anand U., Otto W.R., Facer P., Zebda N., Selmer I., Gunthorpe M.J., Chessell I.P., Sinisi M., Birch R., and Anand P. **2008**. "TRPA1 Receptor Localisation in the Human Peripheral Nervous System and Functional Studies in Cultured Human and Rat Sensory Neurons." *Neuroscience Letters* 438 (2): 221–27. https://doi.org/10.1016/j.neulet.2008.04.007.

Andersson D.A., Filipovic M.R., Gentry C., Eberhardt M., Vastani N., Leffler A., Reeh P., and Bevan S. **2015**. "Streptozotocin Stimulates

the Ion Channel TRPA1 Directly: Involvement of Peroxynitrite." *Journal of Biological Chemistry* 290 (24): 15185–96. https://doi.org/10.1074/jbc.M115.644476.

Andersson D.A., Gentry C., Alenmyr L., Killander D., Lewis S.E., Andersson A., Bucher B., et al. **2011**. "TRPA1 Mediates Spinal Antinociception Induced by Acetaminophen and the Cannabinoid Δ9-Tetrahydrocannabiorcol." *Nature Communications* 2 (1). https://doi.org/10.1038/ncomms1559.

Andersson D.A., Gentry C., Light E., Vastani N., Vallortigara J., Bierhaus A., Fleming T., and Bevan S. **2013**. "Methylglyoxal Evokes Pain by Stimulating TRPA1." *PLoS ONE* 8 (10): 1–9. https://doi.org/10.1371/journal.pone.0077986.

Andersson D.A., Gentry C., Moss S., and Bevan S.. **2008**. "Transient Receptor Potential A1 Is a Sensory Receptor for Multiple Products of Oxidative Stress." *Journal of Neuroscience* 28 (10): 2485–94. https://doi.org/10.1523/JNEUROSCI.5369-07.2008.

Andersson D.A., Nash M., and Bevan S. **2007**. "Modulation of the Cold-Activated Channel TRPM8 by Lysophospholipids and Polyunsaturated Fatty Acids." *Journal of Neuroscience* 27 (12): 3347–55. https://doi.org/10.1523/JNEUROSCI.4846-06.2007.

Andrade E.L., Meotti F.C., and Calixto J.B. **2012**. "TRPA1 Antagonists as Potential Analgesic Drugs." *Pharmacology and Therapeutics* 133 (2): 189–204. https://doi.org/10.1016/j.pharmthera.2011.10.008.

Andrade E.L., Forner S., Bento A.F., Pereira Leite D.F., Dias M.A., Leal P.C., Koepp J., and Calixto J.B. **2011**. "TRPA1 Receptor Modulation Attenuates Bladder Overactivity Induced by Spinal Cord Injury." *American Journal of Physiology. Renal Physiology* 300 (5): 1223–34. https://doi.org/10.1152/ajprenal.00535.2010.

Andrè E., Gatti R., Trevisani M., Preti D., Baraldi P.G., Patacchini R., and Geppetti P. **2009**. "Transient Receptor Potential Ankyrin Receptor 1 Is a Novel Target for Pro-Tussive Agents." *British Journal of Pharmacology* 158 (6): 1621–28. https://doi.org/10.1111/j.1476-5381.2009.00438.x.

Andrè E., Campi B., Materazzi S., Trevisani M., Amadesi S., Massi D., Creminon C., et al. **2008**. "Cigarette Smoke–Induced Neurogenic Inflammation Is Mediated by α,β-Unsaturated Aldehydes and the TRPA1 Receptor in Rodents." *Journal of Clinical Investigation* 118 (7). https://doi.org/10.1172/jci34886.

Andrews M.D., Forselles K.A., Beaumont K., Galan S.R.G., Glossop P.A., Grenie M., Jessiman A., et al. **2015**. "Discovery of a Selective TRPM8 Antagonist with Clinical Efficacy in Cold-Related Pain." *ACS Medicinal Chemistry Letters* 6 (4): 419–24. https://doi.org/10.1021/ml500479v.

Antoniotti S., Fiorio Pla A., Barral S., Scalabrino O., Munaron L., and Lovisolo D. **2006**. "Interaction between TRPC Channel Subunits in Endothelial Cells." *Journal of Receptors and Signal Transduction* 26 (4): 225–40. https://doi.org/10.1080/10799890600784050.

Aragon-Ching J.B., Jain L., Gulley J.L., Arlen P.M., Wright J.J., Steinberg S.M., Draper D., et al. **2009**. "Final Analysis of a Phase II Trial Using Sorafenib for Metastatic Castration-Resistant Prostate Cancer." *BJU International* 103 (12): 1636–40. https://doi.org/10.1111/J.1464-410X.2008.08327.X.

Aramini A., Bianchini G., and Lillini S. **2017**. Preparation of 4-hydroxy-2-phenyl-1,3-thiazol-5-yl methanone derivatives as TRPM8 antagonists. WO2017108632, issued 2017.

Arcas J.M., González A., Gers-Barlag K., González-González O., Bech F., Demirkhanyan L., Zakharian E., Belmonte C., Gomis A., and Viana F. **2019**. "The Immunosuppressant Macrolide Tacrolimus Activates Cold-Sensing TRPM8 Channels." *Journal of Neuroscience* 39 (6): 949–69. https://doi.org/10.1523/JNEUROSCI.1726-18.2018.

Arenas O.M., Zaharieva E.E., Para A., Vásquez-Doorman C., Petersen C.P., and Gallio M. **2017**. "Activation of Planarian TRPA1 by Reactive Oxygen Species Reveals a Conserved Mechanism for Nociception." *Nat Neurosci.* 20 (12): 1686–93. https://doi.org/10.1038/s41593-017-0005-0.

Armisén R., Marcelain K., Simon F., Tapia J.C., Toro J., Quest A.F.G., and Stutzin A. **2011**. "TRPM4 Enhances Cell Proliferation through Up-Regulation of the β-Catenin Signaling Pathway." *Journal of Cellular Physiology* 226 (1): 103–9. https://doi.org/10.1002/jcp.22310.

Asghar M.Y., Magnusson M., Kemppainen K., Sukumaran P., Löf C., Pulli I., Kalhori V., and Törnquist K. **2015**. "Transient Receptor Potential Canonical 1 (TRPC1) Channels as Regulators of Sphingolipid and VEGF Receptor Expression: Implications for Thyroid Cancer Cell Migration and Proliferation." *Journal of Biological Chemistry* 290 (26): 16116–31. https://doi.org/10.1074/jbc.M115.643668.

Asghar M.Y., and Törnquist K. **2020**. "Transient Receptor Potential Canonical (TRPC) Channels as Modulators of Migration and Invasion." *International Journal of Molecular Sciences* 21 (5): 1–15. https://doi.org/10.3390/ijms21051739.

Ashida S., Nakagawa H., Katagiri T., Furihata M., Iiizumi M., Anazawa Y., Tsunoda T., et al. **2004**. "Molecular Features of the Transition from Prostatic Intraepithelial Neoplasia (PIN) to Prostate Cancer: Genome-Wide Gene-Expression Profiles of Prostate Cancers and PINs." *Cancer Research* 64 (17): 5963–72. https://doi.org/10.1158/0008-5472.CAN-04-0020.

Aspenström P. **2004**. "Integration of Signalling Pathways Regulated by Small GTPases and Calcium." *Biochimica et Biophysica Acta - Molecular Cell Research* 1742 (1–3): 51–58. https://doi.org/10.1016/j.bbamcr.2004.09.029.

Asuthkar S., Demirkhanyan L., Mueting S.R., Cohen A., and Zakharian E. **2017**. "High-Throughput Proteome Analysis Reveals Targeted TRPM8 Degradation in Prostate Cancer." *Oncotarget* 8 (8): 12877–90. https://doi.org/10.18632/oncotarget.14178.

Ataga K.I., Smith W.R., De Castro L.M., Swerdlow P., Saunthararajah Y., Castro O., Vichinsky E., et al. **2008**. "Efficacy and Safety of the Gardos Channel Blocker, Senicapoc (ICA-17043), in Patients with Sickle Cell Anemia." *Blood* 111 (8): 3991–97. https://doi.org/10.1182/BLOOD-2007-08-110098.

Atchison J., Kamila S., Nesbitt H., Logan K.A., Nicholas D.M., Fowley C., Davis J., Callan B., McHale A.P., and Callan J.F. **2017**. "Iodinated Cyanine Dyes: A New Class of Sensitisers for Use in NIR Activated Photodynamic Therapy (PDT)." *Chem. Commun.* 53 (12): 2009–12. https://doi.org/10.1039/C6CC09624G.

Atoyan R., Shander D., and Botchkareva N.V. **2009**. "Non-Neuronal Expression of Transient Receptor Potential Type A1 (TRPA1) in Human Skin." *Journal of Investigative Dermatology* 129 (9): 2312–15. https://doi.org/10.1038/jid.2009.58.

Auer-grumbach M., Olschewski A., Papić L., Kremer H., and Meriel E. **2012**. "UKPMC Funders Group Alterations in the Ankyrin Domain of TRPV4 Cause Congenital" 42 (2): 160–64. https://doi.org/10.1038/ng.508.Alterations.

Avirah R.R., Jayaram D.T., Adarsh N., and Ramaiah D.. **2012**. "Squaraine Dyes in PDT: From Basic Design to in Vivo Demonstration." *Org. Biomol. Chem.* 10 (5): 911–20. https://doi.org/10.1039/C1OB06588B.

Azimi I., Milevskiy M.J.G., Kaemmerer E., Turner D., Yapa K.T.D.S., Brown M.A., Thompson E.W., Roberts-Thomson S.J., and Monteith G.R. **2017**. "TRPC1 Is a Differential Regulator of Hypoxia-Mediated Events and Akt Signalling in PTEN-Deficient Breast Cancer Cells." *Journal of Cell Science* 130 (14): 2292–2305. https://doi.org/10.1242/jcs.196659.

Azzouzi A.R., Barret E., Moore C.M., Villers A., Allen C., Scherz A., Muir G., et al. **2013**. "TOOKAD(®) Soluble Vascular-Targeted Photodynamic (VTP) Therapy: Determination of Optimal Treatment Conditions and Assessment of Effects in Patients with Localised Prostate Cancer." *BJU International* 112 (6): 766–74. https://doi.org/10.1111/BJU.12265.

Azzouzi A.R., Vincendeau S., Barret E., Cicco A., Kleinclauss F., van der Poel H.G., Stief C.G., et al. **2017**. "Padeliporfin Vascular-Targeted Photodynamic Therapy versus Active Surveillance in Men with Low-Risk Prostate Cancer (CLIN1001 PCM301): An Open-Label, Phase 3, Randomised Controlled Trial." *The Lancet. Oncology* 18 (2): 181–91. https://doi.org/10.1016/S1470-2045(16)30661-1.

Babes R.M., Selescu T., Domocos D., and Babes A. **2017**. "The Anthelminthic Drug Praziquantel Is a Selective Agonist of the Sensory Transient Receptor Potential Melastatin Type 8 Channel." *Toxicology and Applied Pharmacology* 336 (October): 55–65. https://doi.org/10.1016/j.taap.2017.10.012.

Babič A., Herceg V., Bastien E., Lassalle H.P., Bezdetnaya L., and Lange N. **2018**. "5-Aminolevulinic Acid-Squalene Nanoassemblies for Tumor Photodetection and Therapy: In Vitro Studies." *Nanoscale Research Letters* 13 (1). https://doi.org/10.1186/S11671-017-2408-Y.

Bader M.F., Doussau F., Chasserot-Golaz S., Vitale N., and Gasman S. **2004**. "Coupling Actin and Membrane Dynamics during Calcium-Regulated Exocytosis: A Role for Rho and ARF GTPases." *Biochimica et Biophysica Acta - Molecular Cell Research* 1742 (1–3): 37–49. https://doi.org/10.1016/j.bbamcr.2004.09.028.

Bai C.X., Giamarchi A., Rodat-Despoix L., Padilla F., Downs T., Tsiokas L., and Delmas P. **2008**. "Formation of a New Receptor-Operated Channel by Heteromeric Assembly of TRPP2 and TRPC1 Subunits." *EMBO Reports* 9 (5): 472–79. https://doi.org/10.1038/embor.2008.29.

Baldoli E., Castiglioni S., and Maier J.A.M. **2013**. "Regulation and Function of TRPM7 in Human Endothelial Cells: TRPM7 as a Potential Novel Regulator of Endothelial Function." *PloS One* 8 (3): e59891. https://doi.org/10.1371/journal.pone.0059891.

Baldoli E., and Maier J.A.M. **2012**. "Silencing TRPM7 Mimics the Effects of Magnesium Deficiency in Human Microvascular Endothelial Cells." *Angiogenesis* 15 (1): 47–57. https://doi.org/10.1007/s10456-011-9242-0.

Bandell M., Dubin A.E., Petrus M.J., A., Mathur J., Sun W.H., and Patapoutian A. **2006**. "High-Throughput Random Mutagenesis Screen Reveals TRPM8 Residues Specifically Required for Activation by Menthol." *Nature Neuroscience* 9 (4): 493–500. https://doi.org/10.1038/nn1665.

Bandell M., Macpherson L.J., and Patapoutian A. **2007**. "From Chills to Chilis: Mechanisms for Thermosensation and Chemesthesis via ThermoTRPs." *Current Opinion in Neurobiology* 17 (4): 490–97. https://doi.org/10.1016/j.conb.2007.07.014.

Bandell M., Story G.M., Sun W.H., Viswanath V., Eid S.R., Petrus M.J., Earley T.J., and Patapoutian A. **2004**. "Noxious Cold Ion Channel TRPA1 Is Activated by Pungent Compounds and Bradykinin." *Neuron* 41: 849–57. http://www.neuron.org/cgi/content/full/.

Baptista-Hon D.T., Robertson F.M., Robertson G.B., Owen S. J., Rogers G.W., Lydon E.L., Lee N.H., and Hales T.G. **2014**. "Potent Inhibition by Ropivacaine of Metastatic Colon Cancer SW620 Cell Invasion and NaV1.5 Channel Function." *British Journal of Anaesthesia* 113 Suppl 1 (SUPPL. 1). https://doi.org/10.1093/BJA/AEU104.

Barras A., Boussekey L., Courtade E., and Boukherroub R. **2013**. "Hypericin-Loaded Lipid Nanocapsules for Photodynamic Cancer Therapy in Vitro." *Nanoscale* 5 (21): 10562–72. https://doi.org/10.1039/C3NR02724D.

Barret E., Ahallal Y., Sanchez-Salas R., Galiano M., Cosset J.M., Validire P., MacEk P., et al. **2013**. "Morbidity of Focal Therapy in the Treatment of Localized Prostate Cancer." *European Urology* 63 (4): 618–22. https://doi.org/10.1016/J.EURURO.2012.11.057.

Battaglia L., and Gallarate M. **2012**. "Lipid Nanoparticles: State of the Art, New Preparation Methods and Challenges in Drug Delivery." *Expert Opinion on Drug Delivery* 9 (5): 497–508. https://doi.org/10.1517/17425247.2012.673278.

Bautista D.M., Jordt S.E., Nikai T., Tsuruda P.R., Read A.J., Poblete J., Yamoah E.N., Basbaum A.I., and Julius D. **2006**. "TRPA1 Mediates the Inflammatory Actions of Environmental Irritants and Proalgesic Agents." *Cell* 124 (6): 1269–82. https://doi.org/10.1016/j.cell.2006.02.023.

Bavencoffe A., Gkika D., Kondratskyi A., Beck B., Borowiec A.S., Bidaux G., Busserolles J., et al. **2010**. "The Transient Receptor Potential Channel TRPM8 Is Inhibited via the A2A Adrenoreceptor Signaling Pathway." *Journal of Biological Chemistry* 285 (13): 9410–19. https://doi.org/10.1074/jbc.M109.069377.

Bavencoffe A., Kondratskyi A., Gkika D., Mauroy B., Shuba Y., Prevarskaya N., and Skryma R. **2011**. "Complex Regulation of the TRPM8 Cold Receptor Channel: Role of Arachidonic Acid Release Following M3 Muscarinic Receptor Stimulation." *Journal of Biological Chemistry* 286 (11): 9849–55. https://doi.org/10.1074/jbc.M110.162016.

Beaty B.T., Sharma V.P., Bravo-Cordero J.J., Simpson M.A., Eddy R.J., Koleske A.J., and Condeelis J. **2013**. "B1 Integrin Regulates Arg to Promote Invadopodial Maturation and Matrix Degradation." *Molecular Biology of the Cell* 24 (11): 1661–75. https://doi.org/10.1091/mbc.E12-12-0908.

Beccari A.R., Gemei M., Lo Monte M., Menegatti N., Fanton M., Pedretti A., Bovolenta S., et al. **2017**. "Novel Selective, Potent Naphthyl TRPM8 Antagonists Identified through a Combined Ligand-and Structure-Based Virtual Screening Approach." *Scientific Reports* 7 (1): 1–15. https://doi.org/10.1038/s41598-017-11194-0.

Beck B., Bidaux G., Bavencoffe A., Lemonnier L., Thebault S., Shuba Y., Barrit G., Skryma R., and Prevarskaya N. **2007**. "Prospects for Prostate Cancer Imaging and Therapy Using High-Affinity TRPM8 Activators" 41: 285–94. https://doi.org/10.1016/j.ceca.2006.07.002.

Becker D., Bereiter-Hahn J., and Jendrach M. **2009**. "Functional Interaction of the Cation Channel Transient Receptor Potential Vanilloid 4 (TRPV4) and Actin in Volume Regulation." *European Journal of Cell Biology* 88 (3): 141–52. https://doi.org/10.1016/j.ejcb.2008.10.002.

Becker D., Blasé C., Bereiter-Hahn J., and Jendrach M. **2005**. "TRPV4 Exhibits a Functional Role in Cell-Volume Regulation." *Journal of Cell Science* 118 (11): 2435–40. https://doi.org/10.1242/jcs.02372.

Belvisi M.G., Dubuis M., and Birrell M.A. **2011**. "Transient Receptor Potential A1 Channels: Insights into Cough and Airway Inflammatory Disease." *Chest* 140 (4): 1040–47. https://doi.org/10.1378/chest.10-3327.

Benemei S., and Dussor G. **2019**. "TRP Channels and Migraine: Recent Developments and New Therapeutic Opportunities." *Pharmaceuticals* 12 (2): 1–17. https://doi.org/10.3390/ph12020054.

Berges R.R., Vulkanovic J, Epstein J.I., CarMichel M., Cisek L., Johnson D.E, Veltri R.W., Walsh P.C., and Isaacs J.T. **1995**. "Implication of Cell Kinetic Changes during the Progression of Human Prostatic Cancer." *Clin Cancer Res.* 1 (5): 473–80. https://www.ncbi.nlm.nih.gov/pmc/articles/PMC3624763/pdf/nihms412728.pdf.

Bernardini M., Fiorio Pla A., Prevarskaya N., and Gkika D. **2015**. "Human Transient Receptor Potential (TRP) Channels Expression Profiling in Carcinogenesis." *International Journal of Developmental Biology* 59 (7–9): 399–406. https://doi.org/10.1387/ijdb.150232dg.

Berridge M.J., Lipp P., and Bootman M.D. **2000**. "The Versatility and Universality of Calcium Signalling." *Nature Reviews Molecular Cell Biology* 1 (1): 11–21. https://doi.org/10.1038/35036035.

Berridge M.J., Bootman M.D., and Roderick H.L. **2003**. "CALCIUM SIGNALLING : DYNAMICS, HOMEOSTASIS AND REMODELLING." *Nature Reviews Molecular Cell Biology* 4 (7): 517–29. https://doi.org/10.1038/nrm1155.

Berrout J., Kyriakopoulou E., Moparthi L., Hogea A.S., Berrout L., Ivan C., Lorger M., et al. **2017**. "TRPA1–FGFR2 Binding Event Is a Regulatory Oncogenic Driver Modulated by MiRNA-142-3p." *Nature Communications 2017 8:1* 8 (1): 1–15. https://doi.org/10.1038/s41467-017-00983-w.

Bertamino A., Iraci N., Ostacolo C., Ambrosino P., Musella S., Di Sarno V., Ciaglia T., et al. **2018**. "Identification of a Potent Tryptophan-Based TRPM8 Antagonist with in Vivo Analgesic Activity." *Journal of Medicinal Chemistry* 61 (14): 6140–52. https://doi.org/10.1021/acs.jmedchem.8b00545.

Bertamino A., Ostacolo C., Ambrosino P., Musella S., Di Sarno V., Ciaglia T., Soldovieri M.V., et al. **2016**. "Tryptamine-Based Derivatives as Transient Receptor Potential Melastatin Type 8 (TRPM8) Channel Modulators." *Journal of Medicinal Chemistry* 59 (5): 2179–91. https://doi.org/10.1021/acs.jmedchem.5b01914.

Bessac B.F., Sivula M., Von Hehn C.A., Escalera J., Cohn L., and Jordt S.E. **2008**. "TRPA1 Is a Major Oxidant Sensor in Murine Airway Sensory Neurons." *Journal of Clinical Investigation* 118 (5): 1899–1910. https://doi.org/10.1172/JCI34192.

Betson M., and Braga V.M.M. **2003**. "Tumor Progression : Small GTPases and Loss of Cell – Cell Adhesion." *Bioessays* 25 (5): 452–63. https://doi.org/10.1002/bies.10262.

Bezzerides V.J., Ramsey I.S., Kotecha S., Greka A., and Clapham D.E. **2004**. "Rapid Vesicular Translocation and Insertion of TRP Channels." *Nat Cell Biol.* 6 (8): 709–20. https://doi.org/10.1038/ncb1150.

Bhave G., Hu H.J., Glauner K.S., Zhu W., Wang H., Brasier D.J., Oxford G.S., and Gereau R.W. IV. **2003**. "Protein Kinase C Phosphorylation Sensitizes but Does Not Activate the Capsaicin Receptor Transient Receptor Potential Vanilloid 1 (TRPV1)." *Proceedings of the National Academy of Sciences of the United States of America* 100 (21): 12480–85. https://doi.org/10.1073/pnas.2032100100.

Bidaux G., Roudbaraki M., Merle C., Crépin A., Delcourt P., Slomianny C., Thebault S., et al. **2005**. "Evidence for Specific TRPM8 Expression in Human Prostate Secretory Epithelial Cells: Functional Androgen Receptor Requirement." *Endocrine-Related Cancer* 12 (2): 367–82. https://doi.org/10.1677/erc.1.00969.

Bidaux G., Flourakis M., Thebault S., Zholos A., Beck B., Gkika D., Roudbaraki M., et al. **2007**. "Prostate Cell Differentiation Status Determines Transient Receptor Potential Melastatin Member 8 Channel Subcellular Localization and Function." *Journal of Clinical Investigation* 117 (6): 1647–57. https://doi.org/10.1172/JCI30168.

Bidaux G., Beck B., Zholos A., Gordienko D., Lemonnier L., Flourakis M., Roudbaraki M., et al. **2012**. "Regulation of Activity of Transient Receptor Potential Melastatin 8 (TRPM8) Channel by Its Short Isoforms." *Journal of Biological Chemistry* 287 (5): 2948–62. https://doi.org/10.1074/jbc.M111.270256.

Bidaux G., Borowiec A.S., Dubois C., Delcourt P., Schulz C., Vanden Abeele F., Lepage G., et al. **2016**. "Targeting of Short TRPM8 Isoforms Induces 4TM-TRPM8-Dependent Apoptosis in Prostate Cancer Cells." *Oncotarget* 7 (20): 29063–80. https://doi.org/10.18632/oncotarget.8666.

Bidaux G., Borowiec A.S., Gordienko D., Beck B., Shapovalov G.G., Lemonnier L., Flourakis M., et al. **2015**. "Epidermal TRPM8 Channel Isoform Controls the Balance between Keratinocyte Proliferation and Differentiation in a Cold-Dependent Manner." *Proceedings of the National Academy of Sciences of the United States of America* 112 (26): E3345–54. https://doi.org/10.1073/pnas.1423357112.

Bidaux G., Borowiec A.S., Prevarskaya N., and Gordienko D. **2016**. "Fine-Tuning of eTRPM8 Expression and Activity Conditions Keratinocyte Fate." *Channels* 10 (4): 320–31. https://doi.org/10.1080/19336950.2016.1168551.

Bidaux G., Gordienko D., Shapovalov G., Farfariello V., Borowiec A.S., Iamshanova O., Lemonnier L, et al. **2018**. "4TM-TRPM8 Channels Are New Gatekeepers of the ER-Mitochondria Ca2+ Transfer." *Biochimica et Biophysica Acta - Molecular Cell Research* 1865 (7): 981–94. https://doi.org/10.1016/j.bbamcr.2018.04.007.

Birukova A.A., Smurova K., Birukov K.G., Kaibuchi K., Garcia J.G.N., and Verin A.D. **2004**. "Role of Rho GTPases in Thrombin-Induced Lung Vascular Endothelial Cells Barrier Dysfunction." *Microvascular* 67: 64–77. https://doi.org/10.1016/j.mvr.2003.09.007.

Bledzka K., Smyth S.S., and Plow E.F. **2013**. "Integrin AlphaIIbbeta3: From Discovery to Efficacious Therapeutic Target." *Circulation Research* 112 (8): 1189–1200. https://doi.org/10.1161/CIRCRESAHA.112.300570.Integrin.

Bochenek K., Aebisher D., Międzybrodzka A., Cieślar G., and Kawczyk-Krupka A. **2019**. "Methods for Bladder Cancer Diagnosis – The Role of Autofluorescence and Photodynamic Diagnosis." *Photodiagnosis and Photodynamic Therapy* 27 (March): 141–48.

https://doi.org/10.1016/j.pdpdt.2019.05.036.

Bödding M. **2007**. "TRP Proteins and Cancer." *Cellular Signalling* 19: 617–24. https://doi.org/10.1016/j.cellsig.2006.08.012.

Bödding M., Fecher-Trost C., and Flockerzi V. **2003**. "Store-Operated Ca^{2+} Current and TRPV6 Channels in Lymph Node Prostate Cancer Cells." *Journal of Biological Chemistry* 278 (51): 50872–79. https://doi.org/10.1074/jbc.M308800200.

Bödding M., Wissenbach U., and Flockerzi V. **2007**. "Characterisation of TRPM8 as a Pharmacophore Receptor." *Cell Calcium* 42 (6): 618–28. https://doi.org/10.1016/j.ceca.2007.03.005.

Boettner B., and Van Aelst L. **2009**. "Control of Cell Adhesion Dynamics by Rap1 Signaling." *Current Opinion in Cell Biology* 21 (5): 684–93. https://doi.org/10.1016/j.ceb.2009.06.004.

Bolanz K.A., Hediger M.A., and Landowski C.P. **2008**. "The Role of TRPV6 in Breast Carcinogenesis." *Molecular Cancer Therapeutics* 7 (2): 271–79. https://doi.org/10.1158/1535-7163.MCT-07-0478.

Bomben V.C., Turner K.L., Barclay T.C., and Sontheimer H. **2011**. "Transient Receptor Potential Canonical Channels Are Essential for Chemotactic Migration of Human Malignant Gliomas." *J Cell Physiol.* 226 (7): 1879–88. https://doi.org/10.1161/CIRCULATIONAHA.110.956839.

Bonkhoff H., Fixemer T., and Remberger K. **1998**. "Relation between Bcl-2, Cell Proliferation, and the Androgen Receptor Status in Prostate Tissue and Precursors of Prostate Cancer." *Prostate* 34 (4): 251–58. https://doi.org/10.1002/(SICI)1097-0045(19980301)34:4<251::AID-PROS2>3.0.CO;2-K.

Boonstra M.C., De Geus S.W.L., Prevoo H.A.J.M., Hawinkels L.J.A.C., Van De Velde C.J.H., Kuppen P.J.K., Vahrmeijer A.L., and Sier C.F.M.. **2016**. "Selecting Targets for Tumor Imaging: An Overview of Cancer-Associated Membrane Proteins." *Biomarkers in Cancer* 8: BIC.S38542. https://doi.org/10.4137/bic.s38542.

Borowiec A-S., Sion B., Chalmel F., Rolland A.D., Lemonnier L., De Clerck T., Bokhobza A, et al. **2016**. "Cold_menthol TRPM8 Receptors Initiate the Cold-shock Response and Protect Germ Cells from Cold-shock–Induced Oxidation _ Enhanced Reader.Pdf." *FASEB Journal* 30 (9): 3155–70. https://doi.org/10.1096/fj.201600257R.

Borrelli F., Pagano E., Romano B., Panzera S., Maiello F., Coppola D., De Petrocellis L., Buono L., Orlando P., and Izzo A.A. **2014**. "Colon Carcinogenesis Is Inhibited by the TRPM8 Antagonist Cannabigerol, a Cannabis-Derived Non-Psychotropic Cannabinoid." *Carcinogenesis* 35 (12): 2787–97. https://doi.org/10.1093/carcin/bgu205.

Bos J.L. **1989**. "Ras Oncogenes in Human Cancer: A Review." *Cancer Research* 49 (17): 4682–89.

Boustany C.E., Bidaux G., Enfissi A., Delcourt P., Prevarskaya N., and Capiod T. **2008**. "Capacitative Calcium Entry and Transient Receptor Potential Canonical 6 Expression Control Human Hepatoma Cell Proliferation." *Hepatology* 47 (6): 2068–77. https://doi.org/10.1002/hep.22263.

Boustan, C.E., Katsogiannou M., Delcourt P., Dewailly E., Prevarskaya N., Borowiec A.S., and Capiod T. **2010**. "Differential Roles of STIM1, STIM2 and Orai1 in the Control of Cell Proliferation and SOCE Amplitude in HEK293 Cells." *Cell Calcium*. https://doi.org/10.1016/j.ceca.2010.01.006.

Brauchi S., Orio P., and Latorre R. **2004**. "Clues to Understanding Cold Sensation: Thermodynamics and Electrophysiological Analysis of the Cold Receptor TRPM8." *Proc Natl Acad Sci U S A* 101 (43): 15494–99.

Bräunig J., Mergler S., Jyrch S., Hoefig C.S., Rosowski M., Mittag J., Biebermann H., and Khajavi N. **2018**. "3-Iodothyronamine Activates a Set of Membrane Proteins in Murine Hypothalamic Cell Lines." *Frontiers in Endocrinology* 9 (SEP): 1–12. https://doi.org/10.3389/fendo.2018.00523.

Brittain J.M., Duarte D.B., Wilson S.M., Zhu W., Ballard C., Johnson P.L., Liu N., et al. **2011**. "Suppression of Inflammatory and Neuropathic Pain by Uncoupling CRMP-2 from the Presynaptic Ca^{2+} Channel Complex." *Nat Med.* 17 (7): 822–29. https://doi.org/10.1038/nm.2345.Suppression.

Brossa A., Buono L., Fallo S., Fiorio Pla A., Munaron L., and Bussolati B. **2019**. "Alternative Strategies to Inhibit Tumor Vascularization." *International Journal of Molecular Sciences* 20 (24). https://doi.org/10.3390/ijms20246180.

Brown G.T., and Murray G.I. **2015**. "Current Mechanistic Insights into the Roles of Matrix Metalloproteinases in Tumour Invasion and Metastasis." *Journal of Pathology* 237 (3): 273–81. https://doi.org/10.1002/path.4586.

Brownlee M. **2001**. "Biochemistry and Molecular Cell Biology of Diabetic Complications." *Nature* 414 (December): 813–20.

Bryan B.A., and D'Amore P.A. **2007**. "What Tangled Webs They Weave: Rho-GTPase Control of Angiogenesis." *Cellular and Molecular*

Life Sciences 64 (16): 2053–65. https://doi.org/10.1007/s00018-007-7008-z.

Btesh J., Fischer M.J.M., Stott K., and McNaughton P.A. **2013**. "Mapping the Binding Site of TRPV1 on AKAP79: Implications for Inflammatory Hyperalgesia." *Journal of Neuroscience* 33 (21): 9184–93. https://doi.org/10.1523/JNEUROSCI.4991-12.2013.

Caceres A.I., Brackmann M., Elia M.D., Bessac B.F., Del Camino D., D'Amours M., Witek J.A.S., et al. **2009**. "A Sensory Neuronal Ion Channel Essential for Airway Inflammation and Hyperreactivity in Asthma." *Proceedings of the National Academy of Sciences of the United States of America* 106 (22): 9099–9104. https://doi.org/10.1073/pnas.0900591106.

Caceres A.I., Liu B., Jabba S.V., Achanta S., Morris J.B., and Jordt S.E. **2017**. "Transient Receptor Potential Cation Channel Subfamily M Member 8 Channels Mediate the Anti-Inflammatory Effects of Eucalyptol." *British Journal of Pharmacology* 174 (9): 867–79. https://doi.org/10.1111/bph.13760.

Cáceres M., Ortiz L., Recabarren T., Romero A., Colombo A., Leiva-Salcedo E., Varela D., et al. **2015**. "TRPM4 Is a Novel Component of the Adhesome Required for Focal Adhesion Disassembly, Migration and Contractility." *PLoS ONE* 10 (6): 1–23. https://doi.org/10.1371/journal.pone.0130540.

Cai N., Lou L., Al-Saadi N., Tetteh S., and Runnels L.W. **2018**. "The Kinase Activity of the Channel-Kinase Protein TRPM7 Regulates Stability and Localization of the TRPM7 Channel in Polarized Epithelial Cells." *Journal of Biological Chemistry* 293 (29): 11491–504. https://doi.org/10.1074/jbc.RA118.001925.

Canales J., Morales D., Blanco C., Rivas J., Diaz N., Angelopoulos I., and Cerda O. **2019**. "A Tr(i)p to Cell Migration: New Roles of Trp Channels in Mechanotransduction and Cancer." *Frontiers in Physiology* 10 (JUN): 1–14. https://doi.org/10.3389/fphys.2019.00757.

Cao D.S., Zhong L., Hsieh T.H., Abooj M., Bishnoi M., Hughes L., and Premkumar L.S. **2012**. "Expression of Transient Receptor Potential Ankyrin 1 (TRPA1) and Its Role in Insulin Release from Rat Pancreatic Beta Cells." *PLoS ONE* 7 (5). https://doi.org/10.1371/journal.pone.0038005.

Cao E., Liao M., Cheng Y., and Julius D. **2013**. "TRPV1 Structures in Distinct Conformations Reveal Activation Mechanisms." *Nature* 504 (7478): 113–18. https://doi.org/10.1038/NATURE12823.

Cao E. **2020**. "Structural Mechanisms of Transient Receptor Potential Ion Channels." *The Journal of General Physiology* 152 (3). https://doi.org/10.1085/JGP.201811998.

Cao R., Meng Z., Liu T., Wang G., Qian G., and Cao T. **2016**. "Decreased TRPM7 Inhibits Activities and Induces Apoptosis of Bladder Cancer Cells via ERK1 / 2 Pathway." *Oncotarget* 7 (45): 72941–60.

Cappelli H.C., Kanugula A.K., Adapala R.K., Amin V., Sharma P., Midha P., Paruchuri S., and Thodeti C.K. **2019**. "Mechanosensitive TRPV4 Channels Stabilize VE-Cadherin Junctions to Regulate Tumor Vascular Integrity and Metastasis." *Cancer Letters* 442: 15–20. https://doi.org/10.1016/j.canlet.2018.07.042.

Caprodossi S., Lucciarini R., Amantini C., Nabissi M., Canesin G., Ballarini P., Di Spilimbergo A., et al. **2008**. "Transient Receptor Potential Vanilloid Type 2 (TRPV2) Expression in Normal Urothelium and in Urothelial Carcinoma of Human Bladder: Correlation with the Pathologic Stage." *European Urology* 54 (3): 612–20. https://doi.org/10.1016/j.eururo.2007.10.016.

Carmeliet P., and Jain R.K. **2000**. "Angiogenesis in Cancer and Other Diseases." *Nature* 407 (6801): 249–57. https://doi.org/10.1038/35025220.

Carmeliet P. **2005**. "Angiogenesis in Life, Disease and Medicine." *Nature* 438 (7070): 932–36. https://doi.org/10.1038/nature04478.

Carmona G., Go S., Orlandi A., Ba T., Jugold M., Kiessling F., Henschler R., Zeiher A.M., Dimmeler S., and Chavakis E. **2009**. "Role of the Small GTPase Rap1 for Integrin Activity Regulation in Endothelial Cells and Angiogenesis." *Blood J. Am. Soc. Hematol.* 113 (2): 488–97. https://doi.org/10.1182/blood-2008-02-138438.The.

Castano A.P., Demidova T.N., and Hamblin M.R. **2004**. "Mechanisms in Photodynamic Therapy: Part One - Photosensitizers, Photochemistry and Cellular Localization." *Photodiagnosis and Photodynamic Therapy*. Elsevier. https://doi.org/10.1016/S1572-1000(05)00007-4.

Caterina M.J. **2007**. "Transient Receptor Potential Ion Channels as Participants in Thermosensation and Thermoregulation." *American Journal of Physiology - Regulatory Integrative and Comparative Physiology* 292 (1): 64–76. https://doi.org/10.1152/ajpregu.00446.2006.

Caterina M.J., and Pang Z. **2016**. "TRP Channels in Skin Biology and Pathophysiology." *Pharmaceuticals* 9 (4). https://doi.org/10.3390/ph9040077.

Caterina, M.J., Schumacher M.A., Tominaga M., Rosen T.A., Levine J.D., and Julius D. **1997**. "The Capsaicin Receptor: A Heat-Activated Ion Channel in the Pain Pathway." *Nature* 389 (6653): 816–24. https://doi.org/10.1038/39807.

Chan P., Ding H.T, Liederer B.M., Mao J., Belloni P., Chen L., Gao S.S., et al. 2021. "Translational and Pharmacokinetic-Pharmacodynamic Application for the Clinical Development of GDC-0334, a Novel TRPA1 Inhibitor." *Clinical and Translational Science* 14 (5): 1945–54. https://doi.org/10.1111/cts.13049.

Chandel N.S., Trzyna W.C., McClintock D.S., and Schumacker P.T. **2000**. "Role of Oxidants in NF-KB Activation and TNF-α Gene Transcription Induced by Hypoxia and Endotoxin." *The Journal of Immunology* 165 (2): 1013–21. https://doi.org/10.4049/jimmunol.165.2.1013.

Chen G.L., Lei M., Zhou L.P., Zeng B., and Zou F. **2016**. "Borneol Is a TRPM8 Agonist That Increases Ocular Surface Wetness." *PLoS ONE* 11 (7): 1–15. https://doi.org/10.1371/journal.pone.0158868.

Chen H., and Terrett J.A. **2020**. "Transient Receptor Potential Ankyrin 1 (TRPA1) Antagonists: A Patent Review (2015–2019)." *Expert Opinion on Therapeutic Patents* 0 (0). https://doi.org/10.1080/13543776.2020.1797679.

Chen J.P., Wang J., Luan Y., Wang C.X., Li W.H., Zhang J.B., Sha D., et al. **2015**. "TRPM7 Promotes the Metastatic Process in Human Nasopharyngeal Carcinoma." *Cancer Letters* 356 (2): 483–90. https://doi.org/10.1016/j.canlet.2014.09.032.

Chen J., Joshi S.K., Didomenico S., Perner R.J., Mikusa J.P., Gauvin D.M., Segreti J.A., et al. **2011**. "Selective Blockade of TRPA1 Channel Attenuates Pathological Pain without Altering Noxious Cold Sensation or Body Temperature Regulation." *Pain* 152 (5): 1165–72. https://doi.org/10.1016/j.pain.2011.01.049.

Chen L., Cao R., Wang G., Yuan L., Qian G., Guo Z., Wu C.L., Wang X., and Xiao Y. **2017**. "Downregulation of TRPM7 Suppressed Migration and Invasion by Regulating Epithelial – Mesenchymal Transition in Prostate Cancer Cells." *Medical Oncology* 34 (7): 1–11. https://doi.org/10.1007/s12032-017-0987-1.

Chen Y., Chatterjee S., Lisok A., Minn I., Pullambhatla M., Wharram B., Wang Y., et al. **2017**. "A PSMA-Targeted Theranostic Agent for Photodynamic Therapy." *Journal of Photochemistry and Photobiology. B, Biology* 167 (February): 111–16. https://doi.org/10.1016/J.JPHOTOBIOL.2016.12.018.

Chen Y., Zhang X., Yang T., Bi R., Huang Z., Ding H., Li J., and Zhang J. **2019**. "Emerging Structural Biology of TRPM Subfamily Channels." *Cell Calcium* 79 (January): 75–79. https://doi.org/10.1016/j.ceca.2019.02.011.

Chen Z., Zhu Y., Dong Y., Zhang P., Han X., Jin J., and Ma X. **2017**. "Overexpression of TrpC5 Promotes Tumor Metastasis via the HIF-1α-Twist Signaling Pathway in Colon Cancer." *Clinical Science* 131 (19): 2439–50. https://doi.org/10.1042/CS20171069.

Cheng H.W., James A.F., Foster R.R., Hancox J.C., and Bates D.O. **2006**. "VEGF Activates Receptor-Operated Cation Channels in Human Microvascular Endothelial Cells." *Arteriosclerosis, Thrombosis, and Vascular Biology*. https://doi.org/10.1161/01.ATV.0000231518.86795.0f.

Cheng W., Sun C., and Zheng J. **2010**. "Heteromerization of TRP Channel Subunits: Extending Functional Diversity." *Protein and Cell* 1 (9): 802–10. https://doi.org/10.1007/s13238-010-0108-9.

Cherfils J., and Zeghouf M. **2013**. "Regulation of Small GTPases by GEFs, GAPs, and GDIs." *Physiological Reviews* 93 (1): 269–309. https://doi.org/10.1152/physrev.00003.2012.

Chernov-Rogan T., Gianti E., Liu C., Villemure E., Cridland A.P., Hu X., Ballini E., et al. **2019**. "TRPA1 Modulation by Piperidine Carboxamides Suggests an Evolutionarily Conserved Binding Site and Gating Mechanism." *Proceedings of the National Academy of Sciences of the United States of America* 116 (51): 26008–19. https://doi.org/10.1073/pnas.1913929116.

Chigurupati S., Venkataraman R., Barrera D., Naganathan A., Madan M., Paul L., Pattisapu J.V., et al. **2010**. "Receptor Channel TRPC6 Is a Key Mediator of Notch-Driven Glioblastoma Growth and Invasiveness." *Cancer Research* 6 (11): 418–28. https://doi.org/10.1158/0008-5472.CAN-09-2654.

Chodon D., Guilbert A., Dhennin-Duthille I., Gautier M., Telliez M.S., Sevestre H., and Ouadid-Ahidouch H. **2010**. "Estrogen Regulation of TRPM8 Expression in Breast Cancer Cells." *BMC Cancer* 10. https://doi.org/10.1186/1471-2407-10-212.

Chrzanowska-Wodnicka M. **2010**. "Regulation of Angiogenesis by a Small GTPase Rap1." *Vascular Pharmacology* 53 (1–2): 1–10. https://doi.org/10.1016/j.vph.2010.03.003.

Chrzanowska-Wodnicka M., Kraus A.E., Gale D., White Ii G.C., and Vansluys J. **2008**. "Defective Angiogenesis , Endothelial Migration, Proliferation , and MAPK Signaling in Rap1b-Deficient Mice." *Blood* 111 (5): 2647–56. https://doi.org/10.1182/blood-2007-08-109710.The.

Chumakova L., Patron A., Priest C., Karanewsky D.S., Kimmich R., Boren B.C., Hammaker J.R., Chumakov V., Zhao W., and Noncovich A. **2014**. Heterocycles and related compounds useful as modulators of TRPM8 and their preparation. WO2014130582, issued 2014.

Chun J.N., Lim J.M., Kang Y., Kim E.H., Shin Y.C., Kim H.G., Jang D., et al. **2014**. "A Network Perspective on Unraveling the Role of TRP Channels in Biology and Disease." *Pflugers Archiv : European Journal of Physiology* 466 (2): 173–82. https://doi.org/10.1007/S00424-013-1292-2.

Chung C.L., Lin Y.S., Chan N.J., Chen Y.Y., and Hsu C.C. **2020**. "Hypersensitivity of Airway Reflexes Induced by Hydrogen Sulfide: Role of TRPA1 Receptors." *International Journal of Molecular Sciences* 21 (11): 1–18. https://doi.org/10.3390/ijms21113929.

Chung H.K., Rathor N., Wang S.R., Wang J.Y., and Rao J.N. **2015**. "RhoA Enhances Store-Operated Ca^{2+} Entry and Intestinal Epithelial Restitution by Interacting with TRPC1 after Wounding." *American Journal of Physiology - Gastrointestinal and Liver Physiology* 309 (9): G759–67. https://doi.org/10.1152/ajpgi.00185.2015.

Clapham D.E. **2015**. "Pain-Sensing TRPA1 Channel Resolved." *Nature* 520: 439–41.

Clark K., Langeslag M., Figdor C.G., and van Leeuwen F.N. **2007**. "Myosin II and Mechanotransduction: A Balancing Act." *Trends in Cell Biology* 17 (4): 178–86. https://doi.org/10.1016/j.tcb.2007.02.002.

Clark K., Middelbeek J., Lasonder E., Dulyaninova N.G., Morrice A., Ryazanov A.G., Bresnick A.R., Figdor C.G., and Van F.N. **2008**. "TRPM7 Regulates Myosin IIA Filament Stability and Protein Localization by Heavy Chain Phosphorylation" 378 (4): 790–803. https://doi.org/10.1016/j.

Clayton N.S., and Ridley A.J. **2020**. "Targeting Rho GTPase Signaling Networks in Cancer." *Front Cell Dev Biol.* 8: 1–12. https://doi.org/10.3389/fcell.2020.00222.

Copeland K.W., Boezio A.A., Cheung E., Lee J., Olivieri P., Schenkel L.B., Wan Q., et al. **2014**. "Development of Novel Azabenzofuran TRPA1 Antagonists as in Vivo Tools." *Bioorganic and Medicinal Chemistry Letters* 24 (15): 3464–68. https://doi.org/10.1016/j.bmcl.2014.05.069.

Corbi-Verge C., and Kim P.M. **2016**. "Motif Mediated Protein-Protein Interactions as Drug Targets." *Cell Communication and Signaling* 14 (1): 8. https://doi.org/10.1186/s12964-016-0131-4.

Cordero-Morales J.F., Gracheva E.O., and Julius D. **2011**. "Cytoplasmic Ankyrin Repeats of Transient Receptor Potential A1 (TRPA1) Dictate Sensitivity to Thermal and Chemical Stimuli." *Proceedings of the National Academy of Sciences of the United States of America* 108 (46). https://doi.org/10.1073/pnas.1114124108.

Corey D.P., Garcia-Añoveros J., Holt J.R., Kwan K.Y., Lin S.Y., Vollrath M.A., Amalfitano A., et al. **2004**. "TRPA1 Is a Candidate for the Mechanosensitive Transduction Channel of Vertebrate Hair Cells." *Nature* 432 (7018): 723–30. https://doi.org/10.1038/nature03066.

Correll R.N., Pang C., Niedowicz D.M., Finlin B.S., and Andres D.A. **2008**. "The RGK Family of GTP-Binding Proteins: Regulators of Voltage-Dependent Calcium Channels and Cytoskeleton Remodeling." *Cellular Signalling* 20 (2): 292–300. https://doi.org/10.1016/j.cellsig.2007.10.028.

Cosens D.J., and Manning A. **1969**. "Abnormal Electroretinogram from a Drosophila Mutant." *Nature* 224 (5216): 285–87. https://doi.org/10.1038/224285a0.

Csordás G., Várnai P., Golenár T., Roy S., Purkins G., Schneider T.G., Balla T., and Hajnóczky G.. **2010**. "Imaging Interorganelle Contacts and Local Calcium Dynamics at the ER-Mitochondrial Interface." *Molecular Cell* 39 (1): 121–32. https://doi.org/10.1016/j.molcel.2010.06.029.

Cullen P.J. **2003**. "Calcium Signalling: The Ups and Downs of Protein Kinase C." *Current Biology* 13 (18): 699–701. https://doi.org/10.1016/j.cub.2003.08.041.

Cullen P.J., and Lockyer P.J. **2002**. "Integration of Calcium and Ras Signalling." *Nature Reviews Molecular Cell Biology* 3 (5): 339–48. https://doi.org/10.1038/nrm808.

Curcio-Morelli, C., Zhang P., Venugopal B., Charles F.A., Browning M.F., Cantiello H.F., and Slaugenhaupt S.A. **2009**. "Functional Multimerization of Mucolipin Channel Proteins." *J Cell Physiol* 222 (2): 328–35. https://doi.org/10.1002/jcp.21956.

Cvetkov T.L., Huynh K.W., Cohen M.R., and Moiseenkova-Bell V.Y. **2011**. "Molecular Architecture and Subunit Organization of TRPA1 Ion Channel Revealed by Electron Microscopy." *Journal of Biological Chemistry* 286 (44): 38168–76. https://doi.org/10.1074/jbc.M111.288993.

Czifra G., Varga A., Nyeste K., Marincsák R., Tóth B.I., Kovács I., Kovács L., and Bíró T. **2009**. "Induction of Apoptosis in Prostate Tumor PC-3 Cellsand Inhibition of Xenograft Prostate Tumor Growthby the Vanilloid Capsaicin." *Journal of Cancer Research and Clinical Oncology* 135 (4): 507–14. https://doi.org/10.1007/s00432-008-0482-3.

D'Alessandro G., Catalano M., Sciaccaluga M., Chece G., Cipriani R., Rosito M., Grimaldi A., et al. **2013**. "KCa3.1 Channels Are Involved in the Infiltrative Behavior of Glioblastoma in Vivo." *Cell Death & Disease* 4 (8). https://doi.org/10.1038/CDDIS.2013.279.

Dąbrowski J.M., and Arnaut L.G. **2015**. "Photodynamic Therapy (PDT) of Cancer: From Local to Systemic Treatment." *Photochemical and Photobiological Sciences* 14 (10): 1765–80. https://doi.org/10.1039/c5pp00132c.

Dąbrowski J.M., Pucelik B., Regiel-Futyra A., Brindell M., Mazuryk O., Kyzioł A., Stochel G., Macyk W., and Arnaut L.G. **2016**. *Engineering of Relevant Photodynamic Processes through Structural Modifications of Metallotetrapyrrolic Photosensitizers*. *Coordination Chemistry Reviews*. Vol. 325. Elsevier B.V. https://doi.org/10.1016/j.ccr.2016.06.007.

Daehne S., and Koenig W. **1922**. *Polymethine Dyes 1.*

Dai Y. **2016**. "TRPs and Pain." *Seminars in Immunopathology* 38: 277–91. https://doi.org/10.1007/s00281-015-0526-0.

Dai Y., Wang S., Tominaga M., Yamamoto S., Fukuoka T., Higashi T., Kobayashi K., Obata K., Yamanaka H., and Noguchi K. **2007**. "Sensitization of TRPA1 by PAR2 Contributes to the Sensation of Inflammatory Pain." *Journal of Clinical Investigation* 117 (7): 1979–87. https://doi.org/10.1172/JCI30951.

Dang Y., and Guan J. **2020**. "Nanoparticle-Based Drug Delivery Systems for Cancer Therapy." *Smart Materials in Medicine* 1 (March): 10–19. https://doi.org/10.1016/j.smaim.2020.04.001.

Davis F.M., Azimi I., Faville R.A., Peters A.A., Jalink K., Putney J.W Jr, Goodhill G.J., Thompson E.W., and Roberts-Thomson S.J. **2014**. "Induction of Epithelial – Mesenchymal Transition (EMT) in Breast Cancer Cells Is Calcium Signal Dependent." *Oncogene* 33 (18): 2307–16. https://doi.org/10.1038/onc.2013.187.

DeFeo-Jones D., Garsky V.M., Wong B.K., Feng D.M., Bolyar T., Haskell K., Kiefer D.M., Leander K., McAvoy E., et al. **2000**. "A Peptide – Doxorubicin ' Prodrug ' Activated by Prostate- Specific Antigen Selectively Kills Prostate Tumor Cells Positive for Prostate-Specific Antigen *in Vivo*." *Nat Med.* 6 (11): 1248–52. https://doi.org/10.1038/81351.

De La Torre-Martínez R., Bonache M.A., Llabrés-Campaner P.J., Balsera B., Fernández-Carvajal A., Fernández-Ballester G., Ferrer-Montiel A., Pérez De Vega M.J., and González-Muñiz R. **2017**. "Synthesis, High-Throughput Screening and Pharmacological Characterization of β-Lactam Derivatives as TRPM8 Antagonists." *Scientific Reports* 7 (1): 1–13. https://doi.org/10.1038/s41598-017-10913-x.

De Logu F., Li Puma S., Landini L., Tuccinardi T., Poli G., Preti D., De Siena G., et al. **2019**. "The Acyl-Glucuronide Metabolite of Ibuprofen Has Analgesic and Anti-Inflammatory Effects via the TRPA1 Channel." *Pharmacological Research* 142 (December 2018): 127–39. https://doi.org/10.1016/j.phrs.2019.02.019.

Déliot N., and Constantin B. **2015**. "Plasma Membrane Calcium Channels in Cancer: Alterations and Consequences for Cell Proliferation and Migration." *Biochimica et Biophysica Acta - Biomembranes* 1848 (10): 2512–22. https://doi.org/10.1016/j.bbamem.2015.06.009.

Denham J.W., Steigler A., Lamb D.S., Joseph D., Turner S., Matthews J., Atkinson C., et al. **2011**. "Short-Term Neoadjuvant Androgen Deprivation and Radiotherapy for Locally Advanced Prostate Cancer: 10-Year Data from the TROG 96.01 Randomised Trial." *The Lancet Oncology* 12 (5): 451–59. https://doi.org/10.1016/S1470-2045(11)70063-8.

De Petrocellis L., Arroyo F.J., Orlando P., Schiano Moriello A., Vitale R.M., Amodeo P., Sánchez A., et al. **2016**. "Tetrahydroisoquinoline-Derived Urea and 2,5-Diketopiperazine Derivatives as Selective Antagonists of the Transient Receptor Potential Melastatin 8 (TRPM8) Channel Receptor and Antiprostate Cancer Agents." *Journal of Medicinal Chemistry* 59 (12): 5661–83. https://doi.org/10.1021/acs.jmedchem.5b01448.

De Petrocellis L., Ligresti A., Schiano Moriello A., Allarà M., Bisogno T., Petrosino S., Stott C.G., and Di Marzo V.. **2011**. "Effects of Cannabinoids and Cannabinoid-Enriched Cannabis Extracts on TRP Channels and Endocannabinoid Metabolic Enzymes." *British Journal of Pharmacology* 163 (7): 1479–94. https://doi.org/10.1111/j.1476-5381.2010.01166.x.

De Petrocellis L., Vellani V., Schiano-Moriello A., Marini P., Magherini P.C., Orlando P., and Di Marzo V. **2008**. "Plant-Derived Cannabinoids Modulate the Activity of Transient Receptor Potential Channels of Ankyrin Type-1 and Melastatin Type-8." *Journal of Pharmacology and Experimental Therapeutics* 325 (3): 1007–15. https://doi.org/10.1124/jpet.107.134809.

Derouiche S., Warnier M., Mariot P., Gosset P., Mauroy B., Bonnal J.L., Slomianny C., Delcourt P., Prevarskaya N., and Roudbaraki M. **2013**. "Bisphenol A Stimulates Human Prostate Cancer Cell Migration via Remodelling of Calcium Signalling." *SpringerPlus* 2

(1): 1–16. https://doi.org/10.1186/2193-1801-2-54.

Desai B.N., Krapivinsky G., Navarro B., Krapivinsky L., Carter B.C., Febvay S., Delling M., et al. **2012**. "Cleavage of TRPM7 Releases the Kinase Domain from the Ion Channel and Regulates Its Participation in Fas-Induced Apoptosis." *Developmental Cell* 22 (6): 1149–62. https://doi.org/10.1016/j.devcel.2012.04.006.

Dhennin-Duthille I., Gautier M., Faouzi M., Brevet M., Vaudry D., Ahidouch A., and Ouadid-ahidouch H. **2011**. "Cellular Physiology and Biochemistry - High Expression of Transient Receptor Potential Channels in Human Breast Cancer Epithelial Cells and Tissues: Correlation with Pathological Parameters," 813–22.

Di Donato M., Ostacolo C., Giovannelli P., Di Sarno V., Gomez Monterrey I.M., Campiglia P., Migliaccio A., Bertamino A., and Castoria G. **2021**. "Therapeutic Potential of TRPM8 Antagonists in Prostate Cancer." *Scientific Reports* 11 (1): 1–16. https://doi.org/10.1038/s41598-021-02675-4.

Dietrich A. **2019**. "Transient Receptor Potential Channels in Cardiac Health and Disease." *Nature Reviews Cardiology* 8 (5): 413. https://doi.org/10.3390/cells8050413.

Doerner J.F., Gisselmann G., Hatt H., and Wetzel C.H. **2007**. "Transient Receptor Potential Channel A1 Is Directly Gated by Calcium Ions." *Journal of Biological Chemistry* 282 (18): 13180–89. https://doi.org/10.1074/jbc.M607849200.

Dong H., Shim K.N., Li J.M.J., Estrema C., Ornelas T.A., Nguyen F., Liu S., et al. **2010**. "Molecular Mechanisms Underlying Ca^{2+}-Mediated Motility of Human Pancreatic Duct Cells." *American Journal of Physiology - Cell Physiology* 299 (6): 1493–1503. https://doi.org/10.1152/ajpcell.00242.2010.

Dong X-P, Cheng X., Mills E., Delling M., Wang F., Kurz T., and Xu H. **2008**. "The Type IV Mucolipidosis-Associated Protein TRPML1 Is an Endo-Lysosomal Iron Release Channel." *Nature* 455 (7215): 992–96. https://doi.org/10.1038/nature07311.

Dougherty T.J., Gomer C.J., Henderson B.W., Jori G., and Korbelik D. **1998**. "Photodynamic Therapy." *J. Natl. Cancer Inst* 90 (12): 889–905. https://books.google.co.jp/books?id=bG0oDwAAQBAJ.

Dougherty T.J., Cooper M.T., and Mang T.S. **1990**. "Cutaneous Phototoxic Occurrences in Patients Receiving Photofrin®." *Lasers in Surgery and Medicine* 10 (5): 485–88. https://doi.org/10.1002/lsm.1900100514.

Dragoni S., Laforenza U., Bonetti E., Lodola F., Bottino C., Berra-Romani R., Bongio G.C., et al. **2011**. "Vascular Endothelial Growth Factor Stimulates Endothelial Colony Forming Cells Proliferation and Tubulogenesis by Inducing Oscillations in Intracellular Ca^{2+} Concentration." *Stem Cells* 29 (11): 1898–1907. https://doi.org/10.1002/stem.734.

Dragoni S., Reforgiato M., Zuccolo E., Poletto V., Lodola F., Ruffinatti F.A., Bonetti E., et al. **2015**. "Dysregulation of VEGF-Induced Proangiogenic Ca^{2+} Oscillations in Primary Myelofibrosis-Derived Endothelial Colony-Forming Cells." *Experimental Hematology* 43 (12): 1019-1030.e3. https://doi.org/10.1016/j.exphem.2015.09.002.

Driffort V., Gillet L., Bon E., Marionneau-Lambot S., Oullier T., Joulin V., Collin C., et al. **2014**. "Ranolazine Inhibits NaV1.5-Mediated Breast Cancer Cell Invasiveness and Lung Colonization." *Molecular Cancer* 13 (1). https://doi.org/10.1186/1476-4598-13-264.

Dror Michaelson M., Regan M.M., Oh W.K., Kaufman D.S., Olivier K., Michaelson S.Z., Spicer B., Gurski C., Kantoff P.W., and Smith M.R. **2009**. "Phase II Study of Sunitinib in Men with Advanced Prostate Cancer." *Annals of Oncology : Official Journal of the European Society for Medical Oncology* 20 (5): 913–20. https://doi.org/10.1093/ANNONC/MDP111.

Du J., Wong W.Y., Sun L., Huang Y., and Yao X. **2012**. "Protein Kinase G Inhibits Flow-Induced Ca2+ Entry into Collecting Duct Cells." *J Am Soc Nephrol.* 23 (7): 1172–80.

Du K.L., Mick R., Busch T.M., Zhu T.C., Finlay J.C., Yu G., Yodh A.G., et al. **2006**. "Preliminary Results of Interstitial Motexafin Lutetium-Mediated PDT for Prostate Cancer." *Lasers in Surgery and Medicine* 38 (5): 427–34. https://doi.org/10.1002/lsm.20341.

Du S., Araki I., Kobayashi H., Zakoji H., Sawada N., and Takeda M. **2008**. "Differential Expression Profile of Cold (TRPA1) and Cool (TRPM8) Receptors in Human Urogenital Organs." *Urology* 72 (2): 450–55. https://doi.org/10.1016/j.urology.2007.11.127.

Du S., Araki I., Yoshiyama M., Nomura T., and Takeda M. **2007**. "Transient Receptor Potential Channel A1 Involved in Sensory Transduction of Rat Urinary Bladder Through C-Fiber Pathway." *Urology* 70 (4): 826–31. https://doi.org/10.1016/j.urology.2007.06.1110.

Duitama M., Moreno Y., Santander S.P., Casas Z., Sutachan J.J., Torres Y.P., and Albarracín S.L. **2022**. "TRP Channels as Molecular Targets to Relieve Cancer Pain." *Biomolecules* 12 (1). https://doi.org/10.3390/biom12010001.

Duke University. **2017**. Small molecule dual-inhibitors of TRPV4 and TRPA1 for sanitizing and anesthetizing. WO2017177200, issued 2017.

Duncan L.M., Deeds J., Hunter J., Shao J., Holmgren L.M., Woolf E.A., Tepper R.I., and Shyjan A.W. **1998**. "Down-Regulation of the Novel Gene Melastatin Correlates with Potential for Melanoma Metastasis." *Cancer Research* 58 (7): 1515–20.

Dussor G., and Cao Y-Q. **2016**. "TRPM8 and Migraine." *Headache* 56 (9): 1406–17. https://doi.org/10.1111/head.12948.

Dyba T., Randi G., Bray F., Martos C., Giusti F., Nicholson N., Gavin A., et al. **2021**. "The European Cancer Burden in 2020: Incidence and Mortality Estimates for 40 Countries and 25 Major Cancers." *European Journal of Cancer* 157 (November): 308–47. https://doi.org/10.1016/J.EJCA.2021.07.039.

EA Pharma Co., Ltd. **2017**. Heterocyclic sulfonamide derivative and medicine containing same. WO2017135462, issued 2017.

Earley S., and Brayden J.E. **2015**. "Transient Receptor Potential Channels in the Vasculature." *Physiological Reviews* 95 (2): 645–90. https://doi.org/10.1152/physrev.00026.2014.

Eberhardt M., Dux M., Namer B., Miljkovic J., Cordasic N., Will C., Kichko T.I., et al. **2015**. "H_2S and NO Cooperatively Regulate Vascular Tone by Activating a Neuroendocrine HNO–TRPA1–CGRP Signalling Pathway - Supplement." *Nature Communications* 5: 4381.

Eberhardt M.J., Filipovic M.R., Leffler A., De La Roche J., Kistner K., Fischer M.J., Fleming T., et al. **2012**. "Methylglyoxal Activates Nociceptors through Transient Receptor Potential Channel A1 (TRPA1): A Possible Mechanism of Metabolic Neuropathies." *Journal of Biological Chemistry* 287 (34): 28291–306. https://doi.org/10.1074/jbc.M111.328674.

Egan T.J., Acũna M.A., Zenobi-Wong M., Zeilhofer H.U., and Urech D. **2016**. "Effects of N-Glycosylation of the Human Cation Channel TRPA1 on Agonist-Sensitivity." *Bioscience Reports* 36 (5): 1–12. https://doi.org/10.1042/BSR20160149.

Eiber M., Fendler W.P., Rowe S.P., Calais J., Hofman M.S., Maurer T., Schwarzenboeck S.M., Kratowchil C., Herrmann K., and Giesel F.L. **2017**. "Prostate-Specific Membrane Antigen Ligands for Imaging and Therapy." *Journal of Nuclear Medicine : Official Publication, Society of Nuclear Medicine* 58 (Suppl 2): 67S-76S. https://doi.org/10.2967/JNUMED.116.186767.

Eid S.R., Crown E.D., Moore E.L., Liang H.A., Choong K.C., Dima S., Henze D.A., Kane S.A., and Urban M.O. **2008**. "HC-030031, a TRPA1 Selective Antagonist, Attenuates Inflammatory- and Neuropathy-Induced Mechanical Hypersensitivity." *Molecular Pain* 4: 1–10. https://doi.org/10.1186/1744-8069-4-48.

Elbaz M., Ahirwar D., Xiaoli Z., Zhou X., Lustberg M., Nasser M.W., Shilo K., and Ganju R.K. **2018**. "TRPV2 Is a Novel Biomarker and Therapeutic Target in Triple Negative Breast Cancer." *Oncotarget* 9 (71): 33459–70. https://doi.org/10.18632/oncotarget.9663.

Eli-Lilly, and Company. **2019**. Inhibiting the Transient Receptor Potential A1 ion channel. WO2019152465, issued 2019.

Engel M.A., Becker C., Reeh P.W., and Neurath M.F. **2011**. "Role of Sensory Neurons in Colitis: Increasing Evidence for a Neuroimmune Link in the Gut." *Inflammatory Bowel Diseases* 17 (4): 1030–33. https://doi.org/10.1002/ibd.21422.

Escárcega R.O., Fuentes-Alexandro S., García-Carrasco M., Gatica A., and Zamora A. **2007**. "The Transcription Factor Nuclear Factor-Kappa B and Cancer." *Clinical Oncology* 19 (2): 154–61. https://doi.org/10.1016/j.clon.2006.11.013.

Eymerit-Morin C., Zidane M., Lebdai S., Triau S., Azzouzi A.R., and Rousselet M.C. **2013**. "Histopathology of Prostate Tissue after Vascular-Targeted Photodynamic Therapy for Localized Prostate Cancer." *Virchows Archiv : An International Journal of Pathology* 463 (4): 547–52. https://doi.org/10.1007/S00428-013-1454-9.

Fabian A., Fortmann T., Dieterich P., Riethmüller C., Schön P., Mally S., Nilius B., and Schwab A. **2008**. "TRPC1 Channels Regulate Directionality of Migrating Cells." *Pflugers Archiv European Journal of Physiology* 457 (2): 475–84. https://doi.org/10.1007/s00424-008-0515-4.

Fajardo O., Meseguer V., Belmonte C., and Viana F. **2008**. "TRPA1 Channels: Novel Targets of 1,4-Dihydropyridines." *Channels* 2 (6): 429–38. https://doi.org/10.4161/chan.2.6.7126.

Fang D., and Setaluri V. **2000**. "Expression and Up-Regulation of Alternatively Spliced Transcripts of Melastatin, a Melanoma Metastasis-Related Gene, in Human Melanoma Cells." *Biochemical and Biophysical Research Communications* 279 (1): 53–61. https://doi.org/10.1006/bbrc.2000.3894.

Fang J., Islam W., and Maeda H. **2020**. "Exploiting the Dynamics of the EPR Effect and Strategies to Improve the Therapeutic Effects of Nanomedicines by Using EPR Effect Enhancers." *Advanced Drug Delivery Reviews* 157: 142–60. https://doi.org/10.1016/j.addr.2020.06.005.

Faouzi M., Kilch T, Horgen F.D., Fleig A., and Penner R. **2017**. "The TRPM7 Channel Kinase Regulates Store-Operated Calcium Entry." *Journal of Physiology* 595 (10): 3165–80. https://doi.org/10.1113/JP274006.

Farco J.A., and Grundmann O. **2013**. "Menthol--Pharmacology of an Important Naturally Medicinal 'Cool.'" *Mini Rev Med Chem* 13 (1): 124–31.

"FDA Briefing Document Oncologic Drugs Advisory Committee Meeting NDA 212578/S000 Padeliporfin Di-Potassium (TOOKAD) Applicant: Steba Oncology, Inc." 2020. US National Library of Medicine. **2020**. https://clinicaltrials.gov/ct2/show/NCT01310894.

Fels B., Bulk E., Pethő Z., and Schwab A. **2018**. "The Role of TRP Channels in the Metastatic Cascade." *Pharmaceuticals* 11 (2). https://doi.org/10.3390/ph11020048.

Fernandes E.S., Vong C.T., Quek S., Cheong J., Awal S., Gentry C., Aubdool A.A., et al. **2013**. "Superoxide Generation and Leukocyte Accumulation: Key Elements in the Mediation of Leukotriene B4-Induced Itch by Transient Receptor Potential Ankyrin 1 and Transient Receptor Potential Vanilloid 1." *FASEB Journal* 27 (4): 1664–73. https://doi.org/10.1096/fj.12-221218.

Fernández J.A., Skryma R., Bidaux G., Magleby K.L., Scholfield C.N., McGeown J.G., Prevarskaya N., and Zholos A.V.. **2012**. "Short Isoforms of the Cold Receptor TRPM8 Inhibit Channel Gating by Mimicking Heat Action Rather than Chemical Inhibitors." *Journal of Biological Chemistry* 287 (5): 2963–70. https://doi.org/10.1074/jbc.M111.272823.

Ferrer Montiel A., Fernandez Carvajal A., Belmonte Martinez A., Gallar Martinez J., De la Torre R., Genazzani A., Tron G.C., and Mercalli V. **2017**. Preparation and therapeutical uses of triazole derivatives as TRPM8 receptor agonists. WO2017125634, issued 2017.

Fidanzi-Dugas C., Liagre B., Chemin G., Perraud A., Carrion C., Couquet C.Y., Granet R., Sol V., and Léger D.Y.. **2017**. "Analysis of the *in Vitro* and *in Vivo* Effects of Photodynamic Therapy on Prostate Cancer by Using New Photosensitizers, Protoporphyrin IX-Polyamine Derivatives." *Biochimica et Biophysica Acta. General Subjects* 1861 (7): 1676–90. https://doi.org/10.1016/J.BBAGEN.2017.02.003.

Fiorio Pla A., Ong H.L., Cheng K.T., Brossa A., Bussolati B., Lockwich T., Paria B., Munaron L., and Ambudkar I.S.S. **2012**. "TRPV4 Mediates Tumor-Derived Endothelial Cell Migration via Arachidonic Acid-Activated Actin Remodeling." *Oncogene* 31 (2): 200–212. https://doi.org/10.1016/j.physbeh.2017.03.040.

Fiorio Pla A., and Gkika D. **2013**. "Emerging Role of TRP Channels in Cell Migration: From Tumor Vascularization to Metastasis." *Frontiers in Physiology* 4 (311): 1–12. https://doi.org/10.3389/fphys.2013.00311.

Fiorio Pla A., and Munaron L. **2014**. "Functional Properties of Ion Channels and Transporters in Tumour Vascularization." *Philosophical Transactions of the Royal Society B: Biological Sciences* 369 (1638). https://doi.org/10.1098/rstb.2013.0103.

Fischer A., Rosen A.C., Ensslin C.J., Wu S., and Lacouture M.E. **2013**. "Pruritus to Anticancer Agents Targeting the EGFR, BRAF, and CTLA-4." *Dermatologic Therapy* 26 (2): 135–48. https://doi.org/10.1111/dth.12027.

Fisher M.J., Btesh J., and McNaughton P.A. **2013**. "Disrupting Sensitization of Transient Receptor Potential Vanilloid Subtype 1 Inhibits Inflammatory Hyperalgesia." *Journal of Neuroscience* 33 (17): 7407–14. https://doi.org/10.1523/JNEUROSCI.3721-12.2013.

Fixemer T., Wissenbach U., Flockerzi V., and Bonkhoff H. **2003**. "Expression of the Ca2þ-Selective Cation Channel TRPV6 in Human Prostatecancer: A Novel Prognostic Marker for Tumor Progression." *Oncogene* 22: 7858–61. https://doi.org/10.1038/sj.onc.1206895.

Fliniaux I., Germain E., Farfariello V., and Prevarskaya N.. **2018**. "TRPs and Ca^{2+} in Cell Death and Survival." *Cell Calcium*. Elsevier Ltd. https://doi.org/10.1016/j.ceca.2017.07.002.

Folkman J. **2006**. "Angiogenesis." *Annual Review of Medicine* 57: 1–18. https://doi.org/10.1146/annurev.med.57.121304.131306.

Fossati N., Willemse P.P.M., Van den Broeck T., van den Bergh R.C.N., Yuan C.Y., Briers E., Bellmunt J., et al. **2017**. "The Benefits and Harms of Different Extents of Lymph Node Dissection During Radical Prostatectomy for Prostate Cancer: A Systematic Review." *European Urology* 72 (1): 84–109. https://doi.org/10.1016/j.eururo.2016.12.003.

Franco S.J., and Huttenlocher A. **2005**. "Regulating Cell Migration: Calpains Make the Cut." *Journal of Cell Science* 118 (17): 3829–38. https://doi.org/10.1242/jcs.02562.

Fuessel S., Sickert D., Meye A., Klenk U., Schmidt U., Schmitz M., Rost A-K, Weigle B., Kiessling A., and Wirth M.P. **2003**. "Multiple Tumor Marker Analyses (PSA, HK2, PSCA, Trp-P8) in Primary Prostate Cancers Using Quantitative RT-PCR." *Int J Oncol* 23 (1): 221–28.

Fuessel S., Meye A., Schmitz M., Zastrow S., Linné C., Richter K., Lobel B., et al. **2006**. "Vaccination of Hormone-Refractory Prostate Cancer Patients With Peptide Cocktail-Loaded Dendritic Cells: Results of a Phase I Clinical Trial." *The Prostate* 66: 811–21.

Fujiwara Y., and Minor D.L. **2008**. "X-Ray Crystal Structure of a TRPM Assembly Domain Reveals an Antiparallel Four-Stranded Coiled-Coil." *Journal of Molecular Biology* 383 (4): 854–70. https://doi.org/10.1016/j.jmb.2008.08.059.

Galderma Research & Development. **2018**. TRPA1 antagonists for use in the treatment of atopic dermatitis. WO2018109155, issued 2018.

Gallin W.J., and Greenberg M.E. **1995**. "Calcium Regulation of Gene Expression in Neurons: The Mode of Entry Matters." *Current Opinion in Neurobiology* 5 (3): 367–74. https://doi.org/10.1016/0959-4388(95)80050-6.

Gao G., Wang W., Tadagavadi R.K., Briley N.E., Love M.I., Miller B.A., and Reeves W.B. **2014**. "TRPM2 Mediates Ischemic Kidney Injury and Oxidant Stress through RAC1." *J Clin Invest.* 124 (11): 4989–5001. https://doi.org/10.1172/JCI76042.us.

Gao H., Chen X., Du X., Guan B., Liu Y., and Zhang H. **2011**. "EGF Enhances the Migration of Cancer Cells by Up-Regulation of TRPM7." *Cell Calcium* 50 (6): 559–68. https://doi.org/10.1016/j.ceca.2011.09.003.

Gardiner J.C., Kirkup A.J., Curry J., Humphreys S., O'Regan P., Postlethwaite M., Young K.C., et al. **2014**. "The Role of TRPM8 in the Guinea-Pig Bladder-Cooling Reflex Investigated Using a Novel TRPM8 Antagonist." *European Journal of Pharmacology* 740: 398–409. https://doi.org/10.1016/j.ejphar.2014.07.022.

Garsky V.M., Lumma P.K., Feng D.M., Wai J., Ramjit H.G., Sardana M.K., Oliff A., Jones R.E., DeFeo-Jones D., and Freidinger R.M. **2001**. "The Synthesis of a Prodrug of Doxorubicin Designed to Provide Reduced Systemic Toxicity and Greater Target Efficacy." *Journal of Medicinal Chemistry* 44 (24): 4216–24. https://doi.org/10.1021/jm0101996.

Gaston T.E., and Friedman D. **2017**. "Pharmacology of Cannabinoids in the Treatment of Epilepsy." *Epilepsy and Behavior* 70: 313–18. https://doi.org/10.1016/j.yebeh.2016.11.016.

Gaudet R. **2008**. "A Primer on Ankyrin Repeat Function in TRP Channels and Beyond." *Mol Biosyst* 4 (5): 372–79. https://doi.org/10.1039/b801481g.A.

Ge R.g, Tai Y., Sun Y., Zhou K., Yang S., Cheng T., Zou Q., Shen F., and Wang Y. **2009**. "Critical Role of TRPC6 Channels in VEGF-Mediated Angiogenesis." *Cancer Letters* 283 (1): 43–51. https://doi.org/10.1016/j.canlet.2009.03.023.

Genova T., Grolez G.P., Camillo C., Bernardini M., Bokhobza A., Richard E., Scianna M., et al. **2017**. "TRPM8 Inhibits Endothelial Cell Migration via a Nonchannel Function by Trapping the Small GTPase Rap1." *Journal of Cell Biology* 216 (7): 2107–30. https://doi.org/10.1083/jcb.201506024.

Genovesi S., Moro R., Vignoli B., De Felice D., Canossa M., Montironi R., Carbone F.G., Barbareschi M., Lunardi A., and Alaimo A. **2022**. "Trpm8 Expression in Human and Mouse Castration Resistant Prostate Adenocarcinoma Paves the Way for the Preclinical Development of TRPM8-Based Targeted Therapies." *Biomolecules*. https://doi.org/10.3390/biom12020193.

Ghosh K., Thodeti C.K., Dudley A.C., Mammoto A., Klagsbrun M., and Ingber D.E. **2008**. "Tumor-Derived Endothelial Cells Exhibit Aberrant Rho-Mediated Mechanosensing and Abnormal Angiogenesis in Vitro" 105 (32).

Gill I.S., Azzouzi A.R., Emberton M., Coleman J.A., Coeytaux E., Scherz A., and Scardino P.T. **2018**. "Randomized Trial of Partial Gland Ablation with Vascular Targeted Phototherapy versus Active Surveillance for Low Risk Prostate Cancer: Extended Followup and Analyses of Effectiveness." *Journal of Urology* 200 (4): 786–93. https://doi.org/10.1016/j.juro.2018.05.121.

Gilmore T.D. **2006**. "Introduction to NF-KB: Players, Pathways, Perspectives." *Oncogene* 25 (51): 6680–84. https://doi.org/10.1038/sj.onc.1209954.

Gkika D., Flourakis M., Lemonnier L., and Prevarskaya N. **2010**. "PSA Reduces Prostate Cancer Cell Motility by Stimulating TRPM8 Activity and Plasma Membrane Expression." *Oncogene* 29 (32): 4611–16. https://doi.org/10.1038/onc.2010.210.

Gkika D., Lemonnier L., Shapovalov G., Gordienko D., Poux C., Bernardini M., Bokhobza A., et al. **2015**. "TRP Channel-Associated Factors Are a Novel Protein Family That Regulates TRPM8 Trafficking and Activity." *Journal of Cell Biology* 208 (1): 89–107. https://doi.org/10.1083/jcb.201402076.

Gkika D., and Prevarskaya N. **2009**. "Molecular Mechanisms of TRP Regulation in Tumor Growth and Metastasis." *BBA - Molecular Cell Research* 1793 (6): 953–58. https://doi.org/10.1016/j.bbamcr.2008.11.010.

———. **2011**. "TRP Channels in Prostate Cancer : The Good , the Bad and the Ugly ?" *Asian J Androl.* 13 (5): 673–76. https://doi.org/10.1038/aja.2011.18.

Gleason D.F., Mellinger G.T., and Ardving L.J. **1974**. "Prediction of Prognosis for Prostatic Adenocarcinoma by Combined Histological Grading and Clinical Staging." *The Journal of Urology* 111 (1): 58–64. https://doi.org/10.1016/S0022-5347(17)59889-4.

Glenmark Pharmaceuticals. **2010**. Thienopyrimidinedione derivatives as trpa1 modulators. WO2010109334A2, issued 2010.

———. **2015**. Pharmaceutical composition comprising a TRPA1 antagonist and an analgesic agent. WO2015056094, issued 2015.

———. **2016**. TRPA1 antagonist for the treatment of pain associated to diabetic neuropathic pain. WO2016042501, issued 2016.

Gollnick S.O., and Brackett C.M. **2010**. "Enhancement of Anti-Tumor Immunity by Photodynamic Therapy." *Immunologic Research* 46 (1–3): 216–26. https://doi.org/10.1007/s12026-009-8119-4.

Gómez-Vicente V., Donovan M., and Cotter T.G. **2005**. "Multiple Death Pathways in Retina-Derived 661W Cells Following Growth Factor Deprivation: Crosstalk between Caspases and Calpains." *Cell Death and Differentiation* 12 (7): 796–804. https://doi.org/10.1038/sj.cdd.4401621.

González-Muñiz R., Angeles Bonache M., Martín-Escura C., and Gómez-Monterrey I. **2019**. "Recent Progress in TRPM8 Modulation: An Update." *International Journal of Molecular Sciences* 20 (11): 1–22. https://doi.org/10.3390/ijms20112618.

Gordetsky J., and Epstein J. **2016**. "Grading of Prostatic Adenocarcinoma: Current State and Prognostic Implications." *Diagnostic Pathology* 11 (1). https://doi.org/10.1186/S13000-016-0478-2.

Gratzke C., Streng T., Waldkirch E., Sigl K., Stief C., Andersson K.E., and Hedlund P. **2009**. "Transient Receptor Potential A1 (TRPA1) Activity in the Human Urethra-Evidence for a Functional Role for TRPA1 in the Outflow Region." *European Urology* 55 (3): 696–704. https://doi.org/10.1016/j.eururo.2008.04.042.

Gratzke C., Weinhold P., Reich O., Seitz M., Schlenker B., Stief C.G., Andersson K.E., and Hedlund P. **2010**. "Transient Receptor Potential A1 and Cannabinoid Receptor Activity in Human Normal and Hyperplastic Prostate: Relation to Nerves and Interstitial Cells." *European Urology* 57 (5): 902–10. https://doi.org/10.1016/j.eururo.2009.08.019.

Greka A., Navarro B., Oancea E., Duggan A., and Clapham D.E. **2003**. "TRPC5 Is a Regulator of Hippocampal Neurite Length and Growth Cone Morphology." *Nat Neurosci.* 6 (8): 837–45.

Grgic I., Eichler I., Heinau P., Si H., Brakemeier S., Hoyer J., and Köhler R. **2005**. "Selective Blockade of the Intermediate-Conductance Ca^{2+}-Activated K^+ Channel Suppresses Proliferation of Microvascular and Macrovascular Endothelial Cells and Angiogenesis *in Vivo*." *Arteriosclerosis, Thrombosis, and Vascular Biology* 25 (4): 704–9. https://doi.org/10.1161/01.ATV.0000156399.12787.5C.

Grimaldi N., Andrade F., Segovia N., Ferrer-Tasies L., Sala S., Veciana J., and Ventosa N. **2016**. "Lipid-Based Nanovesicles for Nanomedicine." *Chemical Society Reviews* 45 (23): 6520–45. https://doi.org/10.1039/c6cs00409a.

Grolez G.P., Hammadi M., Barras A., Gordienko D., Slomianny C., Völkel P., Angrand P.O., et al. **2019**. "Encapsulation of a TRPM8 Agonist, WS12, in Lipid Nanocapsules Potentiates PC3 Prostate Cancer Cell Migration Inhibition through Channel Activation." *Scientific Reports* 9 (1): 7926. https://doi.org/10.1038/s41598-019-44452-4.

Grolez G.P., Gordiendko D., Clarisse M., Hammadi M., Desruelles E., Fromont G., Prevarskaya N., Slomianny C., and Gkika D. **2019**. "TRPM8-Androgen Receptor Association within Lipid Rafts Promotes Prostate Cancer Cell Migration." *Cell Death & Disease* 10 (9): 652. https://doi.org/10.1038/s41419-019-1891-8.

Gualdani R., Ceruti S., Magni G., Merli D., Di Cesare Mannelli L., Francesconi O., Richichi B., et al. **2015**. "Lipoic-Based TRPA1/TRPV1 Antagonist to Treat Orofacial Pain." *ACS Chemical Neuroscience* 6 (3): 380–85. https://doi.org/10.1021/cn500248u.

Guéguinou M., Harnois T., Crottes D., Uguen A., Deliot N., Gambade A., Chantôme A., et al. **2016**. "SK3/TRPC1/Orai1 Complex Regulates SOCE-Dependent Colon Cancer Cell Migration: A Novel Opportunity to Modulate Anti- EGFR MAb Action by the Alkyl-Lipid Ohmline." *Oncotarget* 7 (24): 36168–84. https://doi.org/10.18632/oncotarget.8786.

Guilbert A., Gautier M., Dhennin-Duthille I., Rybarczyk P., Sahni J., Sevestre H., Scharenberg A.M., and Ouadid-Ahidouch H. **2013**. "Transient Receptor Potential Melastatin 7 Is Involved in Oestrogen Receptor-Negative Metastatic Breast Cancer Cells Migration through Its Kinase Domain." *European Journal of Cancer* 49 (17): 3694–3707. https://doi.org/10.1016/j.ejca.2013.07.008.

Guilbert A., Dhennin-Duthille I., Hiani Y.E.L., Haren N., Khorsi H., Sevestre H., Ahidouch A., and Ouadid-Ahidouch H. **2008**. "Expression of TRPC6 Channels in Human Epithelial Breast Cancer Cells." *BMC Cancer* 8: 1–11. https://doi.org/10.1186/1471-2407-8-125.

Gunnarsson O., Schelin S., Brudin L., Carlsson S., and Damber J.E. **2019**. "Triple Treatment of High-Risk Prostate Cancer. A Matched Cohort Study with up to 19 Years Follow-up Comparing Survival Outcomes after Triple Treatment and Treatment with Hormones and Radiotherapy." *Scandinavian Journal of Urology* 53 (2–3): 102–8. https://doi.org/10.1080/21681805.2019.1600580.

Habault J., and Poyet J.L. **2019**. "Recent Advances in Cell Penetrating Peptide-Based Anticancer Therapies." *Molecules* 24 (5): 927. https://doi.org/10.3390/molecules24050927.

Haglind E., Carlsson S., Stranne J., Wallerstedt A., Wilderäng U., Thorsteinsdottir T., Lagerkvist M., et al. **2015**. "Urinary Incontinence and Erectile Dysfunction after Robotic Versus Open Radical Prostatectomy: A Prospective, Controlled, Nonrandomised Trial." *European Urology* 68 (2): 216–25. https://doi.org/10.1016/j.eururo.2015.02.029.

Hamdollah Z., Hamdollah M.A., Glass C.A., Magnussen A., Hancox J.C., and Bates D.O. **2008**. "VEGF-Mediated Elevated Intracellular Calcium and Angiogenesis in Human Microvascular Endothelial Cells *In Vitro* Are Inhibited by Dominant Negative TRPC6." *Microcirculation* 15 (7): 605–14. https://doi.org/10.1080/10739680802220323.

Hamdy F.C., Donovan J.L., Lane J.A., Mason M., Metcalfe C., Holding P., Davis M., et al. **2016**. "10-Year Outcomes after Monitoring, Surgery, or Radiotherapy for Localized Prostate Cancer." *New England Journal of Medicine* 375 (15): 1415–24. https://doi.org/10.1056/nejmoa1606220.

Hantute-Ghesquier A., Haustrate A., Prevarskaya N., and 'V Lehen'kyi. **2018**. "TRPM Family Channels in Cancer." *Pharmaceuticals* 11 (58). https://doi.org/10.3390/ph11020058.

Hardie R.C., and Minke B. **1992**. "The Trp Gene Is Essential for a Light-Activated Ca^{2+} Channel in Drosophila Photoreceptors." *Neuron* 8 (4): 643–51.

Harmatys K.M., Overchuk M., Chen J., Ding L., Chen Y., Pomper M.G., and Zheng G. **2018**. "Tuning Pharmacokinetics to Improve Tumor Accumulation of a Prostate-Specific Membrane Antigen-Targeted Phototheranostic Agent." *Bioconjugate Chemistry* 29 (11): 3746–56. https://doi.org/10.1021/ACS.BIOCONJCHEM.8B00636.

Haws H.J., Mcneil M.A., and Hansen M.D.H. **2016**. "Control of Cell Mechanics by RhoA and Calcium Fl Uxes during Epithelial Scattering." *Tissue Barriers* 4 (3): 1–15. https://doi.org/10.1080/21688370.2016.1187326.

Hayashi T., Kondo T., Ishimatsu M., Takeya M., Igata S., Nakamura K.I., and Matsuoka K. **2011**. "Function and Expression Pattern of TRPM8 in Bladder Afferent Neurons Associated with Bladder Outlet Obstruction in Rats." *Autonomic Neuroscience: Basic and Clinical* 164 (1–2): 27–33. https://doi.org/10.1016/j.autneu.2011.05.006.

Hecquet C.M., Ahmmed G.U., Vogel S.M., and Malik A.B. **2008**. "Role of TRPM2 Channel in Mediating H_2O_2-Induced Ca^{2+} Entry and Endothelial Hyperpermeability." *Circulation Research* 102 (3): 347–55. https://doi.org/10.1161/CIRCRESAHA.107.160176.

Heidtmann H.H., Nettelbeck D.M., Mingels A., Jäger R., Welker H.G., and Kontermann R.E. **1999**. "Generation of Angiostatin-like Fragments from Plasminogen by Prostate-Specific Antigen." *British Journal of Cancer* 81 (8): 1269–73. https://doi.org/10.1038/sj.bjc.6692167.

Heit J.J., Apelqvist A.A., Gu X., Winslow M.M., Neilson J.R., Crabtree G.R., and Kim S.K. **2006**. "Calcineurin/NFAT Signalling Regulates Pancreatic β-Cell Growth and Function." *Nature* 443 (7109): 345–49. https://doi.org/10.1038/nature05097.

Henshall S.M., Afar D.E.H., Hiller J., Horvath L.G., Quinn D.I., Rasiah K.K., Gish K., et al. **2003**. "Survival Analysis of Genome-Wide Gene Expression Profiles of Prostate Cancers Identifies New Prognostic Targets of Disease Relapse." *Cancer Research* 63 (14): 4196–4203.

Herz J.M., and Kesicki E.A. **2015**. TRPA1 modulators. WO2015103060A1, issued 2015.

Hicks K., Neil R.G.O., Dubinsky W.S., Brown R.C., Hicks K., O Neil R.G., Dubinsky W.S., and Brown R.C. **2010**. "TRPC-Mediated Actin-Myosin Contraction Is Critical for BBB Disruption Following Hypoxic Stress." *Am J Physiol Cell Physiol* 298: 1583–93. https://doi.org/10.1152/ajpcell.00458.2009.

Himmel N.J., and Cox D.N. **2020**. "Transient Receptor Potential Channels: Current Perspectives on Evolution, Structure, Function and Nomenclature." *Proceedings of the Royal Society B: Biological Sciences* 287 (1933): 20201309. https://doi.org/10.1098/rspb.2020.1309.

Hinman A., Chuang H.H., Bautista D.M., and Julius D. **2006**. "TRP Channel Activation by Reversible Covalent Modification." *Proceedings of the National Academy of Sciences of the United States of America* 103 (51): 19564–68. https://doi.org/10.1073/pnas.0609598103.

Hirasawa H., Kawamura N., and Kobauashi J. **2016**. TRPM8 inhibitors containing α-substituted glycine amides. JP2016094407, issued 2016.

Hirasawa, H., Tanada F., Mutai Y., Fushimi N., Kobayashi Y., and Kijima Y. **2018**a. Method for the preparation of pyrazole derivatives. JP2018108988A, issued 2018.

———. **2018**b. Pharmaceutical composition containing pyrazole derivatives as TRPM8 inhibitors. JP2018100269, issued 2018.

Ho H-H., Chang C-S., Ho W-C., Liao S-Y., and Wu C-H. **2010**. "Anti-Metastasis Effects of Gallic Acid on Gastric Cancer Cells Involves Inhibition of NF-kB Activity and Downregulation of PI3K/ AKT/Small GTPase Signals." *Food and Chemical Toxicology* 48 (8–9): 2508–16. https://doi.org/10.1016/j.fct.2010.06.024.

Hoag G.E. **2017**. Topical analgesic pain relief formulations, manufacture and methods of use thereof. WO2017059088A8, issued 2017.

Hobbs G.A., Der C.J., and Rossman K.L. **2016**. "RAS Isoforms and Mutations in Cancer at a Glance." *Journal of Cell Science* 129 (7): 1287–92. https://doi.org/10.1242/jcs.182873.

Hoefig C.S., Zucchi R., and Köhrle J. **2016**. "Thyronamines and Derivatives: Physiological Relevance, Pharmacological Actions, and Future Research Directions." *Thyroid* 26 (12): 1656–73. https://doi.org/10.1089/thy.2016.0178.

Hoenderop J.G.J., Voets T., Hoefs S., Weidema F., Prenen J., Nilius B., and Bindels R.J.M. **2003**. "Homo- and Heterotetrameric Architecture of the Epithelial Ca^{2+} Channels TRPV5 and TRPV6." *The EMBO Journal* 22 (4): 2–11.

Hoenderop J.G.J., Nilius B., and Bindels R.J.M. **2005**. "Calcium Absorption across Epithelia." *Physiological Reviews* 85 (1): 373–422. https://doi.org/10.1152/physrev.00003.2004.

Hoffmann F., LaRoche, and Genentech. **2018**. Sulfonyl pyridyl TRP inhibitors. WO2018029288, issued 2018.

———. **2019**. Oxadiazole transient receptor potential channel inhibitors. WO2019182925, issued 2019.

Hofmann T., Schaefer M., Schultz G., and Gudermann T. **2002**. "Subunit Composition of Mammalian Transient Receptor Potential Channels in Living Cells." *Proceedings of the National Academy of Sciences of the United States of America* 99 (11): 7461–66. https://doi.org/10.1073/pnas.102596199.

Holzer P. **2011**. "Transient Receptor Potential (TRP) Channels as Drug Targets for Diseases of the Digestive System." *Pharmacology and Therapeutics* 131 (1): 142–70. https://doi.org/10.1016/j.pharmthera.2011.03.006.

Holzmann C., Kappel S., Kilch T., Jochum M.M., Urban S.K., Jung V., Stöckle M., Rother K., Greiner M., and Peinelt C. **2015**. "Transient Receptor Potential Melastatin 4 Channel Contributes to Migration of Androgen-Insensitive Prostate Cancer Cells." *Oncotarget* 6 (39): 41783–93. https://doi.org/10.18632/oncotarget.6157.

Hong X., and Yu J.J. **2019**. "MicroRNA-150 Suppresses Epithelial-Mesenchymal Transition, Invasion, and Metastasis in Prostate Cancer through the TRPM4-Mediated β-Catenin Signaling Pathway." *American Journal of Physiology - Cell Physiology* 316 (4): C463–80. https://doi.org/10.1152/ajpcell.00142.2018.

Horne D.B., Biswas K., Brown J., Bartberger M.D., Clarine J., Davis C.D., Gore V.K., et al. **2018**. "Discovery of TRPM8 Antagonist (S)-6-(((3-Fluoro-4-(Trifluoromethoxy)Phenyl)(3-Fluoropyridin-2-Yl)Methyl)Carbamoyl)Nicotinic Acid (AMG 333), a Clinical Candidate for the Treatment of Migraine." *Journal of Medicinal Chemistry* 61 (18): 8186–8201. https://doi.org/10.1021/acs.jmedchem.8b00518.

Horne D.B., Tamayo N.A., Bartberger M.D., Bo Y., Clarine J., Davis C.D., Gore V.K., et al. **2014**. "Optimization of Potency and Pharmacokinetic Properties of Tetrahydroisoquinoline Transient Receptor Potential Melastatin 8 (TRPM8) Antagonists." *Journal of Medicinal Chemistry* 57 (7): 2989–3004. https://doi.org/10.1021/jm401955h.

House C.D., Dar Wang B., Ceniccola K., Williams R., Simaan M., Olender J., Patel V., et al. **2015**. "Voltage-Gated Na^{+} Channel Activity Increases Colon Cancer Transcriptional Activity and Invasion Via Persistent MAPK Signaling." *Scientific Reports* 5 (June). https://doi.org/10.1038/SREP11541.

Hoyer-Hansen M., and Jaattela M. **2007**. "Connecting Endoplasmic Reticulum Stress Toautophagy by Unfolded Protein Response and Calcium." *Cell Death and Differentiation* 14: 1576–82. https://doi.org/10.1038/sj.cdd.4402200.

Huang F., Ni M., Zhang J.M., Li D.J., and Shen F.M. **2017**. "TRPM8 Downregulation by Angiotensin II in Vascular Smooth Muscle Cells Is Involved in Hypertension." *Molecular Medicine Reports* 15 (4): 1900–1908. https://doi.org/10.3892/mmr.2017.6158.

Huang X., He Y., Dubuc A.M., Hashizume R., Zhang W, Reimand J., Yang H., et al. **2015**. "EAG2 Potassium Channel with Evolutionarily Conserved Function as a Brain Tumor Target." *Nature Neuroscience* 18 (9): 1236–46. https://doi.org/10.1038/nn.4088.

Huang Y.W., Chang S.J., Harn H.I-C, Huang H.T., Lin H.H., Shen M.R., Tang M.J., and Chiu W.T. **2015**. "Mechanosensitive Store-Operated Calcium Entry Regulates the Formation of Cell Polarity." *Journal of Cellular Physiology* 230 (9): 2086–97. https://doi.org/10.1002/jcp.24936.

Huang Y., Fliegert R., Guse A.H., Lü W., and Du J. **2020**. "A Structural Overview of the Ion Channels of the TRPM Family." *Cell Calcium*

85 (September 2019): 102111. https://doi.org/10.1016/j.ceca.2019.102111.

Huggins C., and Hodges C.V. **1972**. "Studies on Prostatic Cancer. I. The Effect of Castration, of Estrogen and Androgen Injection on Serum Phosphatases in Metastatic Carcinoma of the Prostate." *CA: A Cancer Journal for Clinicians* 22 (4): 293–97. https://doi.org/10.3322/CANJCLIN.22.4.232.

Hydra Biosciences. **2007**. TRPA1 inhibitors for treating pain. WO2007073505, issued 2007.

Iamshanova O., Fiorio Pla A., and Prevarskaya N. **2017**. "Molecular Mechanisms of Tumour Invasion: Regulation by Calcium Signals." *Journal of Physiology* 595 (10): 3063–75. https://doi.org/10.1113/JP272844.

Iftinca M., Hamid J., Chen L., Varela D., Tadayonnejad R., Altier C., Turner R.W., and Zamponi G.W. **2007**. "Regulation of T-Type Calcium Channels by Rho-Associated Kinase." *Nature Neuroscience* 10 (7): 854–60. https://doi.org/10.1038/nn1921.

Igarashi P., and Somlo S. **2002**. "Genetics and Pathogenesis of Polycystic Kidney Disease." *Journal of the American Society of Nephrology* 13 (9): 2384–98. https://doi.org/10.1097/01.ASN.0000028643.17901.42.

Imbrici P., Nicolotti O., Leonetti F., Conte D., and Liantonio A. **2018**. "Ion Channels in Drug Discovery and Safety Pharmacology." *Methods in Molecular Biology* 1800: 313–26. https://doi.org/10.1007/978-1-4939-7899-1_15.

Inoue K.i, and Xiong Z.G. **2009**. "Silencing TRPM7 Promotes Growth/Proliferation and Nitric Oxide Production of Vascular Endothelial Cells via the ERK Pathway." *Cardiovascular Research* 83 (3): 547–57. https://doi.org/10.1093/cvr/cvp153.

Izquierdo C., Martín-Martínez M., Gómez-Monterrey I., and González-Muñiz R. **2021**. "TRPM8 Channels: Advances in Structural Studies and Pharmacological Modulation." *International Journal of Molecular Sciences*. https://doi.org/10.3390/ijms22168502.

Jabłońska-Trypuć A., Matejczyk M., and Rosochacki S. **2016**. "Matrix Metalloproteinases (MMPs), the Main Extracellular Matrix (ECM) Enzymes in Collagen Degradation, as a Target for Anticancer Drugs Enzymes in Collagen Degradation, as a Target for Anticancer Drugs." *J Enzyme Inhib Med Chem.* 31 (sup1): 177–83. https://doi.org/10.3109/14756366.2016.1161620.

Jacob A., Jing J., Lee J., Schedin P., Gilbert S.M., Peden A.A., Junutula J.R., and Prekeris R. **2013**. "Rab40b Regulates Trafficking of MMP2 and MMP9 during Invadopodia Formation and Invasion of Breast Cancer Cells." *J Cell Sci.* 126 (Pt20): 4647–58. https://doi.org/10.1242/jcs.126573.

Jacquart A., Kéramidas M., Vollaire J., Boisgard R., Pottier G., Rustique E., Mittler F., et al. **2013**. "LipImage™ 815: Novel Dye-Loaded Lipid Nanoparticles for Long-Term and Sensitive in Vivo near-Infrared Fluorescence Imaging." *Journal of Biomedical Optics* 18 (10): 101311 1-9. https://doi.org/10.1117/1.JBO.18.10.101311.

Jahchan N.S., Dudley J.T., Mazur P.K., Flores N., Yang D., Palmerton A., Zmoos A.F., et al. **2013**. "A Drug Repositioning Approach Identifies Tricyclic Antidepressants as Inhibitors of Small Cell Lung Cancer and Other Neuroendocrine Tumors." *Cancer Discovery* 3 (12): 1364–77. https://doi.org/10.1158/2159-8290.CD-13-0183.

Janssen Pharmaceutical. **2010**. Heterocyclic amides as modulators of trpa1. WO2010141805, issued 2010.

Janssens A., Gees M., Toth B.I., Ghosh D., Mulier M., Vennekens R., Vriens J., Talavera K., and Voets T. **2016**. "Definition of Two Agonist Types at the Mammalian Cold-Activated Channel TRPM8." *ELife* 5 (JULY): 1–21. https://doi.org/10.7554/eLife.17240.

Jaquemar D., Schenker T., and Trueb B. **1999**. "An Ankyrin-like Protein with Transmembrane Domains Is Specifically Lost after Oncogenic Transformation of Human Fibroblasts." *J Biol Chem* 274: 7325–33. https://doi.org/10.1074/jbc.274.11.7325.

Jeske N.A., Diogenes A., Ruparel N.B., Fehrenbacher J.C., Henry M., Akopian A.N., and Hargreaves K.M. **2008**. "A-Kinase Anchoring Protein Mediates TRPV1 Thermal Hyperalgesia through PKA Phosphorylation of TRPV1." *Pain* 138 (3): 604–16. https://doi.org/10.1016/j.pain.2008.02.022.A-Kinase.

Jiang L., Gamper N., and Beech D.J. **2011**. "Properties and Therapeutic Potential of Transient Receptor Potential Channels with Putative Roles in Adversity: Focus on TRPC5, TRPM2 and TRPA1." *Current Drug Targets* 12 (5): 724–36. https://doi.org/10.2174/138945011795378568.

Johnson C.D., Melanaphy D., Purse A., Stokesberry S.A., Dickson P., and Zholos A.V. **2009**. "Transient Receptor Potential Melastatin 8 Channel Involvement in the Regulation of Vascular Tone." *American Journal of Physiology - Heart and Circulatory Physiology* 296 (6). https://doi.org/10.1152/ajpheart.01112.2008.

Johnson J.D., Han Z., Otani K., Ye H., Zhang Y., Wu H., Horikawa Y., Misler S.,. Bell G.I., and Polonsky K.S. **2004**. "RyR2 and Calpain-10 Delineate a Novel Apoptosis Pathway in Pancreatic Islets." *Journal of Biological Chemistry* 279 (23): 24794–802. https://doi.org/10.1074/jbc.M401216200.

Jordt S.E., Bautista D.M., Chuang H.H., McKemy D.D., Zygmunt P.M., Högestätt E.D., Meng I.D., and Julius D. **2004**. "Mustard Oils and Cannabinoids Excite Sensory Nerve Fibres through the TRP Channel ANKTM1." *Nature* 427 (6971): 260–65. https://doi.org/10.1038/nature02282.

Julius D. **2022**. "David Julius - Nobel Prize Lecture." Outreach AB 2022. https://www.nobelprize.org/prizes/medicine/2021/julius/lecture/.

Jung S., Strotmann R., Schultz G., and Plant T.D. **2002**. "TRCP6 Is a Candidate Channel Involved in Receptor Stimulated Cation Currents in A7r5 Smooth Muscle Cells." *American Journal of Physiology - Cell Physiology* 282 (2 51-2): 347–59. https://doi.org/10.1152/ajpcell.00283.2001.

Kaneko Y., and Szallasi A. **2014**. "Transient Receptor Potential (TRP) Channels: A Clinical Perspective." *British Journal of Pharmacology*. John Wiley and Sons Inc. https://doi.org/10.1111/bph.12414.

Kang K., Pulver S.R., Panzano V.C., Chang E.C., Griffith L.C., Theobald D.L., and Garrity P.A. **2010**. "Analysis of Drosophila TRPA1 Reveals an Ancient Origin for Human Chemical Nociception" 464 (7288): 597–600. https://doi.org/10.1038/nature08848.Analysis.

Kang R.H., Jang J.E., Huh E., Kang S.J., Ahn D.R., Kang J.S., Sailor M.J., et al. **2020**. "A Brain Tumor-Homing Tetra-Peptide Delivers a Nano-Therapeutic for More Effective Treatment of a Mouse Model of Glioblastoma." *Nanoscale Horizons* 5 (8): 1213–25. https://doi.org/10.1039/d0nh00077a.

Kanzaki M., Zhang Y.Q., Mashima H., Li L., Shibata H., and Kojima I. **1999**. "Translocation of a Calcium-Permeable Cation Channel Induced by Insulin-like Growth Factor-I." *Nature Cell Biology* 1 (3): 165–70. https://doi.org/10.1038/11086.

Kao Corporation. **2015**. Irritation relieving agent. WO2015002095, issued 2015.

Karashima Y., Damann N., Prenen J., Talavera K., Segal A., Voets T., and Nilius B. **2007**. "Bimodal Action of Menthol on the Transient Receptor Potential Channel TRPA1." *Journal of Neuroscience* 27 (37): 9874–84. https://doi.org/10.1523/JNEUROSCI.2221-07.2007.

Kato T., Sakamoto T., Niwa Y., Sawamoto D., and Otani N.K.M. **2017**. Preparation of aromatic carboxylic acida mides having TRPM8 blocking effect. JP2017214290, issued 2017.

Katterle Y., Brandt B.H., Dowdy S.F., Niggemann B., Zänker K.S., and Dittmar T. **2004**. "Antitumour Effects of PLC-Γ1-(SH2)2-TAT Fusion Proteins on EGFR/c-ErbB-2-Positive Breast Cancer Cells." *British Journal of Cancer* 90 (1): 230–35. https://doi.org/10.1038/sj.bjc.6601506.

Kazantzis K.T., Koutsonikoli K., Mavroidi B., Zachariadis M., Alexiou P., Pelecanou M., Politopoulos K., Alexandratou E., and Sagnou M. **2020**. "Curcumin Derivatives as Photosensitizers in Photodynamic Therapy: Photophysical Properties and in Vitro Studies with Prostate Cancer Cells." *Photochemical & Photobiological Sciences : Official Journal of the European Photochemistry Association and the European Society for Photobiology* 19 (2): 193–206. https://doi.org/10.1039/C9PP00375D.

Khajavi N., Mergler S., and Biebermann H. **2017**. "3-Iodothyronamine, a Novel Endogenous Modulator of Transient Receptor Potential Melastatin 8?" *Frontiers in Endocrinology* 8 (AUG): 1–7. https://doi.org/10.3389/fendo.2017.00198.

Khajavi N., Reinach P.S., Slavi N., Skrzypski M., Lucius A., Strauß O., Köhrle J., and Mergler S. **2015**. "Thyronamine Induces TRPM8 Channel Activation in Human Conjunctival Epithelial Cells." *Cellular Signalling*. https://doi.org/10.1016/j.cellsig.2014.11.015.

Kida N., Sokabe T., Kashio M., Haruna K., Mizuno Y., Suga Y., Nishikawa K., et al. **2012**. "Importance of Transient Receptor Potential Vanilloid 4 (TRPV4) in Epidermal Barrier Function in Human Skin Keratinocytes." *Pflugers Archiv European Journal of Physiology* 463 (5): 715–25. https://doi.org/10.1007/s00424-012-1081-3.

Kiessling A., Füssel S., Schmitz M., Stevanovic S., Meye A., Weigle B., Klenk U., Wirth M.P., and Rieber E.P. **2003**. "Identification of an HLA-A*0201-Restricted T-Cell Epitope Derived from the Prostate Cancer-Associated Protein Trp-P8." *Prostate* 56 (4): 270–79. https://doi.org/10.1002/pros.10265.

Kim A.Y., Tang Z., Liu Q., Patel K.N., Maag D., Geng Y., and Dong X. **2008**. "Pirt, a Phosphoinositide-Binding Protein, Functions as a Regulatory Subunit of TRPV1." *Cell* 133 (3): 475–85. https://doi.org/10.1016/j.cell.2008.02.053.

Kim J.G., Islam R., Cho J.Y., Jeong H., Cap K.C., Park Y., Hossain A.J., and Park J.B. **2018**. "Regulation of RhoA GTPase and Various Transcription Factors in the RhoA Pathway." *Journal of Cellular Physiology* 233 (9): 6381–92. https://doi.org/10.1002/jcp.26487.

Kim M.M., and Darafsheh A. **2020**. "Light Sources and Dosimetry Techniques for Photodynamic Therapy." *Photochemistry and Photobiology* 96 (2): 280–94. https://doi.org/10.1111/php.13219.

Kim S.H., Nam J.H., Park E.J., Kim B.J., Kim S.J., So I., and Jeon J.H. **2009**. "Menthol Regulates TRPM8-Independent Processes in PC-3 Prostate Cancer Cells." *Biochimica et Biophysica Acta - Molecular Basis of Disease* 1792 (1): 33–38. https://doi.org/10.1016/j.bbadis.2008.09.012.

Kirchherr A-K, Briel A., and Ma K. **2009**. "Stabilization of Indocyanine Green by Encapsulation within Micellar Systems." *Molecular Pharmaceutics* 6 (2): 480–91.

Kobayashi J.I., Hirasawa H., Ozawa T., Ozawa T., Takeda H., Fujimori Y., Nakanishi O., Kamada N., and Ikeda T. **2017**. "Synthesis and Optimization of Novel α-Phenylglycinamides as Selective TRPM8 Antagonists." *Bioorganic and Medicinal Chemistry* 25 (2): 727–42. https://doi.org/10.1016/j.bmc.2016.11.049.

Köhler R., Degenhardt C., Kühn M., Runkel N., Paul M., and Hoyer J. **2000**. "Expression and Function of Endothelial Ca(2+)-Activated K(+) Channels in Human Mesenteric Artery: A Single-Cell Reverse Transcriptase-Polymerase Chain Reaction and Electrophysiological Study in Situ." *Circulation Research* 87 (6): 496–503. https://doi.org/10.1161/01.RES.87.6.496.

Koike T., Kuzuya M., Asai T., Kanda S., and Cheng X.W. **2000**. "Activation of MMP-2 by Clostridium Difficile Toxin B in Bovine Smooth Muscle Cells" 46: 43–46. https://doi.org/10.1006/bbrc.2000.3630.

Koivisto A., Jalava N., Bratty R., and Pertovaara A. **2018**. "TRPA1 Antagonists for Pain Relief." *Pharmaceuticals*. http://www.embase.com/search/results?subaction=viewrecord&from=export&id=L624872945%0Ahttp://dx.doi.org/10.3390/ph11040117.

Koivisto A., Hukkanen M., Saarnilehto M., Chapman H., Kuokkanen K., Wei H., Viisanen H., Kerman K.E., Lindstedt K., and Pertovaara A. **2012**. "Inhibiting TRPA1 Ion Channel Reduces Loss of Cutaneous Nerve Fiber Function in Diabetic Animals: Sustained Activation of the TRPA1 Channel Contributes to the Pathogenesis of Peripheral Diabetic Neuropathy." *Pharmacological Research* 65 (1): 149–58. https://doi.org/10.1016/j.phrs.2011.10.006.

Koivisto A.P., Belvisi M.G., Gaudet R., and Szallasi A. **2021**. "Advances in TRP Channel Drug Discovery: From Target Validation to Clinical Studies." *Nature Reviews Drug Discovery*, 1–19. https://doi.org/10.1038/s41573-021-00268-4.

Koopman W.J.H., Bosch R.R., Van Emst-De Vries S.E., Spaargaren M., De Pont J.J.H.H.M., and Willems P.H.G.M. **2003**. "R-Ras Alters Ca^{2+} Homeostasis by Increasing the Ca^{2+} Leak across the Endoplasmic Reticular Membrane." *Journal of Biological Chemistry* 278 (16): 13672–79. https://doi.org/10.1074/jbc.M211256200.

Kraft R., and Harteneck C. **2005**. "The Mammalian Melastatin-Related Transient Receptor Potential Cation Channels: An Overview." *Pflugers Archiv European Journal of Physiology* 451 (1): 204–11. https://doi.org/10.1007/s00424-005-1428-0.

Kremeyer B., Lopera F., Cox J.J., Momin A., Rugiero F., Marsh S., Woods C.G., et al. **2010**. "A Gain-of-Function Mutation in TRPA1 Causes Familial Episodic Pain Syndrome." *Neuron* 66 (5): 671–80. https://doi.org/10.1016/j.neuron.2010.04.030.

Kriete A., and Mayo K.L. **2009**. "Atypical Pathways of NF-KB Activation and Aging." *Experimental Gerontology* 44 (4): 250–55. https://doi.org/10.1016/j.exger.2008.12.005.

Kuo Y.J., Chung C.H., and Huang T.F. **2019**. "From Discovery of Snake Venom Disintegrins to a Safer Therapeutic Antithrombotic Agent." *Toxins* 11 (7): 1–11. https://doi.org/10.3390/toxins11070372.

Kwan K.Y., Allchorne A.J., Vollrath M.A., Christensen A.P., Zhang D.S., Woolf C.J., and Corey D.P. **2006**. "TRPA1 Contributes to Cold, Mechanical, and Chemical Nociception but Is Not Essential for Hair-Cell Transduction." *Neuron* 50 (2): 277–89. https://doi.org/10.1016/j.neuron.2006.03.042.

Laínez S., Valente P., Ontoria-Oviedo I., Estévez-Herrera J., Camprubí-Robles M., Ferrer-Montiel A., and Planells-Cases R. **2010**. "GABA A Receptor Associated Protein (GABARAP) Modulates TRPV1 Expression and Channel Function and Desensitization." *The FASEB Journal* 24 (6): 1958–70. https://doi.org/10.1096/fj.09-151472.

Lange I., Yamamoto S., Partida-Sanchez S., Mori Y., Fleig A., and Penner R. **2009**. "TRPM2 Functions as a Lysosomal Ca^{2+}-Release Channel in β Cells." *Sci Signal.* 2 (71): ra23. https://doi.org/10.1126/scisignal.2000278.

Langeslag M., Clark K., Moolenaar W.H., Van Leeuwen F.N., and Jalink K. **2007**. "Activation of TRPM7 Channels by Phospholipase C-Coupled Receptor Agonists." *Journal of Biological Chemistry* 282 (1): 232–39. https://doi.org/10.1074/jbc.M605300200.

Laragione T., Cheng K.F., Tanner M.R., He M., Beeton C., Al-Abed Y., and Gulko P.S. **2015**. "The cation channel TRPV2 is a new suppressor of arthritis severity, joint damage and synovial fibroblast invasion." *Clin Immunol.* 158 (2): 183–92. https://doi.org/10.1016/j.clim.2015.04.001.THE.

Laragione T., Harris C., and Gulko P.S. **2019**. "TRPV2 Suppresses Rac1 and RhoA Activation and Invasion in Rheumatoid Arthritis Fibroblast-like Synoviocytes." *International Immunopharmacology* 70: 268–73. https://doi.org/10.1016/j.intimp.2019.02.051.

Lashinger E.S.R., Steiginga M.S., Hieble J.P., Leon L.A., Gardner S.D., Nagilla R., Davenport E.A., Hoffman B.E.,. Laping N.J., and Su X. **2008**. "AMTB, a TRPM8 Channel Blocker: Evidence in Rats for Activity in Overactive Bladder and Painful Bladder Syndrome." *American Journal of Physiology - Renal Physiology* 295 (3): 803–10. https://doi.org/10.1152/ajprenal.90269.2008.

Lastraioli E., Iorio J., and Arcangeli A. **2015**. "Ion Channel Expression as Promising Cancer Biomarker." *Biochimica et Biophysica Acta - Biomembranes* 1848 (10): 2685–2702. https://doi.org/10.1016/j.bbamem.2014.12.016.

Laursen W.J., Anderson E.O., Hoffstaetter L.J., Bagriantsev S.N., and Gracheva E.O. **2015**. "Species-Specific Temperature Sensitivity of TRPA1." *Temperature* 2 (2): 214–26. https://doi.org/10.1080/23328940.2014.1000702.

Lazzeri M., Vannucchi M.G., Spinelli M., Bizzoco E., Beneforti P., Turini D., and Faussone-Pellegrini M.S. **2005**. "Transient Receptor Potential Vanilloid Type 1 (TRPV1) Expression Changes from Normal Urothelium to Transitional Cell Carcinoma of Human Bladder." *European Urology* 48 (4): 691–98. https://doi.org/10.1016/j.eururo.2005.05.018.

Leamy A.W., Shukla P., McAlexander M.A., Carr M.J., and Ghatta S. **2011**. "Curcumin ((E,E)-1,7-Bis(4-Hydroxy-3-Methoxyphenyl)-1,6-Heptadiene-3,5-Dione) Activates and Desensitizes the Nociceptor Ion Channel TRPA1." *Neuroscience Letters* 503 (3): 157–62. https://doi.org/10.1016/j.neulet.2011.07.054.

Lebdai S., Bigot P., Leroux P.A., Berthelot L.P., Maulaz P., and Azzouzi A.R. **2017**. "Vascular Targeted Photodynamic Therapy with Padeliporfin for Low Risk Prostate Cancer Treatment: Midterm Oncologic Outcomes." *The Journal of Urology* 198 (2): 335–44. https://doi.org/10.1016/J.JURO.2017.03.119.

Lebdai S., Villers A., Barret E., Nedelcu C., Bigot P., and Azzouzi A.R. **2015**. "Feasibility, Safety, and Efficacy of Salvage Radical Prostatectomy after Tookad® Soluble Focal Treatment for Localized Prostate Cancer." *World Journal of Urology* 33 (7): 965–71. https://doi.org/10.1007/S00345-015-1493-8.

Lee G., Abdi K., Jiang Y., Michaely P., Bennett V., and Marszalek P.E. **2006**. "Nanospring Behaviour of Ankyrin Repeats." *Nature* 440 (7081): 246–49. https://doi.org/10.1038/nature04437.

Lee K.J., Wang W., Padaki R., Bi V., Plewa C.A., and Gavva N.R. **2014**. "Mouse Monoclonal Antibodies to Transient Receptor Potential Ankyrin 1 Act as Antagonists of Multiple Modes of Channel Activation." *Journal of Pharmacology and Experimental Therapeutics* 350 (2): 223–31. https://doi.org/10.1124/jpet.114.215574.

Lee W.H., Choong L.Y., Jin T.H., Mon N.N., Chong S., Liew C.S., Putti T., Lu S.Y., Harteneck C., and Lim Y.P. **2017**. "TRPV4 Plays a Role in Breast Cancer Cell Migration via Ca^{2+}-Dependent Activation of AKT and Downregulation of E-Cadherin Cell Cortex Protein." *Oncogenesis* 6 (5): e338. https://doi.org/10.1038/oncsis.2017.39.

Lee W.H., Choong L.Y., Mon N.N., Lu S., Lin Q., Pang B., Yan B., Sri V., Krishna R., Singh H., Zea T.T., Thiery J.P., Lim C.T., Boon P., Tan O., Johansson M., et al. **2016**. "TRPV4 Regulates Breast Cancer Cell Extravasation, Stiffness and Actin Cortex." *Scientific Reports* 6: 27903. https://doi.org/10.1038/srep27903.

———. **2016**. "TRPV4 Regulates Breast Cancer Cell Extravasation , Stiffness and Actin Cortex." *Scientific Reports* 6: 27903. https://doi.org/10.1038/srep27903.

Legay C.M., Gorobets E., Iftinca M., Ramachandran R., Altier C., and Derksen D.J. **2016**. "Natural-Product-Derived Transient Receptor Potential Melastatin 8 (TRPM8) Channel Modulators." *Organic Letters* 18 (11): 2746–49. https://doi.org/10.1021/acs.orglett.6b01222.

Lehen'kyi V., Flourakis M., Skryma R., and Prevarskaya N. **2007**. "TRPV6 Channel Controls Prostate Cancer Cell Proliferation via Ca^{2+}/NFAT-Dependent Pathways." *Oncogene* 26 (52): 7380–85. https://doi.org/10.1038/sj.onc.1210545.

Lehen'kyi V., and Prevarskaya N. **2011**. "Oncogenic TRP Channels." In *Transient Receptor Potential Channels. Advances in Experimental Medicine and Biology*, edited by M. Islam, 929–45. Springer.

Lehen'kyi V., Raphaël M., and Prevarskaya N. **2012**. "The Role of the TRPV6 Channel in Cancer." *Journal of Physiology* 590 (6): 1369–76. https://doi.org/10.1113/jphysiol.2011.225862.

Lehto S.G., Weyer A.D., Zhang M., Youngblood B.D., Wang J., Wang W., Kerstein P.C., et al. **2015**. "AMG2850, a Potent and Selective TRPM8 Antagonist, Is Not Effective in Rat Models of Inflammatory Mechanical Hypersensitivity and Neuropathic Tactile Allodynia." *Naunyn-Schmiedeberg's Archives of Pharmacology* 388 (4): 465–76. https://doi.org/10.1007/s00210-015-1090-9.

Lei Z., Ishizuka O., Imamura T., Noguchi W., Yamagishi T., Yokoyama H., Kurizaki Y., et al. **2013**. "Functional Roles of Transient Receptor Potential Melastatin 8 (TRPM8) Channels in the Cold Stress-Induced Detrusor Overactivity Pathways in Conscious Rats." *Neurourol Urodyn.* 32 (April): 500–504. https://doi.org/10.1002/nau.

Lepannetier S., Zanou N., Yerna X., Emeriau N., Dufour I., Masquelier J., Muccioli G., Tajeddine N., and Gailly P. **2016**. "Sphingosine-

1-Phosphate-Activated TRPC1 Channel Controls Chemotaxis of Glioblastoma Cells." *Cell Calcium* 60 (6): 373–83. https://doi.org/10.1016/j.ceca.2016.09.002.

Li B., Zhao M., and Zhang F. **2020**. "Rational Design of Near-Infrared-II Organic Molecular Dyes for Bioimaging and Biosensing." *ACS Materials Letters* 2 (8): 905–17. https://doi.org/10.1021/ACSMATERIALSLETT.0C00157/ASSET/IMAGES/LARGE/TZ0C00157_0013.JPEG.

Li M., Li Q., Yang G., Kolosov V.P., Perelman J.M., and Zhou X.D. **2011**. "Cold Temperature Induces Mucin Hypersecretion from Normal Human Bronchial Epithelial Cells in Vitro through a Transient Receptor Potential Melastatin 8 (TRPM8)-Mediated Mechanism." *Journal of Allergy and Clinical Immunology* 128 (3): 626-634.e5. https://doi.org/10.1016/j.jaci.2011.04.032.

Li S., Balmain A., and Counter C.M. **2018**. "A Model for RAS Mutation Patterns in Cancers: Finding the Sweet Spot." *Nature Reviews Cancer* 18 (12): 767–77. https://doi.org/10.1038/s41568-018-0076-6.

Liao M., Cao E., Julius D., and Cheng Y. **2013**. "Structure of the TRPV1 Ion Channel Determined by Electron Cryo- Microscopy." *Nature* 504 (7478): 107–12. https://doi.org/10.1038/nature12822.Structure.

Lieu T., Jayaweera G., Zhao P., Poole D.P., Jensen D., Grace M., Mcintyre P., et al. **2014**. "The Bile Acid Receptor TGR5 Activates the TRPA1 Channel to Induce Itch in Mice." *Gastroenterology* 147 (6): 1417–28. https://doi.org/10.1053/j.gastro.2014.08.042.

Lima A.M., Dal Pizzol C., Monteiro F.B.F., Creczynski-Pasa T.B., Andrade G.P., Ribeiro A.O., and Perussi J.R. **2013**. "Hypericin Encapsulated in Solid Lipid Nanoparticles: Phototoxicity and Photodynamic Efficiency." *Journal of Photochemistry and Photobiology B: Biology* 125: 146–54. https://doi.org/10.1016/j.jphotobiol.2013.05.010.

Lin C.M., Ma J.M., Zhang L., Hao Z.Y., Zhou J., Zhou Z.Y., Shi H.Q., Zhang Y.F., Shao E.M., and Liang C.Z. **2015**. "Inhibition of Transient Receptor Potential Melastain 7 Enhances Apoptosis Induced by TRAIL in PC-3 Cells." *Asian Pacific Journal of Cancer Prevention* 16 (10): 4469–75. https://doi.org/10.7314/APJCP.2015.16.10.4469.

Lintschinger B., Balzer-Geldsetzer M., Baskaran T., Graier W.F., Romanin C., Zhu M.X., and Groschner K. **2000**. "Coassembly of Trp1 and Trp3 Proteins Generates Diacylglycerol- and Ca2+-Sensitive Cation Channels." *Journal of Biological Chemistry* 275 (36): 27799–805. https://doi.org/10.1074/jbc.M002705200.

Lis A., Wissenbach U., and Philipp S.E. **2005**. "Transcriptional Regulation and Processing Increase the Functional Variability of TRPM Channels." *Naunyn-Schmiedeberg's Archives of Pharmacology* 371 (4): 315–24. https://doi.org/10.1007/s00210-005-1050-x.

Litan A., and Langhans S.A. **2015**. "Cancer as a Channelopathy: Ion Channels and Pumps in Tumor Development and Progression." *Frontiers in Cellular Neuroscience* 9 (March): 1–11. https://doi.org/10.3389/fncel.2015.00086.

Liu B., and Qin F. **2005**. "Functional Control of Cold- and Menthol-Sensitive TRPM8 Ion Channels by Phosphatidylinositol 4,5-Bisphosphate." *Journal of Neuroscience* 25 (7): 1674–81. https://doi.org/10.1523/JNEUROSCI.3632-04.2005.

Liu C.H., Wang T., Postma M., Obukhov A.G., Montell C., and Hardie R.C. **2007**. "*In Vivo* Identification and Manipulation of the Ca^{2+} Selectivity Filter in the Drosophila Transient Receptor Potential Channel." *Journal of Neuroscience* 27 (3): 604–15. https://doi.org/10.1523/JNEUROSCI.4099-06.2007.

Liu F., Bardhan K., Yang D., Thangaraju M., Ganapathy V., Waller J.L., Liles G.B., Lee J.R., and Liu K. **2012**. "NF-KB Directly Regulates Fas Transcription to Modulate Fas-Mediated Apoptosis and Tumor Suppression." *Journal of Biological Chemistry* 287 (30): 25530–40. https://doi.org/10.1074/jbc.M112.356279.

Liu J., Chen Y., Shuai S., and Ding D. **2014**. "TRPM8 Promotes Aggressiveness of Breast Cancer Cells by Regulating EMT via Activating AKT / GSK-3 β Pathway." *Tumour Biol.* 35 (9): 8969–77. https://doi.org/10.1007/s13277-014-2077-8.

Liu K., Xu S-H., Chen Z., Zeng Q-X., Li Z-J., and Chen Z-M. **2018**. "TRPM7 Overexpression Enhances the Cancer Stem Cell-like and Metastatic Phenotypes of Lung Cancer through Modulation of the Hsp90 α / UPA / MMP2 Signaling Pathway." *BMC Cancer* 18 (1): 1167.

Liu L., Wu N., Wang Y., Zhang X., Xia B., Tang J., Cai J., and Zhao Z. **2019**. "TRPM7 Promotes the Epithelial – Mesenchymal Transition in Ovarian Cancer through the Calcium-Related PI3K / AKT Oncogenic Signaling." *J Exp Clin Cancer Res.* 38 (1): 106–21.

Liu T., Wu L.Y., Choi J.K., and Berkman C.E. **2010**. "Targeted Photodynamic Therapy for Prostate Cancer: Inducing Apoptosis via Activation of the Caspase-8/-3 Cascade Pathway." *International Journal of Oncology* 36 (4). https://doi.org/10.3892/IJO_00000553.

Liu T., Fang Z., Wang G., Shi M., Wang X., Jiang K., Yang Z., et al. **2016**. "Anti-Tumor Activity of the TRPM8 Inhibitor BCTC in Prostate Cancer DU145 Cells." *Oncology Letters* 11 (1): 182–88. https://doi.org/10.3892/ol.2015.3854.

Liu T., Wu L.Y., and Berkman C.E. **2010**. "Prostate-Specific Membrane Antigen-Targeted Photodynamic Therapy Induces Rapid Cytoskeletal Disruption." *Cancer Letters* 296 (1): 106–12. https://doi.org/10.1016/J.CANLET.2010.04.003.

Liu T., Wu L.Y., Choi J.K., and Berkman C.E. **2009**. "*In Vitro* Targeted Photodynamic Therapy with a Pyropheophorbide--a Conjugated Inhibitor of Prostate-Specific Membrane Antigen." *The Prostate* 69 (6): 585–94. https://doi.org/10.1002/PROS.20909.

Llense F., and Etienne-Manneville S. **2015**. "Front-to-Rear Polarity in Migrating Cells." In *Cell Polarity 1*, edited by Ebnet Klaus, 115–46. Springer. https://doi.org/10.1007/978-3-319-14463-4_5.

Lu Z-R., and Qiao P. **2018**. "Drug Delivery in Cancer Therapy, Quo Vadis." *Molecular Pharmaceutics* 15: 3603–16.

Luan L., Fang W., Liu W., Tian M., Ni Y., Chen X., and Yu X. **2016**. "Phthalocyanine-CRGD Conjugate: Synthesis, Photophysical Properties and in Vitro Biological Activity for Targeting Photodynamic Therapy." *Organic & Biomolecular Chemistry* 14 (10): 2985–92. https://doi.org/10.1039/C6OB00099A.

Lucius A., Khajavi N., Reinach P.S., Köhrle J., Dhandapani P., Huimann P., Ljubojevic N., Grötzinger C., and Mergler S. **2016**. "3-Iodothyronamine Increases Transient Receptor Potential Melastatin Channel 8 (TRPM8) Activity in Immortalized Human Corneal Epithelial Cells." *Cellular Signalling* 28 (3): 136–47. https://doi.org/10.1016/j.cellsig.2015.12.005.

Luo S., Zhang E., Su Y., Cheng T., and Shi C. **2011**. "A Review of NIR Dyes in Cancer Targeting and Imaging." *Biomaterials* 32 (29): 7127–38. https://doi.org/10.1016/j.biomaterials.2011.06.024.

Luo Y., Wu J.Y., Lu M.H., Shi Z., Na N., and Di J-M. **2016**. "Carvacrol Alleviates Prostate Cancer Cell Proliferation , Migration , and Invasion through Regulation of PI3K / Akt and MAPK Signaling Pathways" 2016.

Lütje S., Rijpkema M., Franssen G.M., Fracasso G., Helfrich W., Eek A., Oyen W.J., Colombatti M., and Boerman O.C. **2014**. "Dual-Modality Image-Guided Surgery of Prostate Cancer with a Radiolabeled Fluorescent Anti-PSMA Monoclonal Antibody." *Journal of Nuclear Medicine : Official Publication, Society of Nuclear Medicine* 55 (6): 995–1001. https://doi.org/10.2967/JNUMED.114.138180.

Lysechko T.L., Cheung S.M.S., and Ostergaard H.L. **2010**. "Regulation of the Tyrosine Kinase Pyk2 by Calcium Is through Production of Reactive Oxygen Species in Cytotoxic T Lymphocytes." *Journal of Biological Chemistry* 285 (41): 31174–84. https://doi.org/10.1074/jbc.M110.118265.

Ma S., Yu H., Zhao Z., Luo Z., Chen J., Ni Y., Jin R., et al. **2012**. "Activation of the Cold-Sensing TRPM8 Channel Triggers UCP1-Dependent Thermogenesis and Prevents Obesity." *Journal of Molecular Cell Biology* 4 (2): 88–96. https://doi.org/10.1093/jmcb/mjs001.

Mabonga L., and Kappo A.P. **2019**. "Protein-Protein Interaction Modulators: Advances, Successes and Remaining Challenges." *Biophysical Reviews* 11 (4): 559–81. https://doi.org/10.1007/s12551-019-00570-x.

———. **2020**. "Peptidomimetics: A Synthetic Tool for Inhibiting Protein–Protein Interactions in Cancer." *International Journal of Peptide Research and Therapeutics*. https://doi.org/10.1007/s10989-019-09831-5.

Macpherson L.J., Dubin A.E., Evans M.J., Marr F., Schultz P.G., Cravatt B.F., and Patapoutian A. **2007**. "Noxious Compounds Activate TRPA1 Ion Channels through Covalent Modification of Cysteines." *Nature* 445 (7127): 541–45. https://doi.org/10.1038/nature05544.

Macpherson L.J., Geierstanger B.H., Viswanath V., Bandell M., Eid S.R., Hwang S.W., and Patapoutian A. **2005**. "The Pungency of Garlic: Activation of TRPA1 and TRPV1 in Response to Allicin." *Current Biology* 15 (10): 929–34. https://doi.org/10.1016/j.cub.2005.04.018.

Mader C.C., Oser M., Magalhaes M.A.O., Bravo-Cordero J.J., Condeelis J., Koleske A.J., and Gil-Henn H. **2011**. "An EGFR-Src-Arg-Cortactin Pathway Mediates Functional Maturation of Invadopodia and Breast Cancer Cell Invasion." *Cancer Research* 71 (5): 1730–41. https://doi.org/10.1158/0008-5472.CAN-10-1432.

Mahieu F., Owsianik G., Verbert L., Janssens A., De Smedt H., Nilius B., and Voets T. **2007**. "TRPM8-Independent Menthol-Induced Ca^{2+} Release from Endoplasmic Reticulum and Golgi." *Journal of Biological Chemistry* 282 (5): 3325–36. https://doi.org/10.1074/jbc.M605213200.

Malagarie-Cazenave S., Olea-Herrero N., Vara D., and Díaz-Laviada I. **2009**. "Capsaicin, a Component of Red Peppers, Induces Expression of Androgen Receptor via PI3K and MAPK Pathways in Prostate LNCaP Cells." *FEBS Letters* 583 (1): 141–47. https://doi.org/10.1016/j.febslet.2008.11.038.

Mälkiä A., Madrid R., Meseguer V., De La Peña E., Valero M., Belmonte C., and Viana F. **2007**. "Bidirectional Shifts of TRPM8 Channel Gating by Temperature and Chemical Agents Modulate the Cold Sensitivity of Mammalian Thermoreceptors." *Journal of Physiology* 581 (1): 155–74. https://doi.org/10.1113/jphysiol.2006.123059.

Mälkiä A., Pertusa M, Fernández-Ballester G., Ferrer-Montiel A., and Viana F. **2009**. "Differential Role of the Menthol-Binding Residue Y745 in the Antagonism of Thermally Gated TRPM8 Channels." *Molecular Pain* 5: 1–13. https://doi.org/10.1186/1744-8069-5-62.

Mandom Corporation. **2018**. TRPA1 activity inhibitor. WO2018180460, issued 2018.

Marasa B.S., Rao J.N., Zou T., Liu L., Keledjian K.M., Zhang A.H., Xiao L., Chen J., Turner D.J., and Wang J.Y. **2006**. "Induced TRPC1 Expression Sensitizes Intestinal Epithelial Cells to Apoptosis by Inhibiting NF-kB Activation through Ca^{2+} Influx." *Biochemical Journal* 397 (1): 77–87. https://doi.org/10.1042/BJ20060124.

Martínez-Jabaloyas J.M., March-Villalba J.A., Navarro-García M.M., and Dasi F. **2013**. "Anti-Angiogenic Therapies in Prostate Cancer." *Expert Opinion on Biological Therapy* 13 (1): 1–5. https://doi.org/10.1517/14712598.2013.733366.

Martínez R., Stühmer W., Martin S., Schell J., Reichmann A., Rohde V., and Pardo L. **2015**. "Analysis of the Expression of Kv10.1 Potassium Channel in Patients with Brain Metastases and Glioblastoma Multiforme: Impact on Survival." *BMC Cancer* 15 (1). https://doi.org/10.1186/S12885-015-1848-Y.

Matsumoto Y., and Maller J.L. **2002**. "Calcium, Calmodulin, and CaMKII Requirement for Initiation of Centrosome Duplication in Xenopus Egg Extracts." *Science* 295 (5554): 499–502. https://doi.org/10.1126/science.1065693.

Matta J.A., Cornett P.M., Miyares R.L., Abe K., Sahibzada N., and Ahern G.P. **2008**. "General Anesthetics Activate a Nociceptive Ion Channel to Enhance Pain and Inflammation." *Proceedings of the National Academy of Sciences of the United States of America* 105 (25): 8784–89. https://doi.org/10.1073/pnas.0711038105.

Mayor R., and Etienne-Manneville S. **2016**. "The Front and Rear of Collective Cell Migration." *Nature Reviews Molecular Cell Biology* 17 (2): 97–109. https://doi.org/10.1038/nrm.2015.14.

McConkey D.J., and Orrenius S. **1997**. "The Role of Calcium in the Regulation of Apoptosis." *Biochemical and Biophysical Research Communications*. https://doi.org/10.1006/bbrc.1997.7409.

McKemy D.D., Neuhausser W.M., and Julius D. **2002**. "Identification of a Cold Receptor Reveals a General Role for TRP Channels in Thermosensation." *Nature* 416 (6876): 52–58. https://doi.org/10.1038/nature719.

McNamara C.R., Mandel-Brehm J., Bautista D.M., Siemens J., Deranian K.L., Zhao M., Hayward N.J., et al. **2007**. "TRPA1 Mediates Formalin-Induced Pain." *Proceedings of the National Academy of Sciences of the United States of America* 104 (33): 13525–30. https://doi.org/10.1073/pnas.0705924104.

Mehta D., Ahmmed G.U., Paria B.C., Holinstat M., Voyno-Yasenetskaya T., Tiruppathi C., Minshall R.D., and Malik A.B. **2003**. "RhoA Interaction with Inositol 1,4,5-Trisphosphate Receptor and Transient Receptor Potential Channel-1 Regulates Ca^{2+} Entry: Role in Signaling Increased Endothelial Permeability." *Journal of Biological Chemistry* 278 (35): 33492–500. https://doi.org/10.1074/jbc.M302401200.

Meng X., Cai C., Wu J., Cai S., Ye C., Chen H., Yang Z., Zeng H., Shen Q., and Zou F. **2013**. "TRPM7 Mediates Breast Cancer Cell Migration and Invasion through the MAPK Pathway." *Cancer Letters* 333 (1): 96–102. https://doi.org/10.1016/j.canlet.2013.01.031.

Meotti F.C., Forner S., Lima-Garcia J.F., Viana A.F., and Calixto J.B. **2013**. "Antagonism of the Transient Receptor Potential Ankyrin 1 (TRPA1) Attenuates Hyperalgesia and Urinary Bladder Overactivity in Cyclophosphamide-Induced Haemorrhagic Cystitis." *Chemico-Biological Interactions* 203 (2): 440–47. https://doi.org/10.1016/j.cbi.2013.03.008.

Mergler S., Cheng Y., Skosyrski S., Garreis F., Pietrzak P., Kociok N., Dwarakanath A., Reinach P.S., and Kakkassery V. **2012**. "Altered Calcium Regulation by Thermosensitive Transient Receptor Potential Channels in Etoposide-Resistant WERI-Rb1 Retinoblastoma Cells." *Experimental Eye Research*. https://doi.org/10.1016/j.exer.2011.12.002.

Mérian J., Boisgard R., Bayle P.A., Bardet M., Tavitian B., and Texier I. **2015**. "Comparative Biodistribution in Mice of Cyanine Dyes Loaded in Lipid Nanoparticles." *European Journal of Pharmaceutics and Biopharmaceutics* 93: 1–10. https://doi.org/10.1016/j.ejpb.2015.03.019.

Meseguer V., Karashima Y., Talavera K., D'Hoedt D., Donovan-Rodríguez T., Viana F., Nilius B., and Voets T. **2008**. "Transient Receptor Potential Channels in Sensory Neurons Are Targets of the Antimycotic Agent Clotrimazole." *Journal of Neuroscience* 28 (3): 576–86. https://doi.org/10.1523/JNEUROSCI.4772-07.2008.

Michaelson M.D., Oudard S., Houede N., Maurina T., Chuan Ou Y., Sengeløv L., Daugaard G., et al. **2014**. "Randomized, Placebo-Controlled, Phase III Trial of Sunitinib plus Prednisone versus Prednisone Alone in Progressive, Metastatic, Castration-Resistant Prostate Cancer." *Journal of Clinical Oncology : Official Journal of the American Society of Clinical Oncology* 32 (2): 76–82. https://doi.org/10.1200/JCO.2012.48.5268.

Middelbeek J., Kuipers A.J., Henneman L., Visser D., Eidhof I., Van Horssen R., Wieringa B., et al. **2012**. "TRPM7 Is Required for Breast Tumor Cell Metastasis." *Cancer Research* 72 (16): 4250–61. https://doi.org/10.1158/0008-5472.CAN-11-3863.

Middelbeek J., Vrenken K., Visser D., Lasonder E., Koster J., Jalink K., Clark K., and van Leeuwen F.N. **2016**. "The TRPM7 Interactome Defines a Cytoskeletal Complex Linked to Neuroblastoma Progression." *European Journal of Cell Biology* 95 (11): 465–74. https://doi.org/10.1016/j.ejcb.2016.06.008.

Min X.J., Li H., Hou S.C., He W., Liu J., Hu B., and Wang J. **2011**. "Dysfunction of Volume-Sensitive Chloride Channels Contributes to Cisplatin Resistance in Human Lung Adenocarcinoma Cells." *Experimental Biology and Medicine (Maywood, N.J.)* 236 (4): 483–91. https://doi.org/10.1258/EBM.2011.010297.

Minke B., Wu C., and Pak W.L. **1975**. "Induction of Photoreceptor Voltage Noise in the Dark in Drosophila Mutant." *Nature* 258 (5530): 84–87. https://doi.org/10.1038/258084a0.

Misery L., Santerre A., Batardière A., Hornez N., Nedelec A.S., Le Caër F., Bourgeois P., Huet F., and Neufang G. **2019**. "Real-Life Study of Anti-Itching Effects of a Cream Containing Menthoxypropanediol, a TRPM8 Agonist, in Atopic Dermatitis Patients." *Journal of the European Academy of Dermatology and Venereology* 33 (2): e67–69. https://doi.org/10.1111/jdv.15199.

Mishra A.K., and Lambright D.G. **2016**. "Small GTPases and Their GAPs." *Biopolymers* 105 (8): 431–48. https://doi.org/10.1002/bip.22833.

Misra U.K., Mowery Y.M., Gawdi G., and Pizzo S.V. **2011**. "Loss of Cell Surface TFII-I Promotes Apoptosis in Prostate Cancer Cells Stimulated with Activated A_2 -Macroglobulin." *J Cell Biochem.* 112 (6): 1685–95. https://doi.org/10.1002/jcb.23083.Loss.

Mittal M., Urao N., Hecquet C.M., Zhang M., Sudhahar V., Gao X.P., Komarova Y., Ushio-Fukai M., and Malik A.B. **2015**. "Novel Role of ROS-Activated Trp Melastatin Channel-2 (TRPM2) in Mediating Angiogenesis and Post-Ischemic Neovascularisation." *Arterioscler Thromb Vasc Biol.* 35 (4): 877–87. https://doi.org/10.1161/ATVBAHA.114.304802.

Moccia F., Negri S., Shekha M., Faris P., and Guerra G. **2019**. "Endothelial Ca^{2+} Signaling, Angiogenesis and Vasculogenesis: Just What It Takes to Make a Blood Vessel." *International Journal of Molecular Sciences* 20 (16): 3962. https://doi.org/10.3390/ijms20163962.

Moissoglu K., and Schwartz M.A. **2014**. "Spatial and Temporal Control of Rho GTPase Functions." *Cellular Logistics* 4 (2): e943618. https://doi.org/10.4161/21592780.2014.943618.

Monet M., Gkika D., Lehen'kyi V., Pourtier A., Vanden Abeele F., Bidaux G., Juvin V., Rassendren F., Humez S., and Prevarsakaya N. **2009**. "Lysophospholipids Stimulate Prostate Cancer Cell Migration via TRPV2 Channel Activation." *Biochimica et Biophysica Acta - Molecular Cell Research* 1793 (3): 528–39. https://doi.org/10.1016/j.bbamcr.2009.01.003.

Monet M., Lehen'kyi V., Gackiere F., Firlej V., Vandenberghe M., Roudbaraki M., Gkika D., et al. **2010**. "Role of Cationic Channel TRPV2 in Promoting Prostate Cancer Migration and Progression to Androgen Resistance." *Cancer Research* 70 (3): 1225–35. https://doi.org/10.1158/0008-5472.CAN-09-2205.

Monteith G.R., Prevarskaya N., and Roberts-Thomson S.J. **2017**. "The Calcium–Cancer Signalling Nexus." *Nature Reviews Cancer* 17 (6): 367–80. https://doi.org/10.1038/nrc.2017.18.

Monteith G.R., McAndrew D., Faddy H.M., and Roberts-Thomson S.J. **2007**. "Calcium and Cancer: Targeting Ca^{2+} Transport." *Nature Reviews Cancer* 7 (7): 519–30. https://doi.org/10.1038/nrc2171.

Montell C., and Rubin G.M. **1989**. "Molecular Characterization of the Drosophila Trp Locus: A Putative Integral Membrane Protein Required for Phototransduction." *Neuron* 2 (4): 1313–23.

Montell C. **2011**. "The History of TRP Channels, a Commentary and Reflection." *Pflugers Archiv European Journal of Physiology* 461 (5): 499–506. https://doi.org/10.1007/s00424-010-0920-3.

Montell C., Jones K., Hafen E., and Rubin G. **1985**. "Rescue of the Drosophila Phototransduction Mutation Trp by Germline Transformation." *Science* 230 (4729): 1040–43. https://doi.org/10.1126/science.3933112.

Moore C.M., Nathan T.R., Lees W.R., Mosse C.A., Freeman A., Emberton M., and Bown S.G. **2006**. "Photodynamic Therapy Using Meso Tetra Hydroxy Phenyl Chlorin (MTHPC) in Early Prostate Cancer." *Lasers in Surgery and Medicine* 38 (5): 356–63. https://doi.org/10.1002/LSM.20275.

Moore C.M., Azzouzi A.R., Barret E., Villers A., Muir G.H., Barber N.J., Bott S., et al. **2015**. "Determination of Optimal Drug Dose and Light Dose Index to Achieve Minimally Invasive Focal Ablation of Localised Prostate Cancer Using WST11-Vascular-Targeted Photodynamic (VTP) Therapy." *BJU International* 116 (6): 888–96. https://doi.org/10.1111/BJU.12816.

Moore C.M., Pendse D., and Emberton M. **2009**. "Photodynamic Therapy for Prostate Cancer - A Review of Current Status and Future Promise." *Nature Clinical Practice Urology* 6 (1): 18–30. https://doi.org/10.1038/ncpuro1274.

Moran M.M. **2018**. "TRP Channels as Potential Drug Targets." *Annual Review of Pharmacology and Toxicology* 58: 309–30. https://doi.org/10.1146/annurev-pharmtox-010617-052832.

Moran M.M., McAlexander M.A., Bíró T., and Szallasi A. **2011**. "Transient Receptor Potential Channels as Therapeutic Targets." *Nature Reviews Drug Discovery*. https://doi.org/10.1038/nrd3456.

Moran M.M., and Szallasi A. **2018**. "Targeting Nociceptive Transient Receptor Potential Channels to Treat Chronic Pain: Current State of the Field." *British Journal of Pharmacology* 175 (12): 2185–2203. https://doi.org/10.1111/bph.14044.

Morelli M.B., Amantini C., Nabissi M., Liberati S., Cardinali C., Farfariello V., Tomassoni D., et al. **2014**. "Cross-Talk between Alpha1D-Adrenoceptors and Transient Receptor Potential Vanilloid Type 1 Triggers Prostate Cancer Cell Proliferation." *BMC Cancer* 14 (1): 1–13. https://doi.org/10.1186/1471-2407-14-921.

Morelli M.B., Amantini C., Liberati S., Santoni M., and Nabissi M. **2013**. "TRP Channels: New Potential Therapeutic Approaches in CNS Neuropathies." *CNS Neurol Disord Drug Targets* 12 (2): 274–93. https://doi.org/10.2174/18715273113129990056.

Morenilla-Palao C., Pertusa M., Meseguer V., Cabedo H., and Viana F. **2009**. "Lipid Raft Segregation Modulates TRPM8 Channel Activity." *Journal of Biological Chemistry* 284 (14): 9215–24. https://doi.org/10.1074/jbc.M807228200.

Moriconi A., Bianchini G., Colagioia S., Brandolini L., Aramini A., Liberati C., and Bovolenta S. **2013**. TRPM8 antagonists. Patent 2013.RPM8 antagonists. Patent. WO2013092711, issued 2013.

Mottet N., van den Bergh R.C.N., Briers E., Van den Broeck T., Cumberbatch M.G., De Santis M., Fanti S., et al. **2021**. "EAU-EANM-ESTRO-ESUR-SIOG Guidelines on Prostate Cancer—2020 Update. Part 1: Screening, Diagnosis, and Local Treatment with Curative Intent." *European Urology* 79 (2): 243–62. https://doi.org/10.1016/j.eururo.2020.09.042.

Mrkonjić S., Garcia-Elias A., Pardo-Pastor C., Bazellières E., Trepat X., Vriens J., Ghosh D., Voets T., Vicente R., and Valverde M.A. **2015**. "TRPV4 Participates in the Establishment of Trailing Adhesions and Directional Persistence of Migrating Cells." *Pflugers Archiv European Journal of Physiology* 467 (10): 2107–19. https://doi.org/10.1007/s00424-014-1679-8.

Mukerji G., Yiangou Y., Corcoran S.L., Selmer I.S., and Smith G.D. **2006**. "Cool and Menthol Receptor TRPM8 in Human Urinary Bladder Disorders and Clinical Correlations." *BMC Urol* 6 (6): 1. https://doi.org/10.1186/1471-2490-6-6.

Mukhopadhyay I., Gomes P., Aranake S., Shetty M., Karnik P., Damle M., Kuruganti S., Thorat S., and Khairatkar-Joshi N. **2011**. "Expression of Functional TRPA1 Receptor on Human Lung Fibroblast and Epithelial Cells." *Journal of Receptors and Signal Transduction* 31 (5): 350–58. https://doi.org/10.3109/10799893.2011.602413.

Munaron L. **2015**. "Systems Biology of Ion Channels and Transporters in Tumor Angiogenesis: An Omics View." *Biochimica et Biophysica Acta - Biomembranes* 1848 (10): 2647–56. https://doi.org/10.1016/j.bbamem.2014.10.031.

Nagasawa M., and Kojima I. **2015**. "Translocation of TRPV2 Channel Induced by Focal Administration of Mechanical Stress." *Physiological Reports* 3: e12296. https://doi.org/10.14814/phy2.12296.

Nagasawa M., Nakagawa Y., Tanaka S., and Kojima I. **2007**. "Chemotactic Peptide FMetLeuPhe Induces Translocation of the TRPV2 Channel in Macrophages." *Journal of Cellular Physiology* 210 (3): 692–702. https://doi.org/10.1002/jcp.20883.

Nagata K., Duggan A., Kumar G., and García-Añoveros J. **2005**. "Nociceptor and Hair Cell Transducer Properties of TRPA1, a Channel for Pain and Hearing." *Journal of Neuroscience* 25 (16): 4052–61. https://doi.org/10.1523/JNEUROSCI.0013-05.2005.

Nagatomo K., and Kubo Y. **2008**. "Caffeine Activates Mouse TRPA1 Channels but Suppresses Human TRPA1 Channels." *Proceedings of the National Academy of Sciences of the United States of America* 105 (45): 17373–78. https://doi.org/10.1073/pnas.0809769105.

Nakayama K., Nakayama M., Iwabuchi M., Terawaki H., Sato T., Kohno M., and Ito S. **2008**. "Plasma α-Oxoaldehyde Levels in Diabetic and Nondiabetic Chronic Kidney Disease Patients." *American Journal of Nephrology* 28 (6): 871–78. https://doi.org/10.1159/000139653.

Nalli M., Ortar G., Schiano Moriello A., Morera E., Di Marzo V., and De Petrocellis L. **2016**. "TRPA1 Channels as Targets for Resveratrol and Related Stilbenoids." *Bioorganic and Medicinal Chemistry Letters* 26 (3): 899–902. https://doi.org/10.1016/j.bmcl.2015.12.065.

Nalli M., Ortar G, Schiano Moriello A., Morera E., Di Marzo V., and De Petrocellis L. **2017**. "Effects of Curcumin and Curcumin Analogues on TRP Channels." *Fitoterapia* 122 (July): 126–31. https://doi.org/10.1016/j.fitote.2017.09.007.

Narayan G., Bourdon V., Chaganti S., Arias-Pulido H., Nandula S.V., Rao P.H., Gissmann L., et al. **2007**. "Gene Dosage Alterations Revealed by CDNA Microarray Analysis in Cervical Cancer: Identification of Candidate Amplified and Overexpressed Genes." *Genes Chromosomes Cancer* 46 (4): 373–84. https://doi.org/10.1002/gcc.20418.

Naseri N., Valizadeh H., and Zakeri-Milani P. **2015**. "Solid Lipid Nanoparticles and Nanostructured Lipid Carriers: Structure Preparation and Application." *Advanced Pharmaceutical Bulletin* 5 (3): 305–13. https://doi.org/10.15171/apb.2015.043.

Nassini R., Fusi C., Materazzi S., Coppi E., Tuccinardi T., Marone I.M., De Logu F., et al. **2015**. "The TRPA1 Channel Mediates the Analgesic Action of Dipyrone and Pyrazolone Derivatives." *British Journal of Pharmacology* 172 (13): 3397–3411. https://doi.org/10.1111/bph.13129.

Nassini R., Materazzi S., Andrè E., Sartiani L., Aldini G., Trevisani M., Carnini C., et al. **2010**. "Acetaminophen, via Its Reactive Metabolite N -Acetyl- p -Benzo-Quinoneimine and Transient Receptor Potential Ankyrin-1 Stimulation, Causes Neurogenic Inflammation in the Airways and Other Tissues in Rodents ." *The FASEB Journal* 24 (12): 4904–16. https://doi.org/10.1096/fj.10-162438.

Nassini R., Pedretti P., Moretto N., Fusi C., Carnini C., Facchinetti F., Viscomi A.R., et al. **2012**. "Transient Receptor Potential Ankyrin 1 Channel Localized to Non-Neuronal Airway Cells Promotes Non-Neurogenic Inflammation." *PLoS ONE* 7 (8). https://doi.org/10.1371/journal.pone.0042454.

Nathan T.R., Whitelaw D.E., Chang S.C., Lees W.R., Ripley P.M., Payne H., Jones L., et al. **2002**. "Photodynamic Therapy for Prostate Cancer Recurrence after Radiotherapy: A Phase I Study." *The Journal of Urology* 168 (4 Pt 1): 1427–32. https://doi.org/10.1097/01.JU.0000030000.81684.7E.

"National Cancer Institute -Surveillance, Epidemiology, and End Result Program." 2022. 2022. seer.cancer.gov.

Navarro F.P., Creusat G., Frochot C., Moussaron A., Verhille M., Vanderesse R., Thomann J.S., et al. **2014**. "Preparation and Characterization of MTHPC-Loaded Solid Lipid Nanoparticles for Photodynamic Therapy." *Journal of Photochemistry and Photobiology B: Biology* 130: 161–69. https://doi.org/10.1016/j.jphotobiol.2013.11.007.

Negri S., Faris P., Berra-Romani R., Guerra G., and Moccia F. **2020**. "Endothelial Transient Receptor Potential Channels and Vascular Remodeling: Extracellular Ca^{2+} Entry for Angiogenesis, Arteriogenesis and Vasculogenesis." *Frontiers in Physiology* 10 (January): 1–23. https://doi.org/10.3389/fphys.2019.01618.

Nelson M., Yang M., Dowle A.A., Thomas J.R., and Brackenbury W.J. **2015**. "The Sodium Channel-Blocking Antiepileptic Drug Phenytoin Inhibits Breast Tumour Growth and Metastasis." *Molecular Cancer* 14 (1). https://doi.org/10.1186/S12943-014-0277-X.

Nilius B., Owsianik G., Voets T., and Peters J.A. **2007**. *Transient Receptor Potential Cation Channels in Disease*. *Physiological Reviews*. Vol. 87. https://doi.org/10.1152/physrev.00021.2006.

Nilius B. **2013**. "Introduction (Transient Receptor Potential TRP Channels as Therapeutic Drug Targets: Next Round!)." *Current Topics in Medicinal Chemistry* 13 (3): 244–46. https://doi.org/10.2174/1568026611313030002.

Nilius B., Appendino G., and Owsianik G.. **2012**. "The Transient Receptor Potential Channel TRPA1: From Gene to Pathophysiology." *Pflugers Archiv European Journal of Physiology* 464 (5): 425–58. https://doi.org/10.1007/s00424-012-1158-z.

Nilius B., and Owsianik G. **2010**. "Transient Receptor Potential Channelopathies." *Pflugers Archiv European Journal of Physiology* 460 (2): 437–50. https://doi.org/10.1007/s00424-010-0788-2.

———. **2011**. "The Transient Receptor Potential Family of Ion Channels." *Genome Biology* 12 (3): 218. https://doi.org/10.1186/gb-2011-12-3-218.

Nilius B., Owsianik G., and Voets T. **2008**. "Transient Receptor Potential Channels Meet Phosphoinositides." *EMBO Journal* 27 (21): 2809–16. https://doi.org/10.1038/emboj.2008.217.

Nilius B., and Szallasi A. **2014**. "Transient Receptor Potential Channels as Drug Targets: From the Science of Basic Research to the Art of Medicine." *Pharmacological Reviews* 66 (3): 676–814. https://doi.org/10.1124/pr.113.008268.

Nilius B., Talavera K., Owsianik G., Prenen J., Droogmans G., and Voets T. **2005**. "Gating of TRP Channels: A Voltage Connection?" *Journal of Physiology* 567 (1): 35–44. https://doi.org/10.1113/jphysiol.2005.088377.

Noncovich A., Priest C., Ung J., Patron A.P., Servant G., Brust P., Servant N., et al. **2017**. "Discovery and Development of a Novel Class of Phenoxyacetyl Amides as Highly Potent TRPM8 Agonists for Use as Cooling Agents." *Bioorganic and Medicinal Chemistry Letters* 27 (16): 3931–38. https://doi.org/10.1016/j.bmcl.2017.04.003.

Noren D.P., Chou W.H., Lee S.H., Qutub A.A., Warmflash A., Wagner D.S., Popel A.S., and Levchenko A. **2017**. "Endothelial Cells Decode VEGF-Mediated Ca^{2+} Signaling Patterns to Produce Distinct Functional Responses." *Sci Signal.* 9 (416): ra20. https://doi.org/10.1126/scisignal.aad3188.

Noweski A., Roosen A., Lebdai S., Barret E., Emberton M., Benzaghou F., Apfelbeck M., et al. **2019**. "Medium-Term Follow-up of Vascular-Targeted Photodynamic Therapy of Localized Prostate Cancer Using TOOKAD Soluble WST-11 (Phase II Trials)." *European Urology Focus* 5 (6): 1022–28. https://doi.org/10.1016/J.EUF.2018.04.003.

Nozadze I., Tsiklauri N., Gurtskaia G., and Tsagareli M.G. **2016**. "Role of Thermo TRPA1 and TRPV1 Channels in Heat, Cold, and Mechanical Nociception of Rats." *Behavioural Pharmacologyhav* 27: 29–36.

Nozadze I., Tsiklauri N., Gurtskaia G., Abzianidze E., and Tsagareli M.G. **2016**. "TRP Channels in Thermal Pain Sensation." In *Systemic, Cellular and Molecular Mechanisms of Physiological Functions and Their Disorders*, 271–87. New York: Nova Biomedical.

Nozadze I., Tsiklauri N., Gurtskaia G.,, and Tsagareli M.G. **2019**. "Agonist-Evoked Hyperalgesia and Allodynia: The Role of Transient Receptor Potential Channels in Pain and Itch." In *Hyperalgesia and Allodynia: A Closer Look. Symptoms, Mechanisms and Treatment*, edited by MG Tsagareli, 151–74. New York: Nova.

Nyman E., Franzén B., Nolting A., Klement G., Liu G., Nilsson M., Rosén A., et al. **2013**. "*In Vitro* Pharmacological Characterization of a Novel TRPA1 Antagonist and Proof of Mechanism in a Human Dental Pulp Model." *Journal of Pain Research* 6: 59–70. https://doi.org/10.2147/JPR.S37567.

Ohkawara S., Tanaka-Kagawa T., Furukawa Y., and Jinno H. **2012**. "Methylglyoxal Activates the Human Transient Receptor Potential Ankyrin 1 Channel." *Journal of Toxicological Sciences* 37 (4): 831–35. https://doi.org/10.2131/jts.37.831.

Ohmi M., Shishido Y., Inoue T., Ando K., Fujiuchi A., Yamada A., Watanabe S., and Kawamura K. **2014**. "Identification of a Novel 2-Pyridyl-Benzensulfonamide Derivative, RQ-00203078, as a Selective and Orally Active TRPM8 Antagonist." *Bioorganic and Medicinal Chemistry Letters* 24 (23): 5364–68. https://doi.org/10.1016/j.bmcl.2014.10.074.

Okamoto Y., Ohkubo T., Ikebe T., and Yamazaki J.U.N. **2012**. "Blockade of TRPM8 Activity Reduces the Invasion Potential of Oral Squamous Carcinoma Cell Lines," 1431–40. https://doi.org/10.3892/ijo.2012.1340.

Onoe S., Temma T., Shimizu Y., Ono M., and Saji H. **2014**. "Investigation of Cyanine Dyes for *in Vivo* Optical Imaging of Altered Mitochondrial Membrane Potential in Tumors." *Cancer Medicine* 3 (4): 775–86. https://doi.org/10.1002/cam4.252.

Ordá, P., Hernández-Ortego P., Vara H., Fernández-Peña C., Reimúndez A., Morenilla-Palao C., Guadaño-Ferraz A., et al. **2021**. "Expression of the Cold Thermoreceptor TRPM8 in Rodent Brain Thermoregulatory Circuits." *J Comp Neurol* 529 (1): 234–56.

Orrenius S., Zhivotovsky B., and Nicotera P. **2003**. "Regulation of Cell Death: The Calcium-Apoptosis Link." *Nature Reviews Molecular Cell Biology* 4 (7): 552–65. https://doi.org/10.1038/nrm1150.

Osuchowski M., Bartusik-Aebisher D., Osuchowski F., and Aebisher D. **2021**. "Photodynamic Therapy for Prostate Cancer – A Narrative Review." *Photodiagnosis and Photodynamic Therapy* 33. https://doi.org/10.1016/j.pdpdt.2020.102158.

Ou-yang Q., Li B., Xu M., and Liang H. **2018**. "TRPV4 Promotes the Migration and Invasion of Glioma Cells via AKT/Rac1 Signaling." *Biochemical and Biophysical Research Communications* 503 (2): 876–81. https://doi.org/10.1016/j.bbrc.2018.06.090.

Oulidi A., Bokhobza A., Gkika D., Vanden Abeele F., Lehen'kyi V., Ouafik L.H., Mauroy B., and Prevarskaya N. **2013**. "TRPV2 Mediates Adrenomedullin Stimulation of Prostate and Urothelial Cancer Cell Adhesion , Migration and Invasion." *PloS One* 8 (5): 1–7. https://doi.org/10.1371/journal.pone.0064885.

Overchuk M., Damen M.P.F., Harmatys K.M., Pomper M.G., Chen J., and Zheng G. **2020**. "Long-Circulating Prostate-Specific Membrane Antigen-Targeted NIR Phototheranostic Agent." *Photochemistry and Photobiology* 96 (3): 718–24. https://doi.org/10.1111/PHP.13181.

Owsianik G., Talavera K., Voets T., and Nilius B. **2006**. *Permeation and Selectivity of TRP Channels*. *Annual Review of Physiology*. Vol. 68. https://doi.org/10.1146/annurev.physiol.68.040204.101406.

Palumbo J.M. **2017**. Composition for treating or preventing vasomotor symptoms. WO2017217351, issued 2017.

Parekh A.B. **2011**. "Decoding Cytosolic Ca2+ Oscillations." *Trends in Biochemical Sciences* 36 (2): 78–87. https://doi.org/10.1016/j.tibs.2010.07.013.

Parekh A.B., Fleig A., and Penner R. **1997**. "The Store-Operated Calcium Current I(CRAC): Nonlinear Activation by InsP3 and Dissociation from Calcium Release." *Cell* 89 (6): 973–80. https://doi.org/10.1016/S0092-8674(00)80282-2.

Park J., Choi Y., Chang H., Um W., Ryu J.H., and Kwon I.C. **2019**. "Alliance with EPR Effect: Combined Strategies to Improve the EPR Effect in the Tumor Microenvironment." *Theranostics* 9 (26): 8073–90. https://doi.org/10.7150/thno.37198.

Park J., Shim M.K., Jin M., Rhyu M.R., and Lee Y.J. **2016**. "Methyl Syringate, a TRPA1 Agonist Represses Hypoxia-Induced Cyclooxygenase-2 in Lung Cancer Cells." *Phytomedicine* 23 (3): 324–29. https://doi.org/10.1016/j.phymed.2016.01.009.

Park S., Lee S., Park E.K., Kang M.J., So I., Jeon J.H., and Chun J.N. **2017**. "TGFβ1 Induces Stress Fiber Formation through Upregulation of TRPC6 in Vascular Smooth Muscle Cells." *Biochemical and Biophysical Research Communications* 483 (1): 129–34. https://doi.org/10.1016/j.bbrc.2016.12.179.

Parveen S., Misra R., and Sahoo S.K. **2012**. "Nanoparticles: A Boon to Drug Delivery, Therapeutics, Diagnostics and Imaging." *Nanomedicine: Nanotechnology, Biology, and Medicine* 8 (2): 147–66. https://doi.org/10.1016/j.nano.2011.05.016.

Patapoutian A., and Jegla T.J. **2007**. Methods and compositions for treating hyperalgesia. WO2007098252, issued 2007.

Patapoutian A., Tate S., and Woolf C.J. **2009**. "Transient Receptor Potential Channels: Targeting Pain at the Source." *Nature Reviews Drug Discovery* 8 (1): 55–68. https://doi.org/10.1038/nrd2757.

Patel R., Gonçalves L., Newman R., Jiang F.L., Goldby A., Reeve J., Hendrick A., et al. **2014**. "Novel TRPM8 Antagonist Attenuates Cold Hypersensitivity after Peripheral Nerve Injury in Rats." *Journal of Pharmacology and Experimental Therapeutics* 349 (4): 47–55. https://doi.org/10.1124/jpet.113.211243.

Paulsen C.E., Armache J.P., Gao Y., Cheng Y., and Julius D. **2015**. "Structure of the TRPA1 Ion Channel Suggests Regulatory Mechanisms." *Nature* 525 (7570): 552. https://doi.org/10.1038/nature14871.

Pedersen S.F., Owsianik G., and Nilius B. **2005**. "TRP Channels: An Overview." *Cell Calcium* 38 (3-4 SPEC. ISS.): 233–52. https://doi.org/10.1016/j.ceca.2005.06.028.

Pedretti A., Labozzetta A., Lo Monte M., Beccari A.R., Moriconi A., and Vistoli G. **2011**. "Exploring the Activation Mechanism of TRPM8 Channel by Targeted MD Simulations." *Biochemical and Biophysical Research Communications* 414 (1): 14–19. https://doi.org/10.1016/j.bbrc.2011.08.134.

Pedretti A., Marconi C., Bettinelli I., and Vistoli G. **2009**. "Comparative Modeling of the Quaternary Structure for the Human TRPM8 Channel and Analysis of Its Binding Features." *Biochimica et Biophysica Acta - Biomembranes* 1788 (5): 973–82. https://doi.org/10.1016/j.bbamem.2009.02.007.

Peer D., Karp J.M., Hong S., Farokhzad O.C., Margalit R., and Langer R. **2007**. "Nanocarriers as an Emerging Platform for Cancer Therapy." *Nature Nanotechnology* 2 (12): 751–60. https://doi.org/10.1038/nnano.2007.387.

Peier A.M., Moqrich A., Hergarden A.C., Reeve A.J., Andersson D.A., Story G.M., Earley T.J., et al. **2002**. "A TRP Channel That Senses Cold Stimuli and Menthol." *Cell* 108 (5): 705–15. https://doi.org/10.1016/s0092-8674(02)00652-9.

Pelton K., Freeman M.R., and Solomon K.R. **2012**. "Cholesterol and Prostate Cancer." *Current Opinion in Pharmacology* 12 (6): 751–59. https://doi.org/10.1016/j.coph.2012.07.006.

Peng J.B., Zhuang L., Berger U.V., Adam R.M., Williams B.J., Brown E.M., Hediger M.A., and Freeman M.R. **2001**. "CaT1 Expression Correlates with Tumor Grade in Prostate Cancer." *Biochemical and Biophysical Research Communications* 282 (3): 729–34. https://doi.org/10.1006/bbrc.2001.4638.

Peng M., Wang Z., Yang Z., Tao L., Liu Q., Yi L., and Wang X. **2015**. "Overexpression of Short TRPM8 Variant α Promotes Cell Migration and Invasion, and Decreases Starvation-Induced Apoptosis in Prostate Cancer LNCaP Cells." *Oncology Letters* 10 (3): 1378–84. https://doi.org/10.3892/ol.2015.3373.

Pérez de Vega M.J., Ferrer-Montiel A., and González-Muñiz R. **2018**. "Recent Progress in Non-Opioid Analgesic Peptides." *Archives of Biochemistry and Biophysics* 660 (October): 36–52. https://doi.org/10.1016/j.abb.2018.10.011.

Pérez de Vega M.J., Gómez-Monterrey I., Ferrer-Montiel A., and González-Muñiz R. **2016**. "Transient Receptor Potential Melastatin 8 Channel (TRPM8) Modulation: Cool Entryway for Treating Pain and Cancer." *Journal of Medicinal Chemistry* 59 (22): 10006–29. https://doi.org/10.1021/acs.jmedchem.6b00305.

Pergolizzi J.V., Taylor R., LeQuang J.A., and Raffa R.B. **2018**. "The Role and Mechanism of Action of Menthol in Topical Analgesic Products." *Journal of Clinical Pharmacy and Therapeutics* 43 (3): 313–19. https://doi.org/10.1111/jcpt.12679.

Perner R.J., Kort M.E., Didomenico S., Chen J., and Vasudevan A. **2009**. TRPA1 ANTAGONISTS. WO2009089082, issued 2009.

Pfizer. **2016**. N-(2-alkyleneimino-3-phenylpropyl)acetamide compounds and their use against pain and pruritus via inhibition of

TRPA1 channels. WO2016067143, issued 2016.

Phelan K.D., Mock M.M., Kretz O., Shwe U.T., Kozhemyakin M., Greenfield L.J., Dietrich A., et al. **2012**. "Heteromeric Canonical Transient Receptor Potential 1 and 4 Channels Play a Critical Role in Epileptiform Burst Firing and Seizure-Induced Neurodegeneration." *Molecular Pharmacology* 81 (3): 384–92. https://doi.org/10.1124/mol.111.075341.

Pigozzi D., Ducret T., Tajeddine N., Gala J.L., Tombal B., and Gailly P. **2006**. "Calcium Store Contents Control the Expression of TRPC1, TRPC3 and TRPV6 Proteins in LNCaP Prostate Cancer Cell Line." *Cell Calcium* 39 (5): 401–15. https://doi.org/10.1016/j.ceca.2006.01.003.

Pinton P., Giorgi C., Siviero R., Zecchini E., and Rizzuto R. **2008**. "Calcium and Apoptosis: ER-Mitochondria Ca^{2+} Transfer in the Control of Apoptosis." *Oncogene* 27 (50): 6407–18. https://doi.org/10.1038/jid.2014.371.

Piscatelli J.A., Ban J., Lucas A.T., and Zamboni W.C. **2021**. "Complex Factors and Challenges That Affect the Pharmacology, Safety and Efficacy of Nanocarrier Drug Delivery Systems." *Pharmaceutics*. https://doi.org/10.3390/pharmaceutics13010114.

Planells-Cases R., and Ferrer-Montiel A. **2007**. "TRP Channel Trafficking." In *TRP Ion Channel Function in Sensory Transduction and Cellular Signaling Cascades*, edited by WB and Heller S Liedtke, 319–30. CRC Press/Taylor & Francis.

Pocock T.M., Foster R.R., and Bates D.O. **2004**. "Evidence of a Role for TRPC Channels in VEGF-Mediated Increased Vascular Permeability *in Vivo*." *American Journal of Physiology - Heart and Circulatory Physiology* 286 (3 55-3): 1015–26. https://doi.org/10.1152/ajpheart.00826.2003.

Pollastro F., De Petrocellis L., Schiano-Moriello A., Chianese G., Heyman H., Appendino G., and Taglialatela-Scafati O. **2017**. "Amorfrutin-Type Phytocannabinoids from Helichrysum Umbraculigerum." *Fitoterapia* 123 (September): 13–17. https://doi.org/10.1016/j.fitote.2017.09.010.

Preise D., Scherz A., and Salomon Y. **2011**. "Antitumor Immunity Promoted by Vascular Occluding Therapy: Lessons from Vascular-Targeted Photodynamic Therapy (VTP)." *Photochemical & Photobiological Sciences* 10 (5): 681. https://doi.org/10.1039/c0pp00315h.

Premkumar L.S., Raisinghani M., Pingle S.C., Long C., and Pimentel F. **2005**. "Downregulation of Transient Receptor Potential Melastatin 8 by Protein Kinase C-Mediated Dephosphorylation." *Journal of Neuroscience* 25 (49): 11322–29. https://doi.org/10.1523/JNEUROSCI.3006-05.2005.

Preti D., Szallasi A., and Patacchini R. **2012**. *TRP Channels as Therapeutic Targets in Airway Disorders: A Patent Review*. *Expert Opinion on Therapeutic Patents*. Vol. 22. https://doi.org/10.1517/13543776.2012.696099.

Prevarskaya N., Flourakis M., Bidaux G., Thebault S., and Skryma R. **2007**. "Differential Role of TRP Channels in Prostate Cancer." *Biochemical Society Transactions* 35 (1): 133–35. https://doi.org/10.1042/BST0350133.

Prevarskaya N., Skryma R., Bidaux G., Flourakis M., and Shuba Y. **2007**. "Ion Channels in Death and Differentiation of Prostate Cancer Cells." *Cell Death and Differentiation* 14 (7): 1295–1304. https://doi.org/10.1038/sj.cdd.4402162.

Prevarskaya N., Skryma R., and Shuba Y. **2018**. "Ion Channels in Cancer: Are Cancer Hallmarks Oncochannelopathies?" *Physiological Reviews* 98 (2): 559–621. https://doi.org/10.1152/physrev.00044.2016.

———. **2004**. "Ca^{2+} Homeostasis in Apoptotic Resistance of Prostate Cancer Cells." *Biochemical and Biophysical Research Communications* 322 (4): 1326–35. https://doi.org/10.1016/j.bbrc.2004.08.037.

———. **2010**. "Ion Channels and the Hallmarks of Cancer." *Trends in Molecular Medicine* 16 (3): 107–21. https://doi.org/10.1016/j.molmed.2010.01.005.

Prevarskaya N., Zhang L., and Barritt G. **2007**. "TRP Channels in Cancer." *Biochimica et Biophysica Acta - Molecular Basis of Disease* 1772 (8): 937–46. https://doi.org/10.1016/j.bbadis.2007.05.006.

Priest C., Noncovich A., Patron A., and Ung J. **2012**. Preparation of heteroaryl amide compounds useful as modulators of TRPM8. Patent. WO2012061698, issued 2012.

Prior I.A., Lewis P.D., and Mattos C. **2012**. "A Comprehensive Survey of Ras Mutations in Cancer." *Cancer Research* 72 (10): 2457–67. https://doi.org/10.1158/0008-5472.CAN-11-2612.A.

Qian X., Francis M., Solodushko V., Earley S., and Taylor M.S. **2013**. "Recruitment of Dynamic Endothelial Ca^{2+} Signals by the TRPA1 Channel Activator AITC in Rat Cerebral Arteries." *Microcirculation* 20 (2): 138–48. https://doi.org/10.1111/micc.12004.Recruitment.

Qin N., Neeper M.P., Liu Y., Hutchinson T.L., Lubin M.L., and Flores C.M. **2008**. "TRPV2 Is Activated by Cannabidiol and Mediates CGRP Release in Cultured Rat Dorsal Root Ganglion Neurons." *Journal of Neuroscience* 28 (24): 6231–38. https://doi.org/10.1523/JNEUROSCI.0504-08.2008.

Radresa O., Dahllöf H., Nyman E., Nolting A., Albert J.S., and Raboisson P. **2013**. "Roles of TRPA1 in Pain Pathophysiology and Implications for the Development of a New Class of Analgesic Drugs." *The Open Pain Journal* 6 (1): 137–53. https://doi.org/10.2174/1876386301306010137.

Ramachandran R., Hyun E., Zhao L., Lapointe T.K., Chapman K., Hirot C.L., Ghosh S., et al. **2013**. "TRPM8 Activation Attenuates Inflammatory Responses in Mouse Models of Colitis." *Proceedings of the National Academy of Sciences of the United States of America* 110 (18): 7476–81. https://doi.org/10.1073/pnas.1217431110.

Ramaiah D., Eckert I., Arun K.T., Weidenfeller L., and Epe B. **2004**. "Squaraine Dyes for Photodynamic Therapy: Mechanism of Cytotoxicity and DNA Damage Induced by Halogenated Squaraine Dyes Plus Light (>600 Nm)." *Photochemistry and Photobiology* 79 (1): 99. https://doi.org/10.1111/j.1751-1097.2004.tb09863.x.

Ramaiah D., Eckert I., Arun K.T., Weidenfeller L., and Epe B. **2002**. "Squaraine Dyes for Photodynamic Therapy: Study of Their Cytotoxicity and Genotoxicity in Bacteria and Mammalian Cells." *Photochemistry and Photobiology* 76 (6): 672–77. https://doi.org/10.1562/0031-8655(2002)076<0672:SDFPTS>2.0.CO;2.

Ramaiah D., Joy A., Chandrasekhar N., Eldho N.V., Das S., and George M.V. **1997**. "Halogenated Squaraine Dyes as Potential Photochemotherapeutic Agents. Synthesis and Study of Photophysical Properties and Quantum Efficiencies of Singlet Oxygen Generation." *Photochemistry and Photobiology* 65 (5): 783–90. https://doi.org/10.1111/j.1751-1097.1997.tb01925.x.

Rampino T., Gregorini M., Guidetti C., Broggini M., Marchini S., Bonomi R., Maggio M., et al. **2007**. "KCNA1 and TRPC6 Ion Channels and NHE1 Exchanger Operate the Biological Outcome of HGF / Scatter Factor in Renal Tubular Cells" 25 (December): 382–91. https://doi.org/10.1080/08977190801892184.

Raphaël M., Lehen'kyi V., Vandenberghe M., Beck B., Khalimonchyk S., Vanden Abeele F., Farsetti L., et al. **2014**. "TRPV6 Calcium Channel Translocates to the Plasma Membrane via Orai1-Mediated Mechanism and Controls Cancer Cell Survival." *Proceedings of the National Academy of Sciences of the United States of America* 111 (37): E3870–79. https://doi.org/10.1073/pnas.1413409111.

Rapozzi V., Beverina L., Salice P., Pagani G.A., Camerin M., and Xodo L.E. **2010**. "Photooxidation and Phototoxicity of π-Extended Squaraines." *Journal of Medicinal Chemistry* 53 (5): 2188–96. https://doi.org/10.1021/jm901727j.

Ray M., Wei Lee Y., Scaletti F., Yu R., and Rotello V.M. **2017**. "Intracellular Delivery of Proteins by Nanocarriers." *Nanomedicine* 12 (8): 941–52. https://doi.org/10.2217/nnm-2016-0393.

Reaume A.G., Cong W., Greenway F., and Coulter A. **2018**. Treatment of adipocytes. WO2018191166A1, issued 2018.

Rech J.C., Eckert W.A., Maher M.P., Banke T., Bhattacharya A., and Wickenden A.D. **2010**. "Recent Advances in the Biology and Medicinal Chemistry of TRPA1." *Future Medicinal Chemistry* 2 (5): 843–58. https://doi.org/10.4155/fmc.10.29.

Redmond R.W., Kochevar I.E., Krieg M., Smith G., and Mcgimpsey W.G. **1997**. "Excited State Relaxation in Cyanine Dyes: A Remarkably Efficient Reverse Intersystem Crossing from Upper Triplet Levels." *J. Phys. Chem. A* 101 (15): 2773–77. http://nathan.instras.com/ResearchProposalDB/doc-37.pdf.

Renard P., Zachary M.D., Bougelet C., Mirault M.E., Haegeman G., Remacle J., and Raes M. **1997**. "Effects of Antioxidant Enzyme Modulations on Interleukin-1-Induced Nuclear Factor Kappa B Activation." *Biochemical Pharmacology* 53 (2): 149–60. https://doi.org/10.1016/S0006-2952(96)00645-4.

Riccio A., Medhurst A.D., Mattei C., Kelsell R.E., Calver A.R., Randall A.D., Benham C.D., and Pangalos M.N. **2002**. "MRNA Distribution Analysis of Human TRPC Family in CNS and Peripheral Tissues." *Molecular Brain Research* 109 (1–2): 95–104. https://doi.org/10.1016/S0169-328X(02)00527-2.

Ridley A.J. **2001**. "Rho Family Proteins : Coordinating Cell Responses" 11 (12): 471–77.

Roche J. **2018**. "The Epithelial-to-Mesenchymal Transition in Cancer." *Cancers* 10 (3): 10–13. https://doi.org/10.3390/cancers10020052.

Roderick H.L., and Cook. S.J. **2008**. "Ca^{2+} Signalling Checkpoints in Cancer: Remodelling Ca2+ for Cancer Cell Proliferation and Survival." *Nature Reviews Cancer* 8 (5): 361–75. https://doi.org/10.1038/nrc2374.

Rodrigues de Carvalho A.M., Freire Vasconcelos L., Moura Rocha N.F., Vasconcelos Rios E.R., Dias M.L., de França Fonteles M.M., Macêdo Gaspar M., Barbosa Filho J.M., Chavez Gutierrez S.J., and Florenço de Sousa F.C. **2018**. "Antinociceptive Activity of

Riparin II from Aniba Riparia: Further Elucidation of the Possible Mechanisms." *Chemico-Biological Interactions* 287 (March): 49–56. https://doi.org/10.1016/j.cbi.2018.04.003.

Rohács T., Lopes C.M.B., Michailidis I., and Logothetis D.E. **2005**. "PI(4,5)P2 Regulates the Activation and Desensitization of TRPM8 Channels through the TRP Domain." *Nature Neuroscience* 8 (5): 626–34. https://doi.org/10.1038/nn1451.

Rokhlin O.W., Taghiyev A.F., Bayer K.U., Bumcrot D., Koteliansk V.E., Glover R.A., and Cohen M.B. **2007**. "Calcium/Calmodulin-Dependent Kinase II Plays an Important Role in Prostate Cancer Cell Survival." *Cancer Biology and Therapy* 6 (5): 732–42. https://doi.org/10.4161/cbt.6.5.3975.

Romano B., Borrelli F., Fasolino I., Capasso R., Piscitelli F., Cascio M.G., Pertwee R.G., et al. **2013**. "The Cannabinoid TRPA1 Agonist Cannabichromene Inhibits Nitric Oxide Production in Macrophages and Ameliorates Murine Colitis." *British Journal of Pharmacology* 169 (1): 213–29. https://doi.org/10.1111/bph.12120.

Rooney L., Vidal A., D'Souza A.M., Devereux N., Masick B., Boissel V., West R., et al. **2014**. "Discovery, Optimization, and Biological Evaluation of 5-(2- (Trifluoromethyl)Phenyl)Indazoles as a Novel Class of Transient Receptor Potential A1 (TRPA1) Antagonists." *Journal of Medicinal Chemistry* 57 (12): 5129–40. https://doi.org/10.1021/jm401986p.

Rosenblum D., Joshi N., Tao W., Karp J.M., and Peer D. **2018**. "Progress and Challenges towards Targeted Delivery of Cancer Therapeutics." *Nature Communications* 9 (1). https://doi.org/10.1038/s41467-018-03705-y.

Rybarczyk P., Gautier M., Hague F., Dhennin-Duthille I., Chatelain D., Kerr-Conte J., Pattou F., Regimbeau J.M., Sevestre H., and Ouadid-Ahidouch H. **2012**. "Transient Receptor Potential Melastatin-Related 7 Channel Is Overexpressed in Human Pancreatic Ductal Adenocarcinomas and Regulates Human Pancreatic Cancer Cell Migration." *International Journal of Cancer* 131 (6): 851–61. https://doi.org/10.1002/ijc.27487.

Rybarczyk P., Vanlaeys A., Brassart B., Dhennin-Duthille I., Chatelain D., Sevestre H., Ouadid-Ahidouch H., and Gautier M. **2017**. "The Transient Receptor Potential Melastatin 7 Channel Regulates Pancreatic Cancer Cell Invasion through the Hsp90 α/UPA/ MMP2." *Neoplasia* 19 (4): 288–300. https://doi.org/10.1016/j.neo.2017.01.004.

Ryckmans T., Aubdool A.A., Bodkin J.V., Cox P., Brain S.D., Dupont T., Fairman E., et al. **2011**. "Design and Pharmacological Evaluation of PF-4840154, a Non-Electrophilic Reference Agonist of the TrpA1 Channel." *Bioorganic and Medicinal Chemistry Letters* 21 (16): 4857–59. https://doi.org/10.1016/j.bmcl.2011.06.035.

Saarnilehto M., Chapman H., Savinko T., Lindstedt K., Lauerma A., and Koivisto A. **2014**. "Contact Sensitizer 2,4-Dinitrochlorobenzene Is a Highly Potent Human TRPA1 Agonist." *European Journal of Allergy and Clinical Immunology* 69: 1424–27.

Sabnis A.S., Reilly C.A., Veranth J.M., and Yost G.S. **2008**. "Increased Transcription of Cytokine Genes in Human Lung Epithelial Cells through Activation of a TRPM8 Variant by Cold Temperatures." *American Journal of Physiology - Lung Cellular and Molecular Physiology* 295 (1): 194–200. https://doi.org/10.1152/ajplung.00072.2008.

Sabnis A.S., Shadid M., Yost G.S., and Reilly C.A. **2008**. "Human Lung Epithelial Cells Express a Functional Cold-Sensing TRPM8 Variant." *American Journal of Respiratory Cell and Molecular Biology* 39 (4): 466–74. https://doi.org/10.1165/rcmb.2007-0440OC.

Sadofsky L.R., Boa A.N., Maher S.A., Birrell M.A., Belvisi M.G., and Morice A.H. **2011**. "TRPA1 Is Activated by Direct Addition of Cysteine Residues to the N-Hydroxysuccinyl Esters of Acrylic and Cinnamic Acids." *Pharmacological Research* 63 (1): 30–36. https://doi.org/10.1016/j.phrs.2010.11.004.

Sagredo A.I., Sagredo E.A., Cappelli C., Báez P., Andaur R.E., Blanco C., Tapia J.C., et al. **2018**. "TRPM4 Regulates Akt/GSK3-β Activity and Enhances β-Catenin Signaling and Cell Proliferation in Prostate Cancer Cells." *Molecular Oncology* 12 (2): 151–65. https://doi.org/10.1002/1878-0261.12100.

Sagredo A.I., Sagredo E.A., Pola V., Echeverría C., Andaur R., Michea L., Stutzin A., Simon F., Marcelain K., and Armisén R. **2019**. "TRPM4 Channel Is Involved in Regulating Epithelial to Mesenchymal Transition, Migration, and Invasion of Prostate Cancer Cell Lines." *Journal of Cellular Physiology* 234 (3): 2037–50. https://doi.org/10.1002/jcp.27371.

Sahai E., and Marshall C.J. **2002**. "RHO - GTPases and Cancer." *Nature Reviews Cancer* 2 (2): 133–42. https://doi.org/10.1038/nrc725.

Saldías M.P., Maureira D., Orellana-Serradell O., Silva I., Lavanderos B., Cruz P., Torres C., Cáceres M., and Cerda O. **2021**. "TRP Channels Interactome as a Novel Therapeutic Target in Breast Cancer." *Frontiers in Oncology* 11 (June): 621614. https://doi.org/10.3389/FONC.2021.621614.

Sánchez A.M., Sánchez M.G., Malagarie-Cazenave S., Olea N., and Díaz-Laviada I. **2006**. "Induction of Apoptosis in Prostate Tumor PC-3 Cells and Inhibition of Xenograft Prostate Tumor Growth by the Vanilloid Capsaicin." *Apoptosis* 11 (1): 89–99. https://doi.org/10.1007/s10495-005-3275-z.

Sánchez A.M., Sánchez M.G., Collado B., Malagarie-Cazenave S., Olea N., Carmena M.J., Prieto J.C., and Díaz-Laviada I. **2005**. "Expression of the Transient Receptor Potential Vanilloid 1 (TRPV1) in LNCaP and PC-3 Prostate Cancer Cells and in Human Prostate Tissue." *European Journal of Pharmacology* 515 (1–3): 20–27. https://doi.org/10.1016/j.ejphar.2005.04.010.

Santella L., Kyozuka K., Hoving S., Munchbach M., Quadroni M., Dainese P., Zamparelli C., James P., and Carafoli E.. **2000**. "Breakdown of Cytoskeletal Proteins during Meiosis of Starfish Oocytes and Proteolysis Induced by Calpain." *Experimental Cell Research* 259 (1): 117–26. https://doi.org/10.1006/excr.2000.4969.

Santibáñez J.F., Kocic J., Fabra A., Cano A., and Quintanilla M. **2010**. "Rac1 Modulates TGF- b 1-Mediated Epithelial Cell Plasticity and MMP9 Production in Transformed Keratinocytes." *FEBS Letters* 584 (11): 2305–10. https://doi.org/10.1016/j.febslet.2010.03.042.

Sanvicens N., Gómez-Vicente V., Masip I., Messeguer A., and Cotter T.G. **2004**. "Oxidative Stress-Induced Apoptosis in Retinal Photoreceptor Cells Is Mediated by Calpains and Caspases and Blocked by the Oxygen Radical Scavenger CR-6." *Journal of Biological Chemistry* 279 (38): 39268–78. https://doi.org/10.1074/jbc.M402202200.

Scarpellino G., Munaron L., Cantelmo A.R., and Fiorio Pla A. **2020**. "Calcium-Permeable Channels in Tumor Vascularization: Peculiar Sensors of Microenvironmental Chemical and Physical Cues." *Rev Physiol Biochem Pharmacol.* https://doi.org/10.1007/112_2020_32.

Schanze N., Jacobi S.F., Rijntjes E., Mergler S., Del Olmo M., Hoefig C.S., Khajavi N., et al. **2017**. "3-Iodothyronamine Decreases Expression of Genes Involved in Iodide Metabolism in Mouse Thyroids and Inhibits Iodide Uptake in PCCL3 Thyrocytes." *Thyroid* 27 (1): 11–22. https://doi.org/10.1089/thy.2016.0182.

Schattling B., Steinbach K., Thies E., Kruse M., Menigoz A., Ufer F., Flockerzi V., et al. **2012**. "TRPM4 Cation Channel Mediates Axonal and Neuronal Degeneration in Experimental Autoimmune Encephalomyelitis and Multiple Sclerosis." *Nature Medicine*. https://doi.org/10.1038/nm.3015.

Schenkel L.B., Olivieri P.R., Boezio A.A., Deak H.L., Emkey R., Graceffa R.F., Gunaydin H., et al. **2016**. "Optimization of a Novel Quinazolinone-Based Series of Transient Receptor Potential A1 (TRPA1) Antagonists Demonstrating Potent *in Vivo* Activity." *Journal of Medicinal Chemistry* 59 (6): 2794–2809. https://doi.org/10.1021/acs.jmedchem.6b00039.

Schinke E.N., Bii V., Nalla A., Rae D.T., Tedrick L., Meadows G.G., and Trobridge G.D. **2014**. "A Novel Approach to Identify Driver Genes Involved in Androgen-Independent Prostate Cancer." *Molecular Cancer* 13 (1): 1–12. https://doi.org/10.1186/1476-4598-13-120.

Schmidt U., Fuessel S., Koch R., Baretton G.B., Lohse A., Tomasetti S., Unversucht S., Froehner M., Wirth M.P., and Meye A. **2006**. "Quantitative Multi-Gene Expression Profiling of Primary Prostate Cancer." *The Prostate* 66 (14): 1521–34. https://doi.org/10.1002/pros.20490.

Schulie A.J., Yeh C.Y., Orang B.N., Pa O.J., Hopkin M.P., Moutal A., Khanna R., Sun D., Justic J.A., and Aizenman E.. **2020**. "Targeted Disruption of Kv2.1-VAPA Association Provides Neuroprotection against Ischemic Stroke in Mice by Declustering Kv2.1 Channels." *Science Advances* 6 (27): eaaz8110. https://doi.org/10.1126/sciadv.aaz8110.

Schwarz E.C. **2007**. "TRP Channels in Lymphocytes." In *Transient Receptor Potential (TRP) Channels. Handbook of Experimental Pharmacology*, edited by V Flockerzi and B Nilius, vol 179. Springer, Berlin, Heidelberg. https://doi.org/10.1007/978-3-540-34891-7_26.

Schwarz E.C., Wissenbach U., Niemeyer B.A., Strauß B., Philipp S.E., Flockerzi V., and Hoth M. **2006**. "TRPV6 Potentiates Calcium-Dependent Cell Proliferation." *Cell Calcium* 39 (2): 163–73. https://doi.org/10.1016/j.ceca.2005.10.006.

Scott D.E., Bayly A.R., Abell C., and Skidmore J. **2016**. "Small Molecules, Big Targets: Drug Discovery Faces the Protein-Protein Interaction Challenge." *Nature Reviews Drug Discovery* 15 (8): 533–50. https://doi.org/10.1038/nrd.2016.29.

Sculptoreanu A., Kullmann F.A., Artim D.E., Bazley F.A., Schopfer F., Woodcock S., Freeman B.A., and De Groat W.C. **2010**. "Nitro-Oleic Acid Inhibits Firing and Activates TRPV1- and TRPA1-Mediated Inward Currents in Dorsal Root Ganglion Neurons from Adult Male Rats." *Journal of Pharmacology and Experimental Therapeutics* 333 (3): 883–95. https://doi.org/10.1124/jpet.109.163154.

Sée V., Rajala N.K.M., Spiller D.G., and White M.R.H. 2004. "Calcium-Dependent Regulation of the Cell Cycle *via* a Novel MAPK-NF-KB Pathway in Swiss 3T3 Cells." *Journal of Cell Biology* 166 (5): 661–72. https://doi.org/10.1083/jcb.200402136.

Seiz J.R., Klinke J., Scharlibbe L., Lohfink D., and Heipel M. **2020**. "Different Signaling and Functionality of Rac1 and Rac1b in the Progression of Lung Adenocarcinoma." *Biol. Chem.* 401 (4): 517–31. https://doi.org/10.1515/hsz-2019-0329.

Selitrennik M., and Lev S. **2015**. "PYK2 Integrates Growth Factor and Cytokine Receptors Signaling and Potentiates Breast Cancer Invasion via a Positive Feedback Loop." *Oncotarget* 6 (26): 22214–26. https://doi.org/10.18632/oncotarget.4257.

Senapati S., Mahanta A.K., Kumar S., and Maiti P. **2018**. "Controlled Drug Delivery Vehicles for Cancer Treatment and Their Performance." *Signal Transduction and Targeted Therapy* 3 (1): 1–19. https://doi.org/10.1038/s41392-017-0004-3.

Serpe L., Ellena S., Barbero N., Foglietta F., Prandini F., Gallo M.P., Levi R., Barolo C., Canaparo R., and Visentin S. **2016**. "Squaraines Bearing Halogenated Moieties as Anticancer Photosensitizers: Synthesis, Characterization and Biological Evaluation." *European Journal of Medicinal Chemistry* 113: 187–97. https://doi.org/10.1016/j.ejmech.2016.02.035.

Shafeekh K.M., Soumya M.S., Rahim M.A., Abraham A., and Das S. **2014**. "Synthesis and Characterization of Near-Infrared Absorbing Water Soluble Squaraines and Study of Their Photodynamic Effects in DLA Live Cells." *Photochemistry and Photobiology* 90 (3): 585–95. https://doi.org/10.1111/php.12236.

Shafirstein G., Bellnier D., Oakley E., Hamilton S., Potasek M., Beeson K., and Parilov E. **2017**. "Interstitial Photodynamic Therapy—a Focused Review." *Cancers* 9 (2): 1–14. https://doi.org/10.3390/cancers9020012.

Shapovalov G., Gkika D., Devilliers M., Kondratskyi A., Gordienko D., Busserolles J., Bokhobza A., Eschalier A., Skryma R., and Prevarskaya N. **2013**. "Opiates Modulate Thermosensation by Internalizing Cold Receptor TRPM8." *Cell Reports* 4 (3): 504–15. https://doi.org/10.1016/j.celrep.2013.07.002.

Shapovalov G., Ritaine A., Skryma R., and Prevarskaya N. **2016**. "Role of TRP Ion Channels in Cancer and Tumorigenesis." *Seminars in Immunopathology* 38 (3): 357–69. https://doi.org/10.1007/s00281-015-0525-1.

Shariat S.F., Semjonow A., Lilja H., Savage C., Vickers A.J., and Bjartell A. **2011**. "Tumor Markers in Prostate Cancer I: Blood-Based Markers." *Acta Oncologica (Stockholm, Sweden)* 50 Suppl 1 (Suppl 1): 61–75. https://doi.org/10.3109/0284186X.2010.542174.

Shariat S.F., Canto E.I., Kattan M.W., and Slawin K.M. **2004**. "Beyond Prostate-Specific Antigen: New Serologic Biomarkers for Improved Diagnosis and Management of Prostate Cancer." *Reviews in Urology* 6 (2): 58–72. http://www.ncbi.nlm.nih.gov/pubmed/16985579%0Ahttp://www.pubmedcentral.nih.gov/articlerender.fcgi?artid=PMC1472815.

Sheikh M.S., and Huang Y. **2003**. "Death Receptor Activation Complexes: It Takes Two to Activate TNF Receptor 1." *Cell Cycle (Georgetown, Tex.)* 2 (6): 549–51. https://doi.org/10.4161/cc.2.6.566.

Shi C., Wu J.B., and Pan D. **2016**. "Review on Near-Infrared Heptamethine Cyanine Dyes as Theranostic Agents for Tumor Imaging, Targeting, and Photodynamic Therapy." *Journal of Biomedical Optics* 21 (5): 50901. https://doi.org/10.1117/1.JBO.21.5.050901.

Shi J., Kantoff P.W., Wooster R., and Farokhzad O.C. **2017**. "Cancer Nanomedicine: Progress, Challenges and Opportunities." *Nat Rev Cancer* 17 (1): 20–38. https://doi.org/10.1038/nrc.2016.108.Cancer.

Shibata Y., Ugawa S., Imura M., Kubota Y., Ueda T., Kojima Y., Ishida Y., et al. **2011**. "TRPM8-Expressing Dorsal Root Ganglion Neurons Project Dichotomizing Axons to Both Skin and Bladder in Rats." *NeuroReport* 22 (2): 61–67. https://doi.org/10.1097/WNR.0b013e3283424c9c.

Shields J.M., Pruitt K., Shaub A., and Der C.J. **2000**. "Understanding Ras : ' It Ain ' t over ' Til It ' s over '." *Trends Cell Biol.* 10 (4): 147–54. https://doi.org/10.1016/s0962-8924(00)01740-2.

Shin Y.C., Shin S.Y., Chun J.N., Cho H.S., Lim J.M., Kim H.G., So I., Kwon D., and Jeon J.H.. **2012**. "TRIP Database 2.0: A Manually Curated Information Hub for Accessing TRP Channel Interaction Network." *PLOS ONE* 7 (10): e47165. https://doi.org/10.1371/JOURNAL.PONE.0047165.

Shirai T., Kumihashi K., Sakasai M., Kusuoku H., Shibuya Y., and Ohuchi A. **2017**. "Identification of a Novel TRPM8 Agonist from Nutmeg: A Promising Cooling Compound." *ACS Medicinal Chemistry Letters* 8 (7): 715–19. https://doi.org/10.1021/acsmedchemlett.7b00104.

Shishido Y., and Ohmi M. **2017**. Preparation of imidazolinone derivatives as TRPM8 antagonist. WO2017043092, issued 2017.

Siegel R.L., Miller K.D., Fuchs H.E., and Jemal A. **2022**. "Cancer Statistics, 2022." *CA: A Cancer Journal for Clinicians* 72 (1): 7–33. https://doi.org/10.3322/caac.21708.

Silva D.F., De Almeida M.M., Chaves C.G., Braz A.L., Gomes M.A., Pinho-Da-Silva L., Luiz Pesquero J., et al. **2015**. "TRPM8 Channel Activation Induced by Monoterpenoid Rotundifolone Underlies Mesenteric Artery Relaxation." *PLoS ONE*. https://doi.org/10.1371/journal.pone.0143171.

Silva E.F.F., Pimenta F.M., Pedersen B.W., Blaikie F.H., Bosio G.N., Breitenbach T., Westberg M., et al. **2016**. "Intracellular Singlet Oxygen Photosensitizers: On the Road to Solving the Problems of Sensitizer Degradation, Bleaching and Relocalization." *Integr. Biol.* 8 (2): 177–93. http://xlink.rsc.org/?DOI=C5IB00295H.

Simon A.R., Vikis H.G., Steward S., Fanburg B.L., Cochran B.H., and Guan K-L. **2000**. "Regulation of STAT3 by Direct Binding to the Racl GTPase." *Science* 290 (5489): 144–47.

Singh I., Knezevic N., Ahmmed G.U., Kini V., Malik A.B., and Mehta D. **2007**. "Gαq -TRPC6-Mediated Ca^{2+} Entry Induces RhoA Activation and Resultant Endothelial Cell Shape Change in Response to Thrombin." *J. Biol. Chem* 282 (11): 7833–43. https://doi.org/10.1074/jbc.M608288200.

Singh J., Manickam P., Shmoish M., Natik S., Denyer G., Handelsman D., Wei Gong D., and Dong Q. **2006**. "Annotation of Androgen Dependence to Human Prostate Cancer-Associated Genes by Microarray Analysis of Mouse Prostate." *Cancer Letters* 237 (2): 298–304. https://doi.org/10.1016/j.canlet.2005.06.008.

Sisignano M., Park C.K., Angioni C., Zhang D.D., von Hehn C., Cobos E.J., Ghasemlou N., et al. **2012**. "5,6-EET Is Released upon Neuronal Activity and Induces Mechanical Pain Hypersensitivity via TRPA1 on Central Afferent Terminals." *Journal of Neuroscience* 32 (18): 6364–72. https://doi.org/10.1523/JNEUROSCI.5793-11.2012.

Skryma R., Prevarskaya N., Gkika D., and Shuba Y. **2011**. "From Urgency to Frequency: Facts and Controversies of TRPs in the Lower Urinary Tract." *Nat Rev Urol* 8: 617–30. https://doi.org/10.1038/nrurol.2011.142.

Smedler E., and Uhlén P. **2014**. "Frequency Decoding of Calcium Oscillations." *Biochimica et Biophysica Acta - General Subjects* 1840 (3): 964–69. https://doi.org/10.1016/j.bbagen.2013.11.015.

Smedlund K., Tano J.Y., and Vazquez G.. **2010**. "The Constitutive Function of Native TRPC3 Channels Modulates Vascular Cell Adhesion Molecule-1 Expression in Coronary Endothelial Cells through Nuclear Factor Kb Signaling." *Circulation Research* 106 (9): 1479–88. https://doi.org/10.1161/CIRCRESAHA.109.213314.

Smith M.A., and Schnellmann R.G. **2012**. "Calpains, Mitochondria, and Apoptosis." *Cardiovascular Research* 96 (1): 32–37. https://doi.org/10.1093/cvr/cvs163.

Smith P.K., and Nilius B. **2013**. "Transient Receptor Potentials (TRPs) and Anaphylaxis." *Current Allergy and Asthma Reports* 13 (1): 93–100. https://doi.org/10.1007/s11882-012-0301-4.

Sokabe T., and Tominaga M. **2010**. "The TRPV4 Cation Channel." *Communicative & Integrative Biology* 3 (6): 619–21. https://doi.org/10.4161/cib.3.6.13461.

Song Y., Peng x., Porta A., Takanaga H., Peng J-B, Hediger M.A., Fleet J.C., and Christakos S. **2003**. "Calcium Transporter 1 and Epithelial Calcium ChannelMessenger Ribonucleic Acid Are Differentially Regulatedby 1,25 Dihydroxyvitamin D3in the Intestine and Kidneyof Mice." *Endocrinology* 144 (9): 3885–94. https://doi.org/10.1210/en.2003-0314.

Sotomayor M., Corey D.P., and Schulten K. **2005**. "In Search of the Hair-Cell Gating Spring: Elastic Properties of Ankyrin and Cadherin Repeats." *Structure* 13 (4): 669–82. https://doi.org/10.1016/j.str.2005.03.001.

Soumya M.S., Shafeekh K.M., Das S., and Abraham A. **2014**. "Symmetrical Diiodinated Squaraine as an Efficient Photosensitizer for PDT Applications: Evidence from Photodynamic and Toxicological Aspects." *Chemico-Biological Interactions* 222: 44–49. https://doi.org/10.1016/j.cbi.2014.08.006.

Sreejith S., Joseph J., Lin M., Menon N.V., Borah P., Ng H.J., Loong Y.X., Kang Y., Yu S.W.K, and Zhao Y. **2015**. "Near-Infrared Squaraine Dye Encapsulated Micelles for in Vivo Fluorescence and Photoacoustic Bimodal Imaging." *ACS Nano* 9 (6): 5695–5704. https://doi.org/10.1021/acsnano.5b02172.

Stamm S., Ben-Ari S., Rafalska I., Tang Y., Zhang Z., Toiber D., Thanaraj T.A., and Soreq H. **2005**. "Function of Alternative Splicing." *Gene* 344: 1–20. https://doi.org/10.1016/j.gene.2004.10.022.

Ständer S., Augustin M., Roggenkamp D., Blome C., Heitkemper T., Worthmann A.C., and Neufang G. **2017**. "Novel TRPM8 Agonist Cooling Compound against Chronic Itch: Results from a Randomized, Double-Blind, Controlled, Pilot Study in Dry Skin." *Journal of the European Academy of Dermatology and Venereology* 31 (6): 1064–68. https://doi.org/10.1111/jdv.14041.

Starkus J.G., Fleig A., and Penner R. **2010**. "The Calcium-Permeable Non-Selective Cation Channel TRPM2 Is Modulated by Cellular Acidification." *Journal of Physiology* 588 (8): 1227–40. https://doi.org/10.1113/jphysiol.2010.187476.

Steinbild S., Mross K., Frost A., Morant R., Gillessen S., Dittrich C., Strumberg D., et al. **2007**. "A Clinical Phase II Study with Sorafenib in Patients with Progressive Hormone-Refractory Prostate Cancer: A Study of the CESAR Central European Society for Anticancer Drug Research-EWIV." *British Journal of Cancer* 97 (11): 1480–85. https://doi.org/10.1038/SJ.BJC.6604064.

Stenmark H. **2009**. "Rab GTPases as Coordinators of Vesicle Traffic." *Nature Reviews Molecular Cell Biology* 10 (8): 513–25. https://doi.org/10.1038/nrm2728.

Stewart J.M. **2020**. "TRPV6 as a Target for Cancer Therapy." *Journal of Cancer* 11 (2): 374–87. https://doi.org/10.7150/jca.31640.

Story G.M., Peier A.M., Reeve A.J., Eid S.R., Mosbacher J., Hricik T.R., Earley T.J., et al. **2003**. "ANKTM1, a TRP-like Channel Expressed in Nociceptive Neurons, Is Activated by Cold Temperatures." *Cell* 112 (6): 819–29. https://doi.org/10.1016/S0092-8674(03)00158-2.

Streng T., Axelsson H.E., Hedlund P., Andersson D.A., Jordt S.E., Bevan S., Andersson K.E., Högestätt E.D., and Zygmunt P.M. **2008**. "Distribution and Function of the Hydrogen Sulfide-Sensitive TRPA1 Ion Channel in Rat Urinary Bladder." *European Urology* 53 (2): 391–400. https://doi.org/10.1016/j.eururo.2007.10.024.

Strübing C., Krapivinsky G., Krapivinsky L., and Clapham D.E. **2001**. "TRPC1 and TRPC5 Form a Novel Cation Channel in Mammalian Brain." *Neuron* 29 (3): 645–55. https://doi.org/10.1016/S0896-6273(01)00240-9.

Su L-T., Liu W., Chen H-C, Gonzalez-Pagan O., Habas R., Runnels L.W., and Jun N-. **2011**. "TRPM7 Regulates Polarized Cell Movements." *Biochem J* 434 (3): 513–21. https://doi.org/10.1042/BJ20101678.

Subkowski T., Bollschweiler C., Wittenberg J., Krohn M., and Zinke H. **2010**. Screening for low molecular-weight modulators of the cold-menthol receptor TRPM8 for therapeutic and cosmetic use. WO2010026094, issued 2010.

Subkowski T., Bollschweiler C., Wittenberg J., Siegel W., and Pelzer R. **2013**. Preparation of spiro compounds as low molecular weight modulators of the cold-menthol receptor TRPM8 and use thereof. WO2013041621, issued 2013.

Subramaniam, Bavani, Zahid H. Siddik, and Noor Hasima Nagoor. 2020. "Optimization of Nanostructured Lipid Carriers: Understanding the Types, Designs, and Parameters in the Process of Formulations." *Journal of Nanoparticle Research* 22 (6). https://doi.org/10.1007/s11051-020-04848-0.

Sumoza-Toledo A., Espinoza-Gabriel M.I., and Montiel-Condado D. **2016**. "Evaluación Del Canal TRPM2 Como Biomarcador En Cáncer de Mama Mediante El Análisis de Bases de Datos Públicos." *Boletin Medico Del Hospital Infantil de Mexico* 73 (6): 397–404. https://doi.org/10.1016/j.bmhimx.2016.10.001.

Sun J., Yang T., Wang P., Ma S., Zhu Z., Pu Y., Li L., et al. **2014**. "Activation of Cold-Sensing Transient Receptor Potential Melastatin Subtype 8 Antagonizes Vasoconstriction and Hypertension through Attenuating RhoA/Rho Kinase Pathway." *Hypertension* 63 (6): 1354–63. https://doi.org/10.1161/HYPERTENSIONAHA.113.02573.

Sun L., Yau H.Y., Wong W.Y., Li R.A., Huang Y., and Yao X. **2012**. "Role of TRPM2 in H_2O_2-Induced Cell Apoptosis in Endothelial Cells." *PLoS ONE* 7 (8): 1–10. https://doi.org/10.1371/journal.pone.0043186.

Sun Y., Sukumaran P., Varma A., Derry S., and Sahmoun A.E. **2014**. "Cholesterol-Induced Activation of TRPM7 Regulate Cell Proliferation, Migration, and Viability of Human Prostate Cells." *Biochim Biophys Acta* 1843 (9): 1839–50. https://doi.org/10.1016/j.bbamcr.2014.04.019.

Sun Y., Selvaraj S., Varma A., Derry S., Sahmoun A.E., and Singh B.B. **2013**. "Increase in Serum Ca^{2+}/Mg^{2+} Ratio Promotes Proliferation of Prostate Cancer Cells by Activating TRPM7 Channels." *Journal of Biological Chemistry* 288 (1): 255–63. https://doi.org/10.1074/jbc.M112.393918.

Sung H., Ferlay J., Siegel R.L., Laversanne M., Soerjomataram I., Jemal A., and Bray F. **2021**. "Global Cancer Statistics 2020: GLOBOCAN Estimates of Incidence and Mortality Worldwide for 36 Cancers in 185 Countries." *CA: A Cancer Journal for Clinicians* 71 (3): 209–49. https://doi.org/10.3322/caac.21660.

Suo Y., Wang Z., Zubcevic L., Hsu A.L., He Q., Borgnia M.J., Ji R.R., and Lee S.Y.. **2020**. "Structural Insights into Electrophile Irritant Sensing by the Human TRPA1 Channel." *Neuron* 105 (5): 882-894.e5. https://doi.org/10.1016/j.neuron.2019.11.023.

Surburg H., Backes M., Oertling H., Machinek A., Loges H, Simchen U, Subkowski T, Bollschweiler C, Wittenberg J, and Siegel W. **2011**. Use of physiological cooling active ingredients such as transient receptor potential cation channel 8 modulator for achieving cooling effect on skin or mucous membrane. WO2011061330, issued 2011.

Suri A., and Szallasi A. **2008**. "The Emerging Role of TRPV1 in Diabetes and Obesity." *Trends in Pharmacological Sciences* 29 (1): 29–36. https://doi.org/10.1016/j.tips.2007.10.016.

Svensmark J.H., and Brakebusch C. **2019**. "Rho GTPases in Cancer: Friend or Foe?" *Oncogene* 38 (50): 7447–56. https://doi.org/10.1038/s41388-019-0963-7.

Taberner F.J., López-Córdoba A., Fernández-Ballester G., Korchev Y., and Ferrer-Montiel A. **2014**. "The Region Adjacent to the C-End

of the Inner Gate in Transient Receptor Potential Melastatin 8 (TRPM8) Channels." *Journal of Biological Chemistry* 289 (41): 28579–94. https://doi.org/10.1074/jbc.M114.577478.

Tajima N., Schönherr K., Niedling S., Kaatz M., Kanno H., Schönherr R., and Heinemann S.H. **2006**. "Ca^{2+}-Activated K^+ Channels in Human Melanoma Cells Are up-Regulated by Hypoxia Involving Hypoxia-Inducible Factor-1alpha and the von Hippel-Lindau Protein." *The Journal of Physiology* 571 (Pt 2): 349–59. https://doi.org/10.1113/JPHYSIOL.2005.096818.

Takahashi N., Kuwaki T., Kiyonaka S., Numata T., Kozai D., Mizuno Y., Yamamoto S., et al. **2011**. "TRPA1 Underlies a Sensing Mechanism for O_2." *Nature Chemical Biology* 7 (10): 701–11. https://doi.org/10.1038/nchembio.640.

Takahashi N., Mizuno Y., Kozai D., Yamamoto S., Kiyonaka S., Shibata T., Uchida K., and Mori Y. **2008**. "Molecular Characterization of TRPA1 Channel Activation by Cysteine-Reactive Inflammatory Mediators." *Channels* 2 (4): 287–98. https://doi.org/10.4161/chan.2.4.6745.

Takahashi N., and Mori Y. **2011**. "TRP Channels as Sensors and Signal Integrators of Redox Status Changes." *Frontiers in Pharmacology* OCT (October): 1–11. https://doi.org/10.3389/fphar.2011.00058.

Takaishi M., Fujita F., Uchida K., Yamamoto S., Shimizu M.S., Uotsu C.H., Shimizu M., and Tominaga M. **2012**. "1,8-Cineole, a TRPM8 Agonist, Is a Novel Natural Antagonist of Human TRPA1." *Molecular Pain* 8. https://doi.org/10.1186/1744-8069-8-86.

Takaishi M., Uchida K., Fujita F., and Tominaga M. **2014**. "Inhibitory Effects of Monoterpenes on Human TRPA1 and the Structural Basis of Their Activity." *Journal of Physiological Sciences* 64 (1): 47–57. https://doi.org/10.1007/s12576-013-0289-0.

Takaya J., Mio K., Shiraishi T., Kurokawa T., Otsuka S., Mori Y., and Uesugi M. **2015**. "A Potent and Site-Selective Agonist of TRPA1." *Journal of the American Chemical Society* 137 (50): 15859–64. https://doi.org/10.1021/jacs.5b10162.

Talavera K., Nilius B., and Voets T. **2008**. "Neuronal TRP Channels: Thermometers, Pathfinders and Life-Savers." *Trends in Neurosciences* 31 (6): 287–95.

Talavera K., Gees M., Karashima Y., Meseguer V.M., Vanoirbeek J.A.J., Damann N., Everaerts W., et al. **2009**. "Nicotine Activates the Chemosensory Cation Channel TRPA1." *Nature Neuroscience* 12 (10): 1293–99. https://doi.org/10.1038/nn.2379.

Tan X., Luo S., Wang D., Su Y., Cheng T., and Shi C. **2012**. "A NIR Heptamethine Dye with Intrinsic Cancer Targeting, Imaging and Photosensitizing Properties." *Biomaterials* 33 (7): 2230–39. https://doi.org/10.1016/j.biomaterials.2011.11.081.

Taneja S.S., Bennett J., Coleman J., Grubb R., Andriole G., Reiter R.E., Marks L., Azzouzi A.R., and Emberton M. **2016**. "Final Results of a Phase I/II Multicenter Trial of WST11 Vascular Targeted Photodynamic Therapy for Hemi-Ablation of the Prostate in Men with Unilateral Low Risk Prostate Cancer Performed in the United States." *The Journal of Urology* 196 (4): 1096–1104. https://doi.org/10.1016/J.JURO.2016.05.113.

Taylor-Clark T.E., Mcalexander M.A., Nassenstein C., Sheardown S.A., Wilson S., Thornton J., Carr M.J., and Undem B.J. **2008**. "Relative Contributions of TRPA1 and TRPV1 Channels in the Activation of Vagal Bronchopulmonary C-Fibres by the Endogenous Autacoid 4-Oxononenal." *Journal of Physiology* 586 (14): 3447–59. https://doi.org/10.1113/jphysiol.2008.153585.

Taylor-Clark T.E., Kiros F., Carr M.J., and McAlexander M.A. **2009**. "Transient Receptor Potential Ankyrin 1 Mediates Toluene Diisocyanate-Evoked Respiratory Irritation." *American Journal of Respiratory Cell and Molecular Biology* 40 (6): 756–62. https://doi.org/10.1165/rcmb.2008-0292OC.

Texier I., Goutayer M., Da Silva A., Guyon L., Djaker N., Josserand V., Neumann E., Bibette J., and Vinet F. **2009**. "Cyanine-Loaded Lipid Nanoparticles for Improved in Vivo Fluorescence Imaging." *Journal of Biomedical Optics* 14 (5): 054005 1-11. https://doi.org/10.1117/1.3213606.

Thebault S., Flourakis M., Vanoverberghe K., Vandermoere F., Roudbaraki M., Lehen'kyi V., Slomianny C., et al. **2006**. "Differential Role of Transient Receptor Potential Channels in Ca^{2+} Entry and Proliferation of Prostate Cancer Epithelial Cells." *Cancer Research* 66 (4): 2038–47. https://doi.org/10.1158/0008-5472.CAN-05-0376.

Thebault S., Lemonnier L., Bidaux G., Flourakis M., Bavencoffe A., Gordienko D., Roudbaraki M, et al. **2005**. "Novel Role of Cold/Menthol-Sensitive Transient Receptor Potential Melastatine Family Member 8 (TRPM8) in the Activation of Store-Operated Channels in LNCaP Human Prostate Cancer Epithelial Cells." *Journal of Biological Chemistry* 280 (47): 39423–35. https://doi.org/10.1074/jbc.M503544200.

Thodeti C.K., Matthews B., Ravi A., Mammoto A., Ghosh K., Bracha A.L., and Ingber D.E. **2009**. "TRPV4 Channels Mediate Cyclic Strain-Induced Endothelial Cell Reorientation through Integrin-to-Integrin Signaling." *Circulation Research* 104 (9): 1123–30. https://doi.org/10.1161/CIRCRESAHA.108.192930.

Thodeti C.K., Paruchuri S., and Meszaros J.G. **2013**. "A TRP to Cardiac Fibroblast Differentiation." *Channels* 7 (3): 211–14.

https://doi.org/10.4161/chan.24328.

Thoppil R.J., Cappelli H.C., Adapala R.K., Kanugula A.K., Paruchuri S., and Thodeti C.K. **2016**. "TRPV4 Channels Regulate Tumor Angiogenesis *via* Modulation of Rho/Rho Kinase Pathway." *Oncotarget* 7 (18): 25849–61. https://doi.org/10.18632/oncotarget.8405.

Tian D., Jacobo S.M.P., Billing D., Rozkalne A., Gage S.D., Anagnostou T., Pavenstädt H., et al. **2010**. "Antagonistic Regulation Od Actin Dynamics and Cell Motility by TRPC5 and TRPC6 Channels." *Sci Signal.* 3 (145): ra77. https://doi.org/10.1126/scisignal.2001200.Antagonistic.

Todak A. **2020**. "FDA Committee Votes against Approval of Tookad for Localized Prostate Cancer." *HemOnc Today*. https://www.healio.com/news/hematology-oncology/20200226/fda-committee-votes-against-approval-of-tookad-for-localized-prostate-cancer.

Tomasek J.J., Vaughan M.B., Kropp B.P., Gabbiani G., Martin M.D., Haaksma C.J., and Hinz B. **2006**. "Contraction of Myofibroblasts in Granulation Tissue Is Dependent on Rho/Rho Kinase/Myosin Light Chain Phosphatase Activity." *Wound Repair Regen.* 14 (3): 313–20. https://doi.org/10.1111/j.1743-6109.2006.00126.x.

Trabulsi E.J., Rumble R.B., Jadvar H., Hope T., Pomper M., Turkbey B., Rosenkrantz A.B., et al. **2020**. "Optimum Imaging Strategies for Advanced Prostate Cancer: ASCO Guideline." *Journal of Clinical Oncology* 38 (17): 1963–96. https://doi.org/10.1200/JCO.19.02757.

Trachtenberg J., Bogaards A., Weersink R.A., Haider M.A., Evans A., McCluskey S.A., Scherz A., et al. **2007**. "Vascular Targeted Photodynamic Therapy With Palladium-Bacteriopheophorbide Photosensitizer for Recurrent Prostate Cancer Following Definitive Radiation Therapy: Assessment of Safety and Treatment Response." *Journal of Urology* 178 (5): 1974–79. https://doi.org/10.1016/j.juro.2007.07.036.

Trachtenberg J., Weersink R.A., Davidson S.R.H., Haider M.A., Bogaards A., Gertner M.R., Evans A., et al. **2008**. "Vascular-Targeted Photodynamic Therapy (Padoporfin, WST09) for Recurrent Prostate Cancer after Failure of External Beam Radiotherapy: A Study of Escalating Light Doses." *BJU International* 102 (5): 556–62. https://doi.org/10.1111/j.1464-410X.2008.07753.x.

Trevisan G., Rossato M.F., Hoffmeister C., Oliveira S.M., Silva C.R., Matheus F.C., Mello G.C., Antunes E., Prediger R.D.S., and Ferreira J. **2013**. "Mechanisms Involved in Abdominal Nociception Induced by Either TRPV1 or TRPA1 Stimulation of Rat Peritoneum." *European Journal of Pharmacology* 714 (1–3): 332–44. https://doi.org/10.1016/j.ejphar.2013.07.029.

Trevisan G., Rossato M.F., Tonello R., Hoffmeister C., Klafke J.Z., Rosa F., Pinheiro K.V., et al. **2014**. "Gallic Acid Functions as a TRPA1 Antagonist with Relevant Antinociceptive and Antiedematogenic Effects in Mice." *Naunyn-Schmiedeberg's Archives of Pharmacology* 387 (7): 679–89. https://doi.org/10.1007/s00210-014-0978-0.

Trevisani M., Siemens J., Materazzi S., Bautista D.M., Nassini R., Campi B., Imamachi N., et al. **2007**. "4-Hydroxynonenal, an Endogenous Aldehyde, Causes Pain and Neurogenic Inflammation through Activation of the Irritant Receptor TRPA1." *Proceedings of the National Academy of Sciences of the United States of America* 104 (33): 13519–24. https://doi.org/10.1073/pnas.0705923104.

Tsagareli M.G., Nozadze I., Tsiklauri N., and Gurtskaia G. **2018**. "Non-Steroidal Anti-Inflammatory Drugs Attenuate Agonist-Evoked Activation of Transient Receptor Potential Channels." *Biomedicine and Pharmacotherapy* 97 (October 2017): 745–51. https://doi.org/10.1016/j.biopha.2017.10.131.

Tsagareli M.G., and Nozadze I. **2020**. "An Overview on Transient Receptor Potential Channels Superfamily." *Behavioural Pharmacology* 31 (5): 413–34. https://doi.org/10.1097/FBP.0000000000000524.

Tsagareli M.G., Tsiklauri N., Zanotto K.L., Carstens M.I., Klein A.H., Sawyer C.M., Gurtskaia G., Abzianidze E., and Carstens E. **2010**. "Behavioral Evidence of Thermal Hyperalgesia and Mechanical Allodynia Induced by Intradermal Cinnamaldehyde in Rats." *Neuroscience Letters* 473 (3): 233–36. https://doi.org/10.1016/j.neulet.2010.02.056.

Tsagareli M.G., Tsiklauri N., and Gurtskaia G.. **2019**. "TRPA1 Channel Is Involved in SLIGRL-Evoked Thermal and Mechanical Hyperalgesia in Mice." *Medical Sciences* 7 (4): 62. https://doi.org/10.3390/medsci7040062.

Tsavaler L., Shapero M.H., Morkowski S., and Laus R. **2001**. "Trp-P8, a Novel Prostate-Specific Gene, Is up-Regulated in Prostate Cancer and Other Malignancies and Shares High Homology with Transient Receptor Potential Calcium Channel Proteins." *Cancer Research* 61 (9): 3760–69.

Tsutsumi M., Denda S., Ikeyama K., Goto M., and Denda M. **2010**. "Exposure to Low Temperature Induces Elevation of Intracellular Calcium in Cultured Human Keratinocytes." *Journal of Investigative Dermatology* 130 (7): 1945–48. https://doi.org/10.1038/jid.2010.33.

Tu C.L., Chang W., and Bikle D.D. **2005**. "Phospholipase Cγ1 Is Required for Activation of Store-Operated Channels in Human Keratinocytes." *Journal of Investigative Dermatology* 124 (1): 187–97. https://doi.org/10.1111/j.0022-202X.2004.23544.x.

Uchida K., Miura Y., Nagai M., and Tominaga M. **2012**. "Isothiocyanates from Wasabia Japonica Activate Transient Receptor Potential Ankyrin 1 Channel." *Chemical Senses* 37 (9): 809–18. https://doi.org/10.1093/chemse/bjs065.

Ungefroren H., Witte D., and Lehnert H. **2018**. "The Role of Small GTPases of the Rho/Rac Family in TGF-β-Induced EMT and Cell Motility in Cancer." *Developmental Dynamics* 247 (3): 451–61. https://doi.org/10.1002/dvdy.24505.

University, Duke. **2016**. TRPA1 and TRPV4 inhibitors and methods of using the same for organ-specific inflammation and itch. WO2016028325, issued 2016.

Urata T., Mori N., and Fukuwatari T. **2017**. "Vagus Nerve Is Involved in the Changes in Body Temperature Induced by Intragastric Administration of 1,8-Cineole via TRPM8 in Mice." *Neuroscience Letters* 650: 65–71. https://doi.org/10.1016/j.neulet.2017.04.018.

Valerio M., Ahmed H.U., Emberton M., Lawrentschuk N., Lazzeri M., Montironi R., Nguyen P.L., Trachtenberg J., and Polascik T.J. **2014**. "The Role of Focal Therapy in the Management of Localised Prostate Cancer: A Systematic Review." *European Urology* 66 (4): 732–51. https://doi.org/10.1016/j.eururo.2013.05.048.

Valero M.L., Mello de Queiroz F., Stühmer W., Viana F., and Pardo L.A. **2012**. "TRPM8 Ion Channels Differentially Modulate Proliferation and Cell Cycle Distribution of Normal and Cancer Prostate Cells." *PLoS ONE* 7 (12): 2–13. https://doi.org/10.1371/journal.pone.0051825.

Van Cromphaut S.J., Rummens K., Stockmans I., Van Herck E., Dijcks F.A., Ederveen A.G.H., Carmeliet P., Verhaeghe J., Bouillon R., and Carmeliet G. **2003**. "Intestinal Calcium Transporter Genes Are Upregulated by Estrogens and the Reproductive Cycle Through Vitamin D Receptor-Independent Mechanisms." *Journal of Bone and Mineral Research* 18 (10): 1725–36. https://doi.org/10.1359/jbmr.2003.18.10.1725.

Vancauwenberghe E., Noyer L., Derouiche S., Lemonnier L., Gosset P., Sadofsky L.R., Mariot P., et al. **2017**. "Activation of Mutated TRPA1 Ion Channel by Resveratrol in Human Prostate Cancer Associated Fibroblasts (CAF)." *Molecular Carcinogenesis* 56 (8): 1851–67. https://doi.org/10.1002/mc.22642.

Vanden Abeele F., Lemonnier L., Thébault S., Lepage G., Parys J.B., Shuba Y., Skryma R., and Prevarskaya N. **2004**. "Two Types of Store-Operated Ca^{2+} Channels with Different Activation Modes and Molecular Origin in LNCaP Human Prostate Cancer Epithelial Cells." *Journal of Biological Chemistry* 279 (29): 30326–37. https://doi.org/10.1074/jbc.M400106200.

Vanden Abeele F., Roudbaraki M., Shuba Y., Skryma R., and Prevarskaya N. **2003**. "Store-Operated Ca^{2+} Current in Prostate Cancer Epithelial Cells: Role of Endogenous Ca^{2+} Transporter Type 1." *Journal of Biological Chemistry* 278 (17): 15381–89. https://doi.org/10.1074/jbc.M212106200.

Vanden Abeele F., Skryma R., Shuba Y., Van Coppenolle F., Slomianny C., Roudbaraki M., Mauroy B., Wuytack F., and Prevarskaya N. **2002**. "Bcl-2-Dependent Modulation of Ca^{2+} Homeostasis and Store-Operated Channels in Prostate Cancer Cells." *Cancer Cell* 1 (2): 169–79. https://doi.org/10.1016/S1535-6108(02)00034-X.

Vanden Abeele F., Zholos A., Bidaux G., Shuba Y., Thebault S., Beck B., Flourakis M., Panchin Y., Rman Skryma R., and Prevarskaya N. **2006**. "Ca^{2+}-Independent Phospholipase A2-Dependent Gating of TRPM8 by Lysophospholipids." *Journal of Biological Chemistry* 281 (52): 40174–82. https://doi.org/10.1074/jbc.M605779200.

Van Haute C., De Ridder D., and Nilius B. **2010**. "TRP Channels in Human Prostate." *The ScientificWorldJournal* 10: 1597–1611. https://doi.org/10.1100/tsw.2010.149.

Vanoverberghe K., Vanden Abeele F., Mariot P., Lepage G., Roudbaraki M., Bonnal J.L., Mauroy B., Shuba Y., Skryma R., and Prevarskaya N. **2004**. "Ca^{2+} Homeostasis and Apoptotic Resistance of Neuroendocrine-Differentiated Prostate Cancer Cells." *Cell Death and Differentiation* 11 (3): 321–30. https://doi.org/10.1038/sj.cdd.4401375.

Velazco M.I., Wuensche L., and Deladoey P. **2000**. Use of cubebol as a flavoring ingredient. EP1040765, issued 2000.

Vennekens R., and Nilius B. **2007**. "Insights into TRPM4 Function, Regulation and Physiological Role." In *Transient Receptor Potential (TRP) Channels. Handbook of Experimental Pharmacology*, edited by V. Flockerzi and B. Nilius, 179:269–85. Springer. https://doi.org/10.1007/978-3-540-34891-7_16.

Vennekens R., Menigoz A., and Nilius B. **2012**. "TRPs in the Brain." In *Reviews of Physiology, Biochemistry and Pharmacology*, Vol. 163. Springer, Berlin, Heidelberg. https://doi.org/10.1007/112_2012_8.

Verigos K., Stripp D.C.H., Mick R., Zhu T.C., Whittington R., Smith D., Dimofte A., et al. **2006**. "Updated Results of a Phase I Trial of

Motexafin Lutetium-Mediated Interstitial Photodynamic Therapy in Patients with Locally Recurrent Prostate Cancer." *Journal of Environmental Pathology, Toxicology and Oncology : Official Organ of the International Society for Environmental Toxicology and Cancer* 25 (1–2): 373–87. https://doi.org/10.1615/JENVIRONPATHOLTOXICOLONCOL.V25.I1-2.230.

Vetter I.R., and Wittinghofer A. **2001**. "The Guanine Nucleotide-Binding Switch in Three Dimensions." *Science* 294 (5545): 1299–1304. https://doi.org/10.1126/science.1062023.

Viana F. **2016**. "TRPA1 Channels: Molecular Sentinels of Cellular Stress and Tissue Damage." *Journal of Physiology* 594 (15): 4151–69. https://doi.org/10.1113/JP270935.

Voets T., Droogmans G., Wissenbach U., Janssens A., Flockerzi V., and Nilius B. **2004**. "The Principle of Temperature-Dependent Gating in Cold- and Heat-Sensitive TRP Channels." *Nature* 430 (7001): 748–54. https://doi.org/10.1038/nature02732.

Vrenken K.S., Jalink K., van Leeuwen F.N., and Middelbeek J. **2015**. "Beyond Ion-Conduction: Channel-Dependent and -Independent Roles of TRP Channels during Development and Tissue Homeostasis." *Biochimica et Biophysica Acta - Molecular Cell Research* 1863 (6): 1436–46. https://doi.org/10.1016/j.bbamcr.2015.11.008.

Vriens J., Janssens A., Prenen J., Nilius B., and Wondergem R. **2004**. "TRPV Channels and Modulation by Hepatocyte Growth Factor / Scatter Factor in Human Hepatoblastoma (HepG2) Cells." *Cell Calcium* 36 (1): 19–28. https://doi.org/10.1016/j.ceca.2003.11.006.

Walcher L., Budde C., Böhm A., Reinach P.S., Dhandapani P., Ljubojevic N., Schweiger M.W., et al. **2018**. "Induced Transactivation of TRPV1 in Human Uveal Melanoma Cells." *Frontiers in Pharmacology* 9 (NOV). https://doi.org/10.3389/fphar.2018.01234.

Wang C., Hu H.Z., Colton C.K., Wood J.D., and Zhu M.X. **2004**. "An Alternative Splicing Product of the Murine Trpv1 Gene Dominant Negatively Modulates the Activity of TRPV1 Channels." *Journal of Biological Chemistry* 279 (36): 37423–30. https://doi.org/10.1074/jbc.M407205200.

Wang D., Li X., Liu J., Li J., Li L.J., and Qiu M.X. **2014**. "Effects of TRPC6 on Invasibility of Low-Differentiated Prostate Cancer Cells." *Asian Pacific Journal of Tropical Medicine* 7 (1): 44–47. https://doi.org/10.1016/S1995-7645(13)60190-X.

Wang Q., Huang L., and Yue J.. **2017**. "Oxidative Stress Activates the TRPM2-Ca^{2+} -CaMKII-ROS Signaling Loop to Induce Cell Death in Cancer Cells." *BBA - Molecular Cell Research* 1864 (6): 957–67. https://doi.org/10.1016/j.bbamcr.2016.12.014.

Wang S., Dai Y., Fukuoka T., Yamanaka H., Kobayashi K., Obata K., Cui X., Tominaga M., and Noguchi K. **2008**. "Phospholipase C and Protein Kinase A Mediate Bradykinin Sensitization of TRPA1: A Molecular Mechanism of Inflammatory Pain." *Brain* 131 (5): 1241–51. https://doi.org/10.1093/brain/awn060.

Wang S., Zhai C., Zhang Y., Yu Y., Zhang Y., Lianghui M., Li S., and Qiao Y. **2016**. "Cardamonin, a Novel Antagonist of HTRPA1 Cation Channel, Reveals Therapeutic Mechanism of Pathological Pain." *Molecules*. https://doi.org/10.3390/molecules21091145.

Wang X., Tsui B., Ramamurthy G., Zhang P., Meyers J., Kenney M.E., Kiechle J., Ponsky L., and Basilion J.P. **2016**. "Theranostic Agents for Photodynamic Therapy of Prostate Cancer by Targeting Prostate-Specific Membrane Antigen." *Molecular Cancer Therapeutics* 15 (8): 1834–44. https://doi.org/10.1158/1535-7163.MCT-15-0722.

Wang Y., Yue D., Li K., Liu Y-L., Ren C-S., and Wang P. **2010**. "The Role of TRPC6 in HGF-Induced Cell Proliferation of Human Prostate Cancer DU145 and PC3 Cells." *Nature Publishing Group* 12 (6): 841–52. https://doi.org/10.1038/aja.2010.85.

Wang Y., Wang X., Yang Z., Zhu G., Chen D., and Meng Z. **2012**. "Menthol Inhibits the Proliferation and Motility of Prostate Cancer DU145 Cells." *Pathology and Oncology Research* 18 (4): 903–10. https://doi.org/10.1007/s12253-012-9520-1.

Wang Y., He H., Srivastava N., Vikarunnessa S., Chen Y.B., Jiang J., Cowan C.W., and Zhang X. **2012**. "Plexins Are GTPase-Activating Proteins for Rap and Are Activated by Induced Dimerization." *Science Signaling* 5 (207): 1–25. https://doi.org/10.1126/scisignal.2002636.

Waning J., Vriens J., Owsianik G., and Stuwe L., Mally S., Fabian A., Frippiat, C., Nilius B., Schwab A. **2007**. "A Novel Function of Capsaicin-Sensitive TRPV1 Channels : Involvement in Cell Migration" 42: 17–25. https://doi.org/10.1016/j.ceca.2006.11.005.

Watanabe H., Iino K., Ohba T., and Ito H. **2013**. "Possible Involvement of TRP Channels in Cardiac Hypertrophy and Arrhythmia." *Curr Top Med Chem* 13 (3): 283–94. https://doi.org/10.2174/1568026611313030006.

Watanabe R., Hanaoka H., Sato K., Nagaya T., Harada T., Mitsunaga M., Kim I., et al. **2015**. "Photoimmunotherapy Targeting Prostate-Specific Membrane Antigen: Are Antibody Fragments as Effective as Antibodies?" *Journal of Nuclear Medicine : Official Publication, Society of Nuclear Medicine* 56 (1): 140–44. https://doi.org/10.2967/JNUMED.114.149526.

Weber K., Erben R.G., Rump A., and Adamski J. **2001**. "Gene Structure and Regulation of the Murine Epithelial Calcium Channels

ECaC1 and 2." *Biochemical and Biophysical Research Communications* 289 (5): 1287–94. https://doi.org/10.1006/bbrc.2001.6121.

Wei C., Wang X., Chen M., Ouyang K., Song L-S., and Cheng H. **2009**. "Calcium Flickers Steer Cell Migration." *Nature* 457 (7231): 901–5. https://doi.org/10.1038/nature07577.Calcium.

Wei C., Wang X., Chen M., Ouyang K., Zheng M., and Cheng H. **2010**. "Flickering Calcium Microdomains Signal Turning of Migrating Cells." *Canadian Journal of Physiology and Pharmacology* 88 (2): 105–10. https://doi.org/10.1139/Y09-118.

Wei E.T. **2015**. Di-isopropyl-phosphinoyl-alkanes as topical agents for the treatment of sensory discomfort. US20150164924A1, issued 2015.

———. **2017**. Dialkyl-phosphinoyl-alkane (Dapa) compounds and compositions for treatment of lower gastrointestinal tract disorders. US20170189428A1, issued 2017.

Wei H., Hamalainen M.M., Saarnilehto M., Koivisto A., and Pertovaara A. **2009**. "Attenuation of Mechanical Hypersensitivity by AnAntagonist of the TRPA1 Ion Channel in Diabetic Animals." *Anesthesiology* 111: 147–54.

Weis S.M., and Cheresh D.A. **2005**. "Pathophysiological Consequences of VEGF-Induced Vascular Permeability." *Nature* 437 (7058): 497–504. https://doi.org/10.1038/nature03987.

Wellington K., and Keam S.J. **2006**. "Bicalutamide 150mg: A Review of Its Use in the Treatment of Locally Advanced Prostate Cancer." *Drugs* 66 (6): 837–50. https://doi.org/10.2165/00003495-200666060-00007.

Weng H.J., Patel K.N., Jeske N.A., Bierbower S.M., Zou W., Tiwari V., Zheng Q., et al. **2015**. "Tmem100 Is a Regulator of TRPA1-TRPV1 Complex and Contributes to Persistent Pain." *Neuron* 85 (4): 833–46. https://doi.org/10.1016/j.neuron.2014.12.065.

Wes P.D., Chevesich J., Jeromin A., Rosenberg C., Stetten G., and Montell C. **1995**. "TRPC1, a Human Homolog of a Drosophila Store-Operated Channel." *Proceedings of the National Academy of Sciences of the United States of America* 92 (21): 9652–56. https://doi.org/10.1073/pnas.92.21.9652.

Weyer A.D., and Lehto S.G. **2017**. "Development of TRPM8 Antagonists to Treat Chronic Pain and Migraine." *Pharmaceuticals* 10 (2): 1–9. https://doi.org/10.3390/ph10020037.

Willette R.N., Bao W., Nerurkar S., Yue T.I., Doe C.P., Stankus G., Turner G.H., et al. **2008**. "Systemic Activation of the Transient Receptor Potential Vanilloid Subtype 4 Channel Causes Endothelial Failure and Circulatory Collapse: Part 2." *Journal of Pharmacology and Experimental Therapeutics* 326 (2): 443–52. https://doi.org/10.1124/jpet.107.134551.

Willis D.N., Liu B., Ha M.A., Jordt S-E, and Morris J.B. **2011**. "Menthol Attenuates Respiratory Irritation Responses To Multiple Cigarette Smoke Irritants." *FASEB* 25: 4434–4444. https://doi.org/10.1164/ajrccm-conference.2012.185.1_meetingabstracts.a6745.

Wilson S.R., Gerhold K.A., Bifolck-Fisher A., Liu Q., Patel K.N., Dong X., and Bautista D.M. **2011**. "TRPA1 Is Required for Histamine-Independent, Mas-Related G Protein-Coupled Receptor-Mediated Itch." *Nat Neurosci.* 14 (5): 595–602. https://doi.org/10.1038/nn.2789.TRPA1.

Winn M.P., Conlon P.J., Lynn K.L., Farrington M.K., Creazzo T., Hawkins A.F., Daskalakis N., et al. **2005**. "Medicine: A Mutation in the TRPC6 Cation Channel Causes Familial Focal Segmental Glomerulosclerosis." *Science* 308 (5729): 1801–4. https://doi.org/10.1126/science.1106215.

Wissenbach U., Niemeyer B.A., and Flockerzi V. **2004**. "TRP Channels as Potential Drug Targets." *Biology of the Cell* 96 (1): 47–54. https://doi.org/10.1146/annurev-pharmtox-010617-052832.

Wissenbach U., Niemeyer B.A., Fixemer T., Schneidewind A., Trost C., Cavalié A., Reus K., Meese E., Bonkhoff H., and Flockerzi V. **2001**. "Expression of CaT-like, a Novel Calcium-Selective Channel, Correlates with the Malignancy of Prostate Cancer." *Journal of Biological Chemistry* 276 (22): 19461–68. https://doi.org/10.1074/jbc.M009895200.

Wondergem R., Ecay T.W., Mahieu F., Owsianik G., and Nilius B. **2008**. "HGF/SF and Menthol Increase Human Glioblastoma Cell Calcium and Migration" 372: 210–15. https://doi.org/10.1016/j.bbrc.2008.05.032.

"World Cancer Research Fund International." **2022**. wcrf.org.

Wos J.A., Yelm K.E., Bunke G.M., Frederick H.A., Reilly M., Haught J.C., Sreekrishna K.T., and Lin Y. **2017**. Synthesis of cyclohexane ester derivatives useful as cooling sensates in consumer products. WO2017106279, issued 2017.

Wu H-Y., Tomizawa K., and Matsui H. **2007**. "Calpain-Calcineurin Signaling in the Pathogenesis of Calcium-Dependent Disorder." *Acta Med. Okayama* 61 (3): 123–37.

Wu L.J., Sweet T.B., and Clapham D.E. **2010**. "International Union of Basic and Clinical Pharmacology. LXXVI. Current Progress in the Mammalian TRP Ion Channel Family." *Pharmacological Reviews* 62 (3): 381–404. https://doi.org/10.1124/pr.110.002725.

Xiao N., Jiang L.M., Ge B., Zhang T.Y., Zhao X.K., and Zhou X. **2014**. "Over-Expression of TRPM8 Is Associated with Poor Prognosis in Urothelial Carcinoma of Bladder." *Tumor Biology* 35 (11): 11499–504. https://doi.org/10.1007/s13277-014-2480-1.

Xie J., Bi Y., Zhang H., Dong S., Teng L., Lee R.J., and Yang Z. **2020**. "Cell-Penetrating Peptides in Diagnosis and Treatment of Human Diseases: From Preclinical Research to Clinical Application." *Frontiers in Pharmacology* 11 (May): 697. https://doi.org/10.3389/fphar.2020.00697.

Xie R., Xu J., Xiao Y., Wu J., Wan H., Tang B., Liu J., et al. **2017**. "Calcium Promotes Human Gastric Cancer via a Novel Coupling of Calcium-Sensing Receptor and TRPV4 Channel." *Cancer Research* 77 (23): 6499–6512. https://doi.org/10.1158/0008-5472.CAN-17-0360.

Xin H., Tanaka H., Yamaguchi M., Takemori S., Nakamura A., and Kohama K. **2005**. "Vanilloid Receptor Expressed in the Sarcoplasmic Reticulum of Rat Skeletal Muscle." *Biochemical and Biophysical Research Communications* 332 (3): 756–62. https://doi.org/10.1016/j.bbrc.2005.05.016.

Xing H., Ling J.X., Chen M., Johnson R.D., Tominaga M., Wang C.Y., and Gu J. **2008**. "TRPM8 Mechanism of Autonomic Nerve Response to Cold in Respiratory Airway." *Molecular Pain* 4: 1–9. https://doi.org/10.1186/1744-8069-4-22.

Xu H., Blair N.T., and Clapham D.E. **2005**. "Camphor Activates and Strongly Desensitizes the Transient Receptor Potential Vanilloid Subtype 1 Channel in a Vanilloid-Independent Mechanism." *Journal of Neuroscience* 25 (39): 8924–37. https://doi.org/10.1523/JNEUROSCI.2574-05.2005.

Xu S-Z., Muraki K., Zeng F., Li J., Sukumar P., Dedman A.M., Flemming P.K., et al. **2006**. "A Sphingosine-1 – Phosphate – Activated Calcium Channel Controlling Vascular Smooth Muscle Cell Motility." *Cellular Pharmacology* 98 (11): 1381–89. https://doi.org/10.1161/01.RES.0000225284.36490.a2.A.

Xu X., Shawn Z., Moebius F., Gill D.L., and Montell C. **2001**. "Regulation of Melastatin, a TRP-Related Protein, through Interaction with a Cytoplasmic Isoform." *Proceedings of the National Academy of Sciences of the United States of America* 98 (19): 10692–97. https://doi.org/10.1073/pnas.191360198.

Yallapu M.M., Khan S., Maher D.M., Ebeling M.C., Sundram V., Chauhan N., Ganju A., et al. **2014**. "Anti-Cancer Activity of Curcumin Loaded Nanoparticles in Prostate Cancer." *Biomaterials* 35 (30): 8635–48. https://doi.org/10.1016/j.biomaterials.2014.06.040.

Yamaguchi H., Yoshida S., Muroi E., Yoshida N., Kawamura M., Kouchi Z., Nakamura Y., Sakai R., and Fukami K. **2011**. "Phosphoinositide 3-Kinase Signaling Pathway Mediated by P110α Regulates Invadopodia Formation." *Journal of Cell Biology* 193 (7): 1275–88. https://doi.org/10.1083/jcb.201009126.

Yamamoto S., Egashira N., Tsuda M., and Masuda S. **2018**. "Riluzole Prevents Oxaliplatin-Induced Cold Allodynia via Inhibition of Overexpression of Transient Receptor Potential Melastatin 8 in Rats." *Journal of Pharmacological Sciences*. https://doi.org/10.1016/j.jphs.2018.10.006.

Yang D., and Kim J. **2020**. "Emerging Role of Transient Receptor Potential (TRP) Channels in Cancer Progression." *BMB Reports* 53 (3): 125–32.

Yang J.M., Li F., Liu Q., Rüedi M., Wei E.T., Lentsman M., Lee H.S., Choi W., Kim S.J., and Yoon K.C. **2017**. "A Novel TRPM8 Agonist Relieves Dry Eye Discomfort." *BMC Ophthalmology* 17 (1): 1–15. https://doi.org/10.1186/s12886-017-0495-2.

Yang J.M., Wei E.T., Kim S.J., and Yoon K.C. **2018**. "TRPM8 Channels and Dry Eye." *Pharmaceuticals* 11 (4): 1–7. https://doi.org/10.3390/ph11040125.

Yang J., Liu W., Lu X., Fu Y., Li L., and Luo Y. **2015**. "High Expression of Small GTPase Rab3D Promotes Cancer Progression and Metastasis." *Oncotarget* 6 (13): 11125–38.

Yang X., Shi C., Tong R., Qian W., Zhau H.E., Wang R., Zhu G., et al. **2010**. "Near IR Heptamethine Cyanine Dye-Mediated Cancer Imaging." *Clinical Cancer Research* 16 (10): 2833–44. https://doi.org/10.1158/1078-0432.CCR-10-0059.

Yang Z.H., Wang X.H., Wang H.P., and Hu L.Q. **2009**. "Effects of TRPM8 on the Proliferation and Motility of Prostate Cancer PC-3 Cells." *Asian Journal of Andrology* 11 (2): 157–65. https://doi.org/10.1038/aja.2009.1.

Yarwood S., Cullen P.J., and Kupzig S. **2006**. "The GAP1 Family of GTPase-Activating Proteins : Spatial and Temporal Regulators of Small GTPase Signalling." *Biochemical Society Transactions* 34 (5): 846–50.

Yee N.S., Kazi A.A., Li Q., Yang Z., Berg A., and Yee R.K. **2015**. "Aberrant Over-Expression of TRPM7 Ion Channels in Pancreatic Cancer:

Required for Cancer Cell Invasion and Implicated in Tumor Growth and Metastasis." *Biology Open* 4 (4): 507–14. https://doi.org/10.1242/bio.20137088.

Yelm K.E., Wos J.A., Bunke G.M., Frederick H., Haught J.C., Hoke S.H., and Sreekrishna K.T. **2017**. Synthesis of aryl cyclohexane carboxamide derivatives useful as sensates in consumer products. Patent. WO2017125634, issued 2017.

Yi X., Zhang J., Yan F., Lu Z., Huang J., Pan C., Yuan J., et al. **2016**. "Synthesis of IR-780 Dye-Conjugated Abiraterone for Prostate Cancer Imaging and Therapy." *International Journal of Oncology* 49 (5): 1911–20. https://doi.org/10.3892/IJO.2016.3693.

Yin Y., Le S.C., Hsu A.L., Borgnia M.J., Yang H., and Lee S.Y. **2019**. "Structural Basis of Cooling Agent and Lipid Sensing by the Cold-Activated TRPM8 Channel." *Science* 363 (6430): eaav9334. https://doi.org/10.1126/science.aav9334.

Yin Y., Wu M., Zubcevic L., Borschel W.F., Lander G.C., and Lee S.Y. **2018**. "Structure of the Cold- And Menthol-Sensing Ion Channel TRPM8." *Science* 359 (6372): 237–41. https://doi.org/10.1126/science.aan4325.

Yossepowitch O., Briganti A., Eastham J.A., Epstein J., Graefen M., Montironi R., and Touijer K. **2014**. "Positive Surgical Margins after Radical Prostatectomy: A Systematic Review and Contemporary Update." *European Urology* 65 (2): 303–13. https://doi.org/10.1016/J.EURURO.2013.07.039.

Yu L., Wang S., Kogure Y., Yamamoto S., Noguchi K., and Dai Y. **2013**. "Modulation of TRP Channels by Resveratrol and Other Stilbenoids." *Molecular Pain* 9 (1): 1. https://doi.org/10.1186/1744-8069-9-3.

Yu M.K., Park J., and Jon S. **2012**. "Targeting Strategies for Multifunctional Nanoparticles in Cancer Imaging and Therapy." *Theranostics* 2 (1): 3–44. https://doi.org/10.7150/thno.3463.

Yu Y., Sweeney M., Zhang S., Platoshyn O., Landsberg J., Rothman A., and Yuan J.X.J. **2003**. "PDGF Stimulates Pulmonary Vascular Smooth Muscle Cell Proliferation by Upregulating TRPC6 Expression." *American Journal of Physiology - Cell Physiology* 284 (2 53-2): 316–30. https://doi.org/10.1152/ajpcell.00125.2002.

Yudin Y., and Rohacs T. **2012**. "Regulation of TRPM8 Channel Activity." *Mol Cell Endocrinol.* 353 (1–2): 68–74. https://doi.org/10.1016/j.mce.2011.10.023.Regulation.

Yue D., Wang Y., Xiao J.Y., Wang P., and Ren C.S. **2009**. "Expression of TRPC6 in Benign and Malignant Human Prostate Tissues." *Asian Journal of Andrology* 11 (5): 541–47. https://doi.org/10.1038/aja.2009.53.

Zaak D., Sroka R., Höppner M., Khoder W., Reich O., Tritschler S., Muschter R., Knüchel R., and Hofstetter A. **2003**. "Photodynamic Therapy by Means of 5-ALA Induced PPIX in Human Prostate Cancer – Preliminary Results." *Medical Laser Application* 18 (1): 91–95. https://doi.org/10.1078/1615-1615-00092.

Zahra F.T., Sajib M.S., Ichiyama Y., Akwii R.G., Tullar P.E., Cobos C., Minchew S.A., et al. **2019**. "Endothelial RhoA GTPase Is Essential for in Vitro Endothelial Functions but Dispensable for Physiological in Vivo Angiogenesis." *Scientific Reports* 9 (1): 1–15. https://doi.org/10.1038/s41598-019-48053-z.

Zaorsky N.G., Davis B.J., Nguyen P.L., Showalter T.N., Hoskin P.J., Yoshioka Y., Morton G.C., and Horwitz E.M. **2017**. "The Evolution of Brachytherapy for Prostate Cancer." *Nature Reviews Urology* 14 (7): 415–39. https://doi.org/10.1038/nrurol.2017.76.

Zeng X., Sikka S.C., Huang L., Sun C., Xu C., Jia D., Abdel-Mageed A.B., Pottle J.E., Taylor J.T., and Li M. **2010**. "Novel Role for the Transient Receptor Potential Channel TRPM2 in Prostate Cancer Cell Proliferation." *Prostate Cancer and Prostatic Diseases* 13 (2): 195–201. https://doi.org/10.1038/pcan.2009.55.

Zeng Z., Inoue K., Sun H., Leng T., Feng X., Zhu L., and Xiong Z.G. **2015**. "TRPM7 Regulates Vascular Endothelial Cell Adhesion and Tube Formation." *American Journal of Physiology - Cell Physiology* 308 (4): C308–18. https://doi.org/10.1152/ajpcell.00275.2013.

Zeng Z., Leng T., Feng X., Sun H., Inoue K., Zhu L., and Xiong Z.G. **2015**. "Silencing TRPM7 in Mouse Cortical Astrocytes Impairs Cell Proliferation and Migration via ERK and JNK Signaling Pathways." *PLoS ONE* 10 (3): 1–19. https://doi.org/10.1371/journal.pone.0119912.

Zhang B., Zhang Y., Wang Z.X., and Zheng Y. **2000**. "The Role of Mg^{2+} Cofactor in the Guanine Nucleotide Exchange and GTP Hydrolysis Reactions of Rho Family GTP-Binding Proteins." *Journal of Biological Chemistry* 275 (33): 25299–307. https://doi.org/10.1074/jbc.M001027200.

Zhang C., Wang S., Xiao J., Tan X., Zhu Y., Su Y., Cheng T., and Shi C. **2010**. "Sentinel Lymph Node Mapping by a Near-Infrared Fluorescent Heptamethine Dye." *Biomaterials* 31 (7): 1911–17. https://doi.org/10.1016/j.biomaterials.2009.11.061.

Zhang D., Zhao Y.X., Qiao Z.Y., Mayerhöffer U., Spenst P., Li X.J., Würthner F., and Wang H. **2014**. "Nano-Confined Squaraine Dye Assemblies: New Photoacoustic and near-Infrared Fluorescence Dual-Modular Imaging Probes in Vivo." *Bioconjugate*

Chemistry 25 (11): 2021–29. https://doi.org/10.1021/bc5003983.

Zhang L., and Barritt G.J. **2004**. "Evidence That TRPM8 Is an Androgen-Dependent Ca2+ Channel Required for the Survival of Prostate Cancer Cells." *Cancer Research* 64 (22): 8365–73. https://doi.org/10.1158/0008-5472.CAN-04-2146.

Zhang S.S., Wen J., Yang F., Cai X.L., Yang H., Luo K.J., Liu Q.W., et al. **2013**. "High Expression of Transient Potential Receptor C6 Correlated with Poor Prognosis in Patients with Esophageal Squamous Cell Carcinoma." *Medical Oncology* 30 (3). https://doi.org/10.1007/s12032-013-0607-7.

Zhang X., Mak S., Li L., Parra A., Denlinger B., Belmonte C., and McNaughton P.A. **2012**. "Direct Inhibition of the Cold-Activated TRPM8 Ion Channel by Gαq." *Nature Cell Biology* 14 (8): 850–58. https://doi.org/10.1038/NCB2529.

Zhang Y-W., and Vande Woude G.F. **2003**. "HGF SF-met Signaling in the Control of Branching Morphogenesis and Invasion." *Journal of Cellular Biochemistry* 88: 408–17. https://doi.org/10.1002/jcb.10358.

Zhang Y., Qin W., Zhang L., Wu X., Du N., Hu Y., Li X, et al. **2015**. "MicroRNA-26a Prevents Endothelial Cell Apoptosis by Directly Targeting TRPC6 in the Setting of Atherosclerosis." *Scientific Reports* 5: 1–10. https://doi.org/10.1038/srep09401.

Zhao H., Grossman H.B., Spitz M.R., Lerner S.P., Zhang K., and Wu X. **2003**. "Plasma Levels of Insulin-like Growth Factor-1 and Binding Protein-3, and Their Association with Bladder Cancer Risk." *Journal of Urology* 169 (2): 714–17. https://doi.org/10.1097/01.ju.0000036380.10325.2a.

Zhao W., and Xu H. **2016**. "High Expression of TRPM8 Predicts Poor Prognosis in Patients with Osteosarcoma." *Oncology Letters* 12 (2): 1373–79. https://doi.org/10.3892/ol.2016.4764.

Zhiqi S., Soltani M.H., Bhat K.M.R., Sangha N., Fang D., Hunter J.J., and Setaluri V. **2004**. "Human Melastatin 1 (TRPM1) Is Regulated by MITF and Produces Multiple Polypeptide Isoforms in Melanocytes and Melanoma." *Melanoma Research* 14 (6): 509–16. https://doi.org/10.1097/00008390-200412000-00011.

Zholos A., Johnson C., Burdyga T., and Melanaphy D. **2011**. "TRPM Channels in the Vasculature." In *Transient Receptor Potential Channels. Advances in Experimental Medicine and Biology*, edited by M. Islam, 707–29. Springer, Dordrecht. https://doi.org/10.1007/978-94-007-0265-3_37.

Zhou K., Zhang S.S., Yan Y., and Zhao S. **2014**. "Overexpression of Transient Receptor Potential Vanilloid 2 Is Associated with Poor Prognosis in Patients with Esophageal Squamous Cell Carcinoma." *Medical Oncology* 31 (7). https://doi.org/10.1007/s12032-014-0017-5.

Zhu Z., Luo Z., Ma S., and Liu D. **2011**. "TRP Channels and Their Implications in Metabolic Diseases." *Pflugers Archiv European Journal of Physiology* 461 (2): 211–23. https://doi.org/10.1007/s00424-010-0902-5.

Zhuang L., Peng J.B., Tou L., Takanaga H., Adam R.M., Hediger M.A., and Freeman M.R. **2002**. "Calcium-Selective Ion Channel, CaT1, Is Apically Localized in Gastrointestinal Tract Epithelia and Is Aberrantly Expressed in Human Malignancies." *Laboratory Investigation* 82 (12): 1755–64. https://doi.org/10.1097/01.LAB.0000043910.41414.E7.

Zhuge Y., and Xu J. **2001**. "Rac1 Mediates Type I Collagen-Dependent MMP-2 Activation." *J Biol Chem* 276 (19): 16248–56. https://doi.org/10.10974/jbc.M01090200.

Ziglioli F., Frattini A., Maestroni U., Dinale F., Ciufifeda M., and Cortellini P. **2009**. "Vanilloid-Mediated Apoptosis in Prostate Cancer Cells through a TRPV-1 Dependent and a TRPV-1-Independent Mechanism." *Acta Biomed.* 80 (1): 13–20.

Zoppoli P., Calice G., Laurino S., Ruggieri V., La Rocca F., La Torre G., Ciuffi M., et al. **2019**. "TRPV2 Calcium Channel Gene Expression and Outcomes in Gastric Cancer Patients: A Clinically Relevant Association." *Journal of Clinical Medicine* 8 (5): 662. https://doi.org/10.3390/jcm8050662.

Zurborg S., Yurgionas B., Jira J.A., Caspani O., and Heppenstall P.A. **2007**. "Direct Activation of the Ion Channel TRPA1 by Ca^{2+}." *Nature Neuroscience* 10 (3): 277–79. https://doi.org/10.1038/nn1843.

Zygmunt P.M., and Hogestatt E.D. **2014**. "TRPA1." In *Mammalian Transient Receptor Potential (TRP) Cation Channels*, edited by B Nilius and V Flockerzi, 583–560. Springer Berlin Heidelberg.

2. PhD PROJECT

Context: biomedical challenges

The development of metastases is currently the leading cause of cancer death worldwide. Prostate cancer is no exception. Indeed, although the 5-year relative survival for PCa is 100% as long as it is diagnosed as localized, it drops dramatically to 32.3% for patients in whom it has metastasized, thus making prostate cancer the second deadliest cancer among men ("National Cancer Institute -Surveillance, Epidemiology, and End Result Program" 2022; Siegel et al. 2022). Hence the need for more sensitive diagnostic methods that allow early diagnosis of the neoplasm and new and innovative treatment methods that reduce the onset of relapses and the development of metastasis as well as allow even the most advanced metastatic forms to be effectively treated. For instance, in the conventional treatment of localized prostate tumors, radical prostatectomy may have severe side effects including incontinence and erectile dysfunction (Haglind et al. 2015), and androgen deprivation therapy (ADT) may lead to untreatable androgen-independent relapses. For patients with metastatic castration-resistant prostate cancer (mCRPC), no effective treatments are currently available and their median life expectancy is less than 3 years (Siegel et al. 2022). My Ph.D. project fits into the context of the need to develop new therapeutic strategies to more effectively fight prostate cancer.

Understanding the mechanisms by which tumor metastases can spread throughout the body is critical to improving the prognosis of mCRPC patients. Metastasis is generally defined as the spread of malignant cells from the primary tumor through the lymph or blood circulation to establish secondary growth in a distant organ. We know that the ability to migrate is a fundamental prerequisite for a cancer cell to effectively escape the primary tumor, invade adjacent tissues, and then enter circulation. At the same time, the migration of endothelial cells is also necessary to ensure the formation of new tumor vessels that allow the diffusion of oxygen and nutrients to the new tumor sites. Therefore, tissue invasion and angiogenesis, which are two of the main hallmarks of cancer, both underlie the migratory capacity of epithelial and endothelial cancer cells (Hanahan and Weinberg 2011). Ca^{2+} signaling is certainly implicated in tumor progression as well as in the regulation of angiogenesis due to its central and multifaceted role in the control of cell motility and proliferation (Monteith, Prevarskaya, and Roberts-Thomson 2017). Hence not surprisingly, in recent years, an ever-increasing interest has been directed to the study of ion channels and their implications in the development of cancer, so much so as to lead to the definition of cancer hallmarks as "oncochannelopathies" (Prevarskaya, Skryma, and Shuba 2018). Interestingly, many FDA-approved drugs targeting Ca^{2+} channels currently used to treat a variety of pathological conditions are being evaluated for cancer repurposing (Prevarskaya, Skryma, and Shuba 2018). Among the ion channels, the superfamily of TRP channels has attracted particular interest, revealing an appealing de-regulation during cancer development and progression (Nilius et al. 2007). This deregulation causes a significant alteration of the spatial and temporal

patterns of the intracellular distribution of Ca^{2+} and consequently interferes with multiple downstream effectors involved in the pathophysiology of cancer, which influence tumor growth, invasion, and vascularization (Prevarskaya, Skryma, and Shuba 2018). For this reason, several TRP proteins have been proposed as valuable markers in predicting the progress of cancers and potential targets for pharmaceutical treatment of many tumor forms including PCa (Tsavaler et al. 2001; Fuessel et al. 2003; Wissenbach, Niemeyer, and Flockerzi 2004; Yang and Kim 2020).

However, a big challenge in cancer therapy, beyond the discovery of new molecular targets, is represented by the ability to translate new research findings into clinical efficacy, that is to reduce the gap between "drug discovery" and "drug delivery". Indeed, the development of new innovative anticancer therapies is mainly hindered by the fact that therapeutic agents including TRP activators/inhibitors often suffer of poor solubility and stability in physiological conditions thus compromising their bioavailability and therapeutic action *in vivo*. This is, for example, the case of most photosensitizers proposed for the photodynamic treatment (PDT) of some types of tumors including PCa, which has recently emerged as a useful therapeutic approach to improve the outcome of conventional therapies and reduce the development of metastatic cancer stages. The translation of many drugs into clinical practice is also dramatically hampered by the risk of adverse effects associated with the non-specific distribution of therapeutic agents in healthy tissues. Both these challenges could be efficiently overcome by the use of nanodelivery systems, which can improve the solubility and the pharmacokinetic profile of lipophilic drugs as well as drive their delivery to the tumor, thus optimizing drug bioavailability and therapeutic action in the desired sites while limiting side effects.

Aims

In this context, the main **general objective** of my Ph.D. thesis was to explore the potential of TRP channels as innovative targets to treat metastatic PCa. More specifically, the first aim was to delineate the molecular mechanisms involving TRP in PCa progression. For this purpose, I investigated the role of TRP channels regulating Ca^{2+} signature in PCa cells and PCa vasculature focusing on the channels that affect cell migration, a common key step in tumor vascularization and invasion. Secondly, taking into account the challenges faced in clinical practice by many therapeutic agents, I focused on the development of new tools to improve drug delivery. In particular, I assessed the use of lipid nanoparticles to increase the solubility of a new class of polymethine dyes that are emerging as promising candidates for PDT applications as well as cancer imaging.

For greater clarity, the results of my Ph.D. project have been divided into two main chapters which will be briefly described below (1. Functional role of TRP channels in prostate cancer progression; 2. Lipid nanoparticles as drug delivery systems: incorporation of polymethine dyes) and will be matched in **Chapters 3** and **4**. The first chapter is about the functional characterization of TRP channels' roles in PCa progression (**Chapters 3.1** and **4.1**): it is divided into two different subsections referring respectively to the impact of TRP in PCa angiogenesis (**Chapters 3.1.1** and **4.1.1**) and PCa invasion (**Chapters 3.1.2** and **4.1.2**). The second chapter includes data on the development of lipid nanoparticles as drug delivery systems (**Chapters 3.2** and **4.2**). Below is a more detailed description of the specific aims of the thesis.

1. Functional role of TRP channels in prostate cancer progression

1.1 Role of TRPA1 in prostate cancer angiogenesis

During the first year of my Ph.D. I took part in a project already in progress on the role of TRP channels in prostate cancer angiogenesis contributing to a research article published on "*Cancers*" in July 2019 (Bernardini *et al*., "TRANSIENT RECEPTOR POTENTIAL CHANNEL EXPRESSION SIGNATURES IN TUMOR-DERIVED ENDOTHELIAL CELLS: FUNCTIONAL ROLES IN PROSTATE CANCER ANGIOGENESIS", *Cancers*, 2019 Jul 9; 7(11):956; doi: 10.3390/cancers11070956). In particular, through a qPCR screening of endothelial cells derived from human prostate cancer (PTEC), previously characterized in our laboratories (Fiorio Pla et al. 2014), four "prostate-associated" TRP genes were found significantly and specifically deregulated in PTEC (TRPA1, TRPV2, TRPC3, and TRPC6). My first aim was to validate this signature in PTEC both at the protein level and from a functional point of view. Then, looking at the functional role of the four 'prostate-associated' channels in PTEC, I mainly focused on the role of TRPA1 in controlling cell motility, thus deepening TRPA1 involvement in PCa angiogenesis (see **Chapter 3.1.1** and **Chapter 4.1.1**). In particular, I contributed to the aforementioned publication by performing cell cultures, Western Blot analyses, Ca^{2+} imaging experiments and Transwell migration assays (see Materials and Methods in **Chapter 4.1.1**).

1.2 Role of TRPM8 in prostate cancer invasion

Starting from the second year of my Ph.D. I focused on the role of TRP channels in prostate cancer invasion. More specifically, I deepened the intriguing role of TRPM8 previously established by our groups in regulating the motility of epithelial prostate cancer cells (Bidaux et al. 2007; Gkika et al. 2010; Gkika et al. 2015; Grolez et al. 2019; Grolez et al. 2019). Starting from the evidence of an inhibitory effect of TRPM8 on PCa cell migration, which has been the subject of the laboratory of Cell Physiology in Lille for several years, I investigated the mechanism through which TRPM8 may exert this function on PCa cells. In particular, I

focused on the possible interaction between TRPM8 and the small GTPase Rap1A, which plays a key role in controlling cell adhesion and motility and which we previously found to interact with TRPM8 in endothelial cells thus affecting cell migration (Genova et al. 2017). These results made up the bulk of my Ph.D. work and were recently published in an article I contributed to as first author (Chinigò *et al*., "TRPM8-RAP1A INTERACTION SITES AS CRITICAL DETERMINANTS FOR ADHESION AND MIGRATION OF PROSTATE AND OTHER EPITHELIAL CANCER CELLS", *Cancers*, 2022 April 30, 14(9):2261; doi: 10.3390/cancers14092261).

Finally, to further support TRPM8 as a promising candidate for blocking the progression of PCa to its lethal metastatic form, we evaluated the role of TRPM8 *in vivo* using an orthotopic xenograft mouse model. These data have been recently accepted for publication by the "*International Journal of Molecular Sciences*" and I participated in the publication as second author (Grolez *et al*., "TRPM8 AS AN ANTI-TUMORAL TARGET IN PROSTATE CANCER GROWTH AND METASTASIS DISSEMINATION" *International Journal of Molecular Sciences,* 2022 Jun 15, 23(12):6672; doi: 10.3390/ijms23126672).

Briefly, I contributed to this project by performing cell cultures, Western Blot analyses, plasmid cloning and cell transfection procedures, co-immunoprecipitation and active Rap1 pull-down assays, Live-cell and Ca^{2+} imaging experiments, random and transwell migration assays, adhesion assays, micro-fluidic co-coltures, cell viability tests and confocal analyses (see Materials and Methods in **Chapter 3.1.2**).

These two studies will be included in **Chapter 3.1.2** and discussed in **Chapter 3.1.2**.

2. Lipid nanoparticles as drug delivery systems: incorporation of polymethine dyes for Photodynamic Therapy.

During my Ph.D. I also took part in a project concerning another innovative therapeutic approach to target PCa in its early localized stage, i.e. photodynamic therapy (Osuchowski et al. 2021). This project has been conducted in collaboration with the Department of Organic Chemistry of the University of Turin which synthesized new organic dyes belonging to the family of polymethine dyes (PMD) which revealed a great potential as photosensitizers for PDT application (Serpe et al. 2016; Ciubini et al. 2019). In this context, I mainly focused on the characterization of nanodelivery systems suitable for improving the solubility and therefore the *in vivo* bioavailability of this new class of photosensitizers. In particular, I incorporated two PMD into solid lipid nanoparticles (SLN) and characterized them from a physicochemical as well as biological point of view. These data were recently published in an article of which I am the first author (Chinigò *et al*., "POLYMETHINE DYES-LOADED SOLID LIPID NANOPARTICLES (SLN) AS PROMISING PHOTOSENSITIZERS FOR BIOMEDICAL APPLICATIONS", *Spectrochimica Acta Part A: Mol Biomol Spectrosc.,* 2022 April 15, 271:120909; doi: 10.1016/j.saa.2022.120909*"*). I contributed to this publication by performing all the experiments, from

the synthesis and physico-chemical characterization of the nanosystems to cellular assays and confocal analysis (see Materials and Methods in **Chapter 3.2**). Furthermore, I actively contributed to a project on the incorporation of PMD into another type of lipid nanoparticles, namely quatsomes, conducted in collaboration with the Institut de Ciència de Materials of Barcelona (Bordignon *et al*., "QUATSOMES AS POWERFUL NANOVESICLES FOR PHOTODYNAMIC THERAPY", article in preparation). The results of the incorporation of PMD into lipid nanoparticles will be included in **Chapter 3.2** and discussed in **Chapter 4.2**.

Research project management

I performed my Ph.D. project in co-tutorship between the Laboratory of Cellular and Molecular Angiogenesis (DBIOS) of the University of Turin (Italy) under the supervision of Prof. Alessandra Fiorio Pla and the Laboratory of Cell Physiology (INSERM U1003) of the University of Lille (France) where I spent one year under the supervision of Prof. Dimitra Gkika (current affiliation: Laboratory of Cancer Heterogeneity, Plasticity, and Resistance to Therapies, Centre Oscar Lambret, University of Lille). The complementary background competencies of the two research units, allowed me to study in-depth the physiopathological roles of TRP channels affecting both PCa invasion and angiogenesis. Indeed, the Laboratory of Cell Physiology of the University of Lille headed by Natalia Prevarskaya boasts great expertise on TRP channels and Ca^{2+} signal in cancer with a particular focus on PCa and the identification of new prognostic and therapeutic agents which make it a Laboratory of Excellence in Ion Channels Science and Therapeutics. At the same time, the Laboratory of Cellular and Molecular Angiogenesis of the University of Turin headed by Luca Munaron, is specialized in tumor vascularization with a focus on Ca^{2+} signals regulating endothelial cells' physiopathology. Thanks to the solid collaboration between these two laboratories, which has been going on for several years, during my three-year traineeship as Ph.D. student I was able to contribute to the field of TRP channels in cancer with the publication of two reviews as first author and three research articles including one as first author.

Furthermore, at the University of Turin, I had the opportunity to carry out a research project started during my Master's Degree in collaboration with the Department of Organic Chemistry of the University of Turin. In particular, the project on PDT was conducted in collaboration with Prof. Claudia Barolo, Nadia Barbero (Department of Organic Chemistry), and Prof. Sonjia Visentin (Department of Molecular Biotechnology and Health Sciences). Finally, the development of lipid nanosystems for drug delivery involved collaborations with the Institut de Ciència de Materials of Barcelona and the Turin company Nanovector Srl specialized in drug

delivery. This side research project led to the publication of a research article of which I am the first author and the writing of three other manuscripts currently in preparation.

References

Bidaux G., Flourakis M., Thebault S., Zholos A., Beck B., Gkika D., Roudbaraki M., et al. **2007**. "Prostate Cell Differentiation Status Determines Transient Receptor Potential Melastatin Member 8 Channel Subcellular Localization and Function." *Journal of Clinical Investigation* 117 (6): 1647–57. https://doi.org/10.1172/JCI30168.

Ciubini B., Visentin S., Serpe L., Canaparo R., Fin A., and Barbero N. **2019**. "Design and Synthesis of Symmetrical Pentamethine Cyanine Dyes as NIR Photosensitizers for PDT." *Dyes and Pigments* 160: 806–13. https://doi.org/10.1016/j.dyepig.2018.09.009.

Fiorio Pla A., Brossa A., Bernardini M., Genova T., Grolez G., Villers A., Leroy X., Prevarskaya N., Gkika D., and Bussolati B. **2014**. "Differential Sensitivity of Prostate Tumor Derived Endothelial Cells to Sorafenib and Sunitinib." *BMC Cancer* 14 (January). https://doi.org/10.1186/1471-2407-14-939.

Fuessel S., Sickert D., Meye A., Klenk U., Schmidt U., Schmitz M., Rost A-K, Weigle B., Kiessling A., and Wirth M.P. **2003**. "Multiple Tumor Marker Analyses (PSA, HK2, PSCA, Trp-P8) in Primary Prostate Cancers Using Quantitative RT-PCR." *Int J Oncol* 23 (1): 221–28.

Genova T., Grolez G.P., Camillo C., Bernardini M,, Bokhobza A., Richard E., Scianna M., et al. **2017**. "TRPM8 Inhibits Endothelial Cell Migration via a Nonchannel Function by Trapping the Small GTPase Rap1." *Journal of Cell Biology* 216 (7): 2107–30. https://doi.org/10.1083/jcb.201506024.

Gkika D., Flourakis M., Lemonnier L., and Prevarskaya N. **2010**. "PSA Reduces Prostate Cancer Cell Motility by Stimulating TRPM8 Activity and Plasma Membrane Expression." *Oncogene* 29 (32): 4611–16. https://doi.org/10.1038/onc.2010.210.

Gkika D., Lemonnier L., Shapovalov G., Gordienko D., Poux C., Bernardini M., Bokhobza A., et al. **2015**. "TRP Channel-Associated Factors Are a Novel Protein Family That Regulates TRPM8 Trafficking and Activity." *Journal of Cell Biology* 208 (1): 89–107. https://doi.org/10.1083/jcb.201402076.

Grolez G.P., Hammadi M., Barras A., Gordienko D., Slomianny C., Völkel P., Angrand P.O., et al. **2019**. "Encapsulation of a TRPM8 Agonist, WS12, in Lipid Nanocapsules Potentiates PC3 Prostate Cancer Cell Migration Inhibition through Channel Activation." *Scientific Reports* 9 (1): 7926. https://doi.org/10.1038/s41598-019-44452-4.

Grolez G.P., Gordiendko D., Clarisse M., Hammadi M., Desruelles E., Fromont G., Prevarskaya N., Slomianny C., and Gkika D. **2019**. "TRPM8-Androgen Receptor Association within Lipid Rafts Promotes Prostate Cancer Cell Migration." *Cell Death & Disease* 10 (9): 652. https://doi.org/10.1038/s41419-019-1891-8.

Haglind E., Carlsson S., Stranne J., Wallerstedt A., Wilderäng U., Thorsteinsdottir T., Lagerkvist M., et al. **2015**. "Urinary Incontinence and Erectile Dysfunction after Robotic Versus Open Radical Prostatectomy: A Prospective, Controlled, Nonrandomised Trial." *European Urology* 68 (2): 216–25. https://doi.org/10.1016/j.eururo.2015.02.029.

Hanahan D., and Weinberg R.A. **2011**. "Review Hallmarks of Cancer : The Next Generation." *Cell* 144 (5): 646–74. https://doi.org/10.1016/j.cell.2011.02.013.

Monteith G.R., Prevarskaya N., and Thomson S.J.R. **2017**. "The Calcium–Cancer Signalling Nexus." *Nature Reviews Cancer* 17 (6): 367–80. https://doi.org/10.1038/nrc.2017.18.

"National Cancer Institute -Surveillance, Epidemiology, and End Result Program." **2022**. seer.cancer.gov.

Nilius B., Owsianik G., Voets T., and Peters J.A. **2007**. *Transient Receptor Potential Cation Channels in Disease*. *Physiological Reviews*. Vol. 87. https://doi.org/10.1152/physrev.00021.2006.

Osuchowski M., Bartusik-Aebisher D., Osuchowski F., and Aebisher D. **2021**. "Photodynamic Therapy for Prostate Cancer – A Narrative Review." *Photodiagnosis and Photodynamic Therapy* 33. https://doi.org/10.1016/j.pdpdt.2020.102158.

Prevarskaya N., Skryma R., and Shuba Y. **2018**. "Ion Channels in Cancer: Are Cancer Hallmarks Oncochannelopathies?" *Physiological Reviews* 98 (2): 559–621. https://doi.org/10.1152/physrev.00044.2016.

Serpe L., Ellena S., Barbero N., Foglietta F., Prandini F., Gallo M.P., Levi R., Barolo C., Canaparo R., and Visentin S. **2016**. "Squaraines Bearing Halogenated Moieties as Anticancer Photosensitizers: Synthesis, Characterization and Biological Evaluation." *European Journal of Medicinal Chemistry* 113: 187–97. https://doi.org/10.1016/j.ejmech.2016.02.035.

Siegel R.L., Miller K.D., Fuchs H.E., and Jemal A. **2022**. "Cancer Statistics, 2022." *CA: A Cancer Journal for Clinicians* 72 (1): 7–33. https://doi.org/10.3322/caac.21708.

Tsavaler L., Shapero M.H., Morkowski S., and Laus R. **2001**. "Trp-P8, a Novel Prostate-Specific Gene, Is up-Regulated in Prostate Cancer and Other Malignancies and Shares High Homology with Transient Receptor Potential Calcium Channel Proteins." *Cancer Research* 61 (9): 3760–69.

Wissenbach U., Niemeyer B.A., and Flockerzi V. **2004**. "TRP Channels as Potential Drug Targets." *Biology of the Cell* 96 (1): 47–54. https://doi.org/10.1146/annurev-pharmtox-010617-052832.

Yang D., and Kim J. **2020**. "Emerging Role of Transient Receptor Potential (TRP) Channels in Cancer Progression." *BMB Reports* 53 (3): 125–32.

3. RESULTS

3.1.1 Role of TRPA1 in prostate cancer angiogenesis

"Transient Receptor Potential Channel Expression Signatures in Tumor-Derived Endothelial Cells: Functional Roles in Prostate Cancer Angiogenesis"

Michela Bernardini[1,2,3], Alessia Brossa[4], **Giorgia Chinigò**[1,2,3], Guillaume P. Grolez[1,2], Giulia Trimaglio[1,3], Laurent Allart[1,2], Audrey Hulot[5], Guillemette Marot[5,6], Tullio Genova[3], Aditi Joshi[3], Virginie Mattot[7], Gaelle Fromont-Hankard[8], Luca Munaron[3], Benedetta Bussolati[4], Natalia Prevarskaya[1,2], Alessandra Fiorio Pla[1,2,3,†] and Dimitra Gkika[1,2,*,†]

[1] Department, Univ. Lille, Inserm, U1003-PHYCEL-Physiologie Cellulaire, F-59000 Lille, France

[2] Laboratory of Excellence, Ion Channels Science and Therapeutics, Université de Lille, F-59655 Villeneuve d'Ascq, France

[3] Department of Life Science and Systems Biology, University of Torino, postal code Turin, Italy

[4] Department of Molecular Biotechnology and Health Sciences, Molecular Biotechnology Centre, University of Torino, 10126 Turin, Italy

[5] Department, Université de Lille, bilille, F-59000 Lille, France

[6] Department, Université de Lille, Inria, EA 2694, MODAL, F-59000 Lille, France

[7] Institut Pasteur de Lille, Univ. Lille, CNRS, UMR 8161, F-59000 Lille, France

[8] Inserm UMR 1069, Université de Tours, postal code Tours, France

* Correspondence: dimitra.gkika@univ-lille.fr

† These authors contributed equally to this paper.

Bernardini *et al.*, *Cancers.* 2019, 7(11):956

Abstract

Background: Transient receptor potential (TRP) channels control multiple processes involved in cancer progression by modulating cell proliferation, survival, invasion and intravasation, as well as, endothelial cell (EC) biology and tumor angiogenesis. Nonetheless, a complete TRP expression signature in tumor vessels, including in prostate cancer (PCa), is still lacking. Methods: In the present study, we profiled by qPCR the expression of all TRP channels in human prostate tumor-derived ECs (TECs) in comparison with TECs from breast and renal tumors. We further functionally characterized the role of the 'prostate-associated' channels in proliferation, sprout formation and elongation, directed motility guiding, as well as in vitro and in vivo morphogenesis and angiogenesis. Results: We identified three 'prostate-associated' genes whose expression is upregulated in prostate TECs: TRPV2 as a positive modulator of TEC proliferation, TRPC3 as an endothelial PCa cell attraction factor and TRPA1 as a critical TEC angiogenic factor in vitro and in vivo. Conclusions: We provide here the full TRP signature of PCa vascularization among which three play a profound effect on EC biology. These results contribute to explain the aggressive phenotype previously observed in PTEC and provide new putative therapeutic targets.

Keywords: tumor angiogenesis; calcium channel; migration; TRP; prostate cancer

Introduction

Transient receptor potential (TRP) channels form a 28-member superfamily of nonselective channels mostly permeable to both monovalent and divalent cations, which is subgrouped into six main families, namely, TRPC (canonical), TRPV (vanilloid), TRPM (melastatin), TRPP (polycystin), TRPML (mucolipin), and TRPA (ankyrin). Despite their structural similarities, TRP channels are polymodal molecular sensors and are activated by a range of external stimuli (including temperature, light, sound, chemicals, and touch) and changes in local microenvironment [1]. These observations suggest that the physiologically relevant stimulus for any given TRP is governed by the specific cellular context, which dramatically changes during carcinogenesis [2].

Indeed, TRP-activated signaling pathways have profound effects on a variety of physiological and pathological processes, including cancer [3,4]. Accumulating evidence demonstrates that the development of some cancers involves ion channels, thereby classifying these diseases as a special type of '*channelopathy*', called *'oncochannelopathy'* [2,4,5]. Several studies have demonstrated that TRP channels control multiple

aspects of cancer progression at all stages and modulate Ca^{2+}-regulated pathways such as cell proliferation and survival, migration and angiogenesis [2,6]. It is therefore not surprising that the expression of some TRP channels is altered during tumor growth and metastasis, and consequently a TRP expression signature could characterize the phenotype of a tumor, including prostate cancer (PCa) [7]. Several studies have identified and proposed TRP channels as new prognostic and therapeutic targets for PCa [8–12]. In particular, we proposed that at least five TRP members (namely, TRPM8, TRPV6, TRPC6, TRPV2 and TRPA1) could be of particular interest in PCa therapy since their expression and function define and modulate specific stages of PCa progression (for a review see [5]).

Nevertheless, little is known about the role of TRP channels in PCa angiogenesis, even though the crucial role of vascularization in tumor growth, invasion into surrounding tissues and metastasis is well studied. Indeed, as for other cancers, tumor angiogenesis is a well-recognized hallmark of aggressive PCa progression [13]. Immunohistochemical staining on normal and tumor tissues from the prostate showed that the endothelial cell (EC) population is enriched in PCa tissues compared to that in normal tissues, whereas the EC population decreases upon castration and gradually recovers with time [14]. A growing number of studies implicate TRP channels in EC biology, as well as in tumor angiogenesis. Several members of the TRP superfamily (i.e., TRPC1, TRPC4, TRPC6, TRPM7, TRPV1, TRPV4 and TRPM8) appear to be heterogeneously expressed in different EC types and have a key role during multiple functions in ECs, including cell proliferation, survival, motility and tubulogenesis in vitro [15–17]. However, until now, most available data focus on the function of a single channel rather a global view of the regulation of all TRP channels in PCa development and angiogenesis [16].

The definition of a specific expression pattern is of particular interest, as it is now evident that specific stages of cancer progression, such as angiogenesis, are not caused by mutations in the *trp* genes but rather by altered expression of the wild-type protein [4]. Indeed, the aim of this study is to profile the expression of TRP channels during PCa angiogenesis and to identify the specific molecular modulators of this process, thereby identifying novel therapeutic targets. We have therefore analyzed the complete expression profile of all *trp* channels in prostate tumor-derived ECs (TEC). To verify the PCa specificity of the molecular candidates identified, we also profiled *trp* expression signatures in ECs derived from breast and renal tumors. We identified four '*prostate-associated*' genes whose expression is significantly and specifically deregulated in prostate TECs relative to normal ECs. Most importantly, we functionally characterized the role of the '*prostate-associated*' *trp* channels (i.e., *trpa1*, *trpv2*, and *trpc3*) upregulated in TECs in the modulation of key biological processes occurring during angiogenesis, such as EC proliferation, motility, regulation of tubulogenesis *in vitro* and angiogenic sprouting *in vivo*.

Materials and Methods

Chemicals and Drugs

Naltriben methanesulfonate hydrate (NTB), was resuspended in DMSO to a final concentration of 25 mM and stored at −20°C, according to the manufacturer's instructions. Allyl isothiocyanate (AITC) was diluted in DMSO to a final concentration of 10 mM and stored at −20 °C, according to the manufacturer's instructions. L-α-Lysophosphatidylcholine from soybean (LPC) was diluted in ethanol to a final concentration of 20 mM and stored at −20 °C, according to the manufacturer's instructions. 1-Oleoyl-2-acetyl-sn-glycerol (OAG) was diluted in DMSO to a final concentration of 100 mM and stored at −20 °C, according to the manufacturer's instructions. All drugs were purchased from Sigma-Aldrich (St Louis, MO, USA). Fura2-AM calcium probe used in calcium imaging experiments was purchased from (Invitrogen Ltd., Waltham, MA, USA) and dissolved in DMSO to a final concentration of 1 mM and stored at −20 °C.

Cell Cultures and Transfection

Normal glomerular ECs (GEC), breast tumor ECs (BTEC), renal tumor ECs (RTEC) were isolated and characterized as described by Bussolati et al. [19,20,45]. Prostate tumor ECs (PTEC) primary cultures were isolated and characterized as previously described [18]. Normal human prostatic microvascular ECs (HPrMEC) were purchased from ScienCell Research Laboratories (Carlsbad, CA, USA). HMECs were obtained from the derma using an anti-CD31 antibody and MACS. HMECs from the derma were immortalized by the infection of primary cultures with a replication-defective adeno-5/SV40 virus as previously described [46,47]. All endothelial cells were cultured in EndoGRO MV-VEGF medium (Merck Millipore, Darmstadt, Germany) containing 5% fetal bovine serum (FBS). All cell cultures were maintained in incubator (37 °C and 5% CO_2 atmosphere), using Falcon™ plates as supports (about 5000 cells/cm^2) and were used at passage 3 to 12 (for HMEC, GEC, BTEC, and RTEC) or at passage 1 to 5 (for HPrMEC and PTEC). TECs (BTEC, RTEC and PTEC) were cultured on coating of 1% gelatin. When specified, experiments were performed using DMEM, Dulbecco's modified eagle medium (Sigma-Aldrich), with 4500 mg/L glucose, 15 mM HEPES and sodium bicarbonate. DMEM was supplemented with 2% L-glutamine, 0.5% gentamicin, and 0, 2, or 10% FBS. HMEC cells were transfected with NucleofectorTM (Amaxa, Gaithersburg, MD, USA) for Human Primary Endothelial Cells with 2 µg of each construct: human pcDNA3TRPA1 [43], human pcDNA3TRPV2 [11], human pcDNA3.1TRPC3 (Addgene, Watertown, MA 02472, USA plasmid #25902), human pcDNA3TRPC6 (already present in our laboratory), mouse pcDNA3.1TRPM7 (kind gift from Prof. Thomas Guderman). Control experiments were performed by transfecting the empty vector. For siRNA-mediated silencing, PTEC were plated in six-well dishes at a concentration of 6×10^4 cells per well (3 wells/condition) the day before oligofection. Oligofection (Oligofectamine, Thermo Fisher Scientific, Waltham, MA, USA) of siRNA duplexes was performed according

to manufacturer's protocol. Briefly, PTEC were transfected twice (at 0 and 24 h) with 200 pmol siLuc (control, siCNTRL), siTRPA1 or siTRPV2. siRNA against Luciferase (siLuc; Eurogentec, Seraing, Belgium) was used for control silencing. 24 or 48 h after the second oligofection, PTEC were lysed or tested in functional assays. The siTRPA1 sequence is 5'-GGUGGGAUGUUAUUCCAUA(dTdT)-3' [43], and the siTRPV2 sequence is 5'-UAAGAGUCAACCUCAACUAdTdT (dTdT)-3' [32].

Generation of Immortalized PTEC

Primary prostate-derived TEC (PTEC) were infected (at passage 2) with a retrovirus containing a pBABE-puro-hTERT plasmid (Addgene plasmid #1771) [48] and selected using the antibiotic resistance (1 µg/mL puromycin, Gibco, Thermo Fisher Scientific, Waltham, MA, USA) for two weeks. hTERT mRNA was always upregulated in hTERT PTEC as compared with wild type PTEC, as shown in Figure S4c.

Flow Cytometry

hTERT PTEC were detached from plates with a non-enzymatic cell dissociation solution (Sigma-Aldrich), washed and stained (30 min at 4 °C) with the following fluorescein isothiocyanate (FITC)-, phycoerythrin (PE)-, or allophycocyanin (APC)-conjugated antibodies: CD31 (BD Bioscience, Franklin Lakes, NJ, USA), CD105 (from MiltenyiBiotec, Bergisch Gladbach, Germany), VEGFR1 (R&D Systems, Minneapolis, MN, USA). Isotypes (all from MiltenyiBiotec, Bergisch Gladbach, Germany) were used as negative controls. Cells were subjected to cytofluorimetric analysis (FACScan Becton Dickinson, Franklin Lakes, NJ, USA) every other passage.

In Vivo Angiogenesis

Wild type outbred OF1 mice were purchased from Charles River (Wilmington, MA, USA). Sub-retinal injections were performed in three-day-old anesthetized mice by injecting 0.5 µL DMSO (control), 500 µM AITC or 500 µM HC030031. Six-day-old mice were sacrificed by decapitation according to the CNRS recommendation and eyes were enucleated. Retinal cups were dissected under binoculars and briefly fixated using 4% PFA in PBS before whole mount immunostaining. Flat mount retinas were incubated overnight at 4 °C with the rabbit anti-mouse type IV collagen (ab6586, 1 mg/mL, 1:500, Abcam, Cambridge, UK). After washes, retinas were then incubated with the fluorescent secondary antibody donkey anti-rabbit A594 (Invitrogen, 2 mg/mL, 1:500). Retinas were finally washed and mounted in Mowiol before imaging with an AxioImager Z1-Apotome (Carl Zeiss, Marly le Roi, France). All pups derived from a litter were used in one experiment. Experiments were performed two times with six retinas per treatment. The distances between the established retina vascular plexus and the extended vascular sprouts were measured for each condition. VM was authorized to perform experimentation on animals (#59-35066) and experimental procedure has been

deposited to Ministère de l'enseignement supérieur et de la Recherche (French government research department), as per regulations.

Isolation of CD31 Positive Cells from Retinas

Retinas were harvested from six-day-old mouse pups previously sacrificed by decapitation. Retinas were digested with type I collagenase (2 mg/mL, Life Technologies) and DNAse I (10 µg/mL, Roche Life Science, New York, NY, USA) in DMEM for 40'. Cell suspensions were then incubated with 25 µL magnetic beads (Dynabeads Sheep anti-Rat IgG, Life Technologies) previously coated with 1.5 µg anti-CD31 antibody (rat anti-mouse CD31, Becton Dickinson). CD31+ cells were isolated following manufacturer's instructions. Isolated cells were centrifuged and suspended in Trizol for total RNA isolation and RT-qPCR analysis.

Patients and Tissues

Formalin-fixed paraffin-embedded tissue samples containing both normal and tumor areas were obtained from 10 patients treated by radical prostatectomy for prostate cancer. Patients were aged 62 to 70 years old, with PCa classified as ISUP group 2 in 6 cases and group 3 in 4 cases. Serial 3 µm sections of the paraffin blocks were used for immunohistochemistry. Written informed consents were obtained from patients in accordance with the requirements of the medical ethic committee, Comité de Protection des Personnes of Tours Universitary Hospital of the 18th of February (DC-2014-2045).

Immunohistochemistry

Slides were deparaffinized, rehydrated, and heated in citrate buffer pH 6 for antigenic retrieval. After blocking for endogenous peroxidase with 3% hydrogen peroxide, the following antibodies were incubated: TRPA1 (#ACC-037 1:500, 1 h, Alomone Labs, Jerusalem, Israel), TRPV2 (SAB1101376 Sigma, 1:1000, 1 h), TRPC3 (#ACC-016 Alomone, 1:500, 1 h), TRPC6 (#ACC-017 Alomone, 1:300, 1 h). Immunohistochemistry was performed using the streptavidin-biotin-peroxidase method with diaminobenzidine as the chromogen (Kit LSAB, Dakocytomotion, Glostrup, Denmark). Slides were finally counterstained with haematoxylin. Negative controls were obtained after omission of the primary antibody or incubation with an irrelevant antibody. For cryo-sections, retinas were fixed overnight with 4% PFA, rinsed in PBS and then incubated with 30% sucrose before OCT embedding. Retina sections were blocked and permeabilized in PBS 0.25% triton, 5% FBS, 1% BSA for 2 h and incubated overnight at 4 °C with the rabbit anti-TRPA1 antibody (#ACC-037 Alomone, 1:100) and the rat anti-CD31 (Becton Dickinson, 1/100). After washes, sections were incubated with secondary antibody donkey anti-rabbit A488 and donkey anti-Rat A594 for 2 h at room temperature. Sections were then washed and stained with DAPI before mounting in Mowiol. Sections were imaged with a Carl Zeiss AxioImager Z1-Apotome.

Total RNA Extraction and Reverse Transcription

Total RNAs were extracted from cultured cells by Nucleospin RNA II kit (Clontech Laboratories, Mountain View, CA, USA) according to manufacturer's protocol, and subjected to reverse transcription as previously described [49].

Quantitative Real-Time PCR

Real-time qPCR of cDNA was done using qPCR SsoFast™ EvaGreen® Supermix (Bio-Rad, Hercules, CA, USA) on the CFX96 Real-Time PCR Detection System (Bio-Rad). The primers for *trp* channels were designed on the functional region of the channels using Primer3 software (PREMIER Biosoft, Palo Alto, CA, USA) and efficiency was validated on *trp*-coding plasmids and cell lines expressing the channels (Table 1).

TRP Channel		PCR Product Length (nt)
Gene	**NCBI Reference Sequence**	
trpv1	NM_080704.3	101
trpv2	NM_016113.4	94
trpv3	NM_001258205.1	118
trpv4	NM_021625.4	99
trpv5	NM_019841.6	114
trpv6	NM_018646.5	118
trpc1	NM_001251845.1	118
trpc3	NM_001130698.1	112
trpc4	NM_016179.2	90
trpc5	NM_012471.2	111
trpc6	NM_004621.5	95
trpc7	NM_020389.2	110
trpm1	NM_001252020.1	91
trpm2	NM_003307.3	100
trpm3	NM_020952.4	113
trpm4	NM_017636.3	93
trpm5	NM_014555.3	117
trpm6	NM_017662.4	117
trpm7	NM_017672.5	109
trpm8	NM_024080.4	113
trpa1	NM_007332.2	95
trpp2-pkd2	NM_000297.3	110

trpp3-pkd2l1	NM_016112.2	110
trpml1-mcoln1	NM_020533.2	117
trpml2-mcoln2	NM_153259.3	91
trpml3-mcoln3	NM_018298.10	96

Table 1. *Primers for trp channels were designed on the functional region of the channels. Primer3 was used to select the best primer couple for each gene. Primer couples were chosen in order to detect all functional variants described in NCBI.*

The sequences for the *actin* and *hprt* primers are: 5'-CAGCTTCCGGGAAACCAAAGTC-3' and 5'-AATTAAGCCGCAGGCTCCACTC-3' for *18s*; 5'-GGCGTCGTGATTAGTGATGAT-3' and 5'-CGAGCAAGACGTTCAGTCCT-3' for *hprt.* For the qPCR on cDNA from mice retina the following primers were used: 5'- GCAGGTGGAACTTCATACCAACT-3' and 5'-CACTTTGCGTAAGTA CCAGAGTGG-3' for *trpa1*; 5'-CTGCAGGCATCGGCAAA-3' and 5'-GCATTTCGCACACCTGGAT-3' for *CD31*; 5'-GCCATGGATGACGATATCGCTG-3' and 5'-GCCATGGATGACGATATCGCTG-3' for *actin*. *18s* and *hprt* (hypoxanthine-guanine phosphoribosyltransferase) were used as internal controls to normalize variations in RNA extraction and RT efficiency. In order to quantify relative gene expression (Figure 1d, Figure S1a,c,d), the delta-delta Cycle threshold (□□C_T) method was used, calculating the difference between the normalized expression values of tumor and normal samples: $2^{-\Delta\Delta C_T}$, where $\Delta\Delta\mathrm{Ct} = (\Delta\mathrm{C}_{\mathrm{T}\ target\ gene,\mathrm{tumor}} - \Delta\mathrm{C}_{T\ ref\ gene,\mathrm{tumor}}) - (\mathrm{mean}\ \Delta\mathrm{C}_{\mathrm{T}\ target\ gene,\mathrm{normal}} - \mathrm{mean}\ \Delta\mathrm{C}_{\mathrm{T}\ ref\ gene,\mathrm{normal}})$. In dispersion graphics (Figure 1e), values are expressed as mean $Log_{10}\ (\frac{C_{T,target\ gene}}{C_{T,18s}})$ of at least three independent experiments. All screened ECs did not show differences in the expression of the two internal controls used for the screening, *18s* and *hprt* (Figure S1a), showing that there were no significant variations in the amount of input cDNA that could interfere with the differential profiling. Prior to the definition of the TEC differential profile, we had to assess the correct healthy counterpart to be used for PTEC. We therefore plotted the mRNA expression of two normal EC cell lines, namely dermal HMEC and prostatic HPrMEC, of the different *trp* channels (expressed as the Logarithm of the corrected qPCR threshold cycle (C_T) values). As shown in Figure S1b, the values are very poorly correlated: most of the values of HMEC are stable in contrast to the values of HPrMEC, showing the necessity of a prostate specific EC model as healthy counterpart for our studies. In light of these results, we decided to use HPrMEC as the healthy counterpart of PTEC.

Western Blot

Conditions for SDS–PAGE and western blotting were as previously described [8]. Polyvinylidene fluoride membranes were properly blocked in 5% bovin sieric albumin (BSA) in TNT buffer (0.1 M Tris-Cl pH 7.5, 150 mM NaCl, 0.1% Tween-20) for 30 s and then incubated over night with anti-TRPA1 (#ACC-037, Alomone, 1:200), anti-TRPC3 (#ACC-016, Alomone, 1:500), anti-TRPC6 (#ACC-017, Alomone, 1:200), or anti-TRPV2

(SAB1101376, Sigma, 1:500), anti-β-actin (A5316, Sigma, 1:1000) primary antibodies, following manufacturer's instructions. The membrane was then washed using TNT containing 0.1% Tween 20 and incubated with the appropriate HRP-conjugated secondary antibodies (SantaCruz, Dallas, TX, USA). Membranes were treated with either Femto or Dura enhanced chemiluminescence (ECL) reagents (ThermoFisher, Thermo Fisher Scientific, Waltham, MA, USA) for 1 or 5 minutes respectively, and exposed by Amersham Imager 600 (GE Healthcare, Little Chalfont, UK). To quantify the differences in protein expression, the ratio between TRP channels and actin expression was evaluated using Fiji, ImageJ software (https://imagej.net/Fiji).

Calcium Imaging

Cells were seeded on gelatin-coated glass coverslips at a density of 5000 cells/cm^2 at 24 h before the experiments. Cells were starved in DMEM 5% FBS for at least 2 h before the experiments. Cells were next loaded (45 s at 37 °C) with 2 µM Fura-2 AM, for ratiometric cytosolic calcium concentration ($[Ca^{2+}]_i$) measurements. During experiments, cells were maintained in standard extracellular solution of the following composition: 154 mM NaCl, 4 mM KCl, 2 mM $CaCl_2$, 1 mM $MgCl_2$, 5 mM HEPES, 5.5 mM glucose. Solution pH was adjusted to 7.35 using NaOH. 4 h before experiments cells were starved in DMEM 2% FBS. Fluorescence measurements were made using a Polychrome V spectrofluorimeter (TILL Photonics, Munich, Germany) attached to an Olympus ×51 microscope (Olympus, Tokyo, Japan) and Metafluor Imaging System (Molecular Devices, Sunnyvale, CA, USA). $[Ca^{2+}]_i$ was measured using ratiometric probe Fura-2-AM and quantified according to Fiorio Pla et al. [50].

Cell Viability and Proliferation Assay

Cells were transfected by NucleofectorTM (Amaxa, Gaithersburg, MA, USA) with 2 µg of each construct and plated (1600 cells/well) on 96-well plates in EndoGRO MV-VEGF medium. 20 h after transfection, cells were starved in DMEM containing 2% FBS for 4 h. After starvation, EndoGRO MV-VEGF and DMEM 2% FBS with or without agents to be tested were added (12 wells/condition) to cutured cells. EndoGRO MV-VEGF was used as positive control, whereas 2% FBS served as negative control. 24, 48 and 72 h after treatments, cells were washed with PBS and colored using the CellTiter 96 AQueous Non-Radioactive cell proliferation assay (Promega, Madison, WI, USA). Assays were performed by adding 40 µL of MTS-containing solution to each culture well and absorbance was recorded at 495 nm in a microplate reader (Dinnex Technologies MR422, Thermo Labsystems, Philadelphia, PA,USA) after 2 and 4 h of incubation.

For siRNA-mediated silencing on hTERT PTEC, Oligofection (Oligofectamine, Life Science) of siRNA duplexes was performed twice (at 0 and 24 h) with 200 pmol siLuc (control, siCNTRL) or siTRPV2 (see also "Cell cultures and transfection" section). 6 h after the second pulse hTERT PTEC were plated (2500 cells/well)

on 96-well plates in EndoGRO MV-VEGF medium. Proliferation was evaluated using Cell Proliferation ELISA, BrdU (colorimetric, Roche) following manufacturer instruction. Briefly, 48 h after the first pulse, cells were labelled with BrDU 10 µL/well overnight. ELISA assay was performed by adding Add 100 µL/ well anti-BrdU-POD working solution for 90 minutes and subsequently adding 100 µL/well Substrate solution until color development is sufficient for photometric detection (5–30 min). Absorbance was measureed the absorbance of the samples in the microplate reader at 370 nm (reference wavelength: approx. 492 nm).

Scratch-Wound Healing Assay

Cells were transfected by NucleofectorTM with 2 µg of each construct, as previously described, and plated (10×10^4 cells/well) using EndoGRO MV-VEGF on 24-well culture plates coated with 1% gelatin. 20 h after transfection, cell monolayers were starved for 4 h in DMEM 0% FBS. Motility assay was performed by generating a wound in the confluent cellular monolayers by means of a P10-pipette tip. Floating cells were removed by two washes in PBS solution, and monolayers were treated with test conditions (in duplicate). Complete EndoGRO 5% FBS was used as positive control, whereas DMEM 0% FBS served as negative control. Experiments were performed using a Nikon Eclipse Ti (Nikon Corporation, Tokyo, Japan) inverted microscope equipped with a A.S.I. MS-2000 stage and a OkoLab incubator (to keep cells at 37 °C and 5% CO_2). Images were acquired at 2 h time intervals for 5 time points, using a Nikon Plan 4×/0.10 objective and a CCD camera. Within two subsequent time points, MetaMorph software (Molecular Devices) was used to measure the distance covered by cells to close the “wound area” (four field measurements for each image, at least 10 fields for each condition analyzed in each independent experiment) and to calculate migration rate (%).

Random Migration Assay

HMEC were transfected by NucleofectorTM with 2 µg of each construct. Cells were plated (1.5×10^4 cells/well), using EndoGRO MV-VEGF for HMEC on 24-well culture plates coated with 1% gelatin. 20 h after transfection, cells were starved for 4 h in DMEM 0%. EndoGRO 5% FBS was used as positive control, whereas DMEM 0% FBS was the negative control for HMEC. Experiments were performed using the same set-up described for the wound healing assays but using a Nikon Plan 10×/0.10 objective. Images were acquired for 10 h every 10 min using MetaMorph software. Image stacks were analyzed with ImageJ software and at least 500 cells/condition were tracked. Migration rate (µm/s) is obtained by measuring the distance covered by cells between two subsequent time points after conversion of pixels to micrometers. Directional migration index, or cell persistence, was calculated as the Euclidean distance from the initial position of each cell to the final point of its path (i.e., straight line from initial to final positions) divided by the total path length (sum of the distances covered between each acquisition). The value obtained was then normalized to the total

duration of the cell tracking and then multiplied by the square root of the cell tracking duration, as previously described [49].

Cell Attraction Assay

HMEC (10×10^4 cells/well) and PTEC (5×10^4 cells/well) were plated in 24-well plates (2 wells/condition) using EndoGRO MV-VEGF medium. After 24 h, Transwell® permeable supports (6.5 mm inserts with an 8 µm pore polycarbonate membrane) were equilibrated for 20 s at 37 °C using RPMI 0% FBS medium. The equilibrated Transwell® inserts were then placed over the wells containing the previously plated HMEC and PTEC. PC3 cells (5×10^4 cells/insert) were seeded in the Transwell® inserts using RPMI 0% FBS and incubated for 24 h. Transwell® inserts were then washed in PBS twice and fixed in methanol for 30'. PC3 cells were then colored with 0.5% Crystal Violet in methanol for 20 s at room temperature and after washed in PBS. PC3 cells that did not migrate thought the membrane pores were removed from the upper side of the membrane using a cotton bud. PC3 cells that migrated thought the membrane pores were then counted using an Eclipse Ti-E Nikon microscope with a 10×/0.25 NA Plan objective.

2D chemotaxis assay

6 µL of PC3 cell suspension (3×10^6 cells/mL) were plated in the observation area (3 observation areas/chamber) of a µ-Slide Chemotaxis chamber (ibidi GmbH, Gräfelfing, Germany) using RPMI 10% FBS medium and incubated to allow cell attachment. After 6 h, 65 µL of control medium (EndoGRO basal medium) were added to the right reservoirs of the chamber (3 right reservoirs/chamber). 65 µL of control basal medium or PTEC/HMEC/TRPC3-overexpressing HMEC conditioned medium were added to the left reservoirs of the chamber (3 left reservoirs/chamber). Experiments were performed using the same set-up described for the wound healing assays with a Nikon Plan 10×/0.10 objective. Images of the observations chambers were acquired for 10 h every 10 min using MetaMorph software. Image stacks were analyzed with ImageJ software.

In Vitro Tubulogenesis

In vitro formation of capillary-like structures was studied on growth factor-reduced Matrigel (Corning, Corning, NY, USA) for HMEC and a solution of 40% growth factor-reduced Matrigel and 60% Collagen-I 4 mg/mL gel obtained by mixing 1 M HEPES, 37 g/L NaHCO3, and 5 mg/mL collagen-I in a 1:1:8 ratio (Cultrex 3D Culture Matrix Rat Collagen I, Amsbio) for PTEC-hTERT. HMEC were transfected by NucleofectorTM with 2 µg of each construct, as previously described. 24 h after transfection, cells were seeded (3.5×10^4 cells/ well) onto Matrigel-coated 24-well plates in growth medium containing treatments (in duplicate). For siRNA-mediated silencing on PTEC-hTERT, Oligofection (Oligofectamine, Life Science) of siRNA duplexes was

performed twice (at 0 and 24 h) with 200 pmol siLuc (control, siCNTRL) or siTRPA1 (see also "Cell cultures and transfection" section). EndoGRO 5% FBS was used as positive control and DMEM 10% FBS as negative control. Cell organization onto Matrigel was periodically observed with the same set-up as the one used for wound healing and migration assays using a Nikon Plan 10×/0.10 objective. Images were acquired at 2 h time intervals (10 time points) using MetaMorph software. In order to quantify tubulogenesis images, we used the Angiogenesis Analyzer plugin of the ImageJ software, developed by Gilles Carpentier (ImageJ contribution: Angiogenesis Analyzer. ImageJ News, 5 October 2012). Angiogenesis Analyzer allows the analysis of cellular networks by the detection of different characteristics and constitutive elements of tubules. In order to measure differences in cell ability to from pseudo-capillary structures in vitro, we quantified the number of master junctions and the total master segments length. Master junctions are defined as portions of tree delimited by two junctions, none exclusively implicated with one branch. The total master segment length is the sum of the length of the detected master segments in the analyzed area, where master segments are the elements delimited by two master junctions.

Statistical Analysis

Statistical analysis was performed using R 3.4.2 software and Kaleidagraph Software (Synergy Software, Reading PA, USA). Statistical significance between populations was determined by Student's *t*-test (for normal populations) or non-parametric Wilcoxon-Mann-Whithney test. Differences with *p*-values < 0.05 were considered statistically significant. Heatmap: A heatmap was generated to represent and visualize the relative expression pattern of TRP genes. Figure 1a was produced with Complex Heatmap package 1.14.0. (https://bioconductor.org/packages/release/bioc/html/ComplexHeatmap.html). Euclidean distance and Ward's aggregation criterion were used to perform the hierarchical classification of the channels. The color key displayed in heatmap was prepared by putting the color breaks to log2 fold change values as follows: red, −4 to −2; black, −2 to +2 and green, 2 to 4. Normalization of relative expressions patterns: all experiments, except the ones involving TRPP2, were carried with at least two technical and three biological replicates for each experimental condition. For TRPP2, only two biological replicates were used. All initial values ($\Delta\Delta C_T$) were $\log_2$ transformed in order to stabilize the variance and directly observe the $\log_2$ fold changes (log2FC). Values of technical replicates were averaged before the $\log_2$ transformations. Relative expression pattern was obtained by subtraction of the healthy counterpart to the $\log_2$-averages of each biological sample. Differential analysis: Differential analysis of $\Delta\Delta C_T$ between PTEC1-3 samples and HPrMEC samples was performed with non-parametric Wilcoxon tests for unpaired data, without averaging technical replicates. In order to take into account the multiple testing issue, raw *p*-values were adjusted using the Benjamini-Hochberg method [51], which controls the false discovery rate (FDR). Differences with adjusted *p*-

values < 0.05 were considered statistically significant except for Figure 1b for which significance was at 0.1 (Figure 1b).

Results

1. Identification of the Trp Expression Signature Associated with PTEC

To define a complete '*TRP signature*' for the PCa endothelium, we performed gene expression profiling of TRP channels by means of real-time qPCR in TECs from the prostate and compared the profiles to those of breast and renal tumors. For this purpose, we designed primers targeting the functional region for all members of the TRP channel superfamily (*ankyrin 1*, *trpa1*; *canonical 1-7*, *trpc1-7*; *melastatin 1-8*, *trpm1-8*; *vanilloid 1-6*, *trpv1-6*; *polycystin 2-3*, *trpp2-3*; and *mucolipin 1-3*, *trpm1-3*).

We screened three primary human TEC primary cell lines derived from the prostate (PTEC1-3, corresponding to three different patients), which were previously characterized in our laboratory [18]. We also screened TECs from breast and renal tumors (designated BTEC and RTEC, respectively) [19,20]. Expression profiles of TECs were compared to those of several normal human ECs, namely, human umbilical vein ECs (HUVECs), human microvascular ECs from derma (HMECs), glomerular ECs from the kidney (GECs), and the commercially available human prostatic microvascular ECs (HPrMEC, ScienCell Research Laboratories, Carlsbad, CA 92008, US).

Differential analysis by the C_T method and fold change analysis of the expression values resulting from the qPCR screening were used to select '*prostate-associated*' genes that are deregulated during PCa angiogenesis (Figure 1c).

The $\Delta\Delta C_T$ method was applied to calculate the relative *trp* expression level in both normal ECs and TECs. $\Delta\Delta C_T$ values in TECs were normalized to different normal ECs: PTEC1-3, BTEC and RTEC expression profiles were compared to those of HPrMEC, HMEC and GEC respectively (Figure 1a). As shown in the heatmap (Figure 1a), the complete profiling of *trp* channel expression revealed several genes that are deregulated between normal ECs and TECs. Notably, compared to those in HPrMEC six genes are significantly deregulated in PTEC1-3 (Figure 1b), and among these, *trpa1* is the only upregulated gene (Figure 1d, Figure S1c). To identify a specific profile for PCa vascularization, we compared the expression profiles of TECs from PCa to those of TECs from breast and renal cancers. Four mRNA (i.e., *trpc1*, *trpc4*, *trpm1*, and *trpml1*) are downregulated in all TECs compared to that in normal ECs; moreover, *trpm7* is downregulated in PTEC and RTEC but upregulated in BTEC (Figure 1a, Figure S1c). Based on differential statistical analysis, *trpa1* is the

only '*prostate-associated*' gene (Figure 1c). In fact, in RTEC, *trpa1* expression is barely detectable, and *trpa1* is downregulated relative to that in renal GECs; in BTEC, *trpa1* is expressed at low levels, being downregulated relative to that in HPrMEC and upregulated relative to that in other normal ECs (HUVEC, HMEC and GEC) (Figure 1d). We further analyzed the expression profiles in PTEC, in comparison with HPrMEC (Figure 1e). Notably, twelve genes display at least 2-fold change in their expression relative to those in HPrMEC in at least two patient-derived PTEC (Figure 1e, blue and red dots, Figure 1c). Among these genes, *trpa1*, *trpv2*, and *trpc3* are specifically upregulated in PTEC but not in the other TECs (Figure 1d).

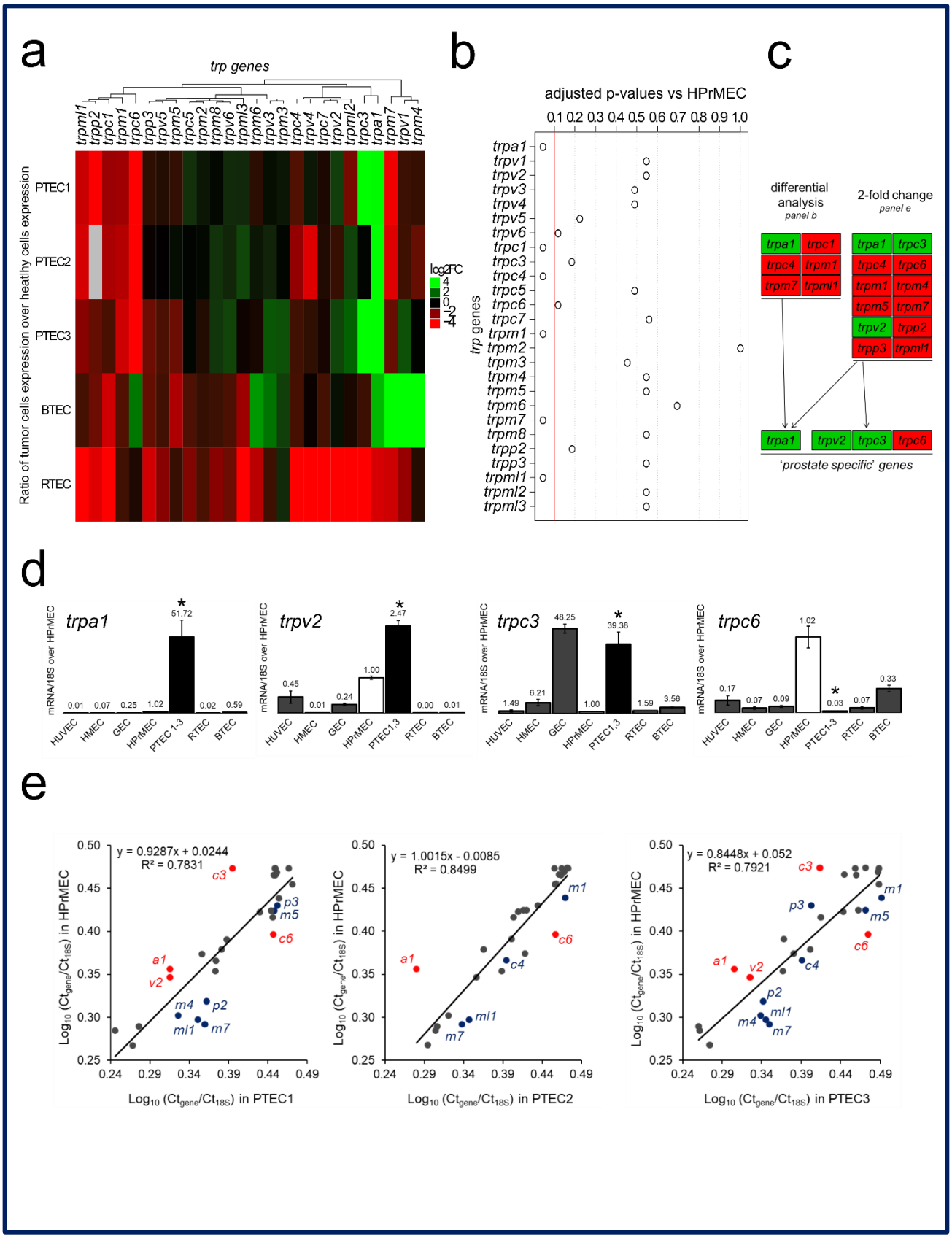

Figure 1. Identification of the trp expression signature in PTEC.

*(**a**) Heatmap showing the relative mRNA expression of the trp genes in TECs of different origins. TEC expression normalized based on normal endothelial counterparts: PTEC1-3 expression is normalized against HPrMEC expression, while BTEC and RTEC expression is normalized against HMEC and GEC expression, respectively. (**b**) Differential analysis of PTEC1-3 and HPrMEC highlighted six genes (i.e., trpa1, trpc1, trpc4, trpm1, trpm7, and trpml1) that are differentially deregulated (adjusted p-value < 0.1, red line), while the other genes did not show significant deregulation. (**c**) Differential analysis identified six genes that are differentially deregulated (panels **a**,**b**), and twelve genes displayed at least 2-fold change in their expression in at least two patient lines (panel **e**). Among these, four channels (trpa1, trpv2, trpc3 and trpc6) were selected as 'prostate-associated'. (**d**) Real-time qPCR analysis of mRNA expression shows that trpa1, trpv2, trpc3 and trpc6 are deregulated in PTEC1-3 relative to those in normal HPrMEC, and the deregulation is observed only in the prostatic tissue but not in the other normal ECs or TECs tested. Values are expressed as the mean ΔΔCT values ± SEM of at least three independent experiments. *: p-value < 0.05. (**e**) Scatter plots showing the expression of trp channels in PTEC1 (left panel), PTEC2 (central panel) and PTEC3 (right panel) relative to that in HPrMEC, as determined by real-time qPCR. Gray dots indicate genes with less than 2-fold change in PTEC relative to those in HPrMEC. Blue dots indicate genes with more than 2-fold change in at least one PTEC line relative to those in HPrMEC. Red dots showing the four 'prostate-associated' genes (i.e., trpa1, trpv2, trpc3, and trpc6), with more than 2-fold change in at least 2 PTEC lines out of three. Correlation values for trp channels are expressed as Log (C_(T,gene x)/C_(T,18s)) in primary PTEC (x-axis) and normal HPrMECs (y-axis).*

In particular, *trpa1*, already identified by differential analysis (Figure 1b,c), is strongly upregulated in PTEC1-3 relative to that in HPrMEC (51.72-fold increase) (Figure 1d, Figure S1d), as well as relative to that in HUVEC and HMEC (where channel expression is barely detectable) and GEC. *Trpv2* is upregulated by greater than 2-fold (2.47-fold increase) in PTEC1 and PTEC3 (PTEC1,3) relative to that in HPrMEC (Figure 1d, Figure S1d) and is overall markedly upregulated compared to that in other normal ECs while; however, in other TECs (RTEC and BTEC) and in normal HMEC, *trpv2* expression is barely detectable (Figure 1d). *Trpc3* is strongly upregulated in PTEC1,3 (39.38-fold increase) relative to that in normal HPrMEC (Figure 1d, Figure S1d), and this up-upregulation is also consistent relative to that in HUVEC and HMEC (Figure 1d). *Trpc3* is downregulated in RTEC relative that in the normal GEC, while in BTEC *trpc3* is downregulated relative to that in HMEC but upregulated relative to that in HUVEC and HPrMEC (Figure 1d). The only *trp* gene showing a specific downregulation in PTEC is *trpc6*, being 34-fold downregulated compared to that in HPrMEC (Figure 1d, Figure S1d). No significant change in *trpc6* expression is observed between RTEC and GECs, while BTEC display upregulation of *trpc6* relative to that in all normal ECs (HUVEC, HMEC, andGEC) but not to HPrMEC (Figure 1d).

These data therefore highlight four channels, namely, *trpa1*, *trpv2*, *trpc3* and *trpc6,* as '*prostate-associated*' (Figure 1c), displaying at least 2-fold change in expression compared to that in normal ECs (Figure 1e, red dots); additionally, these genes show differential regulation in PTEC compared with those in other TECs (Figure 1d).

2. TRPA1, TRPV2, TRPC3 and TRPC6 Expression in PCa Patients

Given that we identified *trpa1*, *trpv2*, *trpc3* and *trpc6* as '*prostate-associated*' genes that are deregulated in PTEC compared to that in normal HPrMEC, we further studied their expression at the protein level in vivo by immunohistochemistry on PCa tissues (Figure 2a,b) from ten patients (see materials and methods section) and in vitro by western blotting on proteins extracted from PTEC1-3 (Figure S2). Immunohistochemical analysis highlighted TRPA1 expression in human PCa tissues, showing positive TRPA1 staining in intratumoral ECs (Figure $2a_{aii}$). In particular, endothelial expression of TRPA1 was observed in tumor areas in all patient tissues (*n* = 10/10), with negative staining on cancer cells in 8 out of 10 patient samples (Figure $2a_{aii}$). In the normal areas of the tissues, we observed focal positive staining in epithelial cells with diffuse staining in ECs in all patients (Figure $2a_{ai}$). We quantified TRPA1 expression by western blotting in PTEC and compared it to the expression in HPrMEC confirming TRPA1 upregulation in all PTEC with a mean increase by 1.78-fold (Figure S2a).

Immunohistochemical analysis in PCa patient samples confirmed TRPV2 overexpression in intratumoral ECs, showing positive expression in seven of 10 patient samples (Figure $2a_{bii}$), with variable expression in tumor cells (Figure $2a_{bii}$). However, TRPV2 expression was not detected in ECs in histologically normal areas (*n* = 0/10) (Figure $2a_{bi}$). The expression pattern at the protein level was confirmed by western blotting, showing TRPV2 overexpression in PTECs compared to that in HPrMEC (Figure S2b), in accordance with the mRNA levels in the different PTEC (Figure S1d).

Immunohistochemistry did not confirm TRPC3 expression patterns in PTEC mRNA profiling, revealing negative TRPC3 staining in ECs in all normal areas (*n* = 10/10 patients) (Figure $2a_{ci}$), but only one tumor area (*n* = 1/10) showed faint positive TRPC3 staining in ECs (Figure $2a_{cii}$). Nevertheless, *trpc3* already shows a certain degree of variability since it is overexpressed in two PTEC (PTEC1,3) out of three. The overexpression pattern detected mRNA profiling was confirmed by western blotting, showing an upregulation in all PTECs (Figure S2c).

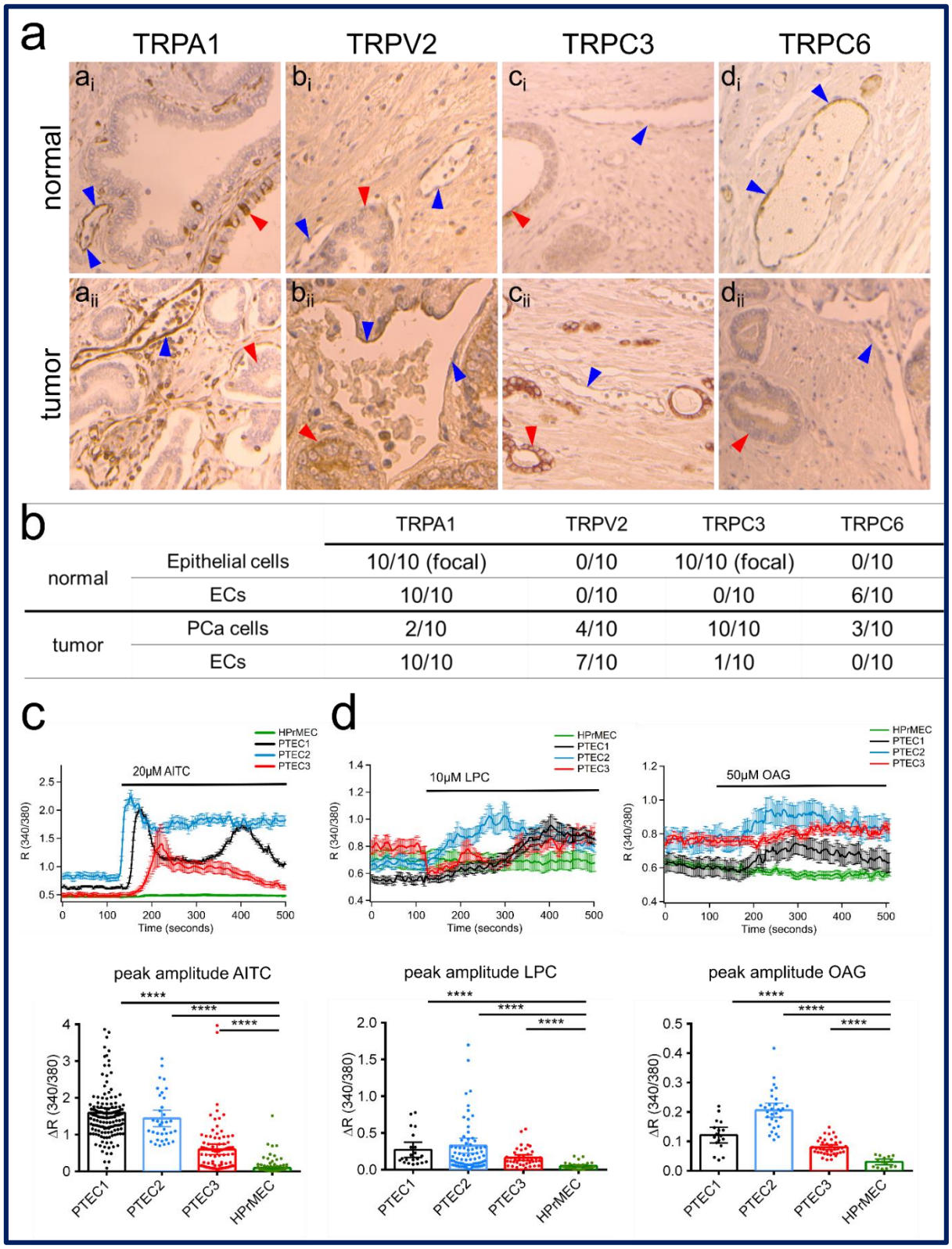

		TRPA1	TRPV2	TRPC3	TRPC6
normal	Epithelial cells	10/10 (focal)	0/10	10/10 (focal)	0/10
	ECs	10/10	0/10	0/10	6/10
tumor	PCa cells	2/10	4/10	10/10	3/10
	ECs	10/10	7/10	1/10	0/10

Figure 2. Protein expression of 'prostate-associated' genes in PTEC and HPrMEC.

*(**a**) (panel **a**$_i$, ×20) TRPA1 expression in normal areas: focal positive staining in epithelial cells (red arrows) and diffuse staining in ECs (blue arrows). (panel **a**$_{ii}$, ×20) In tumor areas, TRPA1 expression is observed in all cases (n = 10/10) in ECs*

*(blue arrows), with negative staining in tumor cells (red arrows). (panel **b**$_i$, ×40) In histologically normal areas, TRPV2 expression is not observed in ECs (n = 0/10) (blue arrows) or epithelial cells (red arrows). (panel **b**$_{ii}$, ×40) Positive endothelial TRPV2 expression was observed in 7 of 10 cases in the tumor areas (blue arrows), with positive staining in cancer cells in 4 cases (red arrow). TRPC3 expression: (panel **c**$_i$, ×40) all normal tissues showed negative staining (n = 10/10) in ECs (blue arrows) with focal positive staining in epithelial cells (red arrow). (panel **c**$_{ii}$, ×10) Only one tumor (n = 1/10) showed faint positive TRPC3 staining on ECs (blue arrow), whereas cancer cells were positive (red arrows) in all cases. (panel **d**$_i$, ×20) TRPC6 expression was observed in ECs in histologically normal tissues (n = 6/10), (panel **d**$_{ii}$, ×40) whereas TRPC6 expression was absent in cancer cells in 7 out of 10 patient samples (red arrows). (**b**) Summary of endothelial and epithelial expression of the four 'prostate-associated' candidates in both normal and tumor areas for the ten patient samples used for immunohistochemical analysis. The patients were 62 to 70 years old, with PCa classified as ISUP group 2 in six cases and group 3 in four cases. Ca^{2+}- imaging traces in response to TRPA1, TRPV2 and TRPC3 agonists respectively (**c**) 20 µM AITC), (**d**) 10 µM LPC and (**e**) 50 µM OAG in PTEC1 (black), PTEC2 (blue) and PTEC3 (red) but not in HPrMEC (green).Traces represents mean ± SEM of cells in the recorded field of one representative experiment. Lower panel: histogram showing peak amplitude of TRP agonist-mediated Ca^{2+} responses (mean ± 95% CI of different cells in the field from at least 3 independent experiments). Statistical significance and ****: p-value < 0.0001 (Kruskal-Wallis test).*

As previously stated, we also identified *trpc6* as a '*prostate-associated*' downregulated gene. Immunohistochemistry for TRPC6 confirmed the qPCR data, as expression of the channel was observed in ECs in normal areas (*n* = 6/10) (Figure 2a$_{di}$), while a negative staining was obtained in ECs in all tumor areas (*n* = 10/10) (Figure 2a$_{dii}$). TRPC6 expression was absent in cancer cells in 7/10 patient samples (Figure 2a$_{dii}$). However, PTEC showed variable expression of TRPC6 at the protein level, as western blotting analysis showed no change in TRPC6 expression at the protein level in PTEC relative to that in HPrMEC (Figure S2d).

Overall, except for TRPC3, the results obtained are consistent at the protein level and the mRNA level determined by qPCR screening, thereby establishing '*prostate-associated*' TRP channels as valid candidates to study at the functional level by defining their role in TEC physiology. We have further studied functional expression of TRPA1, TRPV2 and TRPC3 since up-regulation in mRNA and protein levels do not necessarily correspond to increased channel activity. Ca^{2+} imaging experiments on the three primary cells PTEC 1, 2 and 3 using the agonists of TRPA1 (Figure 2c), TRPV2 (Figure 2d) and TRPC3 (Figure 2e) showed a significant increased Ca^{2+} influx as compared to HPrMEC in accordance with the over-expression of these channels in PTECs.

3. 'Prostate-Associated' TRPV2 Enhances EC Viability

We functionally characterized the role of the three *"prostate-associated"* overexpressed TRP channels (namely, *trpa1*, *trpv2*, and *trpc3*) in TECs. We first assessed the effect of the overexpression of the selected TRP channels in cell viability, a key process in stalk cells during angiogenic sprouting [6,7]. For this purpose, we used HMECs as a cellular model to study the function and role of the selected '*prostate-associated*' channels (*trpa1*, *trpv2*, and *trpc3*) since they exhibit a low or barely detectable expression as shown by qPCR (Figure 1d). For all experiments, we verified the

overexpression and activity of the channels by western blotting and Ca^{2+} imaging experiments, respectively, using the following channel activators: AITC for TRPA1; LPC for TRPV2; and OAG for TRPC3 (Figure S3). Of the three TRP channels analyzed, only TRPV2 significantly increased basal HMEC viabiity by approximately 55% relative to control cells, as evaluated by MTS assays (Figure 3a).

To study the functional role of the channels in PTEC, we immortalized PTEC (hTERT PTEC) by retroviral transfection with telomerase reverse transcriptase (hTERT). To validate the new cell model we performed flow cytometric analysis to confirm endothelial markers expression (Figure S4a). Similarly, to primary PTEC, hTERT PTEC expressed the following endothelial markers: Endoglin, Type I membrane glycoprotein (CD105), Platelet EC adhesion molecule (CD31, PECAM-1), and Vascular Endothelial Growth Factor Receptor1 (VEGFR1, Figure S4a). CD105 and CD31 expression was also confirmed at the mRNA level by qPCR (Figure S4b). Phenotype maintenance was confirmed by flow cytometry analysis of endothelial markers expression at passage 7 (Figure S4a). In addition, androgen receptor (AR) expression was detected in hTERT PTEC (Figure S4e), as previously reported for primary PTEC [18]. In line with this last study, hTERT PTEC cell lines were resistant to sorafenib (Figure S4d), an anti-angiogenic drug currently used in the treatment of several cancers.

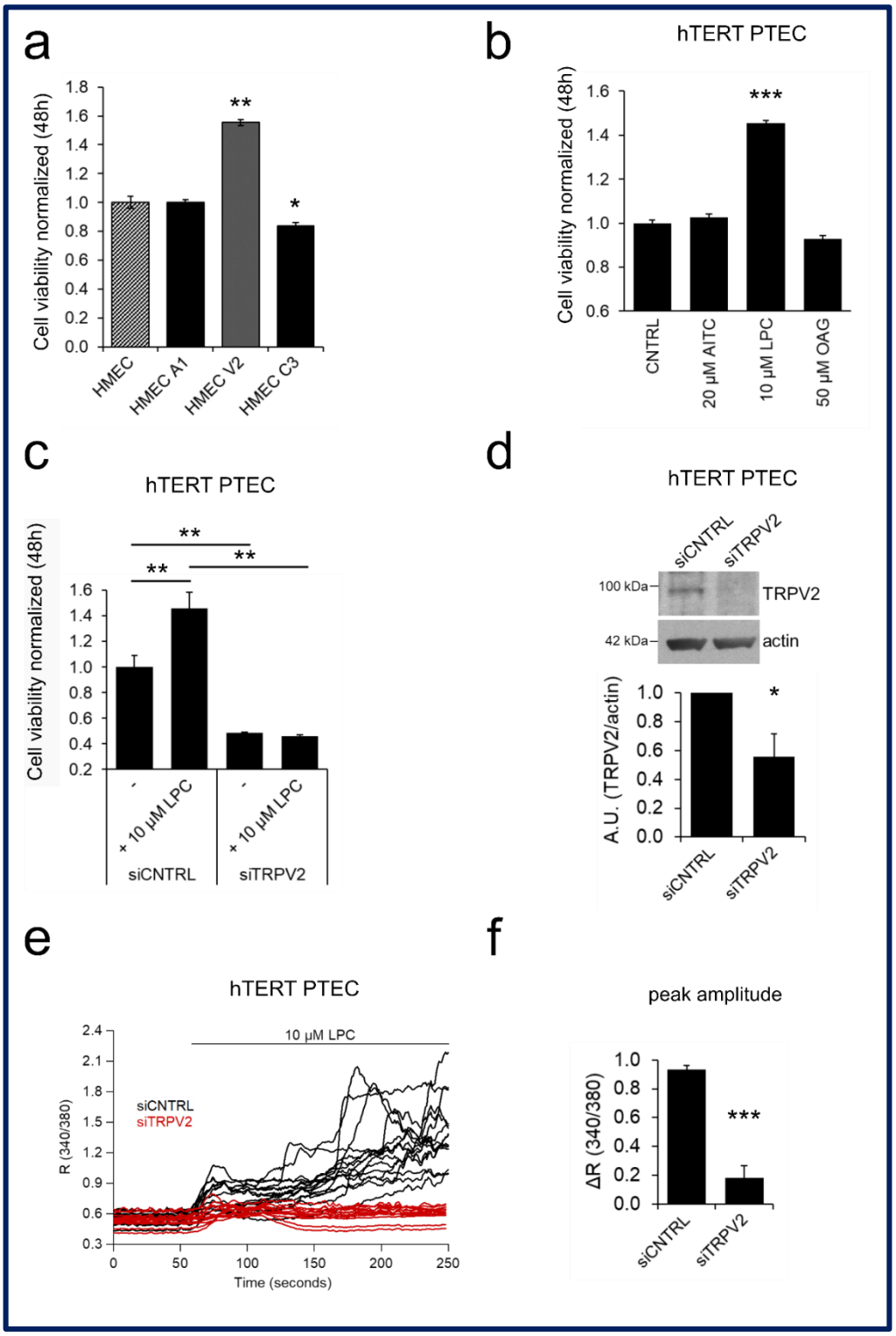

Figure 3. TRPV2 modulates EC viability.

*(**a**) The 'prostate-associated' channels were overexpressed in HMEC to test their effect on cell viability. Of all channels, only TRPV2-overexpression positively modulated proliferation in HMEC, 48 hours after transfection. Statistical significance *: p-value < 0.05 and **: p-value < 0.005 vs HMEC. (**b**) Treatment with the 'prostate-associated' channel agonists shows that 10 µM LPC induces an increase in hTERT PTEC viability 48 h after treatment. Agonists were added to the basal growth medium. Data represent the mean ± SEM of a minimum of three independent experiments. Statistical*

*significance ***: p-value < 0.005 vs. control basal medium. (**c**) Silencing of TRPV2 expression significantly reduced hTERT PTEC viability, under both basal conditions and LPC stimulation and reverted the LPC-induced increase in PTEC viability observed in control cells. Statistical significance **: p-value < 0.005. (**d**) TRPV2 downregulation 48 h after siRNA transfection was verified by western blotting in hTERT PTECs. Histogram showing the quantification of TRPV2 expression relative to actin represented as the mean ± SEM of a minimum of three independent experiments. (**e**) Downregulation of TRPV2 expression was also studied in Ca^{2+} imaging experiments 48 h after siRNA transfection by stimulation with 10 µM LPC in control and TRPV2-silenced hTERT PTEC. Each trace represents the ratio (340/380 nm) of a single cell in the field in one representative experiment.*

We further validated *trp* channel expression and function in hTERT PTEC as compared with PTEC3 (from which the cells were immortalized), HPrMEC and HMEC. Immortalized hTERT PTEC showed equal expression of trpa1, trpv2, trpc3 and trpc6 as compared with PTEC3 cells (Figure 4a). hTERT PTEC protein expression was validated by immunoblot and compared with HPrMEC (Figure 4b). Induction of the endogenous TRPV2, TRPA1 and TRPC3/TRPC6 channels activity in PTEC was functionally validated by Ca^{2+} imaging experiments. Stimulation of hTERT PTEC cells with the agonists of TRPA1, TRPV2 and TRPC3 (20 µM AITC, 10 µM LPC and 50 µM OAG respectively) induced sustained Ca^{2+} influx and increased significantly the maximum amplitude of response in comparison with that in HPrMEC, which barely express the channel proteins (Figure 4c).

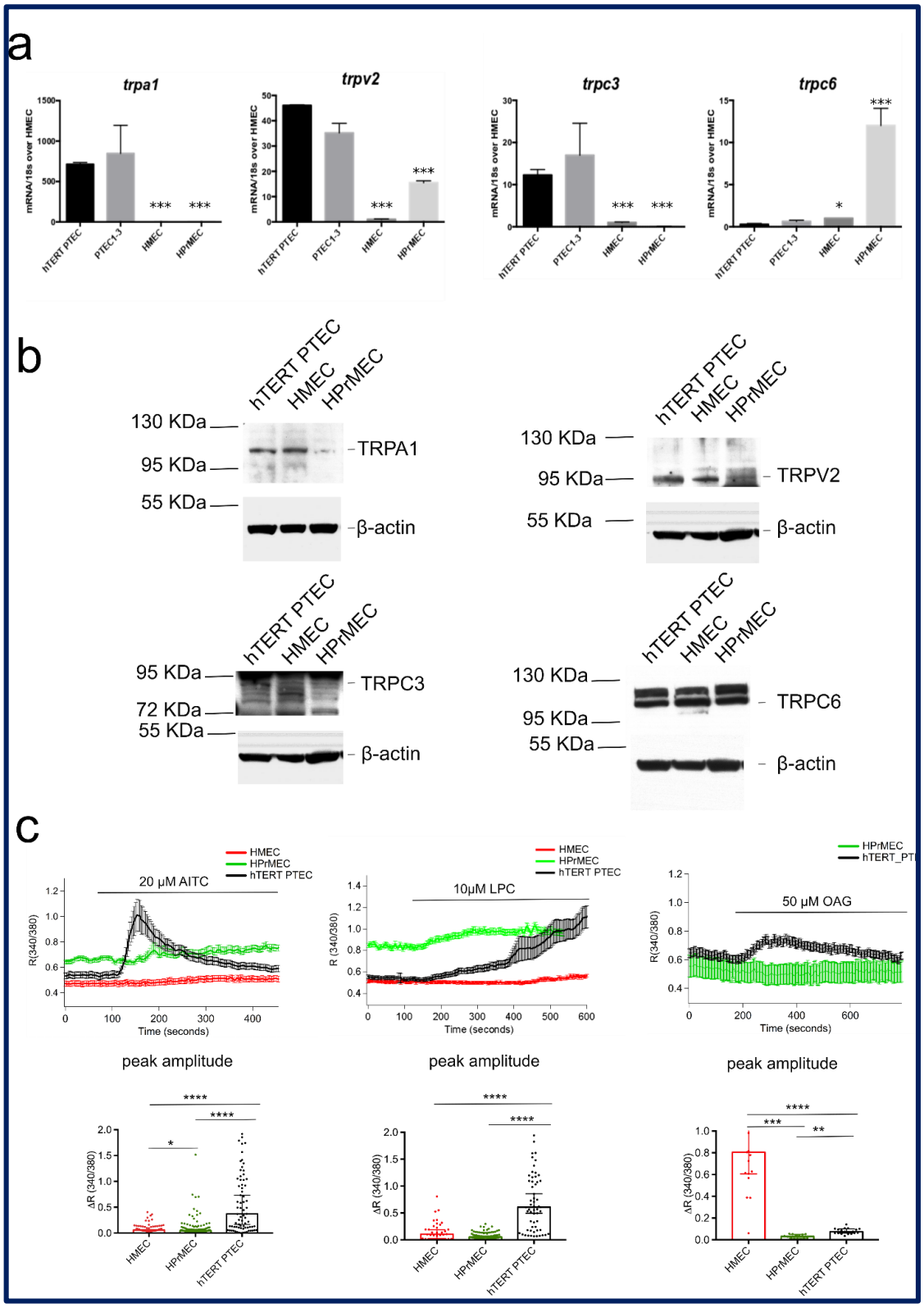

Figure 4. hTERT PTEC validation as cellular model for TEC studies.

a*) Real-time qPCR analysis validating equal amount of mRNA expression if trpa1, trpv2, trpc3 and trpc6 in hTERT PTEC compared to PTEC1-3, as well as deregulated expression compared to HMEC and HPrMEC. Values are expressed as the*

*mean ΔΔCT values ± SEM of three independent experiments. (**b**) Representative immunoblots blots (n = 3) showing similar TRPA1, TRPV2 and TRPC3, and TRPC6 expression in hTERT PTEC compared to PTEC1, 2 and 3. β-actin was used as a loading control. (**c**) Ca^{2+}- imaging traces in response to TRPA1, TRPV2 and TRPC3 agonists respectively 20 µM AITC), 10 µM LPC and 50 µM OAG in HMEC (red), HPrMEC (green) and hTERT PTEC (black). Traces represents mean ± SEM of all cells in the recorded field of one representative experiment. Lower panel: histogram showing peak amplitude of TRP agonist-mediated Ca^{2+} responses (median ± 95% CI of different cells in the field from at least three independent experiments). Statistical significance *: p-value < 0.05, **: p-value < 0.005 and ****: p-value < 0.0001 (Kruskal-Wallis test.).*

Similarly HMEC stimulation with AITC and LPC show barely no Ca^{2+} responses; however OAG promoted a significant increase in $[Ca^{2+}]_i$ probably due to the non-specific activity of OAG and possible activation of TRPC6 (Figure 4c, Figure S4e). Altogether, these data show that hTERT PTEC are suitable as a PTEC model for the study of the selected TRP candidates in cell processes important for EC physiology, such as cell viability, migration, chemotaxis and tubulogenesis. We next assessed whether the activation of the endogenous *trpa1*, *trpv2*, and *trpc3* channels affected the viability of hTERT PTEC. In line with the overexpression results in HMEC (Figure 3a), only treatment with 10 µM LPC (a TRPV2 agonist) induced an increase of approximately 45.5% in hTERT PTEC viability compared to that under control conditions (Figure 3b), confirming the role of endogenous TRPV2 as a positive modulator of EC proliferation. Silencing of TRPV2 expression significantly reduced availability in hTERT PTEC, under both basal conditions and LPC stimulation (Figure 3c). The role of TRPV2 in cell proliferation was confirmed by means of BrDU assay (Figure S4g). Downregulation of TRPV2 expression was verified by Ca^{2+} imaging experiments 48 hours after siRNA transfection after stimulating control and TRPV2-silenced (siTRPV2) hTERT PTEC with 10 µM LPC (Figure 3e,f). Mean TRPV2 downregulation of 44.3% was verified 48 hours after siRNA transfection by means of western blotting (Figure 3d).

4. 'Prostate-Associated' TRPA1 Expression Promotes EC Migration

Cell migration is one of the key steps involved in sprouting angiogenesis that enables endothelial tip cells to function as motile guidance structures that dynamically extend filopodia to explore signals in the tumor microenvironment for directional vessel growth [21]. We thus investigated the role of the four '*prostate-associated*' channels in EC migration. For this purpose, we overexpressed the channels in HMECs to analyze their effect on EC motility by means of scratch wound healing assays. Among the three candidates, overexpression of TRPA1 significantly increased migration in HMEC compared to that in non-transfected cells (Figure 5a). The increase in migration rate was significant from 2 h onward and peaked after 8 hours in TRPA1-overexpressing HMEC compared to that in control cells.

We further investigated the endogenous role of TRPA1 in hTERT PTEC motility, as this channel is strongly up regulated in PTEC compared to that in normal ECs (Figures 1,2). To achieve this goal, we tested the effect of TRPA1 silencing in hTERT PTEC by wound healing experiments (Figure 5b). Compared to siCNTRL

transfection, down regulation of TRPA1 expression in PTEC by means of siRNA transfection induced a significant decrease of 23% in cell migration (siTRPA1) (Figure 5b). Moreover, TRPA1 inhibition by treatment with the channel inhibitor (20 µM HC030031) induced a 41% decrease in migration in control hTERT PTEC (siCNTRL) but not in TRPA1-silenced hTERT PTEC (siTRPA1) (Figure 5b). Next, endogenous functional expression of TRPA1 in hTERT PTEC and HMEC was tested by Ca^{2+} imaging. $[Ca^{2+}]_i$ significantly increased in hTERT PTEC but not in HMEC following stimulation with the TRPA1 channel agonist AITC (20 µM) (Figure 5d). On the other hand, silencing of TRPA1 expression in hTERT PTEC significantly reduced AITC-mediated $[Ca^{2+}]_i$ by 3.26-fold (Figure 5d). Similarly, treatment with two different concentrations (10 µM and 20 µM) of the TRPA1 inhibitor HC030031 dramatically decreased AITC-induced channel activity in hTERT PTEC (Figure 5e). Mean TRPA1 downregulation of 36.8% was verified via western blotting in PTEC 48 h after siRNA transfection (Figure 5c).

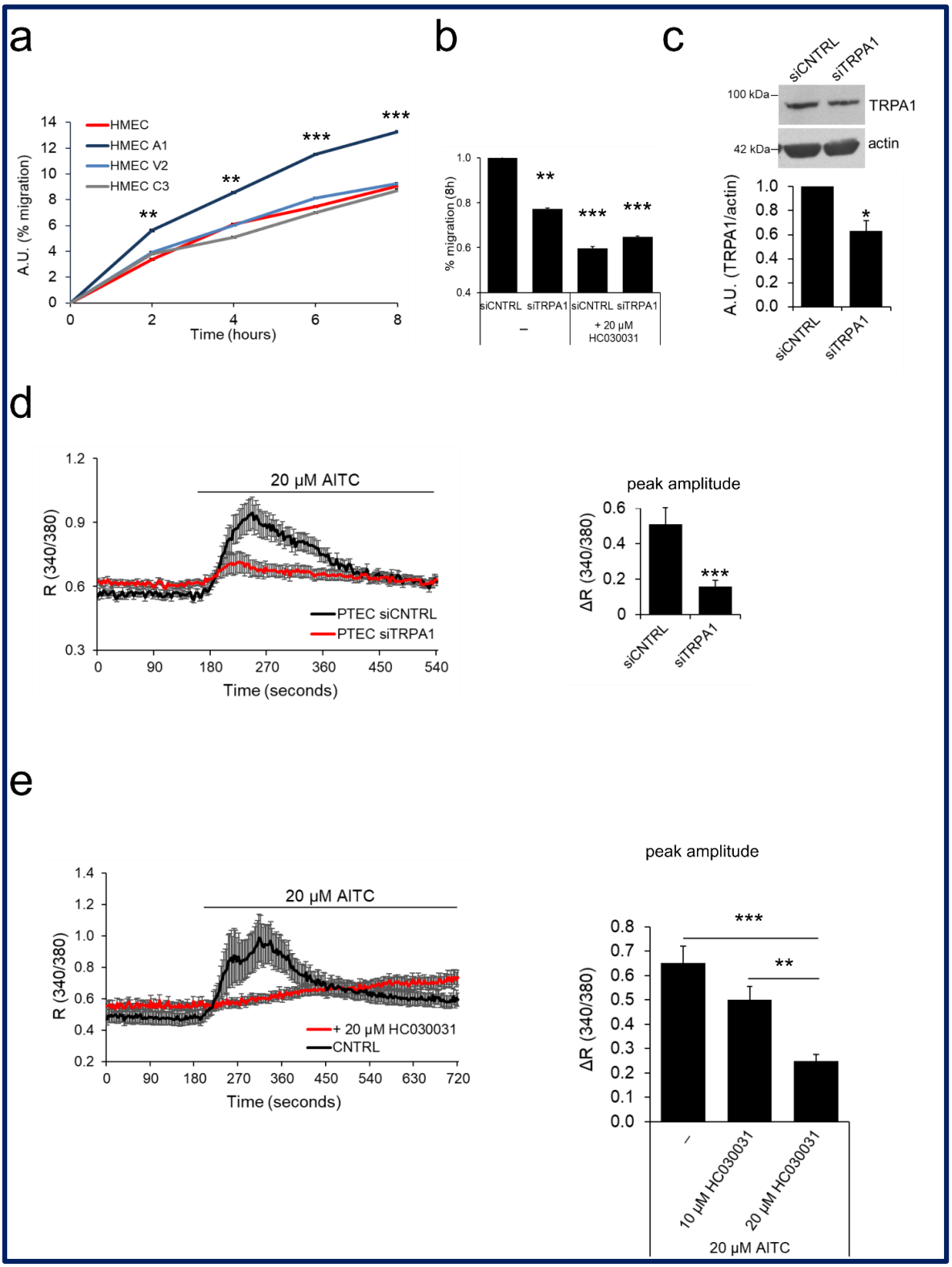

Figure 5. TRPA1 increases EC migration.

*(**a**) The 'prostate-associated' channels were overexpressed in HMECs to test their effect on cell migration. Expression of TRPA1 increased the migration of HMEC relative to control cells in basal medium, as observed by wound healing*

*experiments. Lines show the mean value ± SEM of one out of three independent experiments (24 h after transfection). Statistical significance **: p-value < 0.005 and ***: p-value < 0.0005 vs. HMEC. (**b**) Histogram showing the % migration in wound healing experiments of PTEC transfected with control siRNA (siCNTRL) or siRNA against TRPV2 (siTRPV2), under both basal conditions and 8 h after treatment with TRPA1 inhibitor HC030031. Statistical significance **: p-value < 0.005 and ***: p-value < 0.0005 vs. HMECs. (**c**) TRPA1 downregulation 48 h after siRNA transfection was verified by western blotting. Histogram shows quantification of TRPA1 expression relative to actin represented as the mean + SEM of a minimum of three independent experiments. *: p-value < 0.05. (**d**) Downregulation of TRPA1 expression was verified 72 h after siRNA transfection in Ca^{2+} imaging experiments by stimulation with 20 µM AITC in control PTEC (siCNTRL, black trace) and in PTECs transfected with siRNA against TRPA1 (siTRPA1, red trace). (**e**) TRPA1 activity is inhibited when PTEC are treated with a TRPA1 channel inhibitor (20 µM HC030031) based on Ca^{2+} imaging experiments. For experiments in c, d and e traces show the mean value ± SEM of all cells in the recorded field of one representative experiment (left panel); histograms represent the quantification of the peak amplitude after treatment with AITC (**c**,**d**) or different doses of the channel inhibitor (10 or 20 µM HC030031) in Ca^{2+} imaging experiments (**e**, right panel).*

5. 'Prostate-Associated' TRPC3 Promotes PCa Cell Attraction

TECs have been shown to exert a chemoattractive effect on cancer cell, thus guiding cancer metastasis [22]. We thus considered a possible role of the three *'prostate-associated'* channels that are upregulated in PTEC (*trpa1*, *trpv2* and *trpc3*) in the cross-talk between TECs and PCa cells. In this regard, we showed that hTERT PTEC exert a significantly stronger attractive effect on PCa cells (PC3) in co-culture experiments than do normal ECs (HMEC) (Figure 6a). Moreover, we overexpressed TRPA1, TRPV2 and TRPC3 channels in HMEC and investigated the effect on PC3 cell attraction. TRPC3 overexpression in HMEC induced a significant increase of 219% in PC3 cell attraction compared to that in control cells, mimicking the effect of PTEC that endogenously overexpress the channel (Figure 6a). However, TRPA1 and TRPV2 overexpression in HMECs did not alter PC3 cell attraction compared to that in control HMEC in co-culture experiments (Figure 6a central panel), supporting a specific role for TRPC3 in PCa cell attraction.

We further explored the role of TRPC3 in PCa cell attraction by chemoattraction assays in the presence of hTERT PTEC, TRPC3-overexpressing HMEC, or control HMEC conditioned media (Figure 6b). We observed that compared to HMEC conditioned medium, hTERT PTEC conditioned medium (24-h conditioning) increased PC3 cell migration speed (Figure 6b,c, left panel). Moreover, compared to control HMEC conditioned media, the conditioned medium from TRPC3-overexpressing HMEC significantly promoted PC3 migration via enhancing the directional persistence index but not the speed (Figure 6b,c, central and right panels). These data, together with the results from the transwell migration experiments, confirm that TRPC3 expression is correlated with PCa cell attraction by TECs.

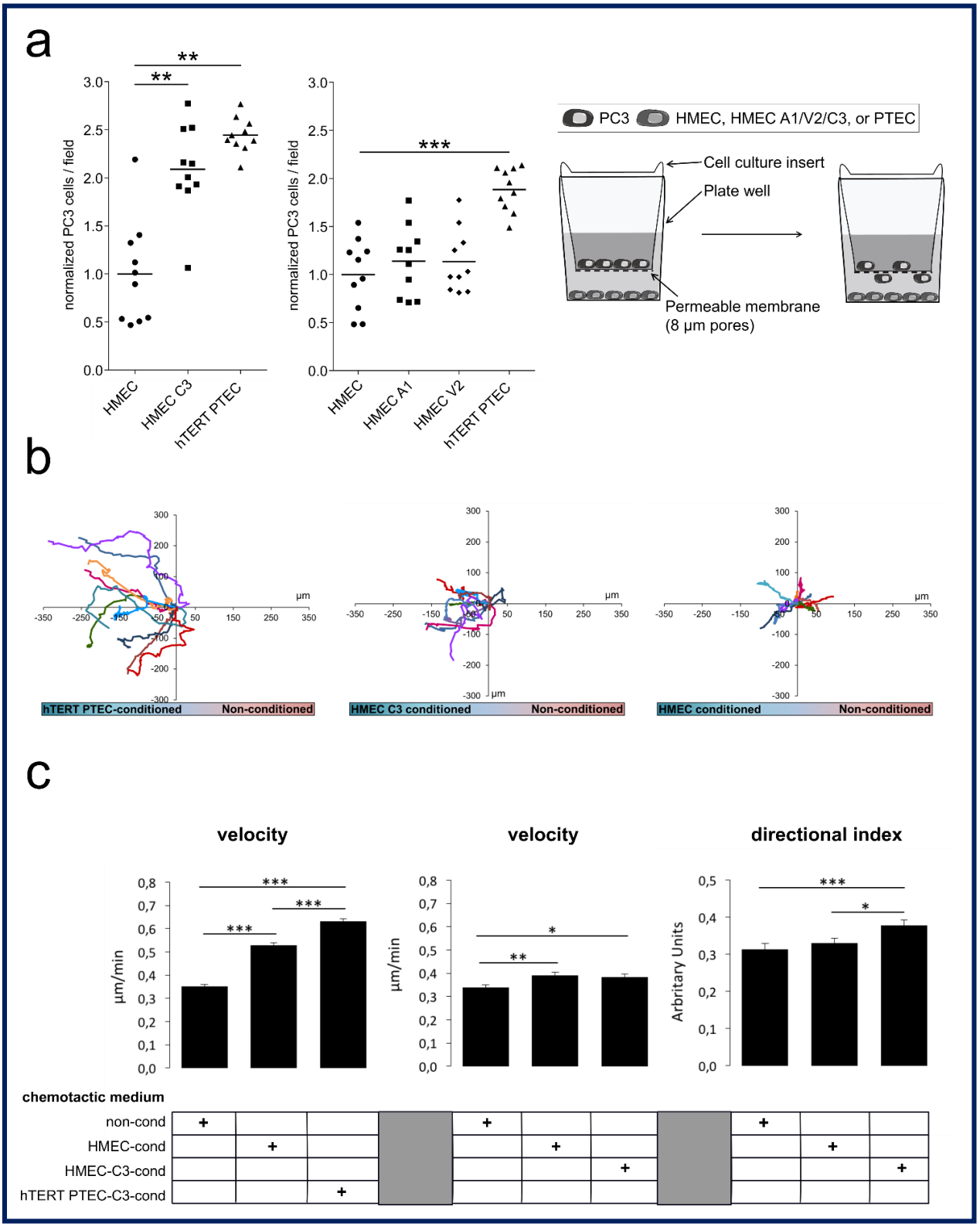

Figure 6. TRPC3 has a role in PCa cell attraction.

*(**a**) PC3 cells were used to study the effect of TRPA1, TRPV2 and TRPC3 on cancer cell attraction. Control HMEC, channel-overexpressing HMEC or hTERT PTEC were plated in multiwell plates, and PC3 cells were plated in the upper chamber of 8 µm-pore culture inserts. hTERT PTEC or TRPC3-overexpressing HMEC (HMEC C3) increased PC3 cells migration through the membrane, quantified 24 h after plating. Each dot indicates the cell number in a single field normalized to PC3 cell count; results are presented as normalized values against co-cultured HMEC, while the continuous line represents the median value of normalized cells/field for each condition (n = 10). The graph shows one representative experiment out of three. Statistical significance: ** p-value < 0.005; *** p-value < 0.0005. Right panel shows the schematic representation of the migration assays used to study PC3 cell migration in co-culture with either hTERT PTEC, TRPA1/V2/C3-overexpressing HMEC, or control HMEC. (**b**) Chemotaxis chambers were used to study hTERT PTEC-directed migration in the presence of hTERT PTEC-, TRPC3-overexpressing HMEC-, HMEC- or non-conditioned (non-cond) media. Compared to HMEC conditioned medium, PTEC conditioned medium (24-h conditioning) increased PC3 cell speed (**c**, left panel), while compared to control HMEC conditioned medium, the conditioned medium from TRPC3-overexpressing HMECs significantly promoted PC3 migration via directional persistence index and not on the speed (**c**, central and right panels). Statistical significance: * p-value < 0.05, ** p-value < 0.005 and *** p-value < 0.0005.*

6. TRPA1 Promotes Vascular Network Formation and Angiogenic Sprouting both In Vitro and In Vivo

The results described above indicate that TRPA1 is a modulator of PTEC migration, raising the question of whether this channel also affects tubulogenesis or in vivo angiogenesis. To investigate this point, we tested TRPA1 and other TRP candidates for their ability to organize into capillary-like structures in vitro. Interestingly, among all the *'prostate-associated'* channels, a significant increase in the capillary-like structure formation was observed in TRPA1-overexpressing HMEC relative to that in control cells (Figure 7a, Figure S5). In particular, for TRPA1 overexpression, we observed a strong and significant increase in the number of *master segments* and a concomitantly significant decrease of number of *isolated segments*, two important parameters of EC organization during network formation (Figure 7a, right panel). The role of endogenous TRPA1 was subsequently studied on hTERT PTEC capillary-like structure formations: both TRPA1 inhibitor HC030031 treatment or TRPA1 down regulation strongly and significantly decreases the number of *master segments* and a significantly increase the number of *isolated segments* (Figure 7a, right panels). These results suggest that in addition to playing an important role in cell migration, TRPA1 exerts a marked effect on in vitro EC morphogenesis, which is one of the key features required for new vessel formation (Figure 7a).

To further confirm the role of TRPA1 in vessel morphogenesis, we performed in vivo experiments by using the well-established in vivo angiogenesis model of postnatal mouse retina. Endogenous TRPA1 is diffusely expressed in postnatal mouse retina but clearly co-localizes with CD31 staining, indicating that TRPA1 is expressed in ECs (Figure 7b). Moreover, TRPA1 expression was detected by qPCR in CD31-positive cells isolated from the whole retina, confirming its expression in retinal ECs (Figure 7c). Subretinal injection of AITC or HC030031 did not alter the overall development of the vascular plexus 3 days after treatment but disturbed the vascular front. Indeed, the front of the growing vasculature appeared more uneven after

injection of the TRPA1 agonist AITC in the subretinal space. This was illustrated by a significant increase of 26.8% in the length of the sprouts (Figure 7e, upper graph, white bars). In addition, when vascular sprouts were counted and classified in terms of their length (<70 µm, 70–150 µm or >150 µm), the number of longer sprouts (>70 µm) was increased after AITC injection (Figure 7f), confirming the irregular growth front of the retinal vascular plexus when TRPA1 is activated. In contrast, the retina vascular front was straighter when the TRPA1 inhibitor HC030031 was injected in the vitreous, confirmed by a 14.1% reduction in the length of the vascular sprouts (Figure 7e, lower graph, white bars) and by an increase in the number of the shorter sprouts (<70 µm) and a decrease in the number of longer sprouts (Figure 7f, lower panel). These data demonstrate an important role of TRPA1 in vascular remodeling (as demonstrated by capillary-like morphology in Matrigel), as well as in vascular sprouting in vivo in the retina. Therefore, we detected an important role of TRPA1 (Figure 7a) by overexpression or inhibition of its basal activity using the TRPA1 blocker HC030031, (Figure 7d) further supporting the role of TRPA1 in vascular remodeling.

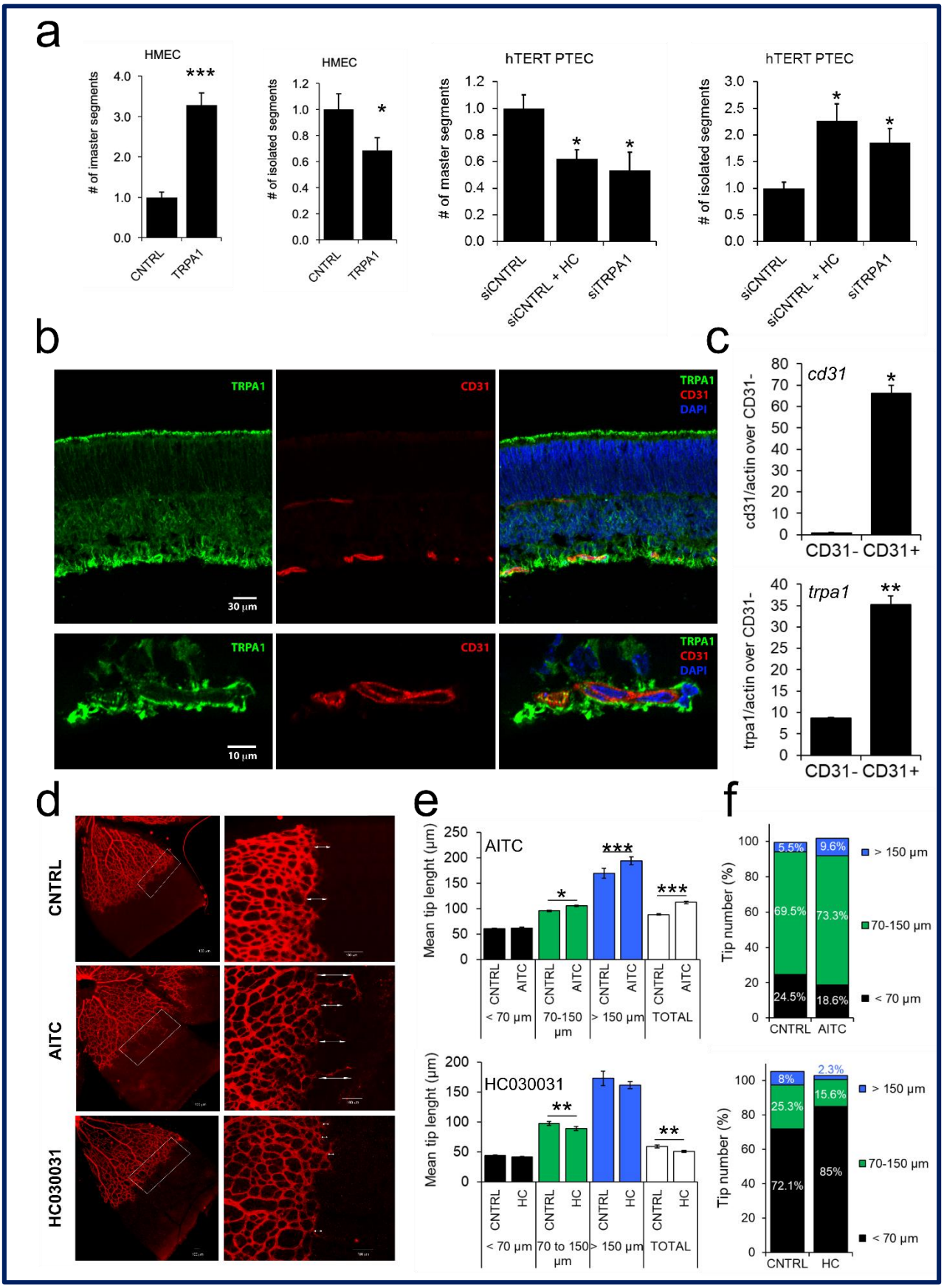

Figure 7. TRPA1 promotes in vitro tubulogenesis and in vivo angiogenesis.

*(**a**) left panels:TRPA1-overexpressing HMEC display increased in vitro tubulogenesis in Matrigel compared to control cells; right panels: TRPA1-downregulating hTERT PTEC display decreased in vitro tubulogenesis in Matrigel/collagenI substrate compared to control cells; bar graphs show the quantification of number of master segment and the number of isolated segments of control HMECs and TRPA1-overexpressing HMECs. Three independent experiments were performed 24 h after overexpression or after II oligofection pulse. (**b**) Endogenous TRPA1 is diffusely expressed in postnatal mouse retina but clearly co-localizes with CD31 staining, indicating that TRPA1 is found in ECs. (**c**, upper panel): analysis of CD31 levels by qPCR in a fraction of CD31-enriched cell population isolated from the mouse retina (CD31+) compared to the depleted cell population (CD31−); (**c**, lower panel): analysis of TRPA1 mRNA expression by qPCR in a fraction of CD3-enriched cell population isolated from the mouse retina (CD31+) compared to the depleted cell population (CD31−). Values are expressed relative to actin expression. Statistical significance *: p-value < 0.05, **: p-value < 0.005 and ***: p-value < 0.0005 vs. control. (**d**) Subretinal injection of AITC or HC030031 did not alter the overall development of the vascular plexus 3 days after treatment, but the front of growing vasculature became uneven after injection of the TRPA1 agonist AITC in the subretinal space. (**e**, upper panel) This was illustrated by a significant increase of 26.8% in the length of sprouts (white bars): quantification of tip cell length during mouse retinal angiogenesis shows that compared to that in controls, tip cell length increased significantly 3 days post-intravitreous injection of 200 µM AITC. (**e**, lower panel**)**: Treatment with TRPA1 inhibitor (200 µM HC030031) induced a decrease in tip cell length. Cell lengths were either classified into three groups according to ranges (<70 µm, 70–150 µm, >150 µm) or considered altogether (total). Bars represent the mean ± SEM of each length range or total grouping. (**f**, upper panel): Percentage of tip cells with each length range shows that treatment with AITC induces a decrease in the number of short tip cells (<70 µm) and an increase in the number of medium and long tip cells (>70 µm). (**f**, lower panel): Inhibition of TRPA1 with HC030031 induces the opposite effect, increasing the number of short tip cells and decreasing the number of medium and long tip cells.*

The significant role of TRPA1 in sprouting angiogenesis intrigued us to evaluate a possible activity of this channel in chemoattraction. In order to verify this hypothesis, we performed migration transwell assays stimulating hTERT PTEC cells in the presence of 20 µM AITC in the lower compartment. Figure 8 clearly shows a chemoattractive effect in cell stimulated with TRPA1 agonist as compared to control (Figure 8a). We next evaluated whether this chemoattractive role was due to specific activation of TRPA1 on migrating cells.

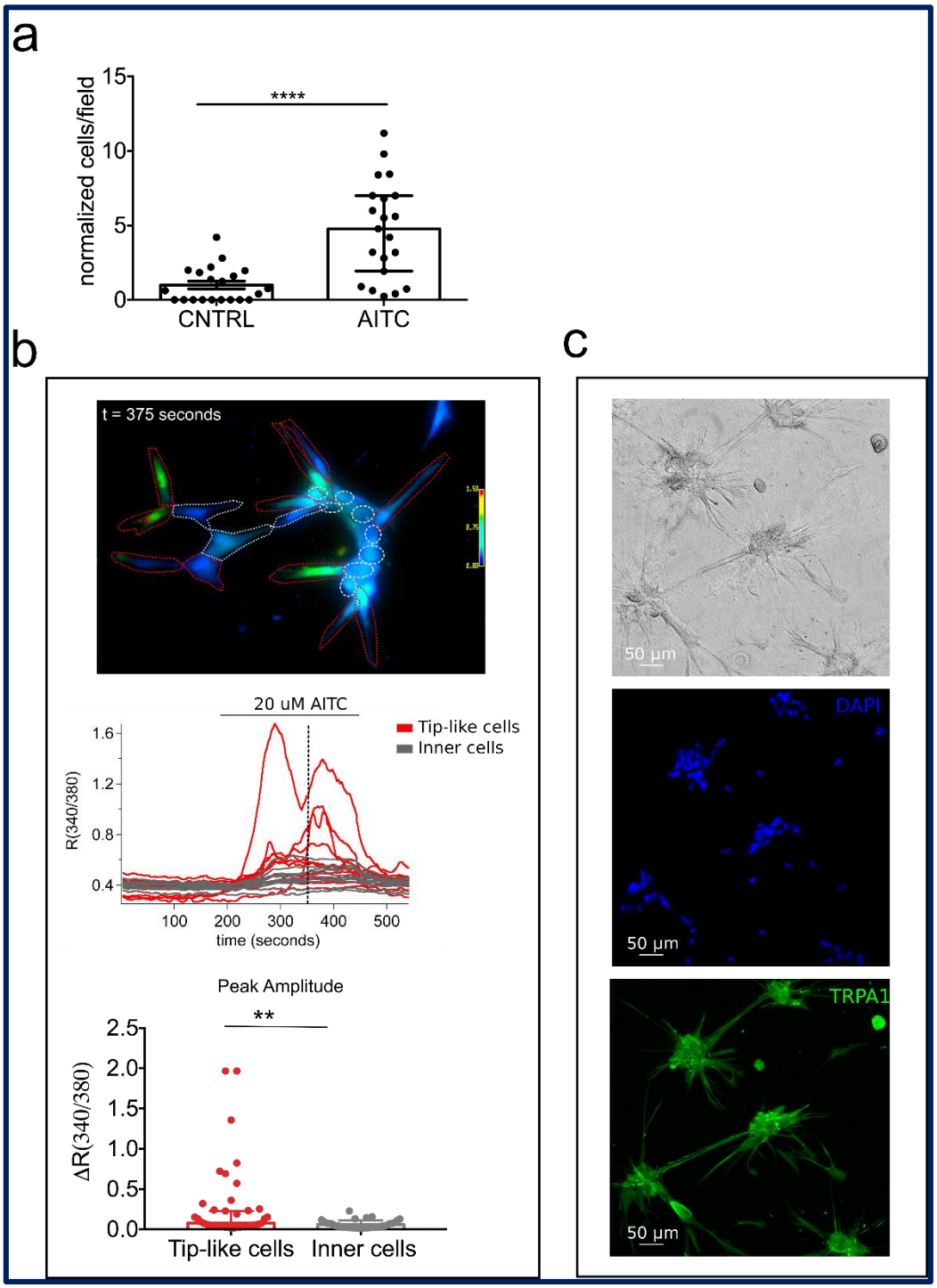

Figure 8. TRPA1 is implicated in PTEC chemotaxis and function in tip-like cells.

*(**a**) hTERT PTEC were plated in the upper chamber of 8 µm-pore culture inserts in the presence or absence of 20 µM AITC. AITC significantly increased hTERT PTEC chemoattraction through the membrane, quantified 24 h after plating. Each dot indicates cell number in a single field normalized to hTERT PTEC cell count; results are presented as normalized values against CNTRL hTERT PTEC (median ± 95% CI of normalized cells in the field cells from 4 independent experiments). Statistical significance ****: p-value < 0.0001 (Mann-Whitney test). (**b**) TRPA1-mediated Ca^{2+} responses in migrating (tip-like) versus non-migrating cells (inner cells). Upper panel: representative field showing 20 µM AITC-induced Ca^{2+} responses in hTERT PTEC plated on Matrigel/collagen substrate. Representative image in pseudocolor showing regions*

*of interest (ROIs) representing "tip-like" cells (red ROIs) or "inner" cells (gray ROIs) at the peak of AITC-induced response (t = 375 seconds as indicated in panel c, dotted line). Middle panel: each trace represents the ratio (340/380 nm) of a single cell in the field from one representative experiment (n = 5 experiments). Lower panel: bar plot showing peak amplitude of AITC-mediated Ca^{2+} responses (median ± 95% CI of different cells in the field from 5 independent experiments). Statistical significance and **: p-value < 0.01 (Mann-Whitney test).* ***(c)*** *Representative images of hTERT PTEC plated on Matrigel/collagen substrate showing phase contrast (upper panel), DAPI (middle panel) and TRPA1 expression in green (lower panel).*

For this purpose we performed Ca^{2+} imaging experiments on hTERT PTEC forming capillary-like structures. Interestingly we observed a specific distribution of TRPA1 activity in hTERT PTEC plated on Matrigel/collagen substrate as compared to 2D culture dishes (Figure 8b). 20 µM AITC induced a strong increase in $[Ca^{2+}]_i$ only in cells engaged in migration (here called "tip-like" cells to recall "tip" cell organization in vessel morphogenesis, Figure 8b,c). These data are in agreement with the role of TRPA1 in vessel morphogenesis and cell migration suggesting an active role for the channel in sprouting angiogenesis and tip cells activation.

Discussion

The present study provides a full TRP channel expression signature in TECs from PCa by shedding light on their expression profile and the role of the most prominent TRP channels in tumor angiogenesis. We identified four '*prostate-associated*' genes (i.e., *trpa1*, *trpv2*, *trpc3,* and *trpc6*), which were deregulated in previously isolated and characterized PTEC [18] compared to those in ECs derived from the healthy prostate. Among them, three '*prostate-associated*' channels (TRPA1, TRPV2, and TRPC3) were overexpressed during PCa angiogenesis and showed proangiogenic activity by exerting effects on the principal EC properties during angiogenesis, particularly EC proliferation, to support sprout formation, directed motility guiding, sprout elongation and in vitro and in vivo morphogenesis regulation.

The study of global changes in *trp* channel expression patterns during physiopathological transitions and disease progression is important for understanding the development of many pathologies, such as cancer [16]. Moreover, a molecular trp signature of a particular cancer could represent a promising prognostic tool for several cancer types. In this regard, several studies have been recently performed, and microarray-assisted expression profiling has identified several ion channel genes (including *trp* channels) to be differentially expressed in tumor tissues relative to those in normal tissues and to contribute to various

extents to pathophysiological hallmarks in breast cancer [23], lung adenocarcinoma [24], glioma [25] or pancreatic ductal adenocarcinoma [26].

Here, we show that TRPV2 is a positive modulator of TEC viability, since LPC-mediated activation of endogenous TRPV2 in PTEC resulted in increased viability and proliferation, and downregulation of the channel by siRNA transfection reverted this effect. These data underline a basal role for TRPV2 even in the absence of agonist stimulation. We confirm the different patterns of *trpv2* mRNA expression obtained by qPCR in PCa vessels by immunohistochemistry on tissues obtained from radical prostatectomies in patients (7 cases out of 10). Even though TRPV2 transcript expression has been reported in human pulmonary artery [27] and umbilical vein [28] ECs, its role in these cells is not described. In circulatory organs, TRPV2 is mainly expressed in smooth muscle cells and participates in mechanosensation [28]. Our study showed, for the first time, a role for TRPV2 in tumor angiogenesis by clearly demonstrating the channel as a positive modulator of EC viability and proliferation. TRPV2 has been previously indirectly implicated in angiogenesis since activation of the channel in fibroblasts by its synthetic cannabinoid agonist (O-1821) was correlated with altered angiogenesis in a mouse model of arthritis [29]. The proangiogenic role we described here for TRPV2 adds another aspect to the tumorigenic properties of TRPV2, since this channel has been positively correlated with tumor progression to the castration-resistant phenotype in PCa [11] and with tumor grade and stage in bladder cancer [30]. In both these urogenital cancers, basal and agonist-induced activity of TRPV2 increased the migratory potential of cancer cells. Lysophospholipids and adrenomedullin stimulate insertion of the channel into the plasma membrane, and the subsequent TRPV2-mediated Ca^{2+} influx increases invasiveness of tumor cells via the direct regulation of key proteases such as MMP2, MMP9, and cathepsin B [11,31,32]. However, in this study, we demonstrated that TRPV2 activation can result in different physiological effects depending on the cell type, since activation of endothelial TRPV2 enhanced cell proliferation rather than cell motility. Because agonists of TRPV2 are implicated not only in tumor progression but also in angiogenesis [33–36, we can speculate that TRPV2 activity could be targeted in both TECs and normal ECs. The use of TRPV2 as an antitumor target is certainly an exciting prospect in drug research but should be considered with caution for cancers other than PCa.

The tumor microenvironment, including the vascular endothelium, plays a critical role in the different phases of tumor progression leading to invasion. The crosstalk between cancer cells and ECs is therefore crucial for both angiogenesis and cancer invasion. Several studies have reported the importance of endothelial-mediated release of growth factors in cancer chemoattraction. In this regard, TECs have been shown to exert a chemoattractive effect on cancer cells, thus guiding cancer cell metastasis in different cancer types [22,37,38]. In line with this, in directed migration experiments, we demonstrate that compared to normal HMEC, PTEC have a strong effect on PCa cell attraction. Our results indicate that this effect may be

due to the expression of TRPC3, which is maintained at high levels in PTEC and downregulated in HMECs. Consistent with this observation, TRPC3 (but not TRPA1 or TRPV2) overexpression in HMEC induced an increase in cell attraction compared to that in control cells. Additionally, PTEC conditioned medium but not HMEC conditioned medium attracted PC3 in directional migration experiments. Moreover, similarly to PTEC conditioned medium, conditioned medium from TRPC3-overexpressing HMECs promoted directional migration of PC3 cells. Although the molecular mechanism underlying EC-driven crosstalk with cancer cells has not been elucidated and requires further studies, we can speculate that TRPC3-mediated Ca^{2+} signaling in TECs may promote the release of growth factors or chemokines, which in turn promote cancer cell migration, as Ca^{2+} signals are known as key players in EC activation in the tumor microenvironment, one of the most relevant steps in tumor progression [4,39].

Finally, we demonstrate that TRPA1 is an important positive modulator of vessel morphogenesis, activating sprouting angiogenesis in vivo and EC migration and tubulogenesis in vitro. We show that endogenous TRPA1 increased wound healing in PTEC and that this effect was inhibited with the downregulation of the channel by siRNA transfection. In line with this, TRPA1 overexpression in HMECs increased cell migration and tubulogenesis in vitro. Most importantly, TRPA1 activation increased angiogenesis in mouse retina, while pharmacological inhibition of TRPA1 caused a decrease in the number of retinal tip cells. Interestingly, the role of Ca^{2+} signals in sprouting angiogenesis has been recently reported in vivo in a zebrafish model [40]. Yokota and coworkers visualized Ca^{2+} dynamics in ECs during sprouting angiogenesis in zebrafish, demonstrating that intracellular Ca^{2+} oscillations occur in ECs exhibiting angiogenic behavior. Dll4/Notch signaling regulates these Ca^{2+} oscillations and is required for the selection of stalk and tip cells during both arterial and venous sprouting [40]. Although whether Dll4/Notch signaling regulates Ca^{2+} stores or Ca^{2+} channels directly or not remains to be delineated, our study suggests TRPA1 as a possible mediator of this pathway, as its activation is clearly involved in vessel sprouting in vivo. In line with these observations we have shown here that TRPA1 agonist induced a strong increase in $[Ca^{2+}]i$ only in cells engaged in migration which we could call “tip-like” cells to recall “tip” cell organization in vessel morphogenesis. These data suggest an active role for the channel in sprouting angiogenesis and tip cells activation. Moreover endothelial TRPA1, it has been previously shown to be selectively expressed in cerebral arteries where it plays a role in vasodilation [41]. Indeed, Ca^{2+} influx via endothelial TRPA1 channels elicits vasodilation in cerebral arteries by a mechanism involving Ca^{2+}-activated K^+ channels and inwardly rectifying K^+ channels in rat myocytes [42]. TRPA1 has also been recently shown to be involved in PCa growth, as its activation by triclosan, a well-established endocrine disruptor, resulted in cytosolic Ca^{2+} influx inducing VEGF secretion by stromal cells, which in turn stimulated epithelial cell proliferation [43]. Moreover, TRPA1 activation by resveratrol induces Ca^{2+} entry, leading to growth factor expression, possibly via the Calcineurin/NFAT

pathway, and secretion of HGF and VEGF, which modulate PCa cell growth, migration and resistance to apoptosis [44].

In summary, we performed a complete expression profiling and functional screening that clearly identified four '*prostate-associated*' genes that are deregulated during PCa vascularization, three of which play profound effects on EC biology. In particular, three out of the selected '*prostate-associated*' channels are overexpressed in PCa ECs and have marked effects on the main EC properties including proliferation (TRPV2), TEC-mediated crosstalk with cancer cells (TRPC3) and angiogenesis (TRPA1). The expression profile and functional data could indeed explain the specific transition of PCa to its aggressive phenotype. PTEC have been previously shown to exhibit aggressive phenotypes typical of TECs: indeed, PTEC have a higher migration rate than normal HMECs and are able to form capillary-like structures both in vitro and in xenografts in SCID mice [18]. These results could be of great importance to explain, at least part, the aggressive phenotype previously observed in PTEC relative to that in normal HUVEC and HMEC [18] and provide new putative therapeutic targets.

Conclusions

We performed a complete expression profiling and functional screening that clearly identified four '*prostate-associated*' genes that are deregulated during PCa vascularization, three of which have profound effects on EC biology. In particular, three out of the selected '*prostate-associated*' channels are overexpressed in PCa ECs and have marked effects on the main EC properties including proliferation (TRPV2), TEC-mediated crosstalk with cancer cells (TRPC3) and angiogenesis (TRPA1). The expression profile and functional data could indeed explain the specific transition of PCa to its aggressive phenotype. PTEC have been previously shown to exhibit aggressive phenotypes typical of TECs: indeed, PTEC have a higher migration rate than normal HMECs and are able to form capillary-like structures both in vitro and in xenografts in SCID mice [18]. These results could be of great importance to explain, at least part, the aggressive phenotype previously observed in PTEC relative to that in normal HUVEC and HMEC [18] and provide new putative therapeutic targets.

Patents

The authors disclose the Report of Invention: "Set de oliginucleotides de qPCR pour l'établissement de profil d'expression du domaine fonctionnel des 26 canaux de type TRP" Reference # DSO2018005437),

Patent Pending (D.G., M.B., N.P.) and thus the exact primer sequences and positions under declaration of invention cannot be stated.

Author Contributions: Conceptualization, B.B., A.F.P. and D.G.; Data curation, M.B., G.C., A.B., G.P.G., G.T., L.A., A.H., T.G., A.J., V.M., G.F.-H., A.F.P. and D.G.; Formal analysis, M.B., G.C., A.B., G.P.G., G.T., A.H., G.M., T.G., A.J., V.M., G.F.-H., A.F.P. and D.G.; Funding acquisition, N.P., A.F.P. and D.G.; Investigation, M.B., A.B., G.P.G., G.T., A.F.P. and D.G.; Methodology, M.B., A.B., G.P.G. and G.T.; Project administration, D.G.; Resources, D.G.; Supervision, G.M., B.B., A.F.P. and D.G.; Validation, G.M. and D.G.; Visualization, M.B.; Writing—original draft, M.B., A.B., G.M., A.F.P. and D.G.; Writing—review & editing, L.M., B.B., A.F.P. and D.G.

Funding: This study was supported by grants from the Ministère de l'Education Nationale and the Institut National de la Santé et de la Recherche Medicale (INSERM). The research of MB, AFP, NP and DG was supported by the Institut National du Cancer (INCa- PLBIO14-213). The research of DG was supported by the Institut Universitaire de France (IUF), the Fondation ARC pour la recherche sur le cancer (PJA 20141202010) and the Association pour la Recherche sur les Tumeurs de la Prostate (ARTP). AFP was supported by AFP was supported by grants from the University of Torino and Compagnia di San Paolo (#Torino_call2014_L2_130); MB was supported by the 2012 and 2018 Université Franco Italienne "Vinci" programs. DG was supported by the SFFR (F 46.2/001). Bilille platform is supported by two investments for the Future Programmes (PIA): 'Institut Français de Bipinformatique' and 'France Genomique'.

Acknowledgments: The authors would like to thank Alexandre Bokhobza and Manon Clarisse (Inserm U1003, PHYCEL laboratory) for technical support, Thomas Guderman for kindly providing the mTRPM7 vectors, Thomas Voets for kindly proving us the hTRPV3, hTRPP3 and hTRPM4 vectors, Christian Harteneck for kindly providing the hTRPM1 and hTRPM3 vectors, and Indu Ambdukar for kindly providing the hTRPC1 vector. The manuscript was edited for English language, grammar, punctuation, spelling and overall style by native English speaking editors of American Journal Experts.

Conflicts of Interest: The authors declare no conflict of interest.

References

1. Clapham, D.E. TRP channels as cellular sensors. *Nature* **2003**, *426*, 517–524.
2. Fiorio Pla, A.; Gkika, D. Emerging role of TRP channels in cell migration: From tumor vascularization to metastasis. *Front. Physiol.* **2013**, *4*, 311, doi:10.3389/fphys.2013.00311.
3. Nilius, B.; Owsianik, G.; Voets, T.; Peters, J.A. Transient receptor potential cation channels in disease. *Physiol. Rev.* **2007**, *87*, 165–217.
4. Prevarskaya, N.; Skryma, R.; Shuba, Y. Ion Channels in Cancer: Are Cancer Hallmarks Oncochannelopathies? *Physiol. Rev.* **2018**, *98*, 559–621, doi:10.1152/physrev.00044.2016.
5. Pedersen, S.F.; Stock, C. Ion channels and transporters in cancer: Pathophysiology, regulation, and clinical potential. *Cancer Res.* **2013**, *73*, 1658–1661, doi:10.1158/0008-5472.CAN-12-4188.
6. Earley, S.; Brayden, J.E. Transient receptor potential channels in the vasculature. *Physiol. Rev.* **2015**, *95*, 645–690, doi:10.1152/physrev.00026.2014.
7. Park, Y.R.; Chun, J.N.; So, I.; Kim, H.J.; Baek, S.; Jeon, J.H.; Shin, S.Y. Data-driven Analysis of TRP Channels in Cancer: Linking Variation in Gene Expression to Clinical Significance. *Cancer Genom. Proteom.* **2016**, *13*, 83–90.
8. Tsavaler, L.; Shapero, M.H.; Morkowski, S.; Laus, R. Trp-p8, a novel prostate-specific gene, is up-regulated in prostate cancer and other malignancies and shares high homology with transient receptor potential calcium channel proteins. *Cancer Res.* **2001**, *61*, 3760–3769.

9. Noyer, L.; Grolez, G.P.; Prevarskaya, N.; Gkika, D.; Lemonnier, L. TRPM8 and prostate: A cold case? *Pflug. Arch.* **2018**, doi:10.1007/s00424-018-2169-1.
10. Bidaux, G.; Flourakis, M.; Thebault, S.; Zholos, A.; Beck, B.; Gkika, D.; Roudbaraki, M.; Bonnal, J.L.; Mauroy, B.; Shuba, Y.; et al. Prostate cell differentiation status determines transient receptor potential melastatin member 8 channel subcellular localization and function. *J. Clin. Investig.* **2007**, *117*, 1647–1657, doi:10.1172/JCI30168.
11. Monet, M.; Lehen'kyi, V.; Gackiere, F.; Firlej, V.; Vandenberghe, M.; Roudbaraki, M.; Gkika, D.; Pourtier, A.; Bidaux, G.; Slomianny, C.; et al. Role of cationic channel TRPV2 in promoting prostate cancer migration and progression to androgen resistance. *Cancer Res.* **2010**, *70*, 1225–1235, doi:10.1158/0008-5472.CAN-09-2205.
12. Lehen'kyi, V.; Flourakis, M.; Skryma, R.; Prevarskaya, N. TRPV6 channel controls prostate cancer cell proliferation via Ca^{2+}/NFAT-dependent pathways. *Oncogene* **2007**, *26*, 7380–7385, doi:10.1038/sj.onc.1210545.
13. Russo, G.; Mischi, M.; Scheepens, W.; De la Rosette, J.J.; Wijkstra, H. Angiogenesis in prostate cancer: Onset, progression and imaging. *BJU Int.* **2012**, *110*, E794–E808, doi:10.1111/j.1464-410X.2012.11444.x.
14. Wang, X.L.S.; Xia, S.; Jiang, Q.; Luo, J.; Li, L.; Yeh, S.; Chang, C. Endothelial cells enhance prostate cancer metastasis via IL-6→androgen receptor→TGF-β→MMP-9 signals. *Mol. Cancer Ther.* **2013**, *12*, 1026–1037, doi:10.1158/1535-7163.MCT-12-0895.
15. Genova, T.; Grolez, G.P.; Camillo, C.; Bernardini, M.; Bokhobza, A.; Richard, E.; Scianna, M.; Lemonnier, L.; Valdembri, D.; Munaron, L.; et al. TRPM8 inhibits endothelial cell migration via a non-channel function by trapping the small GTPase Rap1. *J. Cell Biol.* **2017**, *216*, 2107–2130, doi:10.1083/jcb.201506024.
16. Bernardini, M.; Fiorio Pla, A.; Prevarskaya, N.; Gkika, D. Human transient receptor potential (TRP) channel expression profiling in carcinogenesis. *Int. J. Dev. Biol.* **2015**, *59*, 399–406, doi:10.1387/ijdb.150232dg.
17. Thoppil, R.J.; Cappelli, H.C.; Adapala, R.K.; Kanugula, A.K.; Paruchuri, S.; Thodeti, C.K. TRPV4 channels regulate tumor angiogenesis via modulation of Rho/Rho kinase pathway. *Oncotarget* **2016**, *7*, 25849–25861, doi:10.18632/oncotarget.8405.
18. Fiorio Pla, A.; Brossa, A.; Bernardini, M.; Genova, T.; Grolez, G.; Villers, A.; Leroy, X.; Prevarskaya, N.; Gkika, D.; Bussolati, B. Differential sensitivity of prostate tumor derived endothelial cells to sorafenib and sunitinib. *BMC Cancer* **2014**, *14*, 939, doi:10.1186/1471-2407-14-939.
19. Grange, C.; Bussolati, B.; Bruno, S.; Fonsato, V.; Sapino, A.; Camussi, G. Isolation and characterization of human breast tumor-derived endothelial cells. *Oncol. Rep.* **2006**, *15*, 381–386.
20. Bussolati, B.; Deambrosis, I.; Russo, S.; Deregibus, M.C.; Camussi, G. Altered angiogenesis and survival in human tumor-derived endothelial cells. *FASEB J.* **2003**, *17*, 1159–1161, doi:10.1096/fj.02-0557fje.
21. Eilken, H.M.; Adams, R.H. Dynamics of endothelial cell behavior in sprouting angiogenesis. *Curr. Opin. Cell Biol.* **2010**, *22*, 617–625, doi:10.1016/j.ceb.2010.08.010.
22. Sun, L.; Pan, J.; Yu, L.; Liu, H.; Shu, X.; Sun, L.; Lou, J.; Yang, Z.; Ran, Y. Tumor endothelial cells promote metastasis and cancer stem cell-like phenotype through elevated Epiregulin in esophageal cancer. *Am. J. Cancer Res.* **2016**, *6*, 2277–2288.
23. Ko, J.H.; Ko, E.A.; Gu, W.; Lim, I.; Bang, H.; Zhou, T. Expression profiling of ion channel genes predicts clinical outcome in breast cancer. *Mol. Cancer* **2013**, *12*, 106, doi:10.1186/1476-4598-12-106.
24. Ko, J.H.; Gu, W.; Lim, I.; Bang, H.; Ko, E.A.; Zhou, T. Ion channel gene expression in lung adenocarcinoma: Potential role in prognosis and diagnosis. *PLoS ONE* **2014**, *9*, e86569, doi:10.1371/journal.pone.0086569.
25. Wang, R.; Gurguis, C.I.; Gu, W.; Ko, E.A.; Lim, I.; Bang, H.; Zhou, T.; Ko, J.H. Ion channel gene expression predicts survival in glioma patients. *Sci. Rep.* **2015**, *5*, 11593, doi:10.1038/srep11593.
26. Zaccagnino, A.; Pilarsky, C.; Tawfik, D.; Sebens, S.; Trauzold, A.; Novak, I.; Schwab, A.; Kalthoff, H. In silico analysis of the transportome in human pancreatic ductal adenocarcinoma. *Eur. Biophys. J.* **2016**, *45*, 749–763, doi:10.1007/s00249-016-1171-9.
27. Fantozzi, I.; Zhang, S.; Platoshyn, O.; Remillard, C.V.; Cowling, R.T.; Yuan, J.X. Hypoxia increases AP-1 binding activity by enhancing capacitative Ca^{2+} entry in human pulmonary artery endothelial cells. *Am. J. Physiol. Lung Cell. Mol. Physiol.* **2003**, *285*, L1233–L1245, doi:10.1152/ajplung.00445.2002.
28. Muraki, K.; Shigekawa, M.; Imaizumi, Y. A New Insight into the Function of TRPV2 in Circulatory Organs. In *TRP Ion Channel Function in Sensory Transduction and Cellular Signaling Cascades*; Liedtke, W.B., Heller, S., Eds.; CRC Press: Boca Raton, FL, USA, 2007.
29. Laragione, T.; Cheng, K.F.; Tanner, M.R.; He, M.; Beeton, C.; Al-Abed, Y.; Gulko, P.S. The cation channel Trpv2 is a new suppressor of arthritis severity, joint damage, and synovial fibroblast invasion. *Clin. Immunol.* **2015**, *158*, 183–192, doi:10.1016/j.clim.2015.04.001.

30. Caprodossi, S.; Lucciarini, R.; Amantini, C.; Nabissi, M.; Canesin, G.; Ballarini, P.; Di Spilimbergo, A.; Cardarelli, M.A.; Servi, L.; Mammana, G.; et al. Transient Receptor Potential Vanilloid Type 2 (TRPV2) Expression in Normal Urothelium and in Urothelial Carcinoma of Human Bladder: Correlation with the Pathologic Stage. *Eur. Urol.* **2008**, *54*, 612–620.
31. Monet, M.; Gkika, D.; Lehen'kyi, V.; Pourtier, A.; Vanden Abeele, F.; Bidaux, G.; Juvin, V.; Rassendren, F.; Humez, S.; Prevarskaya, N. Lysophospholipids stimulate prostate cancer cell migration via TRPV2 channel activation. *Biochim. Biophys. Acta* **2009**, *1793*, 528–539, doi:10.1016/j.bbamcr.2009.01.003.
32. Oulidi, A.; Bokhobza, A.; Gkika, D.; Vanden Abeele, F.; Lehen'kyi, V.; Ouafik, L.; Mauroy, B.; Prevarskaya, N. TRPV2 Mediates Adrenomedullin Stimulation of Prostate and Urothelial Cancer Cell Adhesion, Migration and Invasion. *PLoS ONE* **2013**, *8*, e64885, doi:10.1371/journal.pone.0064885.
33. Benyahia, Z.; Dussault, N.; Cayol, M.; Sigaud, R.; Berenguer-Daize, C.; Delfino, C.; Tounsi, A.; Garcia, S.; Martin, P.M.; Mabrouk, K.; et al. Stromal fibroblasts present in breast carcinomas promote tumor growth and angiogenesis through adrenomedullin secretion. *Oncotarget* **2017**, *8*, 15744–15762, doi:10.18632/oncotarget.14999.
34. Linkous, A.G.; Yazlovitskaya, E.M.; Hallahan, D.E. Cytosolic phospholipase A2 and lysophospholipids in tumor angiogenesis. *J. Natl. Cancer Inst.* **2010**, *102*, 1398–1412, doi:10.1093/jnci/djq290.
35. Ochoa-Callejero, L.; Pozo-Rodrigalvarez, A.; Martinez-Murillo, R.; Martinez, A. Lack of adrenomedullin in mouse endothelial cells results in defective angiogenesis, enhanced vascular permeability, less metastasis, and more brain damage. *Sci. Rep.* **2016**, *6*, 33495, doi:10.1038/srep33495.
36. Yamada, T.; Ueda, T.; Shibata, Y.; Ikegami, Y.; Saito, M.; Ishida, Y.; Ugawa, S.; Kohri, K.; Shimada, S. TRPV2 activation induces apoptotic cell death in human T24 bladder cancer cells: A potential therapeutic target for bladder cancer. *Urology* **2010**, *76*, 509, doi:10.1016/j.urology.2010.03.029.
37. Feng, T.; Yu, H.; Xia, Q.; Ma, Y.; Yin, H.; Shen, Y.; Liu, X. Cross-talk mechanism between endothelial cells and hepatocellular carcinoma cells via growth factors and integrin pathway promotes tumor angiogenesis and cell migration. *Oncotarget* **2017**, *8*, 69577–69593, doi:10.18632/oncotarget.18632.
38. Warner, K.A.; Miyazawa, M.; Cordeiro, M.M.; Love, W.J.; Pinsky, M.S.; Neiva, K.G.; Spalding, A.C.; Nor, J.E. Endothelial cells enhance tumor cell invasion through a crosstalk mediated by CXC chemokine signaling. *Neoplasia* **2008**, *10*, 131–139.
39. Lastraioli, E.; Iorio, J.; Arcangeli, A. Ion channel expression as promising cancer biomarker. *Biochim. Biophys. Acta* **2015**, *1848*, 2685–2702, doi:10.1016/j.bbamem.2014.12.016.
40. Yokota, Y.; Nakajima, H.; Wakayama, Y.; Muto, A.; Kawakami, K.; Fukuhara, S.; Mochizuki, N. Endothelial Ca^{2+} oscillations reflect VEGFR signaling-regulated angiogenic capacity in vivo. *Elife* **2015**, *4*, doi:10.7554/eLife.08817.
41. Yanaga, A.; Goto, H.; Nakagawa, T.; Hikiami, H.; Shibahara, N.; Shimada, Y. Cinnamaldehyde induces endothelium-dependent and -independent vasorelaxant action on isolated rat aorta. *Biol. Pharm. Bull.* **2006**, *29*, 2415–2418.
42. Earley, S.; Gonzales, A.L.; Crnich, R. Endothelium-dependent cerebral artery dilation mediated by TRPA1 and Ca^{2+}-Activated K^+ channels. *Circ. Res.* **2009**, *104*, 987–994, doi:10.1161/CIRCRESAHA.108.189530.
43. Derouiche, S.; Mariot, P.; Warnier, M.; Vancauwenberghe, E.; Bidaux, G.; Gosset, P.; Mauroy, B.; Bonnal, J.L.; Slomianny, C.; Delcourt, P.; et al. Activation of TRPA1 Channel by Antibacterial Agent Triclosan Induces VEGF Secretion in Human Prostate Cancer Stromal Cells. *Cancer Prev. Res.* **2017**, *10*, 177–187, doi:10.1158/1940-6207.CAPR-16-0257.
44. Vancauwenberghe, E.; Noyer, L.; Derouiche, S.; Lemonnier, L.; Gosset, P.; Sadofsky, L.R.; Mariot, P.; Warnier, M.; Bokhobza, A.; Slomianny, C.; et al. Activation of mutated TRPA1 ion channel by resveratrol in human prostate cancer associated fibroblasts (CAF). *Mol. Carcinog.* **2017**, *56*, 1851–1867, doi:10.1002/mc.22642.
45. Deregibus, M.C.; Cantaluppi, V.; Calogero, R.; Lo Iacono, M.; Tetta, C.; Biancone, L.; Bruno, S.; Bussolati, B.; Camussi, G. Endothelial progenitor cell derived microvesicles activate an angiogenic program in endothelial cells by a horizontal transfer of mRNA. *Blood* **2007**, *110*, 2440–2448, doi:10.1182/blood-2007-03-078709.
46. Cassoni, P.; Marrocco, T.; Bussolati, B.; Allia, E.; Munaron, L.; Sapino, A.; Bussolati, G. Oxytocin induces proliferation and migration in immortalized human dermal microvascular endothelial cells and human breast tumor-derived endothelial cells. *Mol. Cancer Res.* **2006**, *4*, 351–359, doi:10.1158/1541-7786.MCR-06-0024.
47. Fonsato, V.; Buttiglieri, S.; Deregibus, M.C.; Puntorieri, V.; Bussolati, B.; Camussi, G. Expression of Pax2 in human renal tumor-derived endothelial cells sustains apoptosis resistance and angiogenesis. *Am. J. Pathol.* **2006**, *168*, 706–713, doi:10.2353/ajpath.2006.050776.
48. Counter, C.M.; Hahn, W.C.; Wei, W.; Caddle, S.D.; Beijersbergen, R.L.; Lansdorp, P.M.; Sedivy, J.M.; Weinberg, R.A. Dissociation among in vitro telomerase activity, telomere maintenance, and cellular immortalization. *Proc. Natl. Acad. Sci. USA* **1998**, *95*, 14723–14728.

49. Gkika, D.; Lemonnier, L.; Shapovalov, G.; Gordienko, D.; Poux, C.; Bernardini, M.; Bokhobza, A.; Bidaux, G.; Degerny, C.; Verreman, K.; et al. TRP channel-associated factors are a novel protein family that regulates TRPM8 trafficking and activity. *J. Cell Biol.* **2015**, *208*, 89–107, doi:10.1083/jcb.201402076.
50. Fiorio Pla, A.; Ong, H.L.; Cheng, K.T.; Brossa, A.; Bussolati, B.; Lockwich, T.; Paria, B.; Munaron, L.; Ambudkar, I.S. TRPV4 mediates tumor-derived endothelial cell migration via arachidonic acid-activated actin remodeling. *Oncogene* **2012**, *31*, 200–212, doi:10.1038/onc.2011.231.
51. Li, J.; Shi, Y.; Toga, A.W. Controlling False Discovery Rate in Signal Space for Transformation-Invariant Thresholding of Statistical Maps. *Inf. Process. Med. Imaging* **2015**, *24*, 125–136, doi:10.1007/978-3-319-19992-4_10.

© 2019 by the authors. Licensee MDPI, Basel, Switzerland. This article is an open access article distributed under the terms and conditions of the Creative Commons Attribution (CC BY) license (http://creativecommons.org/licenses/by/4.0/).

Supplementary Materials

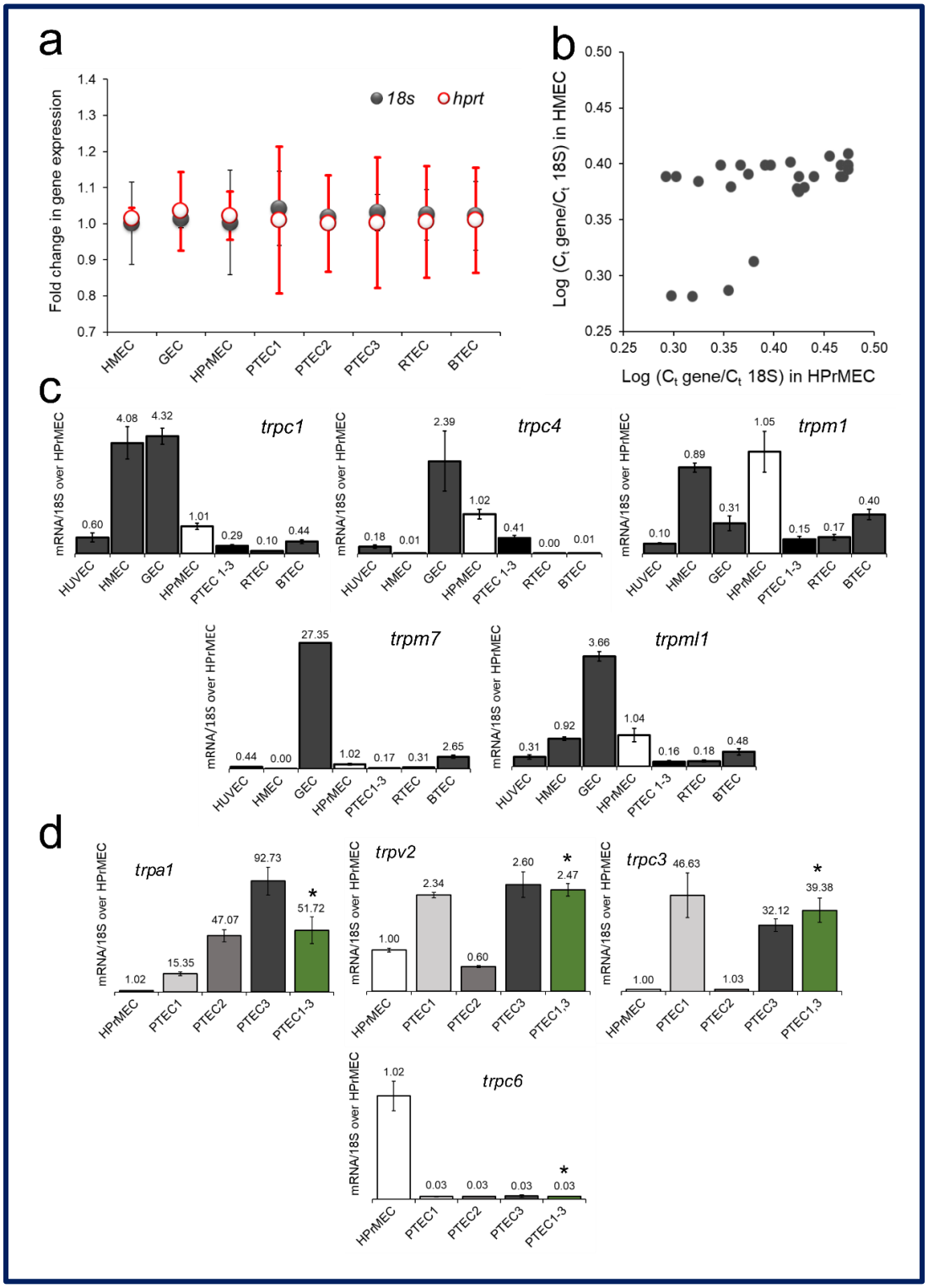

Figure 1S. Assessment of external and internal controls of real-time qPCR used for the normalization of expression data.

(a) *Bar plot showing the relative amount of 18s and hprt mRNAs in normal ECs (HMEC, GEC, and HPrMEC), and in TECs (PTEC1, PTEC2, PTEC3, RTECs, and BTEC). Values are expressed as the mean DDCT values ± SEM of at least three independent experiments.* ***(b)*** *Scatter plots showing the mRNA expression profiles of HPrMEC and HMEC for trp channels, as determined by real-time qPCR. Correlation values for trp channels are expressed as* $Log\ (\frac{C_{T,gene\ x}}{C_{T,18s}})$ *in normal primary HPrMEC (x-axis) and normal HMEC (y-axis).* ***(c)*** *Real-time qPCR analysis of mRNA expression showing that three trp genes (i.e., trpc1, trpc4, and trpml1) are downregulated in all TECs compared to their normal counterparts, while trpm1 is downregulated in PTEC and BTEC but upregulated in RTEC and trpm7 is downregulated in PTEC and RTEC but upregulated in BTEC. Values are expressed as the mean DDCT values ± SEM of at least three independent experiments.* ***(d)*** *mRNA expression profiles from real-time qPCR analysis normalized against the profile in HPrMEC. Values are expressed as the mean DDCT values±SEM. of at least three independent experiments. Statistical significance *: p-value<0.05.*

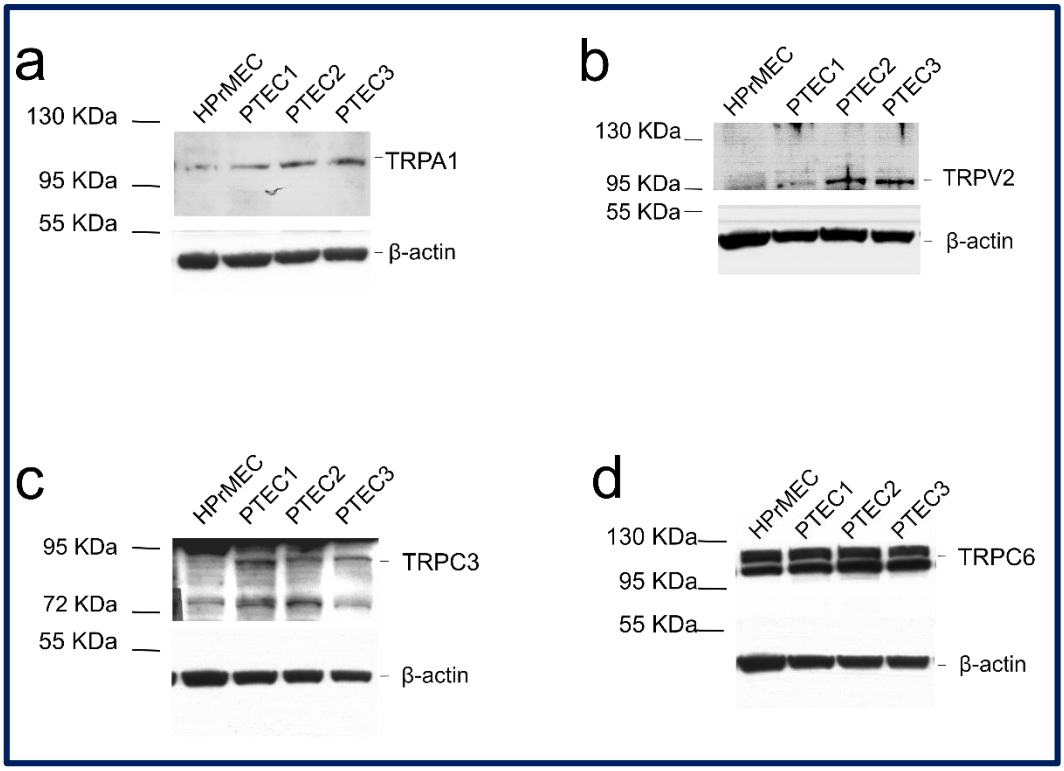

Figure 2S. Assessment of external and internal controls of real-time qPCR used for the normalization of expression.

Representative blots showing TRPA1 (n=2) ***(a)****, TRPV2 (n=4)* ***(b)****, TRPC3 (n=2)* ***(c)****, and TRPC6 (n=2)* ***(d)*** *expression in HPrMEC and PTEC3. Numbers represent quantification of channel expression relative to actin. TRPV2 and TRPC3 channels show differential expression in PTEC2 and PTEC3. In accordance with the mRNA expression data (****Fig. 2A****), compared to those in HPrMEC, TRPV2 and TRPC3 are downregulated in PTEC2 at protein level.*

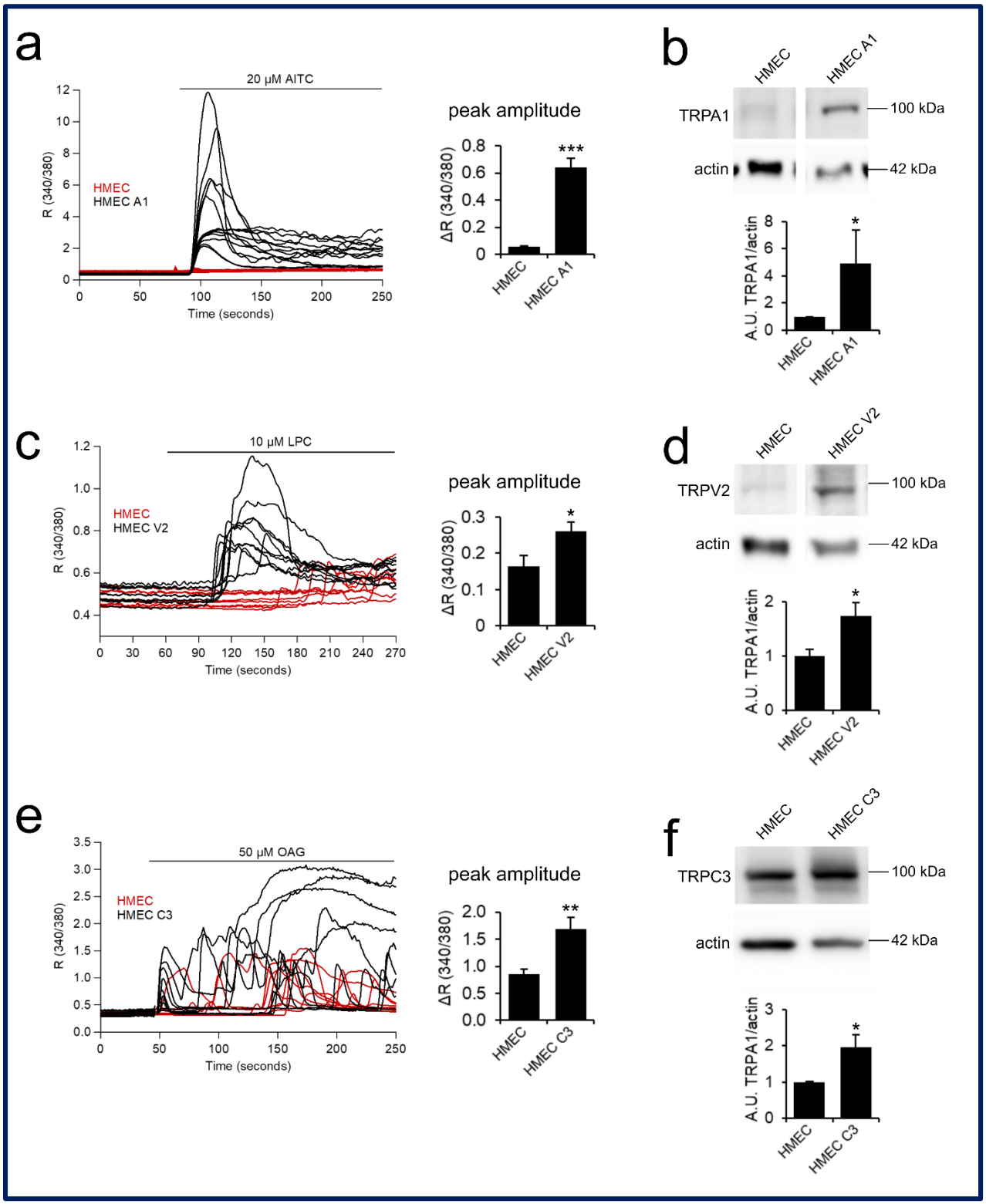

Figure 3S. hTERT PTEC characterization.

(a) *Representative cytofluorimetric analysis of the expression of endothelial markers (CD105, CD31, VEGFR1) in hTERT PTECs at passage 7.* ***(b)*** *Representative qPCR analysis of the expression of endothelial markers (CD31 and CD105) in*

control (total renal tumor cells, CNTRL), primary PTEC and hTERT PTEC at passage 7. ***(c)*** *hTERT PTEC show that hTERT mRNA is upregulated compared with that in wild-type PTECas detected by qPCR experiments.* ***(d)*** *Validation of 'prostate-specific' channels and androgen receptor (AR)* ***(e)*** *Cell viability experiments showed that hTERT PTEC are resistant to 1 µM sorafenib 48 hours after treatment. Proliferation was detected by MTS assays at 48 hours after transfection. Data represented the mean ± SEM of a minimum of three independent experiments. Statistical significance *: p-value<0.05.* ***(f)*** *expression in HMEC and hTERT PTEC. Actin (42 kDa) was used as a loading control.* ***(g)*** *Cell proliferation experiments showed that TRPV2 downregulation in hTERT PTEC significantly inhibits cell proliferation. Proliferation was detected by BrDU assays at 48 hours after siTRPV2 downregulation. Data represented the mean ± SEM of a minimum of three independent experiments. Statistical significance ***: p-value<0.0005.*

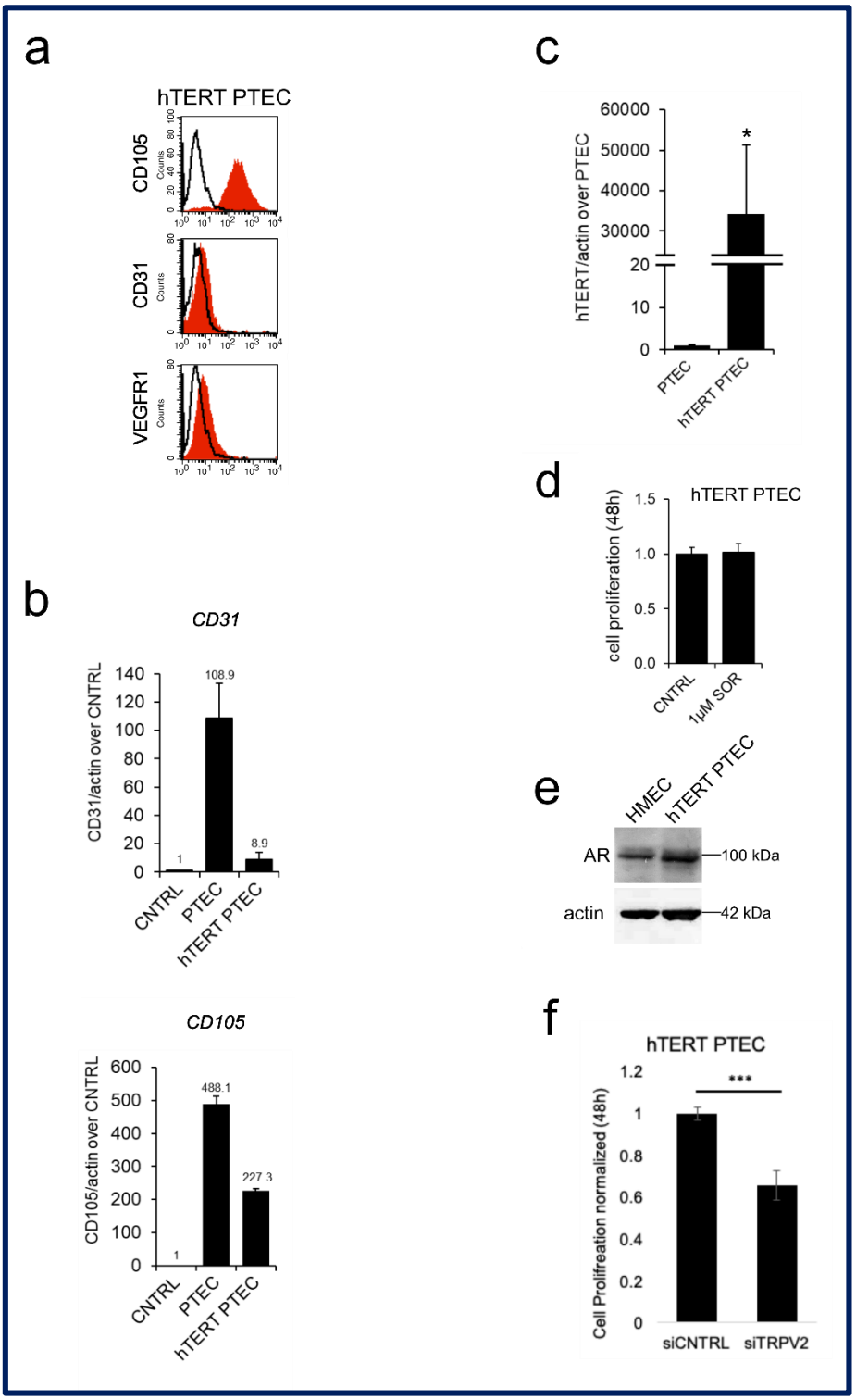

Figure 4S. Validation of 'prostate-specific' channel overexpression in HMECs for their functional characterization in ECs.

Each panel shows Ca^{2+} imaging and western blotting results, with relative quantifications, of control HMECs and HMECs overexpressing the 'prostate-specific' channels. As a control, HMEC were transfected with the empty vector. Ca^{2+} imaging experiments of control HMEC and HMEC-overexpressing the channels show differential channel activity. Peak amplitude

*was evaluated as the mean value±SEM recorded after channel activation with 20 µM AITC for TRPA1 (a) and 10 µM LPC for TRPV2 (c). For TRPC3 (e), each trace represents the ratio (340/380 nm) of a single cell in the field in one representative experiment recorded after channel activation with 50 µM OAG based on at least three independent experiments. Calcium imaging was performed 24 and 48 hours after transfection. (b, d and f) Western blots show one representative experiment performed 24 hours after transfection. Relative quantifications are the mean ± SEM of at least three independent experiments. Statistical significance *: p-value<0.05, **: p-value<0.005 and ***: p-value<0.0005 vs HMECs.*

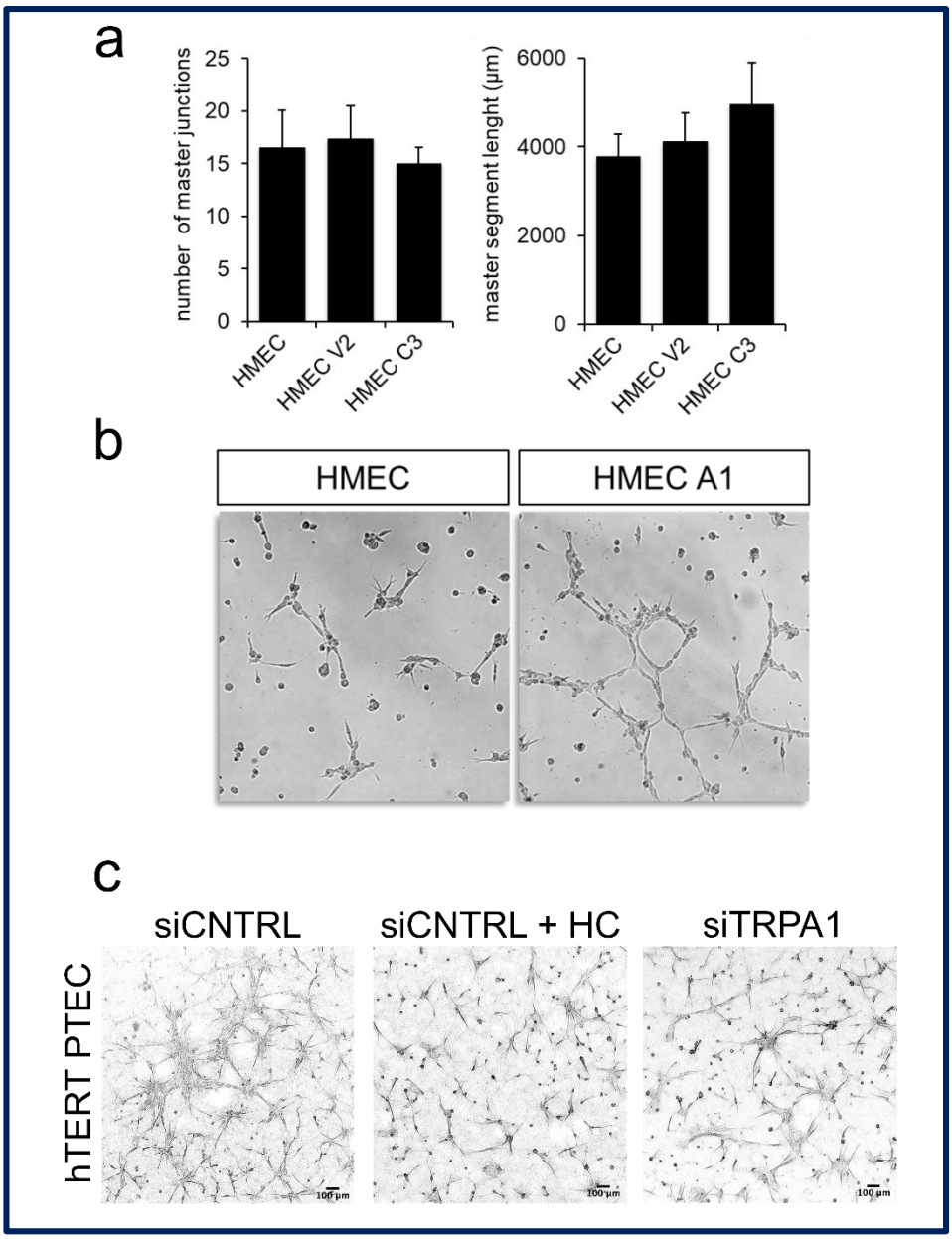

Figure 5S. Validation of 'prostate-specific' channel in tubulogenesis in vitro.

(a) Among all the 'prostate-specific' channels, no effect on the capillary-like structure formation was observed for TRPV2- or TRPC3-overexpressing HMECs compared to control cells. Bar graphs show the quantification of total master segment

length and the number of master junctions of control HMEC and TRPV2- or TRPC3-overexpressing HMEC. Three independent experiments were performed 24 hours after transfection. (b) representative images of CNTRL or TRPA1-overexpressing HMEC 20h after Matrigel seeding; (c) representative images of CNTRL or TRPA1-downregulating hTERT PTEC 20h after Matrigel/collagenI substrate seeding .

3.1.2 Role of TRPM8 in prostate cancer invasion

"TRPM8-Rap1A interaction sites as critical determinants for adhesion and migration of prostate and other epithelial cancer cells"

Giorgia Chinigò[1,2], Guillaume Paul Grolez[2], Madelaine Audero[1,2], Alexandre Bokhobza[2], Michela Bernardini[1], Julien Cicero[3,4], Robert Alain Toillon[3], Quentin Bailleul[2], Luca Visentin[1], Federico Alessandro Ruffinatti[1], Guillaume Brysbaert[5], Marc Lensink[5], Jerome De-Ruyck[5], Anna Rita Cantelmo[2], &, Alessandra Fiorio Pla[1,2,#] and Dimitra Gkika[3,6,7,#,*]

[1] Department of Life Sciences and Systems Biology, University of Torino, 10123 Torino, Italy

[2] INSERM, U1003 - PHYCEL - Physiologie Cellulaire, University of Lille, F-59000 Lille, France

[3] CNRS, INSERM, CHU Lille, Centre Oscar Lambret, UMR 9020-UMR 1277-Canther-Cancer Heterogeneity, Plasticity and Resistance to Therapies, University of Lille, F-59000 Lille, France

[4] UR 2465 – Laboratoire de la Barrière Hémato-Encéphalique (LBHE), University of Artois, F-62300 Lens, France

[5] CNRS, UMR 8576 - UGSF - Unité de Glycobiologie Structurale et Fonctionnelle, University of Lille, F-59000 Lille, France

[6] Department of Molecular and Cell Biology, University of California, Berkeley, Berkeley, CA

[7] Institut Universitaire de France (IUF)

[&] current position: INSERM, U1011-EGID, CHU Lille, Institute Pasteur de Lille, University of Lille, F-59000 Lille, France

[#] equal contribution

[*] Correspondence: dimitra.gkika@univ-lille.fr; Tel.: +33-3-20-43-68-38

Chinigò *et al.*, *Cancers* 2022, 14(9):2261

Abstract

Emerging evidence indicates that TRPM8 channel plays an important role in prostate cancer (PCa) progression, by impairing the motility of these cancer cells. Here, we reveal a novel facet of PCa motility control via direct protein-protein interaction (PPI) of the channel with the small GTPase Rap1A. Functional interaction of the two proteins was assessed by active Rap1 pull-down assays and live-cell imaging experiments. Molecular modelling analysis allowed the identification of four putative residues involved in TRPM8-Rap1A interaction. Point mutations of these sites impaired PPI as shown by GST-pull-down, co-immunoprecipitation, and PLA experiments and revealed their key functional role in the adhesion and migration of PC3 prostate cancer cells. More precisely, TRPM8 inhibits cell migration and adhesion by trapping Rap1A in its GDP-bound inactive form, thus preventing its activation at the plasma membrane. In particular, residues E207 and Y240 in the sequence of TRPM8 and Y32 in that of Rap1A are critical for the interaction between the two proteins not only in PC3 cells but also in cervical (HeLa) and breast (MCF-7) cancer cells. This study deepens our knowledge on the mechanism through which TRPM8 would exert a protective role in cancer progression and provides new insights on the possible use of TRPM8 as a new therapeutic target in cancer treatment.

Keywords: prostate cancer; metastasis; TRPM8; Rap1A; migration; adhesion; GTPase; calcium channel

Introduction

Prostate cancer (PCa) is the most frequently diagnosed cancer among men and the second leading cause of cancer death after lung cancer [1]. PCa poor prognosis is mainly due to metastases. Hence, there is an urgent need to deepen our knowledge on the mechanisms through which the primary tumour can acquire more aggressive phenotypes and therefore the ability to exit the primary site and establish secondary growth in distant organs through lymphatic or blood circulation. Metastasis fundamentally involves cell migration, a complex and multistep process which subtends coordination between cytoskeleton remodelling, cell-substrate adhesion/detachment, and cellular protrusion/contraction [2,3].

Over the past two decades, an increasing set of data has revealed a pivotal role of ion channels, including TRP channels, in many processes underlying the metastatic cascade, making them promising candidates as both molecular biomarkers and therapeutic targets in cancer therapy [4–9]. More specifically, marked changes in TRP proteins expression have been associated with the development and progression of several

cancers depending on their stage [6,10,11]. Interestingly, although most of the best-characterized roles played by TRP channels in the metastatic cascade rely on their channel activity [12], there is growing evidence of pathways that underlie the interaction of TRP channels with different partner proteins, extending interest in TRPs beyond the field of ion channels [13–20]. In this context, particular attention has been paid to the close bidirectional interplay revealed by TRP channels and small GTPase in all phases of the metastatic cascade, including migration, invasion, and tumor vascularization [21]. In most cases, this functional interplay is mediated by calcium (Ca^{2+}) signals, triggered by TRP-mediated Ca^{2+} influx within the cell, which may affect small GTPases activity and their impact on the regulation of cell migration and/or invasion [22–32]. In turn, small GTPase may regulate TRP channels intracellular trafficking to the plasma membrane (PM) or act directly on channel gating, thus impacting their biological functions [22,23,31,33–35]. However, some data revealed alternative regulatory pathways independent of cation homeostasis, through which TRP-small GTPase interplay may affect cancer progression [33,35–37].

Among TRP channels, TRPM8 is one of the most intriguing TRP channels involved in PCa progression, due to its specific and characteristic expression profile. Indeed, *TRPM8* expression was shown to increase in both benign prostate hyperplasia (BPH) and in prostate carcinoma cells characterized by high androgen levels [38], but decrease with tumour progression to the late androgen-insensitive invasive stage [39,40]. This specific expression pattern is attributable to an androgen-dependent regulation of *TRPM8* [41,42]. More specifically, *TRPM8* turned out to be a primary androgen response gene [42,43], since testosterone androgen-receptor complex (AR) is able to directly promote *TRPM8* transcription by binding with androgen-responsive elements present on its gene sequence. Besides the androgen-dependent transcription, testosterone exerts an additional non-genomic rapid effect on TRPM8 channel activity through the AR and translocation of the two proteins in lipid rafts [41]. More specifically, it has been shown that at low concentration, testosterone can promote the physical interaction between TRPM8 and AR within lipid rafts on the PM and consequently an increased AR-mediated inhibition of TRPM8 activity [41]. Consequently, the anti-androgen therapy by downregulating the expression of AR not only greatly reduces the expression of TRPM8 but it also affects the inhibitory action on the control of channel activity, leading PCa cells to an androgen-independent stage in which they relapse with a more aggressive phenotype [40,41]. Consistent with these data, we previously revealed a protective role played by TRPM8 in prostate cancer progression, thanks to its ability to inhibit PCa cells migration *in vitro* and *in vivo* [41,44–46]. Although some data suggest a role of the Ca^{2+}-dependent inactivation of the focal-adhesion kinases (FAK) [47], the exact molecular mechanism by which TRPM8 impairs the motility of epithelial prostate cancer cells is still unclear.

Interestingly, in a previous study, we unveiled that the anti-metastatic function of TRPM8 may be also extended to endothelial cells (ECs), suggesting a TRPM8 involvement also in the angiogenic process [48].

Indeed, endoplasmic reticulum (ER) TRPM8 expression in ECs inhibits cell migration via a direct binding with Rap1A with a subsequent inhibition of inside-out β_1-integrin signalling [48].

Here, we questioned whether the same molecular mechanism showed in ECs underlies the TRPM8-mediated inhibition of cell migration observed in epithelial prostate cancer cells. Previous evidence on TRPM8 interactors confirmed the presence of Rap1A among potential TRPM8 partner proteins in mouse prostate [45]. In this work, we demonstrated that in PCa cells TRPM8 exerts its anti-migratory function through a pore-independent pathway involving the binding to the inactive form of Rap1A and the subsequent inhibition of its activity in promoting cell adhesion. Furthermore, we deepened the TRPM8-Rap1A interaction, identifying and functionally validating the residues involved in its mediation on both fronts. Notably, this interesting new facet of TRPM8 as a Rap1 inhibitor is not limited to PCa but can be extended to other epithelial cancer cell lines. The complete characterization of the molecular mechanisms by which TRPM8 performs its anti-metastatic function could provide new and important insights in view of possible and successful use of TRPM8 as a pharmaceutical target in the treatment of advanced stages of metastatic cancer.

Materials and Methods

Chemicals and drugs

Icilin used as a specific TRPM8 agonist was purchased from Tocris (France), dissolved in DMSO to a final concentration of 20 mM, and stored at -20°C. Fura2-AM calcium probe used in Ca^{2+} imaging experiments was purchased from Invitrogen Ltd (United Kingdom), dissolved in DMSO to a final concentration of 1 mM, and stored at -20°C. Thapsigargin was purchased from Sigma Aldrich (Italy), dissolved in DMSO to a final concentration of 2 mM, and stored at -20°C.

Molecular modelling

As the N- and C-tail of TRPM8 structure was not totally solved by cryo-EM [49], we modelled this tetrameric structure by homology modelling. For this, BLASTP was used to obtain templates similar to the TRPM8 sequence. One template was identified with similarity of over 30% and corresponds to the cryo-EM structure of TRPA1 (Resolution: 4.2 Å, PDB ID: 3J9P) [50]. Using the sequence of TRPM8 and the identified templates, we performed the modelling of one monomer then the full tetrameric form using Modeller [51]. The global structure was subsequently minimized to remove steric clashes.

This model was further used to predict the interaction between TRPM8 and Rap1A, for which a crystal structure existed (Resolution: 1.9 Å, PDB ID: 1C1Y) [52]. This prediction was obtained using a protein-protein algorithm and more specifically the ClusPro2.0 [53] and InterEvDock [54] webservers. Seven residues at the interface between TRPM8 and Rap1A were visually selected, looking at the two first models of InterevDock and three among the five first best models of ClusPro 2 (TRPM8: Glu207, His259, Leu262, Tyr240, Val263; Rap1A: Lys31, Tyr32). For each model, a Residue Interaction Network (RIN) was generated with an in-house C program. A RIN is defined as a network in which each node is a residue, and each edge is a contact detected between two residues in the 3D structure. Here, residue-residue contacts were detected when the distance between them was found between 2.5 Å and 5 Å. Residue Centrality Analyses (RCA) were then performed with the RINspector app [55,56] for Cytoscape [57,58] and Z-scores ≥ 3 were considered as central residues. These residues were shown to be essential for the folding or function of a structure [59,60], therefore constituting good candidates for mutagenesis experiments. Here, we focused on the residues at the interface, central for the quaternary structure and essential for the interaction. Among the visually selected residues listed before, we listed those that were central in at least one of the five models. Four residues out of the seven selected residues were found central in at least one model (TRPM8: Glu207, Tyr240; Rap1A: Lys31, Tyr32) and were chosen for mutagenesis.

Cell cultures

In this work, we used human prostate adenocarcinoma cell line (PC3, ATCC), derived from bone metastasis of prostate cancer, human cervical cancer cell line (HeLa, ECACC), and human breast adenocarcinoma cell line (MCF-7, ECACC). PC3 stably expressing for TRPM8 (PC3M8) were generated by stable transfection of pcDNA4-TRPM8 vector as described in [41]. Cell lines were grown in monolayers using FalconTM plates in RPMI 1640 (Invitrogen Ltd, UK), MEM (Euroclone, Italy) and DMEM High Glucose (Euroclone, Italy) growth medium supplemented with 10% of fetal bovine serum (Pan Biotech), L-glutamine (5 mM; Sigma-Aldrich, France) and PenStrep (100 mg/ml; Sigma-Aldrich, France) for PC3, HeLa, and MCF-7 cells, respectively. PC3-TRPM8 cells were submitted to Zeocin (InvivoGen, US) selection (100 µg/ml) every two passages. Cells were cultured in a humidified atmosphere consisting of 95% air and 5% CO_2 at 37°C and they were used at passages 2 to 15.

Molecular biology

The constructs used for this work were His-tagged-hTRPM8pcDNA4 [61], pGEX6p2, pGEX6p2-TRPM8Nt, pGEX6p2-TRPM8Ct [45], peGFP-Rap1A, pMT2SM-HA-Rap1A, pCMN-TNT-Rap1A (for all Rap constructs wild-type (wt) and S17N) [48], pEGFP-RBD_{RalGDS} [62].

Simple and double mutagenesis for TRPM8 (E207A and Y240A) and Rap1A (K31A and Y32A) are summarized in table 1 and were done by site-directed mutagenesis using *in vitro* mutagenesis (QuikChange Site-directed Mutagenesis kit, Agilent Technologies-Stratagene products and Q5® Site-Directed Mutagenesis Kit);

Vector	Mutation	Fw primer	Rv primer	Kit used
pGEX-TRPM8 Nt	E207A	caatggccacaatattcgcctctgaactcctgctg	cagcaggagttcagaggcgaatattgtggccattg	Agilent kit
pGEX-TRPM8 Nt	Y240A	cttgtgaagtcatccataagggcctgggctaaaaaatagccctc	gagggctatttttagcccaggcccttatggatgacttcacaag	Agilent kit
pCDNA4-TRPM8	E207A	caatggccacaatattcgcctctgaactcctgctg	cagcaggagttcagaggcgaatattgtggccattg	Agilent kit
pCDNA4-TRPM8	Y240A	cttgtgaagtcatccataagggcctgggctaaaaaatagccctc	gagggctatttttagcccaggcccttatggatgacttcacaag	Agilent kit
pCMV-TNT-Rap1A	K31A	gaatcttctatcgttgggtcatatgcttcaacaaaaattccctgaacaaac	gtttgttcagggaatttttgttgaagcatatgacccaacgatagaagattc	Agilent kit
pCMV-TNT-Rap1A	Y32A	cttctatcgttgggtcagctttttcaacaaaaattccctgaacaaactgaac	gttcagtttgttcagggaatttttgttgaaaagctgacccaacgatagaag	Agilent kit
pCMV-TNT-Rap1A	K31A	gaatcttctatcgttgggtcatatgcttcaacaaaaattccctgaacaaac	gtttgttcagggaatttttgttgaagcatatgacccaacgatagaagattc	Agilent kit
pCMV-TNT-Rap1A	Y32A	cttctatcgttgggtcagctttttcaacaaaaattccctgaacaaactgaac	gttcagtttgttcagggaatttttgttgaaaagctgacccaacgatagaag	Agilent kit
peGFP-Rap1A-N17	K31A	agttcagaggcgaatattgtgg	cctgctgatggtgttatc	NEB
peGFP-Rap1A-N17	Y32A	tttagcccaggcccttatggatgac	aaatagccctcagcatcg	NEB
pMT2SM-HA-Rap1A	K31A	gaatcttctatcgttgggtcatatgcttcaacaaaaattccctgaacaaac	gtttgttcagggaatttttgttgaagcatatgacccaacgatagaagattc	Agilent kit
pMT2SM-HA-Rap1A	Y32A	cttctatcgttgggtcagctttttcaacaaaaattccctgaacaaactgaac	gttcagtttgttcagggaatttttgttgaaaagctgacccaacgatagaag	Agilent kit
pMT2SM-HA-Rap1A N17	K31A	gaatcttctatcgttgggtcatatgcttcaacaaaaattccctgaacaaac	gtttgttcagggaatttttgttgaagcatatgacccaacgatagaagattc	Agilent kit
pMT2SM-HA-Rap1A N17	Y32A	cttctatcgttgggtcagctttttcaacaaaaattccctgaacaaactgaac	gttcagtttgttcagggaatttttgttgaaaagctgacccaacgatagaag	Agilent kit

Table 1.[1] *Primers sequences used for single and double mutagenesis of TRPM8 (E207A and Y240A) and Rap1 (K31 and Y32A).*

Gene overexpression in PC3 cells was obtained using Lipofectamine™ 3000 reagents (Invitrogen Ltd, UK), according to manufacturer's instructions, in RPMI 1640 10% FBS growth medium. GFP tagged or human influenza agglutinin (HA) tagged-Rap1 (wild-type, Y32A, K31A, S17N, S17N Y32A and S17N K31A; 0.625-5 µg for transfection) and GFP-tagged as control (5 µg for transfection); pEGFP-RBD_{RalGDS} (1 µg for transfection). Cells were tested 24 h or 48 h after transfection, depending on the assay (24 h for Ca^{2+} imaging experiments, migration and adhesion assays, active Rap1-pull-down assays and live-cells imaging experiments; 48 h for GST-pull-down assays and immunoprecipitation assays).

Western blot analysis

Cells were plated in 6-well culture plates, grown to a confluency of 80%, and then silenced and/or overexpressed according to the protocol described below. Before cell lysis, multiwell plates were kept on ice, washed twice in ice-cold PBS, and then cells were lysed in the presence of RIPA buffer (Pierce® RIPA Buffer, Thermo Fisher Scientific, US); 1% Triton X-100, 1% Na deoxycholate, 150 mM NaCl, 10 mM $NaKPO_4$, pH 7.2) and anti-protease inhibitor cocktail (Sigma-Aldrich P2714, Italy; 1:10). Lysates were vortexed, kept 10 min on ice, sonicated, and then centrifuged at 4°C for 13 min at 13 000 g. Protein concentrations of the supernatant were determined using a bicinchoninic acid (BCA) kit (Sigma-Aldrich) following the manufacturer's instructions.

30 µg of lysates were resuspended in SDS loading buffer, heated 5 min at 95°C or 30 min at 37°, and then loaded and separated on 4-20% pre-cast SDS-PAGE gels (Thermo Fisher Scientific, US) at 130 mV-150 mV. Quick transfer on Polyvinylidene fluoride membranes (PVDF) membranes at 3A, 2.5 V for 15 min was followed. Subsequently, membranes were blocked 30 min in TBST (20 mM Tris, 150 mM NaCl, 0.1% Tween 20, pH 7.6) 5% BSA and then incubated in agitation overnight at 4°C with rabbit anti–Rap1 (Thermo Fisher scientific 1862344; 1:1000 in TBST 5% BSA 0.02% sodium azide), rabbit anti-TRPM8 (Ab 109308; 1:800 in TBST 1% BSA+ sodium azide), and mouse anti-β-actin (Sigma-Aldrich A5316; 1:1000 in TBST 1% BSA 0.02% sodium azide) antibodies. Membranes were then washed with TBST and incubated with the appropriate horseradish peroxidase (HPR)–conjugated antibodies (anti-mouse HRP Thermo Fisher Scientific, 31430; 1:10 000 in TBST 1% BSA and anti-rabbit HRP Santa Cruz Biotechnology, 2054; 1:15 000 in TBST 5% BSA). Chemiluminescence assays were conducted using the Western Lightning Plus-Enhanced Chemiluminescence Substrate (PerkinElmer, Italy). To quantify differences in protein expression, the ratio between overexpressed samples and PC3 wt (each normalized on actin) was evaluated, using Fiji (ImageJ software).

GST-fusion protein and pull-down assay

TRPM8 N- and C-terminal peptides fused with the GST tag were produced from plasmids pGEX6p-2-TRPM8-Nt and pGEX6p-2-TRPM8-Ct and then purified as described previously [45]. GST-fused purified proteins were then incubated with HEK or PC3 cell lysates transfected with pEGFP-Rap1 S17N, pEGFP-Rap1 S17N K31, pEGFP-Rap1 S17N Y32 plasmids.

For the direct interaction assay, Rap1 wt and mutants' coding sequence were *in vitro* translated using the TNT Quick Coupled Transcription/Translation Systems Kit (Promega, US). Briefly, the coding sequences of the proteins of interest were inserted in the pCMV-TNT vectors (Promega, US) as EcoR1-Not1 fragments to produce and translate them *in vitro*, according to the manufacturer's instructions.

Subsequently, TRPM8 GST-fusion proteins were incubated overnight at 4°C with cell lysates or *in vitro* translated proteins. Beads were then washed 4X with the IP buffer and bound proteins were eluted in SDS-PAGE loading buffer, heated at 70°C for 10 min, and separated on 4-20% pre-cast SDS-PAGE gels (Bio-Rad Laboratories Inc., France) starting from 0mV to 130 mV. Quick transfer on PVDF membranes at 2.5 V for 20 min was followed. Membranes were then blocked 2h in TNT (0.1 M Tris-Cl, 150 mM NaCl, 0.1% Tween 20, pH 7.5) 5% BSA and analysed by immunoblotting using rabbit anti-Rap1 (Thermo Fisher Scientific, US, MA5-15052; 1:500 in 1.5% BSA) or mouse anti-GFP (Clontech 632380; 1:1000 in 1% milk) antibody for Rap1 detection. Membranes were incubated with primary antibodies overnight at 4°C in agitation, washed 3 times with TNT 1X (15 mM Tris, 140 mM NaCl, 0,05% Tween, pH = 7.4) and incubated 1h with anti-rabbit secondary antibody (Santa Cruz Biotechnology, Inc; 1:20 000 in 2% BSA) or anti-mouse secondary antibody (Santa Cruz Biotechnology, Inc; 1:50 000 in 1% milk). Chemiluminescence assays were conducted using the SuperSignal West Dura chemiluminescent substrate (Thermo Fischer Scientific, US). TRPM8-Rap1 interaction was quantified as the ratio between IP_{Rap1} and IP_{M8} (both normalized on their own total lysate) and then it was normalized on TRPM8-Rap1 N17 interaction, used as control. Each experiment was repeated at least three times.

Co-Immunoprecipitation assay

PC3M8 were seeded in 100 mm dishes ($30x10^4$ cells/dish) and, 48 h after plating, they were transfected with 5 µg of GFP-Rap1S17N, GFP-Rap1S17N_K31A, GFP-Rap1S17N_Y32A, and GFP- pcDNA3 plasmids. 48 h after transfection, cells were lysed and incubated for 20-30 min on ice in lysis buffer (30 mM Tris HCl, 150 mM NaCl, 1% CHAPS, pH = 7.5, and anti-protease cocktail; Sigma-Aldrich). After centrifugation (12 000 g for 10 min at 4°C) of the lysates, protein concentration was determined by BCA assay (Thermo Fisher Scientific, US) and at least 800 µg of proteins in 500 µl of IP buffer (150 mM NaCl, 20 mM NaH_2PO_4, pH 8) were incubated overnight in rotation at 4°C with 50 µl of His-Tag Dynabeads® (Thermo Fisher Scientific, US), previously extensively washed in 500 µl IP buffer.

Samples were then washed four times in IP buffer, eluted in SDS loading buffer, heated at 95°C for 5 min or at 37° for 30 min, and then separated on 4-20% or 7.5% pre-cast SDS-PAGE gels (Bio-Rad Laboratories Inc., France) starting from 90mV to 130 mV. Total lysate for positive control was prepared with 50 µg of proteins suspended in SDS loading buffer. Quick transfer on PVDF membranes at 3A, 2.5 V for 15 min was followed. Membranes were then blocked 1 h in TNT 5% milk and analysed by immunoblotting using mouse anti-GFP (Clontech 632380; 1:1000 in 1% milk) antibody for Rap1's detection, and rabbit anti-myc (Abcam 9106; 1:1000 in 1% milk) or rabbit anti-TRPM8 (Ab 109308; 1:800 in TBST 1% BSA+ sodium azide) antibodies for TRPM8's detection. Membranes were incubated with primary antibodies overnight at 4°C in agitation, washed 3 times with TNT 1X, and incubated 1 h with secondary antibody (1:50000 in 1% milk). Chemiluminescence assays were conducted using the SuperSignal West Dura chemiluminescent substrate (Thermo Fischer Scientific, US). Each experiment was repeated at least three times.

Proximity Ligation Assay (PLA)

Proximity Ligation Assays (PLA) were performed using Duolink (R) In Situ Red - Starter Kit Goat/Rabbit (Sigma-Aldrich). PC3 cells were seeded ($10x10^4$ cells/dish) on confocal FluoroDish (World Precision Instruments) and then transfected or not with TRPM8 wt or E207A Y240A and Rap1 N17 (1 µg for each plasmid). After fixation, cells were permeabilized with 4% platelet-activating factor for 10 min and then incubated in the blocking buffer (PBS 4% BSA) for 1h and 30 min at room temperature. Primary antibodies diluted in the antibody diluents (rabbit anti–TRPM8 antibody, N571644, 1:200; Antibodies-online; mouse anti-GFP 1:200; Takara) were then added to the cells overnight at 4°C in a humidified chamber. The rest of the protocol was performed according to the manufacturer's instructions. Recordings were performed by confocal imaging (LSM880; ZEISS) using z-stack superposition (Zen black 2010 software; ZEISS). Appropriate controls were performed by incubating PC3 cells with both primary antibodies separately. In order to assess where the interaction between the two proteins occurs, ER staining was assessed 24 h time after transfecting the cells with 0.3 µg of Ds-Red2 plasmid fused to the ER targeting sequence of calreticulin (Ds-Red2 ER probe, Takara Bio Europe, Inc.) in bottom glass dishes.

Live-cell imaging experiments

To study the endogenous activity of Rap1, we performed a set of live-cell GTPase activity assays using the GFP-RBD_{RalGDS} probe. The first set of live-cell imaging experiments was performed on PC3 and PC3M8 and a second one on PC3 overexpressing M8 wt or M8 E207A Y240A (1µg plasmid for transfection).

Cells were seeded on bottom glass dishes coated with 1% gelatin ($5x10^4$ cells/dish) and 48-72 h after plating were transfected (or co-transfected) with 0.5 µg of pEGFP-RalGDS-RBD using Lipofectamine™ 3000 reagents (Invitrogen, Ltd, UK) in RPMI 1640 0% FBS growth medium. 24 h after transfection, cells were

imaged using an LSM 780 confocal microscope equipped with an argon laser. Live cells were kept at 37°C and 5% CO^2 for all experiments, and confocal images were acquired every minute using the "perfect focus" option to maintain the same focal plane. After 10 min of acquisition, cells were stimulated with 10 µM icilin.

Images were acquired using ZEN software and analysed offline with ImageJ. As a direct indication of Rap1 activation, we measured the relative cytoplasmic translocation of GFP-RBD_{RalGDS}, as previously described [63]. Briefly, for each cell, we checked at least four ROIs of identical size around an area of distinct PM fluorescence and around an adjoining region of cytosol without membrane encroachment [48]. The fluorescence intensity (I) was determined for these ROIs at each time point. Relative cytoplasmic translocation (R) was calculated as $R = (I_{cs} - I_m)/I_m$, where I_m and I_{cs} refer to the fluorescence intensities of the regions of interest in the membrane and in the cytosolic compartment, respectively. About 15-20 cells from at least three independent experiments were analysed for each experimental condition. Statistical analysis of the data was performed using Kruskal-Wallis test with *post-hoc* Dunn's test.

Active Rap1 pull-down and detection assay

To study Rap1 activation, we used the Active Rap1 Pull-Down and Detection kit from Thermo Fisher Scientific, according to the manufacturer's instructions as previously described [48]. The detection of GTP-bound Rap1 GTPase was obtained through specific protein interactions with the RalGDS protein-binding domain.

PC3 and PC3 overexpressing TRPM8 cells were seeded in 100 mm dishes and transfected (or co-transfected in ratio 1:1) with Rap1 mutant plasmids or TRPM8 double mutant (see conditions in Results). Pulled-down was performed 24 h after transfection, treating or not the cells with 10 µM icilin for 15 min. Pull-down samples and total lysates used as control were separated on 4-20% pre-cast SDS-PAGE gels (Thermo Fisher Scientific, US) at 130 mV. Quick transfer on PVDF membranes at 3A, 2.5 V for 15 min was followed. Membranes were then blocked 30 min in TBST 5% BSA and analysed by immunoblotting using rabbit anti-Rap1 (Thermo scientific 1862344; 1:1000 in TBST 5% BSA 0.02% sodium azide) antibody for Rap1's detection. Membranes were incubated with primary antibodies overnight at 4°C in agitation, washed 3 times with TBST 1X, and incubated 1 h with secondary antibody (anti-rabbit HRP Santa Cruz Biotechnology 2054; 1:15 000 in TBST 5% BSA). Chemiluminescence assays were conducted using the Western Lightning Plus-ECL (PerkinElmer).

Rap1 activation was quantified as the ratio between the GTP-bound Rap1 fraction (pulled-down) and the amount of Rap1 in total lysates, next normalized on PC3 or PC3M8 as control. At least three independent experiments for each condition were performed and statistical significance was assessed by one sample paired t-test or RM one-way ANOVA without Geisser-Greenhouse correction and with Dunnett's *post-hoc* test.

Cytosolic and ER Ca^{2+} imaging

Cells were seeded on glass coverslips at a density of $0.5x10^4$ cells/dish and were transfected with overexpression plasmids (his tagged-hTRPM8pcDNA4 wt, Y905A, and E207A Y240A; GFP-tagged hTRPM8pcDNA4 wt, empty pcDNA4) at least 48 h after seeding.

Cytosolic Ca^{2+} signals were monitored loading the cells (24 h after transfection) at 37 °C for 30 min with 2 µM Fura-2 AM (Invitrogen), a ratiometric probe used for cytosolic calcium concentration ($[Ca^{2+}]_i$) measurements as previously described [64]. During experiments, cells were maintained in a standard extracellular solution of the following composition: 154 mM NaCl, 4 mM KCl, 2 mM $CaCl_2$, 1 mM $MgCl_2$, 5 mM HEPES, 5.5 mM glucose (NaOH to adjust pH to 7.4). Fluorescence measurements were made using a Polychrome V spectrofluorimeter (TILL Photonics, Munich BioRegio, Germany) attached to an Olympus X51 microscope (Olympus, Tokyo, Japan) and Metafluor Imaging System (Molecular Devices, Sunnyvale, CA USA) for image acquisition using 3-s intervals. Each fluorescent trace (340/380 nm ratio) represents the mean ± SEM of at least 20 traces obtained from one representative experiment. For each condition, at least three independent experiments were performed. The IgorPro software (Wavematrix, Lake Oswego, OR, USA) was used to further analyze fluorescence traces and to calculate the peak amplitude (fluorescence intensity ratio, measured at 510 nm), determined by the difference between the maximum and minimum values of fluorescence intensity recorded in about 300s upon agonist administration. We used the agonist-induced slope change as a criterion to distinguish a cell response to an agonist from the background noise. In PC3 overexpressing TRPM8, only responsive cells were considered for the analysis. Kruskal-Wallis test with *post-hoc* Dunn's test was used for the statistical evaluation of the data.

ER Ca^{2+} signals were monitored by transfecting the cells with the GEM-Cepia1er plasmid (1µg), a Ca^{2+} biosensor targeted to the ER. pCIS GEM-Cepia1er was a gift from Masamitsu Iino (Addgene plasmid #58217; http://n2t.net/addgene:58217; RRID:Addgene_58217) [65]. 24h after GEM-Cepia1er transfection, images were acquired at a magnification of 40X (Nikon Plan 40X/0.10 objective) using a Nikon Eclipse Ti (Nikon Corporation, Tokyo, Japan) inverted microscope equipped on a system integrated by Crisel Instruments (Rome, Italy), controlled with MetaMorph software (Molecular Devices, Sunnyvale, CA, USA), a CCD camera (Q imaging), a filter wheel (Suter Instrument), and a fluorescence lamp with the following excitation and emission settings: excitation 405 ± 20 nm; emission at 460 ± 50 nm and 525 ± 50 nm. During experiments, cells were maintained in a standard extracellular solution of the following composition: 154 mM NaCl, 4 mM KCl, 2 mM $CaCl_2$, 1 mM $MgCl_2$, 5 mM HEPES, 5.5 mM glucose (NaOH to adjust pH to 7.4). Metafluor Imaging System (Molecular Devices, Sunnyvale, CA USA) was used to acquire images at 5-s intervals. The 460/525 nm ratio referring to several ROIs drawn within each cell was recorded and then mediated and normalized on the mean fluorescence signal recorded 100 s before the stimulation ($\Delta F/F_0$). Consequently, a significant

decrease in the $\Delta F/F_0$ ratio revealed an ER Ca^{2+} store depletion. The well-known sarco/endoplasmic reticulum Ca^{2+} ATPase (SERCA) inhibitor thapsigargin (2 µM) was used as a control for ER store depletion. The IgorPro software (Wavematrix, Lake Oswego, OR, USA) was used to further analyze fluorescence traces and to calculate the ER-Ca^{2+} release's slope upon stimulation by icilin and thapsigargin.

Random migration assay

Cells were seeded in 24-well culture plates coated with 1% gelatin ($3x10^4$ cells/well), using RPMI 1640 10% FBS, and incubated at 37°C and 5% CO_2 atmosphere for 24 h. Cells were then transfected with 1 µg of his tagged-hTRPM8pcDNA4 (plasmid wild-type, Y905A, and E207A Y240A) and were treated with 10 µM icilin 24 h after transfection.

The experiment was performed using a Nikon Eclipse Ti (Nikon Corporation, Tokyo, Japan) inverted microscope equipped with an A.S.I. MS-2000 stage, a System integrated by Crisel Instruments (Rome, Italy) for multi-wavelengths and multi-positions widefield time-lapse, CCD camera (Photometrics) and OkoLab incubator, in order to keep cells at 37°C and 5% CO_2. MetaMorph software (Molecular Devices, Sunnyvale, CA, USA) was used to acquire images for 6 h every 10 min, using a Nikon Plan 20X/0.10 objective and a CCD camera.

Image stacks were analysed with ImageJ software, and about 400 cells/condition from three independent experiments were tracked manually using MtrackJ plugin. Cells that exited the imaged field or doubled during the time-lapse acquisition interval were excluded from the analysis. Migration rate (µm/min) is obtained by measuring the distance covered by cells between two consequent time points after conversion of pixel to micrometers. Kruskal-Wallis test with *post-hoc* Dunn's test was used for the statistical evaluation of the data.

Transwell migration assay

Transwell® permeable supports (6.5 mm inserts with an 8 µm pore polycarbonate membrane) were equilibrated for 20 min at 37°C using DMEM 0% FBS medium. The equilibrated Transwell® inserts were then placed into 24-well culture plates (Sarstedt, Germany) containing DMEM 10% FBS. 24 h after transfection with his tagged-hTRPM8pcDNA4 (plasmid wild-type, and E207A Y240A) cells were seeded (2.5x104 cells/insert) in the Transwell® inserts using DMEM 10% FBS and incubated O/N. Transwell® inserts were then washed twice in PBS and the cells that did not migrate through the membrane pores were removed from the upper side of the membrane using a cotton bud. After washing in PBS, cells were fixed in cold ethanol for 20' at 4°C and then stained with DAPI in PBS for 15 min at 37°C. Cells that migrated through the membrane pores were then counted using a Nikon Eclipse Ti (Nikon Corporation, Tokyo, Japan) inverted microscope (4X objective).

Adhesion assay

Cell adhesion was evaluated on 96-well culture plates using a coating of 1% gelatin. 24 h after transfection (see conditions in Results), cells were detached using trypsin for 3 min, carefully counted, and seeded ($0.3x10^4$ cells/well) in 100 µl RPMI 10% FBS growth medium in the presence or absence of 10 µM icilin.

Cells were kept at 37°C and 5% CO_2 for 60 min and then washed twice with PBS with Ca^{2+} and Mg^{2+}. Cells were fixed in ethanol for 20 min at 4°C and then washed twice with PBS with Ca^{2+} and Mg^{2+}. Staining of cell nuclei was performed using 0.2 mM Hoechst for 15 min at room temperature. Then cells were washed again and kept in PBS.

Image acquisition was performed using a Nikon Eclipse Ti (Nikon Corporation, Tokyo, Japan) microscope with a 4X objective and cell nuclei counted using an homemade automatic cell count macro in ImageJ. At least eight wells for each condition were analyzed in each independent experiment and at least three independent experiments were performed for each condition tested. Statistical significance was assessed using Kruskal-Wallis test with *post-hoc* Dunn's test.

Cell viability assay

Cells were seeded in 6-well plates (Sarstedt, Germany) and transfected with 0.625 µg of his tagged-hTRPM8pcDNA4 (TRPM8 wild-type, and E207A Y240A) using LipofectamineTM 3000 reagents (Invitrogen Ltd, UK), according to manufacturer's instructions. 6 h after transfection, the cells were detached, counted accurately, and plated (0.5x104 cells/well) in 96-well black-bottom polystyrene plates (Greiner Bio-One, Austria). 18, 42, and 66 h after incubation at 37 °C (i.e. 24, 48, and 72 h after transfection), cell viability was assessed using CellTiter-Glo® Luminescent Cell Viability Assay (Promega, USA), following manufacturer's instructions. Luminescence was recorded using a microplate reader (FilterMax F5, Multi-Mode Microplate Reader, Molecular Devices) and then analyzed as being proportional to the number of viable cells. For each condition, eight replicates were set up and three independent experiments were performed

Confocal analysis

Cells ($10{\cdot}10^4$ cells/dish) were seeded in 40 mm diameter bottom glass dishes and were transfected with GFP-tagged hTRPM8pcDNA4 wt (1 µg) 24 h after seeding. Cells were incubated at 37°C for 24 h and then washed and incubated with ER-Tracker™ Red (500 nM, Molecular probes®, Invitrogen) for 30 min. After incubation, cells were washed twice with Hanks' Balanced Salt Solution (HBSS) in order to wash off the excess probe and fixed in 4% paraformaldehyde (PAF) at 37°C for 2 min. Images were acquired through a Leica TCS SP8 confocal system (Leica Microsystems, Germany) equipped with an HCX PL APO 63X/1.4 NA oil-immersion objective. GFP-TRPM8 was excited at 488 nm, and ER-Tracker™ Red at 561 nm with DPSS lasers. Images were

acquired on the three coordinates of the space (XYZ planes) with a resolution of 0.081 µm x 0.081 µm x 0.299 µm and were processed and analyzed with ImageJ software (Rasband, W.S., U.S. National Institutes of Health, Bethesda, MA) in order to assess TRPM8 localization in the ER.

Similarly, PC3 cells overexpressing both TRPM8 and Rap1A N17 were analyzed by PLA (see section 2.8, above) and co-localization of PLA dots with ER staining was assessed (Ds-Red ER probe).

Immunohistochemistry

Immunostaining was performed on normal and cancerous prostate tissue arrays (Biomax Inc.). Slides were deparaffinized, rehydrated, and heated in citrate buffer pH 6 for antigenic retrieval. After blocking for endogenous peroxidase with PBS-G Tween (0,2M Glycine + tween 20 0,1%), slides were incubated with goat anti-TRPM8 (ABIN572229, dilution: 1:50) and rabbit anti-Rap1A (ABIN2854404 , dilution: 1:50). Following 3 washing steps, slides were incubated with the corresponding secondary antibodies: Rhodamine Red-X -labeled anti-goat (Jackson ImmunoResearch, dilution: 1:50) and Alexa Fluor 488-labeled anti-rabbit (Jackson ImmunoResearch, dilution: 1:500). Nuclei were counterstained with DAPI (Invitrogen, Life Technologies, Ghent, Belgium). Confocal imaging was performed using an LSM 880 confocal microscope (Carl Zeiss AiryScan, Munich, Germany).

Bioinformatic analysis

Detection of mutations

We retrieved TCGA MuTect2 mutational data from the UCSC Xena databases [66] Using an ad-hoc pipeline [67] we also retrieved up-to-date clinical metadata regarding all patients included in the TCGA study. By combining the metadata with the mutation dataset, we were able to run filtering to find any mutations of interest. For normalization purposes, the protein lengths of Rap1A and TRPM8 were set to be 184 and 1104 amino acids, respectively [68][69].

Differential expression analysis

We retrieved normalized expression data from the UCSC Xena databases, including samples from TCGA, the TARGET and the GTEx projects. We also retrieved metadata for the GTEx samples from the same database portal and used the same TCGA metadata as in the previous analysis. Samples from the TARGET cohort were removed. The samples were divided in "Breast", "Prostate" and "Uterus" cohorts:

• GTEx samples labelled as "Breast" and TCGA samples labelled as "TCGA-BRCA" composed the "Breast" dataset;

• GTEx samples labelled as "Prostate" and TCGA samples labelled as "TCGA-PRAD" composed the "Prostate" dataset;

• GTEx samples labelled as "Uterus" or "Cervix Uteri" and TCGA samples labelled as "TCGA-UCEC" composed the "Uterus" dataset.

The samples were labelled as "healthy", "metastatic", or "not metastatic" based on these criteria ("Metastatic" labelling):

• If the sample was from the TCGA cohort and had an entry in the AJCC "m" category (both clinical or pathologic) reflecting the metastatic nature of the sample, it was labelled as "metastatic";

• If the sample was labelled as having AJCC stage "IV" or equivalent, it was labelled as "metastatic";

• If the sample was labelled with a FIGO stage of "III" or "IV", it was labelled as "metastatic";

• If the sample was from the GTEx cohort, it was labelled as "healthy";

• All other samples were labelled as "not metastatic".

Differential expression analysis was carried out separately on the expression of the two genes in the three distinct cancer cohorts. Normality and homoscedasticity requirements were checked for all cohorts. In particular, for each cohort, residuals within each group were assumed to be normally distributed about group mean if they met either of the following conditions:

• Produced a non-significant p-value under the Kolmogorov-Smirnov two-sided test with the null hypothesis of being drawn from a normal distribution;

• Had sample numerosity greater than 30.

If normality assumptions were not met, the differential expression in said cohort was computed with the Kruskal-Wallis Rank Sum Test followed by Dunn's All-Pairs Rank Comparison *post-hoc* test with Bonferroni multiple comparison correction. Otherwise, an ANOVA (Analysis Of Variance) model was fitted and followed by Tukey's Honest Significant Differences *post-hoc* test. Homoscedasticity of the data was checked for all cohorts analyzed with ANOVA models, and all proved satisfactory.

On the contrary, the Rap1A Breast "Metastatic", Rap1A Prostate "Metastatic", TRPM8 Breast "Metastatic" and TRPM8 Prostate "Metastatic" cohorts did not meet the normality assumptions.

All code used to perform the bioinformatic analysis, as well as further information on how to reproduce the analysis is available on GitHub gists at this url [70].

Statistical analysis

Data are normalized and expressed as means ± SEM when data are normally distributed and as median ± interquartile range when they don't show a normal distribution (Shapiro-Wilk normality test). Statistical analyses were performed using GraphPad Prism software and differences with a p-value < 0.05 were considered statistically significant (*: $P \leq 0.05$; **: $P \leq 0.01$; ***: $P \leq 0.001$; ****: $P \leq 0.0001$). Statistical significance between different conditions was determined by analysis of variance (1way or 2way ANOVA-Kruskal Wallis test) followed by Tukey's or Dunn's multiple comparisons *post-hoc* test to compare more than

two conditions to each other in GST pull-down, Ca^{2+} imaging, and live-cell imaging experiments. Student's t-test or Mann-Whitney test were used to evaluate significance between only two different conditions within one experiment (GST pull-down, immunoprecipitation assay, PLA, active Rap1 pull-down, random migration, and adhesion performed on TRPM8 wt and TRPM8 Y905A/TRPM8 E207A Y240A). One sample t-test or RM one-way ANOVA without Geisser-Greenhouse correction and with Dunnett's *post-hoc* test were used to evaluate significance in migration, adhesion, and active Rap1 pull-down assays.

Results

1. TRPM8 inhibits PC3 migration and adhesion regardless of channel activity

Random migration assays performed on PCa cells from bone metastasis (PC3) confirmed that TRPM8 overexpression leads to a significant reduction in terms of cell migration speed both in the presence and absence of TRPM8 specific agonist icilin (10 µM) (fig. 1a, 1c). To elucidate the underlying mechanism of this biological effect and, taking into account the inhibition observed even in the absence of channel activation, we first assessed whether the ionic flux generated by TRPM8 activation played a role in cell migration. We performed random migration assays in PC3 overexpressing TRPM8 wild-type (wt) or a TRPM8 inactive pore mutant (Y905A), which completely impairs channel activity (fig. S1). As shown in fig. 1b and 1c, cell migration was significantly inhibited in PC3 overexpressing TRPM8 Y905A both in the presence and absence of the channel agonist.

To better characterize TRPM8 inhibitory role, we performed adhesion assays transfecting PC3 cells with TRPM8 wt and plating them on 1% gelatin-coated wells, in the presence or absence of icilin (10 µM). In accordance with cell migration data, overexpression of TRPM8 is correlated with a significant decrease in cell adhesion, even in the absence of the agonist, indicating a role of this channel in inhibiting prostate cancer cell adhesion (fig 1d). In the absence of the agonist, overexpression of TRPM8 pore mutant affected cell adhesion to the same extent as TRPM8 wt (fig. 1e), confirming that the biological effect of TRPM8 on PC3 cells migration and adhesion are not imputable to the pore function of TRPM8 protein (fig. 1b, 1e). However, interestingly icilin (10 µM) stimulation did not inhibit cell adhesion in PC3 cells overexpressing TRPM8 pore mutant (fig. 1e), suggesting a Ca^{2+} involvement.

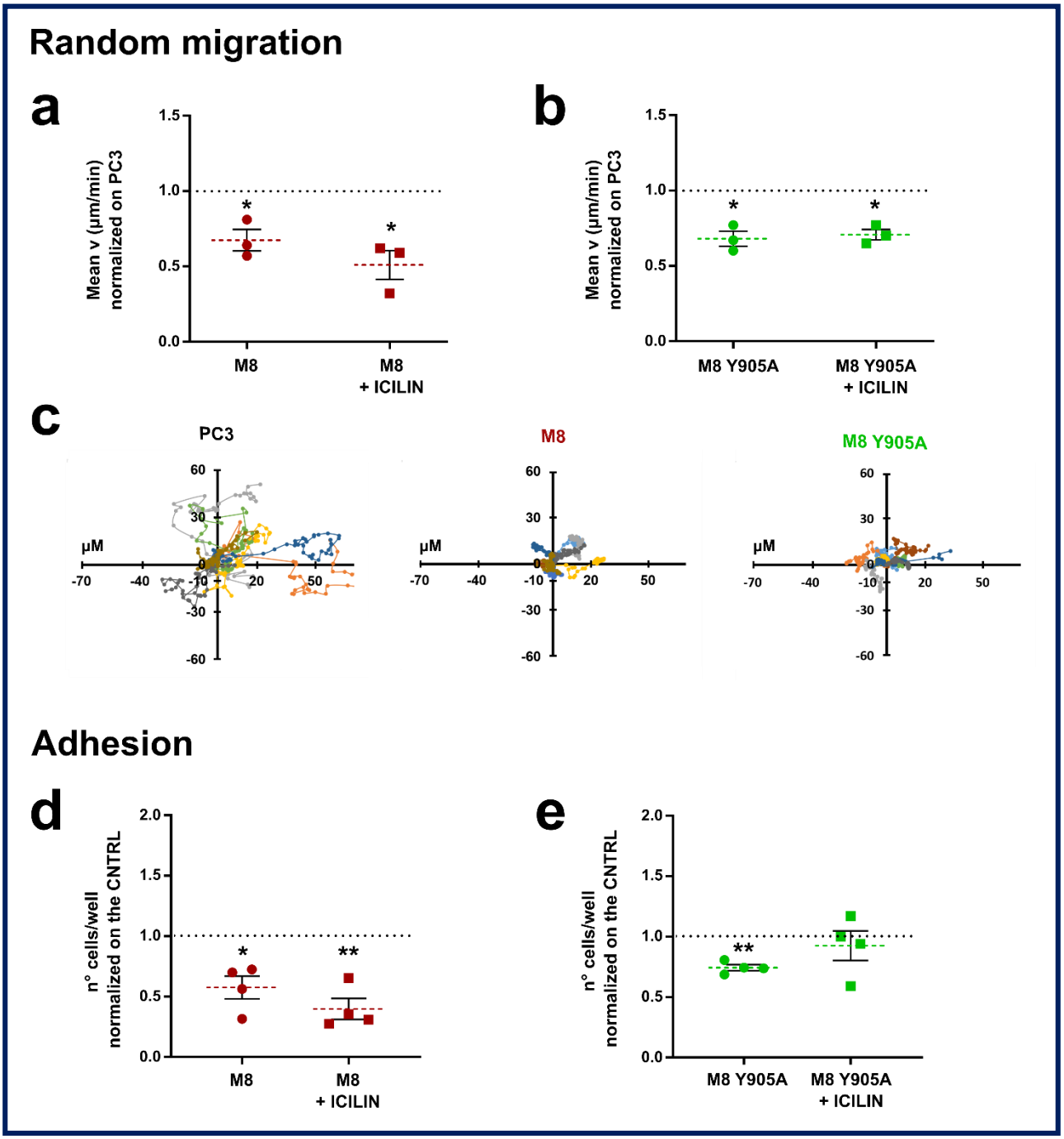

Figure 1. TRPM8 inhibits cell migration and adhesion independently of its channel activity.

*(**a**) Quantification of random migration assays on PC3 overexpressing TRPM8, treated or not with 10 µM icilin. Data are normalized on PC3 or PC3 treated with icilin (controls represented by dot line) and displayed as mean ± SEM of three independent experiments. Statistical significance versus PC3 or PC3 treated with icilin, *: P < 0.05 (One sample t-test).*
*(**b**) Quantification of random migration assays on PC3 overexpressing TRPM8 pore mutant, treated or not with 10 µM icilin. Data are normalized on PC3 or PC3 treated with icilin (controls represented by dot line) and displayed as mean ± SEMof three independent experiments. Statistical significance versus PC3 or PC3 treated with icilin,*: P < 0.05 (One sample t-test).*
*(**c**) Representative migration plots of PC3 (left panel), PC3 overexpressing TRPM8 (central panel) and PC3 overexpressing TRPM8 Y902A (right panel). Each line represents the trajectory of one cell within a 6 h period. Data shown refer to one field of one representative experiment out of three repeats (10 cells for each condition).*

*(**d**) Quantification of adhesion assays on PC3 overexpressing TRPM8 treated or not with icilin (10 µM). Data are normalized on PC3 or PC3 treated with icilin (controls represented by dot line) and displayed as mean ± SEM of four independent experiments. Statistical significance versus PC3 or PC3 treated with icilin *: P < 0.05; **: P < 0.01 (One sample t-test).*
*(**e**) Quantification of adhesion assays on PC3 overexpressing TRPM8 pore mutant treated or not with icilin (10 µM). Data are normalized on PC3 or PC3 treated with icilin (controls represented by dot line) and displayed as mean ± SEM of four independent experiments. Statistical significance versus PC3 or PC3 treated with icilin **: P < 0.01 (One sample t-test).*

2. TRPM8 inhibits Rap1's activity by intracellularly sequestering GDP-bound Rap1

Given the interaction between Rap1A and TRPM8 previously demonstrated [45,48], we further assessed whether Rap1 activation is involved in TRPM8-mediated inhibition of PC3 cells migration by using two distinct approaches. We first performed pull-down assays for GTP-bound Rap1, using GST-RalGDS, which binds active Rap1-GTP (fig. 2a i). PC3 were transfected with TRPM8 (4 µg) and stimulated with 10 µM icilin for 15 min. Interestingly, TRPM8 overexpression led to a decrease of 36% ± 13% of the amount of active Rap1-GTP protein as compared with control PC3 wt transfected with empty vector (fig. 2a ii). At the same time, TRPM8 overexpression doesn't affect the total amount of Rap1 (fig. 2a ii and S2).

The spatiotemporal activation of Rap1 was evaluated by live-cell GTPase activity assays, transfecting PC3 and PC3 stably overexpressing TRPM8 (PC3M8) with the GFP-RBD_{RalGDS} probe. This latter was developed to detect the intracellular spatial and temporal activation of Rap1, exploiting its high bond affinity in the active form (GTP-bounded) for the Ras binding domain (RBD) of the Rap1 effector RalGDS [62,63]. Since the active Rap1 pool localization is restricted to the PM, we considered the membrane recruitment of GFP-RBD as an indirect indication for Rap1 activation, as previously reported [48]. In particular, the cytosolic retention fraction of GFP-RBD upon icilin treatment was measured (see Materials and Methods). In PC3 wt GFP-RBD_{RalGDS} localization at the PM didn't change upon icilin treatment (fig. 2b ii on the top), indicating no changes in Rap1 activation. Conversely, in cells overexpressing TRPM8 the translocation of the active form of Rap1 to the PM was significantly inhibited upon icilin treatment, with a maximal effect on the cytoplasmic translocation 5 min after the treatment, and a partial recovering after 10 min (fig 2b ii on the bottom).

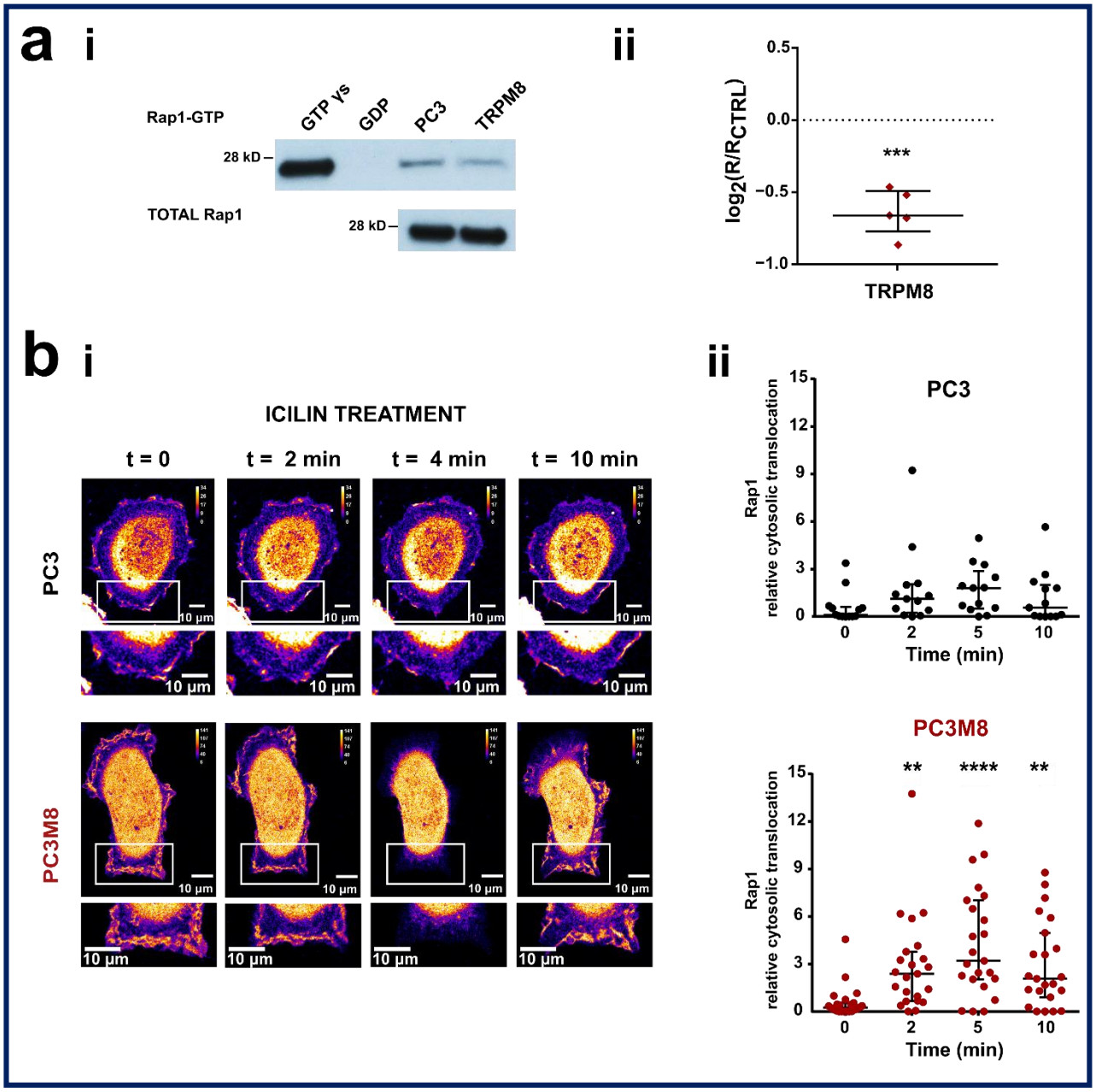

Figure 2. TRPM8 decreases Rap1 activation.

*(**a i**) Active Rap1 pull-down assay on PC3 and PC3 overexpressing TRPM8 . **(ii)** Quantification of the active Rap1 as the ratio between Rap1-GTP over total Rap1 (R) normalized on this ratio on PC3 (R_{CTRL}). Data are expressed as log_2 and shown in the scatter dot plot in which each dot represents one single experiment and lines represent mean ± SEM. Statistical significance versus PC3, ***: P < 0.001 (One sample t-test).*

*(**b i**) Live-cell imaging by confocal microscopy of PC3 and PC3M8 expressing GFP-RBD_{RalGDS} probe. Representative images showing GFP-RBD_{RalGDS} in PC3 and PC3M8 at t=0 and after 2, 4 and 10 min of treatment with 10 µM icilin; the bottom parts of the figures represent enlargement of the inset (white box) for each time point. (**b ii**) Scatter dot plots showing the quantification of GFP-RBD membrane recruitment calculated as cytosol translocation as described in the method section. Each dot represents one cell (83 regions of interest [ROIs] referring to 13 cells for PC3 and 100 ROIs referring to 23 cells for PC3M8) and lines show median ± interquartile range. Statistical significance versus t=0, **: P < 0.005; ****: P < 0.0001 (Kruskal-Wallis test with Dunn's post-hoc test).*

The inhibitory role of TRPM8 on Rap1 activation is compatible with TRPM8 localization in the ER. Indeed, in the ER it could bind Rap1 in its inactive GDP-bound form, thus preventing the GTP exchange and the consequent translocation to the PM, as previously demonstrated for ECs, which, however, express the short isoform of TRPM8 on the ER [48]. On the other hand, when overexpressed in PC3, TRPM8 is located at least in part at the PM [44], favoring Ca^{2+} influx into the cell as shown in figure S1. To test the hypothesis that, once overexpressed in PC3 cells, TRPM8 is also present and functional on the ER membranes, we performed confocal analysis on PC3 cells overexpressing the channel, showing a partial co-localization of TRPM8 with the ER staining (fig. 3a). Moreover, using a Ca^{2+} biosensor targeted to the ER (GEM-Cepia1er), we measured the activity of intracellular TRPM8. Stimulation of PC3 cells overexpressing TRPM8 with icilin (10 µM) induced a Ca^{2+} release from the ER stores in 20% of the cells tested, while no response was detected in CNTRL PC3 overexpressing the empty vector (fig. 3b). Finally, to localize the TRPM8-Rap1 interaction at the cellular level we performed proximity ligation assays on PC3 cells overexpressing both TRPM8 and the inactive form of Rap1 (Rap1 N17), which has been shown to bind TRPM8 *in vitro* [48]. As shown in figure 3c, the protein interaction complexes indicated by fluorescent dots are partially localized on the ER, thus confirming the hypothesis that within the cell TRPM8 acts as a sponge by trapping intracellularly Rap1 in its inactive form, thus avoiding its translocation and activation on the PM.

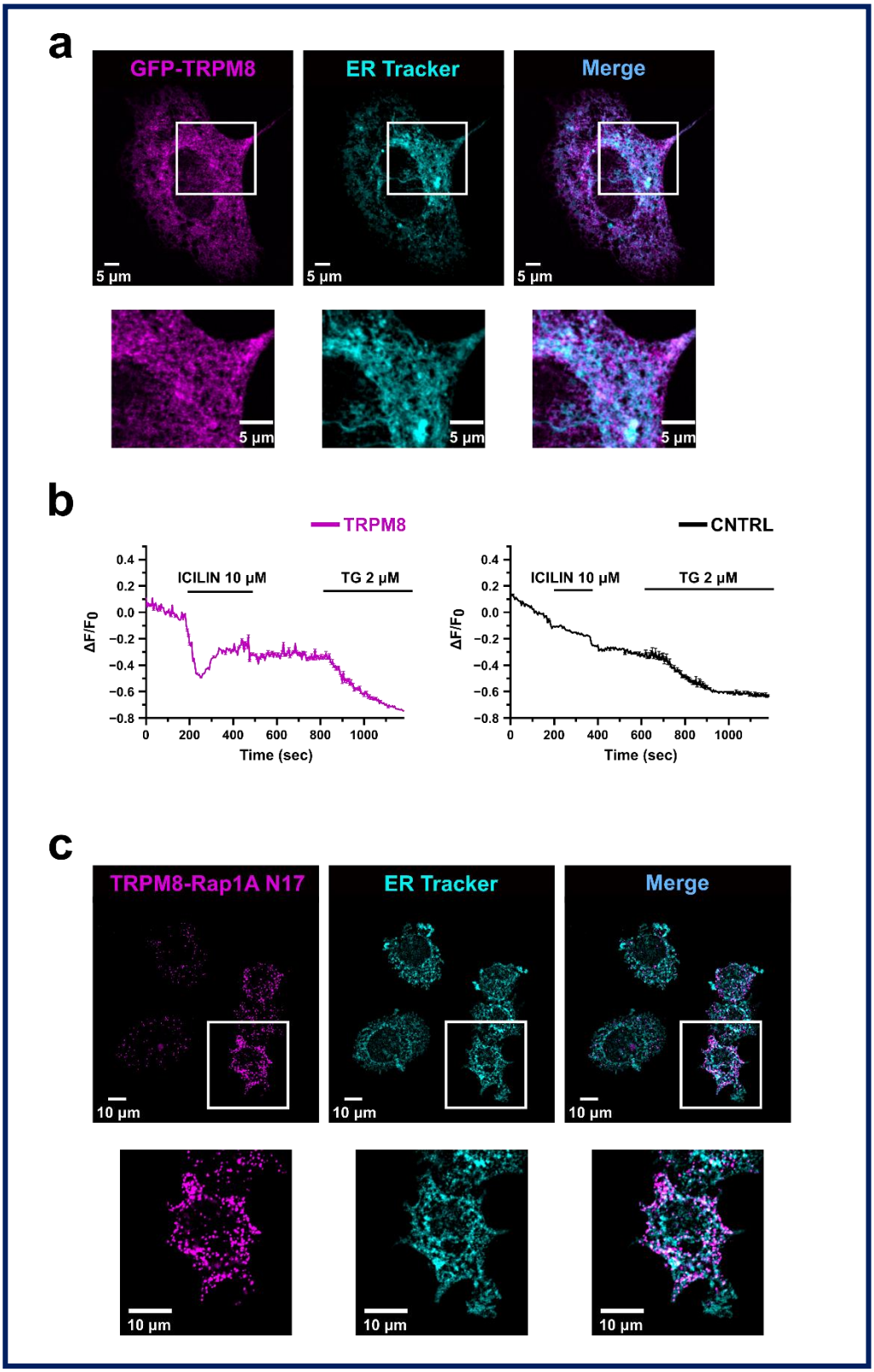

Figure 3. TRPM8 ER localization.

*(**a**) Representative confocal fluorescence images of PC3 cells 24h after transfection with GFP-TRPM8. Magenta signal (on the left) refers to GFP-TRPM8 (excitation at 488 nm), cyan signal (in the center) refers to ER-tracker Red (excitation*

at 561 nm), and light blue in merged image (on the right) indicates overlapped regions; below: zoom on a region of interest indicated by white box. Scale bar: 5 µm.
*(**b**) ER Ca^{2+}-imaging traces in response to TRPM8 agonist (10 µM icilin) and SERCA inhibitor (2 µM thapsigargin) in PC3 transiently overexpressing GFP-TRPM8 (magenta) and PC3 used as control (black). $[Ca^{2+}]_{ER}$ was visualized in PC3 cells expressing GEM-Cepia1er, a Ca^{2+} biosensor targeted to the ER. Traces represent the mean $\Delta F/F_0 \pm$ SEM from different ROIs within one representative cell for each condition (n=7 for PC3, n=3 out of 15 for TRPM8).*
*(**c**) Representative confocal fluorescence images of PC3 cells 24h after transfection with TRPM8 wt and Rap1A N17. Magenta signal (on the left) refers to TRPM8-Rap1A N17 interaction detected as fluorescent PLA dots, cyan signal (in the center) refers to Ds-Red ER probe (excitation at 561 nm), and light blue in merged image (on the right) indicates overlapped regions; below: zoom on a region of interest indicated by white box. Scale bar: 10 µm.*

3. Identification of the residues involved in TRPM8-Rap1 interaction

Aiming to identify putative residues involved in the interaction between Rap1A and TRPM8, a molecular modelling approach has been used. First of all, as the C-tail was not solved for TRPM8 structure, we modelled this tetrameric structure by homology modelling. This model was further used to predict the interaction between TRPM8 and Rap1A, for which a crystal structure existed (PDB ID: 4HDO). This prediction was obtained using a protein-protein algorithm and more specifically the ClusPro2.0 webservers. The docking was performed on one monomer of TRPM8 structure, removing the trans-membrane part of the protein for the calculation. After docking poses were obtained, we superimposed all these poses to the tetrameric structure of TRPM8 and we removed the poses that were not allowed due to unacceptable steric clashes. In the end, we obtained a model that was used to identify hotspots between Rap1A and TRPM8 (fig. 4a). For this purpose, a residue centrality analysis (RCA) and mapping of central residues were performed on the best-scored docking poses TRPM8 and Rap1A (fig. S3). The two best docking poses of InterEvDock and three docking poses of ClusPro were used for residue interaction network generation followed by residue centrality analysis. Only residues at the docking interface were considered. A visual analysis of docking poses was considered and the maximum Z-score values from the residue centrality analyses performed on these docking poses were kept and displayed for four residues of interest, namely Glu207 and Tyr240 for TRPM8 and Lys31 and Tyr32 for Rap1A, respectively. These residues are displayed in stick in the structure (fig. 4c) and proposed for site-directed mutagenesis.

To deepen the clinical relevance of our findings we investigated the presence of point mutations on the key residues identified by molecular modelling in real patients. For the purpose, we used mutational data from the TCGA consortium. The full workflow and results of this analysis are shown in fig. 4b. The pan-cancer dataset included 3,175,929 point missense mutations from a global cohort of 10,182 patients. Of these, 26 mutations occurred on the *RAP1A* gene, and 203 on the *TRPM8* gene. The mutational burden (MB calculated as mutations per patient per megaresidue) of both genes was comparable, and, more precisely 13.88 and 18.06 for *RAP1A* and *TRPM8*, respectively. Filtering for mutations on the codons of residues E207/Y240 of

TRPM8 gene, a single entry (from a single patient) emerged: a transversion on the codon for the Glutamic Acid (E) 207, causing it to become an Aspartic Acid (D). We found no mutations on the codons for K31/Y32 residues of *RAP1A* gene.

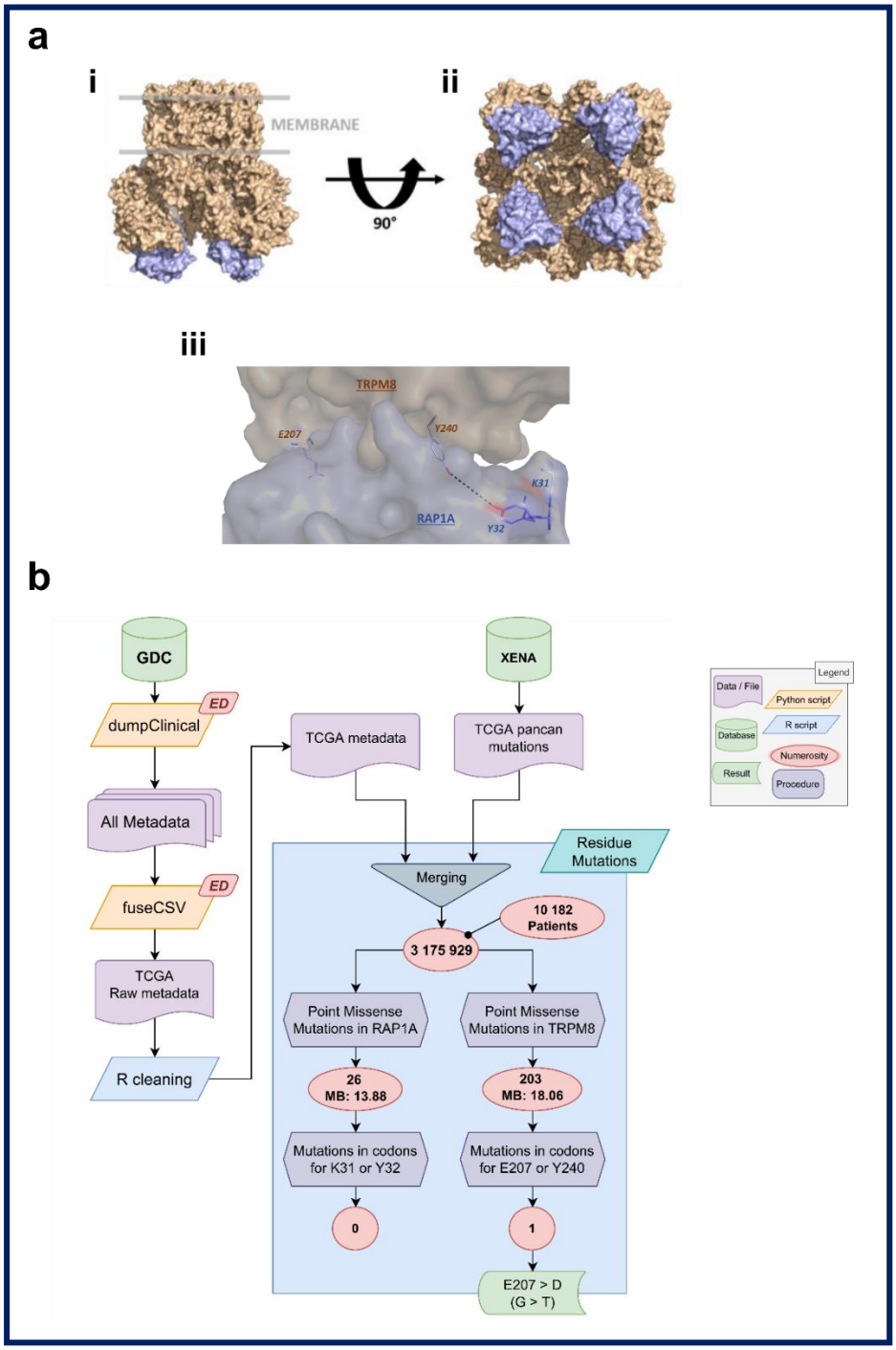

Figure 4. Identification of the residues involved in TRPM8-Rap1 interaction.

*(**a i**) Model of the interaction between TRPM8 (brown surface) and Rap1A (blue surface) obtained after docking simulation. (**ii**) 90° rotation view of the same model showing the tetrameric form of the TRPM8 receptor and the four*

*interacting Rap1 proteins. (**iii**) Focus on residues identified as hotspots after the residue centrality analysis performed on the best docking poses 3.4. (**b**) Workflow followed to investigated the presence of point mutations relative to residues identified by molecular modeling in real patients (n= 10,182).*

4. Characterization of the residues involved in TRPM8-Rap1 interaction.

4.1 Role of the residue Y32 in the interaction of GDP-bound Rap1 with TRPM8 cytosolic N-terminal tail.

As described above, molecular modelling experiments identified two putative critical amino acid residues on Rap1 sequence for the Rap1-TRPM8 interaction: lysine (K) 31 and tyrosine (Y) 32 (fig. 4). We next validated these two putative interaction sites, assessing their effective involvement in Rap1-TRPM8 interaction as well as their functional consequences on protein activity and cellular responses such as migration and adhesion. We started by investigating the role of K31 and Y32 residues in mediating Rap1 N17 interaction with TRPM8 wt. To do that, we produced and purified the TRPM8 N-terminal tail and C-terminal tail fused to GST and then we performed GST pull-down with *in vitro* translated Rap1 mutants (fig. 5a and S4). Results showed that Rap1 N17 mainly directly interacts with TRPM8 cytosolic N-terminal tail (Nt), in agreement with previous data [48], and indicated that both K31A and Y32A mutations significantly decreased Rap1 N17 interaction with TRPM8 Nt, with a total loss of the binding in the case of Y32A (fig. 5a ii).

To further corroborate the contribution of these two residues on the binding of Rap1 N17 with TRPM8 and to validate it also in the cellular context, we generated both mutants by site-directed mutagenesis and assessed their interaction by co-immunoprecipitation assay. PC3M8 cells were transfected with GFP-Rap1 N17 K31A or GFP-Rap1 N17 Y32A mutants and cell lysates were immunoprecipitated for TRPM8 (his-tagged) and then immunoblotted with anti-GFP antibody for Rap1 detection and anti-myc antibody for TRPM8 detection (fig. 5b i). We show that TRPM8 and Rap1 N17 interact in intact prostate cancer cells, validating docking analyses since the point mutation of Y32 in Rap1 sequence significantly weakened the intracellular interaction with TRPM8 (fig. 5b ii).

To further validate the hypothesis that TRPM8 traps the inactive form of Rap1 and thus prevents its activation on the PM, we investigated the functional effects of Rap1 N17 mutant, well-defined in literature as Rap1 dominant-negative due to its ability to significantly reduce GEF activity rate and thereby substantially block Rap1 in its inactive (GDP-bound) form [71]. According to our hypothesis about TRPM8 acting as a sponge for inactive Rap1, pull-down assays for active (GTP-bound) Rap1 showed that in cells overexpressing TRPM8 in the presence of an excess of inactive Rap1 (i.e. overexpressing Rap1 N17) the amount of active Rap1 is higher, although not significantly, with respect to cells overexpressing TRPM8 in the absence of an excess of inactive Rap1 (fig. 5c). Consistently, TRPM8 and Rap1 N17 co-overexpression reverted the TRPM8-mediated inhibition of PC3 adhesion (fig. 5d). More in detail, in the presence and in the absence of icilin we

observed a significant inhibition of cell adhesion both in cells that overexpress TRPM8 alone as previously observed (fig. 5d and 1d) and in cells that overexpress only Rap1 N17. According to the role of Rap1 N17 as dominant-negative, the above inhibition can be explained by overloading the cell with Rap1 in its inactive form. However, the overexpression of both TRPM8 and Rap1 N17 didn't affect PC3 cells adhesion both in the presence and in the absence of icilin (fig. 5d), confirming the tight relationship between the channel and the inactive (GDP-bound) form of Rap1 in mediating cell adhesion independently from the channel activity.

Next, before functionally validating the involvement of K31 and Y32 in Rap1 sequence in mediating the interaction with TRPM8 sequence, we evaluated their possible effects on Rap1 activation (fig. 5e). Interestingly, Rap1 Y32 mutant significantly increased Rap1 activation in PC3 cells (Rap1 Y32 vs CNTRL: * $p<0.05$), whereas Rap1 wt and Rap1 K31 mutant did not alter it (Rap1 wt vs CNTRL: p-value = 0.0833; Rap1 K31 vs CNTRL: p-value = 0.4710). This result could suggest an intrinsic effect of Y32 on Rap1 activation itself even in the absence of TRPM8 and therefore we did not go further in the functional validation of the Rap1 Y32A mutant, as its possible involvement in the interaction with TRPM8 could be altered or masked from an intrinsic activity of the residue on Rap1 properties.

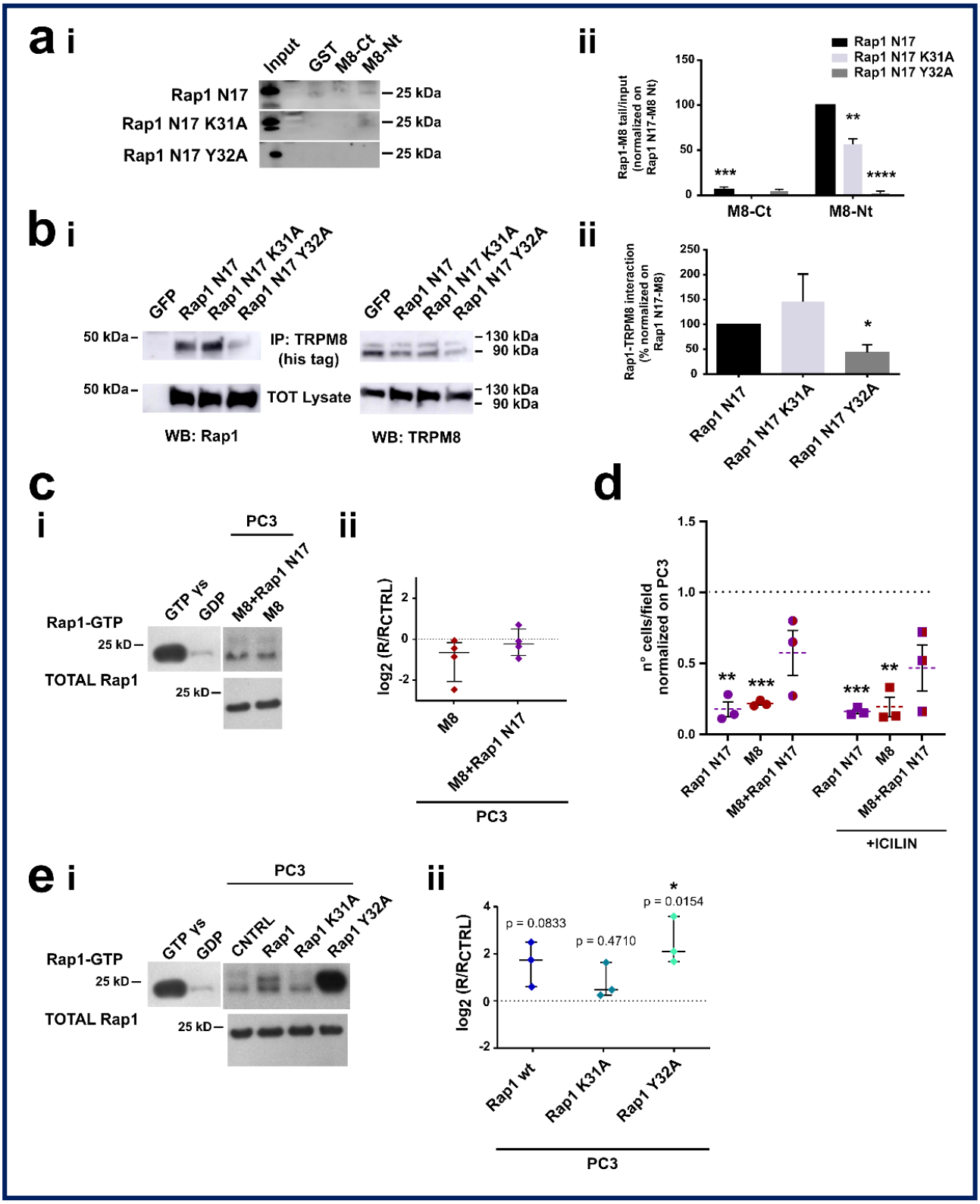

Figure 5. Rap1 mutants' characterization.

*(**a i**) GST pull-down assay on TRPM8 N-terminal tail (M8-Nt), C-terminal tail (M8-Ct), or GST incubated with in vitro translated Rap1 N17, GFP-Rap1 N17 K31A and GFP-Rap1 N17 Y32A. 10% of the in vitro translated Rap1 N17 and mutants were used for the input of the GST pull-down. Western blotting was performed with anti-Rap1 antibody and one*

*representative experiment of three is shown. (**a ii**) Quantification of Rap1-TRPM8 tails interaction normalized on the input. Values are normalized on Rap1 N17-M8 Nt ratio and data are expressed as mean ± SEM. Statistical significance versus Rap1 N17 -TRPM8 Nt: **: P < 0.01; ***: P < 0.001; ****: P < 0.0001 (Two-way ANOVA with Tukey's HSD post-hoc test).*
*(**b i**) Representative immunoprecipitation experiment. PC3M8 cells were transfected with GFP-Rap1 N17, GFP-Rap1 N17 K31A and GFP-Rap1 N17 Y32A plasmids. Cell lysates were immunoprecipitated (IP) for TRPM8 and immunoblotted with anti-GFP antibody for Rap1 detection (panels on the left) and anti-myc antibody for TRPM8 detection (panels on the right). (**b ii**) Quantification of Co-IP experiments on TRPM8 and Rap1 mutants. Data are normalized on TRPM8-Rap N17 interaction and they are expressed as mean ± SEM (n=4). Statistical significance versus TRPM8-Rap1 N17, * = P < 0.05 (Student t-test).*
*(**c i**) Active Rap1 pull-down assay on PC3 stably overexpressing TRPM8 transfected with Rap1 mutants (8 µg). (**c ii**) Quantification of the active Rap1 as the ratio between Rap1-GTP over total Rap1 (R) normalized on this ratio on PC3 (R_{CTRL}). Data are expressed as log_2 and shown in a scatter dot plot in which each dot represents one single experiment and lines represent mean ± SEM. Statistical significance versus PC3 represented by dot line (RM one-way ANOVA without Geisser-Greenhouse correction and with Dunnett's post-hoc test).*
*(**d**) Quantification of adhesion assays on PC3 overexpressing Rap1 N17 (in violet) or TRPM8 (in red) or both Rap1 N17 and TRPM8 (ratio 1:1), treated or not with icilin (10 µM). Data are normalized on PC3 wt (dot line) and displayed as mean ± SEM of three independent experiments. Statistical significance vs PC3 wt, **: P < 0.01; ***: P < 0.001 (One sample t-test).*
*(**e i**) Active Rap1 pull-down assay on PC3 transfected with Rap1 mutants (8 µg). (**e ii**) Quantification of the active Rap1 as the ratio between Rap1-GTP over total Rap1 (R) normalized on this ratio on PC3 (R_{CTRL}). Data are expressed as log_2 and shown in a scatter dot plot in which each dot represents one single experiment and lines represent mean ± SEM. Statistical significance versus PC3 (represented by dot line), *: P < 0.05 (RM one-way ANOVA without Geisser-Greenhouse correction and with Dunnett's post-hoc test).*

4.2 Role of residues E207 and Y240 in the interaction of TRPM8 cytosolic N-terminal tail with GDP-bound Rap1.

After the study and the characterization of Rap1 residues involved in the binding with TRPM8, we focused on TRPM8 residues predicted to be critical for the interaction. Molecular modelling analyses identified two amino acid residues in TRPM8 sequence that may be involved in the binding with Rap1: glutamate (E) 207 and tyrosine (Y) 240 (fig.4). To evaluate the contribution of these two residues on the binding of TRPM8 with inactive Rap1 N17 mutant we performed GST pull-down assays between GST-TRPM8 Ct, GST-TRPM8 Nt, GST-TRPM8 E207A, and GST-TRPM8 Y240A Nt fragments with *in vitro* translated Rap1 N17 (fig. 6a i), Rap1 N17 K31A (fig. 6a ii) and Rap1 N17 Y32A (fig. 6a iii). Indeed, both E207A and Y240A mutations significantly reduced the interaction between TRPM8 Nt wt and Rap1 N17 (fig. 6a, * symbols). Moreover, our data showed that this reduction is even more pronounced in the presence of Rap1 N17 Y32A (fig. 6a, $ symbols), whereas no differences were observed between TRPM8 mutants-Rap1 N17 and TRPM8 mutants-Rap1 K31A interactions. K31 in Rap1 N17 sequence revealed an effect just in the interaction with TRPM8 Nt wt (fig. 6a, # symbols). Overall, these data strongly validated molecular modelling predictions, confirming that all the mutations combined (E207A Y240 on TRPM8 sequence and Y32A on Rap1 N17

sequence) led to a complete loss of TRPM8-Rap1 interaction (fig.6a iv). Since the contribution given by TRPM8 mutants on the interaction with Rap1 N17 was comparable, we decided to generate a single TRPM8 double mutant, carrying both the mutations (TRPM8 E207A Y240A) and we validated it through both GST-pull down (fig. 6b) and Co-IP experiments (fig. 6c). As shown in figures 6b and 6c, TRPM8 double mutant still inhibits the interaction between TRPM8 Nt cytosolic tail and the inactive Rap1 N17. Moreover, we further validated this finding through proximity ligation assay (PLA), showing that in the presence of TRPM8 E207A Y240A the number of dots representing TRPM8-Rap1 complexes is significantly reduced in comparison with TRPM8 wt (fig. 6d).

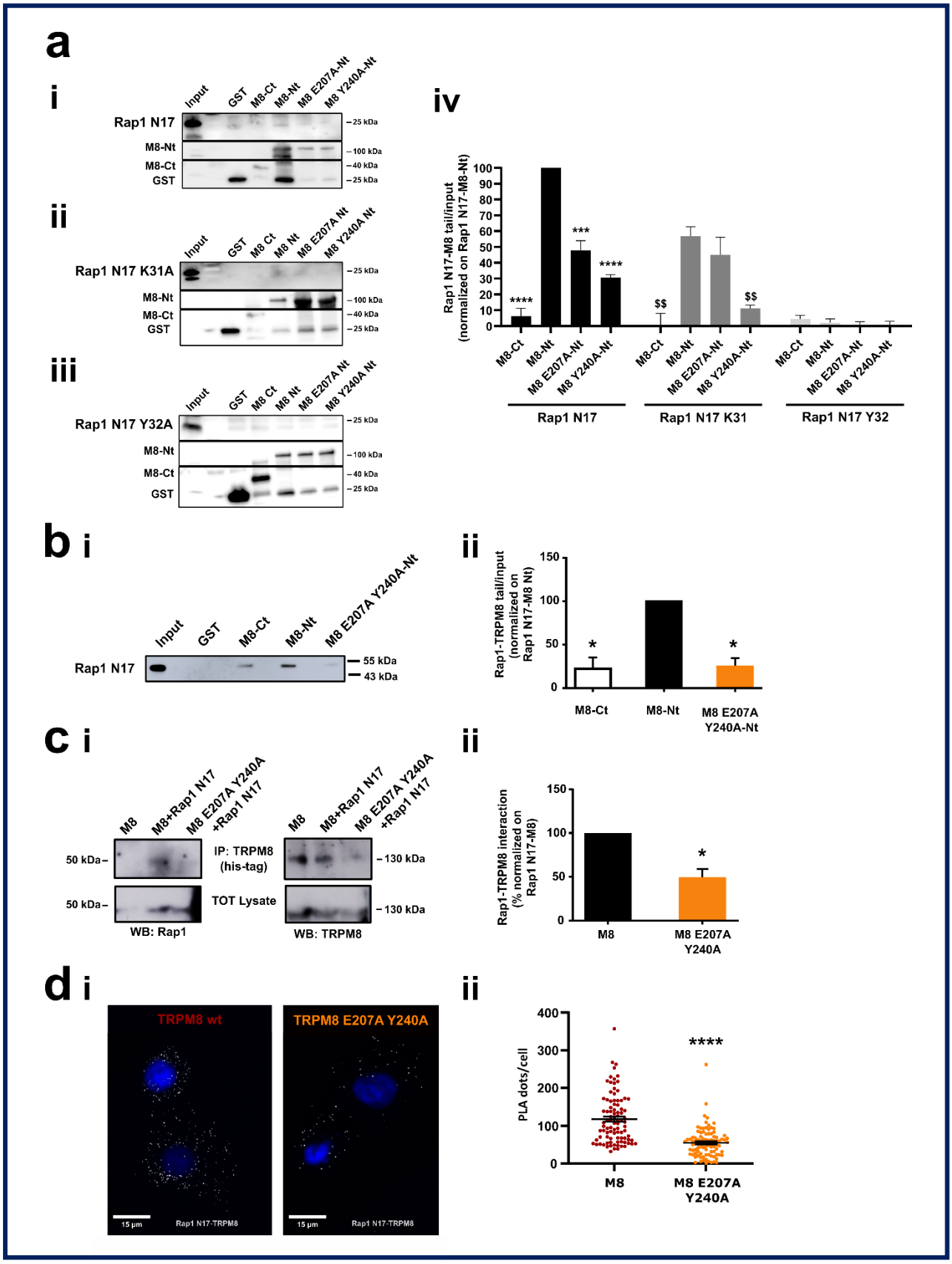

Figure 6. TRPM8 mutants' characterization.

*(**a**) GST pull-down assay on GST, TRPM8 wt C-terminal tail (M8-Ct), TRPM8 wt N-terminal tail (M8-Nt), TRPM8 E207A N-terminal (M8 E207A-Nt) and TRPM8 Y240A N-terminal (M8 Y240A-Nt), incubated with in vitro translated Rap1 N17 (**a i**), Rap1 N17 K31A (**a ii**) and Rap1 N17 Y32A (**a iii**). 5% of the lysates were used for the input of the GST pull-down. Western blotting was performed with anti-Rap1 antibody and one representative experiment out of three is shown. (**a iv**) Quantification of Rap1 N17-TRPM8 tails interaction normalized on the input. Values are normalized on Rap1 N17-M8-Nt ratio and data are expressed as mean ± SEM. Statistical significance versus Rap1 N17-TRPM8-Nt, ***: P < 0.001; ****: P < 0.0001; statistical significance versus Rap1 N17 K31-TRPM8-Nt, $$: P < 0.01 (Student's t-test).*

*(**b i**) GST pull-down assay on GST, M8-Ct, M8-Nt and M8 E207A Y240A-Nt, incubated with lysates of PC3 cells overexpressing GFP-Rap1 N17. 5% of the lysates were used for the input of the GST pull-down. Western blotting was performed with anti–GFP antibody and one representative experiment of three is shown. (**b ii**) Quantification of Rap1 N17-TRPM8 tails interaction normalized on the input. Values are normalized on Rap1 N17-M8 wt-Nt ratio and data are expressed as mean ± SEM (n=3). Statistical significance versus Rap1 N17-TRPM8 wt-Nt, *: P < 0.05 (paired Student's t-test).*

*(**c i**) Representative immunoprecipitation experiment. PC3 cells were transfected with GFP-Rap1 N17 and TRPM8 wt/E207A Y240A plasmid. Cell lysates were immunoprecipitated (IP) for TRPM8 (his-tagged) and immunoblotted with anti-GFP antibody for Rap1 detection (panels on the left) and anti-TRPM8 antibody for TRPM8 detection (panels on the right). (**c ii**) Quantification of Co-IP experiments on TRPM8 and Rap1 N17. Data are normalized on Rap1 N17-TRPM8 (wt) interaction and they are expressed as mean ± SEM (n=4). Statistical significance versus Rap1 N17-TRPM8 (wt), *: P < 0.05 (paired Student t-test).*

*(**d i**) In situ detection of TRPM8/Rap1 interaction in PC3 cells overexpressing TRPM8 (wt or E207A Y240A) and Rap1 N17. TRPM8/Rap1 complexes were monitored as red fluorescent dots using PLA and cell nuclei are visualized in blue (DAPI staining). (**d ii**) Puncta density quantified as mean ± SEM of puncta per cell from three independent experiments (n= 92 for both M8 and M8 E207A Y240A). Statistical significance versus TRPM8 wt, ****: P ≤ 0.0001 (Mann-Whitney test).*

5. TRPM8 E207 Y240 residues revert Rap1-mediated inhibition of cancer cell adhesion and migration.

Given the validation of TRPM8 double mutant showing that E207 and Y240 residues are key players in TRPM8-Rap1A interaction, we functionally validated the interaction. We first characterized the activity of TRPM8 E207A Y240A as a functional ion channel. Ca^{2+} imaging experiments clearly showed that icilin (10 µM) stimulation promotes an increase in $[Ca^{2+}]_i$ in both PC3 overexpressing TRPM8 wt or TRPM8 E207A Y240A as compared with PC3 transfected with empty plasmid (fig. 7a), demonstrating that mutations didn't alter channel activity (not significance between TRPM8 and TRPM8 E207A Y240A – fig. 7a ii).

Next, to validate the functional role of E207A Y240A mutations we performed adhesion assays on PC3 overexpressing TRPM8 wt or TRPM8 E207A Y240A in the presence of icilin (10 µM) (fig. 7b). The results showed that TRPM8 double mutant significantly reverts the inhibition of PC3 cell adhesion induced by TRPM8 wt (fig. 7b). More specifically, in the presence of icilin cell adhesion is inhibited on average by 59% by TRPM8 wt and by 45% by TRPM8 E207A Y240A. Similar results were also obtained by random migration assay, showing that under icilin stimulation (10 µM) TRPM8 E207A Y240 doesn't affect PC3 cells migration speed revealing a significant difference compared to TRPM8 wt (fig. 7c). Aiming to ascertain that this lower inhibitory effect exhibited by the double mutant on migration and adhesion underlies a less marked inhibition

on Rap1 activation, we performed active Rap1 pull-down and live-cell imaging experiments on PC3 cells overexpressing TRPM8 wt or TRPM8 E207A Y240A. Consistent with our hypothesis, E207A Y240A mutations, by reducing the interaction of TRPM8 with Rap1, resulted in less inhibition on the small GTPase activity: the amount of endogenous active (GTP-bound) Rap1 is significantly higher in the presence of TRPM8 double mutant as compared with TRPM8 wt (fig. 7d, TRPM8 wt vs TRPM8 E207A Y240A: *, $p<0.05$). Furthermore, after stimulation with icilin (10 µM), no significant intracellular retention of active Rap1 was mediated by the double mutant (fig. 7e on the bottom). On the contrary, TRPM8 wt showed a significant relative cytoplasmic translocation of active Rap1 (corresponding to an inhibition of its translocation to the PM, as previously described) already 2 min after treatment, which disappears after 10 min (fig. 7e on the top) in agreement with the results previously obtained (fig. 2b).

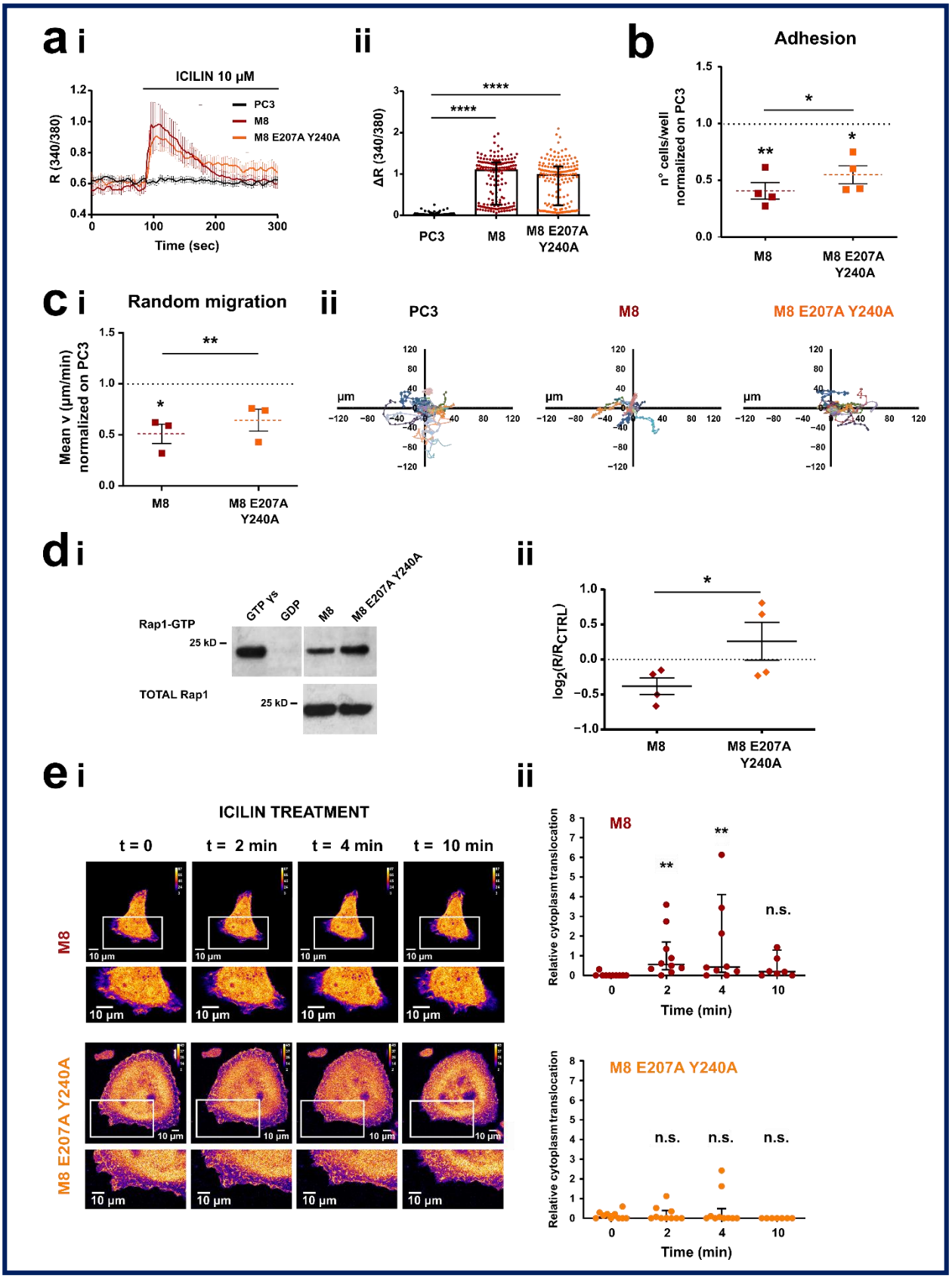

Figure 7. TRPM8 mutant's functional validation.

*(**a i**) Ca^{2+}-imaging traces in response to TRPM8 agonist (10 µM icilin) in PC3 (control in black), PC3 transiently overexpressing TRPM8 (red) and PC3 transiently overexpressing TRPM8 E207A Y240A mutant (orange). Traces represent mean ± SEM of cells in the recorded field of one representative experiment (n=45 for PC3, n=32 for M8 and n=33 for M8 E207A Y240A). (**a ii**) Scatter dot plot showing peak amplitude of icilin-mediated Ca^{2+} responses (median with interquartile range of different cells in the field from at least 7 independent experiments). Only icilin-responsive cells were considered to compare TRPM8 and TRPM8 E207A Y240A channel activity (n=228 for PC3, n=160 for M8 and n=167 for M8 E207A Y240A). Statistical significance versus PC3, ****: P < 0.0001 (Kruskal-Wallis test with Dunn's post-hoc test).*
*(**b**) Quantification of adhesion assays on PC3 overexpressing TRPM8 wt (red) or TRPM8 E207A Y240A (orange) and treated with icilin (10 µM). Data are normalized on PC3 treated with icilin (control represented by dot line) and displayed as mean ± SEM of four independent experiments. Statistical significance versus PC3, *: P < 0.05; **: P < 0.01 (One sample t-test); statistical significance M8 wt vs M8 E207A Y240A, *: P < 0.05 (paired Student t-test).*
*(**c i**) Quantification of random migration assays on PC3 overexpressing TRPM8 wt (red) and PC3 overexpressing TRPM8 E207A Y240A mutant (orange) in the presence of icilin (10 µM). Data are normalized on PC3 treated with icilin (control represented by dot line) and displayed as mean ± SEM of three independent experiments. Statistical significance versus PC3 when not differently specified, *: P < 0.05; **: P < 0.01 (One sample t-test); statistical significance M8 wt vs M8 E207A Y240A, *: P < 0.05 (paired Student t-test). (**c ii**) Representative migration plots of PC3 (left panel), PC3 overexpressing TRPM8 (central panel) and PC3 overexpressing TRPM8 E207A Y240A (right panel). Each line represents the trajectory of one cell within a 6 h period. Data shown refer to one field of one representative experiment out of three (PC3=20 cells; M8= 16 cells; M8 E207A Y240A= 17 cells).*
*(**d i**) Active Rap1 pull-down assay on PC3 overexpressing TRPM8 wt and TRPM8 E207A Y240A (4 µg). (**d ii**) Quantification of the active Rap1 as the ratio between Rap1-GTP over total Rap1 (R) normalized on this ratio on PC3 (R_{CTRL}). Data are expressed as log_2 and shown in a scatter dot plot in which each dot represents one single experiment and lines represent mean ± SEM. Statistical significance *: P < 0.05 (paired Student's t-test).*
*(**e i**) Live-cell imaging by confocal microscopy of PC3 overexpressing TRPM8 wt or TRPM8 E207A Y240A and expressing GFP-RBD_{RalGDS} probe. Representative images showing GFP-RBD_{RalGDS} in PC3+TRPM8 and PC3+ TRPM8 E207AY240A at t=0 and after 2, 5 and 10 min of treatment with 10 µM icilin; the bottom parts of the figures represent enlargement of the inset (white box) for each time point. (**e ii**) Scatter dot plots showing the quantification of GFP-RBD membrane recruitment calculated as cytosol translocation as described in the method section. Each dot represents one cell (51 ROIs referring to 10 cells for TRPM8 and 57 ROIs referring to 10 cells and for TRPM8 E207A Y240A) and lines show median ± interquartile range. Statistical significance versus t=0, **: P < 0.005 (Kruskal-Wallis test with Dunn's post-hoc test).*

6. TRPM8-Rap1 interaction in breast and cervical cancer.

A final set of experiments was performed to evaluate whether the mechanistic model illustrated here on the TRPM8-Rap1 interaction could potentially be generalized beyond prostate cancer. To this purpose, we assessed TRPM8 double mutant on two other tumor cell lines (fig. 8) that do not express TRPM8 endogenously (fig. S2a). We performed adhesion and migration assays on HeLa cells and MCF-7 cells overexpressing TRPM8 wt or TRPM8 E207A Y240A. The TRPM8 transfection was confirmed by Western blot (fig. S2 a i), and Ca^{2+} imaging analyses (fig. S2b). As shown in figure 8a, both HeLa (i) and MCF-7 (ii) cells overexpressing TRPM8 E207A Y240A displayed a significant increase in cell adhesion compared to cells transfected with TRPM8 wt (fig. 8a i, M8 E207A Y240A vs wt in HeLa: **, p<0.01; fig. 8a ii M8 E207A Y240A vs wt in MCF-7: *, p<0.05). As regards cell migration, we observed that in HeLa cells this pathway is not

affected by either TRPM8 wt or TRPM8 E207A Y240A (fig. 8b i). Conversely, TRPM8 wt decreases cell migration in MCF-7 cells, while TRPM8 E207A Y240A does not (fig. 8b ii), thus suggesting an involvement of TRPM8-Rap1 interaction in the control of the migratory phenotype of breast cancer similarly to prostate cancer (fig. 7c). Furthermore, we have verified that this effect is not attributable to reduced cell viability. Indeed, we found that, in correspondence with the greatest overexpression of TRPM8, i.e. 24 h after transfection (fig. S5b), cell viability is not affected in MCF-7 (fig. S5a ii) or in PC3 (fig. S5a i). However, it is interesting to note that disruption of the interaction between TRPM8 and Rap1 mildly reduces the viability of MCF-7 and PC3 (by 7% and 16% respectively), thus suggesting a possible role of TRPM8-Rap1 interaction in preserving the viability of these two cell lines. In contrast, in HeLa cells, which didn't show any TRPM8-mediated inhibition of cell migration, both TRPM8 wt and TRPM8 E207A Y240A showed a slight but significant reduction in cell viability of approximately 14% (fig. S5a iii).

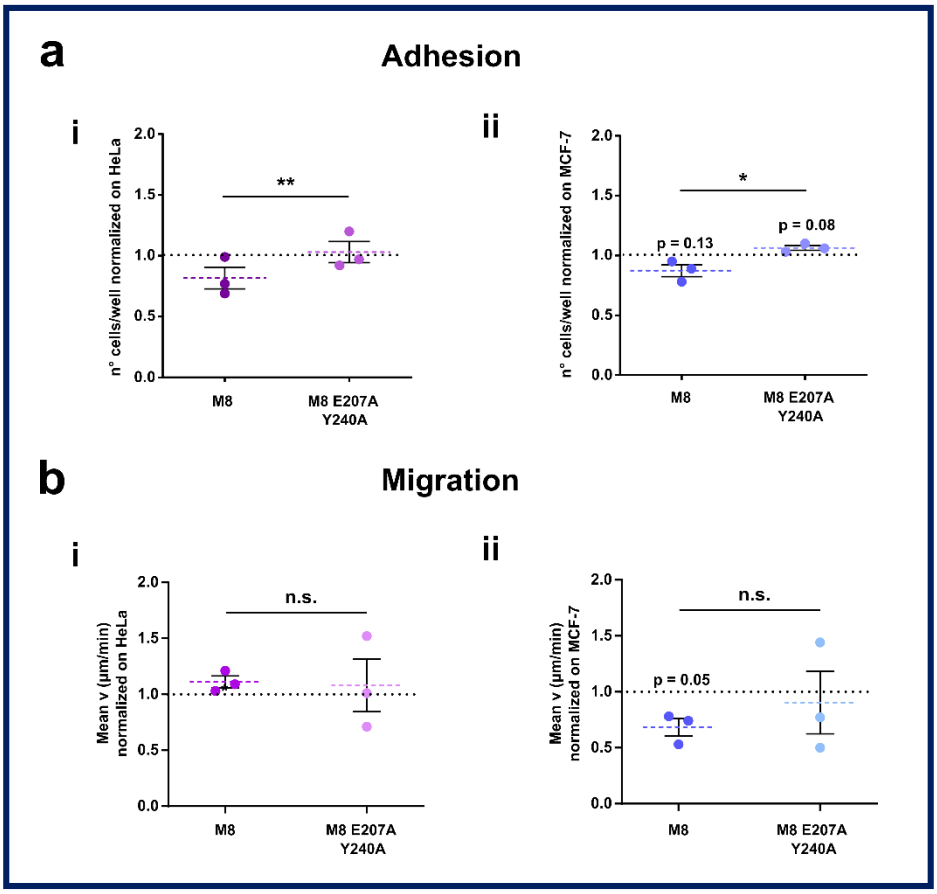

Figure 8. Validation of TRPM8 E207A Y240A on other epithelial cancer cell lines.

*(**a**) Quantification of adhesion assays on HeLa (i) and MCF-7 (ii) cells transfected with TRPM8 wt and TRPM8 E207A Y240A. Data are normalized on control cells (HeLa or MCF-7 cell transfected with empty vector represented by dot lines) and displayed as mean ± SEM of three independent experiments. Statistical significance versus HeLa/MCF-7 wt, *: P <*

*0.05; **: P < 0.01; n.s.: not significant (One sample t-test); statistical significance M8 wt vs M8 E207A Y240A, *: P < 0.05; **: P < 0.01 (paired Student t-test). (**b**) Quantification of transwell migration assays on HeLa (i) and MCF-7 (ii) cells transfected with TRPM8 wt and TRPM8 E207A Y240A. Data are normalized on control cells (dot lines) and displayed as mean ± SEM of three independent experiments. Statistical significance versus HeLa/MCF-7 wt, n.s.: not significant (One sample t-test); statistical significance M8 wt vs M8 E207A Y240A, n.s.: not significant (paired Student t-test).*

Finally, in order to investigate the clinical relevance of TRPM8-Rap1A relative expression in the cancer types for which we studied protein-protein interaction, we used transcriptional data from TCGA and GTEx databases to performe differential expression analysis on both genes. Specifically, we downloaded RNA-Seq data for prostate, breast, and uterine epithelia labeling samples as "healthy", "metastatic" or "not metastatic" based on the clinical criteria described in the Materials and Methods section. Then, differential expression analysis was separately performed on RAP1A and TRPM8 transcript levels in each one of the three cancer cohorts. As shown in figure 9, TRPM8 expression increases in the three types of cancer in “not metastatic” condition compared to healthy samples. The same can be observed when metastatic samples are compared to healthy controls in the uterine cohort but not in the breast and prostate ones. On the other hand, Rap1A expression remains almost unchanged in prostate and breast cancer while it decreases in uterine cancer (in both “metastatic” and “not metastatic” groups). Though the sample size of the “metastatic” group in the prostate cohort is actually too small (n=3) to be really informative about the actual transcriptional profile associated to this condition, these results seem to suggest that prostate and breast cancers both share the same expression profile for RAP1A and TRPM8 genes, in contrast to uterus cohort that showed instead a markedly different transcriptional pattern. Similarly, the cervical cancer cell line was the only in vitro model for which overexpression of TRPM8 failed to reduce migration while instead more markedly affecting cell viability in our experiments, further confirming the functional implications of TRPM8-RAP1A relative expression.

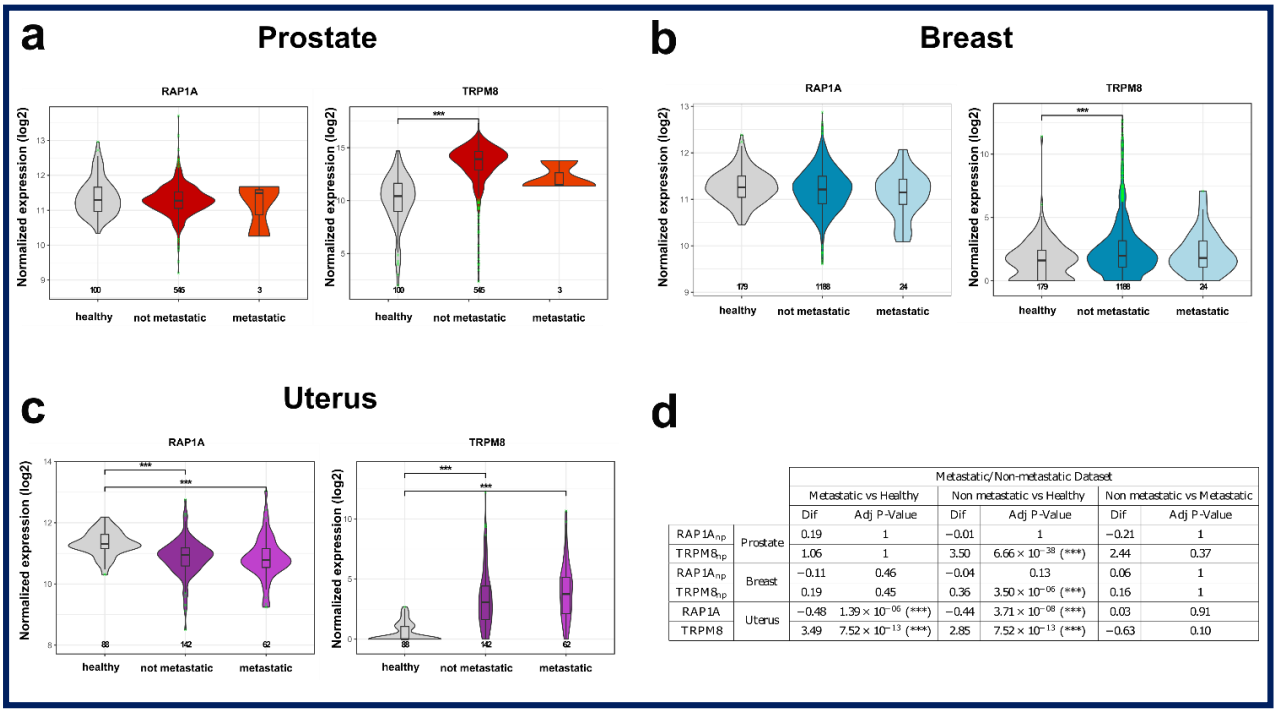

		Metastatic/Non-metastatic Dataset					
		Metastatic vs Healthy		Non metastatic vs Healthy		Non metastatic vs Metastatic	
		Dif	Adj P-Value	Dif	Adj P-Value	Dif	Adj P-Value
$RAP1A_{np}$	Prostate	0.19	1	−0.01	1	−0.21	1
$TRPM8_{np}$	Prostate	1.06	1	3.50	6.66×10^{-38} (***)	2.44	0.37
$RAP1A_{np}$	Breast	−0.11	0.46	−0.04	0.13	0.06	1
$TRPM8_{np}$	Breast	0.19	0.45	0.36	3.50×10^{-06} (***)	0.16	1
RAP1A	Uterus	−0.48	1.39×10^{-06} (***)	−0.44	3.71×10^{-08} (***)	0.03	0.91
TRPM8	Uterus	3.49	7.52×10^{-13} (***)	2.85	7.52×10^{-13} (***)	−0.63	0.10

Figure 9. TRPM8 and Rap1A expression during carcinogenesis in different cancers.

Differential expression analysis on Rap1A and TRPM8 transcripts in prostate (a), breast (b), and uterine (c) healthy and tumor (not metastatic and metastatic) patient samples from GTEx and TCGA databases, respectively. Results of statistical analysis are reported in the table of panel (d). Dif = difference between means; np = nonparametric hypothesis tests (i.e., Kruskal-Wallis H omnibus test and post-hoc Dunn's test). Otherwise, ANOVA and Tukey's HSD post-hoc test were performed.

Discussion

The anti-metastatic role of TRPM8 in prostate cancer due to its ability to impair PCa cells' motility has been suggested in recent years [44,45]. These findings are consistent with an androgen-dependency of TRPM8 expression which results in a strong TRPM8 down-regulation during PCa progression [41,42,72]. Furthermore, it has previously been shown that TRPM8 is also expressed in different ECs and that it is dramatically down-regulated in some tumor-derived ECs, contributing to their more aggressive and pro-angiogenic migratory phenotype [48]. Our data confirmed the key role played by TRPM8 in inhibiting metastatic PCa cells' migration (fig. 1c) and also revealed a role of the channel in the regulation of PC3 cells adhesion (fig. 1a). Consistently with data obtained in ECs [48], TRPM8 seems to exert its inhibitory effect on PCa cells' migration independently from its channel function (fig. 1b, 1e). However, a role for Ca^{2+} influx seems to be important for the adhesion process as demonstrated by the lack of inhibitory effect on cells overexpressing TRPM8 pore mutant (Y905A) stimulated with TRPM8 agonist (fig. 1d, 1e). On the contrary,

the migratory features of PC3 cells transfected with both TRPM8 wt and TRPM8 Y905A didn't show any differences either in the presence of icilin, supporting the hypothesis that TRPM8 effects on cell migration are completely independent of its channel function, as previously demonstrated for ECs [48]. Importantly, we revealed that TRPM8 expression is sufficient to exert its functional effects, inhibiting PC3-extracellular matrix adhesion and PC3 migration, although TRPM8 active stimulation may improve its inhibitory impact on cell adhesion probably through a Ca^{2+}-dependent additive mechanism. Our results are consistent with emerging evidence for pore-independent roles of ion channels [73,74] including TRP channels in many hallmarks of cancer. In particular, the modulation of various intracellular pathways has previously been traced back to the enzymatic properties of some TRP channels [75,76] or to their coupling with other partner proteins that does not necessarily involve their pore activity [13,48,77].

In this regard, among different interactors of TRPM8 [45], our attention was focused on the small GTPase Rap1A, whose central role in the promotion of cell adhesion through the activation of the β_1-integrin signalling pathway is well-known [78,79]. The interaction between TRPM8 and Rap1 was further supported by the partial punctate co-localisation outside the nucleus of the two proteins shown in prostate clinical samples in Supplementary fig. S6. In the last decade, several studies have reported a strong interplay between TRP channels and small GTPases in the modulation of the metastatic cascade [21]. More specifically, TRP channels were found to affect small GTPase activity via both Ca^{2+}-dependent and Ca^{2+}–independent pathways. Conversely, small GTPases may act as TRP channels effectors as well as regulators, by modulating channel trafficking, gene expression, protein-protein interactions (PPIs), and channel gating [21]. Taken together, our results on Rap1 activation clearly show that, as observed in endothelial cells [48], TRPM8 overexpression and its activation by icilin in PC3 cells lead to the intracellular retention of Rap1 in its inactive (GDP-bound) form, decreasing the active (GTP-bound) Rap1 fraction available for the translocation to the PM (fig. 2). We then confirmed that also in intact PC3 cells the TRPM8-mediated inhibition on Rap1 activation is due to physical direct interaction between the channel and the inactive form of Rap1A (fig. 3c and 5a-b). GST pull-down on *in vitro* translated Rap1 proteins had previously shown that TRPM8 N-terminal tail mostly interacts with the inactive (GDP-bound) form of Rap1 (Rap1 N17 mutant) compared to Rap1 wt and its active form (Rap1 V12 mutant) [48]. This interaction was further confirmed in the cellular context in PC3 cells (fig. 3c and 5b). These results are in agreement with our previous data on vascular endothelium, which showed that this coupling affects ECs migration, *in vitro* sprouting and vascular network formation [48].

Our hypothesis on the intracellular trapping of Rap1 in its inactive form by TRPM8 is further corroborated by our data on the subcellular localization of TRPM8-Rap1A interaction. Small GTPases are known to exert their effects on cellular behaviour mainly through a rigorous spatiotemporal regulation to which they and their effectors/modulators are subjected [80–82]. In particular, Rap1A in its active form is

present at the PM, where its activation occurs allowing the β_1-integrin signalling induction [71,79,83], whereas in its nucleotide-free form it is present into cytoplasmic vesicles, but not at the PM [62]. Therefore, the retention of inactive Rap1 would be more consistent with its intracellular localization in close proximity to both TRPM8 and ER. Our analysis on TRPM8-Rap1A N17 complexes revealed a partial co-localization with PC3 ER membrane (fig. 3c), in agreement with previous results obtained in ECs [48]. In PCa it has been extensively highlighted a dual localization of TRPM8 long isoform (130 kD), both on the PM ($TRPM8_{PM}$) and the ER ($TRPM8_{ER}$). This dual localization in the prostate not only is determined by the epithelial cell phenotype and by the androgen status [42,72] but has been also associated with a different channel function in carcinogenesis events, such as proliferation, apoptosis, and migration. More specifically, it has been shown that $TRPM8_{ER}$ can be considered an important factor in controlling apoptosis of advanced PCa metastatic cells [84,85], being capable of influencing the filling of ER stores [61], strictly related to the apoptosis-resistant cell phenotypes, characteristic of advanced prostate cancer [84,86,87]. Our results show that $TRPM8_{ER}$ fraction plays a role in PCa cells' motility, similarly to ECs [48]. On the other hand, this would not exclude a possible Ca^{2+}-mediated involvement of $TRPM8_{PM}$ fraction previously suggested [44]. Overall, we propose that the long $TRPM8_{ER}$ isoform, beyond its Ca^{2+}-dependent impact on cell growth and apoptosis, is also involved in the regulation of PCa migration and adhesion due to its interaction with the small GTPase Rap1A (see graphical abstract – Fig.10). The mechanism here depicted has been further validated by the results obtained through active Rap1 pull-down and adhesion assays performed on PC3 cells overexpressing TRPM8 and the inactive GDP-bound Rap1 N17 mutant. Indeed, the inhibition induced by TRPM8 on Rap1 activation, as well as that on PC3 adhesion, resulted partially reverted in the presence of overexpressed Rap1 N17 (fig. 5c-d). This partial functional reversion could be explained by the saturation of TRPM8 binding sites borne by the excess of inactive Rap1: due to the binding of TRPM8 with Rap1 N17 mutant, the amount of endogenous Rap1 available for the functional switch into the active GTP-bound form free to accomplish its function, promoting cell adhesion, is greater. Consequently, in systems overexpressing both TRPM8 and inactive Rap1, the inhibitory effect on Rap1 activation and cell adhesion is partially reverted. Notably, TRPM8-Rap1A interplay shown here is not the only example of TRPM8 interaction with an inactive GTPase. Indeed, it has been previously described a direct interaction between TRPM8 and the G-protein subunit $G\alpha_q$ even when inactive, which ultimately results in the inhibition of TRPM8 gating [88]. Contemporary, the menthol-mediated activation of TRPM8 was found to exert a metabotropic activity through the functional and structural interaction with $G\alpha_q$ [89]. Overall, there is a close bidirectional interaction between TRPM8 channel and GTPase proteins supported by direct physical interactions: depending on the case, TRPM8 can act as both modulator and effector of this functional coupling.

A major discovery of our study is the identification of the residues involved in the interaction between TRPM8 and Rap1A. These findings could, indeed, give new insights for potential future applications of TRPM8 as therapeutic targets in PCa treatment. Among the two putative residues identified by molecular modelling in the sequence of Rap1A, we demonstrated that the tyrosine (Y) in position 32 is crucial in mediating the interaction of Rap1 N17 with the N-terminal of TRPM8. However, it was difficult to evaluate the functional effect of Y32 mutation in the TRPM8-mediated inhibition of Rap1 activation and cell adhesion, since this mutant seemed to have itself an intrinsic function on Rap1 activation, increasing it also in PC3 cells in the absence of TRPM8 (fig. 5e). These findings are in agreement with recent data that highlighted a central role of Y32 on GTP hydrolysis and effector binding of Ras protein, confirming the possibility that the residue Y32 not only plays a role in mediating Rap1-TRPM8 interaction but may also have an intrinsic functional role on Rap1 activation [90–92]. Indeed, Y32 falls into the so-called switch I, a loop region of small GTPase (residues 30–38) which, together with switch II (59–72), plays a pivotal role in GTPase cycle. More in detail, it has been shown that substantial rearrangements of Switch I, Switch II, and the α3-helix occur during the GTPase switching from the inactive GDP-bound to the active GTP-bound state. These are attributable to a wide range of hydrogen-bonding networks which mainly lead to the loss of the functional water molecules, the positional shift of GTP, fluctuation of Y32, and translocation of Q61 [90]. Moreover, molecular dynamics simulations and Markov state models suggested that alteration of the Y32 chemical environment may cause notable changes in conformation and dynamics of residues surrounding the active site [91]. Therefore, it is evident that Y32 dynamics and orientation can play a direct role in influencing GTPase's properties, such as binding with GTP/GDP, the hydrolysis rate of GTP, the affinity for regulators (GEF and GAP) as well as that for effectors [91]. Consistently, c-Src was found to phosphorylate H/N/KRAS on conserved Tyr32, thus stalling their GTPase cycle in the GTP-bound state and affecting the binding to Raf effector as well as the downstream signalling [92,93]. Taking into account the highly conserved catalytic domain in the Ras-superfamily and the common conformational dynamics shared by Rap1 with Ras proteins [90], it seems possible to assume that tyrosine in position 32 can influence the GTP/GDP cycle of Rap1, influencing its activity as well as its interaction with modulators including TRPM8. Therefore, it is likely that the binding to TRPM8 could engage the hydroxyl group of Y32 and thus prevent the formation of the hydrogen bond with which Y32 contributes to the GTPase transition and therefore the adhesion process.

As regards the putative residues identified by molecular modelling in TRPM8 sequence, i.e. glutamate (E) 207 and tyrosine (Y) 240, both the residues revealed a central role in the interaction with Rap1 N17 (fig. 6). Indeed, in the presence of TRPM8 mutants (TRPM8 E207A, TRPM8 Y240A, and TRPM8 E207A Y240A) TRPM8-Rap1 N17 interaction is significantly compromised, being definitively lost when TRPM8 E207A Y240A is combined to Rap1 N17 Y32A. Although a significant functional difference between TRPM8 wt and TRPM8

E207A Y240A on both cell adhesion and cell migration inhibition is evident, TRPM8 E207A Y240A still inhibits PC3 cells adhesion (Fig. 7b, 7c). This observation could be explained by alternative and potentially Ca^{2+}-mediated modalities disregarding the interaction with Rap1 by which TRPM8 exerts its inhibitory action on cell adhesion. This hypothesis is in agreement with the lack of inhibitory effect on cell adhesion of TRPM8 pore mutant in the presence of icilin (fig. 1e). Another possible explanation is that the two mutations on TRPM8 sequence do not completely disrupt the interaction with endogenous Rap1A. The absence of a total reversion of the functional effects mediated by TRPM8 wt, in addition to the above reasons, could also be influenced by the efficiency of the transient transfection system used. In this regard, it is important to note that the cells were transfected with a rather low amount of TRPM8 plasmid in all experiments, to avoid system saturation with excessive channel expression, and consequently, to avoid the risk of masking the effects of TRPM8 double mutations in impairing TRPM8-Rap1A interaction. Finally, to further support our mechanistic model, we can affirm that the different functional behaviours shown by TRPM8 wt and double mutant, are not imputable to a different channel functionality, since we verified that the two mutations in the cytosolic N-terminus didn't affect the icilin-induced Ca^{2+} flux through the channel, neither qualitatively (fig. 7a i) nor quantitatively in terms of signal peak amplitude or percentage of responding cells (fig. 7a ii). These data confirm once again the pore-independence of this pathway, showing that the inhibitory effect exerted by TRPM8 on Rap1 activation, and consequently on cell adhesion and migration, is, at least in part, due to physical interaction involving, in particular, the residues E207 and Y240 on the N-terminal cytosolic tail of the channel and the residue Y32 on the switch I region of the small GTPase.

To our best knowledge, there are no other examples in the literature of TRP-Rap1 interactions. Moreover, studies reporting TRP channels' physical interaction with other small GTPases like Rac1 and RhoA [25,33,34] did not investigate the putative residues involved in such interactions except for TRPV5/6-Rab11a binding that has been localized in a conserved stretch in the TRPV carboxyl terminus [94]. Therefore, our work is one of the very few examples of a comprehensive characterization of the TRP-small GTPase interaction, revealing not only the biological impact of this interaction on cancer physiology, but also which residues are determinant in this pathway and thus how potentially targeting it in cancer treatment.

Although the pore independence of these inhibitory mechanisms, icilin seems to have an active role in promoting TRPM8-Rap1 interaction, and consequently in the inhibition of Rap1 activation and PC3 cells' migration/adhesion (fig. 1a-d, 2b, 7e). This rather surprising observation raises questions about the possible effects of agonists on TRPM8 in addition to pore gating, and may be explained in light of the crystal structures (ligand-free and ligand-bound) of TRPM8 recently resolved by Yin and co-workers [49,95]. The authors reported cryo-electron microscopy structures (apo, icilin- and WS12-bound) of a full-length avian TRPM8 channel ($TRPM8_{FA}$), with many features common to mammalian TRPM8 channels (83% sequence identity

with human TRPM8), including cold- and menthol-sensitivity and pronounced dependence on phosphatidylinositol 4,5-bisphosphate (PIP_2) [49]. Describing the structural basis for allosteric coupling between PIP_2 and cooling agonists, they demonstrated that both icilin and PIP_2 induce a conformational change by binding to a different region of segment 4b (S4b), that favours the bond of the other [95]. Therefore, the binding of PIP_2 and icilin/WS12 triggers global conformational rearrangements in TRPM8 transmembrane domain (TMD) that are propagated to the cytosolic domain (CD) via extensive intersubunit interactions observed between the TMD and the top layer of the CD ring, mainly mediated by the recently discovered "pre-S1 domain" specific of the TRPM8 structure [49,95]. Consequently, icilin is likely to favour and stabilize conformational changes in TRPM8 N-terminal cytosolic tail where binding to Rap1A occurs, due to the structural rearrangements associated with PIP_2 binding, and thus may improve TRPM8-Rap1A physical and functional coupling.

Notably, our data suggested that the role of TRPM8 as a Rap1 inhibitor is not confined to ECs and PCa cells but may be generalized. Indeed, TRPM8-Rap1 interaction and function have been previously validated in ECs and also confirmed in an overexpression system of HEK cells [48]. Moreover, in this study we demonstrated that the binding of TRPM8 with Rap1, mainly supported by E207 and Y240 residues in its N-terminal tail, affects cell adhesion not only in metastatic PCa cells but also in other cancer models like breast and cervical cancer, though to a different extent (fig. 8). The same is also true for the migratory behavior of breast cancer, but not for that of the cervical. Furthermore, neither the residues of TRPM8 involved in the interaction nor that of Rap1 are mutated in the cohort of patients of all types of cancer analyzed by us (fig. 4b). This bodes well for the potential use of TRPM8, or of the peptide sequence involved in the functional interaction with Rap1 alone, in cancer therapy to prevent and/or block its metastatic degeneration.

Nowadays, TRP channels interactome is an intriguing research field with great potential in cancer therapy. Indeed, disrupting or enhancing PPIs involving TRP channels could be a promising alternative therapeutic approach since allows targeting only the cellular pathways associated with a specific interaction thus minimizing side effects [96]. However, beyond the high specificity shown by peptides against their targets, this approach presents quite a few challenges. First, compared to targeting enzymes or receptors, targeting PPIs is complicated by the broad and less structured interface of these interactions [97]. Second, peptides have poor cell/tissue specificity and membrane penetration capacity. To overcome these limitations, in addition to a deeper mechanistic understanding of these interactions, essential for improving the specificity and selectivity of this innovative approach, the combination of PPI-targeted bioactive peptides with cell-penetrating peptides (CPPs) successfully revealed good cellular uptake and biocompatibility with low side effects *in vivo* [98–100]. Interestingly, a mimetic of the Arg-Gly-Asp tripeptide epitope of fibrinogen able to bind to the αIIbβ3 integrin has been approved by FDA and currently used in therapy as Tirofiban [101].

However, to date, no PPI modulators related to TRP channels have been approved for human treatment. Nevertheless, several *in vivo* studies have highlighted the great therapeutic potential of systemically-administered peptides capable of impairing the association between ion channel and their interactors [102–105]. In this context, a synthetic peptide based on PLC-γ1 SH2 domains, found to interact with TRPC1 [106], revealed an anti-tumoral activity in breast cancer [107]. Similarly, a peptide mimicking the γ-aminobutyric acid type A (GABAA) receptor-associated protein (GABARAP) which interacts with TRPV1 [108] has been proposed as a good candidate to promote TRPV1-associated suppression of breast cancer progression [109]. Furthermore, the design of peptides able to promote TRPV1-TRPA1 interaction could be a promising treatment for pain therapy [110]). Overall, growing evidence supports the use of peptidomimetics to improve currently FDA-approved approaches to fighting cancer [111,112].

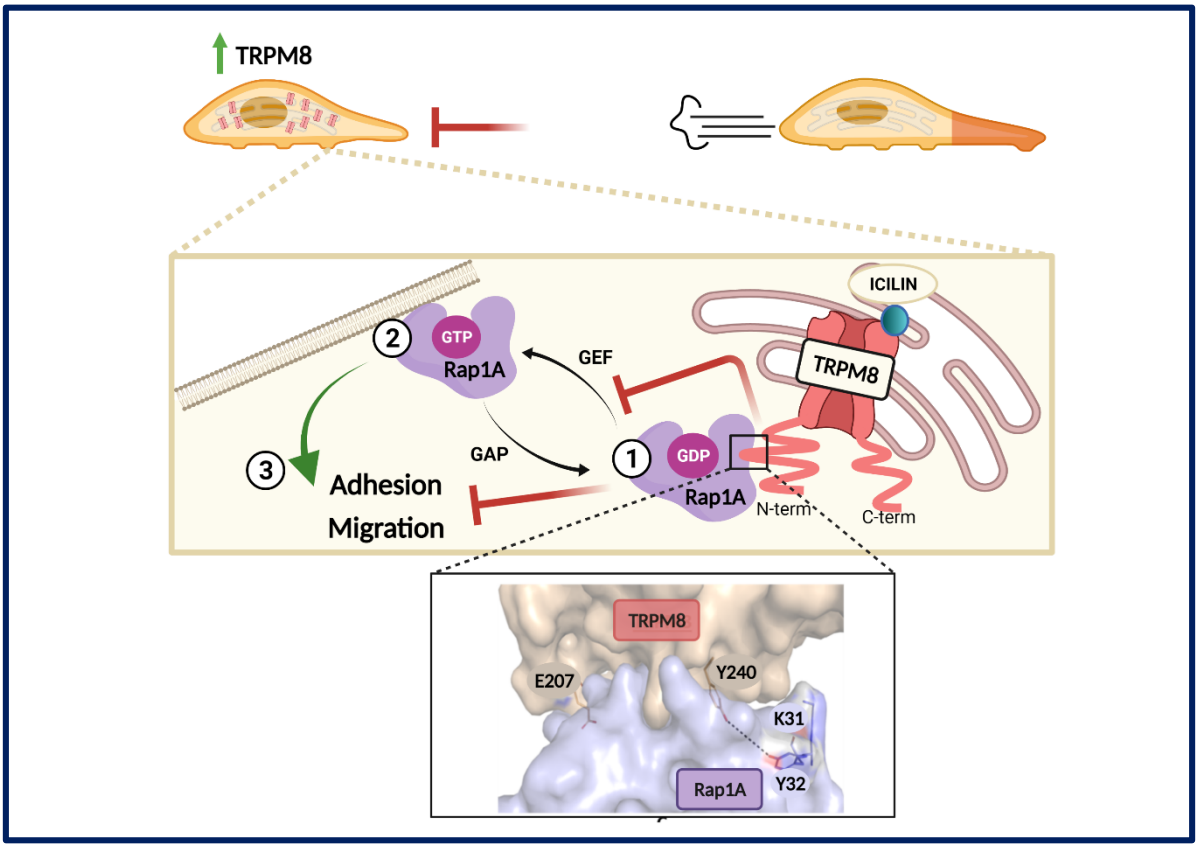

Figure 10. Graphical abstract.

Scheme summarizing the mechanism through which TRPM8 inhibits cell adhesion and migration thanks to the direct interaction with the small GTPase Rap1A.

Conclusions

In this work, we clarified the molecular mechanism through which TRPM8 affects PCa progression by impairing cell motility. We demonstrated that in metastatic PCa cells TRPM8 acts as a sort of GDI-like protein, interacting with the inactive (GDP-bound) form of Rap1A and intracellularly sequestering it into the cytoplasm. This action hinders Rap1 translocation to the PM, where it normally is activated and exerts its positive action on cell adhesion, in principle by promoting the β_1-integrin signalling pathway. Furthermore, we went deeper into the details of this interaction by identifying the residues of the two proteins mainly involved in its mediation: E207 and Y240 on the N-terminal cytosolic tail of the channel and the residue Y32 on the switch I region of the small GTPase. Validation of these residues on different cancer cell lines suggests a broad spectrum of action of this Ca^{2+}-independent TRPM8-Rap1A interplay in terms of control of cell adhesion and migration. Altogether these findings provide new insights into potential therapeutic approaches involving TRPM8 as a target for cancer progression treatments.

Author Contributions: Conceptualization, G.C., D.G. and A.F.P.; methodology, G.C., G.P.G., A.B., M.L., J.D.R., L.V., F.A.R., D.G., A.F.P.; software, A.B., G.B., M.L., J.D.R., L.V., F.A.R.; formal analysis, G.C., G.P.G., M.A., M.B., J.C., G.B., L.V., F.A.R; investigation, G.C., G.P.G., M.A., M.B., A.R.C, M.B., J.C., G.B., A.F.P., D.G,; resources, R.A.T., J.D.R., A.F.P., and D.G.; data curation, G.C., G.P.G., M.A., M.B., G.B., M.L., Q.L., A.F.P., D.G.; writing—original draft preparation, G.C.; writing—review and editing, G.C., A.R.C., D.G. and A.F.P.; visualization, G.C., D.G., A.F.P, J.D.R.; supervision, A.F.P. and D.G.; project administration, A.F.P. and D.G.; funding acquisition, A.F.P. and D.G. All authors have read and agreed to the published version of the manuscript.

Funding: DG is supported by the Institut Universitaire de France (IUF) and France Berkley Fund. GC is supported by University of Torino as part of the PhD Program in Complex Systems for Life Sciences. AFP and GC are supported by Italian Ministry of Instruction, University and Research (MIUR), PRIN grant “Leveraging basic knowledge of ion channel network in cancer for innovative therapeutic strategies (LIONESS)” (grant number 20174TB8KW) and are part of the Associated International Laboratory (CaPANCInv).

Acknowledgments: We thank Dr. Bidaux for providing $TRPM8^{Y905A}$ pore mutant plasmid and Dr. Masamitsu Iino for providing pCIS GEM-Cepia1er plasmid. We thank Mathilde Lebas , Dr. Elodie Richard and Plateforme d'Imagerie BICeL (Campus Cité Scientifique), Dr. Marta Gai and the Open Lab of Advanced Microscopy at the Molecular Biotechnology Center (OLMA@MBC) for technical support.

Conflicts of Interest: The authors declare no conflict of interest

References

1. Sung, H.; Ferlay, J.; Siegel, R.L.; Laversanne, M.; Soerjomataram, I.; Jemal, A.; Bray, F. Global Cancer Statistics 2020: GLOBOCAN Estimates of Incidence and Mortality Worldwide for 36 Cancers in 185 Countries. *CA. Cancer J. Clin.* **2021**, *71*, 209–249, doi:10.3322/caac.21660.
2. Gardel, M.L.; Schneider, I.C.; Aratyn-Schaus, Y.; Waterman, C.M. Mechanical integration of actin and adhesion dynamics in cell migration. *Annu. Rev. Cell Dev. Biol.* **2010**, *26*, 315–333, doi:10.1146/ANNUREV.CELLBIO.011209.122036.

3. Parsons, J.T.; Horwitz, A.R.; Schwartz, M.A. Cell adhesion: integrating cytoskeletal dynamics and cellular tension. *Nat. Rev. Mol. Cell Biol.* **2010**, *11*, 633–643, doi:10.1038/NRM2957.
4. Gkika, D.; Prevarskaya, N. TRP channels in prostate cancer : the good , the bad and the ugly ? *Asian J Androl.* **2011**, *13*, 673–676, doi:10.1038/aja.2011.18.
5. Fiorio Pla, A.; Gkika, D. Emerging role of TRP channels in cell migration: From tumor vascularization to metastasis. *Front. Physiol.* **2013**, *4 NOV*, 1–12, doi:10.3389/fphys.2013.00311.
6. Bernardini, M.; Fiorio Pla, A.; Prevarskaya, N.; Gkika, D. Human transient receptor potential (TRP) channels expression profiling in carcinogenesis. *Int. J. Dev. Biol.* **2015**, *59*, 399–406, doi:10.1387/ijdb.150232dg.
7. Lastraioli, E.; Iorio, J.; Arcangeli, A. Ion channel expression as promising cancer biomarker. *Biochim. Biophys. Acta - Biomembr.* **2015**, *1848*, 2685–2702, doi:10.1016/j.bbamem.2014.12.016.
8. Litan, A.; Langhans, S.A. Cancer as a channelopathy: Ion channels and pumps in tumor development and progression. *Front. Cell. Neurosci.* **2015**, *9*, 1–11, doi:10.3389/fncel.2015.00086.
9. Chinigò, G.; Castel, H.; Chever, O.; Gkika, D. TRP Channels in Brain Tumors. *Front. Cell Dev. Biol.* **2021**, *9*, doi:10.3389/fcell.2021.617801.
10. Tsavaler, L.; Shapero, M.H.; Morkowski, S.; Laus, R. Trp-p8, a novel prostate-specific gene, is up-regulated in prostate cancer and other malignancies and shares high homology with transient receptor potential calcium channel proteins. *Cancer Res.* **2001**, *61*, 3760–3769.
11. Shapovalov, G.; Ritaine, A.; Skryma, R.; Prevarskaya, N. Role of TRP ion channels in cancer and tumorigenesis. *Semin. Immunopathol.* **2016**, *38*, 357–369, doi:10.1007/s00281-015-0525-1.
12. Iamshanova, O.; Fiorio Pla, A.; Prevarskaya, N. Molecular mechanisms of tumour invasion: regulation by calcium signals. *J. Physiol.* **2017**, *595*, 3063–3075, doi:10.1113/JP272844.
13. Vrenken, K.S.; Jalink, K.; van Leeuwen, F.N.; Middelbeek, J. Beyond ion-conduction: Channel-dependent and -independent roles of TRP channels during development and tissue homeostasis. *Biochim. Biophys. Acta - Mol. Cell Res.* **2015**, *1863*, 1436–1446, doi:10.1016/j.bbamcr.2015.11.008.
14. Bödding, M. TRP proteins and cancer. **2007**, *19*, 617–624, doi:10.1016/j.cellsig.2006.08.012.
15. Van De Graaf, S.F.J.; Hoenderop, J.G.J.; Bindels, R.J.M. Regulation of TRPV5 and TRPV6 by associated proteins. *Am. J. Physiol. Renal Physiol.* **2006**, *290*, doi:10.1152/AJPRENAL.00443.2005.
16. Gkika, D.; Mahieu, F.; Niliur, B.; Hoenderop, J.G.J.; Bindels, R.J.M. 80K-H as a new Ca2+ sensor regulating the activity of the epithelial Ca2+ channel transient receptor potential cation channel V5 (TRPV5). *J. Biol. Chem.* **2004**, *279*, 26351–26357, doi:10.1074/JBC.M403801200.
17. Gkika, D.; Topala, C.N.; Hoenderop, J.G.J.; Bindels, R.J.M. The immunophilin FKBP52 inhibits the activity of the epithelial Ca2+ channel TRPV5. *Am. J. Physiol. Renal Physiol.* **2006**, *290*, doi:10.1152/AJPRENAL.00298.2005.
18. Gkika, D.; Topala, C.N.; Chang, Q.; Picard, N.; Thébault, S.; Houillier, P.; Hoenderop, J.G.J.; Bindels, R.J.M. Tissue kallikrein stimulates Ca(2+) reabsorption via PKC-dependent plasma membrane accumulation of TRPV5. *EMBO J.* **2006**, *25*, 4707–4716, doi:10.1038/SJ.EMBOJ.7601357.
19. Sinkins, W.G.; Goel, M.; Estacion, M.; Schilling, W.P. Association of immunophilins with mammalian TRPC channels. *J. Biol. Chem.* **2004**, *279*, 34521–34529, doi:10.1074/JBC.M401156200.
20. Chang, Q.; Hoefs, S.; Van Der Kemp, A.W.; Topala, C.N.; Bindels, R.J.; Hoenderop, J.G. The beta-glucuronidase klotho hydrolyzes and activates the TRPV5 channel. *Science* **2005**, *310*, 490–493, doi:10.1126/SCIENCE.1114245.
21. Chinigò, G.; Fiorio Pla, A.; Gkika, D. TRP Channels and Small GTPases Interplay in the Main Hallmarks of Metastatic Cancer. *Front. Pharmacol.* **2020**, *11*, 1–16, doi:10.3389/fphar.2020.581455.
22. Guéguinou, M.; Harnois, T.; Crottes, D.; Uguen, A.; Deliot, N.; Gambade, A.; Chantôme, A.; Haelters, J.P.; Jaffrès, P.A.; Jourdan, M.L.; et al. SK3/TRPC1/Orai1 complex regulates SOCE-dependent colon cancer cell migration: A novel opportunity to modulate anti- EGFR mAb action by the alkyl-lipid Ohmline. *Oncotarget* **2016**, *7*, 36168–36184, doi:10.18632/oncotarget.8786.
23. Bezzerides, V.J.; Ramsey, I.S.; Kotecha, S.; Greka, A.; Clapham, D.E. Rapid vesicular translocation and insertion of TRP channels. *Nat Cell Biol.* **2004**, *6*, 709–720, doi:10.1038/ncb1150.
24. Singh, I.; Knezevic, N.; Ahmmed, G.U.; Kini, V.; Malik, A.B.; Mehta, D. Gαq -TRPC6-mediated Ca 2+ Entry Induces RhoA Activation and Resultant Endothelial Cell Shape Change in Response to Thrombin. *J. Biol. Chem* **2007**, *282*, 7833–7843, doi:10.1074/jbc.M608288200.
25. Tian, D.; Jacobo, S.M.P.; Billing, D.; Rozkalne, A.; Gage, S.D.; Anagnostou, T.; Pavenstädt, H.; Hsu, H.; Schlondorff, J.; Ramos, A.; et al. Antagonistic regulation od actin dynamics and cell motility by TRPC5 and TRPC6 channels. *Sci Signal.* **2010**, *3*, 1–25, doi:10.1126/scisignal.2001200.Antagonistic.

26. Su, L.; Liu, W.; Chen, H.; An, O.G.A.; Habas, R.; Runnels, L.W.; N-, J. TRPM7 regulates polarized cell movements. *Biochem J* **2011**, *434*, 513–521, doi:10.1042/BJ20101678.
27. Tomasek, J.J.; Vaughan, M.B.; Kropp, B.P.; Gabbiani, G.; Martin, M.D.; Haaksma, C.J.; Hinz, B. Contraction of myofibroblasts in granulation tissue is dependent on Rho / Rho kinase / myosin light chain phosphatase activity. *Wound Repair Regen.* **2006**, *14*, 313–320, doi:10.1111/j.1743-6109.2006.00126.x.
28. Adapala, R.K.; Thoppil, R.J.; Luther, D.J.; Paruchuri, S.; Meszaros, J.G.; Chilian, W.M.; Thodeti, C.K. Cellular Cardiology TRPV4 channels mediate cardiac fi broblast differentiation by integrating mechanical and soluble signals. *J. Mol. Cell. Cardiol.* **2013**, *54*, 45–52, doi:10.1016/j.yjmcc.2012.10.016.
29. Lee, W.H.; Choong, L.Y.; Mon, N.N.; Lu, S.; Lin, Q.; Pang, B.; Yan, B.; Sri, V.; Krishna, R.; Singh, H.; et al. TRPV4 regulates breast cancer cell extravasation, stiffness and actin cortex. *Sci. Rep.* **2016**, *6*, 1–16, doi:10.1038/srep27903.
30. Ou-yang, Q.; Li, B.; Xu, M.; Liang, H. TRPV4 promotes the migration and invasion of glioma cells via AKT/Rac1 signaling. *Biochem. Biophys. Res. Commun.* **2018**, *503*, 876–881, doi:10.1016/j.bbrc.2018.06.090.
31. Gao, G.; Wang, W.; Tadagavadi, R.K.; Briley, N.E.; Love, M.I.; Miller, B.A.; Reeves, W.B. TRPM2 mediates ischemic kidney injury and oxidant stress through RAC1. *J Clin Invest.* **2014**, *124*, 4989–5001, doi:10.1172/JCI76042.us.
32. Laragione, T.; Harris, C.; Gulko, P.S. TRPV2 suppresses Rac1 and RhoA activation and invasion in rheumatoid arthritis fibroblast-like synoviocytes. *Int. Immunopharmacol.* **2019**, *70*, 268–273, doi:10.1016/j.intimp.2019.02.051.
33. Mehta, D.; Ahmmed, G.U.; Paria, B.C.; Holinstat, M.; Voyno-Yasenetskaya, T.; Tiruppathi, C.; Minshall, R.D.; Malik, A.B. RhoA interaction with inositol 1,4,5-trisphosphate receptor and transient receptor potential channel-1 regulates Ca2+ entry: Role in signaling increased endothelial permeability. *J. Biol. Chem.* **2003**, *278*, 33492–33500, doi:10.1074/jbc.M302401200.
34. Chung, H.K.; Rathor, N.; Wang, S.R.; Wang, J.Y.; Rao, J.N. RhoA enhances store-operated Ca2+ entry and intestinal epithelial restitution by interacting with TRPC1 after wounding. *Am. J. Physiol. - Gastrointest. Liver Physiol.* **2015**, *309*, G759–G767, doi:10.1152/ajpgi.00185.2015.
35. Nagasawa, M.; Kojima, I. Translocation of TRPV2 channel induced by focal administration of mechanical stress. *Physiol. Rep.* **2015**, *3*, 1–12, doi:10.14814/phy2.12296.
36. Sun, J.; Yang, T.; Wang, P.; Ma, S.; Zhu, Z.; Pu, Y.; Li, L.; Zhao, Y.; Xiong, S.; Liu, D.; et al. Activation of cold-sensing transient receptor potential melastatin subtype 8 antagonizes vasoconstriction and hypertension through attenuating RhoA/Rho kinase pathway. *Hypertension* **2014**, *63*, 1354–1363, doi:10.1161/HYPERTENSIONAHA.113.02573.
37. Thoppil, R.J.; Cappelli, H.C.; Adapala, R.K.; Kanugula, A.K.; Paruchuri, S.; Thodeti, C.K. TRPV4 channels regulate tumor angiogenesis via modulation of Rho/Rho kinase pathway. *Oncotarget* **2016**, *7*, 25849–25861, doi:10.18632/oncotarget.8405.
38. Tsavaler, L.; Shapero, M.H.; Morkowski, S.; Laus, R. Trp-p8, a novel prostate-specific gene, is up-regulated in prostate cancer and other malignancies and shares high homology with transient receptor potential calcium channel proteins. *Cancer Res.* **2001**, *61*, 3760–3769.
39. Feldman, B.J.; Feldman, D. The development of androgen-independent prostate cancer. *Nat. Rev. Cancer* **2001**, *1*, 34–45, doi:10.1038/35094009.
40. Henshall, S.M.; Afar, D.E.H.; Hiller, J.; Horvath, L.G.; Quinn, D.I.; Rasiah, K.K.; Gish, K.; Willhite, D.; Kench, J.G.; Gardiner-Garden, M.; et al. Survival analysis of genome-wide gene expression profiles of prostate cancers identifies new prognostic targets of disease relapse. *Cancer Res.* **2003**, *63*, 4196–4203.
41. Grolez, G.P.; Gordiendko, D. V.; Clarisse, M.; Hammadi, M.; Desruelles, E.; Fromont, G.; Prevarskaya, N.; Slomianny, C.; Gkika, D. TRPM8-androgen receptor association within lipid rafts promotes prostate cancer cell migration. *Cell Death Dis.* **2019**, *10*, 652, doi:10.1038/s41419-019-1891-8.
42. Bidaux, G.; Roudbaraki, M.; Merle, C.; Crépin, A.; Delcourt, P.; Slomianny, C.; Thebault, S.; Bonnal, J.L.; Benahmed, M.; Cabon, F.; et al. Evidence for specific TRPM8 expression in human prostate secretory epithelial cells: Functional androgen receptor requirement. *Endocr. Relat. Cancer* **2005**, *12*, 367–382, doi:10.1677/erc.1.00969.
43. Zhang, L.; Barritt, G.J. Evidence that TRPM8 is an androgen-dependent Ca2+ channel required for the survival of prostate cancer cells. *Cancer Res.* **2004**, *64*, 8365–8373, doi:10.1158/0008-5472.CAN-04-2146.
44. Gkika, D.; Flourakis, M.; Lemonnier, L.; Prevarskaya, N. PSA reduces prostate cancer cell motility by stimulating TRPM8 activity and plasma membrane expression. *Oncogene* **2010**, *29*, 4611–4616, doi:10.1038/onc.2010.210.
45. Gkika, D.; Lemonnier, L.; Shapovalov, G.; Gordienko, D.; Poux, C.; Bernardini, M.; Bokhobza, A.; Bidaux, G.; Degerny, C.; Verreman, K.; et al. TRP channel-associated factors are a novel protein family that regulates TRPM8 trafficking and activity. *J. Cell Biol.* **2015**, *208*, 89–107, doi:10.1083/jcb.201402076.
46. Grolez, G.P.; Hammadi, M.; Barras, A.; Gordienko, D.; Slomianny, C.; Völkel, P.; Angrand, P.O.; Pinault, M.; Guimaraes, C.; Potier-Cartereau, M.; et al. Encapsulation of a TRPM8 Agonist, WS12, in Lipid Nanocapsules Potentiates PC3 Prostate Cancer Cell Migration Inhibition through Channel Activation. *Sci. Rep.* **2019**, *9*, 1–15, doi:10.1038/s41598-019-44452-4.

47. Yang, Z.H.; Wang, X.H.; Wang, H.P.; Hu, L.Q. Effects of TRPM8 on the proliferation and motility of prostate cancer PC-3 cells. *Asian J. Androl.* **2009**, *11*, 157–165, doi:10.1038/aja.2009.1.
48. Genova, T.; Grolez, G.P.G.P.; Camillo, C.; Bernardini, M.; Bokhobza, A.; Richard, E.; Scianna, M.; Lemonnier, L.; Valdembri, D.; Munaron, L.; et al. TRPM8 inhibits endothelial cell migration via a nonchannel function by trapping the small GTPase Rap1. *J. Cell Biol.* **2017**, *216*, 2107–2130, doi:10.1083/jcb.201506024.
49. Yin, Y.; Wu, M.; Zubcevic, L.; Borschel, W.F.; Lander, G.C.; Lee, S.Y. Structure of the cold- And menthol-sensing ion channel TRPM8. *Science (80-.).* **2018**, *359*, 237–241, doi:10.1126/science.aan4325.
50. Paulsen, C.; Armache, J.; Gao, Y.; Cheng, Y.; Julius, D. Structure of the TRPA1 ion channel suggests regulatory mechanisms. *Nature* **2015**, *520*, 511–517, doi:10.1038/NATURE14367.
51. Sali, A.; Blundell, T. Comparative protein modelling by satisfaction of spatial restraints. *J. Mol. Biol.* **1993**, *234*, 779–815, doi:10.1006/JMBI.1993.1626.
52. Nassar, N.; Horn, G.; Herrmann, C.A.; Scherer, A.; McCormick, F.; Wittinghofer, A. The 2.2 Å crystal structure of the Ras-binding domain of the serine/threonine kinase c-Raf1 in complex with RaplA and a GTP analogue. *Nature* **1995**, *375*, 554–560, doi:10.1038/375554a0.
53. Kozakov, D.; Hall, D.; Xia, B.; Porter, K.; Padhorny, D.; Yueh, C.; Beglov, D.; Vajda, S. The ClusPro web server for protein-protein docking. *Nat. Protoc.* **2017**, *12*, 255–278, doi:10.1038/NPROT.2016.169.
54. Quignot, C.; Rey, J.; Yu, J.; Tufféry, P.; Guerois, R.; Andreani, J. InterEvDock2: an expanded server for protein docking using evolutionary and biological information from homology models and multimeric inputs. *Nucleic Acids Res.* **2018**, *46*, W408, doi:10.1093/NAR/GKY377.
55. Brysbaert, G.; Lorgouilloux, K.; Vranken, W.; Lensink, M. RINspector: a Cytoscape app for centrality analyses and DynaMine flexibility prediction. *Bioinformatics* **2018**, *34*, 294–296, doi:10.1093/BIOINFORMATICS/BTX586.
56. Brysbaert, G.; Mauri, T.; de Ruyck, J.; Lensink, M. Identification of Key Residues in Proteins Through Centrality Analysis and Flexibility Prediction with RINspector. *Curr. Protoc. Bioinforma.* **2019**, *65*, doi:10.1002/CPBI.66.
57. Shannon, P.; Markiel, A.; Ozier, O.; Baliga, N.; Wang, J.; Ramage, D.; Amin, N.; Schwikowski, B.; Ideker, T. Cytoscape: a software environment for integrated models of biomolecular interaction networks. *Genome Res.* **2003**, *13*, 2498–2504, doi:10.1101/GR.1239303.
58. Su, G.; Morris, J.; Demchak, B.; Bader, G. Biological network exploration with Cytoscape 3. *Curr. Protoc. Bioinforma.* **2014**, *47*, 8.13.1-8.13.24, doi:10.1002/0471250953.BI0813S47.
59. Amitai, G.; Shemesh, A.; Sitbon, E.; Shklar, M.; Netanely, D.; Venger, I.; Pietrokovski, S. Network analysis of protein structures identifies functional residues. *J. Mol. Biol.* **2004**, *344*, 1135–1146, doi:10.1016/J.JMB.2004.10.055.
60. del Sol, A.; Fujihashi, H.; Amoros, D.; Nussinov, R. Residues crucial for maintaining short paths in network communication mediate signaling in proteins. *Mol. Syst. Biol.* **2006**, *2*, doi:10.1038/MSB4100063.
61. Thebault, S.; Lemonnier, L.; Bidaux, G.; Flourakis, M.; Bavencoffe, A.; Gordienko, D.; Roudbaraki, M.; Delcourt, P.; Panchin, Y.; Shuba, Y.; et al. Novel role of cold/menthol-sensitive transient receptor potential melastatine family member 8 (TRPM8) in the activation of store-operated channels in LNCaP human prostate cancer epithelial cells. *J. Biol. Chem.* **2005**, *280*, 39423–39435, doi:10.1074/jbc.M503544200.
62. Bivona, T.G.; Wiener, H.H.; Ahearn, I.M.; Silletti, J.; Chiu, V.K.; Philips, M.R. Rap1 up-regulation and activation on plasma membrane regulates T cell adhesion. *J. Cell Biol.* **2004**, *164*, 461–470, doi:10.1083/jcb.200311093.
63. Bivona, T.G.; Quatela, S.; Philips, M.R. Analysis of Ras Activation in Living Cells with GFP-RBD. *Methods Enzymol.* **2006**, *407*, 128–143, doi:10.1016/S0076-6879(05)07012-6.
64. Bernardini, M.; Brossa, A.; Chinigo, G.; Grolez, G.P.; Trimaglio, G.; Allart, L.; Hulot, A.; Marot, G.; Genova, T.; Joshi, A.; et al. Signatures in Tumor-Derived Endothelial Cells : Functional Roles in Prostate Cancer Angiogenesis. **2019**, 1–29.
65. Suzuki, J.; Kanemaru, K.; Ishii, K.; Ohkura, M.; Okubo, Y.; Iino, M. Imaging intraorganellar Ca2+ at subcellular resolution using CEPIA. *Nat. Commun.* **2014**, *5*, 1–13, doi:10.1038/ncomms5153.
66. 66. https://xenabrowser.net/datapages/?dataset=GDC-%0APANCAN.mutect2_snv.tsv&host=https%3A%2F%2Fgdc.xenahubs.net&removeHub=https%0A%3A%2F%2Fxena.treehouse.gi.ucsc.edu%3A443.
67. https://github.com/MrHedmad/Edmund.
68. https://www.ensembl.org/Homo_sapiens/Gene/Summary?db=core;g=ENSG000001164%0A73;r=1:111542218-111716691.
69. https://www.ensembl.org/Homo_sapiens/Gene/Summary?db=core;g=ENSG000001444%0A81;r=2:233917373-234019522.
70. https://gist.github.com/MrHedmad/a53eb36ff1233e45bc638008912c0d35.
71. Reedquist, K.A.; Ross, E.; Koop, E.A.; Wolthuis, R.M.F.; Zwartkruis, F.J.T.; Van Kooyk, Y.; Salmon, M.; Buckley, C.D.; Bos, J.L. The small GTPase, Rap1, mediates CD31-induced integrin adhesion. *J. Cell Biol.* **2000**, *148*, 1151–1158, doi:10.1083/jcb.148.6.1151.

72. Bidaux, G.; Flourakis, M.; Thebault, S.; Zholos, A.; Beck, B.; Gkika, D.; Roudbaraki, M.; Bonnal, J.L.; Mauroy, B.; Shuba, Y.; et al. Prostate cell differentiation status determines transient receptor potential melastatin member 8 channel subcellular localization and function. *J. Clin. Invest.* **2007**, *117*, 1647–1657, doi:10.1172/JCI30168.
73. Pillozzi, S.; Brizzi, M.F.; Bernabei, P.A.; Bartolozzi, B.; Caporale, R.; Basile, V.; Boddi, V.; Pegoraro, L.; Becchetti, A.; Arcangeli, A. VEGFR-1 (FLT-1), β1 integrin, and hERG K+ channel for a macromolecular signaling complex in acute myeloid leukemia: Role in cell migration and clinical outcome. *Blood* **2007**, *110*, 1238–1250, doi:10.1182/blood-2006-02-003772.
74. Negri, S.; Faris, P.; Maniezzi, C.; Pellavio, G.; Spaiardi, P.; Botta, L.; Laforenza, U.; Biella, G.; Moccia, D.F. NMDA receptors elicit flux-independent intracellular Ca2+ signals via metabotropic glutamate receptors and flux-dependent nitric oxide release in human brain microvascular endothelial cells. *Cell Calcium* **2021**, *99*, doi:10.1016/j.ceca.2021.102454.
75. Desai, B.N.; Krapivinsky, G.; Navarro, B.; Krapivinsky, L.; Carter, B.C.; Febvay, S.; Delling, M.; Penumaka, A.; Ramsey, I.S.; Manasian, Y.; et al. Cleavage of TRPM7 Releases the Kinase Domain from the Ion Channel and Regulates Its Participation in Fas-Induced Apoptosis. *Dev. Cell* **2012**, *22*, 1149–1162, doi:10.1016/j.devcel.2012.04.006.
76. Faouzi, M.; Kilch, T.; Horgen, F.D.; Fleig, A.; Penner, R. The TRPM7 channel kinase regulates store-operated calcium entry. *J. Physiol.* **2017**, *595*, 3165–3180, doi:10.1113/JP274006.
77. Joly, D.; Ishibe, S.; Nickel, C.; Yu, Z.; Somlo, S.; Cantley, L. The polycystin 1-C-terminal fragment stimulates ERK-dependent spreading of renal epithelial cells. *J. Biol. Chem.* **2006**, *281*, 26329–26339, doi:10.1074/JBC.M601373200.
78. Bos, J.L. Linking Rap to cell adhesion. *Curr. Opin. Cell Biol.* **2005**, *17*, 123–128, doi:10.1016/j.ceb.2005.02.009.
79. Boettner, B.; Van Aelst, L. Control of cell adhesion dynamics by Rap1 signaling. *Curr. Opin. Cell Biol.* **2009**, *21*, 684–693, doi:10.1016/j.ceb.2009.06.004.
80. Moissoglu, K.; Schwartz, M.A. Spatial and temporal control of Rho GTPase functions. *Cell. Logist.* **2014**, *4*, e943618, doi:10.4161/21592780.2014.943618.
81. Yarwood, S.; Cullen, P.J.; Kupzig, S. The GAP1 family of GTPase-activating proteins : spatial and temporal regulators of small GTPase signalling. *Biochem. Soc. Trans.* **2006**, *34*, 846–850.
82. Cherfils, J.; Zeghouf, M. Regulation of small GTPases by GEFs, GAPs, and GDIs. *Physiol. Rev.* **2013**, *93*, 269–309, doi:10.1152/physrev.00003.2012.
83. Carmona, G.; Go, S.; Orlandi, A.; Ba, T.; Jugold, M.; Kiessling, F.; Henschler, R.; Zeiher, A.M.; Dimmeler, S.; Chavakis, E. Role of the small GTPase Rap1 for integrin activity regulation in endothelial cells and angiogenesis. **2009**, *113*, 488–497, doi:10.1182/blood-2008-02-138438.The.
84. Prevarskaya, N.; Zhang, L.; Barritt, G. TRP channels in cancer. *Biochim. Biophys. Acta - Mol. Basis Dis.* **2007**, *1772*, 937–946, doi:10.1016/j.bbadis.2007.05.006.
85. Skryma, R.; Mariot, P.; Bourhis, X.L.; Coppenolle, F. V; Shuba, Y.; Vanden Abeele, F.; Legrand, G.; Humez, S.; Boilly, B.; Prevarskaya, N. Store depletion and store-operated Ca2+ current in human prostate cancer LNCaP cells: involvement in apoptosis. *J. Physiol.* **2000**, *527 Pt 1*, 71–83.
86. Abeele, F. Vanden; Skryma, R.; Shuba, Y.; Van Coppenolle, F.; Slomianny, C.; Roudbaraki, M.; Mauroy, B.; Wuytack, F.; Prevarskaya, N. Bcl-2-dependent modulation of Ca2+ homeostasis and store-operated channels in prostate cancer cells. *Cancer Cell* **2002**, *1*, 169–179, doi:10.1016/S1535-6108(02)00034-X.
87. Vanoverberghe, K.; Abeele, F. Vanden; Mariot, P.; Lepage, G.; Roudbaraki, M.; Bonnal, J.L.; Mauroy, B.; Shuba, Y.; Skryma, R.; Prevarskaya, N. Ca2+ homeostasis and apoptotic resistance of neuroendocrine-differentiated prostate cancer cells. *Cell Death Differ.* **2004**, *11*, 321–330, doi:10.1038/sj.cdd.4401375.
88. Zhang, X.; Mak, S.; Li, L.; Parra, A.; Denlinger, B.; Belmonte, C.; McNaughton, P.A. Direct inhibition of the cold-Activated TRPM8 ion channel by Gα q. *Nat. Cell Biol.* **2012**, *14*, 850–858, doi:10.1038/ncb2529.
89. Klasen, K.; Hollatz, D.; Zielke, S.; Gisselmann, G.; Hatt, H.; Wetzel, C.H. The TRPM8 ion channel comprises direct Gq protein-activating capacity. *Eur. J. Physiol.* **2012**, *463*, 779–797, doi:10.1007/s00424-012-1098-7.
90. Matsumoto, S.; Miyano, N.; Baba, S.; Liao, J.; Kawamura, T.; Tsuda, C.; Takeda, A.; Yamamoto, M.; Kumasaka, T.; Kataoka, T.; et al. Molecular Mechanism for Conformational Dynamics of Ras·GTP Elucidated from In-Situ Structural Transition in Crystal. *Sci. Rep.* **2016**, *6*, 1–12, doi:10.1038/srep25931.
91. Khaled, M.; Gorfe, A.; Sayyed-Ahmad, A. Conformational and Dynamical Effects of Tyr32 Phosphorylation in K-Ras: Molecular Dynamics Simulation and Markov State Models Analysis. *J. Phys. Chem. B* **2019**, *123*, 7667–7675, doi:10.1021/acs.jpcb.9b05768.
92. Kano, Y.; Gebregiworgis, T.; Marshall, C.B.; Radulovich, N.; Poon, B.P.K.; St-Germain, J.; Cook, J.D.; Valencia-Sama, I.; Grant, B.M.M.; Herrera, S.G.; et al. Tyrosyl phosphorylation of KRAS stalls GTPase cycle via alteration of switch I and II conformation. *Nat. Commun.* **2019**, *10*, doi:10.1038/s41467-018-08115-8.
93. Bunda, S.; Heir, P.; Srikumar, T.; Cook, J.; Burrell, K.; Kano, Y.; JE, L.; G, Z.; B, R.; M, O. Src promotes GTPase activity of Ras via tyrosine 32 phosphorylation. *Proc. Natl. Acad. Sci. U. S. A.* **2014**, *111*, E3785–E3794, doi:10.1073/PNAS.1406559111.

94. van de Graaf, S.F.J.; Chang, Q.; Mensenkamp, A.R.; Hoenderop, J.G.J.; Bindels, R.J.M. Direct Interaction with Rab11a Targets the Epithelial Ca 2+ Channels TRPV5 and TRPV6 to the Plasma Membrane . *Mol. Cell. Biol.* **2006**, *26*, 303–312, doi:10.1128/mcb.26.1.303-312.2006.
95. Yin, Y.; Le, S.C.; Hsu, A.L.; Borgnia, M.J.; Yang, H.; Lee, S.Y. Structural basis of cooling agent and lipid sensing by the cold-activated TRPM8 channel. *Science (80-.).* **2019**, *363*, doi:10.1126/science.aav9334.
96. Mabonga, L.; Kappo, A.P. Protein-protein interaction modulators: advances, successes and remaining challenges. *Biophys. Rev.* **2019**, *11*, 559–581, doi:10.1007/s12551-019-00570-x.
97. Scott, D.E.; Bayly, A.R.; Abell, C.; Skidmore, J. Small molecules, big targets: Drug discovery faces the protein-protein interaction challenge. *Nat. Rev. Drug Discov.* **2016**, *15*, 533–550, doi:10.1038/nrd.2016.29.
98. Habault, J.; Poyet, J.L. Recent advances in cell penetrating peptide-based anticancer therapies. *Molecules* **2019**, *24*, 1–17, doi:10.3390/molecules24050927.
99. Xie, J.; Bi, Y.; Zhang, H.; Dong, S.; Teng, L.; Lee, R.J.; Yang, Z. Cell-Penetrating Peptides in Diagnosis and Treatment of Human Diseases: From Preclinical Research to Clinical Application. *Front. Pharmacol.* **2020**, *11*, 1–23, doi:10.3389/fphar.2020.00697.
100. Kang, R.H.; Jang, J.E.; Huh, E.; Kang, S.J.; Ahn, D.R.; Kang, J.S.; Sailor, M.J.; Yeo, S.G.; Oh, M.S.; Kim, D.; et al. A brain tumor-homing tetra-peptide delivers a nano-therapeutic for more effective treatment of a mouse model of glioblastoma. *Nanoscale Horizons* **2020**, *5*, 1213–1225, doi:10.1039/d0nh00077a.
101. Bledzka, K.; Smyth, S.S.; Plow, E.F. Integrin alphaIIbbeta3: from discovery to efficacious therapeutic target. *Circ. Res.* **2013**, *112*, 1189–1200, doi:10.1161/CIRCRESAHA.112.300570.Integrin.
102. Fisher, M.; Btesh, J.; McNaughton, P. Disrupting Sensitization of Transient Receptor Potential Vanilloid Subtype 1 Inhibits Inflammatory Hyperalgesia. *J. Neurosci.* **2013**, *33*, 7407–14, doi:10.1523/JNEUROSCI.3721-12.2013.
103. Schulie, A.J.; Yeh, C.Y.; Orang, B.N.; Pa, O.J.; Hopkin, M.P.; Moutal, A.; Khanna, R.; Sun, D.; Justic, J.A.; Aizenman, E. Targeted disruption of Kv2.1-VAPA association provides neuroprotection against ischemic stroke in mice by declustering Kv2.1 channels. *Sci. Adv.* **2020**, *6*, 1–14, doi:10.1126/sciadv.aaz8110.
104. Brittain, J.M.; Duarte, D.B.; Wilson, S.M.; Zhu, W.; Ballard, C.; Johnson, P.L.; Liu, N.; Xiong, W.; Ripsch, M.S.; Wang, Y.; et al. Suppression of inflammatory and neuropathic pain by uncoupling CRMP-2 from the presynaptic Ca2+ channel complex. *Nat Med.* **2011**, *17*, 822–829, doi:10.1038/nm.2345.Suppression.
105. Fischer, A.; Rosen, A.C.; Ensslin, C.J.; Wu, S.; Lacouture, M.E. Pruritus to anticancer agents targeting the EGFR, BRAF, and CTLA-4. *Dermatol. Ther.* **2013**, *26*, 135–148, doi:10.1111/dth.12027.
106. Tu, C.L.; Chang, W.; Bikle, D.D. Phospholipase Cγ1 is required for activation of store-operated channels in human keratinocytes. *J. Invest. Dermatol.* **2005**, *124*, 187–197, doi:10.1111/j.0022-202X.2004.23544.x.
107. Katterle, Y.; Brandt, B.H.; Dowdy, S.F.; Niggemann, B.; Zänker, K.S.; Dittmar, T. Antitumour effects of PLC-γ1-(SH2)2-TAT fusion proteins on EGFR/c-erbB-2-positive breast cancer cells. *Br. J. Cancer* **2004**, *90*, 230–235, doi:10.1038/sj.bjc.6601506.
108. Laínez, S.; Valente, P.; Ontoria-Oviedo, I.; Estévez-Herrera, J.; Camprubí-Robles, M.; Ferrer-Montiel, A.; Planells-Cases, R. GABA A receptor associated protein (GABARAP) modulates TRPV1 expression and channel function and desensitization. *FASEB J.* **2010**, *24*, 1958–1970, doi:10.1096/fj.09-151472.
109. Saldías, M.P.; Maureira, D.; Orellana-Serradell, O.; Silva, I.; Lavanderos, B.; Cruz, P.; Torres, C.; Cáceres, M.; Cerda, O. TRP Channels Interactome as a Novel Therapeutic Target in Breast Cancer. *Front. Oncol.* **2021**, *11*, 621614, doi:10.3389/FONC.2021.621614.
110. Weng, H.J.; Patel, K.N.; Jeske, N.A.; Bierbower, S.M.; Zou, W.; Tiwari, V.; Zheng, Q.; Tang, Z.; Mo, G.C.H.; Wang, Y.; et al. Tmem100 Is a Regulator of TRPA1-TRPV1 Complex and Contributes to Persistent Pain. *Neuron* **2015**, *85*, 833–846, doi:10.1016/j.neuron.2014.12.065.
111. Mabonga, L.; Kappo, A.P. Peptidomimetics: A Synthetic Tool for Inhibiting Protein–Protein Interactions in Cancer. *Int. J. Pept. Res. Ther.* 2020, *26*, 225–241.
112. Corbi-Verge, C.; Kim, P.M. Motif mediated protein-protein interactions as drug targets. *Cell Commun. Signal.* **2016**, *14*, 1–12, doi:10.1186/s12964-016-0131-4.

© 2022 by the authors. Licensee MDPI, Basel, Switzerland. This article is an open access article distributed under the terms and conditions of the Creative Commons Attribution (CC BY) license (http://creativecommons.org/licenses/by/4.0/).

Supplementary Materials

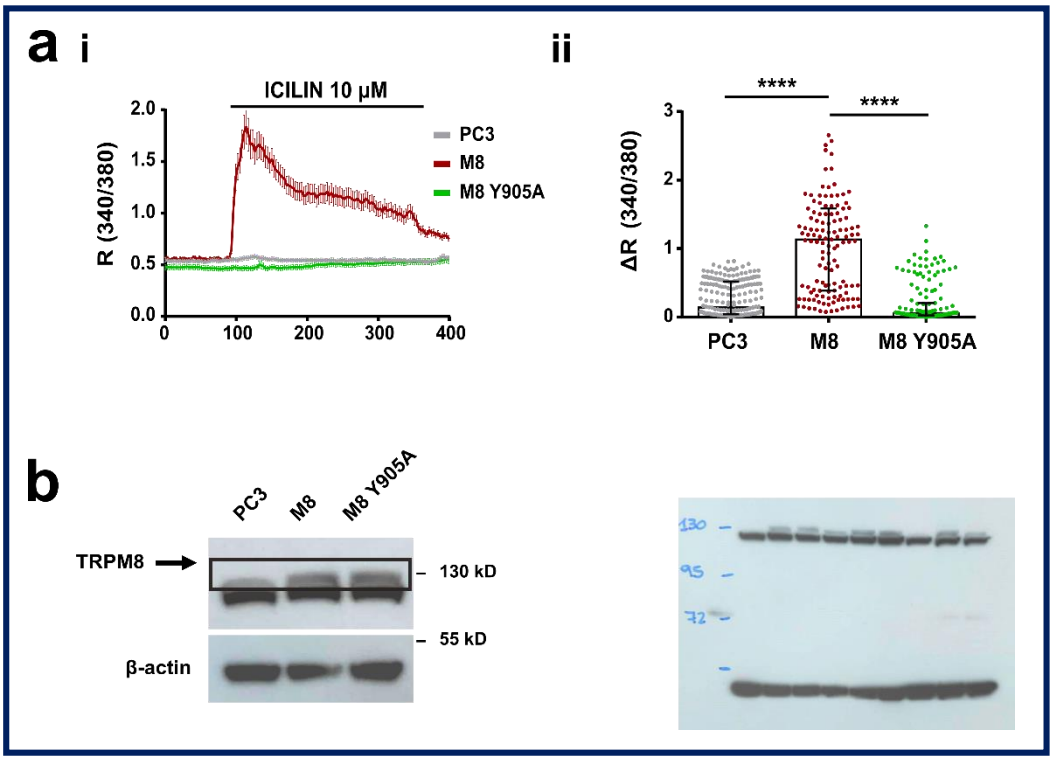

Figure S1. Validation of TRPM8 pore mutant.

*(**a i**) Ca^{2+}-imaging traces in response to TRPM8 agonist (10 µM icilin) in PC3 (grey), PC3 transiently overexpressing TRPM8 (red) and PC3 transiently overexpressing the pore mutant TRPM8 Y905A (green). Traces represent mean ± SEM of cells in the recorded field of one representative experiment (n=33 for PC3, n=24 for M8 and n=25 for M8 Y905A). (**ii**) Scatter dot plot showing peak amplitude of icilin-mediated Ca2+ responses (median with interquartile range of different cells in the field from at least 5 independent experiments). All cells were considered for PC3 and PC3 overexpressing TRPM8 Y905A analysis, only icilin-responsive cells were considered for PC3 overexpressing TRPM8 (n=225 for PC3, n=135 for M8 and n=159 for M8 Y905A). Statistical significance versus PC3 or PC3 overexpressing TRPM8, ****: P < 0.0001 (Kruskal-Wallis test with post-hoc Dunn's test).*

*(**b**) Representative immunoblot showing TRPM8 expression (rabbit anti-TRPM8 Ab109308 1:800) in PC3 cells, PC3 cells overexpressing TRPM8 wt (0.625 µg) and PC3 cells overexpressing TRPM8 Y905A (0.625 µg). β-actin (mouse anti-β-actin Sigma-Aldrich A5316 1:1000) was used as a loading control; the specific bands referring to TRPM8 expression are framed and indicated by the arrows.*

The full uncropped blot is reported on the right. Samples order (from left to right): 1) PC3 CNTRL; 2) PC3+TRPM8 wt; 3) PC3+TRPM8 Y905A; 4) MCF-7 CNTRL; 5) MCF-7+TRPM8 wt; 6) MCF-7+TRPM8 E207A Y240A; 7) HeLa CNTRL; 8) HeLa+TRPM8 wt; 9) HeLa+TRPM8 E207A Y240A.

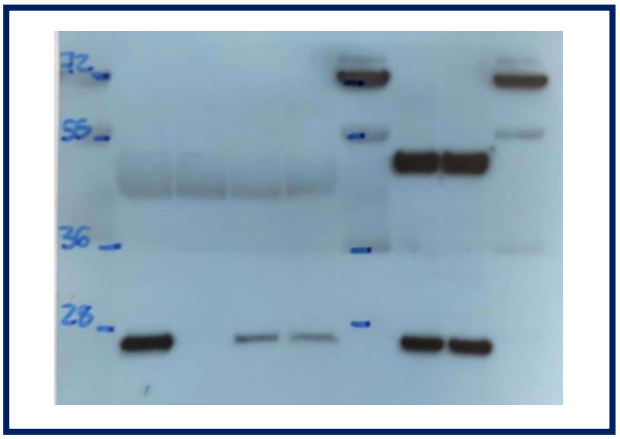

Figure S2. Original uncropped blot referring to Fig. 2ai.

Samples order (from left to right): 1) GTP Ys: 2) GDP; 3) PC3 CNTRL (pulled-down PD); 4) TRPM8 (PD); 5) empty; 6) PC3 CNTRL (total lysates TL); 7) TRPM8 (TL).

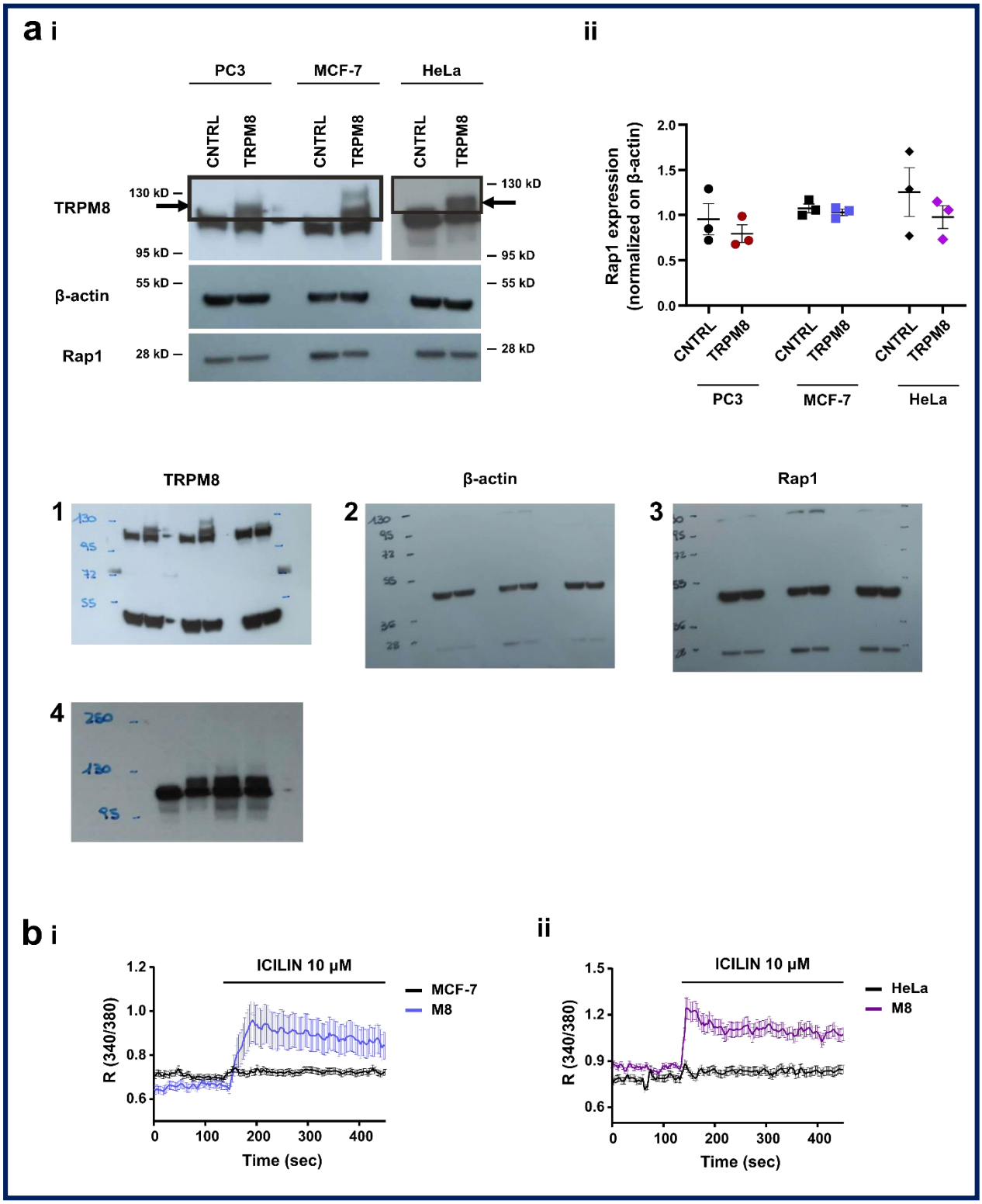

Figure S3. TRPM8 and Rap1A basal expression in PC3, MCF-7, and HeLa cell lines.

(a i) Representative immunoblot showing TRPM8 (rabbit anti-TRPM8 Ab109308 1:800) and Rap1 (rabbit anti-Rap1 Thermo Fisher scientific 1862344) expression in PC3, MCF-7, and HeLa cells wt and overexpressing exogenous TRPM8 wt

(0.625 µg). The specific bands referring to TRPM8 expression are framed and indicated by the arrows. β-actin (mouse anti-β-actin Sigma-Aldrich A5316 1:1000) was used as a loading control and to normalize and quantify (ii) the endogenous amount of Rap1 within cells overexpressing or not TRPM8 (n=3). The original uncropped blots are reported below; samples order in blots 1-3 (from left to right): 1) PC3 wt; 2) PC3+TRPM8; 3) empty; 4) MCF-7 wt; 5) MCF-7+TRPM8; 6) empty; 7) HeLa wt; 8) HeLa+TRPM8; samples order in blot 4 (from left to right): 1) HeLa wt; 2) Hela+TRPM8 (10 µg); 3) HeLa+TRPM8 (30 µg); 4) 3) HeLa+TRPM8 (20 µg).

(b) Ca^{2+}-imaging traces in response to TRPM8 agonist (10 µM icilin) in MCF-7 (i) and HeLa (ii), transiently overexpressing or not TRPM8. Traces represent mean ± SEM of cells in the recorded field of one representative experiment (n=38 for MCF-7 wt, n=29 for MCF-7 M8; n=22 for HeLa CNTRL, n=29 for HeLa M8).

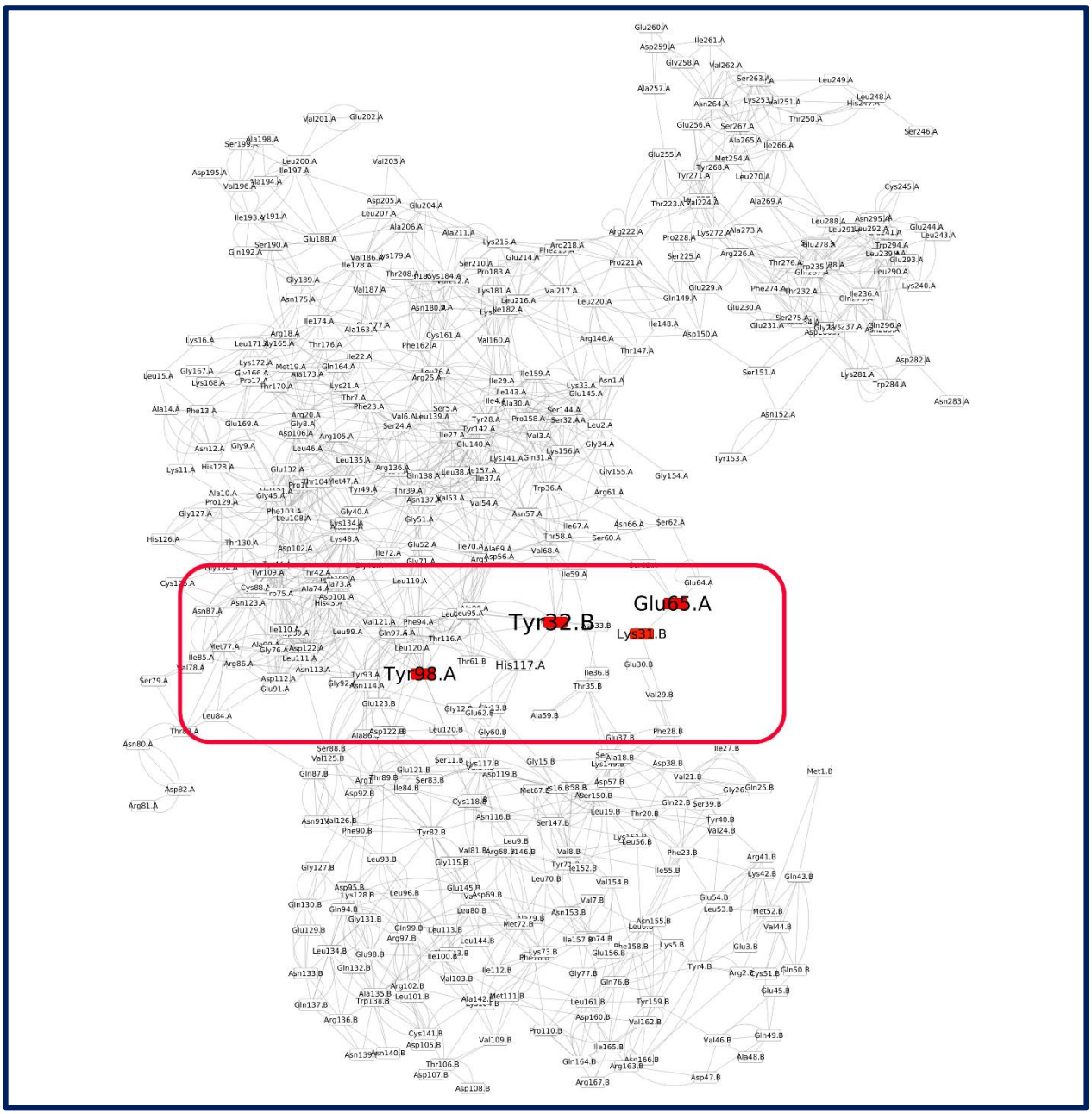

Figure S4. RCA of the interaction between TRPM8 and Rap1A.

The numbering here is slightly modified for TRPM8 by 142 thus His117 is actually His259. Colored in red are the residues considered as central (Z score ≥ 3) in at least one of the five selected docking models. Only central residues at the interface are colored. Chain A corresponds to TRPM8 while B is used for Rap1A.

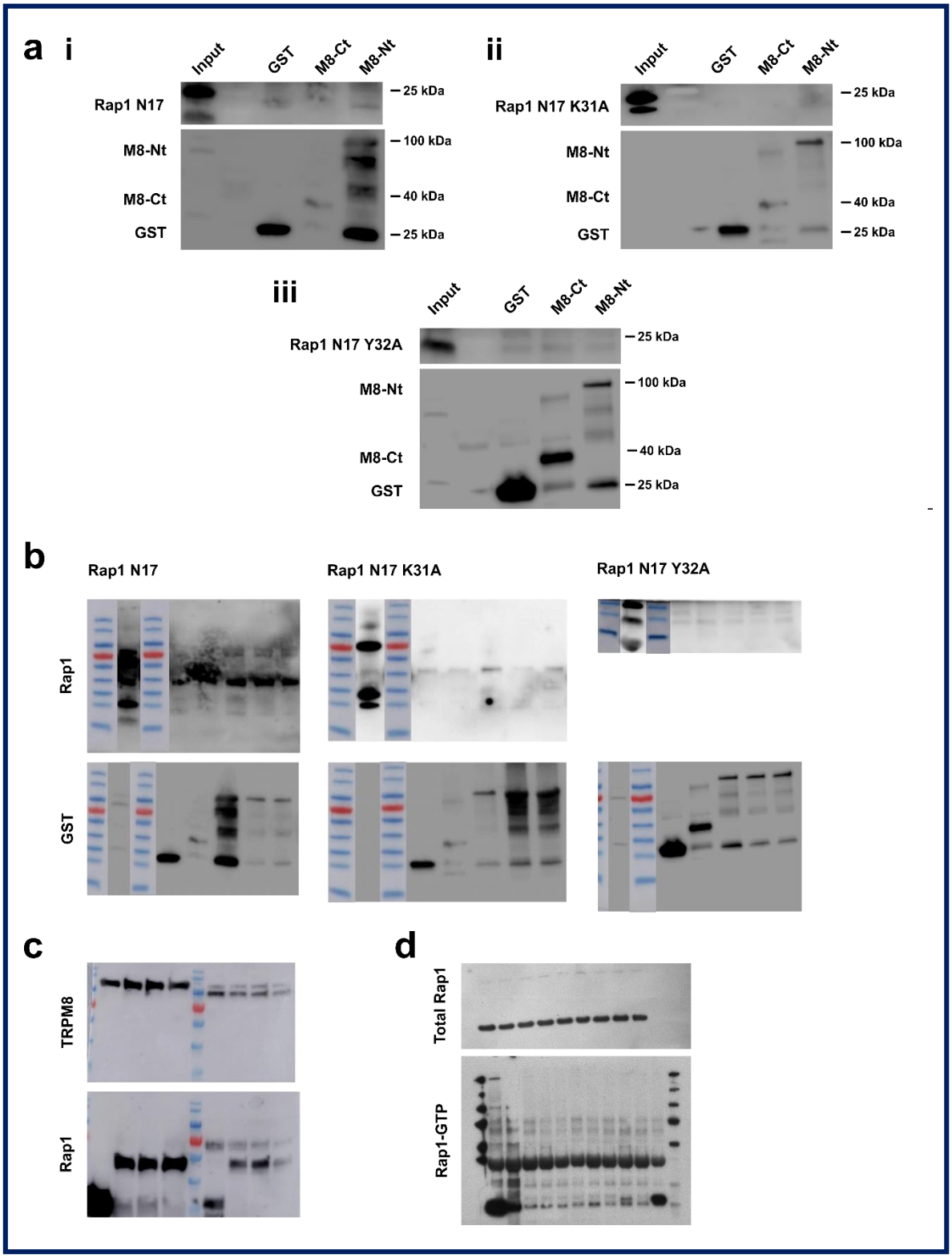

Figure S5. Role of K31 and Y32 in mediating the direct interaction between the inactive (GDP-bound) form of Rap1 and TRPM8 N terminus.

a) GST blots relative to GST pull-down assay described in Fig. 5a (GST-TRPM8 N-terminal tail (M8-Nt), GST-C-terminal tail (M8-Ct), or GST incubated with in vitro translated Rap1 N17 (i), GFP-Rap1 N17 K31A (ii) and GFP-Rap1 N17 Y32A (iii). The interaction of Rap1 mutants with GST-fused TRPM8 N- and C-terminal tail was detected using anti-Rap1 antibody

and anti-GST antibody was used as control for the loading of GST-fused TRPM8 N- and C-terminal tail. One representative experiment of three (the same shown in fig. 5a) is shown.
b) Original uncropped blots referring to GST pull-down assays reported in Fig. 5ai, 6ai, aii, and aiii; samples order (from left to right): 1) MW marker; 2) input; 3) MW marker; 4) GST; 5) TRPM8 Ct-GST; 6) TRPM8 Nt-GST; 7) TRPM8 E207A Nt-GST; 8) TRPM8 Y240A Nt-GST.
c) Original uncropped blots referring to Co-IP experiment reported in Fig. 5bi; samples order (from left to right): 1) MW marker; 2) GFP (total lysates TL); 3) Rap1 N17-GFP (TL); 4) Rap1 N17 K31A-GFP (TL); 5) Rap1 N17 Y32A-GFP (TL); 6) MW marker; 7) GFP (immuno-precipitated IP); 8) Rap1 N17-GFP (IP); 9) Rap1 N17 K31A-GFP (IP); 10) Rap1 N17 Y32A-GFP (IP).
d) Original uncropped blots referring to the active Rap1 pull-down assays reported in Fig. 5ci and 5ei; samples order (from left to right): 1) GTP γs: 2) GDP; 3) TRPM8+Rap1 N17 Y32; 4) TRPM8+Rap1 N17; 5) TRPM8; 6) Rap1 N17 Y32; 7) Rap1 N17; 8) PC3 CNTRL; 9) Rap1 wt; 10) Rap1 K31A; 11) Rap1 Y32A.

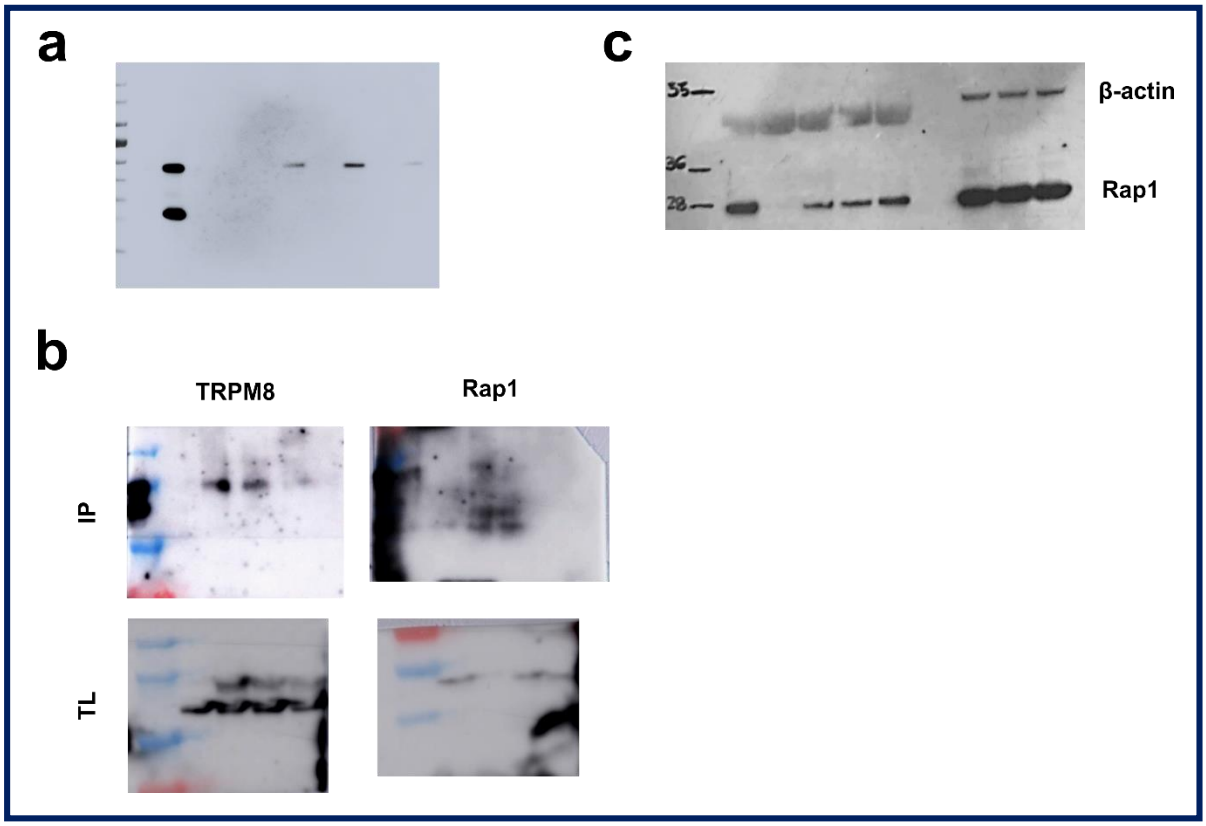

Figure S6. Original uncropped blots referring to Fig. 6 and 7.

***a**) Original uncropped blots referring to GST pull-down assays reported in Fig. 6bi; samples order (from left to right): 1) MW marker; 2) input; 3) GST; 4) TRPM8 Ct-GST; 5) TRPM8 Nt-GST; 6) TRPM8 E207A Y240A Nt-GST.*
***b**) Original uncropped blots referring to Co-IP experiment reported in Fig. 6ci; samples order (from left to right): 1) MW marker; 2) Rap1 N17; 3) TRPM8; 4) TRPM8+Rap1 N17; 5) TRPM8 E207A Y240A+Rap1 N17.*
***c**) Original uncropped blots referring to the active Rap1 pull-down assays reported in Fig. 7di; samples order (from left to right): 1) GTP γs: 2) GDP; 3) PC3 CNTRL (pulled-down PD); 4) TRPM8 (PD); 5) TRPM8 E207A Y240A (PD); 6) empty; 7) PC3 CNTRL (total lysates TL); 8) TRPM8 (TL); 9) TRPM8 E207A Y240A (TL).*

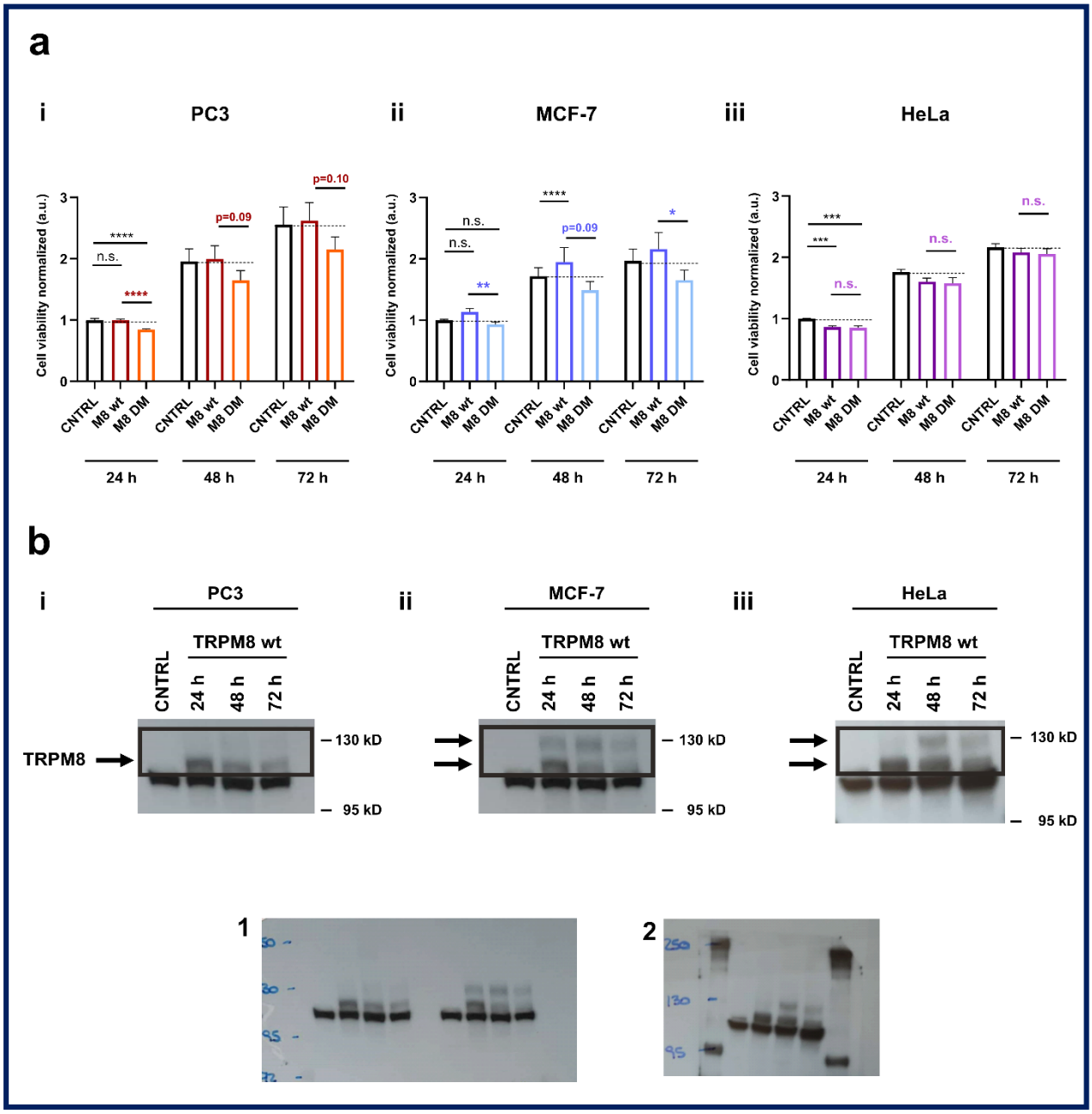

Figure S7. TRPM8-Rap1A interaction in cancer cells viability.

*(**a**) Cell viability of PC3 (**i**), MCF-7 (**ii**) and HeLa (**iii**) cells 24, 48, and 72 h after transfection with 0.625 µg of TRPM8 wt or TRPM8 E207A Y240A (M8 DM). Data are normalized on the CNTRL (cells transfected with empty vector) at 24 h and are represented as mean ± SEM. Data refer to a pool of 3 independent experiments (eight replicates for each experiment). Statistical significance: * p< 0.05, ** p< 0.01, *** < 0.001 **** P< 0.0001 (Kruskal-Wallis test with post-hoc Dunn's test). (**b**) Immunoblot showing TRPM8 overexpression (rabbit anti-TRPM8 Ab109308 1:800) in PC3 (i), MCF-7 (ii) and HeLa (iii) cells 24, 48, and 72 h after transfection with 0.625 µg of TRPM8 wt; The specific bands referring to TRPM8 expression are framed and indicated by the arrows; the original uncropped blots are reported below; samples order in blot 1 (from left to right): 1) PC3 wt; 2) PC3+TRPM8 24 h after transfection; 3) PC3+TRPM8 48 h after transfection; 4) PC3+TRPM8 72 h after transfection; 5) empty; 6) MCF-7 wt; 7) MCF-7+TRPM8 24 h after transfection; 8) MCF-7+TRPM8 48 h after transfection; 9) MCF-7+TRPM8 72 h after transfection; ; samples order in blot 2 (from left to right): 1) HeLa wt; 2) HeLa+TRPM8 24 h after transfection; 3) HeLa+TRPM8 48 h after transfection; 4) HeLa+TRPM8 72 h after transfection.*

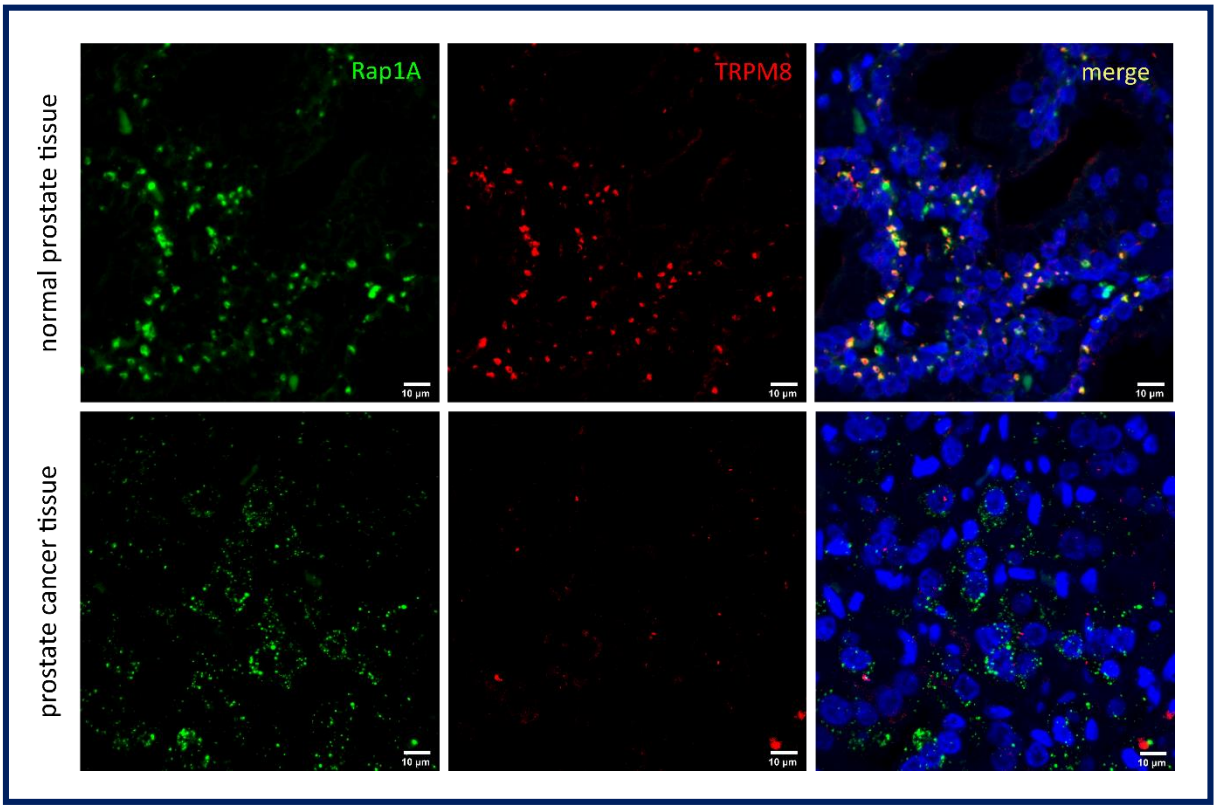

Figure S8. TRPM8-Rap1A interaction in healthy and cancerous prostate tissues.

Representative confocal micrographs of healthy prostate tissue and prostate adenorcarcinoma (Gleason 5) microarrays (Biomax Inc.) stained for Rap1A (green - anti-Rap1A ABIN2854404) and TRPM8 (red - anti-TRPM8 ABIN572229). Nuclei are counterstained with DAPI (blue). Scale bar: 10 µm.

"TRPM8 as an Anti-Tumoral Target in Prostate Cancer Growth and Metastasis Dissemination"

Guillaume P Grolez[1], **Giorgia Chinigò**[1,2], Alexandre Barras[3], Mehdi Hammadi[3], Lucile Noyer[1], Kateryna Kondratska [1], Etmar Bulk[4], Thibauld Oullier[5], Séverine Marionneau-Lambot[5], Marilyne Le Mée[7], Stéphanie Rétif[7], Stéphanie Lerondel[7], Antonino Bongiovanni[8], Tullio Genova[2,6], Sébastien Roger[9], Rabah Boukkerhoub[3], Albrecht Schwab[4], Alessandra Fiorio Pla[1,2,6,] & Dimitra Gkika[10,11,12]

[1] Laboratoire de Physiologie cellulaire, INSERM U1003, Laboratory of Excellence, Ion Channels Science and Therapeutics, University of Lille, F-5900 Villeneuve d'Ascq, France

[2] Department of Life Science and Systems Biology, University of Turin, 10123 Turin, Italy

[3] Univ. Lille, CNRS, Centrale Lille, Univ. Polytechnique Hauts-de-France, UMR 8520 - IEMN, F-59000 Lille, France

[4] Institute of Physiology II, University of Münster, 48149 Münster, Germany

[5] Cancéropôle du Grand Ouest, Plateforme In Vivo, 44000 Nantes, France

[6] Nanostructured Interfaces and Surfaces Centre of Excellence (NIS), University of Turin, Turin, Italy

[7] CNRS UAR44, PHENOMIN-TAAM, 45071 Orléans, France

[8] Univ. Lille, CNRS, Inserm, CHU Lille, Institut Pasteur de Lille, US 41 - UMS 2014 - PLBS, F-59000 Lille, France

[9] Transplantation, Immunologie et Inflammation T2I-EA 4245, Université de Tours, 37044 Tours, France;;

[10] CNRS, INSERM, CHU Lille, Centre Oscar Lambret, UMR 9020-UMR 1277-Canther-Cancer Heterogeneity, Plasticity and Resistance to Therapies, University of Lille, F-59000 Villeneuve d'Ascq, France;

[11] Department of Molecular and Cell Biology, University of California, Berkeley, Berkeley, CA,94720 USA

[12] Institut Universitaire de France (IUF), 75231 Paris, France

[*] Correspondence: dimitra.gkika@univ-lille.fr

Grolez *et al.*, *International Journal of Molecular Sciences* 2022, 23(12):6672

Abstract

In the fight against prostate cancer (PCa), TRPM8 is one of the most promising clinical targets. Indeed, several studies highlighted TRPM8 key involvement in PCa progression due to its impact on cell proliferation, viability and migration. However, data from the literature face some contradictions on the precise role of TRPM8 in prostatic carcinogenesis and are mostly based on *in vitro* studies. The purpose of this study was to clarify the role played by TRPM8 in PCa progression. We used a prostate orthotopic xenograft mouse model, showing that TRPM8 overexpression dramatically limited tumor growth and metastasis dissemination *in vivo*. Mechanistically, our *in vitro* data revealed that TRPM8 inhibits tumor growth by affecting cell proliferation and clonogenic properties of PCa cells. Moreover, TRPM8 impacts on metastatic dissemination mainly impairing cytoskeleton dynamics and focal adhesion formation through the inhibition of Cdc42, Rac1, ERK, and FAK pathways. Lastly, we proved the *in vivo* efficiency of a new tool based on lipid nanocapsules containing WS12 in limiting the TRPM8-positive cells' dissemination in metastatic sites. Our work strongly supports the protective role of TRPM8 on PCa progression, providing new insights for the potential application of TRPM8 as a therapeutic target in PCa treatment.

Keywords: prostate cancer; tumor growth; metastasis dissemination; TRPM8; Rho signaling; ERK; FAK; cell proliferation; trans-endothelial migration; invasion

Introduction

In Western industrialized countries, prostate cancer (PCa) is the most frequently diagnosed cancer and the second most common cause of death among men [1]. In its first stages, PCa develops slowly and remains localized, while in later stages the prostate capsule barrier can be crossed and the tumor becomes invasive, often leading to metastasis in lymph nodes and later mainly in the bone, liver, and lung [2].

Since metastases are the leading cause of cancer-related death, the deepest knowledge about the mechanisms supporting cancer metastasis is crucial in the fight against cancer. Malignant cell transformation is the result of enhanced proliferation, aberrant differentiation, and an impaired ability to die [3]. These alterations finally result in abnormal tissue growth, which can eventually turn into an uncontrolled expansion and invasion, characteristic of cancer. Moreover, to escape from the primary site and colonize distant organs, cancer cells must acquire a more aggressive migratory and invasive phenotype. In this context, several studies pinpointed the central role played by calcium (Ca^{2+}) and ion channels in all the processes associated with the

metastatic cascade [4–7]. In particular, members of the Transient Receptor Potential (TRP) ion channel superfamily were implicated in all the hallmarks of cancer, and their expression levels correlated with the emergence and/or progression of numerous epithelial cancers [8,9]. In addition, it should be noted that besides their transcriptional and translational regulation, ion channel trafficking to the cell surface, as well as plasma membrane stabilization, define channel activity. Therefore, modulation of TRP channels expression/activity on one of these levels may affect intracellular Ca^{2+} concentrations and consequently, processes involved in carcinogenesis, such as proliferation, apoptosis, and migration [10].

In recent decades several lines of evidence highlight a key involvement of the TRP channel TRPM8 in prostate cancer. First, TRPM8 expression varies during cancer progression with a strong expression in the initial PCa stages and loss of expression in the late and more aggressive stages. This differential expression makes TRPM8 a good diagnostic/prognostic marker and, indeed, it is currently used as a clinical marker in some countries [11,12]. Second, several *in vitro* studies reported anti-proliferative [13–15], pro-apoptotic [15,16], and anti-migratory [15,17,18] effects of TRPM8 in PCa cells. However, although an anti-proliferative role was suggested for TRPM8 *in vivo* [14], other studies reported a pro-proliferative role *in vitro* [16,19,20]. More precisely, these *in vitro* studies reported a decrease in the proliferation rate of several PCa cell lines when TRPM8 was inhibited by pharmacological blockers and, to a lesser extent, by siRNA against the channel. Indeed, TRPM8 blockers and siRNA reduced the proliferation in LNCap and DU-145 cells, but not in PC3 cells and PNTA1 cells. Taking into account the broad action of pharmacological blockers and the uncorrelated effects between TRPM8 knock-down expression and cell proliferation, it is difficult to speculate on the physiological relevance of the channel in that case. This data in addition to the antitumorigenic effect of TRPM8 observed in subcutaneous xenograft model in mice [14] illustrate the need of further studies to better confirm and clearly delineate the anti-metastatic role played by TRPM8 in PCa progression.

To shed light on these contradictory data and further support the protective role of TRPM8 *in vivo*, in this study, we explored the effects of TRPM8 overexpression on PCa progression both *in vitro* and *in vivo* using a prostate orthotopic xenograft mouse model. In particular, we evaluated the impact of TRPM8 on primary tumor growth and metastatic dissemination further investigating the molecular mechanisms underlying TRPM8 effects on PCa progression. These findings may provide new insight in view of a potential application of TRPM8 as a therapeutic target in the treatment of PCa using channel-targeting nanotechnologies.

Materials and Methods

Cell culture

Human prostate cancer cells from bone metastasis (PC3, ATCC®) with stable luciferase overexpression (PC3-luc) and PC3 with TRPM8 and luciferase overexpression (PC3-M8-luc) were used in this study. Cells were obtained by stable transfection with pcdna4-TRPM8 and/or pcdna3-luciferase vectors. In order to obtain stable clones, transfected cells were selected using 100µg/ml zeocin (InvivoGen) and/or 700µg/ml geneticin (Sigma-Aldrich) every two passages. PC3 cells were grown in RPMI (Invitrogen) supplemented with 10% of fetal bovine serum (Pan Biotech), L-glutamine (5 mM; Sigma-Aldrich), and PenStrep® (100 mg/ml; Sigma-Aldrich).

Human microvascular endothelial cell line (HMEC-1, ATCC®) was cultured in EndoGRO™ MV-VEGF complete medium (Merck Millipore), supplemented with L-glutamine (5 mM; Sigma-Aldrich), and PenStrep® (100 mg/ml; Sigma-Aldrich).

Lipid nanocapsules formulation

Lipid nanocapsules (LNC) were formulated with a mixture of LabrafacTM Lipophile WL 1349 (caprylic/capric triglyceride), Phospholipon® 90G (soybean lecithin at 97.1% of phosphatidylcholine), and Solutol® HS15 (a mixture of free polyethylene glycol 660 and polyethylene glycol 660 hydroxystearate) generously provided by Gattefosse S.A.S. (Saint-Priest, France), Phospholipid GmbH (Köln, Germany), and Laserson (Etampes, France), respectively. Type I ultrapure water was obtained from a Milli-Q plus system (Millipore, Paris, France). WS-12 was obtained from Tocris (Bio-Techne SAS, France). Other chemical reagents were obtained from Sigma-Aldrich (Saint-Quentin Fallavier, France) and solvents were obtained from Thermo Fischer Scientific (Illkirch, France) and used as received.

Formulation of LNC-WS12 for in vivo experiments: LNC of size 25 nm were prepared with slight modifications in water using a phase inversion method of an oil/water system, as described by Heurtault et al. [11]. Typically, the oil phase containing Labrafac (2.52 g), Solutol (4.08 g) and Phospholipon 90G (0.375 g) was mixed with the appropriate amounts of WS-12 (29 mg, 1% of Labrafac+Phospholipon 90G), Milli-Q water (5.4 mL) and NaCl (660 mg), and heated under magnetic stirring up to 70 °C. The mixture was subjected to 3 temperature cycles from 26 to 76 °C under magnetic stirring. The mixture was then cooled to 45 °C before the addition of 28.2 mL of cold ultrapure water (0 °C). The formulation was stirred at room temperature for another 10 min and was stored in the fridge at 4 °C overnight before purification. Empty LNC were formulated without WS12. The LNC suspensions were purified by dialysis (12000-14000 Da, 4 times) during 2 days in NaCl solution (9 g/L). The purified LNC suspensions were sterilized using syringe filters (0.22 µm) in a sterile plastic tube.

The drug loading of purified LNC suspensions were quantifed by high performance liquid chromatography (HPLC). High performance liquid chromatography (HPLC) analysis was carried out on a Shimadzu LC2010-HT (Shimadzu, Tokyo, Japan) using a 5 µm C18AQ Uptisphere® X-serie 300 Å, 250×4.6 mm column (Interchim, Montluçon, France) heated to 30 °C. The mobile phase consists of a mixture of eluent A (formic acid 0.1% in H2O) and eluent B (formic acid 0.1% in acetonitrile) at a flow rate of 1 mL/min. The isocratic flow (eluent 1) was for 1 min, the linear gradient was 0 to 80% of eluent B in 10 min and further 80% of eluent B for 4 min. The detection was performed at 254 nm. Diluted LNC solutions (by 10) were analyzed by injecting of 40 µL into the column. A stock solution of WS-12 was prepared at 1 mg/mL in DMSO for the calibration curve. Concentrations of 5, 10, 20, 40, 80 and 120 µg/mL of WS-12 in DMSO were prepared from this stock and injected (40 µL) into the column. A calibration curve (Y = 127869*X + 40563, r^2 = 0.9999, LOD = 1.36 µg/mL, LOQ = 4.13 µg/mL) was obtained by linear regression of drug concentration (X, µg/mL) versus the peak area (Y).

In vivo tumor models

Ten-week-old male NMRI Nude Mice (Charles River Laboratories) were injected into the prostate with 2×10^6 PC3-luc or PC3-M8-luc cells (12 mice/condition) suspended in 30 µl PBS while under isoflurane anesthesia. Animal weight was measured every week for 5 weeks and the tumor growth was monitored using bioluminescence (BLI) measurement. To measure BLI, mice were injected with d-luciferin intraperitoneally (150 mg/kg) for 10 min before bioluminescence imaging (ΦimagerTM; BIOSPACE Lab). Photons emitted by cancer cells were counted and expressed in counts per minute (c.p.m.). At necropsy after 5 weeks, *ex vivo* BLI measurement for each collected organ was performed using d-luciferin intraperitoneal injection (150 mg/kg) and results were expressed in counts per minute (c.p.m.).

Unanesthetized twelve-week-old male NSG Mice (Charles River Laboratories) were placed into a plastic restraining device and injected with 5×10^6 PC3-luc or PC3-TRPM8-luc cells suspended in 150 µl PBS (15 mice were injected with PC3-Luc cells, 9 mice with PC3-M8-Luc clone 5 and 6 mice with PC3-M8-Luc clone 2 cells). Cells were injected into the lateral tail vein through a 25-gauge needle, as previously described [51]. Tumor growth was measured every week for 5 weeks using d-luciferin intraperitoneal injection (150 mg/kg) for 10 min before bioluminescence imaging and results were expressed in counts per minute (c.p.m). At necropsy, *ex vivo* BLI measurement for each collected organ was performed, as described above.

To test the toxicity of lipid nanocapsules (LNC), fourteen-week-old male NMRI Nude Mice (Charles River Laboratories) grafted orthotopically with 2×10^6 PC3-M8-luc cells (3 mice/condition) were injected into the lateral caudal vein with empty or WS-12-loaded LNC labeled with DiI at three different concentrations (10, 1, or 0.1 mg/kg diluted in NaCl), free WS-12, or in the solvent (NaCl), for control three times per week for three

weeks. After 3 weeks, mice were sacrificed and the presence of LNC in organs was analyzed using DiI imaging on lysates.

Intracardiac manipulations were performed on 52 six-week-old male NMRI Nude Mice (Charles River Laboratories) bred and housed at the "Small Animal Imaging Center" of the TAAM Unit at the CNRS (Orléans, France) according to referral n°1166 from CECCO n°3 and APAFIS authorization #19911. The mice were anesthetized with an air/2% isoflurane mixture (Piramal, CSP) and then injected in the left ventricle with 2×10^6 PC3-luc clone 11 or PC3-TRPM8-luc clone 2 cells suspended in 100 µL PBS. Starting from D1, mice received 200 µL of a solution containing 2.7% DMSO (control group) or 200 µL containing 0.130 mg of the TRPM8 inhibitor M8B hydrochloride (Bio-techne) diluted in 1X PBS containing 2.7% of DMSO (treated group). Treatments were administered intraperitoneally 3 times a week up to D50. To assess the quality of the injection of cells into the left ventricle and then to perform imaging of tumor proliferation, bioluminescence imaging was performed with an Ivis® Lumina device (Perkin Elmer, USA). Anesthetized mice were imaged by bioluminescence on both the ventral and the dorsal side once a week for 8 weeks upon injection of luciferin (Perkin Elmer, France, supplied by CIPA) at a dose of 2 mg/mouse.

Histology, immunostaining and morphometric analyses

Mouse tissue samples were fixed in 4% PFA overnight at 4 °C, dehydrated, and embedded in paraffin (for 8 µm serial sections). Histology was performed by Trichrome staining (histology core facility of Lille). Before immunofluorescence experiments, the sections underwent deparaffinization: incubation in xylene 2 times x 10 min, then rinsed with 100% ethanol (2 times x 3 minutes), and rehydrated in a decreasing gradient of Ethanol/H20 (100%, 96%, 70%, 30% 5 minutes each) and finally transferred to PBS. The sections were blocked for 30 minutes in blocking buffer (PBS + 10% Donkey serum + 0.3% triton X100), then incubated with primary antibodies in blocking buffer overnight at 4 °C. After three rinses in PBS, the sections were incubated for 90 min at RT with secondary antibodies diluted in blocking buffer. Finally, the sections were rinsed three times in PBS before nuclear staining with DAPI (1:200 in PBS) and mounting with Mowiol. Im-munostainings were performed using the following primary antibodies: Rb-Anti Ki67 (Ab 15580, 1:100); Goat anti-TRPM8 (Antibodies ONLINE, 1:100)

Sections were then incubated with the appropriate fluorescently conjugated sec-ondary antibodies (Dk anti Gt Alexa 488 1:400 Molecular Probes, Dk and Rb Rodhamine 1:250 Jakson Immunoresearch). Nuclei were counterstained with DAPI (Invitrogen, Life Technologies, Ghent, Belgium). For morphometric analyses, mosaic tile images were taken by Axio Scan, Z1 (Zeiss, Jena, Germany) with a ×20 dry objective (NA 0,8). Images were processed with ZEN software (Zeiss Efficient Navigation) and analyzed using the NIH Image J by a sequential operations allowing the tumor area identification, necrotic area identification and cell counting. For each necrotic area, the number of total cells (stained with DAPI) was counted using a fixed threshold,

watershed and analyze particles from 30 to 5000 pixel2. Tumor proliferation was defined as the Ki67+ area and expressed as a percentage of the total nuclei (DAPI+). Apoptosis was measured by TUNEL following manufacturer instruction (DeadEnd™ Fluorometric TUNEL System). Ki67 + cells or apoptotic cells were counted as GFP channel, using a fixed threshold, watershed and analyze particles from 30 to 5000 pixel2. The complete macro is reported in supplementary material as Github.

Confocal imaging was performed using an LSM700 confocal microscope (Carl Zeiss, Munich, Germany).

Flow cytometry assay

Cells were harvested, washed with PBS, and fixed with cold 70% ethanol for 30 minutes. After rinsing with PBS, cells were incubated with an RNase cocktail (Invitrogen) in PBS for 15 minutes, followed by 50 µg/ml propidium iodide (PI; Sigma Aldrich) for 30 minutes at room temperature. After incubation, cells were placed on ice before being analyzed by flow cytometry. Data were acquired with a CyAn ADP flow cytometer (Beckman Coulter) using FL3 channel (488nm excitation, and 640DLP - 613/20 filters). Analysis was performed using Summit software.

Apoptosis assay

Tumor apoptotic cell death was detected and quantified via DeadEndTM Fluorometric TUNEL System Kit (Promega) according to the manufacturer's instruction. For apoptosis analysis of tumor sections, mosaic tile images covering an entire tumor section were acquired and the TUNEL+ area was expressed as a percentage of the total tumor area analyzed.

Clonogenic assay

The ability of the cells to form clones was assessed using a clonogenicity test. PC3-luc and PC3-M8-luc cells were cultured in a 6-well plate at a confluence of 800 cells/well for 2 weeks. The medium containing different treatment conditions (WS12 at 1 and 10 nM, empty LNC, WS12-loaded LNC at 1 and 10 nM, icilin at 10 µM, and M8B at 1 µM) was changed every three days during the time of the experiment. After 2 weeks of incubation, the clones obtained were rinsed with PBS, fixed with methanol, and stained with Crystal violet (Santa Cruz). The number of clones present in each well was counted using the ImageJ software [52] and each condition was normalized to the control condition.

Time-lapse video microscopy

Cells were seeded at low density and kept at 37°C under 5% CO_2 in an incubator chamber for time-lapse video recording (Okolab). Cell movements were monitored with an inverted microscope (Eclipse Ti-E; Nikon) using a 10X/0.25 NA Plan objective lens.

Images were acquired every 10 minutes for a time-lapse of 10 hours with a CCD video camera using NIS-Element software (Nikon). Image stacks were analyzed with ImageJ software and at least 100 cells/condition were manually tracked using the MtrackJ plugin. We excluded dividing cells as well as cells that exited the imaged field during the time-lapse acquisition period. The mean speed parameter was considered for the data analyses. At least 6 fields for each condition were analyzed in each independent experiment. At least three independent experiments were performed for each experimental condition.

Invasion assay

Cells were harvested from the culture dish, 5×10^4 cells in 200 µL of 2% serum medium were transferred to the Transwell inserts coated with Matrigel® (the top compartment, 8-µm pore size, Corning), and 1 mL of 10% serum medium was placed in the lower chamber. Following incubation at 37°C for 22 hours in a cell culture incubator, cells on the upper surface of the filters were removed with cotton swabs, filters were washed with PBS, fixed in methanol, and stained with crystal violet. Cells that had moved to the lower surface of the filter were counted under the microscope. Migrated cells in each field were quantified. Results are presented as relative migration by setting the migrating cell number of control cells as 100.

Trans-endothelial migration assay

To analyze the ability of PC3 and PC3 M8 cells to migrate through an endothelial cell monolayer, we used a video microscopic *in vitro* "extravasation" assay. In brief, a thin basement membrane-like matrix (consisting 1X RPMI, 10 mmol/l HEPES, 0.04 mg/ml laminin, 0.04 mg/ml fibronectin, and 0.32 mg/ml collagen IV, adjusted to pH 7.4) is layered onto thick collagen I layer (containing 1X RPMI, 10 mmol/l HEPES, and 0.8 mg/ml collagen I, adjusted to pH 7.4 and incubated overnight at 37°C in a 12.5 cm^2 flask) for one hour at room temperature. Afterward, 1.7×10^6 HMEC cells are added to the collagen double-layer and incubated for 7–10 days at 37°C, and 5% CO_2. The medium is replaced every 2 days, and when the cells reach confluency, 10 ng/ml TNF-α are added. The next day, 3×10^5 PC3 or PC3-M8 cells and 100 ng/ml epidermal growth factor (EGF) are added with or without senicapoc (30 µmol/l, dissolved in DMSO). Trans-endothelial migration is monitored for 13.5 hours using a ZEISS microscope Axiovert 40C, linked to a video camera (Hamamatsu, Germany). Images are taken in 5-minutes intervals. The analysis is performed using ImageJ. All PC3 and PC3 M8 cells within the given visual field are counted in the first image of the stack (t=0). Then individual cells are tracked. The criterion for trans-endothelial migration is that PC3 or PC3-M8 cells not only settle between but they clearly move underneath the endothelial cells. For these cells, the time point of intrusion into the endothelium is set to represent the beginning of trans-endothelial migration. For the final analysis, the number of transmigrated cells is normalized to the number of PC3 or PC3-M8 cells at t=0. Three independent experiments were performed for each experimental condition.

Microfluidic co-cultures

Blood-vessel formation: The OrganoPlate® 2-lanes (MIMETAS, 9603-400B) containing 96 chips (4.5 mm long gel and perfusion channels - 200 µm × 120 µm (w×h)) was used to reproduce tubular endothelial structures that mimic blood vessels in a microfluidic system [53]. In all experiments rat tail collagen type I (Nalgene) was used as extracellular matrix (ECM) for the cells (in the gel channel). A stock collagen type I solution (5 mg/ml) was neutralized with 10% $NaHCO_3$ (37 g/l) and 10% HEPES buffer (1 M) (Sigma Aldrich) to obtain a final concentration of 4 mg/ml. $NaHCO_3$ and HEPES were mixed in a 1:1 ratio (v/v) and then collagen I was added in a volume corresponding to 4 times the volume of the initial mix (final volume ratio 1:1:8 HEPES/ $NaHCO_3$/Collagen I). Some attracting factors such as FCS and VEGF were added to the ECM. The neutralized collagen was kept on ice and used within 10 minutes. 2µl of the neutralized collagen was added into the inlet of each gel channel and then the device was incubated for 30 minutes at 37°C and 5% CO_2 to allow collagen polymerization; the device was removed from the incubator and kept sterile at room temperature right before cell loading. HMEC cells were dissociated, pelleted and resuspended in complete medium (EndoGRO™ MV-VEGF, Merck Millipore) at a density of 2×10^7 cells/ml. 2 µl of the cell suspension was dispensed into the perfusion channel inlet followed by the addition of 50 µl of culture medium to prevent dehydration of the cell suspension. The OrganoPlate® was placed on its side with gel channels at the bottom and incubated (37° C, 5% CO_2), to allow cells to adhere. After the cells were attached to the gel, the device was rotated back into an upright position and 50 µl of the medium was added to the medium outlet. The device was then placed on a rocking platform (Perfusion rocker, MIMETAS) for continuous perfusion (7° inclination, 8 minutes cycle time). The culture medium was refreshed three times a week and right before each experiment.

Extravasation assay: After transfection with TRPM8 and/or GFP plasmid, PC3 cells were inserted into the tubule (0.2×10^4 cells/line) and the co-culture was imaged 16 hours after PC3 injection using a Leica TCS SP5 confocal system (Leica Microsystems) with magnification 200X. DAPI (1:1000 for 15 minutes, Invitrogen, Life Technologies) was used for nuclear staining and actin was labelled with Rodhamine-phalloidin (1:1000 for 15 minutes, Invitrogen, Life Technologies). The cells that passed through the tubule were counted and they were distinguished into three zones: cells that have passed the tubule and are in the collagen I matrix, cells that are integrated into the tubule, and cells that rested into the tubule.

Western blot analysis

Cells were seeded in Petri dishes with the appropriate medium and grown to a confluency of 80%. Before cell lysis, Petri dishes were kept on ice and washed twice with ice-cold PBS. Cells were lysed with RIPA Buffer (25 mM Tris-HCl pH 7.6, 150 mM NaCl, 1% NP-40, 1% sodium deoxycholate, 0.1% SDS) containing the following protease inhibitors: 2 mg/ml aprotinin, 1 mM Na orthovanadate, 0.1 mM PMSF and 10 mM sodium

fluoride. Lysates were centrifuged at 4°C for 10 minutes at 12 000 g. Protein concentrations were determined using a Bicinchoninic Acid Kit (BCA kit, Sigma) following the manufacturer's instructions. 50 µg of the sample were resuspended in SDS sample buffer, heated at 95°C for 5 minutes, and separated on 10% pre-cast SDS gel (Biorad). Polyvinylidene fluoride membranes were properly blocked and then incubated overnight with ERK1/2 (1:1000, #9102, Cell Signaling), phospho-ERK1/2 Thr402/Tyr204 (1:1000, #9101, Cell Signaling), AKT (1:3000, #9272, Cell Signaling) and Phospho-Akt-Ser473 (1:2000, #4508, Cell Signaling) antibodies. The membrane was then washed with TBS containing 0.1% Tween 20 and incubated with the appropriate horseradish-peroxidase-conjugated antibodies (SantaCruz). Chemiluminescence assays were conducted using the SuperSignal West Dura chemiluminescent substrate (Thermo Fischer Scientific).

Cell signaling pathway assays

Cell signaling activation pathways were analyzed using western blot techniques to study the phosphorylation levels of ERK and FAK using antibodies described above. To quantify the differences in protein phosphorylation, the ratio between non-phosphorylated and phosphorylated protein expression was evaluated using ImageJ software. Cdc42, Rac1, and RhoA activation was evaluated using G-LISA® activation assay kit for Cdc42, Rac1, and RhoA (G-LISA® CDC42 Activation Assay Biochem KitTM, G-LISA® Rac1 Activation Assay Biochem KitTM, G-LISA® RhoA Activation Assay Biochem KitTM; Cytoskeleton). Manufacturer’s instructions were followed for each kit.

Statistical analysis

Data are expressed as means ± SEM. The statistical significance of differences between groups was determined by analysis of variance (ANOVA) followed by pairwise comparison using Tukey’s or Bonferroni’s method for *in vivo* assay, flow cytometry, apoptosis, clonogenic assay, invasion, migration assay, and cell signaling pathway assays. Student t-test was used to analyze trans-endothelial migration assay. Differences with a $P < 0.05$ were considered statistically significant. Statistical analyses were performed using GraphPad Prism 6 software (GraphPad Corporation).

Results

1. TRPM8 overexpression inhibits prostate tumor growth in vivo

To investigate the role played by TRPM8 in prostate tumor growth, we performed an *in vivo* study using mice with a prostate orthotopic graft of PCa cells from bone metastases stably overexpressing (PC3-M8-luc), or not (PC3-luc), TRPM8 channel. We have used two separate clones, named cl2 and cl5, for the PC3-M8-luc assays. These clones were obtained after transfection of PC3-M8 cells with a pcdna-3 luciferase plasmid and then selected using geneticin. Bioluminescence based on the luciferase activity was measured weekly to follow PC3 cell growth and we showed that overexpression of TRPM8 inhibits prostate tumor growth (Fig. 1A and B). More precisely, the overexpression of TRPM8 induced a significant decrease in PCa growth already evident 4 weeks after the orthotopic graft and equal to 93.34 ± 1.81% in PC3-M8-luc cl5 and to 98.04 ± 0.48% in PC3-M8-luc cl2 5 weeks later (Fig. 1A and B).

Following mice sacrifice, prostate tumors were recovered, weighed, and analyzed (Fig 1C-E). In accordance with bioluminescence measurements, we found that TRPM8 overexpression decreased tumor weight by 42.89 ± 7.73 % in PC3-M8-luc cl5 grafts (175.08 ± 23.90 mg for PC3-M8-luc cl5 tumor against 348.6 ± 48.52 mg for PC3-luc tumor) and by 66.31 ± 5.79 % in PC3-M8-luc cl2 grafts (95.83 ± 6.99mg for PC3-M8-luc cl2 tumor against 348.6 ± 49.52 mg for PC3-luc tumor) (Fig. 1C). The comparison of the tumor area between PC3-luc and PC3-M8-luc grafts also confirmed the inhibitory role of TRPM8 in PCa growth, showing a reduction of the tumor area of 79.91 ± 3.28% in PC3-M8-luc cl5 and 64.24 ± 3.41% in PC3-M8-luc cl2 (Fig. 1D). Immunofluorescence and histological analyses were further performed to verify TRPM8 expression in our prostate orthotopic tumor model (Fig. 1E). As shown in figure 1E, the prostatic glandular architecture of PC3-luc orthotopic grafts is severely disorganized when compared to the TRPM8 grafts.

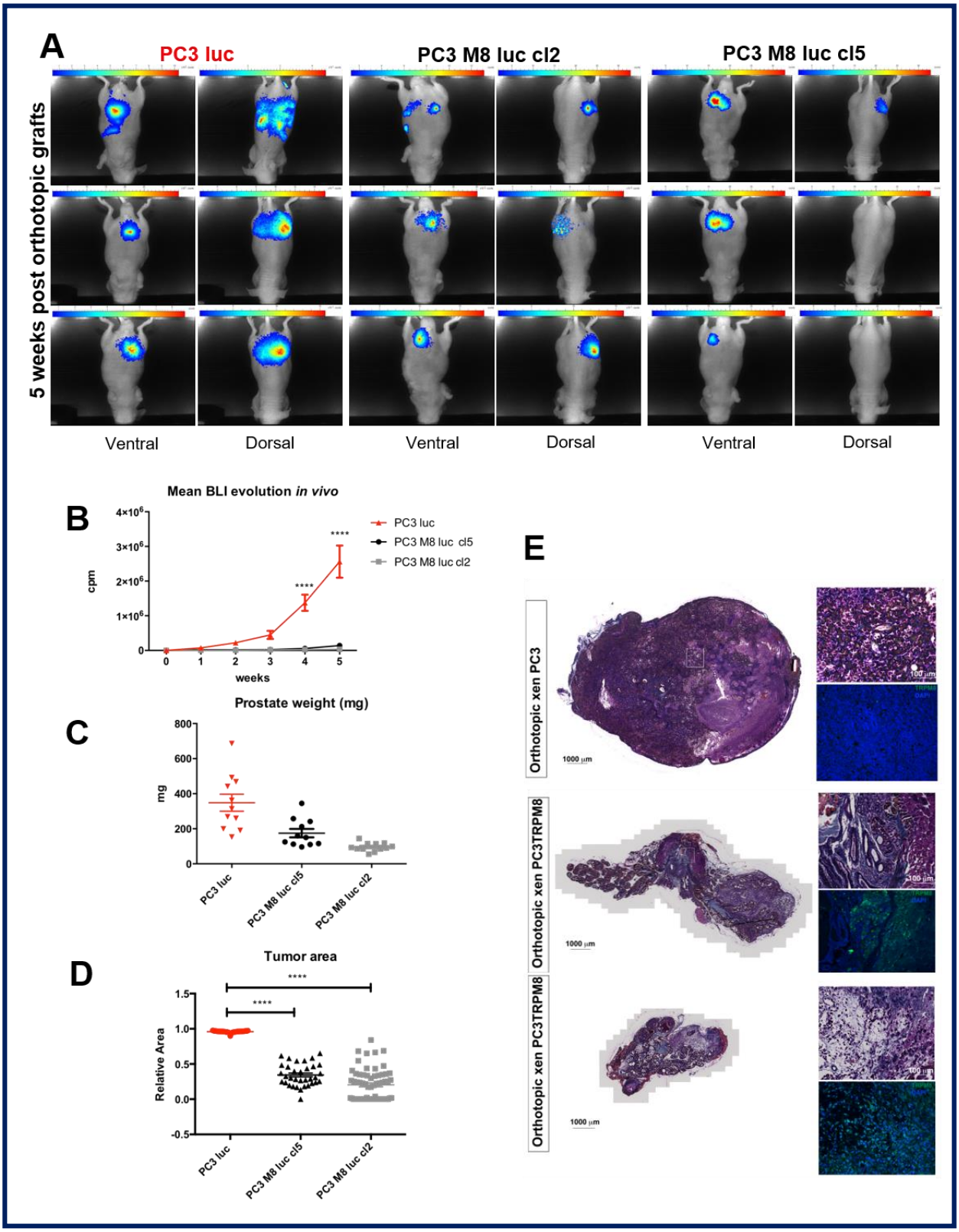

Figure 1. TRPM8 overexpression inhibits prostate primary tumor growth in vivo.

A) Images showing bi-oluminescence from mice grafted with PC3-luc and two clones of TRPM8-overexpressing PC3-M8-luc cells (cl2 and cl5) 5 weeks after orthotopic graft. B) Quantification of bioluminescence from PC3-luc or PC3-M8-luc

*mice xenografts 5 weeks after grafting (n=12 mice/condition; statis-tical significance **** = p <0.00001, 2-way ANOVA with post-hoc Bonferroni test. C) Weight (mg) of prostate tumor from mice 5 weeks after grafting with PC3-luc or PC3-M8-luc (n= 12 mice/condition). D) Quantification of the relative tumor area from PC3-luc or PC3-M8-luc grafts in mice (n=51 for PC3-luc; n=34 for PC3-M8-luc cl5, and n=63 for PC3-M8-luc cl2; statistical sig-nificance, **** = p <0.00001, ordinary one-way ANOVA with post-hoc Tukey's test). E) Histologi-cal analysis of tumors from PC3-luc and PC3-M8-luc mouse xenografts. Immunofluorescence for TRPM8 is represented in green and immunofluorescence for DAPI in blue.*

2. TRPM8 overexpression inhibits cell proliferation and cell clones' formation

To better clarify the mechanism underlying the TRPM8-mediated inhibition of PCa growth observed *in vivo*, we performed histological and immunofluorescence analyses on prostatic tissues extracted from mouse xenografts. In particular, we quantified proliferation and apoptotic markers that could account for the large difference observed between PC3-luc and PC3-M8-luc orthotopic grafts (Fig. 2). The proliferation rate in xenografted mice prostates was assessed by KI67 staining showing that TRPM8 overexpression significantly decreased the proliferative fraction of PC3 cells by 55.7 ± 7.87 % and 88,2 ± 15,87 % in PC3-M8-luc cl 5 and 2, respectively (Fig. 2A and B). Consistently, TRPM8 overexpression in PC3 cells revealed a cell cycle arrest at G_0/G_1 transition with an increase of 6.97 ± 1.21 % of PC3-M8-luc cells in G_0/G_1 phase compared to PC3-luc cells *in vitro* (Fig. 2C). However, this percentage of cell cycle arrest is too limited to explain the large difference found in tumor size and volume due to TRPM8 overexpression (Fig. 1). Therefore, we next evaluated apoptosis in mice cancerous prostates by using the TUNEL assay. As shown in figure 2D, PC3-luc grafts, unlike PC3-M8-luc grafts, include apoptotic and necrotic areas. In agreement, TUNEL quantification *ex vivo* revealed a significant decrease of the apoptotic area in PC3-M8-luc tumors from both the clones compared to PC3-luc tumors by 95.44 ± 14.48 % (Fig. 2D). However, the same assay performed *in vitro* on PC3 cells revealed that TRPM8 overexpression did not induce a significant difference in the number of apoptotic cells (Fig. 2F). This evidence suggests that TRPM8 prevents prostate tumor growth by reducing proliferation rate, without inducing apoptosis.

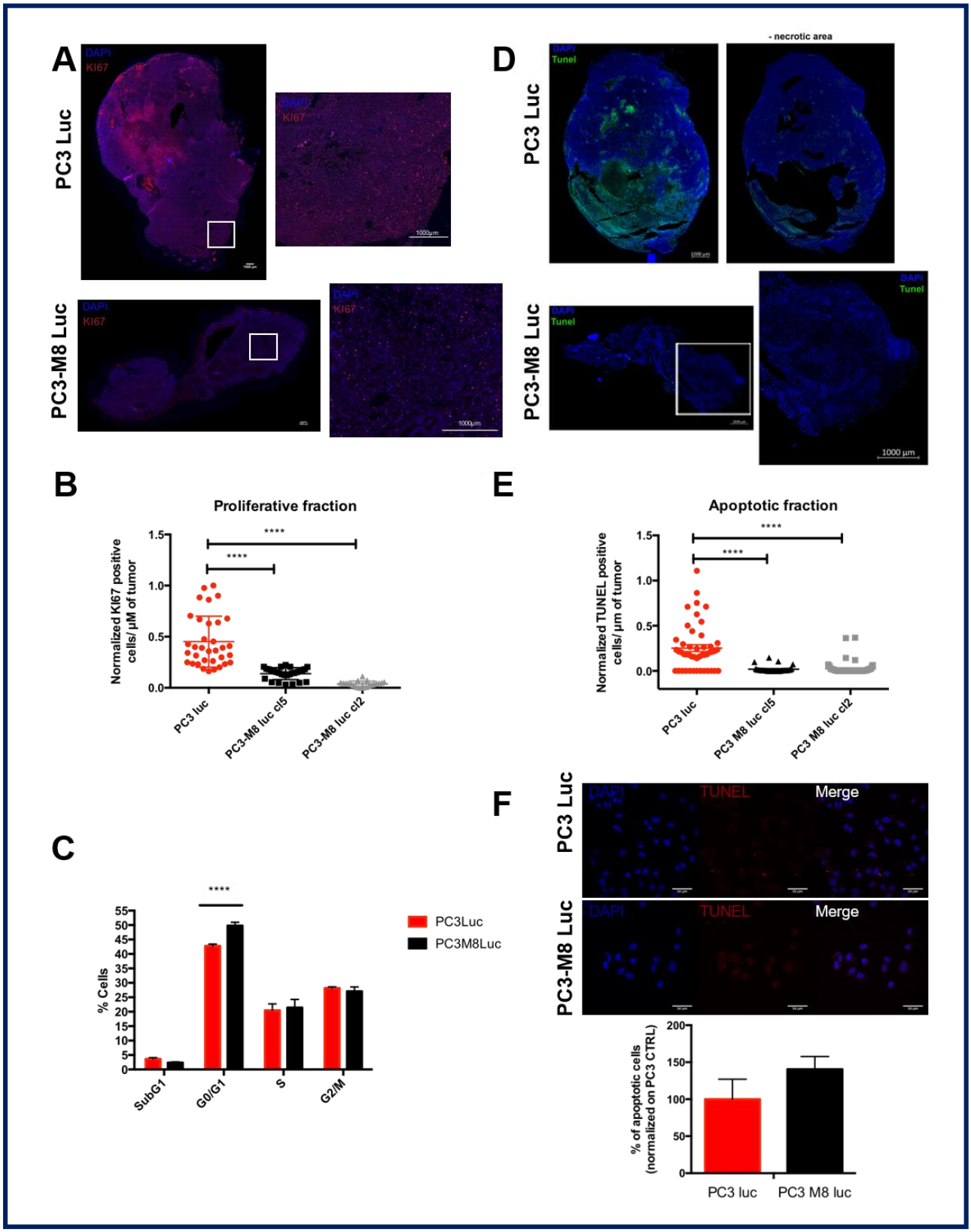

Figure 2. TRPM8 overexpression affects cell proliferation but not apoptosis.

*A) Representative images of Ki67 staining in prostate tumor from PC3-luc or PC3-M8-luc orthotopic grafts. B) Quantification of Ki67 staining on tumors from PC3-luc or PC3-M8-luc grafts. Data are expressed as Ki67 positive cells/µm (n=34 for PC3-luc; n=28 for PC3-M8-luc cl5, and n=21 for PC3-M8-luc cl2; statistical significance: **** = p <0.0001, ordinary one-way ANOVA with post-hoc Tukey's test). C) Flow cytometry assay with propidium iodide on PC3-luc and PC3-M8-luc (n=5 independent assay; statistical significance: **** = p <0.0001, 2-way ANOVA with post-hoc Sidak test). D) Images representing apoptotic fraction (green signal) in tumors from PC3-luc and PC3-M8-luc grafts (necrotic areas were subtracted on tumor from PC3-luc grafts). Cells were labeled with DAPI (blue signal). E) Quantification of apoptotic area in tumors from PC3-luc and PC3-M8-luc grafts. Data are expressed as TUNEL positive cells/µm (n=30 images/condition; statistical significance: **** = p< 0.0001, ordinary one-way ANOVA with post-hoc Tukey's test)., F) Apoptosis assay on PC3-luc and PC3-M8-luc cell lines using TUNEL kit.*

Beyond proliferation and apoptosis, cell capability to form clones plays a crucial role in tumor growth. We therefore performed clonogenic assays with PC3-luc and PC3-M8-luc (Fig. 3A). As shown in figure 3A i, TRPM8 overexpression led to a significant (by 64.12 ± 8.99 %) decrease in the cellular capacity to form clones. Moreover, TRPM8 stimulation with WS12 (10 nM) or icilin (10 µM) further compromised PC3-M8-luc cells' capability to form clones (by 17.97 ± 3.40 % and 27.51 ± 6.61 %, respectively, Fig. 3A iii), whereas no effects were detected on PC3-luc control cells after agonist treatment (Fig. 3A ii). Accordingly, TRPM8 inhibition with the M8B (1µM) antagonist restored the PC3-M8-luc capability to form clones and increased it by 36.27 ± 3.52 % (Fig. 3A iii). To further support these *in vitro* data, analysis of tumors from PC3-luc and PC3-M8-luc orthotopic grafts by DAPI staining was performed. As shown in figure 3B, a higher density of PC3-luc cells was detected as compared to PC3-M8-luc cells in tumor areas (Fig 3 B). More precisely, cell density quantification performed tumor by tumor revealed that, in PC3-luc grafts, cell density was 82.8 ± 14.80 % higher than in PC3-M8-luc cl5 grafts and 41.95 ± 3.27 % higher than in tumors from PC3-M8-luc cl2 grafts ($2.42*10^{-3}$ cells/μm^2 in PC3-luc tumors, $3.8*10^{-4}$ cells/μm^2 in PC3-M8-luc cl5 tumors, and $1.28*10^{-3}$ cells/μm^2 in PC3-M8-luc cl2 tumors) (Fig. 3C). Collectively, our data on PC3-luc and PC3-M8-luc cell lines *in vitro* as well as in xenografted mice prostates demonstrate that the decrease in tumor growth induced by TRPM8 overexpression (Fig. 1) is partly attributable to the TRPM8-induced cell cycle arrest at G_0/G_1 phase as well as to its strong inhibition on PCa cells' clone formation capabilities.

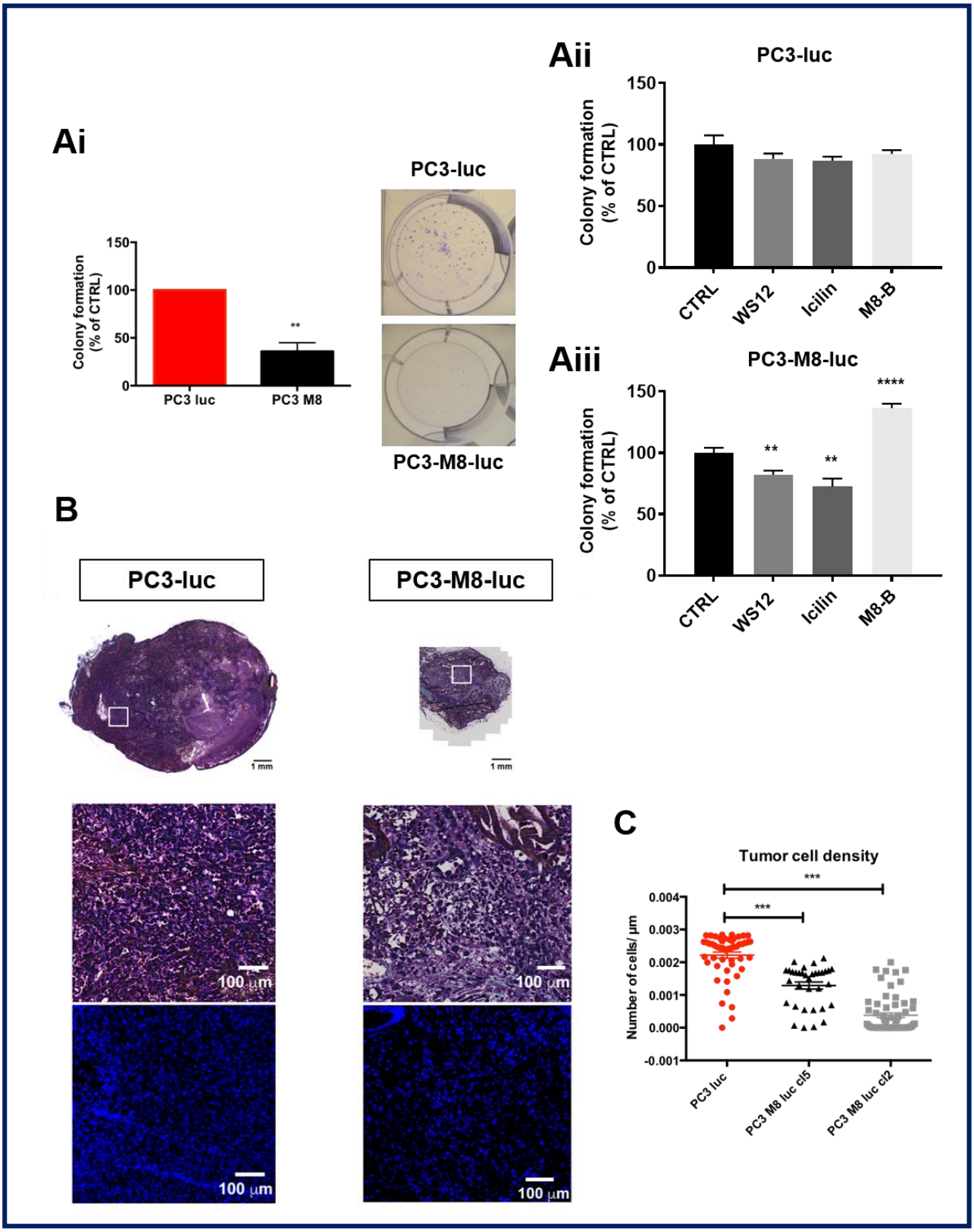

Figure 3. TRPM8 overexpression inhibits clone's formation capability.

*A) In vitro clonogenic assay on PC3-luc and PC3-M8-luc. Cells were seeded at 5*104 cells/well during two weeks and treated (A ii and A iii) or not (A i) with WS-12 (100 nM), icilin (10 µM) or M8-B (1µM). The number of clones was quantified*

*and normalized on control condition (n=6 independent experiments; statistical significance: ** = p <0.01, *** = p <0.001, unpaired Student t-test). B) Images representing DAPI staining in tumor from PC3-luc or PC3-M8-luc grafts. C) Quantification of cells density in tumors from PC3-luc or PC3-M8-luc grafts. Tumor cell density is expressed as number of cell/µm2 (n=50 images/condition; statistical significance: *** = p<0.001, ordinary one-way ANOVA with post-hoc Tukey's test).*

3. TRPM8 overexpression inhibits PCa cell dissemination in vivo and constitutes an efficient anti-migratory target for nanocapsules

To further characterize TRPM8 role in PCa progression, the metastatic dissemination of PC3-luc and PC3-M8-luc from orthotopic grafts shown in figure 1 was analyzed by bioluminescence imaging. As shown in figure 4, we found a higher metastatic rate in mice grafts with PC3-luc as compared to those grafted with TRPM8-overexpressing PC3-M8-luc cancer cells (Fig. 4). In particular, we observed metastases in different sites such as lung, liver, pancreas or kidney which were significantly less abundant in PC3-M8-luc xenografts (Fig. 4A-D). Nevertheless, based on these *in vivo* experiments, we cannot conclude whether TRPM8 overexpression acts also on metastasis dissemination because of the large difference in terms of tumor growth between PC3-luc and PC3-M8-luc orthotopic grafts.

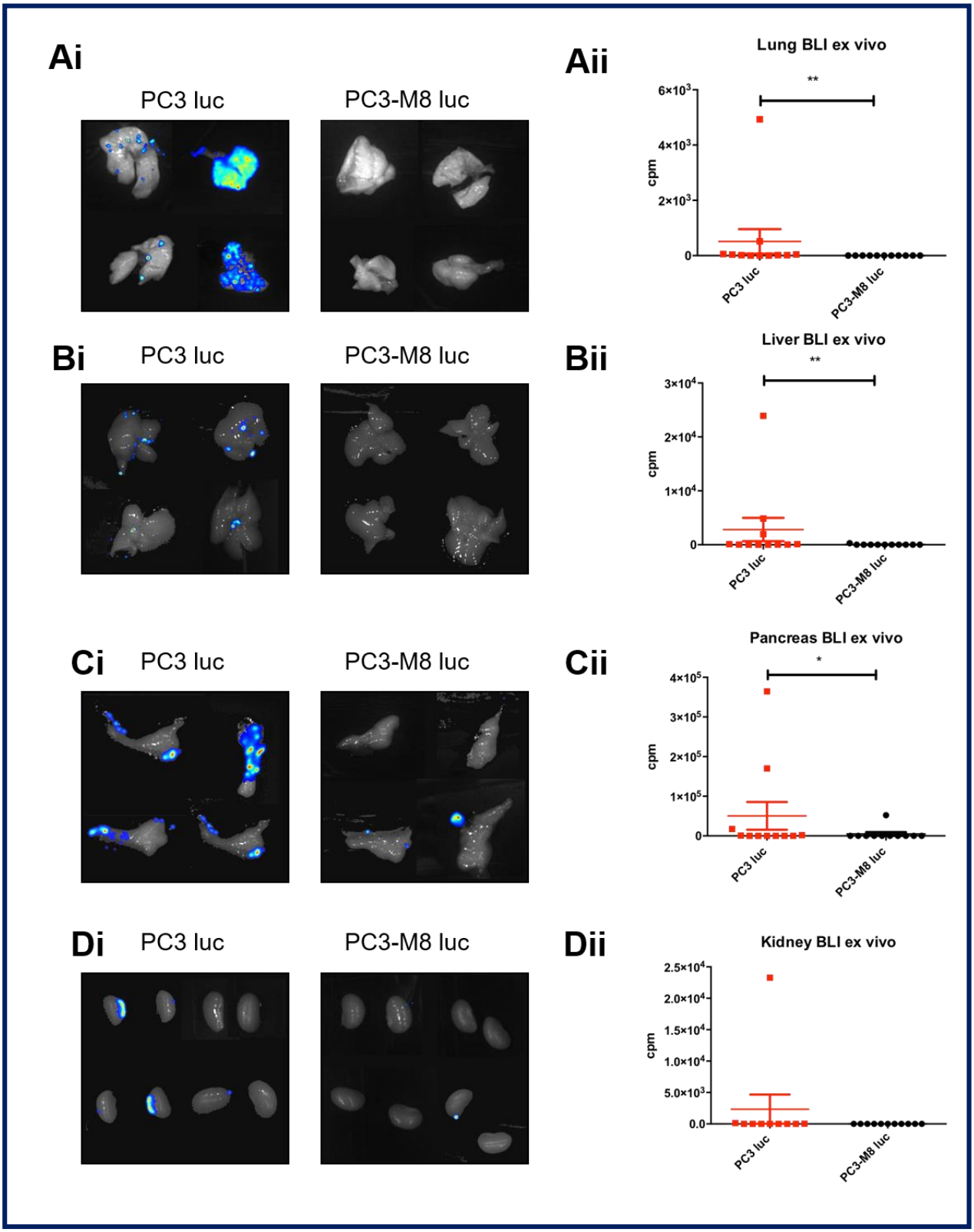

Figure 4. TRPM8 overexpression inhibits PCa cells' metastatic dissemination.

Representative images of bioluminescence in lung (A i), liver (B i), pancreas (C i) and kidney (Di) from mice 5 weeks after orthotopic grafts with PC3-luc or PC3-M8-luc. Quantification of bioluminescence in lung (A ii), liver (B ii), pancreas (C ii)

*and kidney (D ii) from mice 5 weeks after orthotopic grafts (n=11 mice/condition; statistical significance: * = p <0.05; ** = p <0.01, Mann-Whitney test).*

Therefore, we injected PC3-luc and PC3-M8-luc into the tail vein of the mice to more clearly define the role played by TRPM8 on PCa cells dissemination and organ colonization *in vivo*. As shown in figure 5A, PC3-luc cells markedly disseminated into the mice resulting in the development of metastatic tumour 5 weeks after injection, while the injection of PC3-M8-luc cells did not induce any development of metastases (Fig. 5A). More precisely, looking at total mice bioluminescence data (Suppl. 1A), metastasis development was reduced by 97.32 ± 1.75 % after PC3-M8-luc cl2 injection and by 99.45 ± 0.44 % after PC3-M8-luc cl5 injection in comparison with control (PC3-luc) injection. As revealed by bioluminescence imaging performed in different organs after mice sacrifice, PC3-M8-luc injection resulted in very restricted tumor colonization in prostate, liver, kidney, and lung in contrast with PC3-luc (Fig. 5B-E). To further validate TRPM8 involvement in PCa cell dissemination *in vivo*, we injected PC3-luc and PC3-M8-luc intracardially into the left ventricle of NMRI nude mice. Mice were then injected intraperitoneally three times per week with the TRPM8 inhibitor M8B or its solvent for the control group. As shown in figure 5F, we found a significant difference between mice grafted with PC3-luc and PC3-M8-luc in terms of bioluminescent foci, indicating a strong reduction in tumor cell dissemination carried out by TRPM8 (Fig. 5F). Furthermore, TRPM8 inhibition with M8B led to a partial recovery of PCa cells capability to migrate and disseminate through the body. Indeed, we found that mice injected with PC3-M8-luc and treated with M8B for 50 days displayed a significantly higher bioluminescence signal compared to their untreated littermates (Fig. 5F), confirming once again the role of TRPM8 played in this process.

Next, to evaluate the possible involvement of TRPM8 on PCa blood intra- and/or extravasation, trans-endothelial migration assays were performed. As shown in figure 5G, TRPM8 overexpression significantly decreases by 33.85 ± 8.28 % the ability of PCa cells to pass through a monolayer of endothelial cells (statistical significance between PC3 and PC3-M8: p-value = 0.004). To further validate this finding, MIMETAS “Organ-on-chip” technology was used allowing us to compare PC3 and PC3-M8 cells’ behavior within HMEC 3D micro-vessels in a standardized microfluidic platform (Fig. 5H). This assay demonstrated TRPM8 capability to affect the trans-endothelial process reducing PC3 extravasation by 71.90 ± 5.68 %.

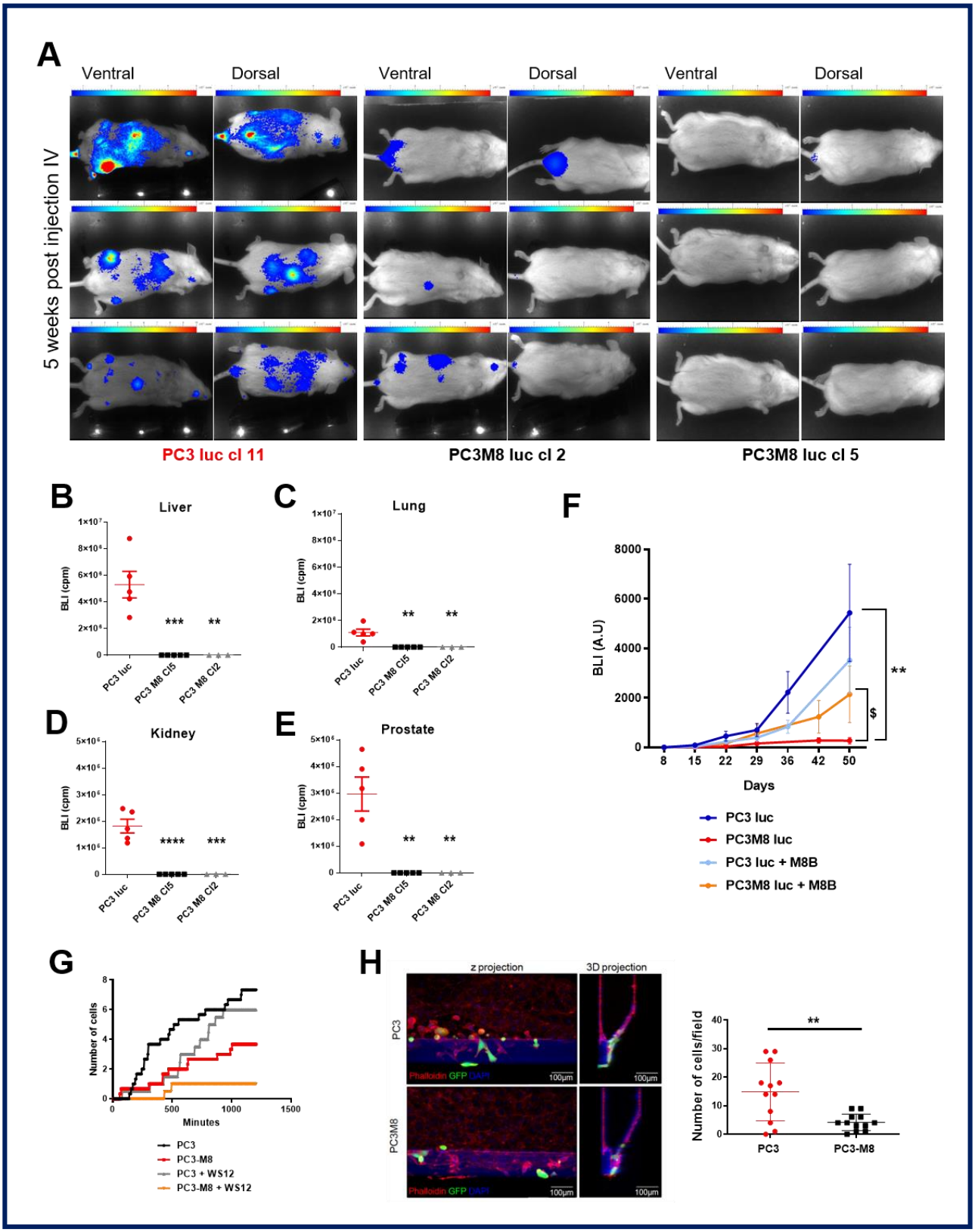

Figure 5. TRPM8 overexpression in PC3 inhibits metastatic dissemination.

PC3-luc or PC3-M8-luc cells were engrafted into NSG mice by tail-vein injection and tumor burden was noninvasively monitored by measuring the bioluminescence signal generated upon subcutaneous administration of luciferin. A)

*Representative bioluminescence images of PC3-luc and PC3-M8-luc in mice, 5 weeks after intravenous injection into the tail vein (n=5 mice/condition). (B-E) Quantification of bioluminescence signal in liver (B), lung (C), kidney (D), and prostate (E) 5 weeks after PC3-luc or PC3-M8-luc tail-vein injection (n=5 mice/condition; statistical significance: ** = p< 0.01, *** = p< 0.001, **** = p< 0.0001, ordinary one-way ANOVA with post-hoc Tukey's test). F) Quantification of bioluminescence in mice after intracardiac injection of PC3-luc or PC3-M8-luc cells in the presence or absence of TRPM8 antagonist M8B (n=5 mice/condition; statistical signif-icance versus PC3 luc: ** = p< 0.01, statistical significance versus PC3M8 luc: $ = p< 0.05, Student's t-test). G) Trans-endothelial assay on PC3 and PC3-M8 cells treated or not with WS12 (10 nM). Data are shown as the number of cells migrated under the endothelial barriers over time (n=5). H) Immunofluorescent staining of microfluidic co-cultures performed on "Organ-on-Chip" systems (Scale bar = 100 µm). Left and central panels: representative confocal images and 3-D reconstruction of cells' extravasation (GFP-tagged cells in green, vessels stained with phalloidin in red, and nu-clei stained with DAPI in blue); Right panel: quantification of PC3 or PC3-M8 extravasated into the matrix (n=12; statistical significance: ** = p<0.01, unpaired t-test).*

Once the anti-metastatic role played by TRPM8 in PCa dissemination was confirmed, we investigated the possibility to use TRPM8 as a therapeutic target in PCa treatment. To do that, a formulation previously developed and characterized [21] containing the TRPM8 agonist WS12 incorporated into lipid nanocapsules (LNC-WS12) was used. First, we evaluated the biocompatibility and biodistribution of LNC *in vivo* after injecting them at three different concentrations (0.1, 1, and 10 mg/kg) into the mice tail vein three times a week for 3 weeks (Fig. 6A). Empty LNC or LNC containing WS12 were not toxic since they didn't increase mice mortality nor change their behavior during the treatment. Concerning the LNC biodistribution, both empty LNC (Fig. 6A i) and LNC-WS12 (Fig. 6A ii) displayed a preferential accumulation in the liver, the spleen, and the kidney, and in the prostate at the two highest at doses (1 and 10 mg of LNC/kg but not with 0.1 mg/kg). Since the highest dose tested (10 mg/kg) showed a strong accumulation in the liver and the lowest (0.1 mg/kg) was early undetectable in the prostate, we chose 1 mg/kg for further *in vivo* investigations in our prostate orthotopic xenografted mouse model. Three days following PC3-M8-luc injection, mice were treated 3 times per week for 5 weeks with empty LNC or LNC-WS12 (1 mg/kg); mice treated with free WS12 or vehicle (CTRL) were used as control. After sacrifice, organs were analyzed by bioluminescence in the primary prostatic tumor as well as in metastatic sites such as liver, lungs, and kidney (Fig. 6B-E). Regarding the primary tumor site, only free WS12 decreased PC3-M8-luc cells in the prostate by 58.64 ± 16.47 % compared to the control condition although no statistical significance was detected (treated with the vehicle i.e. empty LNC). On the other hand, in the liver and lungs, the treatment with LNC-WS12 was the most efficient since it decreased the presence of PC3-M8-luc cells by 82.54 ± 17.45 % and by 73.56 ± 26.43 %, respectively. Finally, concerning the kidney, free WS12 or LNC-WS12 treatment displayed the same effect with a decrease of PC3-M8-luc cells by 78.93 ± 21.06 % in mice treated with free WS12 and 65.99 ± 34.01 % in mice treated with LNC-WS12. Overall, our results clearly show that activation of TRPM8 by WS12, either free or encapsulated in LNC, can effectively reduce the metastatic dissemination of PC3-M8-luc in mice, supporting an anti-metastatic role of the TRPM8 channel in PCa progression.

Results observed *in vivo* were further validated *in vitro* through random migration assays, which confirmed that TRPM8 overexpression significantly reduces cell migration speed by 35.51 ± 1.06 % (Fig. 6F). Moreover, we showed that TRPM8 activation by both free WS12 and LNC-WS12 further decreases *in vitro* cell migration while no effect was observed on PC3-luc cells lacking TRPM8 expression (Fig. 6F). Interestingly, encapsulation of WS12 into LNC resulted in a 10% additional reduction in cell migration. Besides migration, cancer cells need to cross extracellular matrix to reach the bloodstream and colonize a new site other than primary tumor. To study the effect of TRPM8 on PC3 cell invasion, matrigel-coated transwell assays were performed (Fig. 6G). Treatment of PC3-M8-luc cells with LNC-WS12 reduced cell invasiveness more potently than with free WS12, and this effect was even more pronounced than in simple migration assays. Indeed, the activation of TRPM8 by WS12 in its free form reduced the invasiveness of PC3-M8 cells by 13.06 ± 1.32%, while the stimulation of TRPM8 by WS12 encapsulated in LNC reduced it by 32.72 ± 1.83%. No effect on invasion was observed in PC3-luc cells (Suppl. 1B).

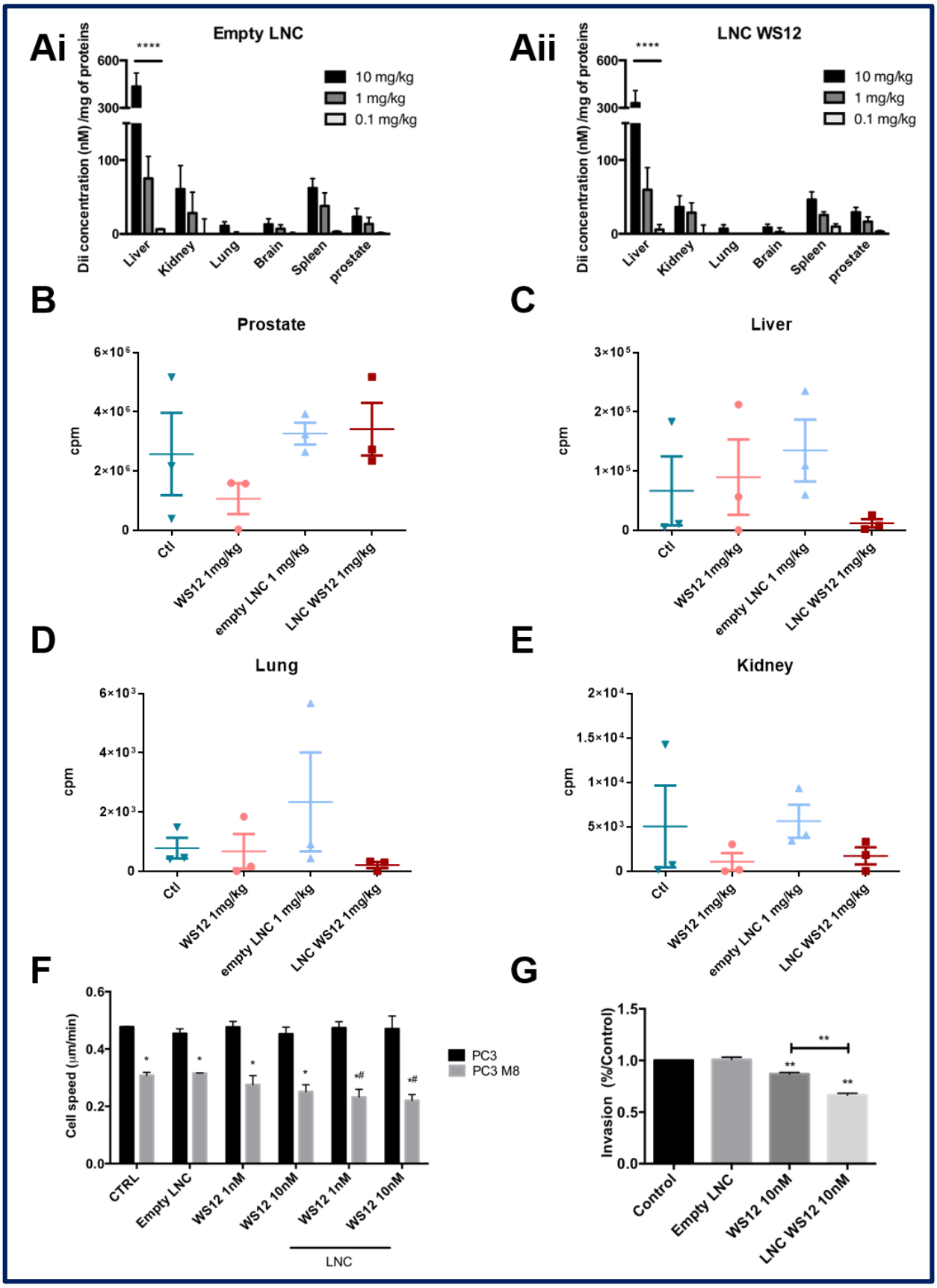

Figure 6. Effects of lipid nanocapsules (LNC) containing a TRPM8 agonist on migratory and invasive properties.

*A) Biodistribution of empty LNC (A i) and LNC WS-12 (A ii) labeled with DiI on mice. Mice were injected 3 times per week for 3 weeks with 10, 1 or 0.1 mg/kg of LNC. Bio-distribution was quantified using DiI concentration per mg of protein in each organ (n=5 mice/condition; statistical significance: **** = p<0.0001, 2-way ANOVA with post-hoc Tukey's test). B-E) Bio-luminescence quantification in mice prostate (B), liver (C), lung (D), and kidney (E) after PC3-M8-luc xenografts and treatment with free WS12, LNC-WS12 or empty LNC 3 times per week for 5 weeks (n=3 mice/condition). F) Random migration assay on PC3 cells stably expressing TRPM8, treated or not with free WS12 or LNC-WS12 (1 or 10 nM) (n=3 independent experiments with globally at least 100 cells/condition; statistical significance between PC3 and PC3-M8 in each condition: * = p< 0.05; statistical significance between PC3-M8 not treated and PC3-M8 treated with 1 and 10 nM of LNC-WS12: # = p< 0.05, 2-way ANOVA with post-hoc Tukey's test). G) Invasion assay of PC3-M8 cells on Matrigel® transwell (n= 3 independent experiments at least; statistical significance versus PC3-M8 cells not treated used as control: ** = p<0.01, RM one-way ANOVA with post-hoc Tukey's test).*

4. TRPM8 activation inhibits different signaling pathways leading to a global reduction of tumor growth and metastasis dissemination

To better elucidate the intracellular pathways underlying the TRPM8 inhibitory effect on PCa growth and metastasis dissemination observed both *in vitro* and *in vivo*, we evaluated different signaling pathways. First, we evaluated the possible impact of TRPM8 overexpression and/or activation on the secretion of matrix metalloproteinases (MMPs) like gelatinases MMP-2 and 9, well-known in promoting cell migration and invasion. However, MMP-2 and MMP-9 secretion was not affected by TRPM8 overexpression nor activation (Fig. 7A and B). Next, we investigated the involvement of small Rho GTPase due to their well-established role in the regulation of cell migration [22]. Activation of small Rho GTPase including Cdc42, Rac1, and RhoA upon TRPM8 overexpression and/or activation was investigated *in vitro* showing that TRPM8 induced a significant decrease of GTP-bound (active) Cdc42 (Fig. 7C) and Rac1 (Fig. 7D) activation, while it did not affect RhoA activity (Fig. 7E). More precisely, TRPM8 overexpression reduced Cdc42 and Rac1 activity by 24.64 ± 7.91% and 15.26 ± 5.17 %, respectively, but that inhibition became significant only after TRPM8 activation by LNC-WS12 (Fig. 7C and D).

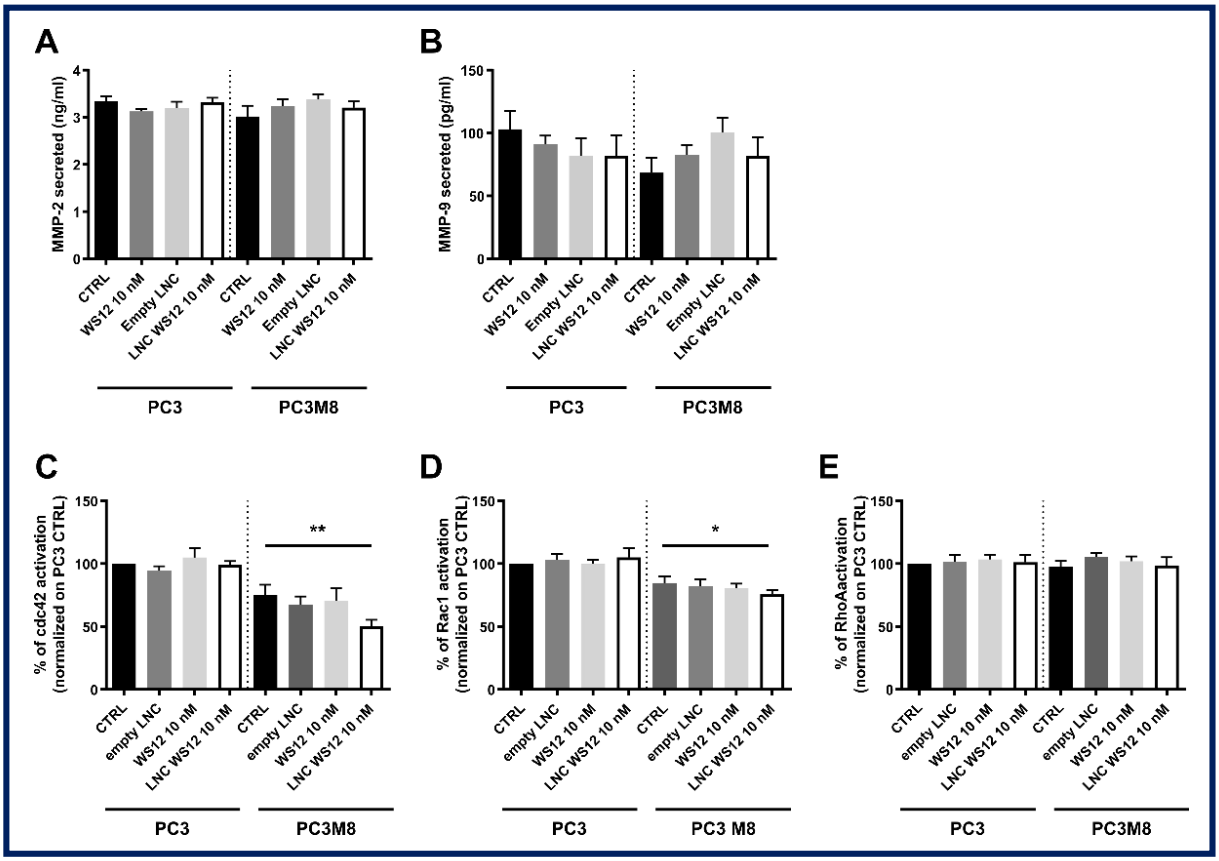

Figure 7. TRPM8 doesn't affect MMPs secretion but modulates Rho-GTPases signaling pathway.

*A-B) MMP-9 (A) and MMP-2 (B) secretion in PC3-luc and PC3-M8-luc treated with WS12 (10 nM), empty LNC, or LNC-WS12 (10 nM); Data are express as mean ± SEM of 6 independent experi-ments (statistical significance: ordinary one-way ANOVA with post-hoc Tukey's test); C-E) Acti-vation of Cdc42 (C), Rac1 (D) and RhoA (E) in PC3-luc and PC3-M8-luc treated with WS12 (10 nM), empty LNC, or LNC-WS12 (10 nM). Data are normalized to the CTRL (PC3-luc) and ex-press as mean ± SEM of 5 independent experiments for each condition (statistical significance: * = P <0.05, ** = P <0.01, ordinary one-way ANOVA with post-hoc Tukey's test).*

Finally, we checked if TRPM8 overexpression and/or activation could affect cell migration through the regulation of focal adhesion. For this purpose, we investigated whether TRPM8 had an impact on extracellular signal-regulated kinases (ERK) and focal adhesion kinase (FAK) phosphorylation (Fig. 8A and 8B, respectively). ERK1/2 and FAK phosphorylation was evaluated by western blot and indicated that TRPM8 overexpression and activation with free WS12 (10 nM) was not sufficient to regulate ERK and FAK activation (Fig. 8). However, TRPM8 activation by LNC-WS12 (10 nM) induced a significant decrease of FAK phosphorylation by 36.4 ± 2.6% and 26.9 ± 2.5 %, respectively (Fig. 8A ii and 8B ii).

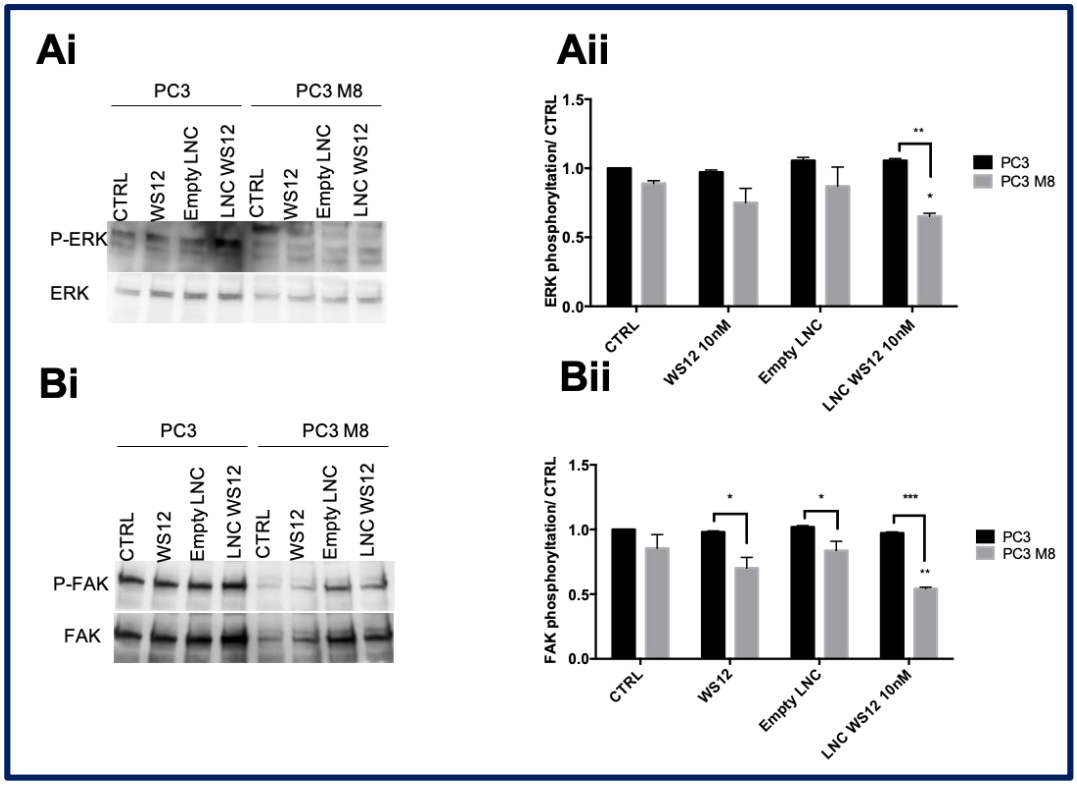

Figure 8. TRPM8 affects ERK and FAK phosphorylation assessed by western blot.

*Representative blots showing ERK (Ai) and FAK (Bi) phosphorylation in PC3-luc and PC3-M8-luc cells treated with WS12 (10 nM), empty LNC, or LNC-WS12 (10 nM); Quantification of ERK (Aii) and FAK (Bii) phosphorylation normalized to the control condition (n=3 independent assays, * = P< 0.05; *** = P< 0.001, two-way ANOVA with post-hoc Tukey's test).*

Discussion

A central role in the regulation of PCa cell progression has been previously ascribed to TRPM8, making it one of the most promising clinical targets in PCa therapy. Currently, TRPM8 is already used as a clinical diagnostic/prognostic marker in some countries [11,12]. Indeed, TRPM8 channel expression changes during PCa progression, revealing an up-regulation in the early stages of both benign prostate hyperplasia and malignant prostate carcinoma followed by a down-regulation and a silencing during late metastatic stages of PCa after the hormonal therapy against androgens [23–25]. This is mainly due to the genomic and non-genomic androgen-dependence of TRPM8 [26,27]: during the anti-androgen therapy, some cells become able to escape this treatment by acquiring a more aggressive androgen-independent phenotype with the subsequent loss of TRPM8 expression/activity. Consistently with this expression profile, several studies

suggested a protective role of TRPM8 in metastatic PCa progression due to its inhibitory impact on PCa cell proliferation, viability, and migration [28]. However, some data reported in the literature are contradictory and, furthermore, most of them are based on *in vitro* studies. In this work, we clarified the role played by TRPM8 on PCa progression *in vivo* mainly focusing on its effects on tumor growth and metastasis dissemination.

TRPM8 revealed an effect on cell proliferation in prostate tumor cells but not in normal prostate cells [20]. However, the role of TRPM8 in the regulation of PCa proliferation and apoptosis was assessed by different groups using several *in vitro* experiments which led to contradictory conclusions. In particular, data from literature reported opposite effects of TRPM8 on the proliferation of different PCa cell lines according to their androgen sensitivity. More specifically, TRPM8 was found essential for cell survival and cell proliferation in PCa cells sensitive to androgens like LNCaP *in vitro* [16,20,29], whereas displayed an anti-proliferative and pro-apoptotic effect on androgen-insensitive PCa cells such as PC3 and DU-145 cells [13–15]. This androgen receptor (AR)-dependency of TRPM8's role in proliferation has also been observed in cells from other cancers such as colon, osteosarcoma, and lung cancer [30–32]. In this context, our *in vivo* investigations support the anti-proliferative role of TRPM8 in PC3 cells, in line with the only other *in vivo* study on TRPM8 reported in the literature by Zhu and co-workers [33]. Indeed, we found that in mice grafted with luminescent PC3 cells overexpressing TRPM8, prostate tumor growth dramatically decreases starting 4 weeks after the orthotopic graft. TRPM8 expression not only reduces tumor weight and area but also affects its histological features, helping to maintain a well-defined glandular tissue. Notably, up to date, no data were available on the tumorigenesis of PCa cells grafted in the prostate. Mechanistically, our *in vitro* data revealed that the inhibition of tumor growth observed *in vivo* is accompanied by a reduction of the proliferative cell fraction and by an increased cell cycle arrest in G_0/G_1 phase induced by TRPM8 overexpression. These findings are in agreement with previous data showing that TRPM8 activation by menthol in DU145 cells [15] and TRPM8 overexpression on PC3 [13] induced G_0/G_1 cell cycle arrest down-regulating cyclin-dependent kinase (Cdk)4 and Cdk6 [13]. Moreover, a significant Proliferating Cell Nuclear Antigen (PCNA) decrease in the presence of TRPM8 has been detected *in vivo* [14]. Nevertheless, contrasting results showed that TRPM8 pharmacological inhibition by BCTC impairs DU145 cell cycle progression downregulating key proteins including protein kinase B, cyclin D1, Cdk2, and Cdk6 and upregulating others like glycogen synthase kinase 3β [34]. Moreover, MAPK pathways seem to may be also involved in the aforementioned pro-proliferative action of TRPM8 in DU145 cells [34]. In this contradictory landscape, our *in vitro* and *in vivo* data further support the anti-proliferative role of TRPM8 in PCa progression. In addition, we observed a concomitant reduction in the apoptotic and necrotic areas *ex vivo* from PC3-M8 tumors compared to PC3 tumors. However, no differences were observed *in vitro* in terms of apoptosis between PC3 and

TRPM8-overexpressing PC3 cells. Therefore, we can conclude that TRPM8 is not directly involved in the control of cell apoptosis and that the difference observed in the apoptotic fraction *ex vivo* would rather be the result of normal tumor growth of PC3 with a necrotic area at the center and an apoptotic area next to it. On the contrary, TRPM8 inhibition or suppression in LNCaP cells leads to the induction of pro-apoptotic pathways supporting a TRPM8-mediated anti-apoptotic mechanism in androgen-sensitive PCa cells [16]. This role may be explained by the androgen-dependent expression of TRPM8 in the ER of LNCaP, from where TRPM8 was shown to induce plasma membrane (PM) store-operated channels (SOC) currents [29], sufficient to induce the apoptotic process [35]. In this context, it has also been demonstrated that LNCaP cells express also a short (19 kDa) TRPM8 isoform, sM8α, able to negatively regulate TRPM8 full-length channels by interaction [36] thus inhibiting apoptosis [37].

Beyond cell proliferation and apoptosis, another cell hallmark that may affect tumor growth is the clonogenic ability of cells. This process seems to contribute the most to the marked differences observed *in vivo* between tumors from PC3 and PC3-TRPM8 orthotopic grafts. Indeed, we showed that the overexpression and especially the activation of TRPM8 significantly inhibit PCa cells' clone formation capabilities. This finding was further supported by the decreased tumor cell density observed *ex vivo* from PC3-TRPM8 tumors with respect to PC3 tumors. The inhibition of Cdc42 and Rac1 activity we observed after TRPM8 overexpression and/or activation could account for such a decrease. Indeed, negative dominant expression of Rac1 or Cdc42 (Rac1-N17 or Cdc42-N17) in kidney cells (MDK cells) was shown to decrease cell-to-cell adhesion explaining the reduced clonogenic ability and tumor cell density [38,39]. Similarly, the active mutant of Rac1 (Rac1-V12) increases paracellular permeability and expression of E-cadherin to promote cell-to-cell adhesion [39,40]. Taken together, the effects of TRPM8 on clonogenic cell ability and, to a lesser extent, on cell proliferation may explain the inhibition on prostate tumor growth observed *in vivo*. However, also the tumor microenvironment must be taken into-account in this kind of considerations since it could affect tumor growth *via* paracrine signaling [41]. The tumor microenvironment is composed of immune cells and fibroblasts which can be modulated by tumor cells and transformed into cancer-associated fibroblasts (CAF). By this transformation, CAF may secret VEGF or interleukin-6 (IL-6) thus affecting angiogenesis and tumor growth [42]. Cellular context could also be involved in the definition of TRPM8 role in cancer progression. Interestingly, an intriguing association between TRPM8 overexpression and a strong reduction of VEGF and microvascular density (MVD) has been suggested *in vivo* [14], thus highlighting a possible TRPM8-mediated anti-angiogenic additional contribution to the observed reduction of tumor growth *in vivo*. Therefore, TRPM8 could be considered a useful target to block PCa growth by using TRPM8 antagonists like capsazepine [16], BCTC [20], cannabigerol [43] as well as TRPM8 agonist including menthol [15,16] and D-3263 [44], according to cancer stages. Nanocarriers loaded with TRPM8 agonists such as WS-12 could

therefore be used in early cancer stages when TRPM8 is highly expressed in order to avoid tumor cell dissemination.

The high cancer-related mortality is mainly due to tumor metastasis. This process mainly relies on cancer cells migration followed by intra- and extravasation into the blood and lymphatic circulation. In this regard, TRPM8 has already been studied and characterized outlining a protective anti-migratory role of TRPM8 *in vitro* [13,15,17,18,21,27,45]. Here, by using orthotopic prostate xenografts and lateral caudal vein injection of PC3 and PC3-TRPM8 in immunocompromised mice, we further demonstrated that TRPM8 exerts an inhibitory action on PCa cells migration *in vivo* as well. Indeed, we showed that TRPM8 overexpression reduces PC3 cells' colonization in primary and distant sites like the liver, kidney, and lung. This outcome is at least partially attributable to the inability of PC3 overexpressing TRPM8 to disseminate to different metastatic sites through the bloodstream by overcoming the vascular barrier. Indeed, *in vitro* trans-endothelial migration assays demonstrated that TRPM8 overexpression strongly inhibits intra- or extravasation of PC3 cells through a monolayer of endothelial cells. This lack of intra- or extravasation due to TRPM8 overexpression could be explained by the TRPM8-induced inhibition of cell adhesion which we have previously described in endothelial cells [18], confirming what had been observed in PCa epithelial cells [14]. Indeed, in endothelial cells, TRPM8-mediated inhibition of cell migration occurs through the direct interaction of the channel with the small GTPase Rap1A and the consequent inhibition of the integrin inside-out pathway, blocking cell adhesion and migration [18]. The TRPM8-mediated inhibition of cell adhesion could also explain in part the decrease we observed in the clonogenic ability of PC3 cells overexpressing TRPM8. TRPM8 overexpression by itself inhibits PCa cell migration and TRPM8 activation by endogenous and exogenous agonists like prostate-specific antigen (PSA), icilin, menthol, and WS12 further enhances the inhibitory effect of metastatic PCa cells' motility [13,14,17,21].

During metastasic dissemination, cancer cells secrete matrix metalloproteinases (MMPs) to degrade the extracellular matrix, facilitating their migration and invasion. Mechanistically, TRPM8 doesn't affect the invasion process since TRPM8 overexpression nor activation affected MMP-2 and MMP-9 secretion in PC3 cells. However, TRPM8 revealed an active role in another key aspect of cell migration, which is the cell capability to create focal adhesion to promote cell movement. This process is regulated by several proteins including some small GTPase belonging to the Rho superfamily like Cdc42, Rac1, and RhoA. These proteins are located at the front of the cell and are responsible for the formation of protrusions and focal adhesions essential for cell adhesion and migration [22]. Interestingly, we found that TRPM8 activation reduced Cdc42 and Rac1 activity, but not that of RhoA. Taking into account the roles played by Cdc42, Rac1 protein, and their effectors in epithelial-to-mesenchymal transition (EMT) through cytoskeleton remodeling [46], the TRPM8-mediated inhibition on cell invasiveness we observed might be explained as a decrease of EMT

through Rac1 and Cdc42 inhibition. Moreover, we showed that TRPM8 activation also inhibits the phosphorylation of two important kinases involved in focal adhesion formation, i.e. ERK and FAK. These findings are in line with other studies reporting a TRPM8-mediated inhibition of DU145 [15] and PC3 cell's motility supported by the down-regulation of phospho-FAK without changing the non-phospho-FAK [13,14]. In addition, we have recently demonstrated that inactivation of TRPM8 by low doses (10 nM) of testosterone significantly increases FAK phosphorylation consequently promoting cell migration [27]. Interestingly, newly identified partner proteins of the channels like PSA, TRP channel–associated factors 1 (TCAF1), and AR were shown to affect TRPM8 expression on the plasma membrane, its opening state, and thus the TRPM8-mediated inhibitory effect on cell migration [17,45,47]. Consistently, the short TRPM8 isoform sM8α, expressed by LNCaP, promotes cell migration acting as an inhibitory partner protein of full-length TRPM8 [37]. Nevertheless, a contrasting study showed that pharmacological inhibition of TRPM8 by BCTC may reduce the speed of PCa DU145 cells[34]. However, most lines of evidence, including the present study, strongly suggest an anti-migratory role of TRPM8, shedding light on the possibility to use TRPM8 agonists like PSA, WS12, and icilin to counteract the metastasis of prostate cancer [17,21].

Since TRPM8 activation reduces the migratory PCa cell potential further than the simple overexpression of the channel, we aimed to develop a molecular tool to target TRPM8 for PCa treatment. In this context, we have recently described the synthesis and the functional characterization of lipid nanocapsules (LNC) containing the TRPM8 agonist WS12 [21]. Nanocarriers were developed and used in several forms such as liposomes, virosomes, solid lipid nanoparticles, polymeric nanoparticles, or protein conjugates to improve drug bioavailability and targeting in cancer therapy [48]. For example, nanoparticles containing the TRPA1 activator, curcumin, efficiently target PCa growth [49]. The LNC we developed are composed of an oily liquid core containing our compound of interest and surrounded by a layer of lecithin and hydrophilic surfactants, which gives them a hybrid structure between polymeric nanocapsules and liposomes (lipoprotein-like structure) [50]. We showed that WS12 encapsulation into LNC potentiates TRPM8 activation and subsequently the TRPM8-mediated inhibition of PCa cells migration *in vitro* [21]. Indeed, the use of nanocarriers not only allows the use of a 10 times lower agonist concentration for the activation of TRPM8, but also ensures more efficient cellular delivery by overcoming the problem associated with the hydrophobicity of most activators of TRPM8. Here, we further support the applicability of this therapeutic approach *in vivo* by injecting LNC-WS12 in our prostate orthotopic xenografted mouse model. We demonstrated that LNC-WS12 efficiently block PCa cell dissemination in particular in the liver and lung where LNC were accumulated after lateral caudal vein tail injection. However, this tool seems to be not very efficient to target primary tumors in the prostate due to the low distribution of LNC on the prostate when injected at 1 mg/kg. Nevertheless, due to their distribution in metastatic sites (lung or liver), LNC-WS12 could be used

to target metastasis dissemination in patients with prostate cancer before anti-androgenic therapy and the subsequent loss of TRPM8 expression [23]. As we have demonstrated that TRPM8 activation inhibits PCa cell trans-endothelial migration, LNC-WS12 could also be efficient to target extravasation of circulating tumor cells if TRPM8 expression is maintained in these cells. Moreover, as mentioned above, since some studies suggest a correlation between TRPM8 role on prostate cancer progression and the androgen-dependent state of PCa cells, the efficacy of LNC-WS12 needs to be tested on androgen-dependent PCa cells.

Overall, this study reinforces the hypothesis that activating TRPM8 could play a protective role in prostate cancer progression, thus supporting its potential application as a powerful therapeutic target antagonizing metastatic transition of PCa.

Conclusions

Our *in vitro* and *in vivo* results shed light on the role of TRPM8 on PCa AR-negative tumor growth and metastasis dissemination. In particular, we showed that TRPM8 overexpression decreased proliferation and clonogenic properties of PCa cells resulting in dramatically limited tumor growth in orthotopic graft mice. In addition to its role on prostate tumor growth, TRPM8 was shown to inhibit PCa cells migration and invasion, leading to a reduced prostate metastasis dissemination in mice. Mechanistically, we demonstrated that TRPM8 activation acts on cytoskeleton dynamics and focal adhesions formation involving the Rho GTPase signaling and, in particular, the inhibition of Cdc42 and Rac1 as well as that of phosphorylation of ERK and FAK. Moreover, we applied lipid nanocapsules (LNC) loaded with TRPM8 agonist, WS12, that can limit the TRPM8-positive cells' dissemination in metastatic sites with better efficiency than treatment with the agonist in its free form. Overall, our results confirm an anti-proliferative and anti-migratory role of TRPM8 on metastatic PCa cells and support the potential therapeutic use of TRPM8 to target PCa progression and PCa metastatic dissemination.

Author Contributions: Conceptualization, D.G.; methodology, G.P.G., E.B., S.M.L., A.F.P., D.G. ; formal analysis, G.P.G., D.G., A.F.P.; investigation, G.P.G., M.H., E.B., A.F.P., K.K., L.N., .M.L., T.O. T.G. A.B., M.L.M, S.R., ; resources, D.G., A.F.P.; data curation, G.P.G, G.C., D.G., A.F.P., S.M.L., S.L.; writing—original draft preparation, G.P.G.; writing—review and editing, G.P.G, G.C., D.G., A.F.P. S.R., L.N., R.B., A.S.; visualization, G.P.G, G.C., D.G., A.F.P.; supervision, D.G., A.F.P., R.B., A.S. S.L.; project administration, D.G.; funding acquisition, D.G., A.F.P., R.B., A.S.. All authors have read and agreed to the published version of the manuscript.

Funding: This research was funded by the Ministère de l'Education Nationale and the Institut National de la Santé et de la Recherche Medicale (INSERM). The research of G.P.G. was supported by the region Hauts-de-France and the University of Lille. The research of D.G. is supported by the Institut Universitaire de France (IUF) and France Berkley Fund. D.G. A.F.P. and R.B. was supported by the Institut National du Cancer (INCa- PLBIO14-213). A.F.P. and G.C. are supported by Italian Ministry of Instruction, University and Research (MIUR), PRIN grant "Leveraging basic knowledge of ion channel network in cancer for innovative thera-peutic strategies (LIONESS)" (grant number 20174TB8KW) and are part of the Associated International Laboratory (CaPANCInv). The authors have no conflicting financial interests.

Institutional Review Board Statement: Animals were handled and cared in accordance with national and institutional guidelines. Protocols were conducted by authorized investigators of the "In Vivo platform" of the Cancéropôle Grand Ouest, Inserm U892 (Nantes, France) and at the TAAM Unit at the CNRS (Orléans, France). The in vivo experiments conducted in the Cancéropôle Grand Ouest, Inserm U892 (Nantes, France) were under the animal care license no. C44278. The project was approved by the French national ethical committee (APAFIS #2837). At the TAAM Unit of the CNRS (Orléans, France) experiments were approved by the French Ministry of Higher Education, Research and Innovation (Ministère de l'Enseignement supérieur, de la Recherche et de l'Innovation, France) under registration #19911..

Acknowledgments: We would like to thank the Flow Core Facility of BioImaging Center Lille - UAR2014-US41-PLBS - (F-59000 Lille, France) for the expert technical assistance.

Conflicts of Interest: The authors declare no conflict of interest

References

1. Sung, H.; Ferlay, J.; Siegel, R.L.; Laversanne, M.; Soerjomataram, I.; Jemal, A.; Bray, F. Global Cancer Statistics 2020: GLO-BOCAN Estimates of Incidence and Mortality Worldwide for 36 Cancers in 185 Countries. CA. Cancer J. Clin. 2021, 71, 209–249, doi:10.3322/caac.21660.
2. Bubendorf, L.; Schöpfer, A.; Wagner, U.; Sauter, G.; Moch, H.; Willi, N.; Gasser, T.C.; Mihatsch, M.J. Metastatic patterns of prostate cancer: An autopsy study of 1,589 patients. Hum. Pathol. 2000, 31, 578–583, doi:10.1053/hp.2000.6698.
3. Hanahan, D.; Weinberg, R.A. Review Hallmarks of Cancer : The Next Generation. Cell 2011, 144, 646–674, doi:10.1016/j.cell.2011.02.013.
4. Flourakis, M.; Prevarskaya, N. Insights into Ca2+ homeostasis of advanced prostate cancer cells. Biochim. Biophys. Acta - Mol. Cell Res. 2009, 1793, 1105–1109, doi:10.1016/j.bbamcr.2009.01.009.
5. Monteith, G.R.; McAndrew, D.; Faddy, H.M.; Roberts-Thomson, S.J. Calcium and cancer: targeting Ca2+ transport. Nat. Rev. Cancer 2007, 7, 519–530, doi:10.1038/nrc2171.
6. Roderick, H.L.; Cook, S.J. Ca2+ signalling checkpoints in cancer: remodelling Ca2+ for cancer cell proliferation and survival. Nat. Rev. Cancer 2008, 8, 361–375, doi:10.1038/nrc2374.
7. Thebault, S.; Flourakis, M.; Vanoverberhe, K.; Vandermoere, F.; Roudbaraki, M.; Lehen'kyi, V.; Slomianny, C.; Beck, B.; Mar-iot, P.; Bonnal, J.; et al. Differential Role of Transient Receptor Potential Channels in Ca2+ Entry and Proliferation of Prostate Cancer Epithelial Cells. Cancer Res. 2006, 66, 2038–2047, doi:10.1158/0008-5472.CAN-05-0376.
8. Fiorio Pla, A.; Gkika, D. Emerging role of TRP channels in cell migration: From tumor vascularization to metastasis. Front. Physiol. 2013, 4 NOV, 1–12, doi:10.3389/fphys.2013.00311.
9. Prevarskaya, N.; Zhang, L.; Barritt, G. TRP channels in cancer. Biochim. Biophys. Acta - Mol. Basis Dis. 2007, 1772, 937–946, doi:10.1016/j.bbadis.2007.05.006.

10. Prevarskaya, N.; Skryma, R.; Shuba, Y. Ion channels in cancer: Are cancer hallmarks oncochannelopathies? Physiol. Rev. 2018, 98, 559–621, doi:10.1152/physrev.00044.2016.
11. Bai, V.U.; Murthy, S.; Chinnakannu, K.; Muhletaler, F.; Tejwani, S.; Barrack, E.R.; Kim, S.H.O.; Menon, M.; Reddy, G.P.V. Androgen regulated TRPM8 expression: A potential mRNA marker for metastatic prostate cancer detection in body fluids. Int. J. Oncol. 2010, doi:10.3892/ijo-00000518.
12. Schmidt, U.; Fuessel, S.; Koch, R.; Baretton, G.B.; Lohse, A.; Tomasetti, S.; Unversucht, S.; Froehner, M.; Wirth, M.P.; Meye, A. Quantitative multi-gene expression profiling of primary prostate cancer. Prostate 2006, 66, 1521–1534, doi:10.1002/pros.20490.
13. Yang, Z.-H.; Wang, X.-H.; Wang, H.-P.; Hu, L.-Q. Effects of TRPM8 on the proliferation and motility of prostate cancer PC-3 cells. Asian J. Androl. 2009, 11, 157–165, doi:10.1038/aja.2009.1.
14. Zhu, G.; Wang, X.; Yang, Z.; Cao, H.; Meng, Z.; Wang, Y.; Chen, D. Effects of TRPM8 on the proliferation and angiogenesis of prostate cancer PC-3 cells in vivo. Oncol. Lett. 2011, 2, 1213–1217, doi:10.3892/ol.2011.410.
15. Wang, Y.; Wang, X.; Yang, Z.; Zhu, G.; Chen, D.; Meng, Z. Menthol inhibits the proliferation and motility of prostate cancer DU145 cells. Pathol. Oncol. Res. 2012, 18, 903–910, doi:10.1007/s12253-012-9520-1.
16. Zhang, L.; Barritt, G.J. Evidence that TRPM8 is an androgen-dependent Ca2+ channel required for the survival of prostate cancer cells. Cancer Res. 2004, 64, 8365–8373, doi:10.1158/0008-5472.CAN-04-2146.
17. Gkika, D.; Flourakis, M.; Lemonnier, L.; Prevarskaya, N. PSA reduces prostate cancer cell motility by stimulating TRPM8 ac-tivity and plasma membrane expression. Oncogene 2010, 29, 4611–4616, doi:10.1038/onc.2010.210.
18. Genova, T.; Grolez, G.P.G.P.; Camillo, C.; Bernardini, M.; Bokhobza, A.; Richard, E.; Scianna, M.; Lemonnier, L.; Valdembri, D.; Munaron, L.; et al. TRPM8 inhibits endothelial cell migration via a nonchannel function by trapping the small GTPase Rap1. J. Cell Biol. 2017, 216, 2107–2130, doi:10.1083/jcb.201506024.
19. Valero, M.; Morenilla-Palao, C.; Belmonte, C.; Viana, F. Pharmacological and functional properties of TRPM8 channels in prostate tumor cells. Pflugers Arch. 2011, 461, 99–114, doi:10.1007/s00424-010-0895-0.
20. Valero, M.L. l.; Mello de Queiroz, F.; Stühmer, W.; Viana, F.; Pardo, L.A. TRPM8 Ion Channels Differentially Modulate Pro-liferation and Cell Cycle Distribution of Normal and Cancer Prostate Cells. PLoS One 2012, 7, 2–13, doi:10.1371/journal.pone.0051825.
21. Grolez, G.P.; Hammadi, M.; Barras, A.; Gordienko, D.; Slomianny, C.; Völkel, P.; Angrand, P.O.; Pinault, M.; Guimaraes, C.; Potier-Cartereau, M.; et al. Encapsulation of a TRPM8 Agonist, WS12, in Lipid Nanocapsules Potentiates PC3 Prostate Can-cer Cell Migration Inhibition through Channel Activation. Sci. Rep. 2019, 9, 1–15, doi:10.1038/s41598-019-44452-4.
22. Millar, F.R.; Janes, S.M.; Giangreco, A. Epithelial cell migration as a potential therapeutic target in early lung cancer. Eur. Respir. Rev. 2017, 26, 160069, doi:10.1183/16000617.0069-2016.
23. Tsavaler, L.; Shapero, M.H.; Morkowski, S.; Laus, R. Trp-p8, a novel prostate-specific gene, is up-regulated in prostate cancer and other malignancies and shares high homology with transient receptor potential calcium channel proteins. Cancer Res. 2001, 61, 3760–3769.
24. Henshall, S.M.; Afar, D.E.H.; Hiller, J.; Horvath, L.G.; Quinn, D.I.; Rasiah, K.K.; Gish, K.; Willhite, D.; Kench, J.G.; Gardi-ner-Garden, M.; et al. Survival analysis of genome-wide gene expression profiles of prostate cancers identifies new prognostic targets of disease relapse. Cancer Res. 2003, 63, 4196–4203.
25. Bidaux, G.; Flourakis, M.; Thebault, S.; Zholos, A.; Beck, B.; Gkika, D.; Roudbaraki, M.; Bonnal, J.L.; Mauroy, B.; Shuba, Y.; et al. Prostate cell differentiation status determines transient receptor potential melastatin member 8 channel subcellular locali-zation and function. J. Clin. Invest. 2007, 117, 1647–1657, doi:10.1172/JCI30168.
26. Bidaux, G.; Roudbaraki, M.; Merle, C.; Crépin, A.; Delcourt, P.; Slomianny, C.; Thebault, S.; Bonnal, J.L.; Benahmed, M.; Ca-bon, F.; et al. Evidence for specific TRPM8 expression in human prostate secretory epithelial cells: Functional androgen re-ceptor requirement. Endocr. Relat. Cancer 2005, 12, 367–382, doi:10.1677/erc.1.00969.
27. Grolez, G.P.; Gordiendko, D. V.; Clarisse, M.; Hammadi, M.; Desruelles, E.; Fromont, G.; Prevarskaya, N.; Slomianny, C.; Gkika, D. TRPM8-androgen receptor association within lipid rafts promotes prostate cancer cell migration. Cell Death Dis. 2019, 10, 652, doi:10.1038/s41419-019-1891-8.
28. Grolez, G.P.; Gkika, D. TRPM8 Puts the Chill on Prostate Cancer. Pharmaceuticals 2016, 9, doi:10.3390/ph9030044.
29. Thebault, S.; Lemonnier, L.; Bidaux, G.; Flourakis, M.; Bavencoffe, A.; Gordienko, D.; Roudbaraki, M.; Delcourt, P.; Panchin, Y.; Shuba, Y.; et al. Novel role of cold/menthol-sensitive transient receptor potential melastatine family member 8 (TRPM8) in the activation of store-operated channels in LNCaP human prostate cancer epithelial cells. J. Biol. Chem. 2005, 280, 39423–39435, doi:10.1074/jbc.M503544200.
30. Borrelli, F.; Pagano, E.; Romano, B.; Panzera, S.; Maiello, F.; Coppola, D.; De Petrocellis, L.; Buono, L.; Orlando, P.; Izzo, A.A. Colon carcinogenesis is inhibited by the TRPM8 antagonist cannabigerol, a Cannabis-derived non-psychotropic cannabinoid. Carcinogenesis 2014, 35, 2787–2797, doi:10.1093/carcin/bgu205.

31. Wang, Y.; Yang, Z.; Meng, Z.; Cao, H.; Zhu, G.; Liu, T.; Wang, X. Knockdown of TRPM8 suppresses cancer malignancy and enhances epirubicin-induced apoptosis in human osteosarcoma cells. Int. J. Biol. Sci. 2013, 10, 90–102, doi:10.7150/ijbs.7738.
32. Du, G.-J.; Li, J.-H.; Liu, W.-J.; Liu, Y.-H.; Zhao, B.; Li, H.-R.; Hou, X.-D.; Li, H.; Qi, X.-X.; Duan, Y.-J. The combination of TRPM8 and TRPA1 expression causes an invasive phenotype in lung cancer. Tumor Biol. 2013, 35, 1251–1261, doi:10.1007/s13277-013-1167-3.
33. Zhu, G.; Wang, X.; Yang, Z.; Cao, H.; Meng, Z.; Wang, Y.; Chen, D. Effects of TRPM8 on the proliferation and angiogenesis of prostate cancer PC-3 cells in vivo. Oncol. Lett. 2011, 2, 1213–1217, doi:10.3892/ol.2011.410.
34. Liu, T.; Fang, Z.; Wang, G.; Shi, M.; Wang, X.; Jiang, K.; Yang, Z.; Cao, R.; Tao, H.; Wang, X.; et al. Anti-tumor activity of the TRPM8 inhibitor BCTC in prostate cancer DU145 cells. Oncol. Lett. 2016, 11, 182–188, doi:10.3892/ol.2015.3854.
35. Wertz, I.E.; Dixit, V.M. Characterization of calcium release-activated apoptosis of LNCaP prostate cancer cells. J. Biol. Chem. 2000, 275, 11470–11477, doi:10.1074/jbc.275.15.11470.
36. Bidaux, G.; Beck, B.; Zholos, A.; Gordienko, D.; Lemonnier, L.; Flourakis, M.; Roudbaraki, M.; Borowiec, A.S.; Fernández, J.; Delcourt, P.; et al. Regulation of activity of transient receptor potential melastatin 8 (TRPM8) channel by its short isoforms. J. Biol. Chem. 2012, 287, 2948–2962, doi:10.1074/jbc.M111.270256.
37. Peng, M.; Wang, Z.; Yang, Z.; Tao, L.; Liu, Q.; Yi, L.; Wang, X. Overexpression of short TRPM8 variant α promotes cell mi-gration and invasion, and decreases starvation-induced apoptosis in prostate cancer LNCaP cells. Oncol. Lett. 2015, 10, 1378–1384, doi:10.3892/ol.2015.3373.
38. Rojas, R.; Ruiz, W.G.; Leung, S.M.; Jou, T.S.; Apodaca, G. Cdc42-dependent modulation of tight junctions and membrane protein traffic in polarized Madin-Darby canine kidney cells. Mol. Biol. Cell 2001, 12, 2257–2274, doi:10.1091/mbc.12.8.2257.
39. Takaishi, K.; Sasaki, T.; Kotani, H.; Nishioka, H.; Takai, Y. Regulation of cell-cell adhesion by Rac and Rho small G proteins in MDCK cells. J. Cell Biol. 1997, 139, 1047–1059, doi:10.1083/jcb.139.4.1047.
40. Braga, V.M.M.; Del Maschio, A.; Machesky, L.; Dejana, E. Regulation of Cadherin Function by Rho and Rac: Modulation by Junction Maturation and Cellular Context. Mol. Biol. Cell 1999, 10, 9–22, doi:10.1091/mbc.10.1.9.
41. Wang, M.; Zhao, J.; Zhang, L.; Wei, F.; Lian, Y.; Wu, Y.; Gong, Z.; Zhang, S.; Zhou, J.; Cao, K.; et al. Role of tumor microen-vironment in tumorigenesis. J. Cancer 2017, 8, 761–773.
42. Nagasaki, T.; Hara, M.; Nakanishi, H.; Takahashi, H.; Sato, M.; Takeyama, H. Interleukin-6 released by colon can-cer-associated fibroblasts is critical for tumour angiogenesis: Anti-interleukin-6 receptor antibody suppressed angiogenesis and inhibited tumour-stroma interaction. Br. J. Cancer 2014, 110, 469–478, doi:10.1038/bjc.2013.748.
43. De Petrocellis, L.; Ligresti, A.; Schiano Moriello, A.; Iappelli, M.; Verde, R.; Stott, C.G.; Cristino, L.; Orlando, P.; Di Marzo, V. Non-THC cannabinoids inhibit prostate carcinoma growth in vitro and in vivo: Pro-apoptotic effects and underlying mecha-nisms. Br. J. Pharmacol. 2013, 168, 79–102, doi:10.1111/j.1476-5381.2012.02027.x.
44. Duncan, D.; Stewart, F.; Frohlich, M.; Urdal, D. Preclinical Evaluation of the Trpm8 Ion Channel Agonist D-3263 for Benign Prostatic Hyperplasia. J. Urol. 2009, 181, 503–503, doi:10.1016/s0022-5347(09)61422-1.
45. Gkika, D.; Lemonnier, L.; Shapovalov, G.; Gordienko, D.; Poux, C.; Bernardini, M.; Bokhobza, A.; Bidaux, G.; Degerny, C.; Verreman, K.; et al. TRP channel-associated factors are a novel protein family that regulates TRPM8 trafficking and activity. J. Cell Biol. 2015, 208, 89–107, doi:10.1083/jcb.201402076.
46. Noren, N.K.; Liu, B.P.; Burridge, K.; Kreft, B. p120 Catenin regulates the actin cytoskeleton via RHO family GTPases. J. Cell Biol. 2000, 150, 567–579, doi:10.1083/jcb.150.3.567.
47. Gkika, D.; Lolignier, S.; Grolez, G.P.; Bavencoffe, A.; Shapovalov, G.; Gordienko, D.; Kondratskyi, A.; Meleine, M.; Prival, L.; Chapuy, E.; et al. Testosterone-androgen receptor: The steroid link inhibiting TRPM8-mediated cold sensitivity. FASEB J. 2020, 34, 7483–7499, doi:10.1096/fj.201902270R.
48. Solaro, R.; Chiellini, F.; Battisti, A. Targeted Delivery of Protein Drugs by Nanocarriers. Materials (Basel). 2010, 3, 1928–1980, doi:10.3390/ma3031928.
49. Yallapu, M.M.; Khan, S.; Maher, D.M.; Ebeling, M.C.; Sundram, V.; Chauhan, N.; Ganju, A.; Balakrishna, S.; Gupta, B.K.; Zafar, N.; et al. Anti-cancer activity of curcumin loaded nanoparticles in prostate cancer. Biomaterials 2014, 35, 8635–8648, doi:10.1016/j.biomaterials.2014.06.040.
50. Huynh, N.T.; Passirani, C.; Saulnier, P.; Benoit, J.P. Lipid nanocapsules: A new platform for nanomedicine. Int. J. Pharm. 2009, 379, 201–209.
51. Driffort, V.; Gillet, L.; Bon, E.; Marionneau-Lambot, S.; Oullier, T.; Joulin, V.; Collin, C.; Pagès, J.C.; Jourdan, M.L.; Chevalier, S.; et al. Ranolazine inhibits NaV1.5-mediated breast cancer cell invasiveness and lung colonization. Mol. Cancer 2014, 13, 264, doi:10.1186/1476-4598-13-264.
52. Rasband, W. ImageJ. U. S. Natl. Institutes Heal. Bethesda, Maryland, USA 2012, //imagej.nih.gov/ij/.

53. Van Duinen, V.; Van Den Heuvel, A.; Trietsch, S.J.; Lanz, H.L.; Van Gils, J.M.; Van Zonneveld, A.J.; Vulto, P.; Hankemeier, T. 96 Perfusable Blood Vessels To Study Vascular Permeability in Vitro. Sci. Rep. 2017, 7, 1–11, doi:10.1038/s41598-017-14716-y.

© 2022 by the authors. Licensee MDPI, Basel, Switzerland. This article is an open access article distributed under the terms and conditions of the Creative Commons Attribution (CC BY) license (http://creativecommons.org/licenses/by/4.0/).

Supplementary Materials

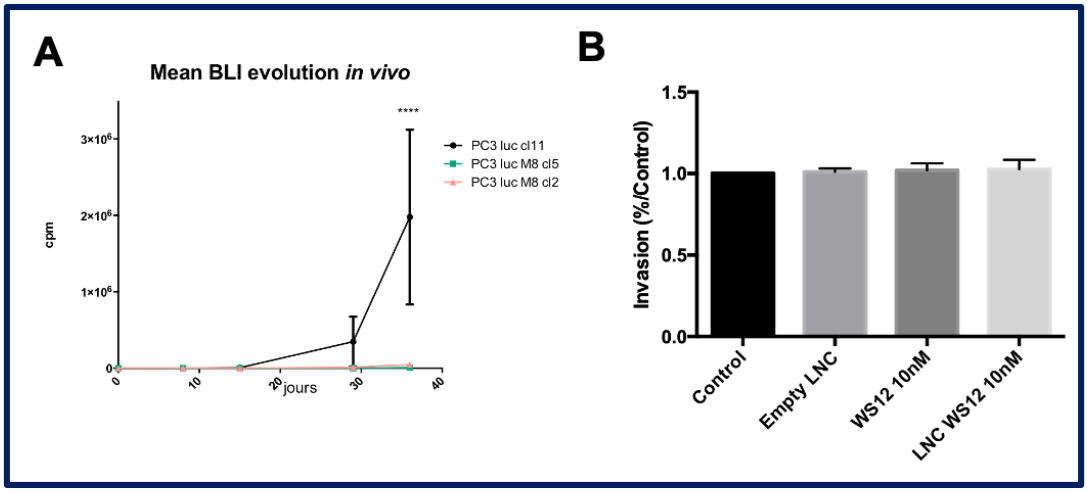

Figure S1. PC3-luc or PC3-M8-luc intravenous injection on mice and invasion assay

*A) Quantification of bioluminescence 5 weeks after PC3-luc or PC3-M8-luc intravenous injection on the mice tail (n= 6 mice/condition; statistical significance: **** = P <0.0001, ordinary one-way ANOVA with post-hoc Bonferroni test). B) Invasion assay using Matrigel® transwell with PC3 cells. Data are normalized to the control and express as mean ± SEM (n=3 independent experiments at least; statistical significance: RM one-way ANOVA with post-hoc Tukey's test).*

3.2 Lipid nanoparticles as nanodelivery systems: incorporation of polymethine dyes

"Polymethine dyes-loaded Solid Lipid Nanoparticles (SLN) as promising photosensitizers for biomedical applications"

Giorgia Chinigò[a*], Ana Gonzalez-Paredes[b1], Alessandra Gilardino[a], Nadia Barbero[c], Claudia Barolo[c,d], Paolo Gasco[b], Alessandra Fiorio Pla[a†] & Sonja Visentin[e†]

[a] University of Torino, Department of Life Sciences and Systems Biology, Via Accademia Albertina 13, 10123 Turin, Italy

[b] Nanovector Srl, Via Livorno 60, 10144, Turin, Italy

[c] University of Torino, Department of Chemistry, NIS Interdepartmental Centre and INSTM Reference Centre, Via Quarello 15a, 10135, Turin, Italy

[d] ICxT Interdepartmental Centre, Lungo Dora Siena 100, 10153 Turin, Italy

[e] University of Torino, Department of Molecular Biotechnology and Health Science, via Quarello 15a, 10135, Turin, Italy.

[1] Present address: NanoMedMol Group, Instituto de Química Medica (IQM), Consejo Superior de Investigaciones Científicas (CSIC), C/Juan de la Cierva 3, 28006, Madrid, Spain

[*] Correspondence: giorgia.chinigo@unito.it

[†] These authors contributed equally to this paper

Chinigò *et al., Spectrochimica Acta Part A,* 2022, *271:120909*

Abstract

Polymethine dyes (PMD) have proved to be excellent candidates in the biomedical field for potential applications in both diagnostic and therapeutic. However, PMD application in biomedicine is hindered by their poor solubility and stability in physiological conditions. Therefore, the incorporation of these dyes in nanosystems could be important to prevent the formation of dye aggregates in aqueous environment and to protect their photophysical characteristics. In the present work, two PMD based on the benzoindolenine ring (bromine benzo-cyanine-C4 and bromine benzo-squaraine-C4) were incorporated into Solid Lipid Nanoparticles (SLN) to solubilize and stabilize them in aqueous solutions. Obtained SLN showed a high incorporation efficiency for both PMD (≈90%) and not only preserved their spectroscopic properties in the NIR region even under physiological conditions but also improved them. Viability assays showed good biocompatibility of both empty and loaded nanocarriers while the cellular uptake and intracellular localization showed the effective internalization in MCF-7 cells, with a partial mitochondrial localization for CY-SLN. Moreover, *in vitro* phototoxicity assay showed that cyanine loaded-SLN (CY-SLN) is more photoactive than the free dye.

Keywords: polymethine dyes, solubility, nanocarrier, SLN, optical imaging, photodynamic activity

Introduction

In the last two decades, strong interest has been attracted to bioimaging and therapeutics of near-infrared (NIR) probes. These dyes, thanks to their emission in the NIR region of the electromagnetic spectrum (650-900 nm), which is characterized by minimal scattering of the excitation light and low self-fluorescence of biological molecules, allow deeper tissue penetration with minimal background interference [1]. Among NIR fluorescent probes, NIR polymethine dyes (PMD), such as pentamethine and heptamethine cyanines (CY) and squaraines (SQ), have been extensively studied for many biomedical applications [1], including *in vivo* optical imaging [2], thanks to their peculiar spectroscopic properties, the easiness in designing, and the simplicity of synthesis of most of PMD and the known structure-properties relationships [3,4]. Some NIR PMD have been shown to enhance *in vivo* characterization of tumors, by significantly improving tumor visualization and allowing detection and identification of small pre-neoplastic lesions and metastasis [2,5]. Moreover, it has recently been shown that a unique group of NIR fluorescent heptamethine cyanine preferentially accumulate in cancer cells without the need for chemical conjugation in many different types

of cancer cells including cultured, circulating and disseminated tumor cells [6–8] , as well as in preclinical models, including mice and dogs [6–10]. More interestingly, many studies have recently highlighted an intrinsic anticancer activity of some PMD, which may be used as efficient agents for photothermal and photodynamic therapy (PDT) [1,11], alternative strategies for the treatment of both oncological and non-oncological diseases [12]. Indeed both cyanine [13–15] and squaraine [16–22] derivatives have shown excellent light-induced toxicity on different types of tumors. Moreover, from data reported in literature, it seems that the presence of a heavy atom in the heterocyclic ring of these dyes leads to greater photodynamic activity, due to the enhancement of the inter-system conversion process, which underlies the singlet oxygen production [15,21,22].

However, the main challenges in the biomedical application of NIR PMD are associated with their structural characteristics, which result in poor solubility and low chemical stability, especially in aqueous solutions [23–27]. In order to overcome this limit, a valid alternative to the synthetic approach is represented by their incorporation into different nanoparticle systems, which may solubilize or shield hydrophobicity of this class of compounds and, therefore, overcome bioavailability challenges [1,28,29]. Indeed, PMD can be successfully loaded into organic nanoparticles, such as micelles [30,31], liposomes [32] and lipid nanoparticles [33–35]. Among these organic nanosystems, in the last decades, solid lipid nanoparticles (SLN) have proved themselves excellent candidates for the targeting and delivery of various diagnostic [36,37] and therapeutic [38] agents, including photosensitizers (PS) [39,40]. Besides the biocompatibility of the excipients used for their formulation and the possibility of being synthesized through relatively simple and inexpensive processes, SLN also possess great kinetic stability [38]. Very few examples of incorporation of PMD within SLN are currently reported in literature, regarding indocyanine green (ICG) and some cyanine derivatives based on the indolenine ring (DiO, DiI, DiD, DiR and IR-780) [34,35,37].

Here, we investigated the possibility of using SLN to increase solubility and stability of some NIR PMD in aqueous solutions in view of possible future applications in the biomedical field. In particular, we entrapped into SLN two symmetrical polymethine dyes (CY and SQ) based on an identical heterocyclic moiety, i.e. a bromo-functionalized benzoindolenine ring. The two dyes differ in the polymethine bridge resulting in a positively charged dye (CY) and a zwitterionic one (SQ) which, in turn, provoque quite different solubility properties in an aqueous solution at physiological pH. In particular, the SQ dye, designed following the successful series of Br-indolenine squaraines showing excellent PDT activity [21], suffers from a very low solubility in aqueous media, preventing its use for biological applications. In the present paper, we showed that SLN not only allow to solubilize PMD in aqueous solution, as aimed but even enhance their spectroscopic performances, making PMD-SLN potential and appealing candidates for *in vivo* imaging and/or PDT applications.

Materials and Methods

Materials

All the chemicals for SQ and CY synthesis were purchased from Merck and were used without any further purification. Epikuron® 200 (soybean lecithin with a phosphatidylcholine content ≥92% - Cargill) was purchased from AVG (Italy), trilaurin and benzylalcohol from Fluka, 2-phenylethanol and PEG-40 stearate (Myrj 52) from Sigma Aldrich. NaCl was supplied by ACEF (Italy). Only freshly distilled water and ultra-pure water (Milli-Q, Millipore, USA) were used. Absolute Ethanol, Tetrahydrofuran and Acetonitrile (HPLC grade) were purchased from Scharlab (Italy).

NovaChem Surfactant 100 (special mix of non-ionic and ionic detergents for Asymmetric Flow Field-Flow Fractionation (AF4) applications) was purchased from Postnova Analytics GmbH (Germany).

Synthesis

(CY) was synthesized as previously reported by some of us [41]. To obtain (SQ), compound 2 (0.45 g, 0.95 mmol) and squaric acid (0.05 g, 0.48 mmol) were introduced in a 10-20 mL microwave vial with a toluene/n-butanol mixture (1:1, 14 mL) and heated at 160 °C for 30 min. After solvent evaporation, Flash column chromatography with 100% CH_2Cl_2 allowed removing all the impurities. Then elution of 100% acetone afforded the squaraine as blue-green crystals (28%).

MS (ESI) [M-H]-: 765.08

^{1}H NMR (200 MHz, DMSO-d6) δ: 8.31 (s, 2H), 8.22-8.15 (m, 2H), 8.02 (d, J = 8 Hz, 2H), 7.79-7.69 (m, 4H), 5.89 (s, 2H), 4.22 (m, 4H), 1.94 (s, 12H), 1.78 (m, 4H), 1.35 (m, 4H), 0.96 (t, J = 6 Hz, 6H).

^{13}C NMR (50MHz, DMSO-d6) δ: δ 182.02, 171.28, 139.71, 134.54, 132.13, 131.39, 130.48, 128.61, 126.88, 123.93, 117.82, 111.03, 86.58, 50.88, 43.60, 29.24, 26.61, 20.16, 13.70.

All microwave reactions were performed in single-mode Biotage Initiator 2.5. TLC were performed on silica gel 60 F254 plates. ESI-MS spectra were recorded using LCQ Thermo Advantage Max spectrometer, with electrospray interface and ion trap as mass analyzer. The flow injection effluent was delivered into the ion source using N_2 as sheath and auxiliary gas. ^{1}H NMR (200 MHz) and ^{13}C NMR (50 MHz) spectra were recorded on a Bruker Avance 200 NMR.

Solid Lipid Nanoparticles (SLN) preparation

Blank (BLK-SLN) and dye-loaded SLN (CY-SLN and SQ-SLN) were prepared in collaboration with Nanovector s.r.l. (Turin, Italy). SLN were prepared by oil-in-water (O/W) warm microemulsion method reported elsewhere [42,43], slightly modified. Briefly, a warm microemulsion was formed by mixing at temperature

above lipids melting point (52° C) an oily phase (lipids and short chain alcohols) with an aqueous phase containing the surfactants. When clear microemulsion was formed, it was dispersed into water at the same temperature (ratio 1:10 v/v) under mechanical stirring (1900 rpm) and left under stirring to achieve room temperature. Dye-loaded SLN were prepared in the same way by adding the PMD (cyanine or squaraine) to the oil phase of the microemulsion. Obtained SLN dispersions were then washed (3X) by tangential flow filtration (TFF) (Vivaflow 50, RC membrane, 100 KDa MWCO, Sartorius Stedim Italy S.r.l.) for purification, all residual solvents were finally reduced at regulatory acceptable concentrations [44]. Each formulation (BLK-SLN, CY-SLN and SQ-SLN) was prepared in triplicate to verify the reproducibility of the synthesis procedure and increase the reliability of data.

Physicochemical characterization

Determination of particle size and surface charge

The average dimension of SLN was evaluated by batch mode Dynamic Light Scattering (DLS), while Zeta potential was measured by Laser Doppler Velocimetry (LDV). For size measurement, SLN dispersions were diluted 1:100 in ultrapure water, whereas for zeta potential measurements samples were diluted 1:50 in NaCl 1mM. All measurements were carried out on Zetasizer-Nano ZS (Malvern Instruments, UK), in triplicate, at 25°C.

Asymmetric Flow Field-Flow fractionation (AF4) characterization

To deeper characterize SLN's size distribution, they were analyzed by AF2000 Asymmetric Flow Field-Flow Fractionation (AF4) instrument (Postnova Analytics GmbH, Germany), which was coupled online to an SPD-20A UV–vis spectrophotometer (Postnova), and a Zetasizer Nano ZS (Malvern Instruments). AF4 was performed in a PMMA channel with a spacer of 350 µm width at the inlet, lined with a regenerated cellulose membrane (cut off 10 KDa). Filtered (0.1 µm Durapore membrane) 0.05% NaCl solution in ultrapure water added with 0.05% Novachem Surfactant 100 was used as the carrier. Samples were diluted 1:2 in the carrier and then manually injected into the system (20 µl). Channel tip flow and focus flow was set to 1 mL/min. The flow rate to the detector was kept at 0.5 mL/min, and the cross flow was set to decrease from 1 mL/min to 0.1 mL/min in 20 min and then to remain constant at 0.1 mL/min for 20 min. The UV detector was set at 280 nm with a sensitivity of 0.001, and the acquisition time for each autocorrelation function in the Zetasizer Nano detector was 3 seconds. The intensity of scattered light (kcount/s) and ζ-average mean diameter (nm) were elaborated using Zetasizer Nano Software. The dimensional range for each analyzed sample was obtained from the integration of the DLS distribution curve.

Entrapment efficiency and chemical composition

Dyes entrapment efficiency was calculated as the ratio between dye concentration in SLN dispersion before washing (BW) by TFF and after 3 washing cycles (A3W) according to the following equation:

$$EE\ (\%) = \frac{[dye]A3W}{[dye]BW} \times 100$$

Washing steps were performed by addition and removal of a fixed amount of water, equal to the volume of dispersion.

Dye concentration was determined after SLN disruption by dilution in tetrahydrofuran (1:100). Absorbance at 692 nm and 672 nm for cyanine and squaraine samples respectively was measured (UV-visible spectrophotometer - HITACHI UH5300). Dyes concentration inside SLN was calculated through the construction of an appropriate calibration line on known concentrations of the dye dissolved in tetrahydrofuran/H_2O (99:1). A linear fit was applied to determine the molar extinction coefficient (ε) as the slope of the line. The analysis was performed in duplicate and the results were considered acceptable once the difference between the determined log ε was less or equal to 0.02 in relevancy to their average.

Phosphatidylcholine (PC) content was also determined by HPLC-UV analysis using a method previously described [45], to confirm the final composition of SLN (i.e. after washing steps) and their chemical stability overtime.

Optical properties of dyes and dye-loaded SLN

Absorbance spectra were recorded on HITACHI UH5300 spectrophotometer (quartz cuvettes, 1 cm pathway length) in ethanol with increasing water content (from 0% to 90%) for dyes' spectroscopic characterization and in 100% ultrapure water for dye-loaded SLN. Cyanine's molar extinction coefficient (ε) in absolute ethanol was obtained from Ciubini *et al.* [41], whereas squaraine's molar extinction coefficient (ε) in absolute ethanol was determined as reported in the same paper [41]. A certain amount of dye (5–7 mg) was dissolved in 10 ml of absolute ethanol. Three diluted solutions in absolute ethanol were prepared by taking aliquots of the stock solution. The diluted solutions were measured by UV–Vis spectroscopy and the absorbance intensities of each solution at the λ_{max} were plotted versus the sample concentration. A linear fit was applied to determine the molar extinction coefficient (ε) as the slope of the line. The analysis was performed in duplicate. Results were considered acceptable once the difference between the determined log ε was less or equal to 0.02 in relevancy to their average.

Fluorescence measurements were recorded on a HORIBA FluoroLog2 (Jobin-Yvon) fluorimeter. Diluted solutions with absorbance around or lower than 0.1 units were used to avoid the presence of aggregates. Because of the low Stokes shift (20 nm for CY and 6 nm for SQ), typical of this class of compounds, emission spectra were obtained by exciting dyes at the wavelength corresponding to the hypsochromic

shoulder showed in absorption spectra (λ_{ex}= 620 nm and 640 nm for cyanine and squaraine respectively). Dyes' fluorescence spectra were recorded in ethanol with increasing water content (from 0% to 90%) and dye-loaded SLN's emission spectra in 100% ultrapure water. Fluorescence lifetimes (τ_f) were measured in DMSO using a nanoLED source (emission at 636 nm, Horiba Jobin-Yvon) and a single photon counting detector (TBX04 Horiba Jobin-Yvon). Fluorescence quantum yields (ϕ) were determined in DMSO using the same instrument with the integrating sphere Quanta-ϕ (Horiba) and De Mello method. Values reported in results correspond to the average of three independent measurements.

Cell culture and cell viability assay

Human microvascular endothelial cell line (HMEC-1, American Type Culture Collection ATCC) were cultured in EndoGRO™ MV-VEGF complete medium (Merck Millipore), complemented with 0.5% gentamicin antibiotic and 5 mM L-glutamine; human breast adenocarcinoma cell line (MCF-7, ATCC) were cultured in Dulbecco's Modified Eagle's Medium-high glucose (DMEM from Euroclone), complemented with 10% Fetal Bovine Serum (FBS from Euroclone), 0.5% gentamicin antibiotic and 5 mM L-glutamine. All cell cultures were maintained in an incubator at 37 °C and 5% CO_2 atmosphere, using Falcon™ plates as supports.

For cell viability, cells ($0.5 \cdot 10^4$ cells/well) were seeded in 96-well plates (Sarstedt, Germany). After 18 h of incubation at 37°C, different dyes concentrations of dye-loaded SLN dispersions (from 10 nM to 1 µM), were added for 24 and 48 h to the culture medium. In order to compare the cytotoxicity of the dye in the free form or after encapsulation, cytotoxicity of cyanine in the free form was tested (diluted from a stock 1mM in DMSO). SQ alone was not tested due to its insolubility in these conditions. For each condition, eight replicates were performed. Cytotoxicity was assessed 24 and 48 h after SLN treatment using CellTiter 96 AQueous Non-Radioactive cell proliferation assay (Promega, USA) following manufacturer's instruction. Briefly, MTS was added (10%) to the culture medium and kept in an incubator for 2 h. Cells without SLN and incubated with complete medium or basal medium without serum and grow factor (EndoGRO starve for HMEC samples and DMEM 0% FBS for MCF-7 samples) were used as positive and negative controls, respectively. Absorbance was then recorded at 490 nm (soluble formazan absorbance) using a microplate reader (FilterMax F5, Multi-Mode Microplate Reader, Molecular Devices). Absorbance values obtained were then analyzed with Excel software (Office, Microsoft) to determine the mean absorbance for each condition after subtraction of the average background (absorbance value of cell medium alone treated with MTS was considered as background). Absorbance values obtained are directly proportional to the number of viable cells.

Photodynamic treatment and phototoxicity assay

To evaluate the photodynamic activity, MCF-7 cells were plated in 96 well plates ($0.5 \cdot 10^4$ cell/well in 200µL of DMEM 10% FBS) and after 6 h were treated with CY-SLN, SQ-SLN and CY at different concentrations (from 10 to 200 nM). Cells were incubated O/N at 37°C and 5% CO_2 and then were irradiated with a light beam intensity of 8 mW/cm^2 for 15 min. For cell irradiation, a compact LED array-based illumination system with a homogeneous illumination area was used. The system was specifically designed and produced by Cicci Research s.r.l (Italy) for *in vitro* PDT tests on cells grown in standard multiwell plates (96-wells). The proposed illumination system includes a RED-LED array (light source with excitation wavelength: 640 nm, and irradiance: 8 mW/cm^2) composed of 96 LEDs in a 12 × 8 arrangement. In addition, both LED-array and 96-multiwell plates were placed into a case to isolate the system during irradiation. 24 h, 48 h and 72 h after LED treatment MTS assay were performed in order to evaluate cell viability. For each monitored time (24 h, 48 h and 72 h) two 96-well plates were prepared: one plate was treated with the light beam and the other one was used as control (not irradiated).

Cellular uptake and intracellular localization

Cells ($50 \cdot 10^4$ cells/dish) were seeded in 10 cm diameter Petri dishes and after three days culture media were removed and replace with fresh culture media. Cells were incubated for 2 h, 6 h, O/N and 24 h with fresh culture media containing the same concentration (100 nM) of cyanine in the free form (CY) or encapsulated into SLN (CY-SLN) and of squaraine encapsulated into SLN (SQ-SLN). Following incubation at 37°C, the medium was removed, cells were trypsinized and the pellet was washed twice with PBS. Proteins were subsequently extracted using 50 µL of RIPA buffer (Pierce® RIPA Buffer, Thermo scientific) and left 1 h on ice. Then cell lysates were sonicated and left on ice for 1 h. After quantification by the BCA Protein Assay proteins were diluted in ethanol to a final concentration of 1 µg/µL. Then cell lysates were diluted 1:10 in ethanol to a final volume of 1 mL and fluorescence emission of the sample was recorded on a spectrofluorimeter (FluoroLog2, Jobin-Yvon - HORIBA).

To assess the intracellular localization of dye-loaded SLN we used Calcein and MitoTracker Red (Molecular probes®, Invitrogen), in order to label and track the whole cellular volume and mitochondria in live cells, respectively. Briefly, $10 \cdot 10^4$ cells were left to attach for 24 h on glass coverslips in a 6-well plate (Sarstedt, Germany) and then incubated O/N with growth medium containing 100 nM of the dye incorporated into SLN (CY-SLN or SQ-SLN) or of the dye in the free form (CY). After incubation, cells were washed and then incubated with Calcein (250 nM) or MitoTracker Red (250 nM) for 30 min. After incubation, wells were washed twice with Hanks' Balanced Salt Solution (HBSS) in order to wash off the excess probe and fixed in 4% paraformaldehyde (PAF) at 37°C for 2 min. Coverslips were then mounted onto a glass slide by DABCO MIX (purchased from Sigma-Aldrich) and observed using a Leica TCS SP8 confocal system (Leica Microsystems,

Germany) equipped with a HCX PL APO 63X/1.4 NA oil-immersion objective. Cyanine and squaraine dyes were excited with a HeNe laser at 633 nm, whereas Calcein and MitoTracker Red were excited with DPSS laser at 561 nm in order to simultaneously detect the probes. Images were acquired on the three coordinates of the space (XYZ planes) with a resolution of 0.081 µm x 0.081 µm x 0.299 µm and were processed and analyzed with ImageJ software (Rasband, W.S., U.S. National Institutes of Health, Bethesda, MA). 3D images with Calcein allowed assessing whether dyes are within the cell or not and Mitotracker Red signals allowed to understand whether dyes co-localize with cell mitochondria (Pearson's correlation coefficient was measured by using ImageJ JACoP plugin).

Statistical analysis

Data are shown as the average of three independent experiments ± SEM (standard error mean). Statistical analyses were performed using Graph-Pad Prism 6.0 software (La Jolla, CA, USA). Statistical significance between populations was determined by analysis of variance (1way ANOVA-Kruskal Wallis test) followed by *post-hoc* Dunn's multiple comparisons test. Differences with p-values <0.05 were considered statistically significant and *: p-value < 0.05, ***: p-value < 0.0005, ****: p-value < 0001.

Results and discussion

1. Synthesis of polymethine dyes

The synthesis of symmetrical brominated pentamethine cyanine and squaraine dyes involved the condensation of the quaternary heterocyclic salts (**2**), bearing an activated methyl group, with a malonodialdehyde derivative and squaric acid, respectively. Compound **1** was obtained from 7-bromo-1,1,2-trimethyl-1Hbenzo[e]indole exploiting the Fischer indole synthesis by reacting (6-bromonaphthalen-2-yl) hydrazine with 3-methylbutan-2-one in glacial acetic acid, as previously described [41]. The quaternization of the benzoindolenine ring to get compound **2**, performed under microwave irradiation, led to an increased acidity of the methyl group which enabled the following condensation reaction (Fig. 1 A) to obtain CY and SQ. The synthesis of the symmetrical cyanine dye is already reported in our previous work [41], while the symmetrical squaraine dye was synthesized in a one-step reaction under microwave heating following our well-established method for indolenine-based squaraines [46] by reacting two equivalents of quaternary heterocyclic salts with squaric acid (Fig. 1 A).

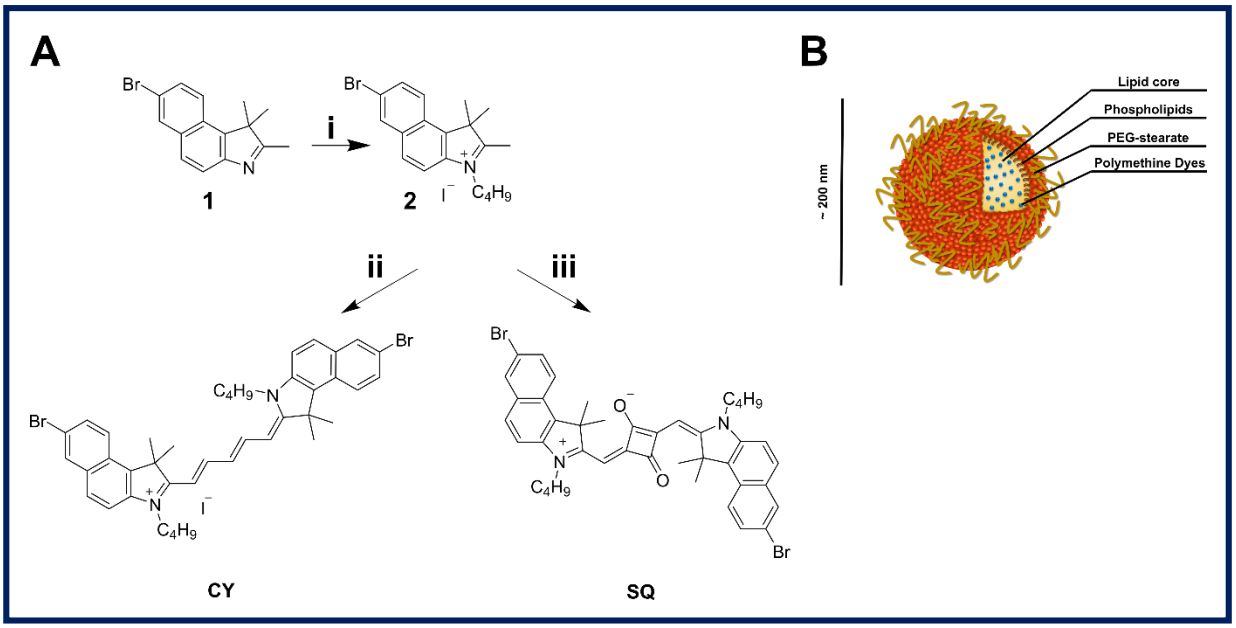

Figure 1. PMD and SLN.

A*) PMD synthesis: (i) acetonitrile, iodobutane, MW, 45 min, 155 °C; (ii) sodium acetate, acetic anhydride, N-((1E,2E)-3-(phenylamino)allylidene)benzenaminium chloride, MW, 10 min, 130 °C; (iii) squaric acid, toluene/n-butanol, MW, 30 min, 160 °C.* ***B****) Schematic representation of dye-loaded SLN synthesized.*

2. Solid Lipid Nanoparticles (SLN) preparation and physicochemical characterization

Solid Lipid Nanoparticles (SLN) and dye-loaded SLN were prepared as reported in the experimental section. Results of SLN physico-chemical characterization through batch mode dynamic light scattering (DLS) after the purification procedure (A3W) are reported in Table 1. BLK-SLN exhibited a mean diameter of 171 nm and a polydispersity index (PDI) lower than 0.20, which indicates the homogeneity of size distribution. On the other hand, the characterization of dye-loaded SLN (CY-SLN and SQ-SLN) revealed higher sizes due to the presence of the PMD within the nanoparticles and slightly higher PDI that remained anyway lower than 0.30. A schematic representation of the dye-loaded SLN synthesized is represented in Figure 1 B. It is important to highlight that synthesized particles have a mean diameter around 200 nm, which is very interesting in cancer applications. Indeed, previous studies on liposomes of different mean size [47] set at 200 nm the threshold size for more effective extravasation of nanoparticles into the tumor tissues *via* the leaky vessels by the enhanced permeability and retention (EPR) effect [48]. Moreover, the presence of the steric stabilizer PEG-40 stearate into the formulation will probably improve the bioavailability of the nanosystem in body fluids and its pharmacokinetic profile after administration for further potential *in vivo* studies [49]. Indeed, PEG chains sterically stabilize nanoparticles and increase their plasma half-life, reducing binding to serum proteins and other opsonic factors [50]. Moreover, both blank and dye-loaded SLN showed

good stability under storage at different temperatures (4, 25 and 40 °C): as shown in Figure S1 A, size and PDI of all SLN did not change over 30 days from their synthesis at all three investigated temperatures.

Regarding the ζ-potential, BLK-SLN showed a value of -11.6 mV, comparable to other SLN prepared with triglycerides [51], suggesting good stability of the dispersion. Comparing ζ-potentials measured on the loaded SLN (Table 1), we observed a significant difference between the two formulations: SQ-SLN showed a negative ζ-potential as well as BLK-SLN, whereas CY-SLN showed an inversion of ζ-potential, which becomes positive. Considering the structures of the two PMD (Fig. 1 B) and the positive charge associated with the cyanine dye, the inversion of the potential observed in the case of CY-SLN can be due to a partial localization of the dye on the particle surface. This effect has been also described for other cyanine dyes incorporated in lipid nanocarriers [52].

SLN	Size (nm)	PDI	ZP (mV)	EE (%)	PC (mg/mL)
BLK-SLN	170.9 ± 22.84	0.152 ± 0.052	-11.6 ± 4.9	-	11.05 ± 1.50
CY-SLN	194.7 ± 27.43	0.258 ± 0.036	+7.8 ± 2.2	89.2 ± 0.4	11.60 ± 1.00
SQ-SLN	203.4 ± 18.43	0.250 ± 0.052	-6.6 ± 2.3	88.9 ± 7.4	9.96 ± 1.78

Table 1. Physicochemical properties of BLK-SLN, SQ-SLN and CY-SLN.

PDI: polydispersity index; ZP: zeta potential, EE: entrapment efficiency; PC: phosphatidylcholine (mean ± SD, n = 3).

Finally, in order to deepen the physico-chemical characterization and to verify the effective size distribution of the formulation obtained through batch mode DLS, SLN were also analyzed by Asymmetric Flow Field-Flow-Fractionation (AF4), an elution-based particle separation technique that allows to separate, detect and measure any sub-populations eventually present in the colloidal sample. This technique is based on the application of a force field (cross flow) perpendicular to the particle transport direction, which allows smaller particles to be transported faster and eluted earlier [53]. AF4 analysis confirmed that all 3 types of SLN prepared were characterized by one main population: the fractograms reported in Figure 2, show an upward trend of hydrodynamic size over the elution peaks. The diameters calculated by analysis of light scattered signals corresponding to peak elution were respectively 143 nm for BLK-SLN (Fig. 2 A), 182 nm for CY-SLN (Fig. 2 B) and 157nm for SQ-SLN (Fig. 2 C). The elution volume (mL), corresponding to the elution time (min), and peak width are displayed in Table 2.

The difference with respect to the diameter obtained from the batch mode DLS measurement may be due to the different ionic composition of the buffer used in AF4, compared to ultrapure water used for the batch mode. Indeed, the different ionic and surfactant composition of the medium alters the nature of the ionic sphere that surrounds the surface of nanoparticles and, consequently, their hydrodynamic radius, which includes not only the diameter of the nanoparticle itself but also the ions included within the slipping plane,

which move together to it in Brownian motion. Moreover, a small shoulder was detected before the elution peak of CY-SLN (6.5 mL <elution volume <10.6 mL). Nevertheless, because of the low intensity of the peak close to the noise threshold, this signal is not attributable to the presence of a sub-population of SLN within the sample; it probably indicates the formation of small micellar systems (64 nm) induced by the surfactants present in the elution medium used (Novachem 0.05% + NaCl 0.05%) and probably related to the different surface characteristics showed by positive ζ-potential of CY-SLN compared with the other formulations [54].

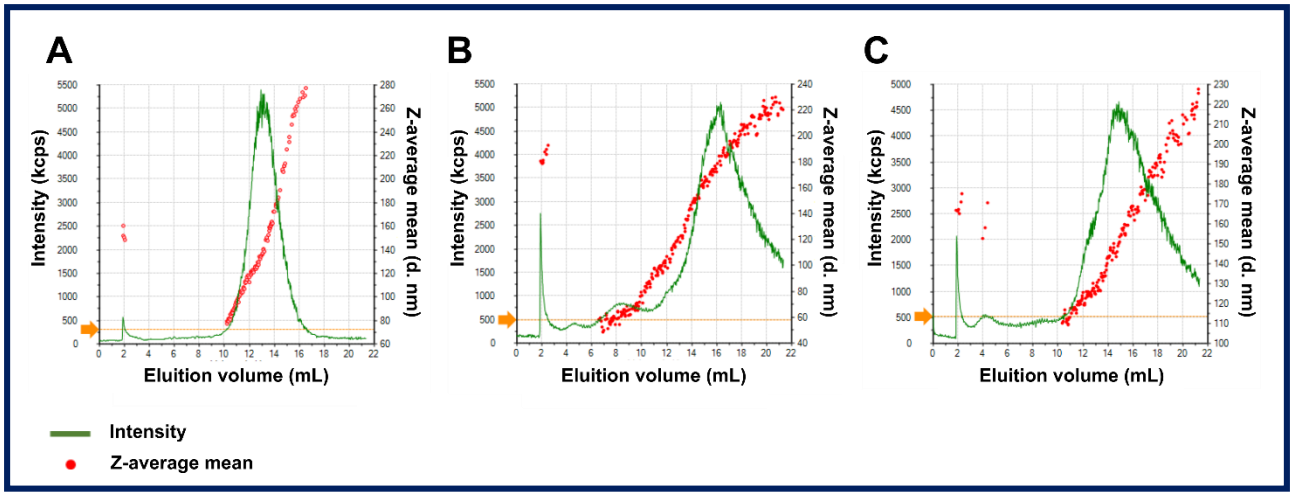

Figure 2. SLN AF4 characterization.

AF4-DLS fractograms of BLK-SLN (A), CY-SLN (B) and SQ-SLN (C) (red dots: z-average mean diameter in nm; green curve: intensity of scattered light in kcount/s; yellow line: noise threshold).

SLN type	Z-average mean diameter (nm)	Elution volume (mL) (initial-final)	Peak width (nm)
BLK-SLN	143	10.5-16	32.0
CY-SLN	182	12.5-21	27.2
SQ-SLN	157	11-20	25.2

Table 2. Particle size obtained from DLS analysis of AF4 fractograms, elution volume (mL) and peak width.

The entrapment efficiency of SLN was very high for both dyes, with values close to 90% (Table 1), showing the efficacy of this type of lipid carrier for the incorporation of hydrophobic molecules. Moreover, the PC concentrations displayed in Table 1 confirmed the final composition of SLN and negligible losses during the purification process, as PC content after 3 washes was about 90% compared to that of non-washed formulations.

3. Dyes and dye-loaded SLN optical characterization

CY and SQ dyes show a narrow absorption band in the NIR, perfectly matching the phototherapeutic window (Fig. 3 A). CY (Fig. 3 A-I) and SQ (Fig. 3 A-II) show similar optical properties in absolute ethanol with an absorbance maximum at 688 (CY) and 668 (SQ) nm, preceded by a hypsochromic shoulder typical for PMD [28] (at about 620 and 640 nm respectively) and emission maxima at 708 (CY) and 674 nm (SQ). CY and SQ exhibit high molar extinction coefficients ($2.08 \cdot 10^5$ and $2.52 \cdot 10^5$ $L \cdot mol^{-1}$ cm^{-1}, respectively, in ethanol) and good quantum yields in organic solvent (36% and 31% respectively in DMSO). The higher molar extinction coefficient showed by SQ as compared to CY is due to the greater rigidity of squaraine derivatives' polymethinic bridge, which reduces photoisomerization phenomena leading to a more stable structure and an optimization of its optical properties with respect to the corresponding cyanine derivative [55].

However, both dyes are poorly soluble in aqueous solutions and this compromises their applicability in the biomedical field. Indeed, as shown in Figures 3 B and 3 C, absorption spectra of CY (Fig. 3 B-I) and SQ (Fig. 3 C-I) in ethanol show a significant change in shape and intensity upon increasing the water content from 0 to 90%, leading to the bleaching of their fluorescent properties (Fig. 3 B-II for CY and Fig. 3 C-II for SQ). The modifications of the absorption spectra upon water addition suggest the rapid aggregate formation of the two dyes in aqueous conditions. This phenomenon is particularly evident in the case of SQ dye, which exhibits a lower solubility than CY in aqueous solution due to its zwitterionic structure.

Interestingly, the incorporation of the PMD into SLN allows to preserve their standard spectroscopic properties even in aqueous solution (Fig. 3 D and 3 E). Indeed, dye-loaded SLN reproduce the same spectroscopic profile exhibited by the dyes not encapsulated in organic solvent with a small bathochromic shift (Table 3). The absorption below 600 nm, shown by dye-loaded SLN, may be due to the Rayleigh scattering from nanoparticles and it is more pronounced in the case of SQ-SLN because of the lower dyes/lipids (w/w) ratio as compared to CY-SLN's one. The quantum yield shown by SQ incorporated into SLN in H_2O is even higher than that exhibited by the dye not encapsulated in DMSO (52% versus 31%) (Table 3). We also evaluated and compared the fluorescence lifetime (τ_f) of the dyes not encapsulated and the dye incorporated into SLN. Fluorescence lifetimes (τ_f) of dyes not encapsulated show mono-exponential decay and are in the nanoseconds range, accordingly with previous results [41]. As regards dye-loaded SLN, the mono-exponential trend of the τ_f indicates a homogeneous dispersion of the dyes within the lipidic nanosystem in both formulations. Moreover, τ_f recorded for dye-loaded SLN in aqueous solution are similar to those obtained for not encapsulated-dyes in organic solvent. Interestingly, squaraine into SLN shows again enhanced optical performances with respect to its not encapsulated form with a fluorescence lifetime even doubled (2.571 versus 1.382). This means that the SQ derivative into SLN gives rise to prolonged fluorescence emission, probably due to an increased stabilization of the fluorophore by the lipidic microenvironment.

Finally, we investigated the stability of the optical properties of the dyes into SLN. Both CY-SLN and SQ-SLN showed good stability until 30 days after formulation (at 4°C and 25°C) and only a small decrease in fluorescence intensity was observed keeping the sample at 40°C (condition of accelerated stability) for 30 days (Fig. S1 B).

These results clearly show that the incorporation of PMD into SLN allows a successful preservation of their optical characteristics, making them suitable candidates for optical imaging.

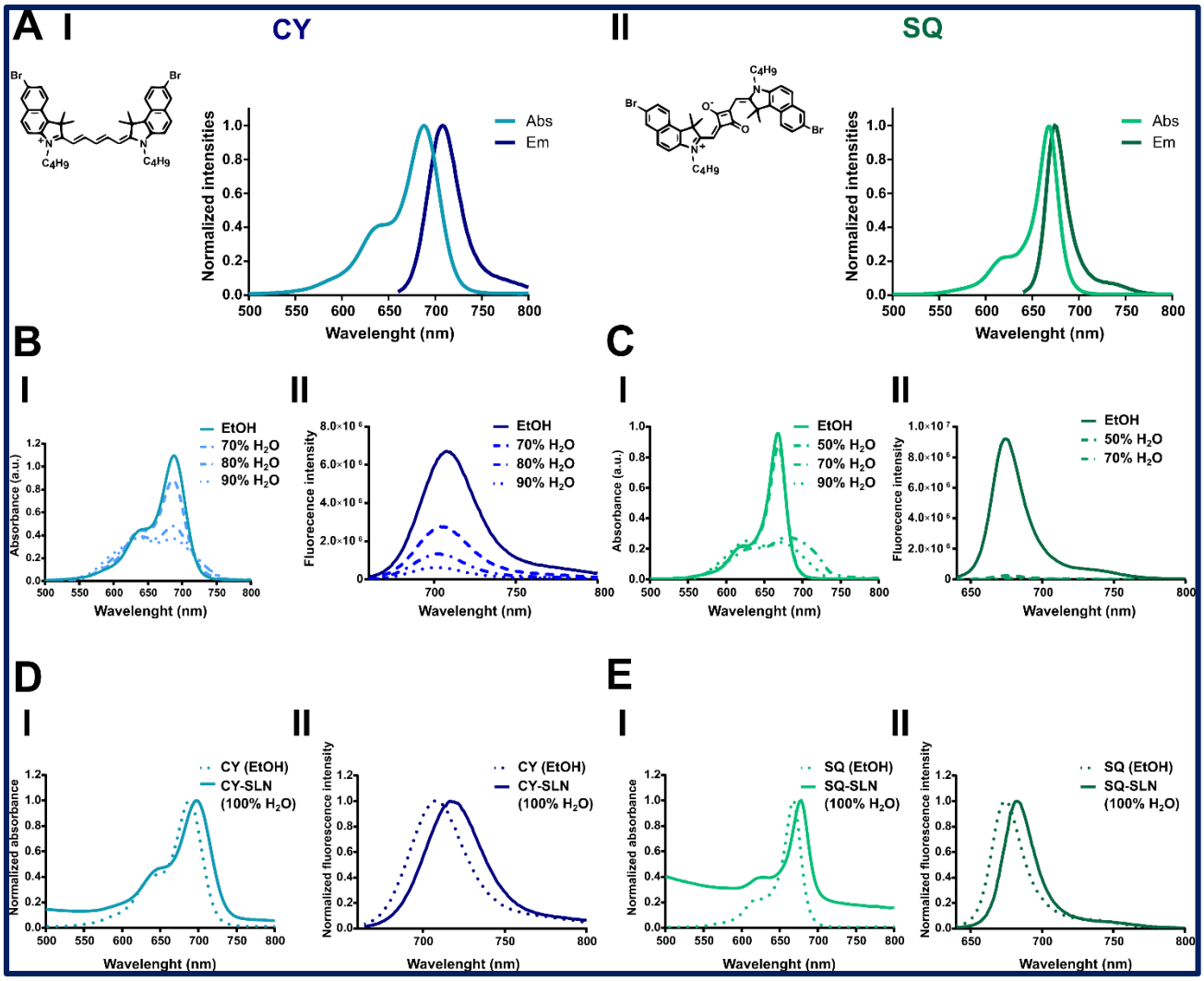

Figure 3. Dyes and dye-loaded SLN optical characterization.

A*) Normalized absorption (abs) and emission (em) spectra of CY (I) and SQ (II) in absolute ethanol. Insets show dyes' structures.* ***B****) Changes in the absorption spectra (I) and in the emission spectra (II) of CY ($5*10^{-6}$ and $5*10^{-7}$ M respectively in absolute ethanol) upon increasing content of water from 0 to 90%. λ_{ex} for emission spectra = 620 nm.* ***C****) Changes in the absorption spectra (I) and in the emission spectra (II) of SQ ($3*10^{-6}$ and $3*10^{-7}$ M respectively in absolute ethanol) upon increasing content of water from 0 to 90%. λ_{ex} for emission spectra = 640 nm.* ***D****) Normalized absorption (I) and*

emission (II) spectra of CY encapsulated into SLN (CY-SLN) in 100% water. Dot lines represent normalized absorption (I) and emission (II) spectra of CY in the free form in absolute ethanol. ***E****) Normalized absorption (I) and emission (II) spectra of SQ encapsulated into SLN (SQ-SLN) in 100% water. Dot lines represent normalized absorption (I) and emission (II) spectra of SQ in the free form in absolute ethanol.*

	absorbance		emission				
	λ_{max} (nm)	ε λ_{max} (L mol^{-1}cm^{-1})	λ_{max} (nm)	ϕ_{fl} (%)		τ_f (ns)	
	EtOH/H_2O	EtOH	EtOH/ H_2O	DMSO	H_20	DMSO	H_20
CY	688	$2.08 \cdot 10^5$	708	36	-	1.570 ± 0.004	-
CY-SLN	698	-	717	-	36	-	1.372 ± 0.004
SQ	668	$2.52 \cdot 10^5$	674	31	-	1.382 ± 0.003	-
SQ-SLN	678	-	682	-	52	-	2.571 ± 0.004

Table 3. Optical properties *of not encapsulated-dyes (CY and SQ) in organic solvent and dye-loaded SLN (CY-SLN and SQ-SLN) in aqueous solution. λmax(abs), λmax(em): dyes absorption and emission maxima, respectively, ε: molar extinction coefficient at the absorption maximum, φfl: fluorescence quantum yield, τf: fluorescence lifetime.*

4. In vitro cell viability of CY-SLN and SQ-SLN

We investigated the inherent cytotoxicity of BLK-SLN, CY-SLN and SQ-SLN using the MTS viability assay on MCF-7 cells. BLK-SLN showed good biocompatibility (Fig. 4 A-I), starting to affect cell viability 24 h after treatment only at the highest lipid concentration tested (about 100 µg/mL, corresponding to a dye concentration of 1.5 µM and 1 µM for CY and SQ, respectively). Regarding dye-loaded SLN, cell viability was tested by varying dyes' concentration into SLN in the nanomolar range, in order to identify the maximum concentration at which treatment can be administered without inducing cytotoxicity. CY cytotoxicity in its free form was also tested and Figure 4 A shows that CY (Fig. 4 A-II) started to affect cell viability from a concentration of 400 nM 24 h after treatment. Surprisingly, once incorporated into SLN CY cytotoxicity increased starting from a concentration of 200 nM 24 h after treatment although with partial recovery at 48h (Fig. 4 A-III). On the contrary, SQ-SLN (Fig. 4 A-IV) are less cytotoxic and do not affect cell viability until a dye concentration of 1 µM. To check the cell-type specificity of the observed CY-SLN cytotoxic effect, we measured CY-SLN cytotoxicity also on endothelial cells (HMECs) and, surprisingly, CY-SLN do not show the same cytotoxic profile shown on MCF-7 (Fig. S2). Indeed, HMECs treated with 200 nM of CY-SLN still show a slight increase in cell viability as compared to the control even 48 h after treatment (Fig. S2). Similar results were also found testing BLK-SLN cytotoxicity on HMECs at lipid concentrations corresponding to those used for CY-SLN treatment (Fig. S2). On the other hand, the cytotoxicity of CY not encapsulated did not show any differences between the two cell types, at least in the concentration range investigated (till 200 nM) (Fig. S2). These results indicate that SLN's and CY-SLN's cytotoxicity is cell type-dependent and it may also suggest that tumor cells may be more sensitive to the dye-loaded nanosystem than normal cells. For the subsequent

characterizations of our nanosystems on tumor cell model (MCF-7) we used SLN with dye concentrations of 100 nM, in order to avoid results affected by any cytotoxic effects (Fig. 5 A-I).

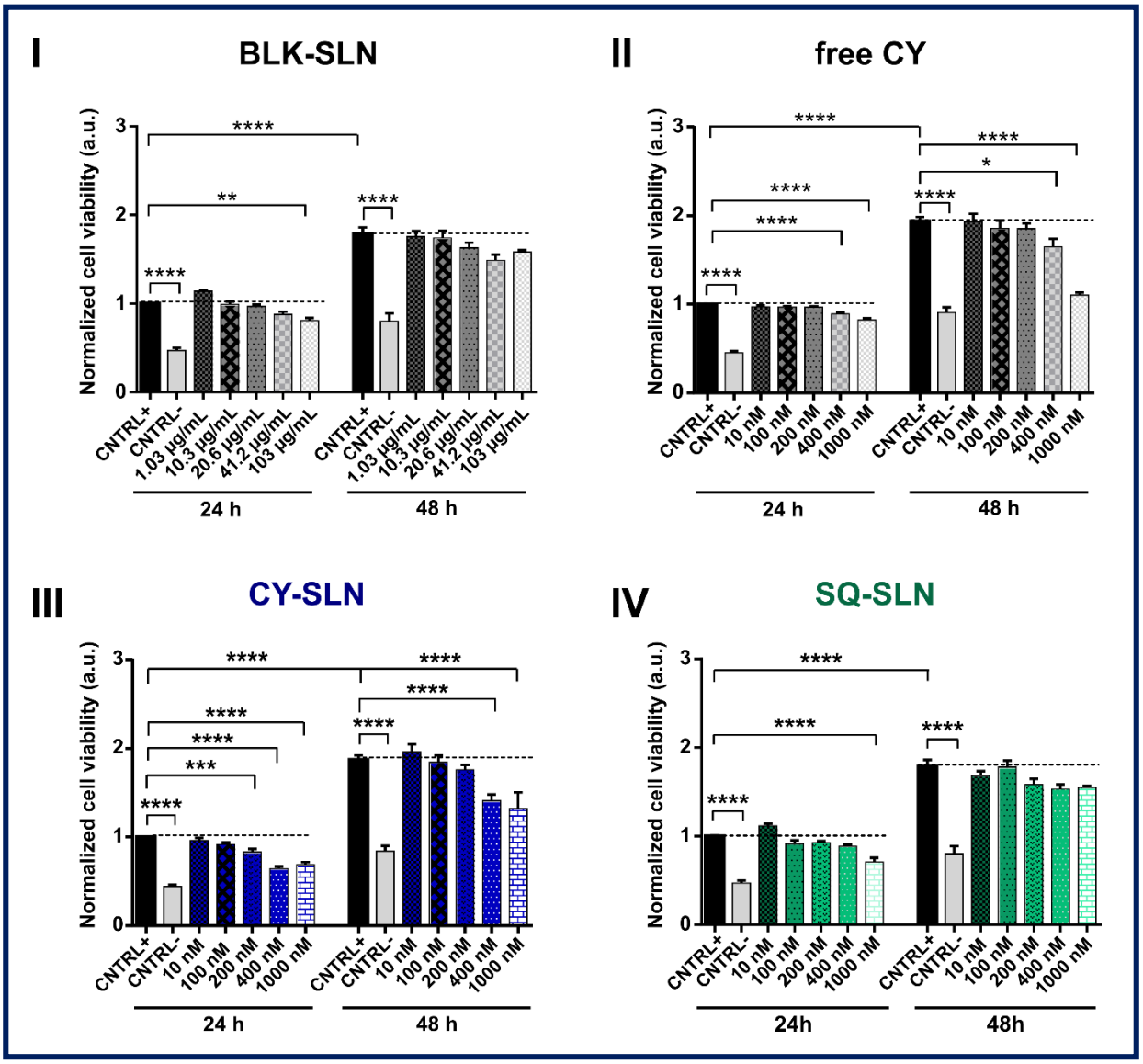

Figure 4. In vitro cytotoxicity of CY-SLN and SQ-SLN on MCF-7.

*Cell viability assays on MCF-7 24 h and 48 h after treatment with different concentrations of BLK-SLN (**I**), free CY (**II**), CY-SLN (**III**) and SQ-SLN (**IV**). For BLK-SLN concentrations refer to phosphatidylcholine content ([PC] from 1.03 to 103 µg/mL), whereas for dye-loaded SLN concentrations refer to dyes incorporated into SLN (from 10 to 1000 nM). Data are normalized on CNTRL+ (MCF-7 untreated) at 24 h and are represented as mean ± SEM. Data refer to a pull of at least 3 independent experiments (eight replicates for each experiment). Statistical significance versus CNTRL+: *** P< 0.001, **** P< 0.0001 (Kruskal-Wallis test with post-hoc Dunn's test).*

5. In vitro photoactivity of CY-SLN and SQ-SLN

In vitro phototoxicity results, illustrated in Figure 5 A-II, do not show any phototoxic effects of not encapsulated CY (100 nM) on MCF-7, but interestingly, highlight a photoactivity of CY after encapsulation into SLN (100 nM) (Fig. 5 A-II). This result may be due to the lower possibility of aggregation of CY encapsulated into SLN, which leads to an increase in the lifetime of the triplet state leading to a more efficient photoactivity. Alternatively, the photoactivity of CY-SLN could be due to a higher local concentration of the dye due to the nanoencapsulation. Notably, BLK-SLN did not show any phototoxicity, meaning that the decrease in cell viability after light beam treatment is exclusively due to the activity of the dye (Fig. 5 A-II). Our results are in agreement with other studies about potential PS loaded into SLN, that have shown how the incorporation of these highly hydrophobic molecules in lipid nanoparticles may increase their photostability and also their singlet oxygen production capacity [39,40]. On the other hand, it has to be noticed that the same CY previously tested in its not encapsulated form resulted in a significant phototoxic activity at 10 nM on HT-1080 [41]. Surely the higher energy fluency rates applied in the previous work (18.0 J/cm^2 versus 7.2 J/cm^2) can at least partially explain the difference in the observed results. However, this difference is probably also attributable to a cell line-dependent sensibility to PMD treatment that emerged even in the dark: indeed, HT-1080 cells showed significant cytotoxicity starting from 100 nM [41], whereas MCF-7 viability was not affected by CY till 400 nM (Fig. 5 A-II). Regarding the squaraine derivative, it was not possible to investigate its phototoxicity in the not encapsulated form because of its insolubility in aqueous solutions. However, SQ-SLN do not show any phototoxic effects at the concentration investigated (100 nM) (Fig. 5 B-I), suggesting that this nanosystem could be used as potential diagnostic tools for *in vivo* fluorescence imaging, but not as a therapeutic tool in photodynamic treatment. On the contrary, preliminary data on CY-SLN suggest that they may be tested in photodynamic treatment of some types of cancer, thanks to its negligible cytotoxicity in the dark and its moderate activity after light beam treatment, enhanced by its incorporation in lipid nanocarriers (Fig. 5 A-I and II).

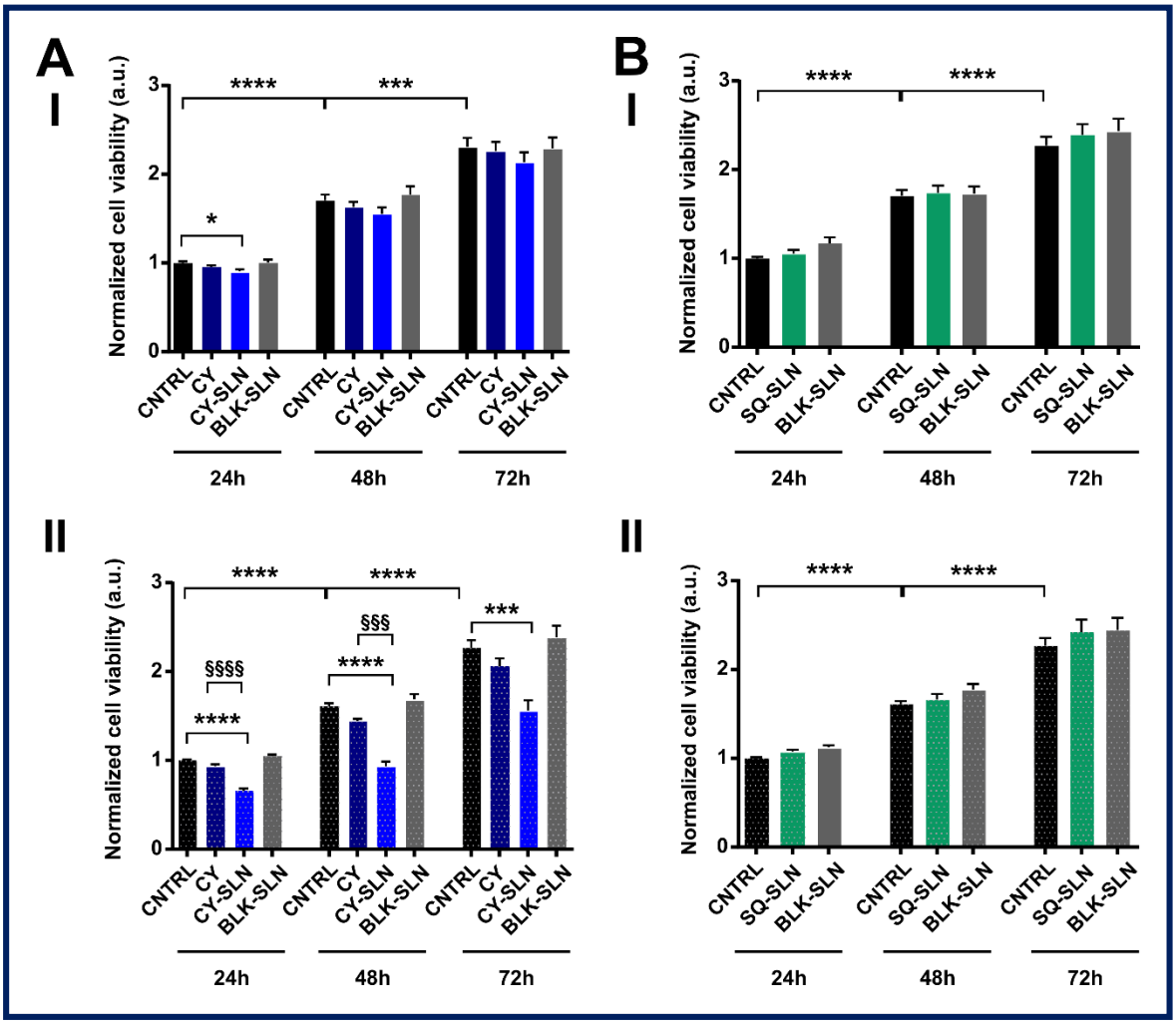

Figure 5. Dyes and dye-loaded SLN in vitro phototoxicity.

A*) Cell viability assays on MCF-7 O/N treated with 100 nM CY (in free form or encapsulated into SLN) kept in the dark (I) or 24 h, 48 h and 72 h after LED irradiation (640 nm, 7.2 J/cm^2) (II).* ***B****) Cell viability assays on MCF-7 O/N treated with 100 nM SQ (encapsulated into SLN) kept in the dark (I) and 24 h, 48 h and 72 h after LED irradiation (640 nm, 7.2 J/cm^2) (II). Data are normalized on CNTRL at 24 h and represented as mean ± SEM. Data refer to 4 independent experiments (eight replicates for each experiment). Statistical significance versus CNTRL (MCF-7 untreated with dyes): * P< 0.05, *** P< 0.001, **** P< 0.0001; statistical significance between free dyes and dye-loaded SLN: §§§ P< 0.001, §§§§ P< 0.0001 (Kruskal-Wallis test with post-hoc Dunn's test).*

6. Cell uptake and intracellular localization

As mentioned in the introduction, the development of good diagnostic and therapeutic agents in biomedicine requires a setup of positive interactions between the molecule and the cellular system. Indeed, the nanosystem must be internalized efficiently and with reasonable timing by the target cell to reach a good drug delivery performance. Therefore, we investigated the cellular uptake and the intracellular localization of SLN. The cell uptake timings of the synthesized fluorescent nanosystems were analyzed by measuring the

fluorescence intensity relative to cell lysates after incubation of MCF-7 cells with CY-SLN and SQ-SLN (dyes concentration: 100 nM) for four different incubation times (2 h, 6 h, O/N and 24 h). An efficient time-dependent accumulation of the dyes was observed in cells treated with dye-loaded SLN, with an appreciable uptake starting from 2 h in both samples (Fig. 6 A-I: CY-SLN, λ_{em} = 708 nm; Fig. 6 A-II: SQ-SLN, λ_{em} = 674 nm). CY-SLN uptake reaches a plateau after O/N incubation (Fig. 6 A-I). The tailing of the peak observed after 24 h incubation is most likely due to the presence of phenol red (λ_{em} = 674 nm at pH 7) in the culture medium. In order to compare the cell uptake of CY not encapsulated and CY-loaded SLN, we performed the same assay on MCF-7 cells treated with 100 nM of CY in culture media for four different incubation times (Fig. S3). At 100 nM, it seems that the presence of the nanocarrier slows down the internalization of the dye. Indeed, comparing Figure 6 A-I and Figure S3 A it results evident that the fluorescence intensities related to the not encapsulated dye are strongly more intense than those relating to the incorporated dye. However, it is difficult to establish a replicable ratio between the two signals because it changes with sample and biological variability (n=3).

In order to verify the effective internalization of the nanosystem into the cell, excluding the possibility that fluorescence signals recorded from cell lysates came from particles attached on the cell surface, we performed confocal laser scan microscopy experiments on MCF-7 cells treated O/N with 100 nM of dyes incorporated into SLN. The whole cellular volume was labeled using Calcein (red signals in Fig. 6 B and S3 B) and images were acquired on the three coordinates of the space (XYZ), allowing to reconstruct the 3D cellular volume and therefore to check whether dyes fluorescent signals were included within the cellular volume or not. Figure 6 B clearly shows that both types of loaded-SLN are internalized by MCF-7 after O/N incubation. Indeed, in cells treated with CY-SLN (Fig. 6 B-I) or SQ-SLN (Fig. 6 B-II) several fluorescent spots were detected (λ_{ex} = 633 nm) within the cell volume labeled with Calcein. Results obtained from samples treated with not encapsulated cyanine show, instead, a greater amount of intracellular labeling and a more widespread and delocalized signal of the dye on the entire cell volume as compared to CY-SLN (Fig. S3 B), suggesting higher internalization of the free CY. This result may be explained on one hand by the cationic nature of CY, which may promote its interaction with the cell surface and on the other hand by the overexpression of organic anion-transporting polypeptide (OATP) channels in tumor cells, which may increase its internalisation [2]. On the contrary, the incorporation of the cyanine derivative into the lipid nanoparticle not only may limit its interaction with the plasma membrane, partially masking the positive charge associated with the dye, but also alters its molecular internalization mechanism, which, in fact, in this case, is mediated by an endocytotic mechanism [56]. Finally, comparing CY (Fig. S3 B) and CY-SLN (Fig. 6 B-I) signals it is also possible to detect the greater compartmentalization of cyanine signal when incorporated within the nanoparticle system:

compared to the non-specific and diffuse signal given by the dye in its free form, incorporation into a solid lipid matrix allows to obtain a more localized signal.

It has been suggested that mitochondria are a major subcellular site for photosensitizer localization and that both cyanine and squaraine dyes localize in mitochondria organelles [2,21]. We, therefore, further investigated the subcellular localization of CY-SLN, staining MCF-7 mitochondria with MitoTracker Red (red signals in Fig. 6 C and S3 C) and evaluated its co-localization with the dye. Figure 6 C shows that CY-SLN is mainly located in close proximity to mitochondrial regions. A partial co-localization with mitochondria was observed also for not encapsulated CY as shown in Figure S3 C, although a more widespread signal of the dye on the entire cell volume was observed. These data suggest that the cyanine derivative, both in its free form and encapsulated into SLN, partially associates with the mitochondria once it has penetrated into the cells and this could be linked to its photodynamic activity (Fig. 5 A-II and [41]).

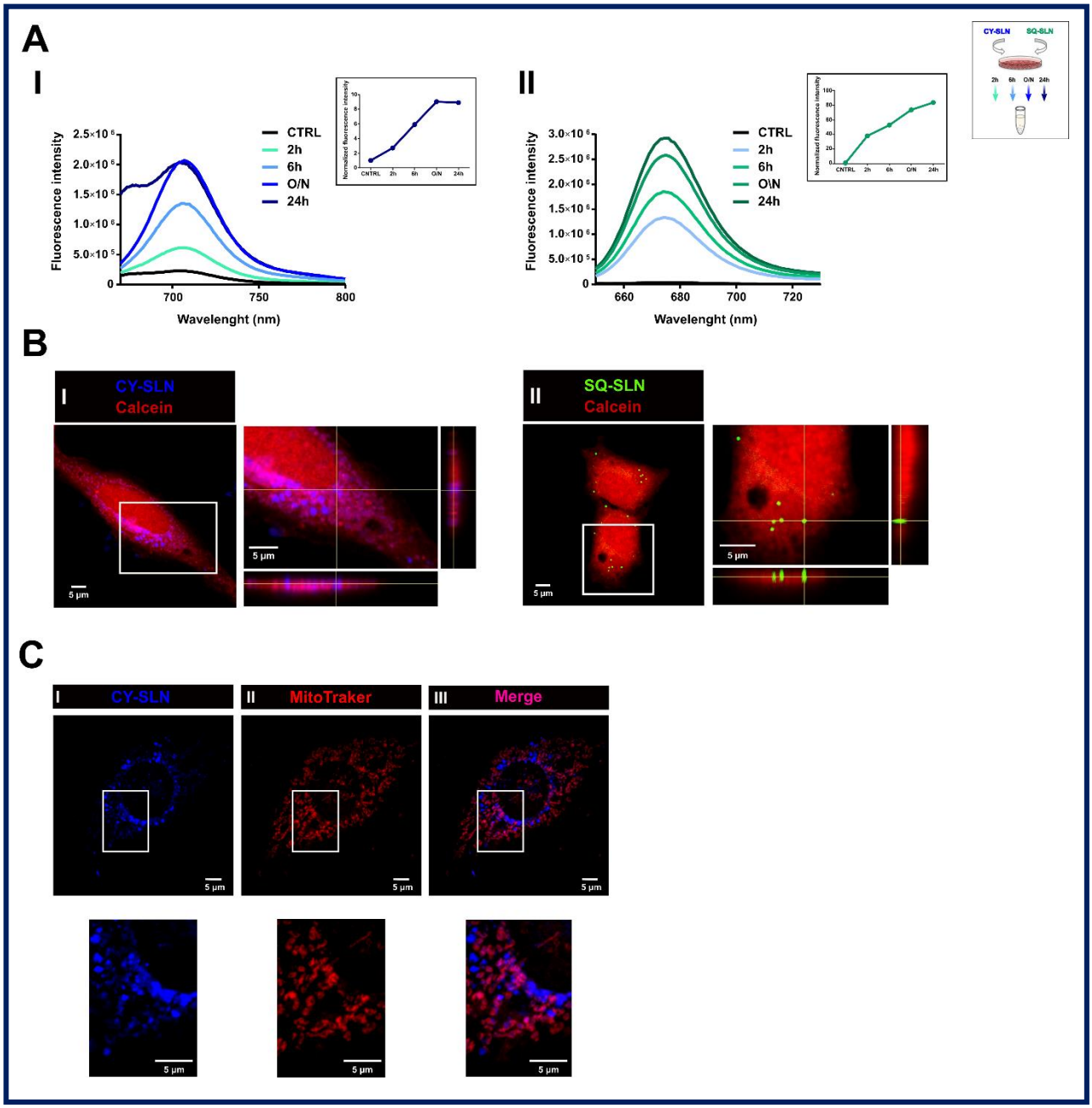

Figure 6. Dye-loaded SLN uptake and intracellular localization.

A*) Fluorescence intensity relative to MCF-7 cellular lysates after incubation with 100 nM CY-SLN (I) or SQ-SLN (II) for increasing time intervals (2 h, 6 h, O/N and 24 h). Emission spectra were recorded excitating CY-SLN and SQ-SLN at 620 and 640 nm, respectively. Insets show the trend over time of fluorescence intensity normalized on the control (untreated cells). Data refer to one representative experiment of at least three. On the right a scheme representing cell uptake assay.*

B*) Representative confocal fluorescence images of MCF-7 cells incubated O/N with either CY-SLN (I) or SQ-SLN (II) at the same concentration (100 nM). Red signal refers to calcein (excitation at 561 nm) and blue/green signal refers to CY-SLN and SQ-SLN respectively (excitation at 633 nm). For each image zoom on a region of interest (indicated by white box) with orthogonal views are reported. Scale bar: 5 µm.*

***C**) Representative confocal fluorescence images of MCF-7 cells incubated O/N with CY-SLN (100 nM). Blue signal in panel I refers to CY-SLN (excitation at 633 nm) and red signal in panel II refers to MitoTracker Red (excitation at 561); panel III: merged image of panel I and II (pink for overlapped regions); below: zoom on a region of interest indicated by white box. Scale bar: 5 µm.*

Conclusions

We successfully incorporated two polymethine dyes (a cyanine CY and a squaraine SQ) based on bromo benzoindolenine ring into SLN in order to overcome their solubility issues in aqueous solutions. Dye-loaded SLN displayed a homogeneous size of <200 nm and high entrapment efficiency, preserving dyes' excellent spectroscopic properties. This study is the first example in the literature of incorporation of a squaraine derivative into SLN, which not only allows the solubilization of this dye (completely insoluble in water), but even enhances its spectroscopic performances with higher ϕ_{fl}. These data, together with the low cytotoxicity of the system and its efficient cellular uptake, suggest that SQ-SLN may be a suitable and appealing candidate as diagnostic agent in *in vivo* optical imaging. On the other hand, CY-SLN, beyond the good optical properties shown, led to a photoactivity on MCF-7 cells. Moreover, CY-SLN seem to have a good uptake and a partial mitochondrial localization, suggesting their potential application as PS for photodynamic anticancer treatment.

In summary, SLN are a valuable delivery strategy for PMD in biomedical applications, although further investigation on *in vivo* models is needed in order to assess the real applicability of these nanosystems in both diagnostic and therapeutic fields.

Author Contributions: SV, AFP and GC conceived the study; GC synthetized nanoparticles and performed chemical characterization and cell culture experiments; GC wrote the paper and designed the figures; AG performed immunofluorescence and confocal acquisitions; NB synthetized PMD; AGP supervised SLN's synthesis and characterization, performed A4F experiments and wrote A4F results; SV, AFP, CB and PG supervised experiments. All authors revised the manuscript.

Funding: This work was supported by the University of Torino (Ricerca Locale ex-60%, Linea A, Bando 2020), by the Fondazione CRT (II tornata 2019 RF.2019.2260) and by Compagnia di San Paolo (Bando ex-post – Anno 2018).

Acknowledgments: We thank Dr. Marta Gai and the Open Lab of Advanced Microscopy at the Molecular Biotechnology Center (OLMA@MBC) for support.

Conflicts of Interest: The authors declare no conflict of interest

References

[1] X. M. Yi, F. L. Wang, W. J. Qin, X. J. Yang, and J. L. Yuan, "Near-infrared fluorescent probes in cancer imaging and therapy: An emerging field," Int. J. Nanomedicine, vol. 9, no. 1, pp. 1347–1365, 2014, doi: 10.2147/IJN.S60206.

[2] C. Shi, J. B. Wu, and D. Pan, "Review on near-infrared heptamethine cyanine dyes as theranostic agents for tumor imaging, targeting, and photodynamic therapy," J. Biomed. Opt., vol. 21, no. 5, p. 50901, 2016, doi: 10.1117/1.JBO.21.5.050901.

[3] N. Barbero, S. Visentin, and G. Viscardi, "The different kinetic behavior of two potential photosensitizers for PDT," J. Photochem. Photobiol. A Chem., vol. 299, pp. 38–43, 2015, doi: 10.1016/j.jphotochem.2014.11.002.

[4] N. Barbero, C. Butnarasu, S. Visentin, and C. Barolo, "Squaraine Dyes: Interaction with Bovine Serum Albumin to Investigate Supramolecular Adducts with Aggregation-Induced Emission (AIE) Properties," Chem. - An Asian J., vol. 14, no. 6, pp. 896–903, 2019, doi: 10.1002/asia.201900055.

[5] W. K. Moon et al., "Enhanced Tumor Detection Using a Folate Receptor-Targeted Near-Infrared Fluorochrome Conjugate," Bioconjug. Chem., vol. 14, no. 3, pp. 539–545, May 2003, doi: 10.1021/bc0340114.

[6] X. Yi et al., "IR-780 dye for near-infrared fluorescence imaging in prostate cancer," Med. Sci. Monit., vol. 21, pp. 511–517, 2015.

[7] C. Shao, C. P. Liao, P. Hu, C. Y. Chu, L. Zhang, and M. H. Bui, "Detection of live circulating tumor cells by a class of near-infrared heptamethine carbocyanine dyes in patients with localized and metastatic prostate cancer," PLoS One, vol. 9, no. 2, p. e88967 1-11, 2014.

[8] X. Yang et al., "Optical imaging of kidney cancer with novel near infra- red heptamethine carbocyanine fluorescent dyes," J. Urol., vol. 189, no. 2, pp. 702–710, 2013, doi: 10.1016/j.jneumeth.2010.08.011.Autogenic.

[9] J. B. Wu et al., "Near-infrared fluorescence imaging of cancer mediated by tumor hypoxia and HIF1alpha/OATPs signaling axis," Biomaterials, vol. 35, no. 28, pp. 8175–8185, Sep. 2014, doi: 10.1016/j.biomaterials.2014.05.073.

[10] C. Shi et al., "Heptamethine carbocyanine dye-mediated near-infrared imaging of canine and human cancers through the HIF-1alpha/OATPs signaling axis," Oncotarget, vol. 5, no. 20, pp. 10114–10126, Oct. 2014, doi: 10.18632/oncotarget.2464.

[11] R. Krejcir et al., "Anticancer pentamethinium salt is a potent photosensitizer inducing mitochondrial disintegration and apoptosis upon red light illumination," J. Photochem. Photobiol. B Biol., vol. 209, no. March, p. 111939, 2020, doi: 10.1016/j.jphotobiol.2020.111939.

[12] A. M. Rkein and D. M. Ozog, "Photodynamic therapy," Dermatol. Clin., vol. 32, no. 3, pp. 415–425, 2014, doi: 10.1016/j.det.2014.03.009.

[13] S. Luo et al., "A multifunctional heptamethine near-infrared dye for cancer theranosis," Biomaterials, vol. 34, no. 9, pp. 2244–2251, 2013.

[14] X. Tan, S. Luo, D. Wang, Y. Su, T. Cheng, and C. Shi, "A NIR heptamethine dye with intrinsic cancer targeting, imaging and photosensitizing properties," Biomaterials, vol. 33, no. 7, pp. 2230–2239, 2012, doi: 10.1016/j.biomaterials.2011.11.081.

[15] J. Atchison et al., "Iodinated cyanine dyes: a new class of sensitisers for use in NIR activated photodynamic therapy (PDT)," Chem. Commun., vol. 53, no. 12, pp. 2009–2012, 2017, doi: 10.1039/C6CC09624G.

[16] D. Ramaiah, I. Eckert, K. T. Arun, L. Weidenfeller, and B. Epe, "Squaraine dyes for photodynamic therapy: study of their cytotoxicity and genotoxicity in bacteria and mammalian cells.," Photochem. Photobiol., vol. 76, no. 6, pp. 672–677, 2002, doi: 10.1562/0031-8655(2002)076<0672:SDFPTS>2.0.CO;2.

[17] D. Ramaiah, I. Eckert, K. T. Arun, L. Weidenfeller, and B. Epe, "Squaraine Dyes for Photodynamic Therapy: Mechanism of Cytotoxicity and DNA Damage Induced by Halogenated Squaraine Dyes Plus Light (>600 nm)," Photochem. Photobiol., vol. 79, no. 1, p. 99, 2004, doi: 10.1562/0031-8655(2004)79<99:sdfptm>2.0.co;2.

[18] V. Rapozzi, L. Beverina, P. Salice, G. A. Pagani, M. Camerin, and L. E. Xodo, "Photooxidation and Phototoxicity of π-Extended Squaraines," J. Med. Chem., vol. 53, no. 5, pp. 2188–2196, Mar. 2010, doi: 10.1021/jm901727j.

[19] R. R. Avirah, D. T. Jayaram, N. Adarsh, and D. Ramaiah, "Squaraine dyes in PDT: from basic design to in vivo demonstration," Org. Biomol. Chem., vol. 10, no. 5, pp. 911–920, 2012, doi: 10.1039/C1OB06588B.

[20] M. S. Soumya, K. M. Shafeekh, S. Das, and A. Abraham, "Symmetrical diiodinated squaraine as an efficient photosensitizer for PDT applications: Evidence from photodynamic and toxicological aspects," Chem. Biol. Interact., vol. 222, pp. 44–49, 2014, doi: 10.1016/j.cbi.2014.08.006.

[21] L. Serpe et al., “Squaraines bearing halogenated moieties as anticancer photosensitizers: Synthesis, characterization and biological evaluation,” Eur. J. Med. Chem., vol. 113, pp. 187–197, 2016, doi: 10.1016/j.ejmech.2016.02.035.

[22] D. Ramaiah, A. Joy, N. Chandrasekhar, N. V. Eldho, S. Das, and M. V. George, “Halogenated Squaraine Dyes as Potential Photochemotherapeutic Agents. Synthesis and Study of Photophysical Properties and Quantum Efficiencies of Singlet Oxygen Generation,” Photochem. Photobiol., vol. 65, no. 5, pp. 783–790, 1997, doi: 10.1111/j.1751-1097.1997.tb01925.x.

[23] N. Lange, W. Szlasa, J. Saczko, and A. Chwiłkowska, “Potential of cyanine derived dyes in photodynamic therapy,” Pharmaceutics, vol. 13, no. 6, pp. 1–17, 2021, doi: 10.3390/pharmaceutics13060818.

[24] K. Ilina, W. M. MacCuaig, M. Laramie, J. N. Jeouty, L. R. McNally, and M. Henary, “Squaraine Dyes: Molecular Design for Different Applications and Remaining Challenges,” Bioconjugate Chemistry, vol. 31, no. 2. pp. 194–213, 2020, doi: 10.1021/acs.bioconjchem.9b00482.

[25] S. Sreejith, P. Carol, P. Chithra, and A. Ajayaghosh, “Squaraine dyes: a mine of molecular materials,” J. Mater. Chem., vol. 18, pp. 264–274, 2008.

[26] H. O. Dickinson, “The aggregation of cyanine dyes in aqueous solution,” Trans. Faraday Soc., vol. 43, pp. 486–491, 1947, doi: 10.1039/TF9474300486.

[27] E. E. Jelley, “Spectral Absorption and Fluorescence of Dyes in the Molecular State,” Nature, vol. 138, pp. 1009–1010, 1936, doi: 10.1038/1381009a0.

[28] G. Alberto et al., “Solid silica nanoparticles as carriers of fluorescent squaraine dyes in aqueous media: Toward a molecular engineering approach,” Colloids Surfaces A Physicochem. Eng. Asp., vol. 568, no. January, pp. 123–130, 2019, doi: 10.1016/j.colsurfa.2019.01.052.

[29] I. Miletto et al., “Mesoporous silica nanoparticles incorporating squaraine-based photosensitizers: A combined experimental and computational approach,” Dalt. Trans., vol. 47, no. 9, pp. 3038–3046, 2018, doi: 10.1039/c7dt03735j.

[30] A. Kirchherr, A. Briel, and K. Ma, “Stabilization of Indocyanine Green by Encapsulation within Micellar Systems,” Mol. Pharm., vol. 6, no. 2, pp. 480–91, 2009.

[31] S. Sreejith et al., “Near-Infrared Squaraine Dye Encapsulated Micelles for in Vivo Fluorescence and Photoacoustic Bimodal Imaging,” ACS Nano, vol. 9, no. 6, pp. 5695–5704, 2015, doi: 10.1021/acsnano.5b02172.

[32] D. Zhang et al., “Nano-confined squaraine dye assemblies: New photoacoustic and near-infrared fluorescence dual-modular imaging probes in vivo,” Bioconjug. Chem., vol. 25, no. 11, pp. 2021–2029, 2014, doi: 10.1021/bc5003983.

[33] I. Texier et al., “Cyanine-loaded lipid nanoparticles for improved in vivo fluorescence imaging,” J. Biomed. Opt., vol. 14, no. 5, pp. 054005 1–11, 2009, doi: 10.1117/1.3213606.

[34] A. Jacquart et al., “LipImageTM 815: novel dye-loaded lipid nanoparticles for long-term and sensitive in vivo near-infrared fluorescence imaging,” J. Biomed. Opt., vol. 18, no. 10, pp. 101311 1–9, 2013, doi: 10.1117/1.JBO.18.10.101311.

[35] J. Mérian, R. Boisgard, P. A. Bayle, M. Bardet, B. Tavitian, and I. Texier, “Comparative biodistribution in mice of cyanine dyes loaded in lipid nanoparticles,” Eur. J. Pharm. Biopharm., vol. 93, pp. 1–10, 2015, doi: 10.1016/j.ejpb.2015.03.019.

[36] S. Morel, E. Terreno, E. Ugazio, S. Aime, and M. R. Gasco, “NMR relaxometric investigations of solid lipid nanoparticles (SLN) containing gadolinium (III) complexes,” Eur. J. Pharm. Biopharm., vol. 45, no. 2, pp. 157–163, 1998.

[37] J. Gravier et al., “Lipidots: competitive organic alternative to quantum dots for in vivo fluorescence imaging,” J. Biomed. Opt., vol. 16, no. 9, pp. 096013 1–10, 2011, doi: 10.1117/1.3625405.

[38] N. Yadav, S. Khatak, U. Vir, and S. Sara, “Solid lipid nanoparticles - a review,” Int. J. Appl. Pharm., vol. 5, no. 2, pp. 8–18, 2013.

[39] A. M. Lima et al., “Hypericin encapsulated in solid lipid nanoparticles: Phototoxicity and photodynamic efficiency,” J. Photochem. Photobiol. B Biol., vol. 125, pp. 146–154, 2013, doi: 10.1016/j.jphotobiol.2013.05.010.

[40] F. P. Navarro et al., “Preparation and characterization of mTHPC-loaded solid lipid nanoparticles for photodynamic therapy,” J. Photochem. Photobiol. B Biol., vol. 130, pp. 161–169, 2014, doi: 10.1016/j.jphotobiol.2013.11.007.

[41] B. Ciubini, S. Visentin, L. Serpe, R. Canaparo, A. Fin, and N. Barbero, “Design and synthesis of symmetrical pentamethine cyanine dyes as NIR photosensitizers for PDT,” Dye. Pigment., vol. 160, pp. 806–813, 2019, doi: 10.1016/j.dyepig.2018.09.009.

[42] M. R. Gasco, L. Priano, G. P. Zara, and H. S. S., “Solid lipid nanoparticles and microemulsions for drug delivery: The CNS,” in Progress in Brain Research, Elsevier, 2009, pp. 181–192.

[43] E. Ugazio, R. Cavalli, and M. R. Gasco, “Incorporation of cyclosporin A in solid lipid nanoparticles (SLN),” Int. J. Pharm, vol. 241, pp. 341–344, 2002.

[44] "ICH guideline Q3C (R6) on impurities: guideline for residual solvents.," in European Medicine Agency, 2016.

[45] A. González-Paredes et al., "Solid lipid nanoparticles for the delivery of anti-microbial oligonucleotides," Eur. J. Pharm. Biopharm., vol. 134, no. November 2018, pp. 166–177, 2019, doi: 10.1016/j.ejpb.2018.11.017.

[46] N. Barbero et al., "Microwave-Assisted Synthesis of Near-Infrared Fluorescent Indole-Based Squaraines," Org. Lett., vol. 17, no. 13, pp. 3306–3309, 2015, doi: 10.1021/acs.orglett.5b01453.

[47] F. Yuan et al., "Vascular permeability in a human tumor xenograft: molecular size dependence and cutoff size.," Cancer Res., vol. 55, no. 17, pp. 3752–6, Sep. 1995.

[48] D. Peer, J. M. Karp, S. Hong, O. C. Farokhzad, R. Margalit, and R. Langer, "Nanocarriers as an emerging platform for cancer therapy," Nat. Nanotechnol., vol. 2, no. 12, pp. 751–760, 2007, doi: 10.1038/nnano.2007.387.

[49] P. L. Turecek, M. J. Bossard, F. Schoetens, and I. A. Ivens, "PEGylation of Biopharmaceuticals: A Review of Chemistry and Nonclinical Safety Information of Approved Drugs," J. Pharm. Sci., vol. 105, no. 2, pp. 460–475, 2016, doi: 10.1016/j.xphs.2015.11.015.

[50] M. Üner and G. Yener, "Importance of solid lipid nanoparticles (SLN) in various administration routes and future perspective," Int. J. Nanomedicine, vol. 2, no. 3, pp. 289–300, 2007.

[51] M. A. Schubert and C. C. Muller-Goymann, "Characterisation of surface-modified solid lipid nanoparticles (SLN): Influence of lecithin and nonionic emulsifier," Eur J Pharm Biopharm, vol. 61, no. 1–2, pp. 77–86, 2005, doi: 10.1016/j.ejpb.2005.03.006.

[52] G. Lollo, A. Gonzalez-paredes, M. Garcia-fuentes, P. Calvo, D. Torres, and M. J. Alonso, "Polyarginine Nanocapsules as a Potential Oral Peptide Delivery Carrier," J. Pharm. Sci., vol. 106, no. 2, pp. 611–618, 2017, doi: 10.1016/j.xphs.2016.09.029.

[53] A. Zattoni, B. Roda, F. Borghi, V. Marassi, and P. Reschiglian, "Flow field-flow fractionation for the analysis of nanoparticles used in drug delivery," J. Pharm. Biomed. Anal., vol. 87, pp. 53–61, 2014, doi: 10.1016/j.jpba.2013.08.018.

[54] F. Caputo et al., "Measuring Particle Size Distribution by Asymmetric Flow Field Flow Fractionation: A Powerful Method for the Preclinical Characterization of Lipid-Based Nanoparticles," Mol. Pharm., vol. 16, no. 2, pp. 756–767, 2019, doi: 10.1021/acs.molpharmaceut.8b01033.

[55] O. A. Mass et al., "Exciton Delocalization in Indolenine Squaraine Aggregates Templated by DNA Holliday Junction Scaffolds," Journal of Physical Chemistry B, vol. 124, no. 43. pp. 9636–9647, 2020, doi: 10.1021/acs.jpcb.0c06480.

[56] T. G. T. Iversen, T. Skotland, and K. Sandvig, "Endocytosis and intracellular transport of nanoparticles: Present knowledge and need for future studies," Nano Today, vol. 6, no. 2, pp. 176–185, 2011, doi: 10.1016/j.nantod.2011.02.003.

Supplementary Materials

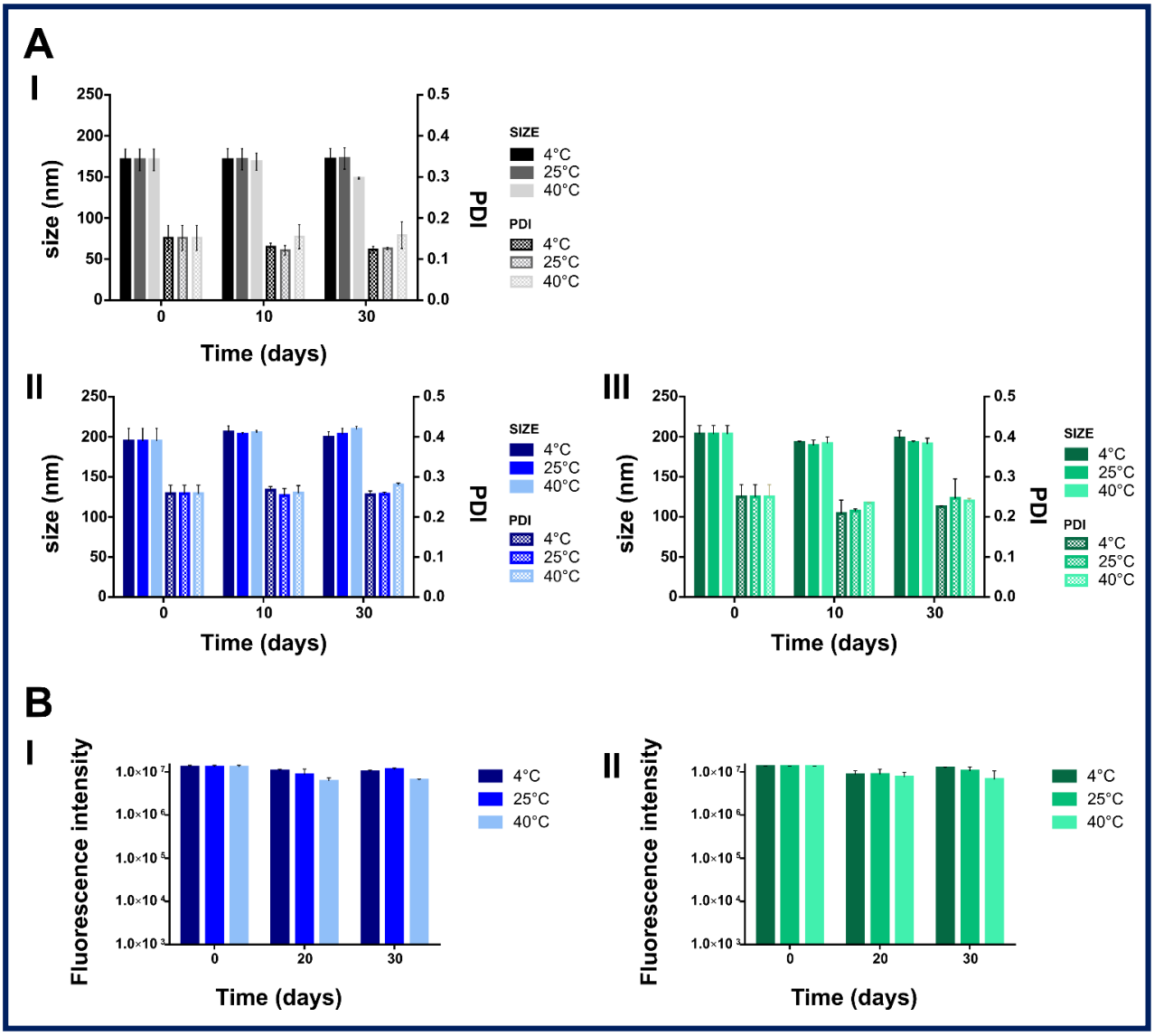

Figure S1. SLN stability.

A*) Change overtime of size and PDI of BLK-SLN (I), CY-SLN (II) and SQ-SLN (III) at three different storage temperature (4°C, 25°C and 40°C).* ***B****) Change overtime of fluorescence intensity of CY-SLN (I) and SQ-SLN (II). Data are expressed as mean ± SEM (n=3).*

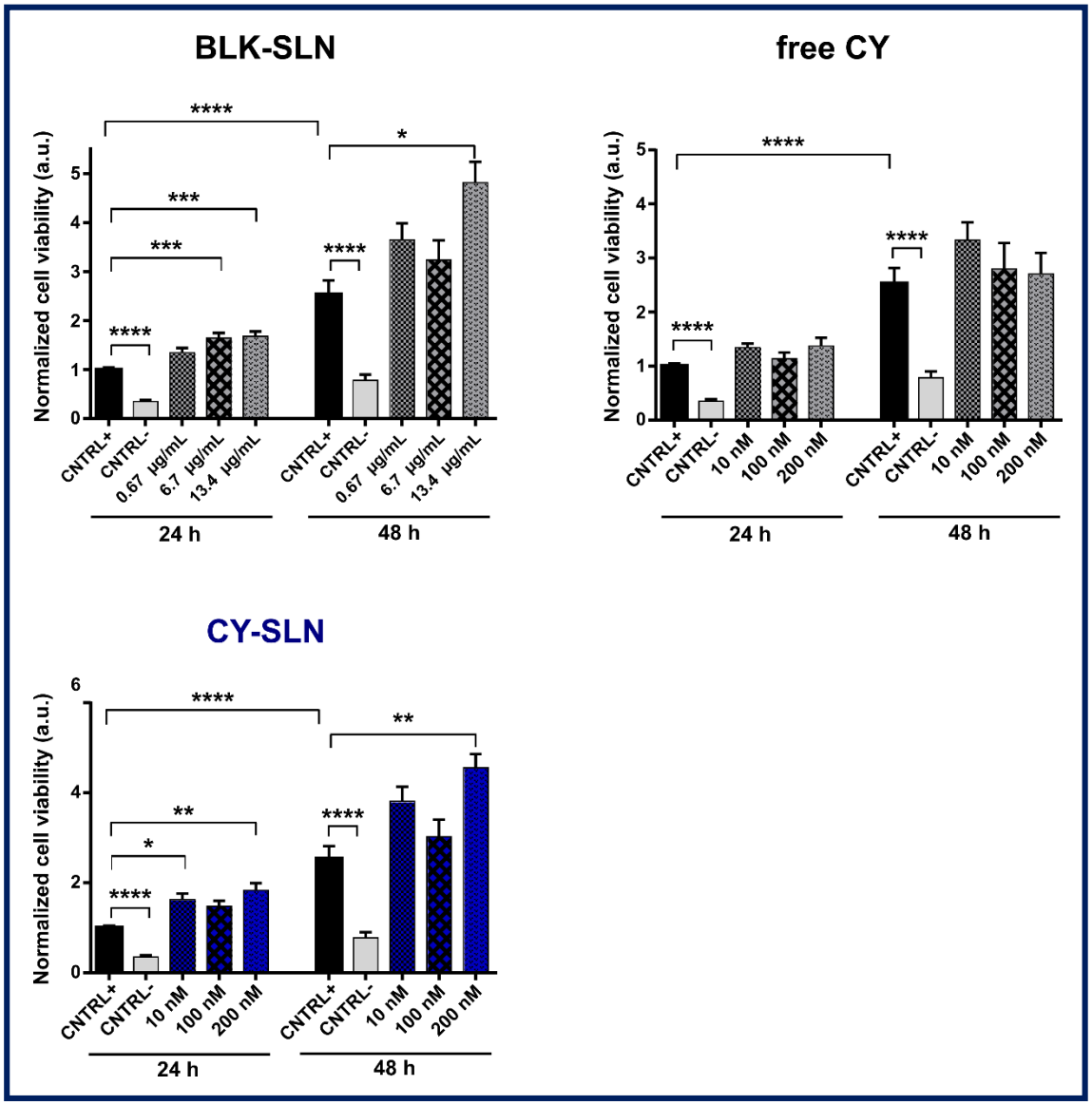

Figure S2. In vitro cytotoxicity of CY-SLN and SQ-SLN on HMEC.

*Cell viability assays on HMEC 24 h and 48 h after treatment with different concentrations of BLK-SLN, free CY and CY-SLN. For dye-loaded SLN concentrations refer to dyes incorporated into SLN (from 10 to 200 nM) whereas for BLK-SLN concentrations refer to phosphatidylcholine content ([PC] from 0.67 to 13.4 µg/mL corresponding to that of loaded-SLN tested. Data are normalized on CNTRL+ at 24 h and are represented as mean ± SEM. Data refer to at least 3 independent experiments (eight replicates for each experiment). Statistical significance versus CNTRL+ (HMEC untreated with dyes): *** P< 0.001, **** P< 0.0001 (Kruskal-Wallis test with post-hoc Dunn's test).*

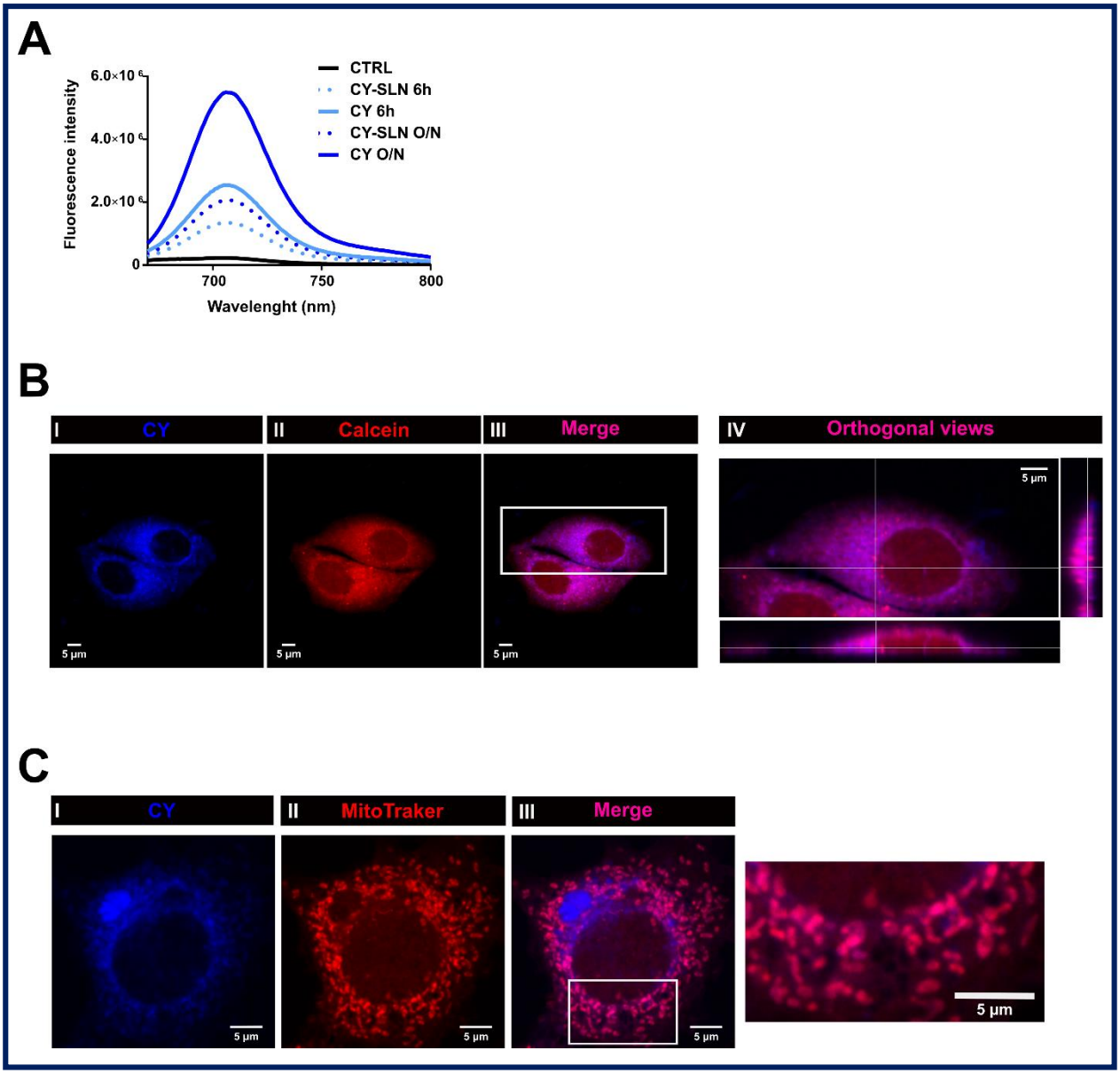

Figure S3. CY uptake and intracellular localization.

A*) Fluorescence intensity relative to MCF-7 cellular lysates after incubation with either CY (continuous lines) or CY-SLN (dot lines) at the same concentration (100 nM) for two different time intervals (6 h and O/N). Data refer to one representative experiment of three.*

B*) Representative confocal fluorescence images of MCF-7 cells incubated O/N with CY (100 nM). Blue signal in panel I refers to dye-loaded SLN (excitation at 633 nm) and red signal in panel II refers to Calcein (excitation at 561 nm); panel III: merged image of panel I and II (pink for overlapped regions); panel IV: zoom on panel III with orthogonal views. Scale bar: 5 µm.*

C*) Representative confocal fluorescence images of MCF-7 cells incubated O/N with CY (100 nM). Blue signal in panel I refers to CY (excitation at 633 nm) and red signal in panel II refers to MitoTracker Red (excitation at 561); panel III: merged image of panel I and II (pink for overlapped regions) with zoom on a region of interest (indicated by white box). Scale bar: 5 µm.*

2022 Elsevier B.V. All rights reserved.

"Quatsomes as powerful nanovesicles for Photodynamic Therapy"

Nicolò Bordignon[a,b], Mariana Kober[b], **Giorgia Chinigò**[a], Carlotta Pontremoli[c], Ettore Sansone[a], Maria Jesus Moran Plata[c], Alessandra Fiorio Pla[a], Nadia Barbero[c*], Judit Morlà[b*], Nora Ventosa[b]

[a] University of Torino, Department of Life Sciences and Systems Biology, Via Accademia Albertina 13, 10123 Turin, Italy

[b] Institut de Ciència de Materials de Barcelona (ICMAB-CSIC), 08193 Bellaterra, Spain

[c] University of Torino, Department of Chemistry, NIS Interdepartmental Centre and INSTM Reference Centre, Via Quarello 15a, 10135, Turin, Italy

[*] equal contribution

Manuscript in preparation

Introduction

Photodynamic Therapy (PDT) is a minimally invasive localized clinical treatment which has been developed in order to treat many diseases including several types of cancer. PDT is based on the presence of three components: a photosensitizer (PS), light and molecular oxygen. Its studies on cells and animals started in 1960s and led to the clinical approval by the FDA of the first photosensitizer, Photophrin, in 1995. [1] [2] In PDT PSs are exposed to light at a specific wavelength, depending on the nature of the molecule in use. After the irradiation, the light is absorbed by the PS, causing the conversion from its ground state (singlet state) to an excited singlet state. Then, the PS can lose energy and return to the ground state or, alternatively, the singlet state can undergo intersystem crossing (ISC), with the formation of an excited triplet state, caused by spin conversion of the electron in the higher energy orbital. From this triplet state the molecule can relax and go back to the singlet state via two different routes: 1) the molecule can reduce the substrate forming radicals, which then reacts with oxygen producing oxygenated radicals (Reactive Oxygen Species, ROS), known as Type I reaction, or 2) the PS can react directly with molecular oxygen, producing singlet oxygen ($^1O_2$), known as Type II reaction [3]. These reactions also explain the importance of oxygen's presence in PDT. Both products then react with cells leading them to apoptosis or necrosis, causing damages in tumor-associated vascular structures and contributing to stimulate the immune response in the host [4] [5].

It is therefore clear the paramount importance of the choice of the right PS. An ideal PS must be non-cytotoxic in the dark but highly cytotoxic after selective irradiation, photo- and chemically stable, non-mutagenic, selective against neoplastic tissues, present an high degree of purity and should absorb light between 600 and 800 nm to promote a deeper tissue penetration and minimize light scattering by tissues [6] [7]. Many PSs have been approved for clinical use during the last 25 years and are now commercialized for different applications *(Photofrin, Ameluz, Metvix, Foscan, Laserphyrin, Visudyne and Redaporfin)* and many others are under clinical trial [8,9]. Even if many of these approved molecules show a porphyrin-based structure, at present different molecules such as Squaraine dyes and Cyanine dyes [10, 11, 12] have been shown to have improved characteristics and can represent promising alternatives as PSs. These molecules show longer absorption wavelengths, higher selectivity and higher purity compared to the so-called "first generation PSs" such as Photofrin [8]. Moreover Squaraines have been proved to have an high clearance rate *in vivo* and good selectivity against neoplastic tissues [10].

Despite the important advances made in the development of improved molecules and formulations, targeting PSs to tumors to avoid the damage of surrounding tissues remains a big challenge. Furthermore, PSs often show high photosensitivity and low hydrophilicity, leading them respectively to photodegradation and aggregation in aqueous media [13]. In order to improve the PSs performances and to protect the

molecules from photodegradation, many conjugation strategies have been tested, leading to the development of several delivery systems, including both organic and inorganic nanoparticles [14].
Regarding organic nanoparticles, the research has been mainly focused on liposomes and polymeric micelles. These vesicles' components form amphiphilic structures in water, enabling the encapsulation of the PS in the hydrophobic core and improving their solubility by exposing their hydrophilic surface to the aqueous environment. Moreover, the carrier can be functionalized with targeting agents, [15-19] or exploit passive targeting with enhanced permeation and retention effect (EPR) [20], leading to a selectivity improvement and providing good results in PDT efficiency. However, one of the main problems of lots of these formulations is represented by the lack of stability over time [21]. Since many vesicles, like liposomes, tend to change morphology and leak the PS over time, they require complex formulations and coatings [22] to overcome these aspects.

To this end, in the present work we employed a different nanovesicle system, namely Quatsomes (QS), as nanocarriers. QS are thermodynamically stable monodispersed nanometric vesicles composed by sterols and quaternary ammonium surfactants [23]. These sterols and surfactants self-assemble in water, forming amphiphilic spherical nanometric structures with high homogeneity. This kind of vesicles has been proved to remain stable for years [23, 24, 25], representing a promising nanocarrier able to overcome stability problems. As a first trial, a well-performing squaraine in PDT, **Br-Sq-C4**, already tested in a previous study by some of us, has been used as a photosensitizer and incorporated inside QSs. The amount of the incorporated dye resulted too low and almost no effect on cell viability was observed. Moreover, some problems correlated to the dye leaking from the nanosystem were also detected. Therefore, to improve the formulation and the PDT activity, we designed and synthesized a similar squaraine bearing longer alkyl chains, i.e. **Br-Sq-C12**, improving its compatibility with the longer chains of the surfactants and thus the incorporation efficiency. Thus, we have prepared QS composed of Cholesterol (Chol) and Sterealkonium Chloride (STK) at different concentrations of **Br-Sq-C12**. These formulations have been proved to have high dye loading efficiency even at the higher tested concentrations. This incorporation efficiency can enable the use of lower amounts of nanovesicles since they can carry higher PSs concentrations, lowering the carriers' cytotoxicity due to the presence of quaternary ammonium surfactants. The formulations under study have been characterized and interrogated *in vitro* for the cytotoxicity and PDT efficiency.

Materials and Methods

Synthesis of Br-Sq-C12 dye

All the chemicals were purchased from Merck, Alfa Aesar or TCI and were used without any further purification. All microwave reactions were performed in single-mode Biotage Initiator 2.5. TLC were performed on silica gel 60 F254 plates. ^{1}H NMR (600 MHz) spectra were recorded on a Bruker Avance 600 NMR in $CDCl_3$.

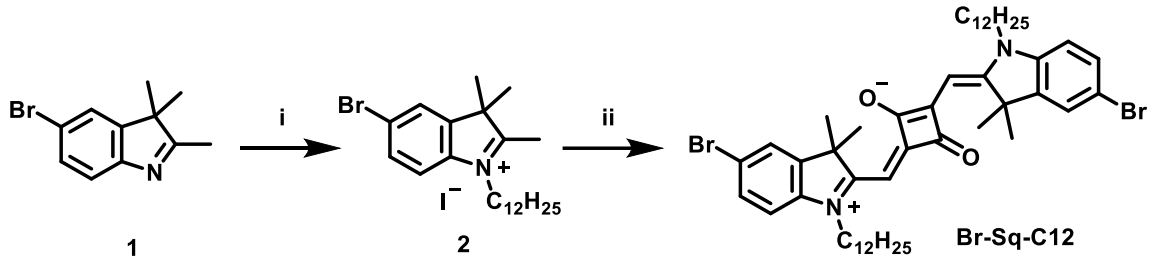

Scheme 1. Synthesis of Br-Sq-C12 dye. *(i) anhydrous acetonitrile, iodododecane, MW, 60 min, 155 °C; (ii) squaric acid, toluene/n-butanol (1:1), MW, 30 min, 160 °C.*

Quaternarization synthesis of indolenine 5-bromo-1-dodecyl-2,3,3-trimethyl-3H-indol-1-ium iodide

5-bromo-2,3,3-trimethyl-3H-indole (**1**) (500 mg, 2.1 mmol), iodododecane (1.6 mL, 6.3 mmol) and anhydrous acetonitrile (10 mL) were introduced in a reaction vial, sealed with a crimp cap and heated in microwave system at 155 °C for 60 min. At the end of the reaction, acetonitrile was removed in the rotavapor and diethyl ether (200 mL) was then poured to precipitate a white-brownish solid which was washed with diethyl ether and filtered (287 mg, 25.5 % yield).

^{1}H NMR (600 MHz, $CDCl_3$): δ 7.78 (dd, J = 8.6, 1.8 Hz, 1H), 7.73 (d, J = 1.8 Hz, 1H), 7.57 (d, J = 8.6 Hz, 1H), 4.65 (t, 2H), 2.99 (s, 3H), 1.68 (s, 6H), 1.24 (m, 20H), 0.87 (t, J = 7.0 Hz, 3H).

^{13}C NMR The compound solubility proved too low to record a ^{13}C NMR spectrum.

Synthesis of Br-Sq-C12

Compound 2 (287 mg, 0.54 mmol), 4-dihydroxycyclobut-3-ene-1,2-dione (30.8 mg, 0.27 mmol) and 5 mL of a mixture of toluene and n-butanol (1:1) were introduced inside a sealed MW vial and heated up to 160 °C for 30 min. The solution turned blue, and the TLC (Pet. Ether:Acetone 8:2) showed reaction completion. After solvent evaporation, a column chromatography (Pet. Ether:Acetone 70:30) afforded **Br-Sq-C12** as a golden solid (140 mg, yield=60%).

^{1}H NMR (600 MHz, $CDCl_3$): δ 7.44 (s, 2H), 7.41 (d, J = 8.3 Hz, 2H), 6.83 (d, J = 8.3 Hz, 2H), 5.94 (s, 2H), 3.92 (s, 4H), 1.77 (s, 12H), 1.24 (m, 40H), 0.87 (t, J = 6.9 Hz, 6H).

^{13}C NMR The compound solubility proved too low to record a ^{13}C NMR spectrum.

Synthesis of Dye-loaded Chol/Stk QS by DELOS-susp

All the formulations described were prepared using the DELOS-susp method [26]. In every preparation 80.40 mg of Cholesterol (PanReac ApplyChem) and 85.50 mg of Stearalkonium (TokyoChemical Industry CO. LTD) (ratio 1:1) were added to the organic phase, composed of ethanol (HPLC grade purity, Avantor Performance Materials Poland S.A.) and a solution of dye in ethanol to reach a total concentration of dye of 200 and 300 µM, in a total volume of organic phase of 3.11 mL. Then CO_2 in the supercritical state was added into the reactor (7.3 mL of volume) to obtain a single-phase solution. After 1 h the solution was depressurized in 25.11 mL of water MilliQ.

The ethanol and the not-incorpored dye were removed by diafiltration, using the KrosFlo® Research IIi TFF System (KR2i) (Repligen, Waltham USA). The column in use was a 100 kDa cut-off mPES hollow fibber column (C04-E100-05-N & C02-E100-05-N, Repligen, Waltham, USA).

Determination of the Dye concentration and loading in Dye-loaded QS

The concentration of dye entrapped in QS was determined by measuring the UV-vis absorbance using an UV-vis spectrophotometer (V-780, Jasco) and a high precision cell (Hellma Analytics) with a pathlength of 1 cm. All the samples were diluted in ethanol in order to disrupt the membrane and release all the entrapped dye molecules. The concentration of **Br-Sq-C12** was determined using the Lambert-Beer law (A = ε l C), knowing that ε (**Br-Sq-C12**) in EtOH = 290484 M^{-1} cm^{-1}.

The dye-loading coefficient was determined by lyophilization of the samples (LyoQuest-80, Telstar) at 193 K and 5 Pa for 5 days. Then the samples were weighted and the loading in mass was determined through Equation 1.

$$dye\ loading = \frac{mass\ of\ dye}{mass\ weighted - mass\ of\ dye}$$

Spectroscopic characterization of free Br-Sq-C12 and Dye-Loaded QSs

UV–Vis spectroscopy

UV–Vis spectra were recorded on a Cary 300 Bio spectrophotometer (Varian, Santa Clara, CA, USA) and a V-780 (Jasco), by using solvents with different polarity in order to investigate the solvatochromic behavior of both the **Br-Sq-C12** and Dye-Loaded QSs. UV–Vis measurements were carried out in the range of 500–800

nm using quartz cuvettes (1 cm pathway length) and were recorded at room temperature. The powders were solubilized and analyzed after proper dilutions in acetone, absolute ethanol (EtOH), methanol (MeOH), double distilled water (ddH_2O) and Dimethyl sulfoxide (DMSO).

Determination of molar extinction coefficient

In order to evaluate the molar extinction coefficient of the Br-Sq-C12, a stock solution (0.5 mM) in Ethanol was prepared and then different diluted solutions were obtained by taking proper aliquots of the stock solution. The diluted solutions were measured by UV–Vis spectroscopy (Cary 300 Bio spectrophotometer) in the range of 500–800 nm using quartz cuvettes with a 1 cm pathway length.

The absorbance intensities of each solution at the λ_{max} were plotted versus the sample concentration. A linear fit was applied to determine the molar extinction coefficient (ε) as the slope of the line. The analysis was performed in duplicate. The obtained data were considered acceptable when the difference between the measured log ε was less or equal to 0.02 in respect to their average.

Fluorescence spectroscopy

Fluorescence emission measurements were acquired in steady state mode and recorded in the range of 595–750 nm using a Horiba Jobin Yvon Fluorolog 3 TCSPC fluorimeter equipped with a 450-W Xenon lamp and a Hamamatsu R928 photomultiplier, by using solvents with different polarity in order to investigate the solvatochromic behavior of both the Br-Sq-C12 and Dye-Loaded QS. The excitation wavelength was different depending on the solvents and was set at the squaraine hypsochromic shoulder previously recorded at the UV–Vis spectra. The powders were solubilized and analyzed after proper dilutions in acetone, absolute ethanol (EtOH), methanol (MeOH), double distilled water (ddH_2O) and Dimethyl sulfoxide (DMSO).

The excitation and emission slits were 5 nm and 5 nm, respectively.

Fluorescence quantum yields (QY) were determined using the same instrument with Quanta-ϕ integrating sphere and De Mello method. The QY were evaluated in absolute Ethanol for the Br-Sq-C12 and in ddH_2O for the Dye-Loaded QSs.

Diluted solutions with absorbance around or lower of 0.1 units were used to avoid the presence of aggregates. The final result is an average of three independent measurements of different dye solutions.

Fluorescence lifetimes (LT) were measured by the time correlated single photon counting method (Horiba Jobin Yvon) using a 636 nm Horiba Jobin Yvon NanoLED as excitation source and an impulse repetition frequency of 1 MHz positioned at 90° with respect to a TBX-04 detector. Lifetimes were calculated using DAS6 decay analysis software. The LT were evaluated in absolute Ethanol for the Br-Sq-C12 and in ddH_2O for the Dye-Loaded QSs.

Physicochemical Characterization and stability of Dye-Loaded QS

Dynamic Light Scattering (DLS)

The mean size and size distribution of the QS loaded with Br-Sq-C12 200 and 300 µM (QS_Sq_200 and QS_Sq_300) were determined by DLS using a Zetasizer Ultra (Malvern Instruments). All the measurements were performed using a fluorescence filter in order to avoid the light absorbance by the samples since the instrument exploits a 633 nm laser.

By analyzing the fluctuations of light scattered, the diffusion coefficient (D) of the particles was determined, and then, using the Stokes-Einstein equation (Equation 2), their hydrodynamic diameter (d_h) was calculated, with the Boltzmann constant (k), the temperature (T), and the viscosity of the solvent (η).

$$D = \frac{kT}{3\pi\eta d_h}$$

Equation 2 – Stokes-Einstein equation

DLS also provides the so-called "polydispersity index" (PDI), which is related to the standard deviation of the gaussian distribution of the nanoparticles population.

All the measurements were performed in triplicate to ensure the reliability of the results.

Electrophoretic Light Scattering (ELS)

ζ-potential (z-pot) measurements were performed with a Zetasizer Ultra (Malvern Instruments) using an incident light ray at 633 nm and measuring the scattered light at 13°. A DTS1070 folded capillary cell (Malvern Instruments) was used, applying a voltage of 40 mV between the gold electrodes.

The z-pot value (ζ) was calculated using the Helmholts-Smoluchowski equation (Equation 3), which employs the relative permittivity of the electrolyte solution (ε_{rs}), the electric permittivity of vacuum (ε_0), and the viscosity (η) of the dispersant.

$$U_e = \frac{\varepsilon_{rs}\varepsilon_0\zeta}{\eta}$$

Equation 3 - Helmholts-Smoluchowski equation

All the measurements were performed in triplicate to ensure the reliability of the results.

Cryogenic transmission electron microscopy

Cryogenic transmission electron microscopy (cryo- TEM) images were acquired with a JEOL JEM microscope (JEOL JEM 2011) operating at 200 kV under low-dose conditions.

The sample was deposited onto the holey carbon grid and then was immediately vitrified by rapid immersion in liquid ethane. The vitrified sample was mounted on a cryo-transfer system (Gatan 626) and introduced into the microscope. Images were recorded on a CCD camera (Gatan Ultrascan US1000).

We performed Cryo-TEM in order to confirm the data obtained during the physicochemical characterization of the samples. Working in cryogenic conditions allowed us to preserve the stability and the physicochemical characteristics of the samples thanks to the process of vitrification [27] of the samples in liquid nitrogen.

Having microscopic images of the samples also allowed us to measure the real nanoparticles' diameters, since DLS can only provide hydrodynamic diameters values. Hydrodynamic diameters values differs from real diameters values because the first parameter takes in account the solvation sphere that forms around the particles due to the surface charge and the ions present in solution [28] [29].

The images were analyzed with the Digital Micrograph 1.8 software.

We used the software Fiji ImageJ 1.52a (Bethesda) to measure the real particles' diameters and to edit them. The geometric diameter of the Quatsomes was measured by analyzing more than 150 single vesicles for each sample using Fiji ImageJ 1.52a.

Evaluation of ROS generation ability with DPBF and DCFH

1,3-Diphenylisobenzofuran (DPBF) was used as scavenger molecules to evaluate Reactive Oxygen Species (ROS) generation, by following the protocol previously described in the literature. In fact, DPBF rapidly reacts with $^1O_2$ forming the colourless *o*-dibenzoylbenzene derivative. The $^1O_2$ scavenger activity can be monitored through a decrease in the electronic absorption band of DBPF at 415 nm. Stock solutions were prepared in DMSO, absolute ethanol and phosphate buffer (2 mM, pH 7.4) respectively for DPBF, Br-Sq-C12 and QS_Sq_300. Each solution was then diluted in phosphate buffer (2 mM, pH 7.4) to obtain the final desired concentration (25 µM for DPBF, 2.5 µM for Squaraine and the proper amount of QS_Sq_300 containing 2.5 µM of Squaraine), placed in a 1 cm quartz cell and irradiated at various time intervals under stirring in an aerated solarbox (Solarbox 3000e, 250 W xenon lamp, CO.FO.ME.GRA). Light was filtered in an optical filter with a 515 nm cut-off, to avoid the DPBF degradation. At predefined time points (30, 60, 90, 120 and 180 sec) absorption spectra were recorded on a Cary 300 Bio spectrophotometer instrument. The decrease in the DBPF absorption contribution at 415 nm was plotted as a function of the irradiation time.

Biological Assays

Cell culture, cell viability and photo-toxicity assay

Human Breast Adenocarcinoma cell line (MCF-7, ECACC) was cultured in DMEM High Glucose (Euroclone, Italy) growth medium complemented with 10% Fetal Bovine Serum (Euroclone, Italy), 100 mg/mL PenStrep (Sigma-Aldrich, Italy), and 2 mM L-glutamine (Sigma-Aldrich, Italy). Cells were cultured in a humidified incubator (HeraCell 150, Heraeus) with 5% CO_2 at 37°C, using Falcon™ plates as supports.

To investigate QS's cytotoxicity, MCF-7 cells ($0.5 \cdot 10^4$ cells/well) were seeded in 96-well plates (Sarstedt, Germany). 6h after plating cells were treated with QS-Blank at two different membrane components' (Chol + Stk) final concentration (10 µg/mL and 2 µg/mL). 24h, 48h, and 72h after treatment, cell viability was assessed using CellTiter 96® AQueous Non-Radioactive cell proliferation assay (Promega, USA) according to the manufacturer's instructions. Briefly, 2h after MTS incubation at 37°C, absorbance at 490 nm was recorded using a microplate reader (FilterMax F5, Multi-Mode Microplate Reader, Molecular Devices). Absorbance values were normalized on the control at 24h and analyzed as being proportional to the number of viable cells. Similarly, the cytotoxicity of QS (2 µg/mL) loaded with increasing dye concentrations (Table 1) was assessed.

To evaluated the photodynamic effect of Br-Sq-C12-loaded QS, MCF-7 cells ($0.5 \cdot 10^4$ cells/well) were seeded in 96-well plates. 6h after plating cells were treated with Br-Sq-C12-loaded QS at the concentrations reported in Table 1 and Br-Sq-C12 in its free form at the same concentrations. After O/N incubation at 37°C and 5% CO_2, the cells were irradiated for 15 min with a RED-LED array (96 LEDs in a 12 × 8 arrangement, excitation wavelength: 640 nm, and irradiance: 8 mW/cm^2) specifically designed and produced by Cicci Research s.r.l (Italy). Cell viability was assessed 24h, 48h, and 72h after irradiation using CellTiter 96® AQueous Non-Radioactive cell proliferation assay (Promega, USA) as described above. The photodynamic effect of Br-Sq-C12-loaded QS was evaluated by comparing the viability of cells treated with Br-Sq-C12-loaded QS or with the same concentration of Br-Sq-C12 in its free form upon irradiation. For each condition, eight technical replicates were set up and three independent experiments were performed.

	QS_Sq_300 *(2,0 µg/mL membrane components)*	***Br-Sq-C12***	***QS_Blank*** *(2 µg/mL membrane components)*
Dye concentration (nM)	85.3	85.3	0

Exposure time (min)	15	15	15
Dilution rate	1:2130	-	1:2397

Table 1. Concentrations (nM) and dilution rates of quatsomes, and exposure times used in PDT tests.

Statistical analysis

Data are shown as the average values of three independent pulled experiments ± standard error mean (SEM). Statistical analyses were performed using Graph-Pad Prism 6.0 software (La Jolla, CA, USA). Statistical significance between different conditions was determined performing t-test or Mann-Whitney test according to populations' distribution (normal or not-normal, respectively). Differences with p-values <0.05 were considered statistically significant and *: p-value < 0.05, ***: p-value < 0.0005, ****: p-value < 0001.

Results and discussion

1. Synthesis of Bromine-Squaraine-C12

The present work started with a preliminary study based on the Quatsomes loading with squaraine Br-Sq-C4, an indolenine-based dye quaternarized with a four-carbon atom chain. Although this dye resulted in an efficient photosensitizer in PDT [Serpe et al. 2016; Dereje et al. 2022], its poor solubility and low chemical stability, especially in aqueous solutions limit its wider use and application. To overcome this drawback, a promising approach is represented by the incorporation into nanoparticle systems to shield its hydrophobicity improving the solubility in physiological conditions. To this purpose, the authors previously reported the incorporation of the same dye and similar structures into different nanoparticle systems proving the effectiveness of this strategy.

As reported in the **SX**, the incorporation into QSs resulted in a limited amount of encapsulated dye as well as dye leaking problems (nearly 70% of Br-Sq-C4 was released after one month). To improve this system, a new squaraine bearing a longer alkyl chain, i.e. Br-Sq-C12, was developed, providing a higher hydrophobicity and promoting its stable incorporation in vesicular membranes. This study outlined the importance of the hydrocarbon chain length for the stabilization of the dye in a vesicular membrane.

The synthesis of Br-Sq-C12 dye (Scheme 1) started with the quaternarization of the bromoindolenine ring (**1**), synthesized as reported in [Serpe 2016], to get compound **2**. This reaction was performed under microwave irradiation and led to an increased acidity of the methyl group promoting the following condensation reaction. The final dye was then obtained in a one-step reaction under microwave heating following our well-established method for indolenine-based squaraines [Barbero 2015 Organic Letters].

2. Preparation of Bromine-Squaraine-C12 loaded Quatsomes for PDT

Stearalkoniumk/Cholesterol (ratio 1:1) Quatsomes (Stk/Chol QS) loaded with Bromine-Squaraine-C12 (Br-Sq-C12) were prepared by DELOS-susp methodology [26] and loaded with two different concentrations of Br-Sq-C12. As a result, we obtained a first batch of QS encapsulating a theoretical concentration of Br-Sq-C12 of 200 µM (QS_Sq_200) and a second batch, encapsulating a theoretical concentration of dye of 300 µM (QS_Sq-C12) (Figure 1). In addition, blank QS were also prepared for sake of comparison with the PS-loaded nanovesicles. All formulations were diafiltrated in order to remove the ethanol and the non-entrapped dye or free membrane components from the solution, finally obtaining three batches of water-suspended filtered nanovesicles (see Materials and methods section for details).

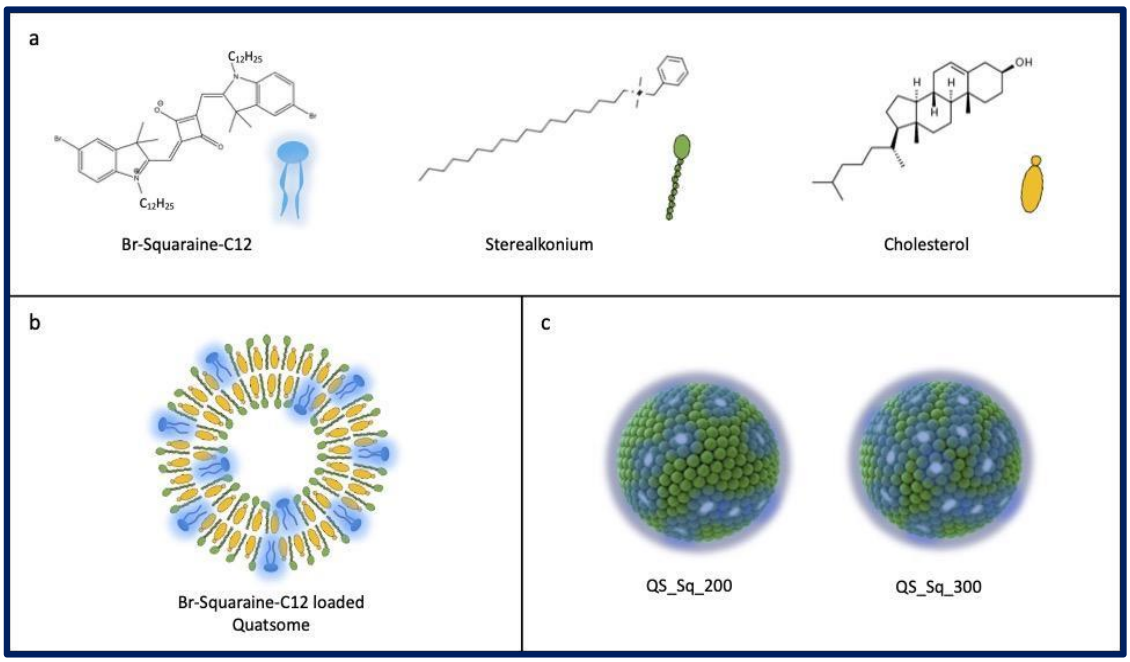

Figure 1. Br-Squaraine-C12 loaded QS.

Br-Squaraine-C12 loaded QS components (a); schematic composition of the dye-loaded quatsomes (b); graphic representation of the products (c)

All formulations showed a very similar membrane components concentration, and so a similar membrane composition (Table 2). Sample QS_Sq_200 showed a higher average dye encapsulation percentage (~80%), while sample QS_Sq_300 showed, as expected, a higher dye loading in mass (L), with a real dye concentration of ~200 µM inside the vesicles. It's important to underline that, even if L it's higher in sample QS_Sq_300, the dye encapsulation seems to be more efficient at the lower concentration, with a higher dye loading encapsulation percentage. This can be due to the chemical structures and their interactions in the membrane, as well as reaching the saturation point of dye concentration at the nanovesicle membrane.

Sample	Theoretical dye concentration (µM)	Real dye concentration (µM)	Average dye encapsulation (%)*	Dye loading in mass ** L	Theoretical membrane components (mg/mL)	Real membrane components (mg/mL)
QS_Blank	/	/	/	/	*5.88*	*4.79*
QS_Sq_200	*200*	*159.02*	*79.51*	*3.20E-2*	*5.88*	*4.42*
QS_Sq_300	*300*	*200.33*	*66.78*	*4.19E-2*	*5.88*	*4.26*

**calculated as* $\frac{real\ dye\ concentration}{theoretical\ dye\ concentration}$

***calculated as* $\frac{mg\ of\ dye}{mg\ of\ membrane\ components}$

Table 2. Summary of the parameters obtained by lyophilization and UV-vis spectroscopy on PMD-loaded quatsomes

3. Spectroscopic characterization

The photochemical properties of both the squaraine dye and dye-loaded QSs in solution are summarized in Table 3.

Samples		Br-Sq-C12	QS_Sq_200	QS_Sq_300
Parameters	ε ($\cdot 10^5$ M cm^{-1})	2.9[3)]		
	λ_{ex} max (nm)	Not soluble[1)], 643[2)], 640[3)], 638[4)], 650[5)]	644[1)], 643[2)], 640[3)], 637[4)], 652[5)]	644[1)], 643[2)], 640[3)], 637[4)], 652[5)]
	λ_{em} max (nm)	Not soluble[1)], 651[2)], 649[3)], 645[4)], 660[5)]	655[1)], 653[2)], 649[3)], 647[4)], 662[5)]	655[1)], 653[2)], 649[3)], 647[4)], 662[5)]
	QY (%)	26[3)]	3[1)]	2[1)]
	τ (ns)	$1.08 \cdot 10^{-9}$ (100%)[3)]	$t_1 = 1.43 \cdot 10^{-9}$ (11%)[1)]	$t_1 = 1.86 \cdot 10^{-9}$ (16%)[1)]
			$t_2 = 2.66 \cdot 10^{-9}$ (89%)[1)]	$t_2 = 2.93 \cdot 10^{-9}$ (84%)[1)]
	χ	1.03[3)]	1.02[1)]	1.00[1)]

Table 3. Photochemical properties of Br-Sq-C12, QS_Sq_200 and QS_Sq_300.

1) Water; 2) Acetone; 3) Ethanol; 4) Methanol; 5) DMSO.

Br-Sq-C12 shows an absorption maximum at around 640 nm in ethanol (Figure 2) with a very high molar extinction coefficient (290,000 $M^{-1}cm^{-1}$). The UV-Vis spectrum is characterized by a narrow absorption band in the NIR, essential requirement for the PDT treatment, and a characteristic hypsochromic shoulder typical for polymethine dyes. The main absorption peak is associated to the $\pi \rightarrow \pi^*$ HOMO–LUMO transitions, mainly localized on the squarainic core; on the other hand, the shoulder at higher energy can be ascribed to the HOMO-LUMO+1 transition. As already observed for other SQs, Br-Sq-C12 shows an excellent fluorescence emission with a maximum emission at 649 nm when dissolved in ethanol, although both the absorption and the fluorescence emission are completely quenched when dissolved in water due to an aggregation caused quenching (ACQ) effect. As shown in Figure 2, the loading into QSs fully overcomes this drawback, increasing the solubility of the dye in aqueous media, with an absorbance and fluorescence emission maxima at 644 nm and 655 nm, respectively.

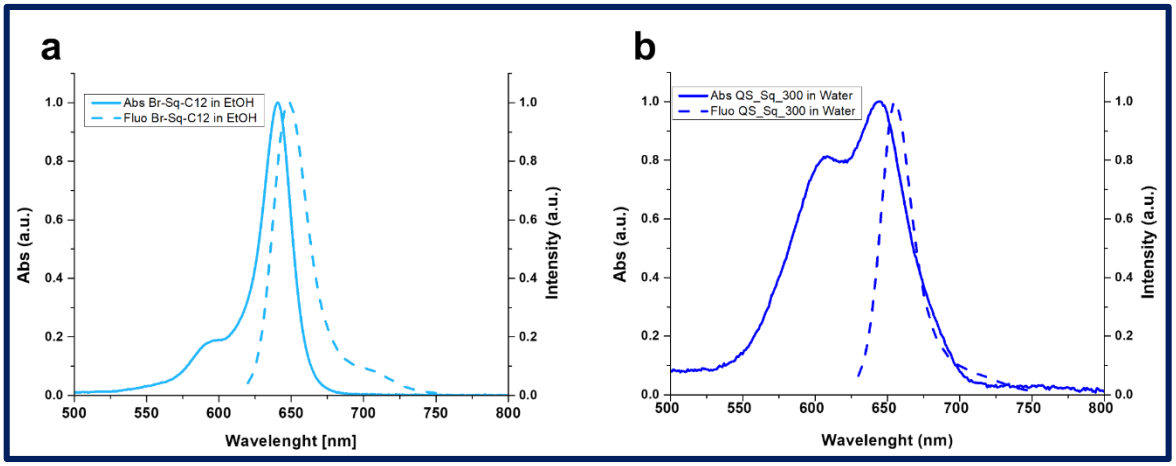

Figure 2. Absorbance and fluorescence spectra of a) free Br-Sq-C12 in ethanol and b) dye-loaded QSs in water.

The solvatochromic effect on both the dye and dye-loaded QSs absorption and emission spectra was also investigated and reported in Table 3. In general, neither the absorption maxima nor the band shape have been affected by the solvent polarity. A slight difference has been observed in the absorption peak maxima in protic or aprotic solvents; in fact, DMSO induced a 15 nm bathochromic shift in comparison to MeOH suggesting a higher polarity of the ground state compared to the excited state. It is worth to notice that both the absorbance and emission maxima of the dye-loaded QSs, irrespective of the amount of incorporated dye, are very close to the values obtained with the free Br-Sq-C12, suggesting that the association with the QS did not change the energies and relative probabilities of the electronic transitions. Fluorescence lifetime and quantum yield of Br-Sq-C12 in ethanol are in the ranges typical for squaraines in organic media. Specifically, Br-Sq-C12 fluorescence lifetime showed monoexponential decay and is in the ns range, as already observed for several squaraines.

By comparing the values obtained for QS_Sq_200 and QS_Sq_300 in water, a bi-functional equations were necessary to fit the decay curves, suggesting that two different types of interactions occurred with the QSs. Specifically, one fluorescence lifetime is slightly longer, while the other ones (*ca.* 85%) increased of *ca.* 2.7 times compared to the free dye. This longer decay could be ascribed to the decrease in rotational/twisting degrees of freedom, confirming a good degree of dye entrapment into the QS vesicles. On the other hand, the shorter lifetime could be due to the presence of a small amount of free dye on the QS surface, leading to a detrimental effect caused by the interaction with highly polar media, such as water.

4. Physicochemical and Photophysical properties

QS_Sq_200 and QS_Sq_300 were interrogated with DLS to determine the mean hydrodynamic diameter and polydispersity index (PDI) at certain dilution (SI). Average hydrodynamic diameter (z-average), PDI and z-

potential average values are summarized in Table 4. Both samples showed similar hydrodynamic diameters (~90 nm) and PDI values (<0,2) (Figure 1a), demonstrating that the population of nanoparticles is highly homogeneous. Also, the values are very similar to the ones obtained from the characterization of blank Quatsomes (QS_Blank), confirming the good reproducibility of the synthesis technique and the fact that the morphology of the vesicles is not affected by dye encapsulation. Z-potential values are comparable between the dye-loaded samples too and abundantly positive (~70 mV), due to the positive charge of Stearalkonium and Br-Sq-C12. This high positively surface charge contributes to the colloidal stability of the nanovesicles [27]. In addition, we performed transmission electron microscopy in cryogenic conditions (Cryo-TEM) in order to confirm the data obtained during the physicochemical characterization of the samples using the DLS. Sample QS_Sq_200 showed high homogeneity in the distribution (Figure 1e and f), as already demonstrated by the low PDI values obtained in DLS. From the analysis of the images, we estimate an average geometric diameter value of the dye loaded QS of 66 ± 20 nm, which differs about 30 nm from the hydrodynamic average diameters observed in DLS (~90 nm). The Cryo-TEM images of sample QS_Sq_300 (Figure 1e and f) confirmed a good homogeneity and, in this case, the real diameters average value measured is 58 ± 18 nm.

Sample	z-average (nm)	z-average standard deviation (nm)	PDI	PDI standard deviation	Average geometric diameter (nm)	z-potential (mV)	z-potential standard deviation (mV)
QS_Blank	*85*	*1*	*0.23*	*0,01*	-	*92*	*3*
QS_Sq_200	*92*	*1*	*0.19*	*0,01*	*66 ± 20*	*67*	*2*
QS_Sq_300	*89*	*0.14*	*0.17*	*0,01*	*58* ± 18	*75*	*2*

Table 4. Summary of DLS and ELS measured parameters.

All values were measured with the same set up (Values obtained by the analysis of diafiltrated samples at dilution 1:10).

Sample QS_Sq_200 showed high homogeneity in the distribution, as proved by the PDI values obtained in DLS (~0,2). From the analysis of the images we manage to measure an average value of diameter of the dye loaded QS of 66 ± 20 nm, which differs about 30 nm from the hydrodynamic average diameters observed in DLS (~90 nm).

The Cryo-TEM images of sample QS_Sq_300 (Figure 3e and f) also confirm the high homogeneity of the population of nanoparticles (PDI < 0,2). In this case the real diameter's average value measured is 58 ± 18 nm.

It's also possible to observe a big dark formation (Figure 3e) which is most likely an artifact.

These values and conclusions are just indicative and to confirm the data obtained in the previous measurements, however it's important to keep in mind that Cryo-TEM is not a representative technique because it just measures a small volume of the sample.

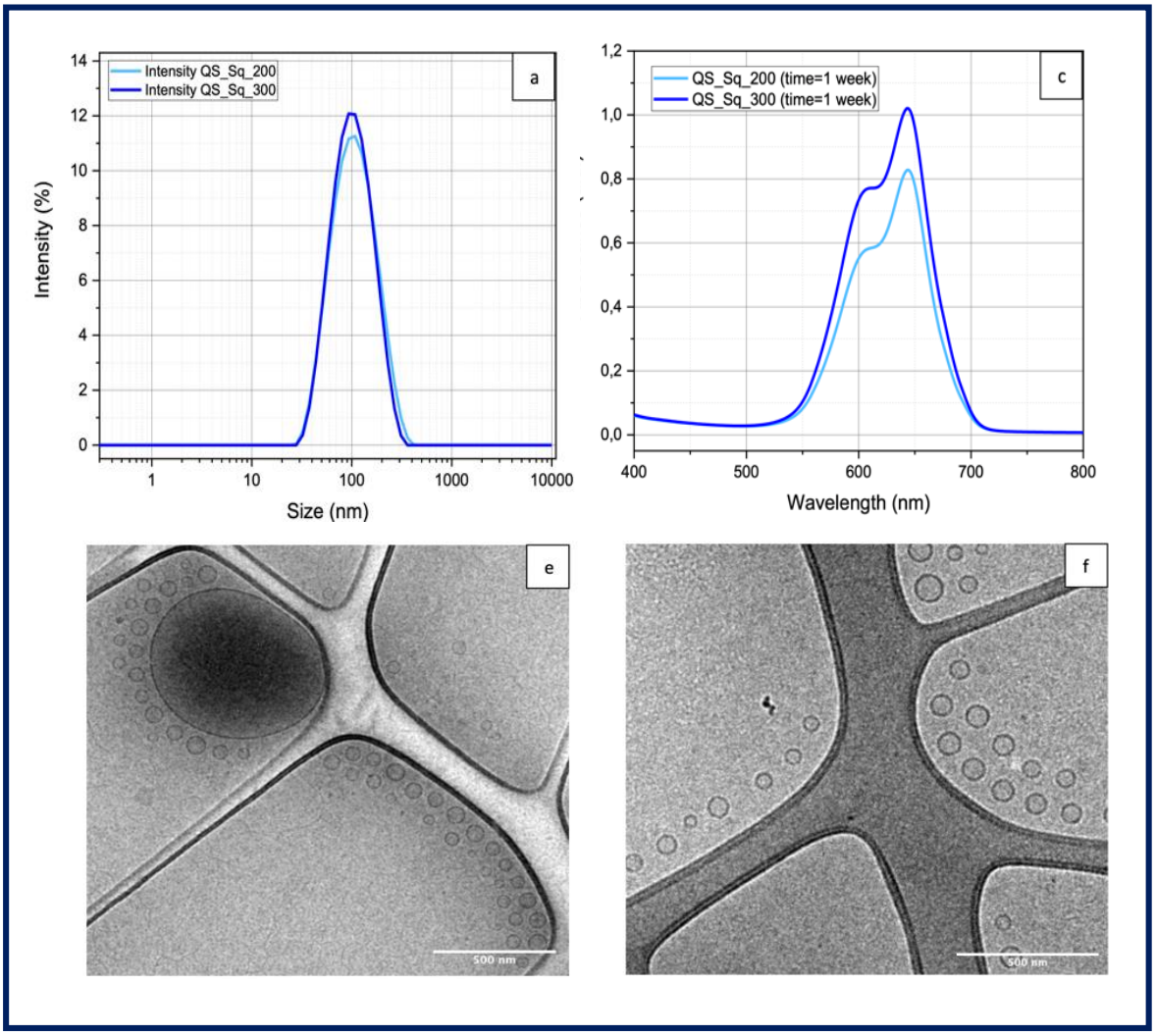

Figure 3. Physicochemical and Photophysical properties of QS-Sq.

Size distribution in DLS of QS_Sq_200 and QS_Sq_300 (a); UV-vis absorbance spectra of QS_Sq_200 and QS_Sq_300 in water (c); cryo-TEM images of sample QS_Sq_200 (e) and QS_Sq_300 (f).
All the presented data refers to diafiltrated samples.

5. Evaluation of colloidal stability and photostability

Previous works on QS have already demonstrated the long colloidal stability, up to a year, of those vesicles [23] [24] [25]. In this work we evaluated the stability on time and photostability of the dye-loaded QS with DLS and fluorescence spectroscopy, respectively. The obtained data proved the dye-loaded nano-vesicular systems to be very stable during at least 10 weeks, with constant Z-average values around 90 nm and optimally low PDI values, always around 0,2 (Figure 4a). In agreement, the Z-potential values (around +70 mV) demonstrated the high stability of the dye-loaded QS (Figure 4b). As mentioned before, the highly positive Z-potential is very likely to contribute to the colloidal stability of the systems [27].

Similarly, photostability was evaluated with periodical UV-vis absorbance measurements up to 3 months. We noticed a lowering of the main absorbance peak at 644 nm during time for both samples in study (Figure 4c), indicating a decrement on the PS concentration at the QS.

The residual dye concentration encapsulated in QS was quantified again 4 months after the production, and the obtained values were 126,09 µM for sample QS_Sq_200 and 181,77 µM for sample QS_Sq_300, resulting in a percentual of dye leaking, respectively, of 20,7% and 9,3% in 4 months.

In order to understand better the phenomenon we followed the variation of the peaks' amplitude in time (ratio peak/shoulder), which can be indicative of the formation of dye aggregates (top right graphs in Figure 4e and f).

Sample QS_Sq_200 presented a continuous decrease in amplitude for both peaks (Figure 4e), as observed for sample QS_Sq_300 too (Figure 2f). In both cases the ratio peak/shoulder was stable around 1,4 during the whole 10 weeks' time (top right graphs in Figure 2e and f) demonstrating that there is no significative dye aggregation out of the QS.

In view of the obtained results we could also assume that the stability of the dyes is not compromised in a major way by the inclusion in QS' membrane at the obtained loadings (0,032 for QS_Sq_20 and 0,042 for QS_Sq_300).

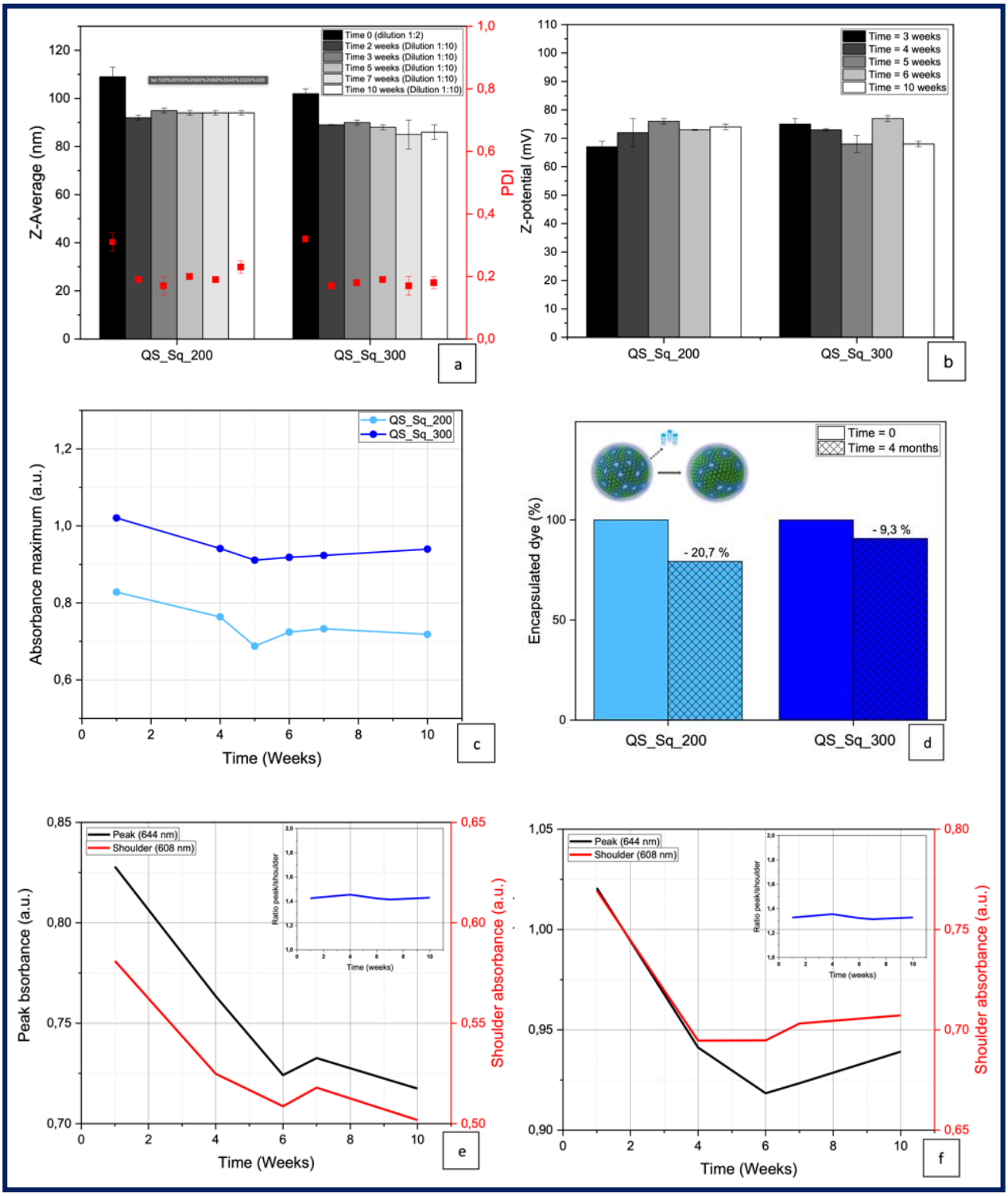

Figure 4. Colloidal stability and photostability of QS-Sq.

DLS bar plot, showing hydrodynamic diameters (z-average) as bars and PDI ad dots (a); ELS bar plot (b)Trend of variation of main absorbance (b); trend of variation of the maximum absorbance peaks in time for both samples (c); dye leaking percentage during 4 months (d); maximum absorbance peak and shoulder trend in time for sample QS_Sq_200 (ratio peak/shoulder trend showed on top-right) (e); maximum absorbance peak and shoulder trend in time for sample QS_Sq_300 (ratio peak/shoulder trend showed on top-right)(f).

6. ROS production

A preliminary evaluation of the ability of both the Br-Sq-C12 and QS_Sq_300 to generate reactive oxygen species (ROS) was carried out by using 1,3-diphenylisobenzofuran (DPBF) as a probe. In fact, DPBF rapidly reacts with ROS generated by the light activated dye, forming the colorless o-dibenzoylbenzene derivative, resulting from the disappearance of DPBF's characteristic absorption band at 415 nm.

The decrease in the DPBF absorption band at 415 nm, as a function of the irradiation time, has been compared to the values obtained by irradiating a standard, the efficient and well-known ROS generator Bengal Rose (BR). As shown in Figure 5, both the free squaraine and the squaraine loaded into QSs possess faster and higher ROS generation ability, compared to the BR. In particular, Br-Sq-C12 is able to promote the complete decay of DPBF absorption within 180 seconds, while the same result was obtained in 10 min for reference BR. This fast ROS generation could be ascribed to the presence of bromine which may facilitate the singlet to triplet state intersystem crossing, due to the well-known heavy atom effect. Moreover, the entrapment of the dye into the QSs seems not to interfere with the ability of the dye to rapidly generate ROS, essential requirement for the PDT activity.

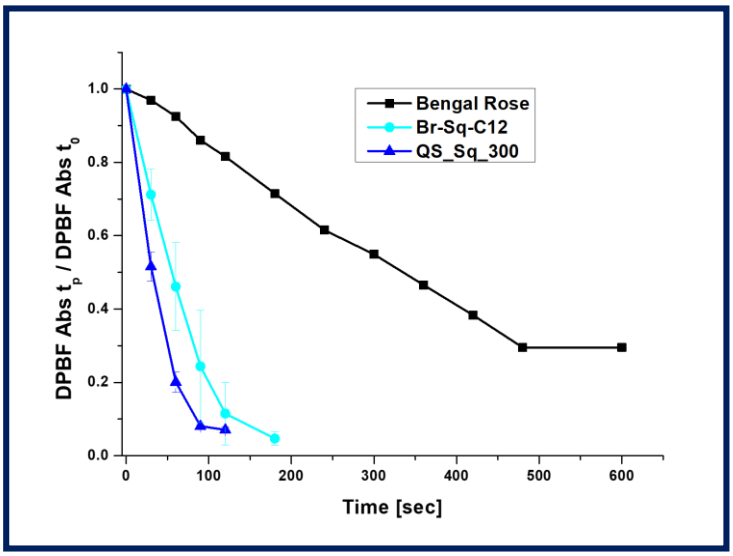

Figure 5. Comparative generation of reactive oxygen species (ROS) by QS_Sq.

7. Cytotoxicity and PDT assays

Despite the outstanding properties of QS, the remarkable cytotoxicity of quaternary ammonium surfactants including Stk could represent a challenge in their *in vivo* application (Zhang et al., 2015). Therefore, to assess QS biocompatibility, we first performed cell viability assays on MCF-7 cells treated with two different concentrations of blank QS, i.e. 10 and 2 µg/mL (Stk/Chol). As shown in figure 6, QS diluted to

a final membrane components' concentration of 10 µg/mL revealed marked cytotoxicity starting 24 h after treatment and occurring up to 72 h (Fig. 6a). On the contrary, QS at 2 µg/mL showed a good biocompatibility on MCF-7 cells (Fig.6b), proving to be significantly less toxic than 10 µg/mL (Fig. 6c). Consequently, for further investigations on the photoactivity of Br-Sq-C12-loaded QS we selected this membrane components' concentration (2 µg/mL) to limit any non-targeted cytotoxicity provided by the carrier itself.

Once selected the optimal blank QS's concentration, we preliminarily tested different loading concentrations of Br-Sq-C12. In particular, we synthesized QS loaded with a theoretical dye-concentration of 50 µM (QS_Sq_50), 100 µM (QS_Sq_100), 200 µM (QS_Sq_200), and 300 µM (QS_Sq_300) corresponding to a real dye concentration of 10 nM, 33 nM, 68 nM, and 85.3 nM respectively (after dilution to 2 µg/mL membrane components). Interestingly, the newly synthesized Sq-loaded nanosystem is slightly more cytotoxic as compared with the unloaded QS at 2 µg/mL although still highly biocompatible compared to SQ at 10 µg/mL (Fig. 6c). This effect is in agreement with previously reported polymethine dyes loaded in solid lipid nanoparticles (Chinigò et al., 2022). Interestingly, all the formulations revealed a significant increase in cell cytotoxicity after light beam irradiation (Fig. 7), which was not observed treating the cells with the same concentration of the dye in its free form. As expected, the photo-activity of the nanosystem is increasing with concentration of the incorporated dye. In particular, QS_Sq_50 proved to induce significant phototoxicity only starting from 72 h after light beam treatment, whereas QS_Sq_100 and QS_Sq_200 displayed a marked photo-induced cytotoxic effect already 24 h after the treatment (Fig. SX). The photoxicity activity of the Sq-loaded quatsome system is reported in Fig. 7: MCF-7 cells treated O/N with QS_Sq_300 (corresponding to 85.3 nM dye effective concentration) revealed a significant reduction in cell viability after light beam irradiation which didn't occur when the cells were treated by same concentration of the dye in its free form (Fig. 7b).

In agreement with previous data obtained on other types of nanosystems (Chinigò et al., 2022), our results clearly demonstrated that the encapsulation within QS highly enhanced dye's photoactivity. It is likely that the nanocarrier, by significantly increasing the local concentration of the dye, in addition to reducing its aggregation phenomena, improves its overall spectroscopic properties. Furthermore, taking into account our results on ROS production (Fig. 3), it is also possible to hypothesize that the relative low photoactivity of the dye in its free form observed *in vitro* on MCF-7 cells may be due to a failure of the molecule to enter the cell, facilitated, on the other hand, by its incorporation into the nanoparticle system.

Of note, the squaraine's concentration usually employed for PDT studies ranges from 1 to 100 µM (Serpe et al., 2016; Rapozzi et al., 2010; Shafeekh et al., 2014). Here, we demonstrated that the use of a nanocarrier system allows to use a much lower concentration of photo-active dye (up to 10-1000 times lower than usual). Taken together our *in vitro* results seems to support the applicability of QS as nanocarriers for PDT application

and highlighted the importance to achieve high dye-loaded nanostructures to optimize their photoactive properties. However, further efforts are needed to optimize the biocompatibility of these nanosystems with a view to future biomedical applicability.

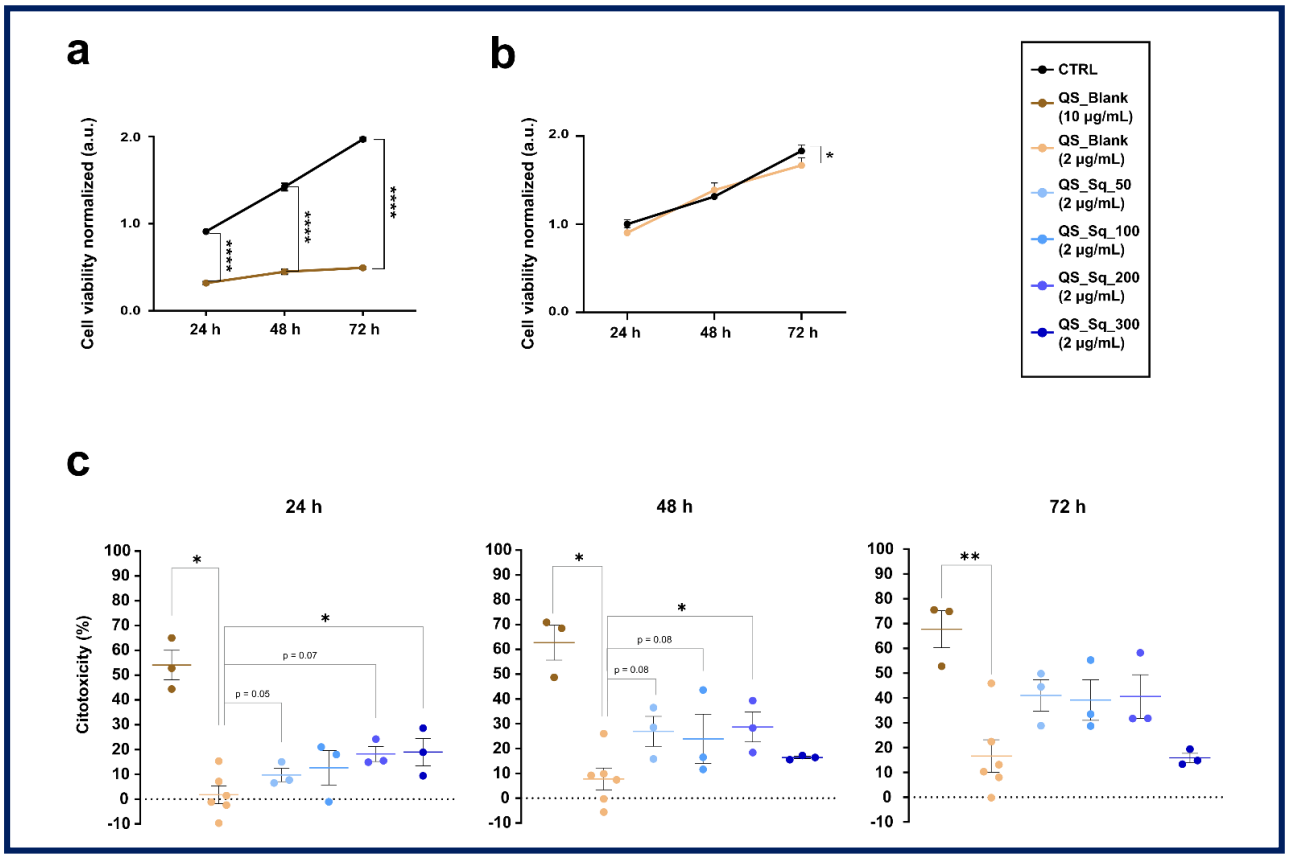

Figure 6. In vitro cytotoxicity of QS and QS-Sq.

*Cell viability assays on MCF-7 O/N treated with QS_blank at two different concentrations of membrane components (Chol + Stk): 10 µg/mL (a) and 2 µg/mL (b). Data refer to one experiment representative of three. Data are normalized on CNTRL at 24 h and represented as mean ± SEM. Statistical significance versus CNTRL (MCF-7 untreated): * P< 0.05, **** P< 0.0001 (t- test or Mann-Whitney test); (c) Percentage of cytotoxicity 24, 48, and 72 h after treatment with 10 µg/mL (brown dots) and 2 µg/mL (beige dots) of QS_blank; light blue and blue dots refer to 2 µg/mL QS loaded with different Sq concentrations. Data are expressed as mean ± SEM of three independent experiments (each dot represents one independent experiment). Statistical significance versus QS_blank 2 µg/mL: * P< 0.05, ** P< 0.01 (RM one-way ANOVA with Dunnett's post-hoc test).*

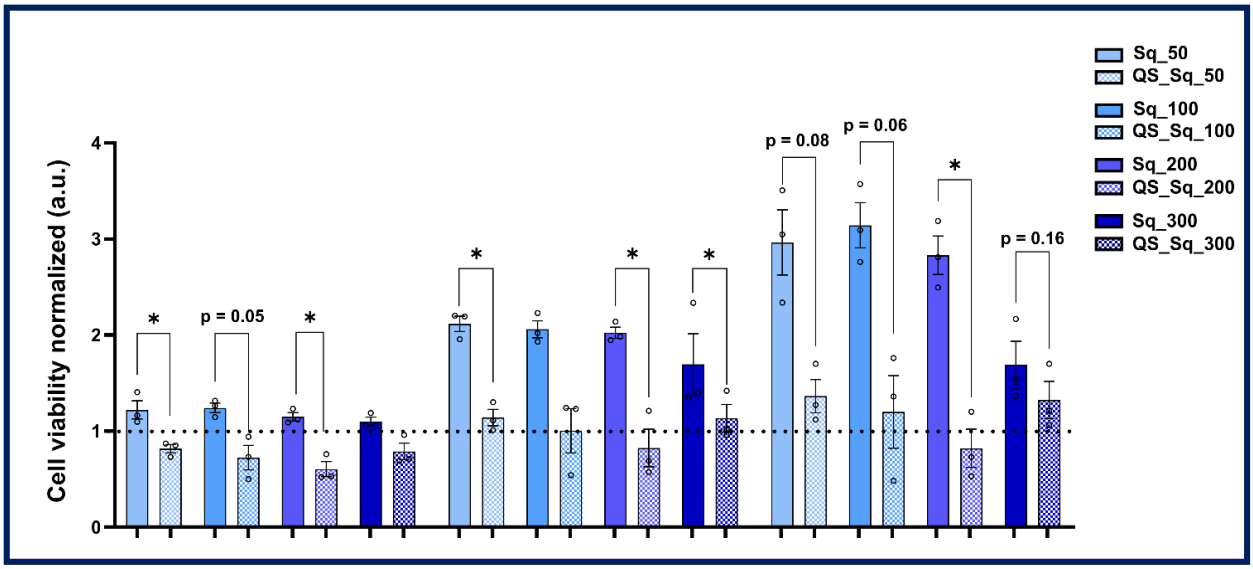

Figure 7. In vitro phototoxicity of QS and QS-Sq.

*Cell viability assays on MCF-7 O/N treated with different concentrations of Br-Sq-C12 in its free form (Sq) or incorporated into 2 µg/mL QS (QS_Sq) 24 h, 48 h, and 72 h after LED irradiation (640 nm, 7.2 J/cm^2). Data are normalized on their own CNTRL (Br-Sq-12 samples on irradiated cells not treated; QS_Sq samples on irradiated cells treated with QS blank) at 24 h (dot line) and represented as mean ± SEM of three independent experiments. Statistical significance between Sq and QS_Sq: * P< 0.05 (paired t- test or Wilcoxon test).*

References

[1] D. Dolmans , D. Fukumura and R. Jain , “Photodynamic therapy for cancer,” Nat Rev Cancer, vol. 3, pp. 380-387, 2003.

[2] Z. Huang, “A review of progress in clinical photodynamic therapy,” Technol Cancer Res Treat, vol. 4, no. 3, pp. 283-293, 2005.

[3] B. W. Henderson and T. J. Dougherty , "How does the photodynamic therapy work?," Photochem Photobiol, vol. 55, pp. 145-157, 1992.

[4] E. Buytaert , M. Dewaele and P. Agostinis , "Molecular effectors of multiple cell death pathways initiated by photodynamic therapy," Biochim Biophys Acta, vol. 1776, pp. 86-107, 2007.

[5] J. Morgan, "Mitochondria-based photodynamic anti-cancer therapy," Adv Drug Deliv Rev, vol. 49, pp. 71-86, 2001.

[6] R. R. Allison , G. H. Downie , R. Cuenca , X. Hu , C. J. H. Childs and C. H. Sibata , "Photosensitizers in clinical PDT," Photodiagnosis Photodyn Ther, vol. 1, pp. 27-42, 2004.

[7] A. E. O'Connor , W. M. Gallagher and A. T. Byrne , "Porphyrin and Nonporphyrin Photosensitizers in Oncology: Preclinical and Clinical Advances in Photodynamic Therapy," Photochem Photobiol, vol. 85, pp. 1053-1074, 2009.

[8] R. Baskaran , J. Lee and S. Yang, "Clinical development of photodynamic agents and therapeutic applications," Biomat Res, vol. 22:25, pp. 1-8, 2018.

[9] J. Berlanda , T. Kiesslich , V. Engelhardt , B. Krammer and K. Plaetzer , "Comparative in vitro study on the characteristics of different photosensitizers employed in PDT," J Photochem Photobiol B, vol. 100, pp. 173-180, 2010.

[10] R. R. Avirah , D. T. Jayaram , N. Adarsh and D. Ramaiah , "Squaraine dyes in PDT: from basic design to in vivo demonstration," Org Biomol Chem, vol. 10, pp. 911-920, 2012.

[11] B. Ciubini , S. Visentin , L. Serpe , R. Canaparo , A. Fin and N. Barbero , "Design and synthesis of symmetrical pentamethine cyanine dyes as NIR photosensitizers for PDT," Dyes Pigm, vol. 160, pp. 806-813, 2019.

[12] S. D'Alessandro and R. Priefer , "Non-porphyrin dyes used as photosensitizers in photodynamic therapy," Journal of Drug Delivery Science and Technology, vol. 60, 2020.

[13] S. Kwiatkowski , B. Knapb , D. Przystupski , J. Saczko , E. Kędzierska , K. Knap-Czop , J. Kotlińska , O. Michel, K. Kotowski and J. Kulbacka , "Photodynamic therapy – mechanisms, photosensitizers and combinations," Biomedicine & Pharmacotherapy, vol. 106, pp. 1098-1107, 2018.

[14] A. Escudero , C. Carrillo-Carriòn , M. C. Castillejos , E. Romero-Ben , C. Rosales-Barrios and N. Khiar , "Photodynamic therapy: photosensitizers and nanostructures," Mater Chem Front, vol. 10, no. 5, pp. 3788-3812, 2021.

[15] J. Son , S. M. Yang , G. Yi , Y. J. Roh , H. Park , J. M. Park , M. G. Choi and H. Koo , "Folate-modified PLGA nanoparticles for tumor-targeted delivery of pheophorbide a in vivo," Biochem Biophys Res Commun, vol. 498, no. 3, pp. 523-528, 2018.

[16] D. Liu , B. Chen , Y. Mo , Z. Wang , T. Qi , Q. Zhang and Y. Wang , "Redox-Activated Porphyrin-Based Liposome Remote-Loaded with Indoleamine 2,3-Dioxygenase (IDO) Inhibitor for Synergistic Photoimmunotherapy through Induction of Immunogenic Cell Death and Blockage of IDO Pathway," Nano Lett, vol. 19, pp. 6964-6976, 2019.

[17] J. Han , W. Park , S. Park and K. Na , "Photosensitizer-Conjugated Hyaluronic Acid-Shielded Polydopamine Nanoparticles for Targeted Photomediated Tumor Therapy," ACS Appl Mater Interfaces, vol. 8, pp. 7739-7747, 2016.

[18] Z. Sheng , D. Hu , M. Zheng , P. Zhao , H. Liu , D. Gao , P. Gong , G. Gao , P. Zhang , Y. Ma and L. Cai , "Smart Human Serum Albumin- Indocyanine Green Nanoparticles Generated by Programmed Assembly for Dual-Modal Imaging-Guided Cancer Synergistic Phototherapy," ACS Nano, vol. 8, no. 12, pp. 12310-12322, 2014.

[19] Y. Dai , B. Wang , Z. Sun , J. Cheng , H. Zhao , K. Wu , P. Sun , Q. Shen , M. Li and Q. Fan , "Multifunctional Theranostic Liposomes Loaded with a Hypoxia- Activated Prodrug for Cascade-Activated Tumor Selective Combination Therapy," ACS Appl Mater Interfaces, vol. 11, pp. 39410-39423, 2019.

[20] H. Meda , J. Wu , T. Sawa , Y. Matsumura and K. Hori , "Tumor vascular permeability and the EPR effect in macromolecular therapeutics: a review," J Controlled Release, vol. 65, pp. 271-284, 200.

[21] N. Grimaldi , F. Andrade , N. Segovia , L. Ferrer-Tasies , S. Sala , J. Veciana and N. Ventosa , "Lipid-based nanovesicles for nanomedicine," Chem Soc Rev, vol. 45, pp. 6520-6545, 2016.

[22] E. H. Lee , S. J. Lim and M. K. Lee , "Chitosan-coated liposomes to stabilize and enhance transdermal delivery of T indocyanine green for photodynamic therapy of melanoma," Carbohydr Polym, vol. 224, 2019.

[23] L. Ferrer-Tasies , E. Moreno-Calvo , M. Cano-Sarabia , M. Aguilella-Arzo , A. Angelova , S. Lesieur , S. Ricart , J. Faraudo , N. Ventosa and J. Veciana , "Quatsomes: vesicles formed by self-assembly of sterols and quaternary ammonium surfactants," Langmuir, vol. 22, pp. 6519-6528, 2013.

[24] J. Morla-Folch , G. Vargas-Nadal , T. Zhao , C. Sissa , A. Ardizzone , S. Kurhuzankau , Kober M, M. Uddin , A. Painelli , J. Veciana , K. D. Belfield and N. Ventosa , "Dye-Loaded Quatsomes Exhibiting FRET as Nanoprobes for Bioimaging," ACS ApplMater Interfaces, vol. 18, pp. 20253-20262, 2020.

[25] G. Vargas-Nadal , M. Munoz-Ubeda , P. Alamo , M. Mitjans , V. Cespedes , M. Kober , E. Gonzalez-Mira , L. Ferrer-Tasies, M. P. Vinardell , R. Mangues , J. Veciana and N. Ventosa , "MKC-Quatsomes: a stable nanovesicle platform for bio-imaging and drug-delivery applications," Nanomedicine, vol. 24, 2020.

[26] I. Cabrera, E. Elizondo, O. Esteban, J. L. Corchero, M. Melgarejo, D. Pulido, A. Córdoba, E. Moreno, U. Unzueta, E. Vazquez, I. Abasolo, S. J. Schwartz, A. Villaverde, F. Albericio, M. Royo, M. F. García-Parajo, N. Ventosa and J. Veciana, "Multifunctional nanovesicle-bioactive conjugates prepared by a one-step scalable method using CO2-expanded solvents," Nano lett, vol. 13, no. 8, p. 3766–3774, 2013.

[27] S. Samimi, N. Maghsoudnia, R. B. Eftekhari and F. Dorkoosh, "Chapter 3 - Lipid-Based Nanoparticles for Drug Delivery Systems," in Characterization and Biology of Nanomaterials for Drug Delivery, 2019, pp. 47-76.

[28] G. M. Fahy, D. R. MacFarlane, C. A. Angell and H. T. Meryman, "Vitrification as an approach to cryopreservation," Cryobiol, vol. 21, no. 4, pp. 407-426, 1984.

[29] R. Pecora, "Dynamic Light Scattering Measurement of Nanometer Particles in Liquids," J Nanopart Res, vol. 2, pp. 123-131, 2000.

[30] Y. Kadam, R. Ganguly, M. Kumbhakar, V. K. Aswal||, P. A. Hassan and P. Bahadur, "Time Dependent Sphere-to-Rod Growth of the Pluronic Micelles: Investigating the Role of Core and Corona Solvation in Determining the Micellar Growth Rate," J Phys Chem, vol. 25, pp. 16296-16302, 2009.

[31] S. Zhang , S. Ding, J. Yu, X. Chen, Q. Lei and W. Fang, "Antibacterial Activity, in Vitro Cytotoxicity, and Cell Cycle Arrest of Gemini Quaternary Ammonium Surfactants," Langmuir, vol. 44, no. 31, pp. 12161-12169, 2015.

[32] "Final Report on the Safety Assessment of Stearalkonium Chloride," J. Am. Coll. Toxicol., vol. 1, no. 2, pp. 57-69, 1990

4. GENERAL DISCUSSION

4.1 TRP channels to target prostate cancer progression

4.1.1 TRPA1 channel to target PCa angiogenesis

Angiogenesis is one of the main hallmarks of cancer (Hanahan and Weinberg 2011) since the formation of new blood vessels is crucial to provide oxygen and nutrients to the tumor as well as to allow metastatic cells to access the bloodstream, allowing them to spread and colonize new sites. PCa, like other highly vascularized solid tumors, is extremely dependent on neovascularization and some tyrosine kinase inhibitors like Sorafenib and Sunitinib have been proposed as anti-angiogenic agents to counter metastatic PCa. However, although the promising results obtained in pre-clinical models, these molecules failed the endpoints in clinical trials (Martínez-Jabaloyas et al. 2013; Michaelson et al. 2009; Michaelson et al. 2014; Aragon-Ching et al. 2009; Steinbild et al. 2007). Hence, the need for novel anti-angiogenic targets. In this regard, TRP channels have attracted a lot of interest in recent years. Indeed, they were found widely expressed in endothelial cells (EC) and aberrant TRP channels expression and/or activity has been correlated with abnormal tumor vascularization. More specifically, some TRP channels have been related to multiple steps of the angiogenic process since they have proved to affect EC cell adhesion and cell migration, vascular remodeling, permeability, tone, and mechanosensing, as well as *in vitro* angiogenesis (Fiorio Pla and Gkika 2013; Munaron 2015). This is basically due to the high sensitivity of some TRP channels to both pro-angiogenic signals and subtle changes in the local microenvironment (Negri et al., 2020; Brossa et al. 2019). However, although at least 14 TRP channels were found to be expressed in EC and endothelial progenitor cells (EPC) (Negri et al. 2020), to date, only TRPV4 has been directly associated with prostate angiogenesis (Adapala et al. 2016; Thoppil et al. 2016; Cappelli et al. 2019). Moreover, until now, most available data focus on the function of a single channel in cancer development and angiogenesis. In order to increase the chances of success in identifying new anti-angiogenic targets, we aimed to obtain a global view of the regulation of all TRP channels in PCa angiogenesis. For this purpose, we used primary Human Prostate Tumor-derived Endothelial Cells (PTEC) previously characterized in our labs (Fiorio Pla et al. 2014). PTEC were proved to be a good model to study the efficacy of anti-angiogenic therapies since they showed expression of androgen and vascular endothelial cell growth factor receptors as well as angiogenic properties including a higher migration rate than normal EC and the ability to form capillary-like structures both *in vitro* and in xenograft in SCID mice (Fiorio Pla et al. 2014). By profiling the expression of TRP channels in PTEC before I started my Ph.D., we identified four "*prostate-associated*" genes characterized by a specific de-regulation accompanied by a functional role in PTEC. Among them, I focused on the role played by TRPA1 in controlling EC motility.

Indeed, the up-regulation of TRPA1 in PTEC compared to the healthy counterpart (HPrMEC) correlates with a higher migratory phenotype. An involvement of TRPA1 in prostatic angiogenesis had been previously suggested by the evidence that TRPA1 activation increase the secretion of VEGF and HGF through a Ca^{2+}-dependent Calcineurin/NFAT pathway in PCa-associated fibroblasts (CAF) and the simultaneously rescue co-cultured PCa cells from apoptosis (Vancauwenberghe et al. 2017). Moreover, TRPA1 also revealed a role in promoting VEGF secretion by stromal cells, which in turn stimulated PCa cell proliferation and tumor growth (Derouiche et al. 2017). Our study further confirmed this hypothesis demonstrating, for the first time, the direct involvement of TRPA1 in PCa angiogenesis and, in particular, in controlling PTEC motility (Bernardini et al. 2019). Indeed, we found that TRPA1 promotes PTEC migration, vascular network formation, and angiogenic sprouting both *in vitro* and *in vivo*. More specifically, we hypothesized a chemoattractive function of TRPA1 during tip cells' activation (Bernardini et al. 2019). Indeed, in sprouting angiogenesis endothelial tip cells function as motile guidance structures that dynamically extend filopodia to explore signals in the tumor microenvironment for directional vessel growth (Eilken and Adams 2010). The role of Ca^{2+} dynamics during sprouting angiogenesis has been recently demonstrated in a zebrafish model, showing that Ca^{2+} oscillations regulated by Dll4/Notch signaling occur in EC exhibiting angiogenic behavior and are required for the selection of stalk and tip cells during both arterial and venous sprouting (Yokota et al. 2015). Although whether Dll4/Notch signaling regulates Ca^{2+} stores or Ca^{2+} channels directly or not remains to be delineated, our results suggest TRPA1 as a possible positive mediator of this pathway.

To note, besides TRPA1 we identified other two TRP channels which are overexpressed in PTEC and showed proangiogenic activity which are TRPV2, and TRPC3. In particular, we observed that TRPV2 increases PTEC viability and proliferation, thus adding another feature to the tumorigenic properties of TRPV2 that have been previously correlated to an enhanced migratory potential of castration-resistant PCa cells (Bernardini et al. 2019). Our data confirmed a previous indirect implication of TRPV2, whose activation in fibroblasts revealed the ability to impair the angiogenic process in a mouse model of arthritis (Laragione et al. 2015). Therefore, TRPV2 appears a very promising candidate to target PCa, due to its potential function on both PCa progression and angiogenesis. As regards TRPC3, we found that it plays a role in controlling the crosstalk between cancer cells and EC in PCa (Bernardini et al. 2019). More specifically, it seems to be involved in the chemoattractive effect exerted by EC on cancer cells in different tumor types (Feng et al. 2017).

Overall, the molecular trp signature we profiled during PCa vascularization could represent a promising prognostic tool in addition to providing new putative therapeutic targets against PCa angiogenesis.

In this regard, the translation of TRPA1 as an anti-angiogenic candidate in the clinic does not seem so unrealistic. Indeed, currently, four TRPA1 antagonists have reached the clinical stage of development

although basically for pain relief. Moreover, the countless patents filed in recent years on TRPA1 inhibitors bode well for the future potential use of this channel in the therapy of advanced PCa.

4.1.2 TRPM8 channels to target PCa invasion

In recent decades, the work undertaken by the Laboratory of Cell Physiology of the University of Lille outlined a key role played by TRPM8 in prostate carcinogenesis. Indeed, after a strong up-regulation in the initial PCa stages, TRPM8 expression results dramatically reduced during late metastatic stages in androgen-independent prostate cancer (Grolez and Gkika 2016; Gkika and Prevarskaya 2009). This expression profile is mainly due to the genomic and non-genomic regulation of TRPM8 by androgens (Zhang and Barritt 2004; Bidaux et al. 2005; Grolez et al. 2019). Consistently, a protective role of TRPM8 in metastatic prostate cancer has been suggested (Grolez and Gkika 2016; Gkika and Prevarskaya 2011). More specifically, TRPM8 was found to impair the motility of PCa cells (Gkika et al. 2010; Wang et al. 2012; Gkika et al. 2015). In addition, anti-proliferative and pro-apoptotic functions of TRPM8 have been described in androgen-insensitive PCa cells such as PC3 and DU-145 cells (Yang et al. 2009; Zhu et al. 2011; Wang et al. 2012; Zhang and Barritt 2004). By contrast, contradictory data referred to a pro-proliferative effect of TRPM8 in PCa cells sensitive to androgens like LNCaP (Zhang and Barritt 2004; Valero et al. 2011; Valero et al. 2012). Thus, it seems that TRPM8 exerts opposite effects on PCa growth according to the androgen sensitivity of the tumor. However, most of the data reported in the literature on TRPM8 impact on PCa growth are based on *in vitro* observations. Therefore, we used a prostate orthotopic xenograft mouse model to shed light on the role of TRPM8 *in vivo*, and, in agreement with the only other *in vivo* study reported in the literature (Zhu et al. 2011), we found that TRPM8 overexpression in PC3 cells significantly reduce tumor growth (Grolez et al. 2022). Mechanistically, this inhibitory action is the result of the TRPM8-mediated induction of cell cycle arrest in G_0/G_1, in agreement with previous studies (Yang et al. 2009; Zhu et al. 2011; Wang et al. 2012). Conversely, the channel seems not directly involved in the control of cell apoptosis, at least in androgen-insensitive PC3 cells. Indeed, data on androgen-insensitive LNCaP cells reported an anti-apoptotic effect of TRPM8 (Zhang and Barritt 2004). This effect is likely induced by the triggering of store-operated channels (SOC) currents on the plasma membrane (PM) by TRPM8 isoform expressed in LNCaP ER (Thebault et al. 2005; Wertz and Dixit 2000) as well as by the inhibitory action exerted by the short TRPM8 isoform sM8α on the full-length isoform present on the PM (Bidaux et al. 2012; Peng et al. 2015). In addition, we observed that the inhibition of tumor growth supported by TRPM8 *in vivo* may be also due to the reduction of PC3 cells' clone formation capabilities (Grolez et al. 2022). In this regard, the inhibition of Cdc42 and Rac1 could explain the reduced tumor cell density observed *ex vivo* thanks to the inhibition of cell-to-cell adhesion (Rojas et al. 2001; Takaishi et al. 1997; Braga et al. 1999).

Furthermore, our *in vivo* data further supported the protective role exerted by TRPM8 on PCa metastasis. Indeed, we demonstrated that TRPM8 overexpression inhibits metastatic dissemination *in vivo* by reducing PC3 cells' colonization both in primary and distant sites including the liver, kidney, and lung. Moreover, we found that the reduced number of metastases formed in the presence of TRPM8 correlated with an impaired ability of PC3 to cross the vascular barrier and thereby colonize distant sites across the bloodstream (Grolez et al. 2022). Previous *in vivo* observations had suggested an additional TRPM8-mediated anti-angiogenic contribution to PCa progression based on an interesting correlation between TRPM8 overexpression and a strong reduction in VEGF and microvascular density (Zhu et al. 2011). Moreover, our group recently stated an anti-migratory function of TRPM8 in EC mediated by the inhibition of the small GTPase Rap1A that is crucial in the promotion of cell adhesion, thus supporting an anti-angiogenic role of this channel during cancer progression (Genova et al. 2017). In this regard, we have shown that the anti-migratory protective role shown by TRPM8 in prostate cancer cells underlies the same molecular mechanism observed in EC. Indeed, we demonstrated that TRPM8 directly interacts with the small GTPase Rap1A in PCa cells as well as in EC (Chinigò et al. 2022). This interaction leads to the intracellular retention of Rap1A in its inactive form, thus preventing its activation and translocation to the PM with the subsequent inhibition of cell adhesion pathway *via* the β1-integrin signaling. This mechanism could at least partially explain the reduced clonogenic capacity as well as the lack of intra- or extravasation through a monolayer of EC we observed in PC3 cells overexpressing TRPM8 (Grolez et al. 2022). The Ca^{2+}-independent interplay between TRPM8 and Rap1A is just one of the interesting examples of an involvement of ion channels in physio-pathological conditions that goes beyond their channel functions (Vrenken et al. 2015; Pillozzi et al. 2007; Negri et al. 2021). Indeed, in recent years growing interest has been shown in signaling pathways that underlie the interaction of TRP channels with different partner proteins (Vrenken et al. 2015; Genova et al. 2017; Joly et al. 2006) and, in particular, for the close bidirectional interplay involving TRP channels and small GTPase in all phases of the metastatic cascade which in some cases are independent of Ca^{2+} signals (Chinigò, Fiorio Pla, and Gkika 2020). Indeed, it has been largely demonstrated that on one hand, TRP channels may affect small GTPase activity *via* both Ca^{2+}-dependent and Ca^{2+}–independent pathways, and on the other hand, small GTPases may act as TRP channels effectors as well as regulators, by modulating channel gating, trafficking, gene expression, and protein-protein interactions (Chinigò, Fiorio Pla, and Gkika 2020). In the case of TRPM8, for example, its direct interaction was found not only with Rap1A but also with other GTPases in their inactive form including the G-protein subunit $G_{\alpha q}$, which leads to the inhibition of TRPM8 gating and, in turn, may be subject to TRPM8-mediated metabotropic regulation (Zhang et al. 2012; Klasen et al. 2012). Going deeper into the characterization of TRPM8-Rap1A interaction in PCa, we identified and functionally validated the residues involved in it (Chinigò et al. 2022). As previously observed in EC, we confirmed that also in PC3 cells the

interaction occurs between the N-terminal tail of TRPM8 and the inactive form of Rap1A in close proximity to ER membranes. More in detail, we demonstrated that the glutamate 207 and the tyrosine 240 in TRPM8 sequence as well as the tyrosine 32 localized in the switch I region of Rap1A play a central role in mediating such interaction (Chinigò et al. 2022). Curiously, we observed that, although the pore-independence of this pathway, the presence of the agonist icilin further increased the TRPM8-mediated inhibition of Rap1 and PC3 cells' migration/adhesion (Chinigò et al. 2022). This observation seems to suggest an active role of icilin in promoting TRPM8-Rap1 interaction, probably due to global conformational rearrangements triggered by the binding of the agonist in TRPM8 transmembrane domain that are propagated to the cytosolic domain where the interaction with Rap1A occur (Yin et al. 2018; 2019). Finally, the importance of the residues we identified as crucial for TRPM8-Rap1A interaction and the subsequent effects on cell migration and adhesion have also been confirmed in other cancer cells including breast (MCF-7) and cervical (HeLa) cancer cells, thus suggesting a broader spectrum of action of TRPM8 as a Rap1 inhibitor, although with a different impact in terms of control of cell adhesion and migration according to the cancer type (Chinigò et al. 2022). Moreover, we have verified that none of these residues are mutated in cohorts of patients of all the types of cancer analyzed by us (Chinigò et al. 2022). This bodes well for the potential use of the TRPM8 sequence, or, more simply, a peptide sequence that mimics the N-terminal tail involved in functional interaction with Rap1 to prevent and/or block cancer metastasis. Indeed, it is interesting to point out that our findings on the mechanistic of the molecular mechanism underlying the anti-metastatic role of TRPM8 in PCa progression, shed light on the possibility to use TRPM8 not only as a "drugable target" but also as a target for the development of peptidomimetics. Acting directly on specific protein-protein interactions is, nowadays, an intriguing field of research with great potential in cancer therapy as it allows to minimize side effects by targeting only the cellular pathways associated with a specific interaction (Mabonga and Kappo 2019; 2020; Tsagareli and Nozadze 2020). Some examples of peptidomimetics that aim to impair some protein-protein interactions involving TRP channels are already present in the literature (Btesh et al. 2013; Fischer, Btesh, and McNaughton 2013; Weng et al. 2015; Katterle et al. 2004; Tu, Chang, and Bikle 2005; Saldías et al. 2021) and could represent a reliable and innovative approach for future perspectives in cancer therapy (Scott et al. 2016; Saldías et al. 2021).

Interestingly, we found that TRPM8-mediated inhibition of PCa invasiveness is not only related to Rap1A but also involves other small GTPase including Cdc42 and Rac1 (Grolez et al. 2022), well-known for their role in mediating focal adhesions formation as well as epithelial-to-mesenchymal transition (EMT) by regulating cytoskeleton remodeling (Noren et al. 2000; Millar, Janes, and Giangreco 2017). Indeed, we observed that TRPM8 inhibits the expression of Cdc42 and Rac1 and inhibits the phosphorylation/activation of ERK and FAK, two crucial kinases involved in focal adhesion formation, in line with other studies (Yang et al. 2009; Zhu et

al. 2011; Wang et al. 2012). By contrast, there is no evidence of an impact of TRPM8 on cell invasion as its overexpression didn't affect the production of matrix metalloproteinases (MMPs) like MMP-2 and MMP-9 in PC3 cells (Grolez et al. 2022). Overall, the reduced metastatic dissemination mediated by TRPM8 *in vivo* can be explained by its ability to impair PCa cell adhesion and migration mainly through the Ca^{2+}-independent inhibition of Rap1A and β_1-integrin signaling and the Ca^{2+}-dependent impairment of focal adhesion formation (Chinigò et al. 2022; Grolez et al. 2022).

All these new mechanistic findings provide new insights for the development of innovative and effective tools targeting TRPM8 to block PCa progression and improve the prognosis of the currently incurable mCRPC phenotypes. To note, all our experiments both *in vitro* and *in vivo* confirmed that TRPM8 overexpression by itself is able to inhibit PC3 cell migration while TRPM8 activation further enhances the inhibitory effect on metastatic PCa cells' motility as previously reported (Yang et al. 2009; Zhu et al. 2011; Gkika et al. 2010; Grolez et al. 2019). This increases the hope of being able to use TRPM8 agonists such as PSA, WS12, and icilin to counteract prostate cancer metastases, but also suggests the possibility to use other approaches like gene therapy or the administration of therapeutic peptide mimicking the channel or part of its structure to use TRPM8 as a molecular target. Altogether, our findings strongly support TRPM8 as one of the most promising clinical targets in PCa therapy. More specifically, peptide therapy could help in improving the prognosis of patients with the more aggressive androgen-independent phenotype induced by androgen deprivation, whereas TRPM8 activation by specific agonists/antagonists could be used in the treatment of earlier phases according to cancer stages and androgen sensitivity.

However, from a clinical perspective, we must not forget the problems associated with the administration of therapeutic agents, be they small molecules or peptides. Indeed, TRP channels' activators/inhibitors, due to their intrinsic lipophilicity, often suffer from poor solubility and stability in physiological conditions thus compromising their bioavailability and therapeutic action *in vivo*. Moreover, a targeted delivery could be necessary to minimize undesirable side effects very common due to the multifunctional roles and the wide expression of TRP channels in many different districts of the body. In this context, the development of efficient nanodelivery systems can be as crucial as the identification of new molecular targets in cancer therapy. As an example, nanoparticles containing the natural anti-cancer curcumin have been proposed to efficiently reduce PCa growth (Yallapu et al. 2014). In this context, our group has very recently developed a molecular tool based on lipid nanocapsules containing WS12 (LNC-WS12) to target TRPM8 for PCa treatment (Grolez et al. 2019). The incorporation of WS12 into this kind of hybrid structure between polymeric nanocapsules and liposomes significantly increases the solubility of the molecule and allows 10 times lower agonist concentration to use for the activation of TRPM8 (Grolez et al. 2019). Interestingly, we demonstrated the applicability of this nanosystem *in vivo*, by showing that the injection of LNC-WS12 in a prostate

orthotopic xenografted mouse model efficiently reduced PCa cell dissemination in particular in the liver and lung. Therefore, our tool could be useful for blocking the spread of metastases in patients who have not yet lost sensitivity to androgens and thus TRPM8 expression (Tsavaler et al. 2001), although its efficiency on androgen-dependent PCa cells needs further investigations to be confirmed. By contrast, due to the low distribution of LNC we observed in the prostate (when injected at a concentration of 1 mg/kg but), LNC-WS12 are not efficient to target primary tumors. In this regard, improving the nanosystem with some strategies of active targeting towards the prostate like the functionalization of LNC using an antibody against PSMA could help to overcome this issue thus extending its applicability also for localized PCa patients. This approach would allow at the same time limiting the possible side effects of TRPM8 activation in clinical applications.

4.2 Lipid nanoparticles as drug delivery systems: incorporation of polymethine dyes

In the same vein used in the studies on TRPM8, we decided to start investigating the possibility of using lipid nanosystems to increase the solubility of a class of near-infrared (NIR) probes that have recently revealed an excellent potential in *in vivo* optical imaging as well as in photodynamic therapy (PDT). PDT is an innovative therapeutic strategy that could help avoid undesirable side effects associated with other treatment approaches and the development of metastatic stages in PCa as well as in other cancer types, thus improving the outcome of therapy.

In recent years, the Department of Organic Chemistry of the University of Turin has synthesized a new class of NIR polymethine dyes (PMD) characterized by easiness in designing, simplicity of synthesis, and peculiar spectroscopic properties. In particular, they focused on the synthesis of cyanines (CY) and squaraines (SQ) based on the indolenine ring, with particular attention to the study of the structure-activity relationship (Serpe et al. 2016; Ciubini et al. 2019). Indeed PMD exhibit a strong structure-properties relationship that allows for obtaining dyes with the desired properties by simply tuning their structure. As an example, it is possible to produce dyes with absorption/emission in the NIR region of the electromagnetic spectrum (650-900 nm), corresponding to the so-called “therapeutic window”, simply by extending the length of the polymethine bridge. Dyes with absorption in the NIR are optimal for biomedical applications since they allow deeper tissue penetration with minimal background interference due to the minimal scattering of the excitation light and low self-fluorescence of biological molecules in that region (Yi et al. 2014). Interestingly, beyond the capability to improve tumor visualization, allowing the detection of small pre-neoplastic lesions and metastasis (Moon et al. 2003; Shi, Wu, and Pan 2016), some PMD revealed a preferential accumulation in cancer cells without the need for chemical conjugation and an intrinsic anticancer activity suitable for PDT applications (Luo et al. 2013; Tan et al. 2012; Ramaiah et al. 2004; Avirah et al. 2012; Soumya et al. 2014). In this regard, it has been demonstrated that the presence of a heavy atom in the heterocyclic ring of these dyes significantly improves their photodynamic activity basically by enhancing the inter-system conversion process and thus singlet oxygen production (Atchison et al. 2017; Ramaiah et al. 1997).

Consistently, in a previous work, we reported the activity of a bromine-substituted squaraine based on the (Br-SQ-C4) with a promising photoactivity (Serpe et al. 2016). However, as well as other PMD, Br-SQ-C4 is inclined to photodegradation and aggregation in aqueous media due to its intrinsic low hydrophilicity (Kwiatkowski et al. 2018). Thus, we employed a lipid-based nanovesicle system, namely Quatsomes (QS), to

improve its performance in physiological conditions for future applications *in vivo*. To improve the efficiency of drug incorporation into QS we had to extend the length of the alkyl chain linked to the quaternary N atom from 4 to 12 carbon atoms (Br-SQ-C12). Moreover, we optimized the formulation by incorporating different dye concentrations into different amounts of Cholesterol (Chol) and Sterealkonium Chloride (STK), the main components of QS formulations. Indeed, the cytotoxicity associated with quaternary ammonium surfactants composing QS such as Stk could represent a challenge in their *in vivo* application. Once fixed QS concentration to 2 µg/mL due to the reasonable biocompatibility showed by this formulation, we tested different loading concentrations of the dye using theoretical dye concentrations ranging from 50 to 300 µM and corresponding to a real concentration from 10 to 85.3 nM respectively. Interestingly, all the formulations were found to significantly increase cell cytotoxicity after light beam irradiation, thus demonstrating that the incorporation of Br-SQ-C12 allows the use of lower doses of the dyes to obtain a suitable photodynamic activity. Indeed, Br-SQ-C12-loaded QS were photoactive starting from a concentration of the dye at least 10 times less compared to the dye in its free form. Of note, the squaraine's concentration usually employed for PDT studies ranges from 1 to 100 µM (Serpe et al. 2016; Rapozzi et al. 2010; Shafeekh et al. 2014) but we demonstrated that the use of a nanocarrier system allows using a concentration of photo-active dye up to 10-1000 times lower than usual.

Similarly, we showed that the encapsulation of PMD within another type of lipid nanocarrier named solid lipid nanoparticles (SLN) highly enhanced the dye's photoactivity (Chinigò et al. 2022b). More specifically, a bromo benzoindolenine cyanine (Br-BCY-C4) which didn't show any phototoxicity in its free form became photoactive upon incorporation into SLN. Our results are in agreement with data in the literature reporting how the incorporation of other promising photosensitizers into SLN improves their physical-chemical properties (Lima et al. 2013; Navarro et al. 2014). A possible explanation, in addition to the higher local concentration of the dye due to the confinement within a nanoparticle, is that the nanocarrier, disfavouring the aggregation phenomena of the compound within the lipid microenvironment, prolongs the life of the triplet state thus leading to a more efficient photoactivity. Interestingly, we observed that the cytotoxic profile of PMD-SLN is cell-type specific (Chinigò et al. 2022b). More specifically, we found that endothelial cells are less sensitive to the nanosystems compared to cancer cells and this could represent a good advantage for future biomedical applications since it might allow for limiting possible side effects.

We efficiently incorporated into SLN also a bromo benzoindolenine squaraine (Br-BSQ-C4), which is completely insoluble in water in its free form due to the high hydrophobicity of the structure (Chinigò et al. 2022b). Unlike the cyanine derivative, this molecule did not show any photoactivity. However, characterizing the optical properties of this nanosystem, we observed that the incorporation of Br-BSQ-C4 into SLN not only allows its solubilization in physiological conditions but also significantly enhances its spectroscopic

properties. Indeed, once encapsulated the dye exhibits a higher quantum yield (52% versus 31%) and a fluorescence lifetime even doubled (2.571 versus 1.382) (Chinigò et al. 2022b). This means that Br-BSQ-C4-loaded SLN gives rise to higher and prolonged fluorescence emission compared to the dye not incorporated probably due to an enhanced stabilization of its structure offered by the lipid microenvironment. Therefore, this nanosystem, although not applicable as a therapeutic tool in photodynamic treatment, could be considered a good diagnostic candidate for *in vivo* fluorescence imaging. Overall, we demonstrated that SLN allow the solubilization of PMD in aqueous solutions preserving and further enhancing their spectroscopic properties. Moreover, SLN revealed high entrapment efficiency, good biocompatibility as well as efficient cellular uptake, thus supporting PMD-loaded SLN as suitable and appealing candidates for both diagnostic and therapeutic purposes.

Taken together our *in vitro* results seems to support the applicability of lipid nanocarriers including QS and SLN for PDT application and highlighted the importance to achieve high dye-loaded nanostructures to optimize their photoactive properties. However, further efforts are needed to optimize the biocompatibility of dye-loaded QS with a view to future biomedical applicability. Moreover, the bioavailability/pharmacokinetic profile *in vivo* of these nanosystems must be investigated in order to evaluate their real applicability in both diagnostic and therapeutic fields.

4.3 References for general discussion

Adapala R.K., Thoppil R.J., Ghosh K., Cappelli H., Dudley A.C., Paruchuri S., Keshamouni V., et al. **2016**. "Activation of Mechanosensitive Ion Channel TRPV4 Normalizes Tumor Vasculature and Improves Cancer Therapy." *J Autism Dev Disord* 35 (3): 314–22. https://doi.org/10.1097/CCM.0b013e31823da96d.Hydrogen.

Aragon-Ching J.B., Jain L., Gulley J.L., Arlen P.M., Wright J.J., Steinberg S.M., Draper D., et al. **2009**. "Final Analysis of a Phase II Trial Using Sorafenib for Metastatic Castration-Resistant Prostate Cancer." *BJU International* 103 (12): 1636–40. https://doi.org/10.1111/J.1464-410X.2008.08327.X.

Atchison J., Kamila S., Nesbitt H., Logan K.A., Nicholas D.M., Fowley C., Davis J., Callan B., McHale A.P., and Callan J.F. **2017**. "Iodinated Cyanine Dyes: A New Class of Sensitisers for Use in NIR Activated Photodynamic Therapy (PDT)." *Chem. Commun.* 53 (12): 2009–12. https://doi.org/10.1039/C6CC09624G.

Avirah R.R., Jayaram D.T., Adarsh N., and Ramaiah D. **2012**. "Squaraine Dyes in PDT: From Basic Design to *in Vivo* Demonstration." *Org. Biomol. Chem.* 10 (5): 911–20. https://doi.org/10.1039/C1OB06588B.

Barras A., Boussekey L., Courtade E., and Boukherroub R. **2013**. "Hypericin-Loaded Lipid Nanocapsules for Photodynamic Cancer Therapy in Vitro." *Nanoscale* 5 (21): 10562–72. https://doi.org/10.1039/C3NR02724D.

Bidaux G., Roudbaraki M., Merle C., Crépin A., Delcourt P., Slomianny C., Thebault S., et al. **2005**. "Evidence for Specific TRPM8 Expression in Human Prostate Secretory Epithelial Cells: Functional Androgen Receptor Requirement." *Endocrine-Related Cancer* 12 (2): 367–82. https://doi.org/10.1677/erc.1.00969.

Bidaux G., Beck B., Zholos A., Gordienko D., Lemonnier L., Flourakis M., Roudbaraki M., et al. **2012**. "Regulation of Activity of Transient Receptor Potential Melastatin 8 (TRPM8) Channel by Its Short Isoforms." *Journal of Biological Chemistry* 287 (5): 2948–62. https://doi.org/10.1074/jbc.M111.270256.

Braga V.M.M., Del Maschio A., Machesky L., and Dejana E.. **1999**. "Regulation of Cadherin Function by Rho and Rac: Modulation by Junction Maturation and Cellular Context." Edited by Richard O. Hynes. *Molecular Biology of the Cell* 10 (1): 9–22. https://doi.org/10.1091/mbc.10.1.9.

Brossa A., Buono L., Fallo S., Fiorio Pla A., Munaron L., and Bussolati B. **2019**. "Alternative Strategies to Inhibit Tumor Vascularization." *International Journal of Molecular Sciences* 20 (24). https://doi.org/10.3390/ijms20246180.

Btesh J., Fischer M.J.M., Stott K., and McNaughton P.A. **2013**. "Mapping the Binding Site of TRPV1 on AKAP79: Implications for Inflammatory Hyperalgesia." *Journal of Neuroscience* 33 (21): 9184–93. https://doi.org/10.1523/JNEUROSCI.4991-12.2013.

Cappelli H.C., Kanugula A.K., Adapala R.K., Amin V., Sharma P., Midha P., Paruchuri S., and Thodeti C.K. **2019**. "Mechanosensitive TRPV4 Channels Stabilize VE-Cadherin Junctions to Regulate Tumor Vascular Integrity and Metastasis." *Cancer Letters* 442: 15–20. https://doi.org/10.1016/j.canlet.2018.07.042.

Chinigò G., Fiorio Pla A., and Gkika, D. **2020**. "TRP Channels and Small GTPases Interplay in the Main Hallmarks of Metastatic Cancer." *Frontiers in Pharmacology* 11: 581455. https://doi.org/10.3389/fphar.2020.581455.

Chinigò G., Grolez G., Audero M., Bokhobza A., Bernardini M., Cicero J., Toillon R.A., Bailleul Q., Visentin L., Ruffinatti FA, Brysbaert G., Lensink M., De-Ruyck J., Cantelmo A.R., Fiorio Pla A. and Gkika D. **2022**. "TRPM8-RAP1A interaction sites as critical determinants for adhesion and migration of prostate and other epithelial cancer cells" *Cancers* 14(9): 2261. https://doi.org/10.3390/cancers14092261

Chinigò G. Gonzalez-Paredes A., Gilardino A., Barbero N., Barolo C., Gasco P., Fiorio Pla A. and Visentin S. **2022**b. "Polymethine dyes-loaded solid lipid nanoparticles (SLN) as promising photosensitizers for biomedical applications" *Spectrochimica Acta Part A: Mol Biomol Spectrosc.* 271:120909. https://doi.org/10.1016/j.saa.2022.120909

Ciubini B., Visentin S., Serpe L., Canaparo R., Fin A., and Barbero N. **2019**. "Design and Synthesis of Symmetrical Pentamethine Cyanine Dyes as NIR Photosensitizers for PDT." *Dyes and Pigments* 160: 806–13. https://doi.org/10.1016/j.dyepig.2018.09.009.

Derouiche S., Mariot P., Warnier M., Vancauwenberghe E., Bidaux G., Gosset P., Mauroy B., et al. **2017**. "Activation of TRPA1 Channel by Antibacterial Agent Triclosan Induces Vegf Secretion in Human Prostate Cancer Stromal Cells." *Cancer Prevention Research* 10 (3): 177–87. https://doi.org/10.1158/1940-6207.CAPR-16-0257/36264/AM/ACTIVATION-OF-TRPA1-CHANNEL-BY-ANTIBACTERIAL-AGENT.

Feng T., Yu H., Xia Q., Ma Y., Yin H., Shen Y., and Liu X. **2017**. "Cross-Talk Mechanism between Endothelial Cells and Hepatocellular Carcinoma Cells via Growth Factors and Integrin Pathway Promotes Tumor Angiogenesis and Cell Migration." *Oncotarget* 8 (41): 69577–93. https://doi.org/10.18632/ONCOTARGET.18632.

Fiorio Pla A., Brossa A., Bernardini M., Genova T., Grolez G., Villers A., Leroy X., Prevarskaya N., Gkika D., and Bussolati B. **2014**. "Differential Sensitivity of Prostate Tumor Derived Endothelial Cells to Sorafenib and Sunitinib." *BMC Cancer* 14 (January): 939. https://doi.org/10.1186/1471-2407-14-939.

Fiorio Pla A., and Gkika D. **2013**. "Emerging Role of TRP Channels in Cell Migration: From Tumor Vascularization to Metastasis." *Frontiers in Physiology* 4 (311): 1–12. https://doi.org/10.3389/fphys.2013.00311.

Fischer M.J.M., Btesh J., and McNaughton P.A. 2013. "Disrupting Sensitization of Transient Receptor Potential Vanilloid Subtype 1 Inhibits Inflammatory Hyperalgesia." *Journal of Neuroscience* 33 (17): 7407–14. https://doi.org/10.1523/JNEUROSCI.3721-12.2013.

Genova T., Grolez G.P., Camillo C., Bernardini M., Bokhobza A., Richard E., Scianna M., et al. **2017**. "TRPM8 Inhibits Endothelial Cell Migration via a Nonchannel Function by Trapping the Small GTPase Rap1." *Journal of Cell Biology* 216 (7): 2107–30. https://doi.org/10.1083/jcb.201506024.

Gkika D., Flourakis M., Lemonnier L., and Prevarskaya N. **2010**. "PSA Reduces Prostate Cancer Cell Motility by Stimulating TRPM8 Activity and Plasma Membrane Expression." *Oncogene* 29 (32): 4611–16. https://doi.org/10.1038/onc.2010.210.

Gkika D., Lemonnier L., Shapovalov G., Gordienko D., Poux C., Bernardini M., Bokhobza A., et al. **2015**. "TRP Channel-Associated Factors Are a Novel Protein Family That Regulates TRPM8 Trafficking and Activity." *Journal of Cell Biology* 208 (1): 89–107. https://doi.org/10.1083/jcb.201402076.

Gkika D., and Prevarskaya N. **2009**. "Molecular Mechanisms of TRP Regulation in Tumor Growth and Metastasis." *BBA - Molecular Cell Research* 1793 (6): 953–58. https://doi.org/10.1016/j.bbamcr.2008.11.010.

———. **2011**. "TRP Channels in Prostate Cancer : The Good , the Bad and the Ugly ?" *Asian J Androl.* 13 (5): 673–76. https://doi.org/10.1038/aja.2011.18.

Grolez G.P., Hammadi M., Barras A., Gordienko D., Slomianny C., Völkel P., Angrand P.O., et al. **2019**. "Encapsulation of a TRPM8 Agonist, WS12, in Lipid Nanocapsules Potentiates PC3 Prostate Cancer Cell Migration Inhibition through Channel Activation." *Scientific Reports* 9 (1): 7926. https://doi.org/10.1038/s41598-019-44452-4.

Grolez G.P., Gordiendko D., Clarisse M., Hammadi M., Desruelles E., Fromont G., Prevarskaya N., Slomianny C., and Gkika D. **2019**. "TRPM8-Androgen Receptor Association within Lipid Rafts Promotes Prostate Cancer Cell Migration." *Cell Death & Disease* 10 (9): 652. https://doi.org/10.1038/s41419-019-1891-8.

Grolez G.P., and Gkika D. **2016**. "TRPM8 Puts the Chill on Prostate Cancer." *Pharmaceuticals* 9 (44). https://doi.org/10.3390/ph9030044.

Grolez G.P., Chinigò G., Barras, A., Hammadi M., Noyer L., Kondraskaya K., Bulk E., Oullier T., Marionneau-Lambot S., Le Mée M., Rétif S., Lerondel S., Bongiovanni A., Genova T., Roger S., Boukkerhoub R., Schwab A., Fiorio Pla A. and Gkika D. **2019**. "TRPM8 as an anti-tumoral target in prostate cancer growth and metastasis dissemination." *International Journal of Molecular Sciences* 23 (12):6672. https://doi.org/10.3390/ijms23126672.

Hanahan D., and Weinberg R.A. **2011**. "Review Hallmarks of Cancer : The Next Generation." *Cell* 144 (5): 646–74. https://doi.org/10.1016/j.cell.2011.02.013.

Joly D., Ishibe S., Nickel C., Yu Z., Somlo S., and Cantley L.G. **2006**. "The Polycystin 1-C-Terminal Fragment Stimulates ERK-Dependent Spreading of Renal Epithelial Cells." *The Journal of Biological Chemistry* 281 (36): 26329–39. https://doi.org/10.1074/JBC.M601373200.

Katterle Y., Brandt B.H., Dowdy S.F., Niggemann B., Zänker K.S., and Dittmar T. **2004**. "Antitumour Effects of PLC-Γ1-(SH2)2-TAT Fusion Proteins on EGFR/c-ErbB-2-Positive Breast Cancer Cells." *British Journal of Cancer* 90 (1): 230–35. https://doi.org/10.1038/sj.bjc.6601506.

Klasen K., Hollatz D., Zielke S., Gisselmann G., Hatt H., and Wetzel C.H. **2012**. "The TRPM8 Ion Channel Comprises Direct Gq Protein-Activating Capacity." *European Journal of Physiology* 463 (6): 779–97. https://doi.org/10.1007/s00424-012-1098-7.

Kwiatkowski S., Knap B., Przystupski D., Saczko J., Kędzierska E., Knap-Czop K., Kotlińska J., Michel O., Kotowski K., and Kulbacka J. **2018**. "Photodynamic Therapy - Mechanisms, Photosensitizers and Combinations." *Biomedicine & Pharmacotherapy = Biomedecine & Pharmacotherapie* 106 (October): 1098–1107. https://doi.org/10.1016/J.BIOPHA.2018.07.049.

Laragione T., Cheng K.F., Tanner M.R., He M., Beeton C., Al-Abed Y., and Gulko P.S. **2015**. "The cation channel TRPV2 is a new suppressor of arthritis severity, joint damage and synovial fibroblast invasion." *Clin Immunol.* 158 (2): 183–92. https://doi.org/10.1016/j.clim.2015.04.001.THE.

Lima A.M., Dal Pizzol C., Monteiro F.B.F., Creczynski-Pasa T.B., Andrade G.P., Ribeiro A.O., and Perussi J.R. **2013**. "Hypericin Encapsulated in Solid Lipid Nanoparticles: Phototoxicity and Photodynamic Efficiency." *Journal of Photochemistry and Photobiology B: Biology* 125: 146–54. https://doi.org/10.1016/j.jphotobiol.2013.05.010.

Luo S., Tan X., Qi Q., Guo Q., Ran X., Zhang L., Zhang E., et al. **2013**. "A Multifunctional Heptamethine Near-Infrared Dye for Cancer Theranosis." *Biomaterials* 34 (9): 2244–51.

Mabonga L., and Kappo A.P. **2019**. "Protein-Protein Interaction Modulators: Advances, Successes and Remaining Challenges." *Biophysical Reviews* 11 (4): 559–81. https://doi.org/10.1007/s12551-019-00570-x.

———. **2020**. "Peptidomimetics: A Synthetic Tool for Inhibiting Protein–Protein Interactions in Cancer." *International Journal of Peptide Research and Therapeutics*. https://doi.org/10.1007/s10989-019-09831-5.

Martínez-Jabaloyas J.M., March-Villalba J.A., Navarro-García M.M., and Dasi F. **2013**. "Anti-Angiogenic Therapies in Prostate Cancer." *Expert Opinion on Biological Therapy* 13 (1): 1–5. https://doi.org/10.1517/14712598.2013.733366.

Michaelson M.D., Regan M.M., Oh W.K., Kaufman D.S., Olivier K., Michaelson S.Z., Spicer B., Gurski C., Kantoff P.W., and Smith M.R. **2009**. "Phase II Study of Sunitinib in Men with Advanced Prostate Cancer." *Annals of Oncology : Official Journal of the European Society for Medical Oncology* 20 (5): 913–20. https://doi.org/10.1093/ANNONC/MDP111.

Michaelson M.D., Oudard S., Houede N., Maurina T., Ou Y.C., Sengeløv L., Daugaard G., et al. **2014**. "Randomized, Placebo-Controlled, Phase III Trial of Sunitinib plus Prednisone versus Prednisone Alone in Progressive, Metastatic, Castration-Resistant Prostate Cancer." *Journal of Clinical Oncology : Official Journal of the American Society of Clinical Oncology* 32 (2): 76–82. https://doi.org/10.1200/JCO.2012.48.5268.

Millar F.R., Janes S.M., and Giangreco A. **2017**. "Epithelial Cell Migration as a Potential Therapeutic Target in Early Lung Cancer." *European Respiratory Review : An Official Journal of the European Respiratory Society* 26 (143): 160069. https://doi.org/10.1183/16000617.0069-2016.

Moon W.K., Lin Y., O'Loughlin T., Tang Y., Kim D-E., Weissleder R., and Tung C-H. **2003**. "Enhanced Tumor Detection Using a Folate Receptor-Targeted Near-Infrared Fluorochrome Conjugate." *Bioconjugate Chemistry* 14 (3): 539–45. https://doi.org/10.1021/bc0340114.

Munaron L. **2015**. "Systems Biology of Ion Channels and Transporters in Tumor Angiogenesis: An Omics View." *Biochimica et Biophysica Acta - Biomembranes* 1848 (10): 2647–56. https://doi.org/10.1016/j.bbamem.2014.10.031.

Navarro F.P., Creusat G., Frochot C., Moussaron A., Verhille M., Vanderesse R., Thomann J.S., et al. **2014**. "Preparation and Characterization of MTHPC-Loaded Solid Lipid Nanoparticles for Photodynamic Therapy." *Journal of Photochemistry and Photobiology B: Biology* 130: 161–69. https://doi.org/10.1016/j.jphotobiol.2013.11.007.

Negri S., Faris P., Berra-Romani R., Guerra G., and Moccia F. **2020**. "Endothelial Transient Receptor Potential Channels and Vascular Remodeling: Extracellular Ca^{2+} Entry for Angiogenesis, Arteriogenesis and Vasculogenesis." *Frontiers in Physiology* 10 (January): 1–23. https://doi.org/10.3389/fphys.2019.01618.

Negri S., Faris P., Maniezzi C., Pellavio G., Spaiardi P., Botta L., Laforenza U., Biella G., and Moccia F. **2021**. "NMDA Receptors Elicit Flux-Independent Intracellular Ca^{2+} Signals via Metabotropic Glutamate Receptors and Flux-Dependent Nitric Oxide Release in Human Brain Microvascular Endothelial Cells." *Cell Calcium* 99 (July): 102454. https://doi.org/10.1016/j.ceca.2021.102454.

Noren N.K., Liu B.P., Burridge K., and Kreft B. **2000**. "P120 Catenin Regulates the Actin Cytoskeleton via RHO Family GTPases." *Journal of Cell Biology* 150 (3): 567–79. https://doi.org/10.1083/jcb.150.3.567.

Peng M., Wang Z., Yang Z., Tao L., Liu Q., Yi L., and Wang X. **2015**. "Overexpression of Short TRPM8 Variant α Promotes Cell Migration and Invasion, and Decreases Starvation-Induced Apoptosis in Prostate Cancer LNCaP Cells." *Oncology Letters* 10 (3): 1378–84. https://doi.org/10.3892/ol.2015.3373.

Pillozzi S., Brizzi M.F., Bernabei P.A., Bartolozzi B., Caporale R., Basile V., Boddi V., Pegoraro L., Becchetti A., and Arcangeli A. **2007**. "VEGFR-1 (FLT-1), B1 Integrin, and HERG K^+ Channel for a Macromolecular Signaling Complex in Acute Myeloid Leukemia: Role in Cell Migration and Clinical Outcome." *Blood* 110 (4): 1238–50. https://doi.org/10.1182/blood-2006-02-003772.

Ramaiah D., Eckert I., Arun K.T., Weidenfeller L., and Epe B. **2004**. "Squaraine Dyes for Photodynamic Therapy: Mechanism of Cytotoxicity and DNA Damage Induced by Halogenated Squaraine Dyes Plus Light (>600 Nm)." *Photochemistry and*

Photobiology 79 (1): 99. https://doi.org/10.1111/j.1751-1097.2004.tb09863.x.

Ramaiah D., Joy A., Chandrasekhar N., Eldho N.V., Das S., and George M.V. **1997**. "Halogenated Squaraine Dyes as Potential Photochemotherapeutic Agents. Synthesis and Study of Photophysical Properties and Quantum Efficiencies of Singlet Oxygen Generation." *Photochemistry and Photobiology* 65 (5): 783–90. https://doi.org/10.1111/j.1751-1097.1997.tb01925.x.

Rapozzi V., Beverina L., Salice P., Pagani G.A., Camerin M., and Xodo L.E. **2010**. "Photooxidation and Phototoxicity of π-Extended Squaraines." *Journal of Medicinal Chemistry* 53 (5): 2188–96. https://doi.org/10.1021/jm901727j.

Rojas R., Ruiz W.G., Leung S.M., Jou T.S., and Apodaca G. **2001**. "Cdc42-Dependent Modulation of Tight Junctions and Membrane Protein Traffic in Polarized Madin-Darby Canine Kidney Cells." *Molecular Biology of the Cell* 12 (8): 2257–74. https://doi.org/10.1091/mbc.12.8.2257.

Saldías M.P., Maureira D., Orellana-Serradell O., Silva I., Lavanderos B., Cruz P., Torres C., Cáceres M., and Cerda O. **2021**. "TRP Channels Interactome as a Novel Therapeutic Target in Breast Cancer." *Frontiers in Oncology* 11 (June): 621614. https://doi.org/10.3389/FONC.2021.621614.

Scott D.E., Bayly A.R., Abell C., and Skidmore J. **2016**. "Small Molecules, Big Targets: Drug Discovery Faces the Protein-Protein Interaction Challenge." *Nature Reviews Drug Discovery* 15 (8): 533–50. https://doi.org/10.1038/nrd.2016.29.

Serpe L., Ellena S., Barbero N., Foglietta F., Prandini F., Gallo M.P., Levi R., Barolo C., Canaparo R., and Visentin S. **2016**. "Squaraines Bearing Halogenated Moieties as Anticancer Photosensitizers: Synthesis, Characterization and Biological Evaluation." *European Journal of Medicinal Chemistry* 113: 187–97. https://doi.org/10.1016/j.ejmech.2016.02.035.

Shafeekh K.M., Soumya M.S., Rahim M.A., Abraham A., and Das S. **2014**. "Synthesis and Characterization of Near-Infrared Absorbing Water Soluble Squaraines and Study of Their Photodynamic Effects in DLA Live Cells." *Photochemistry and Photobiology* 90 (3): 585–95. https://doi.org/10.1111/php.12236.

Shi C., Wu J.B., and Pan D. **2016**. "Review on Near-Infrared Heptamethine Cyanine Dyes as Theranostic Agents for Tumor Imaging, Targeting, and Photodynamic Therapy." *Journal of Biomedical Optics* 21 (5): 50901. https://doi.org/10.1117/1.JBO.21.5.050901.

Soumya M.S., Shafeekh K.M., Das S., and Abraham A. **2014**. "Symmetrical Diiodinated Squaraine as an Efficient Photosensitizer for PDT Applications: Evidence from Photodynamic and Toxicological Aspects." *Chemico-Biological Interactions* 222: 44–49. https://doi.org/10.1016/j.cbi.2014.08.006.

Steinbild S., Mross K., Frost A., Morant R., Gillessen S., Dittrich C., Strumberg D., et al. **2007**. "A Clinical Phase II Study with Sorafenib in Patients with Progressive Hormone-Refractory Prostate Cancer: A Study of the CESAR Central European Society for Anticancer Drug Research-EWIV." *British Journal of Cancer* 97 (11): 1480–85. https://doi.org/10.1038/SJ.BJC.6604064.

Takaishi K., Sasaki T., Kotani H., Nishioka H., and Takai Y. **1997**. "Regulation of Cell-Cell Adhesion by Rac and Rho Small G Proteins in MDCK Cells." *Journal of Cell Biology* 139 (4): 1047–59. https://doi.org/10.1083/jcb.139.4.1047.

Tan X., Luo S., Wang D., Su Y., Cheng T., and Shi C. **2012**. "A NIR Heptamethine Dye with Intrinsic Cancer Targeting, Imaging and Photosensitizing Properties." *Biomaterials* 33 (7): 2230–39. https://doi.org/10.1016/j.biomaterials.2011.11.081.

Thebault S., Lemonnier L., Bidaux G., Flourakis M., Bavencoffe A., Gordienko D., Roudbaraki M., et al. **2005**. "Novel Role of Cold/Menthol-Sensitive Transient Receptor Potential Melastatine Family Member 8 (TRPM8) in the Activation of Store-Operated Channels in LNCaP Human Prostate Cancer Epithelial Cells." *Journal of Biological Chemistry* 280 (47): 39423–35. https://doi.org/10.1074/jbc.M503544200.

Thoppil R.J., Cappelli H.C., Adapala R.K., Kanugula A.K., Paruchuri S., and Thodeti C.K. **2016**. "TRPV4 Channels Regulate Tumor Angiogenesis *via* Modulation of Rho/Rho Kinase Pathway." *Oncotarget* 7 (18): 25849–61. https://doi.org/10.18632/oncotarget.8405.

Tsagareli M.G., and Nozadze I. **2020**. "An Overview on Transient Receptor Potential Channels Superfamily." *Behavioural Pharmacology* 31 (5): 413–34. https://doi.org/10.1097/FBP.0000000000000524.

Tsavaler L., Shapero M.H., Morkowski S., and Laus R. **2001**. "Trp-P8, a Novel Prostate-Specific Gene, Is up-Regulated in Prostate Cancer and Other Malignancies and Shares High Homology with Transient Receptor Potential Calcium Channel Proteins." *Cancer Research* 61 (9): 3760–69.

Tu C.L., Chang W., and Bikle D.D. **2005**. "Phospholipase Cγ1 Is Required for Activation of Store-Operated Channels in Human Keratinocytes." *Journal of Investigative Dermatology* 124 (1): 187–97. https://doi.org/10.1111/j.0022-202X.2004.23544.x.

Valero M.L., Mello de Queiroz F., Stühmer W., Viana F., and Pardo L.A. **2012**. "TRPM8 Ion Channels Differentially Modulate

Proliferation and Cell Cycle Distribution of Normal and Cancer Prostate Cells." *PLoS ONE* 7 (12): 2–13. https://doi.org/10.1371/journal.pone.0051825.

Valero M.L., Morenilla-Palao C., Belmonte C., and Viana F. **2011**. "Pharmacological and Functional Properties of TRPM8 Channels in Prostate Tumor Cells." *Pflugers Archiv : European Journal of Physiology* 461 (1): 99–114. https://doi.org/10.1007/s00424-010-0895-0.

Vancauwenberghe E., Noyer L., Derouiche S., Lemonnier L., Gosset P., Sadofsky L.R., Mariot P., et al. **2017**. "Activation of Mutated TRPA1 Ion Channel by Resveratrol in Human Prostate Cancer Associated Fibroblasts (CAF)." *Molecular Carcinogenesis* 56 (8): 1851–67. https://doi.org/10.1002/mc.22642.

Vrenken K.S., Jalink K., van Leeuwen F.N., and Middelbeek J. **2015**. "Beyond Ion-Conduction: Channel-Dependent and -Independent Roles of TRP Channels during Development and Tissue Homeostasis." *Biochimica et Biophysica Acta - Molecular Cell Research* 1863 (6): 1436–46. https://doi.org/10.1016/j.bbamcr.2015.11.008.

Wang Y., Wang X., Yang Z., Zhu G., Chen D., and Meng Z. **2012**. "Menthol Inhibits the Proliferation and Motility of Prostate Cancer DU145 Cells." *Pathology and Oncology Research* 18 (4): 903–10. https://doi.org/10.1007/s12253-012-9520-1.

Weng H.J., Patel K.N., Jeske N.A., Bierbower S.M., Zou W, Tiwari V., Zheng Q, et al. **2015**. "Tmem100 Is a Regulator of TRPA1-TRPV1 Complex and Contributes to Persistent Pain." *Neuron* 85 (4): 833–46. https://doi.org/10.1016/j.neuron.2014.12.065.

Wertz I.E., and Dixit V.M. **2000**. "Characterization of Calcium Release-Activated Apoptosis of LNCaP Prostate Cancer Cells." *Journal of Biological Chemistry* 275 (15): 11470–77. https://doi.org/10.1074/jbc.275.15.11470.

Yallapu M.M., Khan S., Maher D.M., Ebeling M.C., Sundram V., Chauhan N., Ganju A., et al. **2014**. "Anti-Cancer Activity of Curcumin Loaded Nanoparticles in Prostate Cancer." *Biomaterials* 35 (30): 8635–48. https://doi.org/10.1016/j.biomaterials.2014.06.040.

Yang Z.H., Wang X.H., Wang H.P., and Hu L.Q. **2009**. "Effects of TRPM8 on the Proliferation and Motility of Prostate Cancer PC-3 Cells." *Asian Journal of Andrology* 11 (2): 157–65. https://doi.org/10.1038/aja.2009.1.

Yi X.M., Wang F.L., Qin W.J., Yang X.J., and Yuan J.L. **2014**. "Near-Infrared Fluorescent Probes in Cancer Imaging and Therapy: An Emerging Field." *International Journal of Nanomedicine* 9 (1): 1347–65. https://doi.org/10.2147/IJN.S60206.

Yin Y., Son C. Le, Allen L. Hsu, Mario J. Borgnia, Huanghe Yang, and Seok Yong Lee. **2019**. "Structural Basis of Cooling Agent and Lipid Sensing by the Cold-Activated TRPM8 Channel." *Science* 363 (6430): eaav9334. https://doi.org/10.1126/science.aav9334.

Yin Y., Wu M., Zubcevic L., Borschel W.F., Lander G.C., and Lee S.Y. **2018**. "Structure of the Cold- And Menthol-Sensing Ion Channel TRPM8." *Science* 359 (6372): 237–41. https://doi.org/10.1126/science.aan4325.

Yokota Y., Nakajima H., Wakayama Y., Muto A., Kawakami K., Fukuhara S., and Mochizuki N. **2015**. "Endothelial Ca^{2+} Oscillations Reflect VEGFR Signaling-Regulated Angiogenic Capacity *In Vivo*." *Elife*, no. 4. https://doi.org/10.7554/eLife.08817.

Zhang L., and Barritt G.J. **2004**. "Evidence That TRPM8 Is an Androgen-Dependent Ca^{2+} Channel Required for the Survival of Prostate Cancer Cells." *Cancer Research* 64 (22): 8365–73. https://doi.org/10.1158/0008-5472.CAN-04-2146.

Zhang X., Mak S., Li L., Parra A., Denlinger B., Belmonte C., and McNaughton P.A. **2012**. "Direct Inhibition of the Cold-Activated TRPM8 Ion Channel by GαQ." *Nature Cell Biology* 14 (8): 850–58. https://doi.org/10.1038/ncb2529.

Zhu G., Wang X., Yang Z., Cao H., Meng Z., Wang Y., and Chen D. **2011**. "Effects of TRPM8 on the Proliferation and Angiogenesis of Prostate Cancer PC-3 Cells in Vivo." *Oncology Letters* 2 (6): 1213–17. https://doi.org/10.3892/ol.2011.410.

5. CONCLUSIONS & FUTURE PERSPECTIVES

This Ph.D. project aimed to answer, at least in part, to the urgent need to deepen our knowledge on the mechanisms through which tumors can spread throughout the body, since metastases are currently the leading cause of cancer death worldwide. In particular, I focused on the functional role of TRP channels in PCa progression aiming to identify some promising candidates to treat advanced PCa. Since metastasis fundamentally involves cell migration, I mainly focused on TRP channels which affect the migratory phenotype of both PCa and PTEC cells.

As regards TRP channels involved in EC migration, I identified TRPA1 as a promising candidate to target PCa angiogenesis thanks to its active role in promoting cell migration thus contributing to the more aggressive phenotype shown by tumor-derived compared to normal EC from the prostate. Therefore, TRPA1 antagonists could be explored for future anti-angiogenic therapy of PCa.

As regards the involvement of TRP channels in prostate cancer cells invasiveness, I deepened the previously suggested protective role of TRPM8. We confirmed the anti-metastatic role of the channel *in vivo* and furthermore we characterized one of the mechanism through which it occurs. Interestingly, we found that the process is, at least in part, independent from the channel function and involves a direct interaction with the small GTPase Rap1A. Our results strongly support TRPM8 as a promising clinical target in PCa therapy. More specifically, TRPM8 activation by specific agonists/antagonists could be used in the treatment of earlier phases according to cancer stages and androgen sensitivity, whereas peptide therapy could help in improving the prognosis of patients with the more aggressive androgen-independent phenotype characterized by the loss of TRPM8 expression. As future perspectives, we would like to test the possibility to use TRPM8 not only as a “drugable target” but also as target for the development of a peptide that, mimicking the TRPM8 sequence involved in the interaction with Rap1A, could be used as a therapeutic tool in the treatment of metastatic PCa.

As regards the second aim of my Ph.D. project concerning the use of lipid nanocarriers to fill the gap between “drug discovery” and “drug delivery” our data support the applicability of QS and SLN as suitable nanocarriers for the employ of PMD in biomedical applications including PDT. Certainly, further *in vivo* investigations are needed to confirm our data. Furthermore, I’m currently involved in an ongoing project aimed to investigate the molecular mechanism underlying the photo-induced toxicity of PMD. In particular, we are interested in studying the involvement of Ca^{2+} signals in ROS production and cell death pathways triggered by light beam irradiation. This study could give new insights for the optimization of PMD-based tools as therapeutic agents.

Author’s contributions

Awards

1. **"Best communication"**

   25th School of Physiology and Biophysics (Italian Physiological Society), 2022 May 16th-19th in Anacapri (Italy)

2. **Second Prize "Best Oral presentation"**

   European Young Physiologists' Symposium (Federation of European Physiological Societies – FEPS), 2021 Oct 12th, Virtual Conference

Publications

1. Grolez G.P., **Chinigò G.**, Barras, A., Hammadi M., Noyer L., Kondraskaya K., Bulk E., Oullier T., Marionneau-Lambot S., Le Mée M., Rétif S., Lerondel S., Bongiovanni A., Genova T., Roger S., Boukkerhoub R., Schwab A., Fiorio Pla A. and Gkika D.
   TRPM8 AS AN ANTI-TUMORAL TARGET IN PROSTATE CANCER GROWTH AND METASTASIS DISSEMINATION
   International Journal of Molecular Sciences, 2022 Jun 15, 23(12):6672
   doi: 10.3390/ijms23126672

2. **Chinigò G.,** Grolez G., Audero M., Bokhobza A., Bernardini M., Cicero J., Toillon R.A., Bailleul Q., Visentin L., Ruffinatti FA, Brysbaert G., Lensink M., De-Ruyck J., Cantelmo A.R., Fiorio Pla A. and Gkika D.
   TRPM8-RAP1A INTERACTION SITES AS CRITICAL DETERMINANTS FOR ADHESION AND MIGRATION OF PROSTATE AND OTHER EPITHELIAL CANCER CELLS
   Cancers, 2022 April 30, 14(9):2261
   doi: 10.3390/cancers14092261

3. **Chinigò G.**, Gonzalez-Paredes A., Gilardino A., Barbero N., Barolo C., Gasco P., Fiorio Pla A., Visentin S.
   POLYMETHINE DYES-LOADED SOLID LIPID NANOPARTICLES (SLN) AS PROMISING PHOTOSENSITIZERS FOR BIOMEDICAL APPLICATIONS
   Spectrochimica Acta - Part A: Molecular and Biomolecular Spectroscopy, 2022 April, 271: 120909
   doi: 10.1016/j.saa.2022.120909

4. Petrillo S., Genova T., **Chinigò G**., Roato I., Scarpellino G., Kopecka J., Altruda F., Tolosano E., Riganti C., Mussano F., Munaron L.
   ENDOTHELIAL CELLS PROMOTE OSTEOGENESIS BY ESTABLISHING A FUNCTIONAL AND METABOLIC COUPLING WITH HUMAN MESENCHYMAL STEM CELLS
   Frontiers in Physiology, 2022 January 11, 12: 813547

doi: 10.3389/fphys.2021.813547

5. Roato I., **Chinigò G.**, Genova T., Munaron L. and Mussano F.
ORAL CAVITY AS A SOURCE OF MESENCHYMAL STEM CELLS USEFUL FOR REGENERATIVE MEDICINE IN DENTISTRY
Biomedicines, 2021 August 25, 9(9):1085
doi: 10.3390/biomedicines9091085

6. Mannino G., **Chinigò G.**, Serio G., Genova T., Gentile C., Munaron L. and Bertea C.M.
PROANTHOCYANIDINS AND WHERE TO FIND THEM: A META-ANALYTIC APPROACH TO INVESTIGATE THEIR CHEMISTRY, BIOSYNTHESIS,DISTRIBUTION AND EFFECT ON HUMAN HEALTH
Antioxidants, 2021 July 30, 10(8):1229
doi: 10.3390/antiox10081229

7. Gianfreda F.,Raffone C., Antonacci D., Mussano F., Genova T., **Chinigò G.**, Canullo L. and Bollero P.
EARLY BIOLOGICAL RESPONSE OF AN ULTRA-HYDROPHILIC IMPLANT SURFACE ACTIVATED BY SALTS AND DRY TECHNOLOGY: AN *IN-VITRO* STUDY
Applied Sciences, 2021 June 30, 11(13):6120
doi: 10.3390/app11136120

8. **Chinigò G.**, Castel H., Chever O., Gkika D.
TRP CHANNELS IN BRAIN TUMORS
Frontiers in Cell and Developmental Biology, 2021 Apr 13; 9:617801
doi:10.3389/fcell.2021.617801

9. Mannino G., Iovino P., Lauria A., Genova T., Asteggiano A., Notarbartolo M., Porcu A., Serio G., **Chinigò G.**, Occhipinti A., Capuzzo A., Medana C., Munaron L., Gentile C.
BIOACTIVE TRITERPENES OF PROTIUM HEPTAPHYLLUM GUM RESIN EXTRACT DISPLAY CHOLESTEROL-LOWERING POTENTIAL
International Journal of Molecular Sciences, 2021 Mar 6; 22(5):2664
doi: 10.3390/ijms22052664

10. **Chinigò G.,** Fiorio Pla A., Gkika D.
TRP CHANNELS AND SMALL GTPases INTERPLAY IN THE MAIN HALLMARKS OF METASTATIC CANCER
Frontiers in Pharmacology, 2020 Sept 29 ; 11:581455
doi : 10.3389/fphar.2020.581455

11. Bernardini M., Brossa A., **Chinigò G.**, Grolez G., Trimaglio G., Allart L., Hulot A., Marot G., Genova T., Joshi A., Mattot V., Fromont G., Munaron L., Bussolati B., Prevarskaya N., Fiorio Pla A. And Gkika D.
TRANSIENT RECEPTOR POTENTIAL CHANNEL EXPRESSION SIGNATURES IN TUMOR-DERIVED ENDOTHELIAL CELLS: FUNCTIONAL ROLES IN PROSTATE CANCER ANGIOGENESIS
Cancers, 2019 Jul 9; 7(11):956

Communications

1. **Chinigò G.**, Grolez G., Audero M., Bokhobza A., Bernardini M., Cicero J., Toillon R.A., Bailleul Q., Visentin L., Ruffinatti FA, Brysbaert G., Lensink M., De-Ruyck J., Cantelmo A.R., Fiorio Pla A. and Gkika D.
   TRPM8-RAP1A INTERACTION INHIBITS PROSTATE CANCER CELL ADHESION AND MIGRATION.

   4th European Calcium Channel Conference, 2022 May 24th-28th, in Alpbach, Austria
   Flash talk and Poster presentation

2. **Chinigò G.**, Grolez G., Audero M., Bokhobza A., Bernardini M., Cicero J., Toillon R.A., Bailleul Q., Visentin L., Ruffinatti FA, Brysbaert G., Lensink M., De-Ruyck J., Cantelmo A.R., Fiorio Pla A. and Gkika D.
   TRPM8-RAP1A INTERACTION INHIBITS PROSTATE CANCER CELL ADHESION AND MIGRATION.
   17èmes Journées Cancéropôle Grand Sud-Ouest (GSO), 2021 Nov 17th-19th in Carcassonne, France
   Poster presentation

3. **Chinigò G.**, Grolez G., Audero M., Bokhobza A., Bernardini M., Cicero J., Toillon R.A., Bailleul Q., Visentin L., Ruffinatti FA, Brysbaert G., Lensink M., De-Ruyck J., Cantelmo A.R., Fiorio Pla A. and Gkika D.
   TRPM8-RAP1A INTERACTION INHIBITS PROSTATE CANCER CELL ADHESION AND MIGRATION.

   European Young Physiologists' Symposium (Federation of European Physiological Societies – FEPS), 2021 Oct 12th, Virtual Conference
   Oral communication

4. **Chinigò G.**, Gilardino A., Eccher E., Sansone E., Visentin S., Pontremoli C., Moran Plata M.J., Barbero N., Fiorio Pla A.
   SQUARAINES AS PHOTOSENSITIZERS: A STRUCTURE-FUNCTION ANALYSIS BY MEANS OF *IN VITRO* CYTOTOXICITY TEST AND CALCIUM SIGNALING ASSESSMENT

   Italian Photochemistry Days of the Italian Photochemistry Group (GIF); 2021 Sept 23th-24th, Virtual Congress
   Poster presentation

5. **Chinigò G.**, Grolez G., Audero M., Bokhobza A., Bernardini M., Cicero J., Toillon R.A., Bailleul Q., Visentin L., Ruffinatti FA, Brysbaert G., Lensink M., De-Ruyck J., Cantelmo A.R., Fiorio Pla A. and Gkika D.
   TRPM8-RAP1A INTERACTION INHIBITS PROSTATE CANCER CELL ADHESION AND MIGRATION.

   3rd International Cancer and Ion Channel Congress – Medipol Unv Istanbul, 2021 Sept 16th-18th, Online Congress
   Oral communication

6. **Chinigò G.**, Grolez G., Audero M., Bokhobza A., Bernardini M., Cicero J., Toillon R.A., Bailleul Q., Visentin L., Ruffinatti FA, Brysbaert G., Lensink M., De-Ruyck J., Cantelmo A.R., Fiorio Pla A. and Gkika D.
   TRPM8-RAP1A INTERACTION INHIBITS PROSTATE CANCER CELL ADHESION AND MIGRATION.

   Italian Physiological Society (SIF) Congress; 2021 Sept 8th-9th, Online Congress
   Oral communication

7. **Chinigò G.**, Genova T., Gkika D., Munaron L., Fiorio Pla A.
   BEYOND CHANNEL FUNCTION: TRPM8 IN CELL ADHESION AND MIGRATION.

   Italian Physiological Society (SIF) - Annual Meeting of Young Researchers in Physiology (YRP); 2021 Jul 29th-31th in Bertinoro, Italy
   Oral communication

8. **Chinigò G.**, Gilardino A., Eccher E., Sansone E., Visentin S., Pontremoli C., Moran Plata M.J., Barbero N., Fiorio Pla A.
   SQUARAINES AS PHOTOSENSITIZERS: A STRUCTURE-FUNCTION ANALYSIS BY MEANS OF IN VITRO CYTOTOXICITY TEST AND CALCIUM SIGNALING ASSESSMENT

   Italian Society of Photobiology (SIFB) - XXXII Annual Conference; 2021 Jun 23th-24th, Virtual Conference
   Oral communication

9. **Chinigò G.**, Fiorio Pla A., Visentin S., Barbero N., Barolo C.
   SYNTHESIS AND CHARACTERIZATION OF DYE-LOADED SOLID LIPID NANOPARTICLES FOR POTENTIAL APPLICATIONS IN BIOMEDICINE

   Workshop « Research and Nanomedicine 2019 – IV edizione » ; 2019 Jun 18th in Pavia, Italy
   Oral communication

10. Bernardini M., **Chinigò G.**, Brossa A., Grolez G., Genova T., Mattot V., Fromont-Hankard G., Munaron L., Bussolati B., Prevarskaya N., Fiorio Pla A. & Gkika D.
    TRP EXPRESSION SIGNATURE IN TUMOR-DERIVED ENDOTHELIAL CELLS: FUNCTIONAL ROLES IN PROSTATE CANCER ANGIOGENESIS

    30th Ion Channels Meeting - Association Canaux Ioniques ; 2019 Sept 8th-11th in Sète (Montpellier), France
    Poster presentation

11. Bernardini M., **Chinigò G.**, Brossa A., Grolez G., Genova T., Mattot V., Fromont-Hankard G., Munaron L., Bussolati B., Prevarskaya N., Fiorio Pla A. & Gkika D.
    TRP EXPRESSION SIGNATURE IN TUMOR-DERIVED ENDOTHELIAL CELLS: FUNCTIONAL ROLES IN PROSTATE CANCER ANGIOGENESIS

    Joint meeting of the Federation of European Physiological Societies and the Italian Physiological Society (FEPS-SIF); 2019 Sept 10th-13th in Bologna, Italy **Poster presentation**

Other formative activities

Language courses

36-hours **French course** (obtaining level B1) – University of Lille

30-hours Proficiency **English Course** - Shenker School

Teaching activities

Supervision of 3 Master's degree theses in "Industrial Biotechnologies", 1 Master's degree thesis in "Cellular and Molecular Biology", 3 bachelor students and 1 Erasmus incoming student (Laboratory of Cellular and Molecular Angiogenesis, University of Turin).

Official **co-tutor** of the previous three Master's degree theses

Assistance to the "Cellular and Molecular Biophysics" course (Master's Degree in "Industrial Biotechnology", University of Turin – Prof. Fiorio Pla): theoretical lectures (4h on fluorescence and its applications in Live cell imaging techniques) + practical laboratory exercises

Assistance to the "Physiology" course (Bachelor of "Nursing" University of Turin – Prof. Rastaldo)

Seminars

As part of the Ph.D. didactical program I attended **zeroing courses** in Bioinformatic, Maths, Complex Systems, Statistical Inference and Machine Learning, and **seminars** organized by the University of Turin as well as Journal Club events and webinars organized by both the PhD teaching program of the University of Turin and by the Laboratory of Cell Physiology in Lille.

Attendance to the 25th **School of Physiology and Biophysics** organized by the Italian Physiological Society (SIF), 2022 May 16th-19th, Anacapri (Italy).

Aknowledgements

I would like to thank all the people which contributed to the present Ph.D. thesis.

First of all, thanks to my Tutors Pr. **Alessandra Fiorio Pla** and Pr. **Dimitra Gkika** whose guidance during all these years of PhD has been fundamental for me. Thank you for always trusting me and for teaching me everything I know about scientific research. In particular, I would like to deeply thank Alessandra because if she had not been there, I probably would not have continued my academic career with this PhD: thank you for believing in me since the time of my master's degree and giving me the opportunity to continue this fascinating journey in scientific research. I would also like to thank Myrto not only for his always constant support especially during the months I spent at the University of Lille, but also and above all for helping me improve my scientific curriculum by including me in many collaborations.

I would like also to thank my collegues at the University of Turin **Giorgia Scarpellino**, **Tullio Genova**, and **Federico Ruffinatti**: your presence, your help and your friendship was essential for me during these years. We are a great team because we are more than colleagues and I hope that we will have the opportunity to work together for as long as possible because it is not easy to meet helpful and loving people like you, nor to have the good fortune to work together. Thank also to all the people of the Lab of Cellular and Molecular Angiogenesis in Turin for giving me daily important advice and support: thank to our head Pr. **Luca Munaron** and our technician **Alessandra Gilardino**.

Thank to all the people who I met in the Lab of Cell Physiology in Lille during my stay (Valerio, Natalie, Charlotte, Antoine) and expecially many thanks to **Natalia Prevarskaya** for accepting me in her Lab giving me the opportunity to work in a very active and passionate scientific group. A special thanks that goes beyond their professional and scientific contribution certainly goes to **Lina Mesilmany**, **Madelaine Audero** and **Sylvie Ratoslavova**: thanks for making me feel always at home despite the 1000 km away, I will never forget the affection and comfort that you have been able to give me unconditionally during those particularly complicated months in Lille during, what is more, the pandemic emergency.

Finally, I would like to thank Pr. **Annarosa Arcangeli** and Pr. **Halima Ahidouch-Ouadid** for accepting to review my thesis and for the time you will dedicating in revising my work. Thank also to Pr. **Rosa Angela Cardone** and **Xuefen Le Bourhis** for gently accepting to be part of my jury. Comments and criticisms are essential in our field as well as in life, so all your observations will be of great value to me.

Annex

"TRP channels in Brain Tumors"

Giorgia Chinigò[1,2], Hélène Castel[3], Oana Chever[3] and Dimitra Gkika[4,5*]

[1] Laboratory of Cell Physiology, University of Lille, Department of Life Sciences, Univ. Lille, Inserm, U1003 - PHYCEL - F-59000 Lille, France

[2] Laboratory of Cellular and Molecular Angiogenesis, University of Torino, Department of Life Sciences and Systems Biology, Torino, Italy

[3] Normandie Univ, UNIROUEN, INSERM U1239, DC2N, 76000 Rouen, France, Institute for Research and Innovation in Biomedicine (IRIB), 76000 Rouen, France

[4] University of Lille, CNRS, INSERM, CHU Lille, Centre Oscar Lambret, UMR 9020-UMR 1277-Canther-Cancer Heterogeneity, Plasticity and Resistance to Therapies, F-59000 Lille, France

[5] Institut Universitaire de France (IUF)

[*] Correspondence: dimitra.gkika@univ-lille.fr

Chinigò *et al., Frontiers in Cell and Developmental Biology* 2021, 9:617801

Abstract

Malignant glioma including glioblastoma (GBM) is the most common group of primary brain tumors. Despite standard optimized treatment consisting of extensive resection followed by radiotherapy/concomitant and adjuvant therapy, GBM remains one of the most aggressive human cancers. GBM is a typical example of intra-heterogeneity modeled by different micro-environmental situations, one of the main causes of resistance to conventional treatments. The resistance to treatment is associated with angiogenesis, hypoxic and necrotic tumor areas while heterogeneity would accumulate during glioma cell invasion, supporting recurrence. These complex mechanisms require a focus on potential new molecular actors to consider new treatment options for gliomas. Among emerging and underexplored targets, TRP (transient receptor potential) channels belonging to a superfamily of non-selective cation channels which play critical roles in the responses to a number of external stimuli from the external environment were found to be related to cancer development, including glioma. Here, we discuss the potential as biological markers of diagnosis and prognosis of TRPC6, TRPM8, TRPV4 or TRPV1/V2 being associated with glioma patient overall survival. TRPs-inducing common or distinct mechanisms associated with their Ca2+-channel permeability and/or kinase function were detailed as involving miRNA or secondary effector signaling cascades in turn controlling proliferation, cell cycle, apoptotic pathways, DNA repair, resistance to treatment as well as migration/invasion. These recent observations of the key role played by TRPs such as TRPC6 in GBM growth and invasiveness, TRPV2 in proliferation and glioma-stem cell differentiation and TRPM2 as channel carriers of cytotoxic chemotherapy within glioma cells, should offer new directions for innovation in treatment strategies of high-grade glioma as GBM to overcome high resistance and recurrence.

Key words: ion channel, TRP channel, brain tumor, glioma, glioblastoma

INTRODUCTION

Malignant gliomas are the most prevalent group of primary brain tumors in adults, with an incidence of 8.9 cases per 100,000 persons/year in the US (Ostrom et al. 2015; 2017). Glioblastoma (GBM) remains one of the most aggressive human cancers. Glial tumors or glioma represent a wide spectrum of malignancies including grades II and III oligodendroglioma, grades II and III astrocytoma and glioblastoma from initial classification based on anatomocytopathological criteria related to the morphotypic characteristics and numerous cytonuclear atypologies, accompanied by anaplasia for high-grade glioma (GBM, grade IV) (Louis et al. 2007; Miller and Perry 2007). The diagnosis of GBM was based on the presence of vascular micro-proliferations signs of intense vascularisation, associated with zones of necrosis delimited by a hypoxic pseudopalissadic cellular zone, evidencing important intra-tumoral heterogeneity (Karsy et al. 2012; Alifieris

and Trafalis 2015). Now, brain tumors and glioma are classified according to the histomolecular classification recently published by the World Health Organization (WHO) (Louis et al. 2016), which represents a major clinical improvement for both diagnosis and treatments, as well as patient prognosis. The aim was to implement the histopathological classification with the following molecular signatures: first including mutation in the isocitrate dehydrogenase1/2 (IDH1/2mut) and/or the co-deletion 1p/19q associated with oligodendroglioma or mutation of TP53; second, the l'α-thalassemia mental retardation syndrome X-linked (ATX) or amplification of the epidermal growth factor receptor (EGFR) were associated with GBM IDHwt; finally, while the hypermethylation of the O6-methyl guanine-DNA methyl transferase (MGMT) promoter constitutes an important parameter of the GBM aggressiveness (Louis et al. 2016).

Despite these molecular attempts to stratify glioma patients with the objective to allow personalization of the treatments, the median survival of GBM patients currently ranges from 15 to 17 months, despite a safe maximal surgical resection, radiation/concomitant and adjuvant alkylating-based chemotherapy by temolozomide (TMZ) (Stupp et al. 2005; 2009; Wen and Brandes 2009). However, more than 95% of GBM recur in the margin of the resection cavity, an area in which glioma tumor cells acting as a tumor reservoir are found (Giese et al. 2003). This invasiveness associated with X-ray and/or intrinsic or acquired chemoresistance of the glioma cells and the presence of an intrinsic or acquired blood-brain barrier (BBB), limit the effectiveness and/or the delivery of anti-neoplastic agents and justify the development of new strategies. In agreement, over the last decade, despite very important advances in the field of targeted therapy, none of them, e.g. drug/antibody or combination of small molecule inhibitors, has been shown to be more effective than TMZ or capable of increasing the efficacy of standard therapy in patients with primary or recurrent GBM (Stepanenko and Chekhonin 2018), and no curative treatment is currently identified in GBM. This failure may be explained at least in part by the intratumoral heterogeneity which is a conserved consequence of the GBM micro-environment (Prabhu et al. 2017), referring to the physico-chemical characteristics and matrices interacting with the tumor. Indeed, the GBM heterogeneity is tightly related to angiogenic and hypoxic features as well as invasive processes, thus future strategies should consider targeting mechanisms associated with resistance and invasion. In particular, Watkins and co-workers showed that GBM cells can thus control the regulation of vascular tone, via the release of K+ through K+ channels activated in response to Ca2+, leading to an adaptation of cell volume to facilitate their invasion (Watkins et al. 2014).

TRP (transient receptor potential) channels are a superfamily of cationic tetrameric channels, mostly permeable to Ca^{2+}, involved in various physiological functions, and for the most part sustain calcium homeostasis and calcium signaling. Calcium-dependent mechanisms determine several aspects of brain tumor cell homeostasis including survival, proliferation, invasion or treatment resistance, making TRP channels putative potent modulators of tumorigenesis and glioma progression. Approximately 30 TRPs have

been identified and are classified into TRPA (ankyrin family), TRPC (canonical family), TRPM (melastatin family), TRPN (NomPC family), TRPML (mucolipin family), TRPP (polycystin family) and TRPV (vanilloid family) (Li 2017). These cationic channels have been shown to be gated by many physical or chemical stimuli (temperature, membrane potential, pH, hormones, vitamins …). TRP channels are expressed in various excitable and non-excitable cell types and are present in many organs, including brain, heart, liver, lung, kidney, spleen, muscle, skin, pancreas (Venkatachalam and Montell 2007). Since a decade, TRP channels have attracted much interest in the cancer field and tumorigenesis. Activities of TRP channels have been linked to cell growth, survival or migration, being involved in a plethora of cancers, especially for TRPC, TRPM and TRPV (Prevarskaya, Zhang, and Barritt 2007) Gkika and Prevarskaya 2009; Fiorio Pla and Gkika 2013). Recent research unravels the role of some TRP channels in glioma growth and progression or glioma stem-like cell fate determination. In this review, we will mainly focus on a new class of molecular players, TRP channels emerging in gliomas and for which we will develop three aspects: i) the expression profile and use as clinical markers; ii) the molecular mechanisms through which they act; and iii) their potential use in therapeutics.

TRANSIENT RECEPTOR POTENTIAL (TRP) EXPRESSION PROFILE AND PUTATIVE BIOMARKERS

Changes in expression of TRP channels have been related to cancer development and progression, thus making them valuable diagnostic and/or prognostic markers in several tumor types, including glioma. Furthermore, a strong correlation between clinical-pathological findings and mRNA and/or protein expression of different TRPs has been recently provided. For instance, mRNA encoding TRPC1, TRPC6, TRPM7, TRPM8, TRPV4 and TRPML2 appeared up-regulated in GBM tumor specimens in comparison with normal tissues and their expression was found to increase with glioma tumor grade with the highest mRNA level found in GBM patient samples (Alptekin et al. 2015; Ding et al. 2010). These findings are consistent with a pro-tumorigenic role of these channels in glioma progression and aggressiveness, as described in more detail in the next paragraph. According to a qPCR screening of thirty-three GBM patient tumors, additional mRNA-encoding TRP channels including TRPM2, TRPM3, TRPV1, TRPV2 showed significantly higher expression levels in GBM compared with control normal brain tissues (Alptekin et al. 2015). However, other studies reported opposite results, more consistent with an anti-tumorigenic function of these channels, as confirmed by several experimental data (Amantini et al. 2007; Nabissi et al. 2010; Ying et al. 2013; Morelli et al. 2019). These discrepancies could be due to the relatively low number of patients considered in the first study (Alptekin et al. 2015), which may not be very representative enough while further investigations should now be reconsidered in light of the new molecular GBM patient stratification and the methylome.

Among more than 20 TRP channels investigated, TRPM8 showed the highest mRNA upregulation in GBM as compared with normal brain tissue (Alptekin et al. 2015; Zeng et al. 2019), suggesting a pivotal function of TRPM8 in gliomagenesis. Moreover, TRPM8 expression in human GBM specimens and established GBM cell lines was found to be up-regulated at both mRNA and protein level to a variable extent (Klumpp et al. 2017) and to be significantly correlated with worse patient overall survival (Zeng et al. 2019). Interestingly, it was previously reported that TRPM8 is a primary androgen-responsive gene since its promoter is located downstream an androgen response elements (AREs) to which androgen receptor (AR) may bind once activated by androgens thus promoting TRPM8 expression (Bidaux et al. 2005; Asuthkar et al. 2015). Therefore, TRPM8 overexpression in high-grade glioma might be associated with the documented upregulation of AR in GBM (Yu et al. 2015). Moreover, it has been recently found that AR may also directly regulate TRPM8 channel activity via protein-protein interaction and/or TRPM8 phosphorylation, further accentuating the close TRPM8-androgens relationship (Grolez et al. 2019; Gkika et al. 2020). Similarly to TRPM8, TRPV4 has been shown to positively correlate with glioma progression, since high levels of TRPV4 gene and protein expression were associated with a poorer patient prognosis (Ou-yang et al. 2018). Thus, TRPM8 and TRPV4 may be currently considered promising biomarkers accompanying aggressiveness of glioma and signature of GBM while constituting potential therapeutic targets for future treatment options. TRPML2 expression was also detected in normal astrocytes and neural stem/progenitor cells and to be up-regulated at both mRNA and protein level in glioma to a variable extent, increasing with the pathological grade (Morelli et al. 2016). Such observation was linked to the up-regulation of the transcriptional activator of the TRPML-2 gene Paired box 5 (PAX5) (Valadez and Cuajungco 2015) found in human astrocytoma and correlated with malignancy and pathological grade of glioma (Stuart et al. 1995).

Moreover, the loss of TRPM3, TRPV1, TRPV2 and TRPML1 expression has been proposed as a negative prognostic marker for GBM patients, because of their significant and progressive down-regulation as the tumor grade increases. For instance, a study focusing on the role of miR-204 in high-grade glioma cell lines has revealed a significant down-regulation of TRPM3, due to the hypermethylation of its promoter (Ying et al. 2013). Interestingly, miR-204 is an intronic miRNA located between exons 7 and 8 of the TRPM3 gene and its loss in glioma, due to the high methylation of its host gene TRPM3, is associated with an enhancement in cell migration and cellular stemness (Ying et al. 2013) questioning the direct role of TRPM3 and the indirect regulatory functions of miR-204 via its target genes. Consistently, restoration of miR-204 in LN382T and SNB19 cells orthotopically xenografted in the brains of nude mice suppressed tumorigenesis and invasiveness and increased animal survival (Ying et al. 2013). Taken together, these findings might suggest a potential tumor-suppressive function of TRPM3 in glioma, but further studies are required to clarify its involvement in cancer development and/or progression and to establish whether TRPM3 and miR-204 might cooperate with each other in the pathogenesis of gliomas. Concerning TRPV1 and TRPV2, the preventing role in

gliomagenesis and tumor progression has been more clearly established and characterized (see next paragraph). First, TRPV1 and TRPV2 genes and protein expression appeared inversely correlated with glioma grade, showing an almost undetectable level in GBM (Amantini et al. 2007; Nabissi et al. 2010; Morelli et al. 2016). In particular, a study performed by Nabissi and coworkers has shown that GBM and glioma stem-like cells (GSC) selectively express the TRPV1 5'-untranslated region (5'UTR) variant three (TRPV1v3), one of the four variants resulting from alternative first exon splicing (Nabissi et al. 2016). The 5'UTR can generate different transcripts encoding the same protein but characterized by different stability and translation efficacy (Audic and Hartley 2004; Gebauer and Hentze 2004; Hinnebusch, Ivanov, and Sonenberg 2016) and TRPV1v3 is the most stable TRPV1 5'UTR transcript. In GBM, the mRNA expression of the unique TRPV1v3 variant correlates with the patient's survival, suggesting that its loss or low mRNA expression may represent a potential marker of poor prognosis in GBM patients (Nabissi et al. 2016). Similarly, the clinical relevance of the overexpression of TRPV2 in GBM was confirmed through the analysis of the TRPV2-interactome based signature using a systematic proteomics and computational analysis approach (Doñate-Macián et al. 2018), predicting GBM patient overall survival. Indeed, high TRPV2 interactome protein expression was correlated with tumor progression, recurrence, TMZ-resistance and a poor prognosis (Doñate-Macián et al. 2018). Finally, also TRPML1 might have a potential role as a negative prognostic marker for GBM patients (Morelli et al. 2019) since TRPML1 mRNA down-regulation or loss strongly correlates with reduced overall survival in GBM patients. However, additional studies are needed in order to further investigate the relationship between TRPML1 expression and lower glioma grades (Morelli et al. 2019). However, TRPML1 expression at mRNA and protein levels displayed variability within patient samples and its subcellular localization may also be distinct since TRPML1 is mainly expressed in the late endosome/lysosome of normal cells while found in endolysosomes and as dot spots in the nuclear cell compartment in glioma cells (Morelli et al. 2019). The mechanisms underlying this nuclear localization in tumor cells and the effects of this specific localization are not completely characterized, although it has been shown that TRPML1 is able to bind DNA somehow and thus, it might affect the transcription of some genes involved in tumor progression (Morelli et al. 2019).

Together, these studies highlight that some TRPM, TRPV and/or TRPML channels overexpressed in glioma should be considered as predictive and specific biomarkers of high-grade glioma and GBM, and through changes in their permeability to cations they may play a role in GBM aggressiveness.

MOLECULAR MECHANISMS OF TRP CHANNELS ACTION

TRP channels have revealed a direct involvement in determining many hallmarks of glioma and GBM (Table 1), including some typical histological cellular abnormalities (Bomben and Sontheimer 2008), its relentless growth, and its intrinsic severe aggressiveness due to its high capability to diffuse into the non-

neoplastic brain parenchyma, which contributes to treatments resistance and bad prognosis (Demuth and Berens 2004; Schwartzbaum et al. 2006; Liu et al. 2018). TRP channels may exert both anti-tumorigenic and pro-tumorigenic functions in gliomas and the main TRPs-mediated signaling pathways associated with gliomas progression are schematically summarized in figure 1. Most of the TRP channels involved in gliomagenesis and tumor progression were found to affect more than one cellular process related to carcinogenesis. In this chapter, we will therefore discuss the molecular mechanisms by which each TRP affects cancer cell behavior, subgrouping them into subfamilies.

	Expression					
CHANNEL	**HEALTHY**	**TUMOR PROGRESSION**	**BIOLOGICAL EFFECT**	**MECHANISM**	**POTENTIAL THERAPEUTIC TOOLS**	**REFERENCES**
TRPC1	yes	↑	Cell growth (+) Cell migration (+)	↑ Cytokinesis ↑Chemotaxis	TRPC1/SPK/PI3K inhibitors	(Bomben and Sontheimer 2008) (Bomben and Sontheimer 2010) (Bomben et al. 2011) (Lepannetier et al. 2016)
TRPC6	low	↑	Cell growth (+) Cell migration (+) Angiogenesis (+) Radioresistance (+)	→ NFAT → RhoA → NFAT ↑ G_2/M (Cdc25C)	TRPC6/ NFAT inhibitors	(Ding et al. 2010); (Chigurupati et al. 2010) (Chigurupati et al. 2010) (Ding et al. 2010)
TRPM2	yes	↑	Cell death (+)	↑ ROS-induced Ca^{2+} influx	TRPM2 gene insertion (+Se and DXT)	(Ishii et al. 2007) (Ertilav et al. 2019)
TRPM3	yes	↑/↓	n.d.	n.d.	n.d.	(Alptekin et al. 2015) (Ying et al. 2013)
TRPM7	yes	↑	Cell growth (+) Cell invasion (+)	↑ STAT3/Notch ┤miR-28-5p┤ Rap1b ┤miR-28-5p┤ Rap1b	TRPM7/STAT3/ Notch/ALDH1 inhibitors miR-28-5p	(Liu et al. 2014) (Wan et al. 2019) (Wan et al. 2019)

			Stem cell renewal and differentiation (+)	STAT3-ALDH1 ↑ Ca^{2+}		(Liu et al. 2014)
TRPM8	yes	↑ (2 different isoforms)	Cell migration (+)	→ BK channels RTK signaling		(Wondergem and Bartley 2009; Klumpp et al. 2017); (Wondergem et al. 2008)
			Cell growth (+)	Ca^{2+} → BK channels → CaMKII ┤ cdc25C ┤ cdc2 MAPK signaling		(Klumpp et al. 2017) (Zeng et al. 2019)
			Cell death (-)	MAPK signaling		(Klumpp et al. 2017); (Zeng et al. 2019)
			Radioresistance (+)	Supporting DNA repair and cell cycle upon genotoxic stress		(Klumpp et al. 2017)
TRPV1	yes	↓	Apoptosis (+)	→ p38 MAPK ↑ ER stress (ATF3)		(Amantini et al. 2007) (Stock et al. 2012)
TRPV2	yes	↓	Cell proliferation (-)	ERK signalling		(Nabissi et al. 2010) (Morelli et al. 2012)
			Apoptosis (+)	Fas signaling		(Nabissi et al. 2010)
			Cell differentiation (+)	↑ GFAP and β_{III}-tubulin expression ↑ Aml-1 a (PI3K/AKT pathway)	CBD	(Morelli et al. 2012) (Nabissi et al. 2015)
			Drug sensitivity (+)	↑ drug uptake ↑ drug-mediated apoptotic pathway	CBD + TMZ/BCNU/ DOXO	(Nabissi et al. 2013) (Nabissi et al. 2015)
TRPV4	yes	↑	Cell migration (+)	AKT/Rac1 signaling	TRPV4 inhibitors (HC- 067047)	(Ou-yang et al. 2018)
TRPA1	n.d.	n.d.	Cell apoptosis (+)	↑ mitochondrial stress	TRPA1 activators	(Deveci et al. 2019)

TRPML1	yes	↓	Cell apoptosis (+) Autophagy (+)			(Morelli et al. 2019)
TRPML2	yes	↑	Cell proliferation (+) Cell apoptosis (-)	PI3K/AKT - ERK 1/2 signaling		(Morelli et al. 2016)

Table 1. TRP channels expression and functionality in gliomas/glioblastomas.

Abbreviations: (+) increase (-) decrease (↑) increment (↓) reduction (→) activation (-┤) inhibition

SPK = sphingosine kinase; PI3K = phosphoinositide-3 kinase; NFAT = nuclear factor of activated T-cells; Se = selenium; DXT = docetaxel; STAT3 = signal transducer and activator of transcription 3; miR-28-5p = miRNA 28-5p; ALDH1 = aldehyde dehydrogenase1; BK = large-conductance Ca2+-activated K+ membrane ion channels; RTK = Met receptor tyrosine kinase; CaMKII = Ca^{2+}/calmodulin-dependent protein kinase II; Cdc25C = M-phase inducer phosphatase 3; Cdc2 = subunit of the M phase-promoting factor; MAPK = mitogen-activated protein kinase; ATF3 = transcription factor-3; CBD = cannabidiol; ERK = extracellular signal-regulated kinase 1/2; GFAP = glial fibrillary acidic protein; Aml-1 a = acute myeloid leukemia variant a; AKT = protein kinase B; TMZ = temozolomide; BCNU = carmustine; DOXO = doxorubicin.

n.d. = not determined

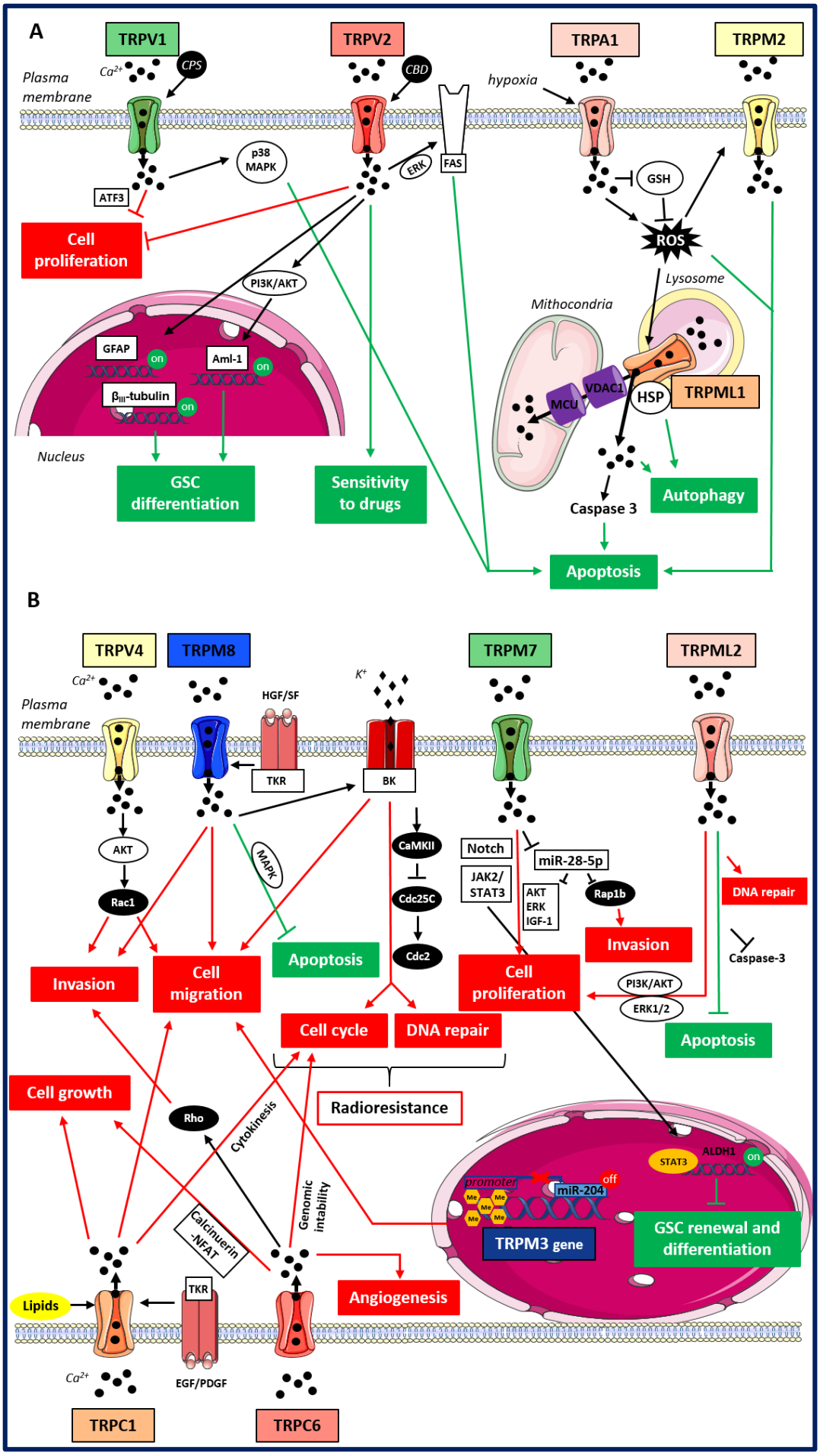
A
TRPV1
TRPV2
TRPA1
TRPM2
Plasma membrane
Ca2+
CPS
CBD
hypoxia
p38 MAPK
ERK
FAS
ATF3
GSH
ROS
Cell proliferation
PI3K/AKT
Lysosome
Mithocondria
GFAP
on
Aml-1
on
βIII-tubulin
on
VDAC1
MCU
HSP
TRPML1
Nucleus
GSC differentiation
Sensitivity to drugs
Caspase 3
Autophagy
Apoptosis
B
TRPV4
TRPM8
TRPM7
TRPML2
Ca2+
K+
HGF/SF
Plasma membrane
TKR
BK
AKT
Rac1
MAPK
CaMKII
Cdc25C
Cdc2
Notch
JAK2/ STAT3
miR-28-5p
AKT ERK IGF-1
Rap1b
DNA repair
Caspase-3
Invasion
Cell migration
Apoptosis
Cell proliferation
Invasion
PI3K/AKT
ERK1/2
Apoptosis
Cell cycle
DNA repair
Radioresistance
Cell growth
Rho
Cytokinesis
Genomic intability
Calcineurin -NFAT
STAT3
ALDH1
on
promoter
off
miR-204
TRPM3 gene
GSC renewal and differentiation
Lipids
TKR
Angiogenesis
Ca2+
EGF/PDGF
TRPC1
TRPC6

Figure 1. TRPs-mediated signaling pathways in gliomas.

A*) Anti-tumorigenic TRPs-mediated signaling pathways in gliomas. Cartoon depicting TRP channels signaling pathways suppressing gliomas progression through the inhibition of pro-tumorigenic pathways (in red) and/or the activation of anti-tumorigenic signaling pathways (in green). TRPM2 and TRPML1 upon ROS activation promote cell apoptosis through an increase in oxidative stress and intracellular Ca^{2+} concentration; due to its localization on the lysosomal membrane TRPML1 may also mediates the autophagic cell death pathway through the interaction with HSP; TRPA1 under hypoxia promotes apoptosis inducing ROS formation and inhibiting antioxidants such as GSH; TRPV1 upon stimulation with CPS triggers the apoptotic pathway through p38 MAPK and reduces glioma expansion via ER pathway in a ATF3-dependent manner; TRPV2 reduces cell proliferation and enhances the Fas-induced apoptosis in an ERK-dependent manner; TRPV2 also acts on cell differentiation since its overexpression is associated with GFAP and βIII-tubulin increased expression and its activation by CBD promotes Aml-1 up-regulation via PI3K/AKT pathway; finally, TRPV2 activation by CBD can improve cell sensitivity to chemotherapeutic agents favoring drug uptake.*

B*) Pro-tumorigenic TRPs-mediated signaling pathways in gliomas. Cartoon depicting TRP channels signaling pathways promoting gliomas progression through the activation of pro-tumorigenic pathways (in red) and/or the inhibition of anti-tumorigenic signaling pathways (in green). TRPC1 affects cell growth and cell proliferation mainly promoting cytokinesis in response to lipid activation, whereas upon stimulation with growth factors it induces chemotactic migration; TRPC6 affects cell proliferation, tumor growth and angiogenesis likely through the Ca^{2+}-induced activation of the calcineurin-NFAT pathway, whereas TRPC6 effects on cell migration might rather involve Rho activation and subsequent actin cytoskeleton rearrangements; TRPV4 promotes cell migration and tumor invasiveness through the AKT-mediated Rac1 activation; TRPM8 supports glioma progression by inhibiting apoptosis through MAPK pathway and impairing the cell cycle through the activation of BK channels and the subsequent CaMKII-mediated inhibition of phosphatases like Cdc25C and Cdc2; TRPM8 effects on cell migration/invasion are also associated with BK channels activation and the function of TRPM8 in aggressiveness and resistance to treatment may also be potentiated by TKR-mediated HGF/SF stimulation; TRPM7 increases glioma cell proliferation and invasion through the down-regulation of miR-28-5p and the subsequent up-regulation of oncogenic signaling pathways involving AKT, ERK, IGF-1 and Rap1b; TRPM7 effects on glioma proliferation may also be mediated by Notch and/or JAK2/STAT3 signaling pathways and through the activation of STAT3; TRPM7 might also be involved in GSC renewal and differentiation thanks to the up-regulation of the well-known GSC marker ALDH1; the hypermethylation of TRPM3 promoter through the down-regulation of miR-204 enhances cell migration; TRPML2 enhances cell proliferation and slows down apoptosis improving DNA repair and inhibiting Caspase 3 likely through PI3K/AKT and ERK1/2 pathways.*

Abbreviations: ROS = reactive oxygen species; HSP = heat shock proteins; GSH = glutathione; CPS = capsaicin; ATF3 = transcription factor-3; CBD = cannabidiol; GFAP = glial fibrillary acidic protein; Aml-1 = acute myeloid leukemia transcription factors; PI3K = phosphoinositide 3-kinases; AKT = protein-kinase B; HGF/SF = hepatocyte growth factor/scatter factor; EGF = epidermal growth factor, PDGF = platelet-derived growth factor, TKR = tyrosine kinase receptor; NFAT = nuclear factor of activated T-cells; MAPK = mitogen-activated protein kinase; BK = big potassium channels; CaMKII = Ca^{2+}/calmodulin-dependent protein kinase II; Cdc25C and Cdc2 = cell division cycle proteins; JAK2 = janus kinase 2 ; STAT3 = signal transducer and activator of transcription 3; ERK = extracellular signal-regulated kinases; IGF-1 = insulin-like growth factor-1; GSC = glioma stem cells; ALDH1 = aldehyde dehydrogenase 1.

Canonical TRPs

It has been suggested that TRPC channels-relayed mechanisms may contribute to some of the most common histopathological hallmarks of GBM such as nuclear atypia and enlarged cell shape (Bomben and Sontheimer 2008). Glioma cell lines and surgical patient-derived tumors have revealed the expression of four TRP channels belonging to the TRP canonical subfamily that are TRPC1, TRPC3, TRPC5, and TRPC6. Further

investigations on their role in glioma cells have suggested an involvement of these channels in a Ca^{2+} influx pathway impacting cellular growth. More specifically, it has been shown that TRPC channels contribute to the resting conductance of glioma cells while their acute pharmacological inhibition with SKF96365 increased membrane resistance of glioma cells and caused a transient hyperpolarization followed by a sustain depolarization of the cells' membrane (Bomben and Sontheimer 2008). Additionally, chronic application of the TRPC inhibitor SKF96365 (from 0 to 5 days) would lead to an almost complete growth arrest at the G2/M phase of GBM D54MG cell cycle, as revealed by FACS analysis (Bomben and Sontheimer 2008). In most cases the blockage of the cell cycle during the G_2/M transition leads to cell death (Stark and Taylor 2006), or in the particular case of D54MG cells, TRPC inhibition was accompanied by a continued growth exhibiting multinuclear and enlarged cells due to incomplete cytokinesis. This phenotype might render impossible a dynamic adaptation of the cell volume to invade the brain parenchyma, through the narrow extracellular brain spaces compatible with less recurrence.

Glioma cells display a depolarized resting membrane potential around -30 mV. Some TRPC channels are opened at rest and contribute to this membrane potentials (Bomben and Sontheimer 2008). Activation of TRPC channels can also lead to membrane potentials fluctuations by various ways. First of all, TRPC channels are non-selective cation channels and they directly depolarize cells following activation. In addition, TRP channels are functionally coupled with other ion channels, so their activation can indirectly lead to depolarizations or hyperpolarizations, depending on the channels involved (Gees, Colsoul, and Nilius 2010). In particular, major conductances of glioma cells are mediated by Ca^{2+}-activated K^+ channels (Ransom, O'Neal, and Sontheimer 2001) and Cl^- channels such as ClC_3 or ClC_2 (Mcferrin and Sontheimer 2006),which both are modulated by TRPC channels. Glioma cells do express many types of channels and transporters (Molenaar 2011; Cuddapah and Sontheimer 2011), which are sensitive to membrane potential fluctuations. Furthermore, glioma cells have been shown to display electrical activities similar to Na^+ spikes, which are sustained by TTX-sensitive voltage-gated Na+ channels (Bordey and Sontheimer 1998). Thus, TRPC channels may impact many voltage-dependent cellular processes and modulate electrical behavior of glioma cells.

Among the TRPCs, TRPC1 and TRPC6 are those for which the mechanism of action has been best characterized in human malignant glioma. For instance, TRPC1 was found to act on several hallmarks of cancer, including growth, cell cycle and migration. Interestingly, all the TRPC1 effects on glioma cell behavior strictly resulted from lipid regulation, e.g. in some cases the channel activity is directly affected by lipids (phosphatidylinositol-(4,5)-bisphosphate PIP_2, phosphoinositides, diacylglycerol, cholesterol, etc.) localized on the plasma membrane, in other cases, it can be by signaling pathways which lead to the production of specific lipids such as sphingolipids. It has been shown that the loss of TRPC1-mediated Ca^{2+} influx upon pharmacological inhibition or constitutive/inducible shRNA silencing, is associated with reduced cell proliferation and incomplete cell division, thus resulting in multinucleated cells similar to those found in

patient biopsies (Bomben and Sontheimer 2010). The important role of TRPC1 in glioma cell division has been also confirmed in vivo through a shRNA knockdown approach on a flank GBM cell tumor model: TRPC1 downregulation led to a significant decrease in tumor size, most likely impairing calcium signaling during cytokinesis (late M-phase) (Bomben and Sontheimer 2010). TRPC1 has also revealed a role in controlling glioma cell migration. In particular, it has been shown that TRPC1 is essential for chemotactic migration in human malignant gliomas in response to chemoattractant growth factors like epidermal growth factor (EGF) and platelet-derived growth factor (PDGF) which affect TRPC1 activity through different signaling pathways (Bomben et al. 2011; Lepannetier et al. 2016). Stimulation with EGF was associated with a re-localization of TRPC1 channel at the leading edge of migrating D54MG glioma cells within lipid rafts, specialized membrane microdomains enriched in cholesterol and sphingolipids (Mollinedo and Gajate 2015). In agreement, it has been shown that both TRPC1 channel activity and lipid raft integrity were required for gliomas chemotaxis (Bomben et al. 2011). Moreover, the disruption of lipid rafts by depletion of cholesterol not only affected chemotaxis but also impaired TRPC currents in whole-cell recordings and decreased store-operated Ca2+ entry (SOCE), confirming a direct interplay between lipid rafts and TRPC1 channels and localized Ca2+ rise in regulating the chemotactic movement of glioma cells (Bomben et al. 2011). It must be noted that TRPC pharmacological inhibition through non-selective inhibitors caused an almost complete loss of chemotactic migration but TRPC1 knockdown through shRNA compromised directional migration but did not eliminate it and did not affect non-directional motility. This suggests TRPC1 specific implication in chemotactic migration and the potential implication of other TRPC channels in migration processes (Bomben et al. 2011). As shown by a more recent study by Lepannetier and coworkers, lipids are not only important for the regulation of TRPC1 at the membrane level, but also through their signaling. The authors shed light on another store-independent mechanism by which TRPC1 may be activated and thus affect cell migration in GBM. In particular, they have shown that PDGF may induce the translocation of TRPC1 from the cytosolic compartment to the front of migrating cells through a mechanism requiring the phosphoinositide-3 kinase (PI3K) and at the same time induces the production of the lipid second messenger sphingosine-1-P (S1P) which in turn, activates TRPC1-mediated Ca^{2+} entry. Indeed, the PDGF-induced Ca^{2+} influx through TRPC1 can be partially inhibited by pretreatment of the cells with a specific inhibitor of the sphingosine kinase (SPK) producing S1P (Lepannetier et al. 2016). However, whether S1P directly or indirectly triggers TRPC1-mediated and store-independent entry of Ca^{2+} channel remains to be clarified (Lepannetier et al. 2016). In any case, it has been well established that both TRPC1 targeting to the leading edge of lamellipodia and its activation by S1P are essential in regulating PDGF-induced chemotaxis in U251 glioblastoma cells (Lepannetier et al. 2016).

Another member of the TRPC subfamily specifically implicated in glioma progression is TRPC6. Indeed, TRPC6 was found to affect different hallmarks of GBM including tumor growth, cell survival, invasiveness and angiogenesis (Chigurupati et al. 2010; Ding et al. 2010). More specifically, it has been

demonstrated that under hypoxia, which is one of the main characteristics of GBM aggressiveness, invasion and resistance to treatment (Flynn et al. 2008), Notch1 activation consequently led to TRPC6 upregulation in primary GBM samples and cell lines (Chigurupati et al. 2010). Indeed, the inhibition/silencing of TRPC6 was associated with a reduction in glioma growth, invasion and angiogenesis. This Notch1-mediated induction of TRPC6 expression in hypoxic U373 cell line was subtype-specific, since other members of the TRPC subfamily were unaffected, indicating that TRPC6 is primarily responsible for the hypoxia-induced sustained increase in the intracellular Ca^{2+} concentration. Additionally, it has been proven that TRPC6 is essential for GBM cell survival, since its downregulation not only suppressed cell growth in vitro and reduced tumor volume in vivo, but also impaired clonogenic ability, induced cell cycle arrest at the G_2/M phase, and enhanced the antiproliferative effect of ionizing radiation.

An accelerated G2 phase progression may lead to an impaired DNA damage checkpoint and thus to an enhanced genomic instability, explaining the TRPC6 association with enhanced glioma cell malignancy. Mechanistically, TRPC6 effects on cell proliferation, tumor growth and angiogenesis seemed to be directly mediated by the Ca^{2+}-induced activation of the calcineurin-NFAT pathway (Chigurupati et al. 2010), whereas TRPC6 effects on cell migration might rather involve Rho activation and subsequent actin cytoskeleton rearrangements (Singh et al. 2007). Together, these data stress a possible role of TRPC6 as a promising therapeutic target in the treatment of human GBM (Ding et al. 2010; Chigurupati et al. 2010).

Melastatin TRPs

Four TRP melastatin subfamily members, TRPM2, TRPM3, TRPM7 and TRPM8, have been implicated in glioma cell growth, proliferation and migration. Among them, TRPM2 and TRPM3 would exert anti-tumorigenic effects, while TRPM7 and TRPM8 may contribute to glioma malignancy.

TRPM2 is known for its role as a sensor of oxidative stress and inductor of necrotic cell death upon activation by reactive oxygen species (ROS) (Naziroglu and Lückhoff 2008; Takahashi et al. 2011). TRPM2 expression likely induced no effect on cell proliferation, migration and invasion. But in A172 human GBM cells the transfection with TRPM2 channels increased cell death induced by H_2O_2 in a Ca^{2+}-dependent manner (Ishii et al. 2007) and in human GBM (DBTRG) cells, TRPM2 activation led to an increase in oxidative stress and intracellular Ca^{2+} concentration, thus promoting GBM cell death through apoptosis (Ertilav et al. 2019). Concerning TRPM3, which is the most recently described melastatin subfamily member, Its roles and action mechanisms were only recently investigated (Zamudio-Bulcock et al. 2011). Like TRPM2, TRPM3 may show a protective role in glioma probably via the miR-204 regulation (Ying et al. 2013), but its function needs further studies.

TRPM7 also controls glioma progression through miRNA regulation in GBM cells with subsequent effects on cell proliferation and invasion (Wan et al. 2019). More specifically, TRPM7 expression can be associated

with a decreased production of miR-28-5p, a tumor suppressor inhibiting the expression of oncogenic signaling pathways involving protein-kinase B (AKT) (Xiao et al. 2018), ERK (J. I. A. Liu et al. 2016), and IGF-1 (Shi and Teng 2015). Accordingly, the downregulation of miR-28-5p caused a significant increase in glioma cell proliferation and invasion. Among miR-28-5p targets, expression of Rap1b appeared as being positively correlated with TRPM7 in GBM and was up-regulated in tumor samples due to the suppression of the repressing role of miR-28-5p (Wan et al. 2019). This miR-28-5p/Rap1b axis shown in gliomagenesis is not the exclusive signaling route in which TRPM7 acts on GBM progression. Indeed, TRPM7 may also regulate the Notch pathway (Liu et al. 2014), recently shown as linked with Rap1b signaling and integrin-mediated cell adhesion in hematopoietic stem cells (Rho et al. 2019). This can be connected with the role of TRPM7 on cell proliferation, migration and invasion in glioma cells and GSCs through the upregulation of JAK2/STAT3 and/or Notch signaling pathways (Liu et al. 2014). Moreover, TRPM7 was found to activate STAT3, which in turn binds to the aldehyde dehydrogenase1 (ALDH1) promoter upregulating the expression of this well-known GSC marker involved in many pathways maintaining stem cell-like state (Rasper et al. 2010), when expanded as spheroids (Liu et al. 2014). Since ALDH1 is functionally involved in self-protection, differentiation, expansion and proliferation (Choudhary et al. 2005; Ma and Allan 2011), this potentially means that TRPM7 is not only implicated in proliferation, migration and invasion, but also in GSC renewal and differentiation. This has to be put into the context that TRPM7 channel exhibits an intrinsic kinase activity, thus supporting that TRPM7 effects on glioma cell growth are mediated by its channel activity while cell migration and invasion required its kinase domain (Wan et al. 2019). The discovery of different cellular and molecular targets affecting gliomas development and progression through their modulation by TRPM7 provides key insights for the development of novel therapeutic agents for glioma treatments.

TRPM8 was found to affect the rate of GBM cell migration by mediating a significant increase in intracellular Ca^{2+} concentration upon stimulation with specific agonists such as menthol and icilin (Wondergem et al. 2008; Wondergem and Bartley 2009; Klumpp et al. 2017). It has been shown that TRPM8 activation by icilin leads to a significant increase in the migration speed and chemotaxis of GBM cells and, consistently, TRPM8 downregulation by RNA interference as well as TRPM8 inhibition by the specific channel blocker BCTC (N-(4-tertiarybutylphenyl)-4-(3-cholorphyridin-2-yl)tetrahydropyrazine-1(2H)-carbox-amide) reduces cell migration rate and decreases transfilter chemotaxis (Klumpp et al. 2017). One of the possible mechanisms through which TRPM8-mediated Ca^{2+} influx may affect cell migration in glioma is by the activation of the large-conductance Ca^{2+}-activated K^+ ion channels (BK channels) (Wondergem and Bartley 2009). BK channels contribute to maintaining the plasma membrane ionic fluxes essential to support cell shrinkage-driven cell migration (Mcferrin and Sontheimer 2006). Interestingly, BK overexpression was detected in human glioma cells (Ransom and Sontheimer 2001) and pharmacological inhibition of BK channels was shown to abolish the menthol-stimulated Ca^{2+} influx within the cell cytoplasm and cell

migration suggesting a key role of TRPM8. TRPM8 activation by agonists has been shown to increase the open probability of single BK channels (Wondergem and Bartley 2009; Klumpp et al. 2017).In agreement, ionizing radiation, known to induce the migration through a Ca^{2+}-mediated activation of BK channels (Steinle et al. 2011; Edalat et al. 2016), has been shown to activate and upregulate TRPM8-mediated Ca^{2+} influx in glioma cells (Klumpp et al. 2017), thus confirming a direct and reciprocal interplay between these two channel families in the control of GBM migration. The function of TRPM8 in aggressiveness and resistance to treatment was suggested by the potentiating impact of hepatocyte growth factor/scatter factor (HGF/SF), a multifunctional effector of cells expressing the Met tyrosine kinase receptor (TKR), on TRPM8-induced Ca^{2+} homeostasis and cell migration. This evidence suggests that TRPM8 might converge to a common HGF/SF and cMET, known to play a role in malignancy of solid tumors including glioma (Laterra et al. 1997; Birchmeier et al. 2003; Wondergem et al. 2008), signaling pathway leading to migration/invasion. An enhancement in the invasion rate of human GBM cells has also been associated with TRPM8 overexpression (Zeng et al. 2019). However, DBTRG cells would express two different variants of TRPM8 (Wondergem et al. 2008) as revealed in Western blot showing a molecular band at 130–140 kDa in the plasma membrane-enriched fraction and consistent with the molecular weight of TRPM8 full-length isoform (Peier et al. 2002), and a second molecular band at 95–100 kDa in microsome- and membrane-enriched fractions more consistent with a truncated TRPM8 splice variant expressed in the endoplasmic reticulum (ER) (Bidaux et al. 2007). The observed greater increase in menthol-induced Ca^{2+} influx among migrating cells compared with non-migrating cells (Wondergem et al. 2008), likely indicates that only migrating cells express full-length TRPM8 protein within the plasma membrane. However, these results have to be taken with caution in a future context of drug therapy, since TRPM8 was shown to have an anti-migratory activity in other cancers including prostate cancer and may play a role in the tumoral and tumor-derived endothelial cells (Gkika et al. 2010, 2015; Genova et al. 2017; Grolez et al. 2019). TRPM8 contribution to GBM progression was found to go far beyond its effects on cell migration and invasion, significantly affecting other determinant processes such as cell cycle, cell survival and radioresistance (Klumpp et al. 2017; Zeng et al. 2019). Indeed, it has been proven that TRPM8 inhibition or knockdown impaired the cell cycle, triggered apoptotic cell death and attenuated DNA repair and clonogenic survival (Klumpp et al. 2017). A recent study by Zeng and coworkers have suggested an involvement of the mitogen-activated protein kinase (MAPK) signaling pathway in TRPM8-mediated effects on cell proliferation and apoptosis, since the expression of the channel was associated with the expression levels of important regulators of these pathways, including extracellular signal-regulated kinase (ERK), cyclin D1 and the apoptosis-related protein Bcl-2 in human glioma cells (Zeng et al. 2019). Moreover, it has been shown that TRPM8 signaling directly regulates the cell cycle, contributing to S phase progression and mitosis. These effects on glioma's cell cycle are most likely mediated by intracellular signaling pathways involving the Ca2+/calmodulin-dependent protein kinase II (CaMKII) and some Cdc phosphatases like Cdc25C and Cdc2,

which control entry into, and progression through, various phases of the cell cycle (Klumpp et al. 2017). More specifically, the TRPM8-mediated Ca^{2+} entry, through the activation of BK channels, may increase the CaMKII activity, which in turn inhibits the Cdc2 subunit of the mitosis-promoting factor likely through the inhibitory phosphorylation of the Cdc25C phosphatase (Klumpp et al. 2017). Finally, TRPM8 channel might also modulate proliferation by dynamically control glioma resting potentials levels, which are key regulator of cell cycle. TRPM8 agonists have been shown to increase the Kir4.1 mediated membrane conductances of glioma cells (Ratto et al. 2020). Kir4.1 is an inward rectifier K^+ channel, with an altered pattern of expression in glioma. In astrocytes, it is responsible for high potassium conductance and hyperpolarized membrane potential (Olsen and Sontheimer 2008). Overexpression of this channel in glioma cell lines D54MG reduces cell proliferation (Higashimori and Sontheimer 2007). Thus, TRPM8 channel by regulating K^+ resting conductances of glioma cells may exert a regulation of cell cycle transitions. Moreover, TRPM8 has also been found to be a contributor to the genotoxic stress response of GBM upon treatment with ionizing radiation, restoring G_1/S transition and S phase progression to levels of unirradiated cells (Klumpp et al. 2017). Interestingly, it has been found that ionizing radiation stimulated TRPM8 availability both in vitro and in vivo and that TRPM8 played a role in the re-entry in mitosis and cell division upon radiation-induced G_2/M arrest, since its knockdown resulted in an impaired DNA repair and a decreased survival of irradiated cells (Klumpp et al. 2017). This, combined with the slowdown of apoptosis in irradiated GBM cells, may explain the enhanced radioresistance acquired by GBM cells overexpressing TRPM8, thus stressing that the key interest of targeting TRPM8 alone or in combination with radiotherapy for future treatments of GBM.

Vanniloid TRPs

Some TRP members of the vanilloid family have been related to gliomagenesis and progression. More specifically, TRPV1 and TRPV2 have revealed a protective role in glioma cells by regulating cell proliferation and survival, stem cell differentiation and sensitivity to drugs, whereas TRPV4 was found to increase cancer cell invasiveness.

The anti-tumorigenic functional role of TRPV1 in gliomas, suggested by its marked downregulation or loss in patients with the shortest overall survival, has been investigated and several findings highlighted a role of TRPV1 in the induction of apoptotic cell death signaling in gliomas (Amantini et al. 2007; Stock et al. 2012). Upon exposure to low doses of the TRPV1 specific agonist capsaicin (CPS), the TRPV1-Ca^{2+} may sustain apoptosis in gliomas through the selective activation of p38 MAPK, but not ERK MAPK (Amantini et al. 2007). More in detail, it has been shown that CPS-mediated TRPV1 activation leads to reduced cell viability, DNA fragmentation, externalization of phosphatidylserine on the outer layer of the plasma membrane, mitochondrial transmembrane potential dissipation, and caspase 3 activation (Amantini et al. 2007). Moreover, TRPV1 translation in GBM was found to be sensitive to interferon-gamma (INF-γ) and to the well-

known autophagic inducer rapamycin (Rap), suggesting a link between TRPV1 channel and autophagy often related to pro-survival in tumors including GBM (Galluzzi et al. 2015) but also in migration (Coly et al. 2017). This biological effect might be achieved by the TRPV1-mediated induction of apoptosis previously reported in GBM cells (Amantini et al. 2007).

One of the mechanisms through which the brain, especially in the juvenile phase, can protect itself against high-grade astrocytoma (HGAs) involves the activation of TRPV1 by neural precursor cells (NPCs), known to show extensive tropism for brain tumors (Mayor et al. 2001). Interestingly, NPCs accumulate at HGA especially in the context of the juvenile brain, exhibiting a high proliferative activity in the stem cell niche (Walzlein et al. 2008), and can release tumor-suppressive factors, such as endovanilloids able to activate TRPV1 expressed by HGA cells (Stock et al. 2012). The activation of the latter would trigger astrocytoma cell death through the ER pathway in a transcription factor-3 (ATF3)-dependent manner, thus reducing glioma expansion mostly in young brain (Stock et al. 2012). In light of these data, the inverse correlation between TRPV1 expression and glioma grade from I to III and the reduced or lost TRPV1 expression found in GBM patients is most likely a mechanism by which tumor cells may evade anti-proliferative and pro-apoptotic signals. This hypothesis is also supported by the finding that TRPV1 is also downregulated in GSCs (Stock et al. 2012), whose resistance to cytotoxic therapies and to pro-apoptotic signals is accepted (Bao, Wu, Mclendon, et al. 2006). Furthermore, the induction of GSCs differentiation was accompanied by $TRPV1_{v3}$ expression at a similar level than found in low-grade glioma, thus confirming a protective role of this channel against aggressiveness (Nabissi et al. 2016).

TRPV2 exerts its anti-tumorigenic function on gliomas through the regulation of several signaling pathways involved in cell proliferation and survival, stem cell differentiation and sensitivity to drugs. Physiologically, the triggering of TRPV2 by agonists/activators such as growth factors, hormones and cannabinoids led to TRPV2 translocation from the endosome to the plasma membrane, where it mediates several pathways associated with cell proliferation and cell death (Liberati et al. 2014). Thus, loss or alterations of TRPV2 expression in cancer cells results in an impairment of these processes, as shown in prostate tumor-derived endothelial cells (Bernardini et al. 2019) and gliomas (Liberati et al. 2014). In gliomas, it has been shown that TRPV2 reduced cell proliferation and increased cell sensitivity to Fas-induced apoptosis in an ERK-dependent manner (Nabissi et al. 2010). Consistently, enhanced cell growth and rescuing from apoptotic cell death was observed when TRPV2 was silencing in U87MG GBM cells. In contrast, TRPV2 upregulation in MZC primary glioma cells, by inducing Fas overexpression led to reduced viability and increased spontaneous as well as Fas-induced apoptosis (Nabissi et al. 2010). Similar findings were also described in GSCs, whose proliferation appeared strongly impaired by TRPV2 pharmacological inhibition or knocking down (Morelli et al. 2012). In GSCs, TRPV2 acts also on differentiation (Morelli et al. 2012; Nabissi et al. 2015). More specifically, TRPV2 overexpression was associated with glial fibrillary acidic protein (GFAP)

and βIII-tubulin increased expression, thus promoting a glial phenotype differentiation while inhibiting GSCs proliferation both in vitro and in vivo. In agreement, TRPV2 silencing or inhibition during differentiation impaired differentiation and reduced GFAP and βIII-tubulin expression (Morelli et al. 2012). Moreover, TRPV2 activation through cannabidiol (CBD) was found to trigger GSCs differentiation activating the autophagic process, in addition to inhibiting GSCs proliferation and clonogenic capability (Nabissi et al. 2015). More specifically, it has been observed that CBD, through the TRPV2-mediated activation of the PI3K/AKT pathway, upregulated the expression of acute myeloid leukemia (Aml-1) transcription factors, known for their pivotal role in GBM proliferation and differentiation. Furthermore, it has also been shown that the spliced variant Aml-1 a, upregulated during GSCs differentiation, directly influenced the expression of TRPV2 by binding its gene promoter (Nabissi et al. 2015), thus establishing a positive feedback circuit, which on the whole caused glial differentiation.

Conversely to TRPV1 and TRPV2, TRPV4 has revealed a pivotal role in promoting glioma progression (Ou-yang et al. 2018). In particular, the tumorigenic potential of TRPV4 comes from its critical involvement in glioma cell migration and invasion. Indeed, it has been demonstrated that TRPV4-mediated Ca^{2+} influx upon stimulation with the selective agonist GSK1016790 A, is able to promote cell migration of glioma cells (Ou-yang et al. 2018), a similar mechanism previously reported in breast cancer (Lee et al. 2017). It was established that TRPV4 effects on cell migration are relayed by phosphorylation of AKT (P-AKT) and activation of Rac1 (Ou-yang et al. 2018), a member of the Rho GTPases family known for its central role in cytoskeleton remodeling, cell motility and cell adhesion as well as for its involvement in the enhanced migration of several tumor types including GBM, colon, colorectal and ovarian cancer (Qin et al. 2017; Guéguinou et al. 2016; Zhou et al. 2018; Guo et al. 2015). Accordingly, TRPV4 blockade, induced by the specific TRPV4 inhibitor HC-067047, was found to decrease motility and invasiveness of U87 glioma cells through a P-AKT and Rac1 signaling pathway (Ou-yang et al. 2018).

Mucolipin TRPs

The two TRP members of mucolipin subfamily have revealed opposite effects on glioma carcinogenesis.

TRPML1 showed a protective role against glioma progression. Indeed, it has been shown that TRPML1 activation by its specific agonist MK6-83 reduced T98 and U251 cell line viability and increased caspase 3-dependent apoptosis. Accordingly, TRPML1 silencing or pharmacological inhibition restored cell viability suppressing the Ca^{2+} influx responsible for apoptosis induction. Furthermore, TRPML1 may also mediate the autophagic cell death pathway, upon cell treatment with the ROS inducer carbonyl cyanide m-chlorophenylhydrazone (CCCP) (Morelli et al. 2019). Indeed, high ROS levels may trigger a TRPML1-mediated lysosomal Ca^{2+} release and the subsequent enhancement of autophagy (Zhang, Yu, and Xu 2016). Accordingly, TRPML1 silencing or inhibition by sphingomyelin pre-treatment reverted CCCP effects. (Morelli

et al. 2019). In this context, it has also been demonstrated that TRPML1, through a large intraluminal loop between its first and second transmembrane domains, may interact with chaperone-mediated autophagy-related proteins such as the heat shock proteins Hsc70, and Hsp40 (Venugopal et al. 2009). Therefore, TRPML1 may exert its cytotoxic effects through two different pathways, e.g. i) it can act as a ROS sensor on the lysosomal membrane and attenuate oxidative cell stress through an autophagy-dependent negative-feedback mechanism (Zhang et al. 2016; Morelli et al. 2019) or ii) it may trigger Ca^{2+} release but no ROS production upon direct activation by its specific agonist, thus inducing apoptosis (Morelli et al. 2019). Moreover, the important role of TRPML1 in controlling intracellular Ca^{2+} homeostasis has been further corroborated by the recent finding of a functional localization of TRPML1 at the so-called "mitochondria-lysosome contact sites" where it mediates a calcium flux from lysosomes to mitochondria adjuvanted by VDAC and MCU on the outer and inner mitochondrial membranes, respectively (Peng, Wong, and Krainc 2020). Consequently, TRPML1 functions go beyond the regulation of lysosomal dynamics and function and, through the control of mitochondrial Ca^{2+} dynamics, can affect other Ca^{2+}-dependent mitochondrial functions, including oxidative phosphorylation, motility, and ROS signaling (Peng, Wong, and Krainc 2020).

Conversely to TRPML1, the other member of the mucolipin family, TRPML2, has revealed a pro-tumorigenic function in glioma progression. Indeed, it has been shown that TRPML2 enhanced glioma cell survival and proliferation (Morelli et al. 2016). More in detail, TRPML2 suppression leads to impaired cell cycle, reduced cell viability and decreased proliferation (Morelli et al. 2016). In addition, its knocking-down was found to induce apoptosis by increasing DNA damage, Ser139 H2AX phosphorylation and caspase-3 activation (Morelli et al. 2016). TRPML2 effects on tumor progression are probably mediated by PI3K/AKT and ERK1/2 pathways, since these pathways remained inactivated in TRPML2-silenced cells (Morelli et al. 2016). Thus, TRPML2 might also be an interesting therapeutic target to control GBM cell survival and proliferation.

THERAPEUTIC TARGETING

Considering the altered expression and the great contribution given by TRP channels to the establishment and progression of glioma, they may be considered very promising new therapeutic molecular targets against which novel drug compounds must be developed. One of the main advantages provided by most TRPs is their accessibility from the extracellular side, which makes them efficient targetable sites via administration of specific TRPs inhibitors or blockers when these channels are overexpressed in high-grade glioma. For instance, some of the TRPC channels by interfering with cytokinesis pathways would be promising targets for the development of drugs able to interfere with the almost unrestrained growth of gliomas, making tumors more susceptible to surgical removal or focal radiotherapy. Moreover, the low specificity of some TRPC

modulators might allow to achieve a higher antitumor effect, through the simultaneous triggering of more than one channel. The progressive understanding of the molecular mechanism underlying TRPC function in glioma has also provided opportunities and arguments in favor of small molecule targeted therapies. Through studies concerning TRPC1 and its specific pharmacological inhibition, the key option by inhibiting SPK or PI3K inhibitors is once again here confirmed to attempt controlling GBM growth and invasiveness. Among TRPC channels, great potential as a promising new candidate for GBM treatment comes from TRPC6. Among TRP, TRPC6 is to date the only one being implicated in GBM angiogenesis suggesting that specific TRPC6 inhibitors could simultaneously target both cancer progression and vascularization, thereby improving the efficacy of standard (radio-chemotherapy) options. The barely detectable TRPC6 expression in normal glial cells should limit the potential side effects on normal glial cells. But a possible impact of TRPC6 blockade on neurons must be considered in regards to the central role of TRPC6 in neuronal functions (Tai et al. 2008; Zhou et al. 2008; Kim, Park, and Kang 2017). A possible strategy to overcome this problem might be the use of viral vectors as a drug delivery system towards glioma cells since adenovirus may target glioma cells more efficiently than neurons (Ding et al. 2010).

As recurrence is due to migration and invasion (and resistance to treatment), pharmacological inhibition of TRPV4 might represent a potential new therapeutic approach in GBM treatment to control migratory and invasive capabilities of GBM cells (Ou-yang et al. 2018). One of the mechanisms through which tumor cells are able to sustain a prolonged survival is by the inhibition of apoptotic pathways (Thompson 1995). In this context, TRPA1 has been recently proposed as a new potential therapeutic target in GBM treatment. Indeed, TRPA1 is a ROS-sensitive cation channel and can subsequently be activated by hypoxia-induced oxidative stress (Naziroğlu 2012; Takahashi et al. 2018). It has been shown that TRPA1 activation following cobalt chloride (CoCl2) treatment with the aim to mimic hypoxia, may increase apoptosis, inflammation and oxidative effects on DBTRG cells (Deveci et al. 2019). More specifically, TRPA1-mediated Ca^{2+} entry was associated with an enhancement of ROS production and mitochondrial membrane depolarization (JC-1). Moreover, TRPA1 activation leads to increased levels of Annexin V, cytokines IL-1β and IL-18, and caspase 3 and 9 and decreased levels of thiol cycle antioxidants (GSH and GSH-Px) (Deveci et al. 2019). These effects were shown attenuated by α-lipoic acid (ALA) treatment, a physiological source of energy for cells which may exert both anti- and pro-oxidant functions (Moini, Packer, and Saris 2002). In glioma cells under hypoxia, ALA likely acts as an antioxidant agent, upregulating GSH and GSH-Px and down-regulating mitochondrial ROS production, thus blocking TRPA1-mediated induction of apoptotic cell death (Deveci et al. 2019). This suggests that targeting and activating TRPA1 or targeting TRPV1 in glioma exhibiting such expression, can restore apoptotic signalings and might provide new insights for the development of alternative therapies against glioma progression.

Besides being potential anti-tumor targets, TRP channels should play a role as “drug carriers” in cancer therapy, facilitating *via* the central pore chemotherapy drug uptake thus improving the efficacy of cancer therapies. For instance, TRPV2 activation by CBD can sensitize GBM cells to chemotherapeutic agents currently used, e.g. TMZ, carmustine (BCNU) and doxorubicin (DOXO) (Nabissi et al. 2013; 2015). The CBD-induced TRPV2 activation was found to increase GSCs sensitivity to cytotoxic effects of alkylating agents like BCNU favoring drug uptake (Nabissi et al. 2013), in synergy with the Ca^{2+}-dependent triggering of apoptotic cell death, a mechanism not found in normal astrocytes (Nabissi et al. 2015). Specifically, by using the natural red fluorescent DOXO, it has been demonstrated that TRPV2 overexpression in MZC glioma cells markedly increased DOXO uptake in a Ca^{2+}-dependent manner, since Ca^{2+} chelation by EGTA completely inhibited the CBD-induced TRPV2-mediated increase of DOXO-positive cells (Nabissi et al. 2013). Similar findings were also observed in hepatocellular carcinoma in which TRPV2 activation by CBD or 2-APB (Aminoethoxydiphenyl borate) was found to improve DOXO permeation into tumor cells, thus corroborating an intriguing role of TRPV2 in increasing tumor cell sensitivity to chemotherapy drugs (Neumann-Raizel et al. 2019). Taking into account other evidence on the role of TRP channels as “drug carriers” thanks to the permeation of chemotherapy agents into the cell through their pore domain (Santoni and Farfariello 2011), it is reasonable to speculate that the activation of TRPV2 channel may cause a conformational change in the pore helix structure, which allow for intracellular nonspecific chemotherapy uptake (Nabissi et al. 2013), opening the route for combinatorial co-administration of TRPV2 specific agonist CBD and lower chemotherapeutic doses to overcome the high resistance of GBM and GSCs to chemotherapeutic agents. In this context, recent developments on the role of the so-called "pore turret", i.e. the region of the extracellular ring that connects the S5 helix to the pore helix, in controlling the upper gate of some TRP channels including TRPV2 (Dosey et al. 2019) have provided new insights into the role of TRPV2 as a drug target to reduce GBM chemoresistance. Indeed, the well-defined pore turret, in addition to allowing the coupling between the lower gate and the upper gate in response to intracellular stimuli stabilizing a fully open un-liganded channel, represents a possible and interesting binding site for extracellular modulators through which it may affect channel activity allowing the passage through the plasma membrane of partially hydrophilic molecules which otherwise could not enter the cell (Dosey et al. 2019).

With a view to looking ahead, some data indicate that TRP channels may constitute targets of gene therapy. It has been recently shown that TRPM2 can promote cell death (Ertilav et al. 2019). Therefore, TRPM2 might represent a good candidate for gene therapy to be used for instance in combination with γ-radiation and/or chemotherapeutic agents to improve the effectiveness of GBM treatments. Preliminary observations indicate that Selenium (Se) tested on GBM cells resistant to Docetaxel (DTX) may improve the apoptotic efficacy of DTX through the activation of TRPM2 by oxidative stress (Ertilav et al. 2019). The cytotoxic effect of DTX likely comes from the formation of excessive mitochondrial ROS and Ca^{2+} influx into

the cells which causes DNA damage by triggering hyperactivation of the DNA nick sensor PARP, thus leading to NAD^+ and ATP depletion and subsequent apoptotic cell death (Ertilav et al. 2019). In this case, Se, in particular, stimulated oxidative stress production in the mitochondria, which in turn activated a TRPM2-mediated Ca^{2+} influx, thus supporting and enhancing the same Ca2+-dependent apoptotic pathway induced by DTX and other chemotherapeutic agents, as seen also in other tumor types (Hazane-Puch et al. 2016) (Çetin et al. 2017). Overall the combination and synergistic activity of Se and DTX in GBM expressing TRPM2 might offer a new option for adjuvant chemotherapy as treatment of GBM.

FUTURE PERSPECTIVES

Increasing understanding of the signaling pathways involved in tumorigenesis has made it possible to identify a wide range of molecular targets involved in self-renewal and proliferation, angiogenesis but also in invasion of GBM cells. A number of therapeutic strategies have therefore been developed during the last decade and few of them have proven to be effective, even though anti-angiogenic treatments appear to be able to provide a 6 month delay for GBM patients before recurrence. It is, therefore, necessary to identify other therapeutic targets that can be combined with anti-angiogenic, cytotoxic, DNA repair inhibitors and/or immunotherapy strategies. In this context, targeting the activity of factors or components expressed by glioma cells themselves and by other cell types of the micro-environment would also be promising. It has also to be considered that main RNAseq and/or transcriptomic databases were constituted by means of the glioma tumor bulk composed of the different populations of GBM cells and other constituents such as endothelial cells, pericytes, reactive astrocytes, macrophages (M_1 and/or M_2), microglial, neurons, and potentially lymphocytes, depending on the level of heterogeneity GBM subgroup. New potential family targets, expressed at the plasma membrane and involved in survival, GSC differentiation, angiogenesis and invasion, constitute a choice option. TRP channels not systematically ubiquitously expressed, potentially playing pleiotropic mechanisms and being overexpressed in pathologic situations such as hypoxia in glioma cells deserve to be more explored, especially since they could be also expressed by other cell types belonging to the tumor micro-environment.

For instance, a direct involvement of TRP channels in vascular endothelial growth factor (VEGF) signaling pathways affecting brain neovascularization and tumor growth it has been proven. GCSs positive for CD133 (human prominin-1/AC 133) not only are capable of self-renewal and proliferation, but also possess the capability to secrete high levels of VEGF (Bao, Wu, Sathornsumetee, et al. 2006; Yao et al. 2008), known to play a crucial role in endothelial cell recruitment and angiogenesis of malignant human gliomas (Fischer et al. 2005; Bian et al. 2006). In GSCs isolated from U87 cell line the production of VEGF and the angiogenic CXCL8 (chemokine interleukin-8) by tumor cells appeared to be mediated by a G protein-coupled receptor

named formylpeptide receptor (FPR) which, upon activation, induces directional migration, growth and angiogenic factors production through a Ca^{2+} mobilization. Although a direct involvement of TRPs in this Ca2+-mediated mechanism has not been highlighted, a GCPR-TRP axis in many signaling pathways is nowadays well established (Veldhuis et al. 2015). Moreover, an interesting crosstalk between TRPM8, TRPV1 and the VEFG receptor (VEGFR) it has been recently characterized in uveal melanoma, suggesting a good potential for TRPM8 as a pharmacological target for blocking brain neovascularization and tumor growth (Walcher et al. 2018). Indeed, it has been demonstrated that in different cell types including corneal epithelial and endothelial cells (Lucius et al. 2016) and uveal melanoma cells (Walcher et al. 2018) the activation of TRPM8 inhibits the VEGF transactivation of TRPV1 and the consequent pro-tumorigenic effects mediated by the VEGFR. These findings further highlighted the central role played by TRPs interactions with other TRP channels, other channels families like that of BK channels, and the GCPRs, in affecting signaling pathways directly involved in carcinogenesis and brain tumor progression. Moreover, they strongly sustain the possible TRPs application in anti-angiogenic therapy.

However, to date, to the best of our knowledge TRPC6 is the only TRP channel directly implicated in GBM angiogenesis. TRPC6 has been found to play a key role in promoting GBM growth, angiogenesis and invasion under hypoxia through Notch1. (Chigurupati et al. 2010). TRPC6 knockdown or NFAT inhibition has been shown to reduce the number of branch points and thus impair the ability of the hypoxic U373MG to induce endothelial cell tube formation in vitro, suggesting a role of TRPC6 in the “vascular mimicry” played by glioma cells (Chigurupati et al. 2010).

Other TRPs among those previously described to have a function in gliomas, such as TRPM2, TRPM7, TRPV2 and TRPV4 have also been found in brain vasculature, thus suggesting a possible double function for these channels in affecting glioma progression (Hatano et al. 2013; Pires and Earley 2017; Ou-yang et al. 2018; Luo et al. 2019) and contributing to GBM angiogenesis. Regarding TRPA1 and TRPC3 not likely described in glioma, some studies highlighted their involvement in other brain vasculature diseases, exerting a protective role against ischemic damage, controlling vasodilation in brain endothelial cells (Sullivan et al. 2016; Pires and Earley 2018). TRPC3, when overexpressed, would lead to an increase in the BBB permeability, leading to vasogenic edema formation (Ryu et al. 2013).

CONCLUSIONS

Taken together all these data suggest a key role of some TRP channels in high-grade glioma development and angiogenesis. The current activators or inhibitors directed against these channels should provide lead compounds and knowledge for future research in the design of drugs targeting simultaneously glioma cells and key components of the micro-environment such as abnormal tumoral vascularization.

Conflicts of Interest: The authors declare that the research was conducted in the absence of any commercial or financial relationships that could be construed as a potential conflict of interest.

Author Contributions: DG and HC provided a rational of the study. GC performed an in-depth analysis of the roles of TRP channels in inducing glioma behavior and generated a preliminary draft. GC, HC, OC and DG performed literature searches and contributed to writing and editing of the content.

Funding: DG is supported by the Institut Universitaire de France (IUF). GC is supported by University of Torino as part of the PhD Program in Complex Systems for Life Sciences. HC and OC's work on glioma invasion and angiogensis are supported by The Ligue contre le Cancer Normandie, Géfluc charity and Fondation ARC.

References

Alifieris, Constantinos, and Dimitrios T. Trafalis. 2015. "Glioblastoma Multiforme: Pathogenesis and Treatment." Pharmacology & Therapeutics 152 (August): 63–82. https://doi.org/10.1016/j.pharmthera.2015.05.005.

Alptekin, M., S. Eroglu, E. Tutar, S. Sencan, M. A. Geyik, M. Ulasli, A. T. Demiryurek, and C. Camci. 2015. "Gene Expressions of TRP Channels in Glioblastoma Multiforme and Relation with Survival." Tumor Biology 36 (12): 9209–13. https://doi.org/10.1007/s13277-015-3577-x.

Amantini, C., M. Mosca, M. Nabissi, R. Lucciarini, S. Caprodossi, A. Arcella, F. Giangaspero, and G. Santoni. 2007. "Capsaicin-Induced Apoptosis of Glioma Cells Is Mediated by TRPV1 Vanilloid Receptor and Requires P38 MAPK Activation." Journal of Neurochemistry 102 (3): 977–90. https://doi.org/10.1111/j.1471-4159.2007.04582.x.

Asuthkar, Swapna, Kiran Kumar Velpula, Pia A Elustondo, and Lusine Demirkhanyan. 2015. "TRPM8 Channel as a Novel Molecular Target in Androgen- Regulated Prostate Cancer Cells." Oncotarget 6 (19): 17221–36.

Audic, Yann, and Rebecca S. Hartley. 2004. "Post-Transcriptional Regulation in Cancer." Biology of the Cell 96 (7): 479–98. https://doi.org/10.1016/j.biolcel.2004.05.002.

Bao, Shideng, Qiulian Wu, Roger E Mclendon, Yueling Hao, Qing Shi, Anita B Hjelmeland, Mark W Dewhirst, Darell D Bigner, and Jeremy N Rich. 2006. "Glioma Stem Cells Promote Radioresistance by Preferential Activation of the DNA Damage Response." Nature 444 (7120): 756–60. https://doi.org/10.1038/nature05236.

Bao, Shideng, Qiulian Wu, Sith Sathornsumetee, Yueling Hao, Zhizhong Li, Anita B. Hjelmeland, Qing Shi, Roger E. McLendon, Darell D. Bigner, and Jeremy N. Rich. 2006. "Stem Cell-like Glioma Cells Promote Tumor Angiogenesis through Vascular Endothelial Growth Factor." Cancer Research 66 (16): 7843–48. https://doi.org/10.1158/0008-5472.CAN-06-1010.

Bernardini, Michela, Alessia Brossa, Giorgia Chinigo, Guillaume P Grolez, Giulia Trimaglio, Laurent Allart, Audrey Hulot, et al. 2019. "Signatures in Tumor-Derived Endothelial Cells : Functional Roles in Prostate Cancer Angiogenesis," 1–29.

Bian, Xiu Wu, Xue Feng Jiang, Jian Hong Chen, Jia Si Bai, Chao Dai, Qing Liang Wang, Jia You Lu, et al. 2006. "Increased Angiogenic Capabilities of Endothelial Cells from Microvessels of Malignant Human Gliomas." International Immunopharmacology 6 (1): 90–99. https://doi.org/10.1016/j.intimp.2005.08.004.

Bidaux, G., M. Roudbaraki, C. Merle, A. Crépin, P. Delcourt, C. Slomianny, S. Thebault, et al. 2005. "Evidence for Specific TRPM8 Expression in Human Prostate Secretory Epithelial Cells: Functional Androgen Receptor Requirement." Endocrine-Related Cancer 12 (2): 367–82. https://doi.org/10.1677/erc.1.00969.

Bidaux, Gabriel, Matthieu Flourakis, Stéphanie Thebault, Alexander Zholos, Benjamin Beck, Dimitra Gkika, Morad Roudbaraki, et al. 2007. "Prostate Cell Differentiation Status Determines Transient Receptor Potential Melastatin Member 8 Channel Subcellular Localization and Function." Journal of Clinical Investigation 117 (6): 1647–57. https://doi.org/10.1172/JCI30168.

Birchmeier, Carmen, Walter Birchmeier, Ermanno Gherardi, and George F Vande Woude. 2003. "Met, Metastasis, Motility and More." Nat Rev Mol Cell Biol 4 (12): 915–25. https://doi.org/10.1038/nrm1261.

Bomben, V. C., and H. Sontheimer. 2010. “Disruption of Transient Receptor Potential Canonical Channel 1 Causes Incomplete Cytokinesis and Slows the Growth of Human Malignant Gliomas.” Glia 58 (10): 1145–56. https://doi.org/10.1038/jid.2014.371.

Bomben, V. C., and H. W. Sontheimer. 2008. “Inhibition of Transient Receptor Potential Canonical Channels Impairs Cytokinesis in Human Malignant Gliomas.” Cell Proliferation 41 (1): 98–121. https://doi.org/10.1111/j.1365-2184.2007.00504.x.

Bomben, V. C., K.L. Turner, T.C. Barclay, and H. Sontheimer. 2011. “Transient Receptor Potential Canonical Channels Are Essential for Chemotactic Migration of Human Malignant Gliomas.” J Cell Physiol. 226 (7): 1879–88. https://doi.org/10.1161/CIRCULATIONAHA.110.956839.

Bordey, Angélique, and Harald Sontheimer. 1998. “Electrophysiological Properties of Human Astrocytic Tumor Cells in Situ: Enigma of Spiking Glial Cells.” Journal of Neurophysiology 79 (5): 2782–93. https://doi.org/10.1152/jn.1998.79.5.2782.

Çetin, Esin Sakallı, Mustafa Nazıroğlu, Bilal Çiğ, İshak Suat Övey, and Pınar Aslan. 2017. “Selenium Potentiates the Anticancer Effect of Cisplatin against Oxidative Stress and Calcium Ion Signaling-Induced Intracellular Toxicity in MCF-7 Breast Cancer Cells : Involvement of the TRPV1 Channel.” J Recept Signal Transduct Res. 37 (1): 84–93. https://doi.org/10.3109/10799893.2016.1160931.

Chigurupati, Srinivasulu, Rajarajeswari Venkataraman, Daniel Barrera, Anusha Naganathan, Meenu Madan, Leena Paul, Jogi V Pattisapu, et al. 2010. “Receptor Channel TRPC6 Is a Key Mediator of Notch-Driven Glioblastoma Growth and Invasiveness.” Cancer Research 6 (11): 418–28. https://doi.org/10.1158/0008-5472.CAN-09-2654.

Choudhary, Sanjeev, Tianlin Xiao, Leoncio A Vergara, Sanjay Srivastava, David Nees, Joram Piatigorsky, and Naseem H Ansari. 2005. “Role of Aldehyde Dehydrogenase Isozymes in the Defense of Rat Lens and Human Lens Epithelial Cells against Oxidative Stress.” Invest Ophthalmol Vis Sci 46 (1): 259–67. https://doi.org/10.1167/iovs.04-0120.

Coly, Pierre Michaël, Pierrick Gandolfo, Hélène Castel, and Fabrice Morin. 2017. “The Autophagy Machinery: A New Player in Chemotactic Cell Migration.” Frontiers in Neuroscience 11 (FEB): 1–11. https://doi.org/10.3389/fnins.2017.00078.

Cuddapah, V.A., and H. Sontheimer. 2011. “Ion Channels and Tranporters in Cancer. 2. Ion Channels and the Control of Cancer Cell Migration.” Am J Physiol Cell Physiol. 301 (3): C541–49. https://doi.org/10.1152/ajpcell.00102.2011.

Demuth, T., and M.E. Berens. 2004. “Molecular Mechanisms of Glioma Cell Migration and Invasion.” J Neurooncol 70 (2): 217–28.

Deveci, Haci Ahmet, Yener Akyuva, Gökhan Nur, and Mustafa Nazıroğlu. 2019. “Alpha Lipoic Acid Attenuates Hypoxia-Induced Apoptosis, Inflammation and Mitochondrial Oxidative Stress via Inhibition of TRPA1 Channel in Human Glioblastoma Cell Line.” Biomedicine and Pharmacotherapy 111 (August 2018): 292–304. https://doi.org/10.1016/j.biopha.2018.12.077.

Ding, Xia, Zhuohao He, Kechun Zhou, Ju Cheng, Hailan Yao, Dongliang Lu, Rong Cai, et al. 2010. “Essential Role of TRPC6 Channels in G2 / M Phase Transition and Development of Human Glioma.” J Natl Cancer Inst 102 (14): 1052–68. https://doi.org/10.1093/jnci/djq217.

Doñate-Macián, Pau, Antonio Gómez, Irene R. Dégano, and Alex Perálvarez-Marín. 2018. “A TRPV2 Interactome-Based Signature for Prognosis in Glioblastoma Patients.” Oncotarget 9 (26): 18400–409. https://doi.org/10.18632/oncotarget.24843.

Dosey, T.L., Z. Wang, G. Fan, Z. Zhang, I.I. Serysheva, W. Chiu, and T.G. Wensel. 2019. “Structures of TRPV2 in Distinct Conformations Provide Insight into Role of the Pore Turret.” Nat Struct Mol Biol 26 (1): 40–49. https://doi.org/10.1038/s41594-018-0168-8.Structures.

Edalat, Lena, Benjamin Stegen, Lukas Klumpp, Erik Haehl, Karin Schilbach, Robert Lukowski, Matthias Kühnle, et al. 2016. “BK K + Channel Blockade Inhibits Radiation-Induced Migration / Brain Infiltration of Glioblastoma Cells.” Oncotarget 7 (12): 14259–78.

Ertilav, Kemal, Mustafa Nazıroğlu, Zeki Serdar Ataizi, and Nady Braidy. 2019. “Selenium Enhances the Apoptotic Efficacy of Docetaxel Through Activation of TRPM2 Channel in DBTRG Glioblastoma Cells.” Neurotoxicity Research 35 (4): 797–808. https://doi.org/10.1007/s12640-019-0009-5.

Fiorio Pla, A., and D. Gkika. 2013. “Emerging Role of TRP Channels in Cell Migration: From Tumor Vascularization to Metastasis.” Front Physiol 4: 311. https://doi.org/10.3389/fphys.2013.00311.

Fischer, Ingeborg, Jean Pierre Gagner, Meng Law, Elizabeth W. Newcomb, and David Zagzag. 2005. “Angiogenesis in Gliomas: Biology and Molecular Pathophysiology.” Brain Pathology 15 (4): 297–310. https://doi.org/10.1111/j.1750-3639.2005.tb00115.x.

Flynn, J. R., L. Wang, D.L. Gillespie, G.J. Stoddard, J.K. Reid, J. Owens, G.B. Ellsworth, K.L. Salzman, A.Y. Kinney, and R.L. Jensen. 2008. “Hypoxia-Regulated Protein Expression, Patient Characteristics, and Preoperative Imaging as Predictors of Survival in Adults With Glioblastoma Multiforme.” Cancer 113 (5): 1032–42.

Galluzzi, Lorenzo, Federico Pietrocola, José Manuel Bravo-San Pedro, Ravi K Amaravadi, Eric H Baehrecke, Francesco Cecconi, Patrice Codogno, et al. 2015. “Autophagy in Malignant Transformation and Cancer Progression.” The EMBO Journal 34 (7): 856–80. https://doi.org/10.15252/embj.201490784.

Gebauer, Fátima, and Matthias W. Hentze. 2004. “Molecular Mechanisms of Translational Control.” Nature Reviews Molecular Cell Biology 5 (10): 827–35. https://doi.org/10.1038/nrm1488.

Gees, Maarten, Barbara Colsoul, and Bernd Nilius. 2010. “The Role of Transient Receptor Potential Cation Channels in Ca2+ Signaling.” Cold Spring Harbor Perspectives in Biology 2 (10): 1–32. https://doi.org/10.1101/cshperspect.a003962.

Genova, Tullio, Guillaume P. Grolez, Chiara Camillo, Michela Bernardini, Alexandre Bokhobza, Elodie Richard, Marco Scianna, et al. 2017. “TRPM8 Inhibits Endothelial Cell Migration via a Nonchannel Function by Trapping the Small GTPase Rap1.” Journal of Cell Biology 216 (7): 2107–30. https://doi.org/10.1083/jcb.201506024.

Giese, A., R. Bjerkvig, M.E. Berens, and M. Westphal. 2003. “Cost of Migration: Invasion of Malignant Gliomas and Implications for Treatment.” Journal of Clinical Oncology 21 (8): 1624–36. https://doi.org/10.1200/JCO.2003.05.063.

Gkika, D., M. Flourakis, L. Lemonnier, and N. Prevarskaya. 2010. “PSA Reduces Prostate Cancer Cell Motility by Stimulating TRPM8 Activity and Plasma Membrane Expression.” Oncogene 29 (32): 4611–16. https://doi.org/10.1038/onc.2010.210.

Gkika, D., L. Lemonnier, G. Shapovalov, D. Gordienko, C. Poux, M. Bernardini, A. Bokhobza, et al. 2015. “TRP Channel-Associated Factors Are a Novel Protein Family That Regulates TRPM8 Trafficking and Activity.” J Cell Biol 208 (1): 89–107. https://doi.org/10.1083/jcb.201402076.

Gkika, D., and N. Prevarskaya. 2009. “Molecular Mechanisms of TRP Regulation in Tumor Growth and Metastasis.” Biochim Biophys Acta 1793 (6): 953–58. https://doi.org/S0167-4889(08)00410-2 [pii] 10.1016/j.bbamcr.2008.11.010.

Gkika, Dimitra, Stéphane Lolignier, Guillaume P. Grolez, Alexis Bavencoffe, Georges Shapovalov, Dmitri Gordienko, Artem Kondratskyi, et al. 2020. “Testosterone-Androgen Receptor: The Steroid Link Inhibiting TRPM8-Mediated Cold Sensitivity.” FASEB Journal 34 (6): 7483–99. https://doi.org/10.1096/fj.201902270R.

Grolez, G. P., M. Hammadi, A. Barras, D. Gordienko, C. Slomianny, P. Völkel, P. O. Angrand, et al. 2019. “Encapsulation of a TRPM8 Agonist, WS12, in Lipid Nanocapsules Potentiates PC3 Prostate Cancer Cell Migration Inhibition through Channel Activation.” Scientific Reports 9 (1): 1–15. https://doi.org/10.1038/s41598-019-44452-4.

Grolez, Guillaume P., Dmitri V. Gordiendko, Manon Clarisse, Mehdi Hammadi, Emilie Desruelles, Gaëlle Fromont, Natalia Prevarskaya, Christian Slomianny, and Dimitra Gkika. 2019. “TRPM8-Androgen Receptor Association within Lipid Rafts Promotes Prostate Cancer Cell Migration.” Cell Death & Disease 10 (9): 652. https://doi.org/10.1038/s41419-019-1891-8.

Guéguinou, Maxime, Thomas Harnois, David Crottes, Arnaud Uguen, Nadine Deliot, Audrey Gambade, Aurélie Chantôme, et al. 2016. “SK3/TRPC1/Orai1 Complex Regulates SOCE-Dependent Colon Cancer Cell Migration: A Novel Opportunity to Modulate Anti- EGFR MAb Action by the Alkyl-Lipid Ohmline.” Oncotarget 7 (24): 36168–84. https://doi.org/10.18632/oncotarget.8786.

Guo, Yuna, S. Ray Kenney, Carolyn Y. Muller, Sarah Adams, Teresa Rutledge, Elsa Romero, Cristina Murray-Krezan, et al. 2015. “R-Ketorolac Targets Cdc42 and Rac1 and Alters Ovarian Cancer Cell Behaviors Critical for Invasion and Metastasis.” Molecular Cancer Therapeutics 14 (10): 2215–27. https://doi.org/10.1158/1535-7163.MCT-15-0419.

Hatano, Noriyuki, Hiroka Suzuki, Yuka Itoh, and Katsuhiko Muraki. 2013. “TRPV4 Partially Participates in Proliferation of Human Brain Capillary Endothelial Cells.” Life Sciences 92 (4–5): 317–24. https://doi.org/10.1016/j.lfs.2013.01.002.

Hazane-Puch, F., J. Arnaud, C. Trocmé, P. Faure, F. Laporte, and P. Champelovier. 2016. “Sodium Selenite Decreased HDAC Activity, Cell Proliferation and Induced Apoptosis in Three Human Glioblastoma Cells.” Anticancer Agents Med Chem 16 (4): 490–500.

Higashimori, Haruki, and Harald Sontheimer. 2007. “Role of Kir4.1 Channels in Growth Control of Glia.” Glia 55 (16): 1668–79. https://doi.org/10.1002/glia.20574.

Hinnebusch, Alan G., Ivaylo P. Ivanov, and Nahum Sonenberg. 2016. “Translational Control by 5’-Untranslated Regions of Eukaryotic MRNAs.” Science 352 (6292): 1413–16. https://doi.org/10.1126/science.aad9868.

Ishii, Masakazu, Akinori Oyama, Tamio Hagiwara, Akira Miyazaki, Yasuo Mori, Yuji Kiuchi, and Shunichi Shimizu. 2007. “Facilitation of H2O2 -Induced A172 Human Glioblastoma Cell Death by Insertion of Oxidative Stress-Sensitive TRPM2 Channels.” Anticancer Research 27 (6B): 3987–92.

Karsy, Michael, Marshall Gelbman, Paarth Shah, Odessa Balumbu, Fred Moy, and Erol Arslan. 2012. “Established and Emerging Variants of Glioblastoma Multiforme: Review of Morphological and Molecular Features.” Folia Neuropathologica 50 (4): 301–21. https://doi.org/10.5114/fn.2012.32361.

Kim, Ji Eun, Jin Young Park, and Tae Cheon Kang. 2017. “TRPC6-Mediated ERK1/2 Activation Regulates Neuronal Excitability via Subcellular Kv4.3 Localization in the Rat Hippocampus.” Frontiers in Cellular Neuroscience 11: 1–16. https://doi.org/10.3389/fncel.2017.00413.

Klumpp, Dominik, Stephanie C. Frank, Lukas Klumpp, Efe C. Sezgin, Marita Eckert, Lena Edalat, Martin Bastmeyer, Daniel Zips, Peter Ruth, and Stephan M. Huber. 2017. “TRPM8 Is Required for Survival and Radioresistance of Glioblastoma Cells.” Oncotarget 8 (56): 95896–913. https://doi.org/10.18632/oncotarget.21436.

Laterra, John, Eliot Rosen, Myeong Nam, Srikanth Ranganathan, Kevin Fielding, and Peter Johnston. 1997. “Scatter Factor / Hepatocyte Growth Factor Expression Enhances Human Glioblastoma Tumorigenicity and Growth.” Biochem Biophys Res Commun 235 (3): 743–47.

Lee, W H, L Y Choong, T H Jin, N N Mon, S Chong, C S Liew, T Putti, S Y Lu, C Harteneck, and Y P Lim. 2017. “TRPV4 Plays a Role in Breast Cancer Cell Migration via Ca2+-Dependent Activation of AKT and Downregulation of E-Cadherin Cell Cortex Protein.” Oncogenesis 6 (5): e338–e338. https://doi.org/10.1038/oncsis.2017.39.

Lepannetier, Sophie, Nadège Zanou, Xavier Yerna, Noémie Emeriau, Inès Dufour, Julien Masquelier, Giulio Muccioli, Nicolas Tajeddine, and Philippe Gailly. 2016. “Sphingosine-1-Phosphate-Activated TRPC1 Channel Controls Chemotaxis of Glioblastoma Cells.” Cell Calcium 60 (6): 373–83. https://doi.org/10.1016/j.ceca.2016.09.002.

Li, Hongyu. 2017. “TRP Channel Classification.” In Transient Receptor Potential Canonical Channels and Brain Diseases, edited by Yizheng Wang, 976:1–8. Dordrecht: Springer Netherlands.

Liberati, S., M.B. Morelli, C. Amantini, M. Santoni, M. Nabissi, C. Cardinali, and G. Santoni. 2014. “Advances in Transient Receptor Potential Vanilloid-2 Channel Expression and Function in Tumor Growth and Progression.” Curr Protein Pept Sci 15 (7): 732–37.

Liu, Ching-ann, Chia-yu Chang, Kuo-wei Hsueh, Hong-lin Su, and Tzyy-wen Chiou. 2018. “Migration / Invasion of Malignant Gliomas and Implications for Therapeutic Treatment.” Int J Mol Sci 19 (4): 1115. https://doi.org/10.3390/ijms19041115.

Liu, J I A, X U E Qing Liu, Ying Liu, Y A N A N Sun, S I Li, and Chun M E I Li. 2016. “MicroRNA 28-5p Regulates ATP-Binding Cassette Transporter A1 via Inhibiting Extracellular Signal-Regulated Kinase 2.” Mol Med Rep 13 (1): 433–40. https://doi.org/10.3892/mmr.2015.4563.

Liu, Mingli, Koichi Inoue, Tiandong Leng, Shanchun Guo, and Zhi-gang Xiong. 2014. “TRPM7 Channels Regulate Glioma Stem Cell through STAT3 and Notch Signaling Pathways.” Cellular Signalling 26 (12): 2773–81. https://doi.org/10.1016/j.cellsig.2014.08.020.

Louis, David N., Hiroko Ohgaki, Otmar D. Wiestler, Webster K. Cavenee, Peter C. Burger, Anne Jouvet, Bernd W. Scheithauer, and Paul Kleihues. 2007. “The 2007 WHO Classification of Tumours of the Central Nervous System.” Acta Neuropathologica 114 (2): 97–109. https://doi.org/10.1007/s00401-007-0243-4.

Louis, David N., Arie Perry, Guido Reifenberger, Andreas von Deimling, Dominique Figarella-Branger, Webster K. Cavenee, Hiroko Ohgaki, Otmar D. Wiestler, Paul Kleihues, and David W. Ellison. 2016. “The 2016 World Health Organization Classification of Tumors of the Central Nervous System: A Summary.” Acta Neuropathologica 131 (6): 803–20. https://doi.org/10.1007/s00401-016-1545-1.

Lucius, Alexander, Noushafarin Khajavi, Peter S. Reinach, Josef Köhrle, Priyavathi Dhandapani, Philipp Huimann, Nina Ljubojevic, Carsten Grötzinger, and Stefan Mergler. 2016. “3-Iodothyronamine Increases Transient Receptor Potential Melastatin Channel 8 (TRPM8) Activity in Immortalized Human Corneal Epithelial Cells.” Cellular Signalling 28 (3): 136–47. https://doi.org/10.1016/j.cellsig.2015.12.005.

Luo, Huilong, Elisa Rossi, Bruno Saubamea, Stéphanie Chasseigneaux, Véronique Cochois, Nina Choublier, Maria Smirnova, et al. 2019. “Cannabidiol Increases Proliferation, Migration, Tubulogenesis, and Integrity of Human Brain Endothelial Cells through TRPV2 Activation.” Molecular Pharmaceutics 16 (3): 1312–26. https://doi.org/10.1021/acs.molpharmaceut.8b01252.

Ma, Irene, and Alison L Allan. 2011. “The Role of Human Aldehyde Dehydrogenase in Normal and Cancer Stem Cells.” Stem Cell Rev Rep 7 (2): 292–306. https://doi.org/10.1007/s12015-010-9208-4.

Mayor, Ugo, Christopher M Johnson, Valerie Daggett, Alice Brown, G Nikolai, Kate A Bower, Shaoxiong Liu, et al. 2001. “Neural Stem Cells Display Extensive Tropism for Pathology in Adult Brain : Evidence from Intracranial Gliomas.” PNAS 97 (23): 12846–51.

Mcferrin, Michael B, and Harald Sontheimer. 2006. “A Role for Ion Channels in Glioma Cell Invasion.” Neuron Glia Biol. 2 (1): 39–49.

Miller, C. Ryan, and Arie Perry. 2007. “Glioblastoma.” Archives of Pathology & Laboratory Medicine 131 (3): 397–406. https://doi.org/10.1043/1543-2165(2007)131[397:G]2.0.CO;2.

Moini, Hadi, Lester Packer, and Nils Erik L. Saris. 2002. “Antioxidant and Prooxidant Activities of α-Lipoic Acid and Dihydrolipoic Acid.” Toxicology and Applied Pharmacology 182 (1): 84–90. https://doi.org/10.1006/taap.2002.9437.

Molenaar, Remco J. 2011. “Ion Channels in Glioblastoma.” ISRN Neurology 2011: 1–7. https://doi.org/10.5402/2011/590249.

Mollinedo, Faustino, and Consuelo Gajate. 2015. “Advances in Biological Regulation Lipid Rafts as Major Platforms for Signaling Regulation in Cancer.” Advances in Biological Regulation 57: 130–46. https://doi.org/10.1016/j.jbior.2014.10.003.

Morelli, Maria Beatrice, Consuelo Amantini, Daniele Tomassoni, Massimo Nabissi, Antonella Arcella, and Giorgio Santoni. 2019. “Transient Receptor Potential Mucolipin-1 Channels in Glioblastoma: Role in Patient’s Survival.” Cancers 11 (4). https://doi.org/10.3390/cancers11040525.

Morelli, Maria Beatrice, Massimo Nabissi, Consuelo Amantini, Valerio Farfariello, Lucia Ricci-Vitiani, Simona Di Martino, Roberto Pallini, et al. 2012. “The Transient Receptor Potential Vanilloid-2 Cation Channel Impairs Glioblastoma Stem-like Cell Proliferation and Promotes Differentiation.” International Journal of Cancer 131 (7): 1067–77. https://doi.org/10.1002/ijc.27588.

Morelli, Maria Beatrice, Massimo Nabissi, Consuelo Amantini, Daniele Tomassoni, Francesco Rossi, Claudio Cardinali, Matteo Santoni, et al. 2016. “Overexpression of Transient Receptor Potential Mucolipin-2 Ion Channels in Gliomas: Role in Tumor Growth and Progression.” Oncotarget 7 (28): 43654–68. https://doi.org/10.18632/oncotarget.9661.

Nabissi, Massimo, Maria Beatrice Morelli, Consuelo Amantini, Valerio Farfariello, Lucia Ricci-Vitiani, Sara Caprodossi, Antonella Arcella, et al. 2010. “TRPV2 Channel Negatively Controls Glioma Cell Proliferation and Resistance to Fas-Induced Apoptosis in ERK-Dependent Manner.” Carcinogenesis 31 (5): 794–803. https://doi.org/10.1093/carcin/bgq019.

Nabissi, Massimo, Maria Beatrice Morelli, Consuelo Amantini, Sonia Liberati, Matteo Santoni, Lucia Ricci-Vitiani, Roberto Pallini, and Giorgio Santoni. 2015. “Cannabidiol Stimulates AML-1a-Dependent Glial Differentiation and Inhibits Glioma Stem-like Cells Proliferation by Inducing Autophagy in a TRPV2-Dependent Manner.” International Journal of Cancer 137 (8): 1855–69. https://doi.org/10.1002/ijc.29573.

Nabissi, Massimo, Maria Beatrice Morelli, Antonietta Arcella, Claudio Cardinali, Matteo Santoni, Giovanni Bernardini, Angela Santoni, Giorgio Santoni, and Consuelo Amantini. 2016. “Post-Transcriptional Regulation of 5’-Untranslated Regions of Human Transient Receptor Potential Vanilloid Type-1 (TRPV-1) Channels: Role in the Survival of Glioma Patients.” Oncotarget 7 (49): 81541–54. https://doi.org/10.18632/oncotarget.13132.

Nabissi, Massimo, Maria Beatrice Morelli, Matteo Santoni, and Giorgio Santoni. 2013. “Triggering of the TRPV2 Channel by Cannabidiol Sensitizes Glioblastoma Cells to Cytotoxic Chemotherapeutic Agents.” Carcinogenesis 34 (1): 48–57. https://doi.org/10.1093/carcin/bgs328.

Naziroğlu, Mustafa. 2012. “Molecular Role of Catalase on Oxidative Stress-Induced Ca2 Signaling and TRP Cation Channel Activation in Nervous System.” Journal of Receptors and Signal Transduction 32 (3): 134–41. https://doi.org/10.3109/10799893.2012.672994.

Naziroglu, Mustafa, and Andreas Lückhoff. 2008. “Effects of Antioxidants on Calcium Influx through TRPM2 Channels in Transfected Cells Activated by Hydrogen Peroxide ☆.” J Neurol Sci 270 (1–2): 152–58. https://doi.org/10.1016/j.jns.2008.03.003.

Neumann-Raizel, Hagit, Asaf Shilo, Shaya Lev, Maxim Mogilevsky, Ben Katz, David Shneor, Yoav D. Shaul, et al. 2019. “2-APB and CBD-Mediated Targeting of Charged Cytotoxic Compounds into Tumor Cells Suggests the Involvement of TRPV2 Channels.” Frontiers in Pharmacology 10: 1–15. https://doi.org/10.3389/fphar.2019.01198.

Olsen, Michelle L., and Harald Sontheimer. 2008. “Functional Implications for Kir4.1 Channels in Glial Biology: From K + Buffering to Cell Differentiation.” Journal of Neurochemistry 107 (3): 589–601. https://doi.org/10.1111/j.1471-4159.2008.05615.x.

Ostrom, Quinn T., Haley Gittleman, Jordonna Fulop, Max Liu, Rachel Blanda, Courtney Kromer, Yingli Wolinsky, Carol Kruchko, and Jill S. Barnholtz-Sloan. 2015. “CBTRUS Statistical Report: Primary Brain and Central Nervous System Tumors Diagnosed in the United States in 2008-2012.” Neuro-Oncology 17 (Suppl 4): iv1–62. https://doi.org/10.1093/neuonc/nov189.

Ostrom, Quinn T., Haley Gittleman, Peter Liao, Toni Vecchione-Koval, Yingli Wolinsky, Carol Kruchko, and Jill S. Barnholtz-Sloan. 2017. “CBTRUS Statistical Report: Primary Brain and Other Central Nervous System Tumors Diagnosed in the United States in 2010–2014.” Neuro-Oncology 19 (suppl_5): v1–88. https://doi.org/10.1093/neuonc/nox158.

Ou-yang, Qing, Bing Li, Minhui Xu, and Hong Liang. 2018. “TRPV4 Promotes the Migration and Invasion of Glioma Cells via AKT/Rac1 Signaling.” Biochemical and Biophysical Research Communications 503 (2): 876–81. https://doi.org/10.1016/j.bbrc.2018.06.090.

Peier, Andrea M, Aziz Moqrich, Anne C Hergarden, Alison J Reeve, David A Andersson, Gina M Story, Taryn J Earley, et al. 2002. “A TRP Channel That Senses Cold Stimuli and Menthol.” Cell 108 (5): 705–15.

Peng, Wesley, Yvette C. Wong, and Dimitri Krainc. 2020. “Mitochondria-Lysosome Contacts Regulate Mitochondrial Ca2+ Dynamics via Lysosomal TRPML1.” Proceedings of the National Academy of Sciences of the United States of America 117 (32): 19266–75. https://doi.org/10.1073/pnas.2003236117.

Pires, P.W., and S. Earley. 2017. “Redox Regulation of Transient Receptor Potential Channels in the Endothelium.” Microcirculation 24 (3). https://doi.org/10.1016/j.physbeh.2017.03.040.

———. 2018. “Neuroprotective Effects of Trpa1 Channels in the Cerebral Endothelium Following Ischemic Stroke.” ELife 7: 1–29. https://doi.org/10.7554/eLife.35316.

Prabhu, Antony, Pravin Kesarwani, Shiva Kant, Stewart F Graham, and Prakash Chinnaiyan. 2017. “Histologically Defined Intratumoral Sequencing Uncovers Evolutionary Cues into Conserved Molecular Events Driving Gliomagenesis.” Neuro-Oncology 19 (12): 1599–1606. https://doi.org/10.1093/neuonc/nox100.

Prevarskaya, Natalia, Lei Zhang, and Greg Barritt. 2007. “TRP Channels in Cancer.” Biochimica et Biophysica Acta - Molecular Basis of Disease 1772 (8): 937–46. https://doi.org/10.1016/j.bbadis.2007.05.006.

Qin, Wenyi, Rong Xiaofeng, Dong Jiangchuan, Chao Yu, and Yang Juan. 2017. “MiR-142 Inhibits the Migration and Invasion of Glioma by Targeting Rac1.” Oncology Reports 38 (3): 1543–50. https://doi.org/10.3892/or.2017.5816.

Ransom, Christopher B., Jeffrey T. O’Neal, and Harald Sontheimer. 2001. “Volume-Activated Chloride Currents Contribute to the Resting Conductance and Invasive Migration of Human Glioma Cells.” Journal of Neuroscience 21 (19): 7674–83. https://doi.org/10.1523/jneurosci.21-19-07674.2001.

Ransom, Christopher B, and Harald Sontheimer. 2001. “BK Channels in Human Glioma Cells.” J Neurophysiol 85 (2): 790–803.

Rasper, Michael, Andrea Schafer, Guido Piontek, Julian Teufel, Gero Brockhoff, Florian Ringel, Stefan Heindl, and Claus Zimmer. 2010. “Aldehyde Dehydrogenase 1 Positive Glioblastoma Cells Show Brain Tumor Stem Cell Capacity ¨.” Neuro-Oncology 12 (10): 1024–33.

Ratto, Daniela, Beatrice Ferrari, Elisa Roda, Federico Brandalise, Stella Siciliani, Fabrizio De Luca, Erica Cecilia Priori, et al. 2020. “Squaring the Circle: A New Study of Inward and Outward-Rectifying Potassium Currents in U251 GBM Cells.” Cellular and Molecular Neurobiology 40 (5): 813–28. https://doi.org/10.1007/s10571-019-00776-3.

Rho, Seung-sik, Isao Kobayashi, Seung-sik Rho, Isao Kobayashi, Eri Oguri-nakamura, Koji Ando, Masakazu Fujiwara, and Naomi Kamimura. 2019. “Rap1b Promotes Notch-Signal-Mediated Hematopoietic Stem Cell Development by Enhancing Integrin-Mediated Cell Adhesion.” Developmental Cell 49 (5): 681-696.e6. https://doi.org/10.1016/j.devcel.2019.03.023.

Ryu, Hea Jin, Ji Eun Kim, Yeon Joo Kim, Ji Yang Kim, Won Il Kim, So Yeon Choi, Min Ju Kim, and Tae Cheon Kang. 2013. “Endothelial Transient Receptor Potential Conical Channel (TRPC)-3 Activation Induces Vasogenic Edema Formation in the Rat Piriform Cortex Following Status Epilepticus.” Cellular and Molecular Neurobiology 33 (4): 575–85. https://doi.org/10.1007/s10571-013-9931-x.

Santoni, Giorgio, and Valerio Farfariello. 2011. “TRP Channels and Cancer: New Targets for Diagnosis and Chemotherapy.” Endocrine, Metabolic & Immune Disorders - Drug Targets 11 (1): 54–67. https://doi.org/10.2174/187153011794982068.

Schwartzbaum, J.A., J.L. Fisher, K.D. Aldape, and M. Wrensch. 2006. “Epidemiology and Molecular Pathology of Glioma.” Nat Clin Pract Neurol 2 (9): 494–503.

Shi, Xiaomin, and Fei Teng. 2015. “Down-Regulated MiR-28-5p in Human Hepatocellular Carcinoma Correlated with Tumor Proliferation and Migration by Targeting.” Molecular and Cellular Biochemistry 408 (1): 283–93. https://doi.org/10.1007/s11010-015-2506-z.

Singh, Itender, Nebojsa Knezevic, Gias U Ahmmed, Vidisha Kini, Asrar B Malik, and Dolly Mehta. 2007. “Gαq -TRPC6-Mediated Ca 2+ Entry Induces RhoA Activation and Resultant Endothelial Cell Shape Change in Response to Thrombin.” J. Biol. Chem 282 (11): 7833–43. https://doi.org/10.1074/jbc.M608288200.

Stark, George R., and William R. Taylor. 2006. “Control of the G2/M Transition.” Molecular Biotechnology 32 (3): 227–48. https://doi.org/10.1385/MB:32:3:227.

Steinle, Marc, Daniela Palme, Milan Misovic, Justine Rudner, Klaus Dittmann, Robert Lukowski, Peter Ruth, and Stephan M Huber. 2011. “Ionizing Radiation Induces Migration of Glioblastoma Cells by Activating BK K + Channels.” Radiotherapy and Oncology 101 (1): 122–26. https://doi.org/10.1016/j.radonc.2011.05.069.

Stepanenko, Aleksei A., and Vladimir P. Chekhonin. 2018. “Recent Advances in Oncolytic Virotherapy and Immunotherapy for Glioblastoma: A Glimmer of Hope in the Search for an Effective Therapy?” Cancers 10 (12). https://doi.org/10.3390/cancers10120492.

Stock, Kristin, Jitender Kumar, Michael Synowitz, Stefania Petrosino, Roberta Imperatore, Ewan St J. Smith, Peter Wend, et al. 2012. “Neural Precursor Cells Induce Cell Death of High-Grade Astrocytomas through Stimulation of TRPV1.” Nature Medicine 18 (8): 1232–38. https://doi.org/10.1038/nm.2827.

Stuart, Edward T., Chrissa Kioussi, Peter Gruss, and Adriano Aguzzi. 1995. “PAX5 Expression Correlates with Increasing Malignancy in Human Astrocytomas.” Clinical Cancer Research 1 (2): 207–14.

Stupp, Roger, Monika E. Hegi, Warren P. Mason, Martin J. van den Bent, Martin J. B. Taphoorn, Robert C. Janzer, Samuel K. Ludwin, et al. 2009. “Effects of Radiotherapy with Concomitant and Adjuvant Temozolomide versus Radiotherapy Alone on Survival in Glioblastoma in a Randomised Phase III Study: 5-Year Analysis of the EORTC-NCIC Trial.” The Lancet. Oncology 10 (5): 459–66. https://doi.org/10.1016/S1470-2045(09)70025-7.

Stupp, Roger, Warren P. Mason, Martin J. van den Bent, Michael Weller, Barbara Fisher, Martin J.B. Taphoorn, Karl Belanger, et al. 2005. “Radiotherapy plus Concomitant and Adjuvant Temozolomide for Glioblastoma.” New England Journal of Medicine 352 (10): 987–96. https://doi.org/10.1056/NEJMoa043330.

Sullivan, Michelle N, Albert L Gonzales, Paulo W Pires, Allison Bruhl, M Dennis Leo, Wencheng Li, Agathe Oulidi, et al. 2016. “Oxygen Species Promote Cerebral Artery Dilation.” Sci Signal 8 (358): 1–26. https://doi.org/10.1126/scisignal.2005659.Localized.

Tai, Yilin, Shengjie Feng, Ruiliang Ge, Wanlu Du, Xiaoxing Zhang, Zhuohao He, and Yizheng Wang. 2008. “TRPC6 Channels Promote Dendritic Growth via the CaMKIV-CREB Pathway.” Journal of Cell Science 121 (14): 2301–7. https://doi.org/10.1242/jcs.026906.

Takahashi, Nobuaki, Hsing Yu Chen, Isaac S. Harris, Daniel G. Stover, Laura M. Selfors, Roderick T. Bronson, Thomas Deraedt, et al. 2018. “Cancer Cells Co-Opt the Neuronal Redox-Sensing Channel TRPA1 to Promote Oxidative-Stress Tolerance.” Cancer Cell 33 (6): 985-1003.e7. https://doi.org/10.1016/j.ccell.2018.05.001.

Takahashi, Nobuaki, Daisuke Kozai, Ryohei Kobayashi, Maximilian Ebert, and Yasuo Mori. 2011. “Cell Calcium Roles of TRPM2 in Oxidative Stress.” Cell Calcium 50 (3): 279–87. https://doi.org/10.1016/j.ceca.2011.04.006.

Thompson, Craig B. 1995. “Apoptosis in the Pathogenesis and Treatment of Disease.” Science 267 (5203): 1456–62.

Valadez, Jessica A., and Math P. Cuajungco. 2015. “PAX5 Is the Transcriptional Activator of Mucolipin-2 (MCOLN2) Gene.” Gene 555 (2): 194–202. https://doi.org/10.1016/j.gene.2014.11.003.

Veldhuis, Nicholas A., Daniel P. Poole, Megan Grace, Peter McIntyre, and Nigel W. Bunnett. 2015. “The g Protein–Coupled Receptor–Transient Receptor Potential Channel Axis: Molecular Insights for Targeting Disorders of Sensation and Inflammation.” Pharmacological Reviews 67 (1): 36–73. https://doi.org/10.1124/pr.114.009555.

Venkatachalam, K., and C. Montell. 2007. “TRP Channels.” Annu Rev Biochem 76: 387–417. https://doi.org/10.1146/annurev.biochem.75.103004.142819.

Venugopal, Bhuvarahamurthy, Nicholas T. Mesires, John C. Kennedy, Cyntia Curcio-Morelli, Janice M. Laplante, J. Fred Dice, and Susan A. Slaugenhaupt. 2009. “Chaperone-Mediated Autophagy Is Defective in Mucolipidosis Type IV.” Journal of Cellular Physiology 219 (2): 344–53. https://doi.org/10.1002/jcp.21676.

Walcher, Lia, Clara Budde, Arina Böhm, Peter S. Reinach, Priyavathi Dhandapani, Nina Ljubojevic, Markus W. Schweiger, et al. 2018. “Induced Transactivation of TRPV1 in Human Uveal Melanoma Cells.” Frontiers in Pharmacology 9 (NOV). https://doi.org/10.3389/fphar.2018.01234.

Walzlein, J-H, M Synowitz, B. Engels, D. S. Markovic, K. Gabrusiewicz, E. Nikolaev, K. Yoshikawa, et al. 2008. “Antitumorigenic Response of Neural Precursors Depends on Subventricular Proliferation and Age.” Stem Cells 26 (11): 2945–54. https://doi.org/10.1634/stemcells.2008-0307.

Wan, Jingwei, Alyssa Aihui Guo, Indrajit Chowdhury, and Shanchun Guo. 2019. “TRPM7 Induces Mechanistic Target of Rap1b Through the Downregulation of MiR-28-5p in Glioma Proliferation and Invasion.” Front Oncol. 9 (1413): 1–14. https://doi.org/10.3389/fonc.2019.01413.

Watkins, Stacey, Stefanie Robel, Ian F. Kimbrough, Stephanie M. Robert, Graham Ellis-Davies, and Harald Sontheimer. 2014. “Disruption of Astrocyte–Vascular Coupling and the Blood–Brain Barrier by Invading Glioma Cells.” Nature Communications 5 (1): 1–15. https://doi.org/10.1038/ncomms5196.

Wen, Patrick Y, and Alba A Brandes. 2009. “Treatment of Recurrent High-Grade Gliomas:” Current Opinion in Neurology 22 (6): 657–64. https://doi.org/10.1097/WCO.0b013e32833229e3.

Wondergem, Robert, and Jeremy W. Bartley. 2009. “Menthol Increases Human Glioblastoma Intracellular Ca2+, BK Channel Activity and Cell Migration.” Journal of Biomedical Science 16 (1): 1–7. https://doi.org/10.1186/1423-0127-16-90.

Wondergem, Robert, Tom W Ecay, Frank Mahieu, Grzegorz Owsianik, and Bernd Nilius. 2008. “Biochemical and Biophysical Research Communications HGF / SF and Menthol Increase Human Glioblastoma Cell Calcium and Migration” 372: 210–15. https://doi.org/10.1016/j.bbrc.2008.05.032.

Xiao, Fangtao, Zhenguo Cheng, Pengliang Wang, Baoheng Gong, Hanwei Huang, Yanan Xing, and Funan Liu. 2018. “MicroRNA-28-5p Inhibits the Migration and Invasion of Gastric Cancer Cells by Suppressing AKT Phosphorylation.” Oncol Lett 15 (6): 9777–85. https://doi.org/10.3892/ol.2018.8603.

Yao, X.H., Y-F Ping, J-H Chen, C-P Xu, D-L Chen, R. Zhang, JM Wang, and X-W Bian. 2008. “Glioblastoma Stem Cells Produce Vascular Endothelial Growth Factor by Activation of a G-Protein Coupled Formylpeptide Receptor FPR.” J Pathol. 215 (4): 369–76. https://doi.org/10.1002/path.2356.Glioblastoma.

Ying, Zhe, Yun Li, Jueheng Wu, Xun Zhu, Yi Yang, Han Tian, Wei Li, Bo Hu, and Shi-yuan Cheng. 2013. “Loss of MiR-204 Expression Enhances Glioma Migration and Stem Cell-like Phenotype.” Cancer Research 73 (2): 990–1000. https://doi.org/10.1158/0008-5472.CAN-12-2895.

Yu, Xiaoming, Yuhua Jiang, Wei Wei, and Ping Cong. 2015. “Androgen Receptor Signaling Regulates Growth of Glioblastoma Multiforme in Men.” Tumour Biol 36 (2): 967–72. https://doi.org/10.1007/s13277-014-2709-z.

Zamudio-Bulcock, P.A., J. Everett, C. Harteneck, and C.F. Valenzuela. 2011. “Activation of Steroid-Sensitive TRPM3 Channels Potentiates Glutamatergic Transmission at Cerebellar Purkinje Neurons From Developing Rats.” Neurochemistry, Journal O F, 474–85. https://doi.org/10.1111/j.1471-4159.2011.07441.x.

Zeng, Jianping, Ye Wu, Siyi Zhuang, Liping Qin, Shushan Hua, Rajneesh Mungur, Jianwei Pan, Yu Zhu, and Renya Zhan. 2019. “Identification of the Role of TRPM8 in Glioblastoma and Its Effect on Proliferation, Apoptosis and Invasion of the U251 Human Glioblastoma Cell Line.” Oncology Reports 42 (4): 1517–26. https://doi.org/10.3892/or.2019.7260.

Zhang, Xiaoli, Xiping Cheng, Lu Yu, Junsheng Yang, Raul Calvo, Samarjit Patnaik, Xin Hu, et al. 2016. “MCOLN1 Is a ROS Sensor in Lysosomes That Regulates Autophagy.” Nature Communications 7 (May). https://doi.org/10.1038/ncomms12109.

Zhang, Xiaoli, Lu Yu, and Haoxing Xu. 2016. “Lysosome Calcium in ROS Regulation of Autophagy.” Autophagy 12 (10): 1954–55. https://doi.org/10.1080/15548627.2016.1212787.

Zhou, Jian, Wanlu Du, Kechun Zhou, Yilin Tai, Hailan Yao, Yichang Jia, Yuqiang Ding, and Yizheng Wang. 2008. “Critical Role of TRPC6 Channels in the Formation of Excitatory Synapses.” Nature Neuroscience 11 (7): 741–43. https://doi.org/10.1038/nn.2127.

Zhou, Kai, Jun Rao, Zhi hua Zhou, Xiao hong Yao, Feng Wu, Jing Yang, Lang Yang, et al. 2018. “RAC1-GTP Promotes Epithelial-Mesenchymal Transition and Invasion of Colorectal Cancer by Activation of STAT3.” Laboratory Investigation 98 (8): 989–98. https://doi.org/10.1038/s41374-018-0071-2.